Jacob Lubliner
Panayiotis Papadopoulos

Introduction to Solid Mechanics

An Integrated Approach

Second Edition

Springer

Introduction to Solid Mechanics

Jacob Lubliner • Panayiotis Papadopoulos

Introduction to Solid Mechanics

An Integrated Approach

Second Edition

Springer

Jacob Lubliner
University of California, Berkeley
Berkeley, CA, USA

Panayiotis Papadopoulos
Department of Mechanical Engineering
University of California, Berkeley
Berkeley, CA, USA

ISBN 978-3-319-18877-5 ISBN 978-3-319-18878-2 (eBook)
DOI 10.1007/978-3-319-18878-2

Library of Congress Control Number: 2015954812

© Springer International Publishing Switzerland 2014, 2017

This work is subject to copyright. All rights are reserved by the Publisher, whether the whole or part of the material is concerned, specifically the rights of translation, reprinting, reuse of illustrations, recitation, broadcasting, reproduction on microfilms or in any other physical way, and transmission or information storage and retrieval, electronic adaptation, computer software, or by similar or dissimilar methodology now known or hereafter developed.

The use of general descriptive names, registered names, trademarks, service marks, etc. in this publication does not imply, even in the absence of a specific statement, that such names are exempt from the relevant protective laws and regulations and therefore free for general use.

The publisher, the authors and the editors are safe to assume that the advice and information in this book are believed to be true and accurate at the date of publication. Neither the publisher nor the authors or the editors give a warranty, express or implied, with respect to the material contained herein or for any errors or omissions that may have been made.

Printed on acid-free paper

This Springer imprint is published by Springer Nature

The registered company is Springer International Publishing AG

The registered company address is: Gewerbestrasse 11, 6330 Cham, Switzerland

Preface

Since the turn of the millennium, it has become common in North American engineering schools and colleges to combine the traditional undergraduate offerings in rigid-body statics (usually called simply "statics") and deformable-body mechanics (known traditionally as "strength of materials" and more recently called "mechanics of materials") into a single introductory course in solid mechanics. Since the textbooks for both of the traditional courses were often the work of a single author or group of authors, the publishing world has found it expedient to create textbooks for the new course by sequentially melding pieces of the existing books, sometimes (but not always) acknowledging the origin by dividing the book into halves titled Statics and Mechanics of Materials.

When a course of the new type was introduced in the College of Engineering of the University of California at Berkeley, we felt that it would be more sensible to treat the material in an integrated way, proceeding from first principles to applications, and we found that the available textbooks forced us (and the students) to move around in a labyrinthine fashion. This experience moved us (JL and PP), with the encouragement of our colleagues, to consider writing a book in which the material would be presented methodically. After three years of work we are ready to present the result to the world of engineering education, in the hope that others teaching introductory solid mechanics might see the subject in a light similar to ours.

The traditional topics of "statics" are covered in the first three chapters, whose respective subjects are (1) forces and moments (including the necessary mathematical preliminaries and a thorough discussion of dimensions and units); (2) equilibrium (beginning with the equilibrium of particle system as studied in elementary physics, and including friction; the concept of work, both real and virtual; and the method of sections in its general sense); and (3) articulated assemblages of rigid members, beginning with a general discussion of the method of joints and covering trusses, frames, machines, chains and cables (with a brief discussion of the relation between cables and arches).

The middle third of the book is devoted to the fundamentals of the mechanics of deformable solids: a chapter each on stress, deformation and strain, and elasticity. All these concepts are developed to their full three-dimensional

aspect, and while only isotropic elasticity is studied in depth, care is taken to define isotropy precisely, and examples of anisotropic elasticity are given for illustration. The chapter on stress includes a section devoted to what we call "simple stress states," that is, the special cases in which stress can be determined by statics alone, and stress-based design is introduced as a consequence. Stress and strain transformations, including the determination of principal axes, are discussed from both the geometric and algebraic points of view. In the chapter on deformation and strain, virtual displacement and virtual work in continua are discussed in detail, both in general and in special cases.

The chapter on elasticity includes sections on static indeterminacy (with introductions to the force and displacements methods), on elastic energy (including the classic energy principles) and on thermoelasticity. The former two sections include a basic introduction to the finite-element method.

The elongation of axially loaded elastic bars is also covered in a section of the elasticity chapter, since the relative simplicity of the problem does not warrant a chapter of its own. The other classic engineering applications of solid mechanics are, on the other hand, covered separately in subsequent chapters: torsion, bending (a chapter each for the basic theory and for additional topics), and buckling.

Singularity functions, whose use is suggested optionally in several contexts (and illustrated in conjunction with bending), are covered in an appendix.

A chapter discussing, in a mostly qualitative way, inelasticity (including a description of various test methods) and material failure (including failure mechanisms and failure criteria), as well as structural failure (including an introduction to ultimate-load analysis), concludes the book.

While the book was conceived with the intent of serving as a text for a one-semester (or one-quarter) course, we have found, after completing it, that the coverage is, in most areas, far more thorough than might be warranted in such a course, and might even serve the needs of a two-term course. With the time constraint of one term, it is likely that several topics or subtopics may have to be omitted because of time constraints. Such omissions are, of course, at the judicious discretion of the instructor, and we will not presume to indicate (as is often done, for example, with asterisks) which topics are to be considered less important than others. We believe that the structure of the book lends itself to a smooth coverage of the material in spite of possible omissions.

Preface to the Second Edition

It took us only a year's experience using this book in teaching the course for which it was designed to realize that it could be improved in a number of ways.

First, we eliminated as many remaining typos as we could find, as well as some visual infelicities largely due to our initial failure to adhere to the publisher's house style.

Second, we found that a number of the topics covered were not suitably illustrated with examples or lacked follow-up exercises. We have tried to compensate for these deficiencies as much as possible.

Third, we decided that the coverage of inelastic behavior in Chapter 11 needed, for the sake of completeness, at least a minimal treatment of viscoelasticity. We have now provided one in the form of an additional subsection in Section 11.2.

We would like to point out that virtually all the non-photographic figures in the book were produced using the LaTeX picture environment, and we would like to express our appreciation to the many developers of the LaTeX packages that made this task feasible.

We were encouraged by our editor at Springer US, Michael Luby, to proceed with the preparation of the second edition with no delay, and we have accordingly done so.

Contents

Preface v

1 Forces and Moments 1
- 1.1 Introduction . . . 1
- 1.2 Review of Vectors . . . 14
- 1.3 Forces . . . 24
- 1.4 Moments . . . 30
- 1.5 Statically Equivalent Force Systems . . . 40

2 Equilibrium 51
- 2.1 Equilibrium of Particle Systems . . . 51
- 2.2 Equilibrium of Rigid Bodies in Two Dimensions . . . 65
- 2.3 Equilibrium of Rigid Bodies in Three Dimensions . . . 88
- 2.4 Method of Sections . . . 98

3 Articulated Assemblages of Rigid Members 107
- 3.1 Method of Joints . . . 107
- 3.2 Two-Dimensional Trusses . . . 115
- 3.3 Three-Dimensional Trusses . . . 127
- 3.4 Frames and Machines . . . 134
- 3.5 Chains and Cables . . . 142

4 Stress 155
- 4.1 Normal Stress, Saint-Venant's Principle . . . 155
- 4.2 Shear Stress . . . 162
- 4.3 Simple Stress States, Stress-Based Design . . . 169
- 4.4 General State of Stress . . . 180
- 4.5 Local Equilibrium Equations . . . 188
- 4.6 Stress Transformation, Principal Stresses, Mohr's Circle . . . 195

5 Deformation and Strain **215**
5.1 Longitudinal Strain 215
5.2 Shear Strain 224
5.3 Displacement, General State of Strain 230
5.4 Strain Transformation, Principal Strains 239

6 Elasticity **247**
6.1 Springs and Hooke's Law (Axial and Shear) 247
6.2 Generalized Hooke's Law 257
6.3 Elongation of Axially Loaded Elastic Bars 273
6.4 Static Indeterminacy in Linearly Elastic Bodies 289
6.5 Elastic Energy 300
6.6 Thermoelastic Properties of Solids 315

7 Torsion **323**
7.1 Torsion of elastic circular bars 323
7.2 Torsion of Non-Circular Thin-Walled Tubes 335
7.3 Compound Shafts 342
7.4 Open Thin-Walled Sections 347

8 Elastic Bending of Beams **353**
8.1 Shear and Bending-Moment Diagrams 353
8.2 Pure Bending of Beams 366
8.3 Bernoulli–Euler Beam Theory 379
8.4 Calculation of Elastic Beam Deflections 391

9 Additional Topics in Bending **405**
9.1 Composite Cross-Sections 405
9.2 Asymmetric Bending of Beams 413
9.3 Shear Stresses in Beams 421
9.4 Stresses in Beams Under Combined Loading 434

10 Elastic Stability and Buckling **441**
10.1 Buckling Fundamentals and Simple Models 441
10.2 Stability and Energy 450
10.3 Buckling of Elastic Columns 456

11 Inelasticity and Material Failure **473**

11.1 Stress-Strain Diagrams 473

11.2 Material Failure 486

11.3 Structural failure 501

Appendix A: Singularity Functions **513**

Appendix B: Tables **517**

Photo Credits **521**

Index **525**

Chapter 1

Forces and Moments

1.1 Introduction

1.1.1 Fundamental Concepts of Solid Mechanics

Mechanics, as a scientific discipline, is the study of the behavior of bodies subject to forces and displacements (and, to some extent, heating and cooling). *Solid mechanics* is the branch of mechanics dealing specifically with solid bodies.* We will begin by defining some of the basic concepts of mechanics.

A *body*, for the purpose of mechanics, is a portion of matter that, at a given moment in time, occupies a certain region in space. If the region occupied by the body can be idealized as being of negligible extent (and thus reducible to a point), the body is called a *particle*. Any body that is not reducible to a single particle will be called a *finite* body. A finite body occupying a connected region every portion of which contains some matter is called a *continuous* body or, simply, a *continuum*. But at any point in a region occupied by a continuum, the matter in its immediate (infinitesimal) neighborhood can also be thought of as constituting a particle, and we may thus speak of the particles (also called material points) of a continuum.

A body is said to undergo a *displacement* when some or all of its particles are moved to occupy different positions in space. The correspondence between the particles and the positions occupied by them at a given time is known as the body's *configuration*. The displacement of a body is said to be *rigid* if the distances between all pairs of particles are the same in any two configurations. Otherwise, the body is said to undergo *deformation*. Bodies that can undergo only rigid displacements are called *rigid bodies*. Bodies that are not rigid are *deformable*.

*While a very precise and general definition of a *solid* body is challenging, we will consider here a body to be solid if all of its material points that are close to each other remain so for a long time even when the body is subject to external loads. Another common characteristic of most solid bodies is that they retain their overall shape even when not confined in a container.

© Springer International Publishing Switzerland 2017

J. Lubliner, P. Papadopoulos, *Introduction to Solid Mechanics*,
DOI 10.1007/978-3-319-18878-2_1

Motion is said to occur when the body occupies a succession of different configurations continuously over time. A *rigid motion* is a motion that involves only rigid displacements.[†] The rate of change, in time, of the position of a particle is its *velocity*. The velocity may in turn change in time, and its rate of change is the *acceleration*. The motion of a body is called *uniform* if the acceleration of all particles is zero; otherwise it is called *accelerated*. The branch of mechanics dealing with the displacement and motion of bodies is called *kinematics*.

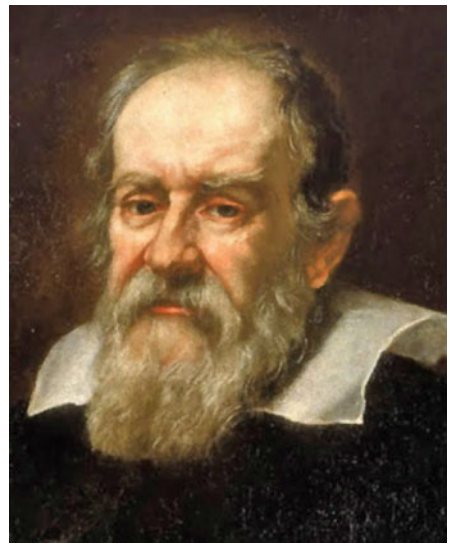

Figure 1.1. Galileo Galilei

Forces are interactions between bodies that cause them to move, and more specifically to accelerate, relative to each other (unless prevented from doing so by other forces). All bodies on or near the earth are subject to the earth's *gravitational force* and, as shown by Galileo[‡] in his famous experiments, will fall toward the center of the earth (unless prevented from doing so by other forces) with the same acceleration; the magnitude of this acceleration is denoted by g.

It was later shown by Newton[§], on the basis of Kepler's[¶] laws of planetary motion, that the magnitude of the acceleration (with respect to a frame of reference based on the "fixed" stars) due to gravitational force between any two bodies (idealized as particles) is inversely proportional to the square of the distance between them, and for each body it is proportional to the quantity

[†]A rigid motion is sometimes also referred to as "rigid-body" motion, although it is clear that rigid motions may be experienced by either rigid or deformable bodies.

[‡]Galileo Galilei (1564-1642) was an Italian physicist and mathematician (Fig. 1.1).

[§]Sir Isaac Newton (1643-1727) was an English physicist and mathematician (Fig. 1.2).

[¶]Johannes Kepler (1571-1630) was a German mathematician and astronomer.

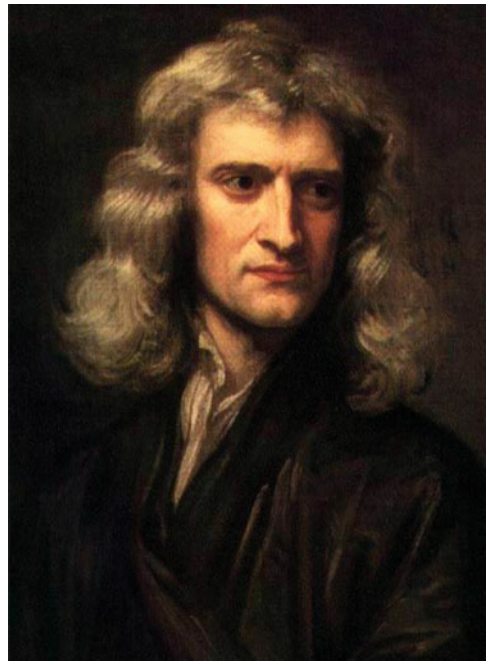

Figure 1.2. Sir Isaac Newton

of matter (or *mass*) of the other body. The product of mass and acceleration is therefore equal and opposite for the two bodies, and may be identified with the force exerted on each body by the other.

If a body's acceleration is zero, then it is at rest or in a uniform motion. In this case, the forces is said to be in *equilibrium*. The study of equilibrium is known as *statics*, and constitutes one the main subjects of this book. Traditionally, statics deals only (or at least primarily) with rigid bodies, while deformable bodies are studied in courses historically called *strength of materials* (or, more recently, *mechanics of materials*). In this book, the statics of rigid *and* deformable solid bodies will be studied in an integrated manner.

1.1.2 Units and Dimensions

The physical quantities already mentioned (distance or length, time, mass, force), as well as others (area, volume, temperature), have magnitudes whose numerical values are expressed in terms of certain reference values called *units*.

Traditionally, units have been defined on the basis of some aspect of everyday human experience or observation. For the measurement of time, for example, the basis was the mean solar day, which is divided into 24 hours, $24 \times 60 = 1440$ minutes and $24 \times 60^2 = 86400$ seconds. Modern scientific convention, on the other hand, favors precise laboratory measurements, and

since the earth's rotation is slowing down, atomic clocks are used to define time intervals. Thus, the fundamental unit of time is the second (abbreviated s)[||], which is nowadays defined as the duration of 9,192,631,770 periods of the radiation corresponding to the transition between the two hyperfine levels of the ground state of the caesium 133 atom.

For the measurement of other quantities, most nations (and even regions) have traditionally had their own customary sets of units. Nowadays, the overwhelming majority of people uses units based on the *metric system* introduced during the French Revolution. Only countries that were once part of the British Empire continue to use units based on the customary ones of England and known as *imperial units*, and only in a small number of these countries (including the United States of America) are these units still primary. The units used in the United States that are derived from the imperial system are known as *United States (US) customary* units.

In the metric system the basic unit of length is the meter[**] (m), originally defined as $1/40,000,000$ of the earth's circumference at the equator but nowadays as the distance traveled by light in $1/299,792,458$ of a second. All other units of length (except some that are used in astronomy) are defined as decimal multiples of the meter and designated with the corresponding prefixes defined in the *Système International* (SI).[††] These include: centi- (c) for 10^{-2}, milli- (m) for 10^{-3}, micro- (μ) for 10^{-6}, nano- (n) for 10^{-9}, pico- (p) for 10^{-12}, kilo- (k) for 10^{3}, mega- (M) for 10^{6}, giga- (G) for 10^{9} and tera- (T) for 10^{12}. The prefixes designating numbers less than one are also used to designate time units smaller than a second, such as the millisecond (ms).

In the US customary system the smallest named unit is the inch (in), officially defined as exactly 25.4 mm (0.0254 m), but originally thought of as the width of one's thumb. Other units are various multiples of the inch: foot (ft = 12 in), yard (yd = 3 ft), and mile (mi = 1,760 yd). Yet other units are found in specialized applications, such as the rod (5.5 yd), chain (4 rods) and furlong (10 chains = 1/8 mi) in surveying, and the fathom (2 yd) in nautical usage.

Measurements of area and volume are expressed in the squares and cubes, respectively, of the units of length. Examples include the square meter (m^2) or the square inch (in^2, also sq in), and the cubic centimeter (cm^3, also cc) or the cubic foot (ft^3, also cu ft). For measurements of land area there are derived units: the hectare (ha = 10^4 m^2) and the acre (the product of one chain and one furlong, or 43,560 ft^2). A commonly used metric unit of volume is the liter or litre (L or l), equal to 10^{-3} m^3; a milliliter (ml) is therefore equal to a cubic centimeter. In North America, the volume of water reservoirs (and hence the volume of large quantities of water in general) is often expressed as

[||] Abbreviations of units are written in roman font and without a period.

[**] It is spelled *metre* in most English-speaking countries, including Canada.

[††] The previously defined atomic-clock-based second is known as the *SI second*.

the product of its area in acres and its depth in feet, resulting in the acre-foot (43,560 ft^3). But the US customary system also has two other sets of units for volume that are not directly related to the units of length. For *liquid* volume, the smallest named unit is the dram, followed by the fluid ounce (8 drams, also 2 tablespoons or 6 teaspoons), cup (8 fluid ounces), pint (2 cups), quart (2 pints). The gallon (4 quarts, also 5 fifths, though the fifth as a beverage quantity is now defined as 750 ml) is defined as 231 cubic inches, while the barrel (used for measurements of petroleum products) is 42 gallons. For *dry* volume (used mainly in agriculture), the smallest units is the (dry) pint, followed by the (dry) quart (2 pints), gallon (4 quarts and equal to 268.8025 cu in), peck (2 gallons) and bushel (4 pecks).[‡‡]

In order to describe quantities that involve both distance and time units, such as velocity and acceleration, the concept of *dimension* is useful. Lengths and distances are said to be of dimension [L]; thus areas and volumes are of dimension $[L]^2$ and $[L]^3$, respectively. The dimension of time is denoted [T], and consequently velocity is of dimension [L]/[T] (or $[L][T]^{-1}$) and acceleration is of dimension $[L]/[T]^2$ (or $[L][T]^{-2}$).

The other physical quantity for which all customary systems, as well as the metric system, have units is *weight*. Operationally, the weight of a body is the smallest force necessary to keep it from falling to earth, whether by a counterweight, a spring or the like. Historically, the basic metric unit of weight is the *gram* (or gramme, g),[§§] defined by a decree of the French National Assembly in 1795 as the weight of a cubic centimeter of pure water at the temperature of melting ice. But, in practice, the basic unit is the *kilogram* (kilogramme, kg), formally defined as the weight of the International Prototype Kilogram, which is a circular right cylinder made of platinum-iridium and stored in the offices of the International Bureau of Weights and Measures in Sèvres, France. Alternative definitions are currently under consideration that would relate the kilogram to fundamental physical constants, rather than a particular object or artifact. Other weight units are formed with the aforementioned SI prefixes, such as the milligram (mg) and microgram (μg). (A weight of 1,000 kg, however, is called a metric ton or tonne, not a megagram).

The English-based customary systems have several different sets of weight units, but the one used for most applications is known as avoirdupois, and is based on the pound (lb), officially defined as 0.45359237 kg and equal to 16 ounces (oz) and also to 7,000 grains (gr). For larger weights, the kilopound (klb = 1,000 lb), commonly called kip, and the (American) ton (2,000 lb) are used.

By the action- reaction law (to be introduced in Ch. 2), weight is equal to

[‡‡]In the United Kingdom and Canada a system of volume units (known as *imperial* units), using the same nomenclature but different definitions, is used semi-officially.

[§§]Note the distinction between g, gram (roman), and g, acceleration due to gravity (italic).

the magnitude of the earth's gravitational force, and therefore to the body's mass (m) times g. The mass could therefore be defined as the weight divided by g, and if the dimension of force is denoted [F], then that of mass is $[\mathrm{F}][\mathrm{L}]^{-1}[\mathrm{T}]^2$.

The concept of weight, however, is specific to objects on or near the earth, while that of mass is universal, and scientists prefer to use universal concepts. Consequently, they have adopted mass, not weight, as the fundamental quantity, with dimension [M], making force a derived quantity with dimension $[\mathrm{M}][\mathrm{L}][\mathrm{T}]^{-2}$. To that end, the metric units that were originally devised for weight were changed into units of mass. A body that weighs one kilogram (as a unit of weight, and therefore force) is defined as having a mass of 1 kg. To indicate the distinction, the force kilogram is denoted kg_f. Since the value of g at sea level on earth is approximately $9.8\ \mathrm{m\cdot s^{-2}}$ (a more accurate value is $g_n = 9.80665\mathrm{m\cdot s^{-2}}$ or, very nearly, $32.17405\ \mathrm{ft\cdot s^{-2}}$), it follows that

$$1\ \mathrm{kg}_f \doteq 9.8\ \mathrm{kg\cdot m\cdot s^{-2}}\ . \tag{1.1}$$

The force kilogram is in everyday use (as are the other metric weight units) in countries where the metric system predominates, even in engineering practice, but the SI has adopted a unit of force of dimension $[\mathrm{M}][\mathrm{L}][\mathrm{T}]^{-2}$ without the numerical factor in Eq. 1.1, namely the newton (N),[¶¶] defined as $\mathrm{N} = \mathrm{kg\cdot m\cdot s^{-2}}$; the millinewton (mN), kilonewton (kN) and meganewton (MN) are defined accordingly. Thus, $1\ \mathrm{kg}_f \doteq 9.8$ N, and a metric ton is about 9.8 kN.

The US customary system, by contrast, has stayed with the pound as a unit of force (sometimes called *pound-force* and denoted lb_f or lbf in order to emphasize this choice), and defined a new unit for mass, the *slug*, equal to $1\ \mathrm{lb}_f\cdot\mathrm{s^2/ft}$. An alternative version of this system, however, uses the pound (pound-mass, lb_m) as the unit of mass, and defines a new unit of force as the *poundal*, equal to $1\ \mathrm{lb}_f\cdot\mathrm{ft\cdot s^{-2}/ft}$. American engineering practice generally follows the former version, as will this book whenever US customary units are used. When using metric units, however, the SI standard will be followed in order to facilitate communication between scientists. [***]

Yet another frequently occurring quantity in engineering and physics that combines the dimensions of force and length is *pressure*, measured as force per unit area (as is a similar quantity known as *stress* that will be introduced in Ch. 4). The basic SI unit of pressure or stress is the pascal ($\mathrm{Pa} = 1\ \mathrm{N\cdot m^{-2}}$), with kilopascal (kPa), megapascal ($\mathrm{MPa} = 1\mathrm{N\cdot mm^{-2}}$) and gigapascal (GPa) defined in the usual way. The US customary systems uses the pound per square foot (psf), pound per square inch (psi) and kilopound per square inch (ksi).

[¶¶] Like other units of measurement named for persons, *newton* is written in lower-case letters but its abbreviation N is capitalized.

[***] A notorious example of the lack of such communication occurred in 1998, when NASA's Mars Climate Orbiter was destroyed because the operations team entered force data in pounds into a navigation program coded in SI units.

Conversions between SI and US units can be found in tabular form in Tables B-1 and B-2 of Appendix B (page 517).

There are two additional important quantities in mechanics whose dimension is [F][L]. One of them is the *moment* of a force, a vector to be defined in Sect. 1.4, whose magnitude in SI units is measured in N·m, and in US customary units in in-lb or ft-lb. The other is the *work*, to be introduced in Sect. 2.1, and the related *energy*. While the dimensions of moment and work (or energy) are the same, it is preferable to use differently named units for them to avoid confusion, and for that reason the joule ($\mathrm{J} = 1\ \mathrm{N \cdot m}$) is used to express work or energy in SI units. The rate of work (or rate of change of energy) per unit time, usually called *power*, is expressed in joules per second, also known as watts ($\mathrm{W} = 1\ \mathrm{J \cdot s^{-1}}$).[†††] A kilowatt-hour (kWh) is, therefore, a unit of energy (equal to 3600 J), which is very popular in denominating commercial or residential energy production or consumption.

There a great many other units in use in various branches of science and engineering, meant to measure quantities that are particular to the discipline, such as the volt and ampere in electricity, the mole in chemistry, and so on. The concept of energy, however, appears in every branch of physical science. In fact, it can be said that every physical process involves a conversion of work into energy, or vice versa, or of energy from one form to another. For this reason, in addition to the standard joule a number of other units are used, in different fields of application, to quantify energy, such as the calorie (cal) in chemistry and biology, the electron-volt (eV) in particle physics, and the British thermal unit (BTU) in heat engineering.

One specific kind of energy is known as *thermal energy*; it represents the energy of the random motion of the atoms and molecules in a body, and is manifested as the body's hotness. It is usually expressed as the *absolute temperature*, measured in degrees Kelvin[‡‡‡] (°K), where the temperature of 0°K is known as the absolute zero (the absence of thermal energy, in the same way that zero mass means the absence of matter). The notion of temperature as a measure of *relative* hotness or coldness, however, was introduced before the concept of absolute zero was known, and conventional temperature is measured relative to an arbitrarily chosen thermal state, such as the freezing point of pure water (273.15°K); the temperature relative to this state, in units of the same size as degrees Kelvin, is the Celsius[§§§] temperature, expressed in degrees Celsius (°C), with the boiling point of water at 100°C. Another unit of temperature, still used in the United States, is the degree Fahrenheit[¶¶¶]

[†††] An old unit of power that is still used occasionally is the horsepower (hp), variously defined as either 745.7 W (in English-speaking countries, taken to be the default definition here) or 735.5 W (on the European continent).

[‡‡‡] William Thomson, 1st Baron Kelvin (1824–1907) was a British physicist and engineer

[§§§] Anders Celsius (1701–1744) was a Swedish astronomer and physicist

[¶¶¶] Daniel Gabriel Fahrenheit (1686–1736) was a German physicist, engineer, and glass blower

(°F); on this scale the freezing and boiling points of water are at 32°F and 212°F, respectively, while absolute zero is at –459.67°F. (When Fahrenheit-size degrees are used to denote absolute temperature they are called degrees Rankine* (°R); thus the numerical value of the absolute temperature in °R is 1.8 times that in °K.) The factor that converts the temperature change in a body into energy change is a property of the body known as its *heat capacity*.

When the degree symbol (°) is used without a following scale symbol (K, C, F or R) then it denotes a degree of arc, a unit of angle measurement representing 1/360 of a full rotation. The SI unit of angular measure is the radian (rad), equal to the angle subtended by a circular arc whose length equals that of the radius (as shown in Fig. 1.3) and representing $1/2\pi$ of a full rotation, so that 1 rad = $(180/\pi)° \doteq 57.2958°$. Since the magnitude of an angle in radians is a ratio of lengths (arc to radius), the angle is a *dimensionless* quantity.

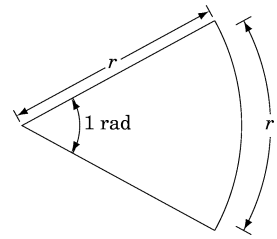

Figure 1.3. Definition of a radian

1.1.3 Arithmetic Precision

A physical quantity is *scalar* if it is fully defined by means of a real number multiplying an appropriate unit. Examples include length, mass, energy and temperature. This number is obtained by measurement or by an arithmetic operation on other measured quantities. Either process is likely to introduce errors, and consequently there is a limit on the precision that can be expected.

Let a scalar a be expressed in decimal form as

$$a \;=\; 0.a_1a_2\ldots a_n\ldots \times 10^k \;, \tag{1.2}$$

where $a_i = 0,1,\ldots,9$, for all $i = 1,2,\ldots,n$, $a_1 \neq 0$, and k is an integer. We say that the scalar a possesses n *significant digits* relative to the exact value a^*, if n is the largest non-negative integer for which

$$\frac{|\,a^* - a\,|}{|\,a^*\,|} \;<\; 0.5\times 10^{-n+1} \;. \tag{1.3}$$

Example 1.1.1: The number 0.314×10^1 approximates π to within three significant digits, since

$$\frac{|\,\pi - 0.314\times 10^1\,|}{|\,\pi\,|} \;=\; 0.000506957\ldots \;<\; 0.5\times 10^{-n+1}$$

for $n = 3$, but not for $n = 4$.

A scalar a, expressed as in Eq. (1.2), may be chopped at the n-th digit, and hence be approximated as

$$a \;\doteq\; 0.a_1a_2\ldots a_n\times 10^k \;. \tag{1.4}$$

*William Rankine (1820–1872) was a British engineer, physicist and mathematician

It is easy to show that chopping at the n-th digit does not necessarily preserve n significant digits (see Exercise **1.1-16**). Alternatively, the scalar a may be rounded at the n-th digit by first adding $0.5 \times 10^{-n+k}$ to its value and then chopping it at the n-th digit. In this case, the resulting approximation to a always preserves at least n significant digits.

Example 1.1.2: Consider the number $0.3141592654\ldots \times 10^1$, which is an estimate of π. If we want to represent this number using only 4 digits, then we may chop it at the fourth digit (leading to 0.3141×10^1) or round it at the fourth digit (leading to 0.3142×10^1).

Rounding (or chopping) is frequently performed on a measured quantity to limit its precision to levels that are meaningful for the purpose served by this quantity. For example, knowing the magnitude of a force to within, say, 10 significant digits (assuming, of course, that such precision is even possible), is most likely unnecessary for any practical engineering design. This is not dissimilar from knowing one's own weight for health-monitoring purposes to within, say, one-hundredth of a pound or kilogram—it is, quite simply, unnecessarily precise information!

Chopping means simply discarding all digits beyond the ones taken as significant. Rounding involves increasing the last retained digit by a unit if the discarded digits represent more than one half. If they represent exactly one half (that is, if the digit to be discarded is 5 with, presumably, any number of zeros following), a common convention (used in such varying disciplines as astronomy and bookkeeping, and known as "odd-even rounding") is to round to the nearest *even* digit. That is, the preceding digit is retained if it is even, and raised by one if it is odd.

Each scalar quantity of interest in solid mechanics is generally assumed to be known to within a certain number of significant digits, which reflects the desired or feasible precision of this quantity. When performing arithmetic operations, it is important to represent scalars with all of their respective significant digits, if possible. As a rule of thumb, when adding or subtracting two scalars,

$$a = 0.a_1a_2\ldots a_n \times 10^k \quad , \quad b = 0.b_1b_2\ldots b_m \times 10^l \, , \tag{1.5}$$

we first "align" them so that the exponents k and l are identical, then we perform the addition or subtraction, and lastly we round or chop the result at the last significant digit shared by both numbers in this aligned format. Likewise, when multiplying or dividing two scalars a and b, the result should have exactly as many significant digits as the least of such digits among a and b.

Example 1.1.3: Adding 0.12345×10^3 and 0.123×10^2 yields 0.1358×10^3 with rounding and 0.1357×10^3 with chopping. Likewise, the product of 0.12345×10^3 and 0.123×10^2 should be 0.151×10^4.

Aside from inexact measurements, another source of imprecision is round-off error, as illustrated in the following example.

Example 1.1.4: Consider the determination of the area of a square that nominally measures 3 m by 3 m, but whose sides, when measured with a tape that reads to the nearest millimeter, turn out to be 3.003 m and 3.004 m. When rounded off to three significant figures, these sides are both 3.00 m and the area is consequently 9.00 m^2. But when the more accurate dimensions are used, the area is, to four significant figures, 9.021 m^2, and therefore the first result is inaccurate in the third significant figure!

To minimize round-off errors, it is desirable, when performing calculations, to retain as much accuracy as is available and round off only the final result. This is especially true when using quantities that are known exactly to within a large number of significant digits, such as the values of numerical or physical constants (like π or g_n).

Unless otherwise specified, the calculations in the examples and exercises in this book are expected to be performed to three significant digits. An example of an exception to this rule is a case where quantities with different orders of magnitude are to be added or subtracted; it is then the number of decimal places rather than the number of significant digits that governs.

1.1.4 Calculating with Dimensional Quantities

Most calculations in mechanics involve quantities that have some physical dimension. When performing such calculations, it is necessary to keep some simple principles in mind.

1. Quantities that are added or subtracted must have the same dimension, and the numerical calculation can be done only if all terms are expressed in the same units.

2. To change units we use the fact that the value of a given quantity is unchanged if it is multiplied by another quantity and then divided by a quantity having the same value as the latter, even if expressed in different units (that is, $b = c \Rightarrow ab/c = a$). Thus, since 1 ft = 12 in, multiplying a quantity by 1 ft and dividing it by 12 in (or vice versa) does not change its value.

Example 1.1.5: Conversion of speed units.
Express a speed of 55 miles per hour in feet per second:

$$55\frac{\text{mi}}{\text{hr}} = 55\frac{\text{mi}}{\text{hr}} \times \frac{5280\text{ft}}{1\text{mi}} \times \frac{1\text{hr}}{3600\text{s}} = \frac{55 \times 5280 \times 1}{1 \times 3600}\ \frac{\text{mi} \times \text{ft} \times \text{hr}}{\text{hr} \times \text{mi} \times \text{s}} = 80.7\frac{\text{ft}}{\text{s}}.$$

3. The arguments of transcendental functions (exponential, hyperbolic, trigonometric and their inverses) must be dimensionless. Of course trigonometric functions, as is well known, can be calculated in terms of either radians or degrees.

Exercises

1.1-1. Consider an automobile that travels at 65 mph. Express its speed in m/sec and km/h.

1.1-2. Identify everyday objects that weigh 0.1 lb, 0.1 kg, 1 lb, 1 kg, 10 lb, and 10 kg.

1.1-3. A person weighs 185 lbs. Express the person's weight in kilograms.

1.1-4. The state of California covers an area of 163,696 square miles. Express this area in square kilometers and acres.

1.1-5. A person stands 6 foot 1-1/2 inches tall. Express the person's height in centimeters.

1.1-6. The maximum thrust of a commercial jet engine is 400 kN. What is the thrust in lb_f?

1.1-7. The pressure in a tire of a road bicycle is 120 psi. Convert the pressure to kPa.

1.1-8. A wind turbine produces power of 1.5 MW. Express the power rating of the turbine in hp.

1.1-9. Express the horsepower (hp) in US customary (ft-lb-s) units.

1.1-10. Blood pressure is normally reported in units of millimeters of mercury (Hg), that is, the pressure exerted on a surface by a 1-mm column of Hg. Given that the density of mercury is approximately 13.5 g/cm^3, convert the normal systolic and diastolic blood pressures of 120 mm Hg and 80 mm Hg, respectively, to Pa.

1.1-11. Convert the data of the preceding exercise to psi.

1.1-12. The normal temperature in the human body is approximately 37 °C. Convert this temperature to °F and °K.

1.1-13. How many significant digits are retained when approximating the square-root of 3 by 1.7321?

1.1-14. Round the following numbers to three significant digits (using odd-even rounding where appropriate): 47.315, 32650, 2.7251, 14.55.

1.1-15. Perform chopping and rounding at the third for $a^* = 1/3$ and $b^* = 2/3$, and comment on the answers.

1.1-16. Perform chopping at the second digit for $a^* = 0.129111\ldots$ and report the number of significant digits that are preserved in this approximation.

1.1-17. Recall that Euler's number e can be defined as $e = \lim_{n\to\infty}\left(1+\frac{1}{n}\right)^n$. Determine the number of significant digits recovered when approximating the preceding formula by $e \doteq \left(1+\frac{1}{n}\right)^n$, for $n = 1,2,\ldots,5$. Plot the number of significant digits attained as a function of n.

1.1-18. Recall the Taylor series expansion of $\cos x$ around $x = 0$, as

$$\cos x \;=\; 1 - \frac{x^2}{2!} + \frac{x^4}{4!} - \ldots \;.$$

Plot the number of significant digits recovered by the preceding formula as a function of the number n of terms considered ($n \le 6$), for the case $x = \pi/3$.

1.1-19. Let $a = 4.1891233$ and $b = 0.012995$ possess three and four significant digits, respectively. Calculate $a+b$, $a-b$, $a\times b$, and a/b and report only the significant digits of the results.

1.1-20. Let $a = 0.1001\times 10^5$ have four significant digits and $b = 0.1\times 10^5$ have one significant digit. What can you say about the difference $a-b$?

1.1-21. Let both $a = 0.1\times 10^8$ and $b = 0.1\times 10^2$ have one significant digit. What can you say about the sum $a+b$?

1.2 Review of Vectors

1.2.1 Definition and Notation

In the context of this book, a *vector* is understood to be a mathematical object endowed with magnitude and direction. A simple example is a directed line segment in space, its magnitude being simply its length. More generally, magnitude is a non-negative measure of size relative to a predefined measure of unity. Direction entails both orientation and sense. The orientation is that of the line, while the sense is defined by the ordering of the end points of the line segment *from* the first point (the "origin" or "tail") *to* the second point (the "head"). Vectors with the same orientation but opposite sense are said to have opposite direction, and if they have the same magnitude they are said to be **equal and opposite**. Vectors are schematically depicted using arrows, as in Fig. 1.4, and are denoted by boldface Latin or Greek letters, such as $\mathbf{A}$, $\mathbf{a}$, $\boldsymbol{\alpha}$, etc. The magnitude of a vector, say $\mathbf{A}$, is usually denoted $|\mathbf{A}|$ or A.

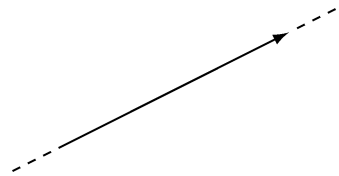

Figure 1.4. Representation of a vector by an arrow

Vector algebra consists of all addition, subtraction, multiplication and division operations involving vectors and, possibly, scalars.

The product of *scalar multiplication* of a vector $\mathbf{A}$ and a scalar α is a vector $\alpha\mathbf{A}$ whose magnitude is $|\alpha||\mathbf{A}|$, and whose direction is the same as that of $\mathbf{A}$ if $\alpha > 0$ and the opposite if $\alpha < 0$. If $\alpha = -1$, the resulting vector $(-1)\mathbf{A}$ (or $-\mathbf{A}$) is the *negative* of $\mathbf{A}$. Multiplying any vector $\mathbf{A}$ by $\alpha = 0$ leads to the *zero vector* $\mathbf{0}$, which has zero magnitude and arbitrary direction. Of course, $\alpha\mathbf{0} = \mathbf{0}$ for any α and also $\mathbf{A} + (-\mathbf{A}) = \mathbf{0}$ for any $\mathbf{A}$. *Division* of a vector by a scalar $\alpha \neq 0$ is just multiplication by $1/\alpha$.

The addition of vectors $\mathbf{A}$ and $\mathbf{B}$ yields a vector $\mathbf{A}+\mathbf{B}$ which satisfies the *parallelogram rule*, as shown in Fig. 1.5a. When the origins of the two vectors $\mathbf{A}$ and $\mathbf{B}$ are made to coincide, the vector $\mathbf{A}+\mathbf{B}$ can be drawn as the arrow starting from the common origin of $\mathbf{A}$ and $\mathbf{B}$ and ending at the opposite vertex of the parallelogram formed by the arrows $\mathbf{A}$ and $\mathbf{B}$. The same result is obtained be making the origin of one of the vectors coincide with the head of the other, and completing the triangle, as shown in Fig. 1.5b.

The parallelogram rule and the definition of scalar multiplication may be used to show that the following properties hold for any vectors $\mathbf{A}$, $\mathbf{B}$, $\mathbf{C}$ and

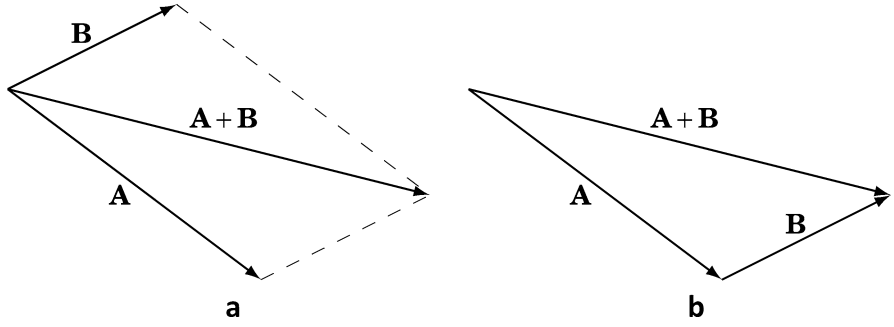

Figure 1.5. Parallelogram rule for vector addition

scalars α, β:

$$\begin{aligned}
&\text{(a)}\ \ \mathbf{A}+\mathbf{B} = \mathbf{B}+\mathbf{A}\,,\\
&\text{(b)}\ \ (\mathbf{A}+\mathbf{B})+\mathbf{C} = \mathbf{A}+(\mathbf{B}+\mathbf{C})\,,\\
&\text{(c)}\ \ \alpha(\mathbf{A}+\mathbf{B}) = \alpha\mathbf{A}+\alpha\mathbf{B})\,,\\
&\text{(d)}\ \ (\alpha+\beta)\mathbf{A} = \alpha\mathbf{A}+\beta\mathbf{A}\,,\\
&\text{(e)}\ \ (\alpha\beta)\mathbf{A} = \alpha(\beta\mathbf{A})\,.
\end{aligned} \tag{1.6}$$

Using the parallelogram rule and the definition of the negative of a given vector, we may easily draw a schematic of the difference $\mathbf{A}-\mathbf{B}$ of two vectors $\mathbf{A}$ and $\mathbf{B}$, as in Fig. 1.6a. A more direct way of getting the same result is shown in Fig. 1.6b.

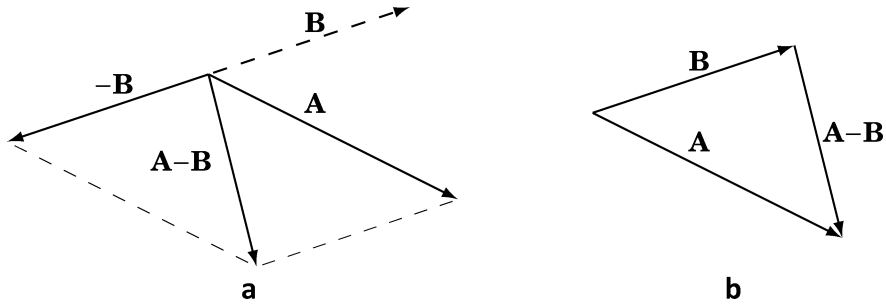

Figure 1.6. Parallelogram rule for vector subtraction

Once subtraction of vectors is defined, it is a simple matter to define differentiation of a vector with respect to a scalar variable. If, say, $\mathbf{W}(s)$ is a vector-valued function of the scalar variable s, then

$$\frac{d\mathbf{W}(s)}{ds} = \lim_{\Delta s\to 0}\frac{\mathbf{W}(s+\Delta s)-\mathbf{W}(s)}{\Delta s}\,. \tag{1.7}$$

In particular, if $\mathbf{r}$ is the *position vector* drawn from a fixed point O to an

arbitrary point that is currently occupied by a moving particle* (so that $\mathbf{r}$ is a function of the time t), then the derivative $d\mathbf{r}/dt$ is the velocity of the particle (denoted $\mathbf{v}$), and the further derivative $d\mathbf{v}/dt = d^2\mathbf{r}/dt^2$ is the acceleration. This result establishes the vectorial nature of velocity and acceleration, and, by the relation between acceleration and force, of force as well.

The parallelogram rule can be also invoked in reverse order to resolve a vector $\mathbf{R}$ into two vectors $\mathbf{A}$ and $\mathbf{B}$ along two given (and distinct) directions, as graphically depicted in Fig. 1.7. In this case, $\mathbf{A}$ and $\mathbf{B}$ are the projections of $\mathbf{R}$ along the two directions.

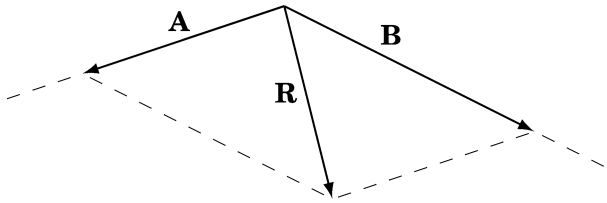

Figure 1.7. Resolution of vector along two given directions

The *dot product* (also known as *scalar product*) of two vectors $\mathbf{A}$ and $\mathbf{B}$, denoted by $\mathbf{A}\cdot\mathbf{B}$, is a scalar whose absolute value is equal to the product of the magnitude of the one vector (say, $\mathbf{A}$) and the magnitude of the projection of the other vector (here, $\mathbf{B}$) along the direction of $\mathbf{A}$. The dot product is a positive (negative) number if $\mathbf{A}$ and the projection of $\mathbf{B}$ along the line of $\mathbf{A}$ have the same (opposite) senses. Using elementary trigonometry, we may write

$$\mathbf{A}\cdot\mathbf{B} \;=\; AB\cos\theta\;, \tag{1.8}$$

where A and B are the respective magnitudes of $\mathbf{A}$ and $\mathbf{B}$, and θ ($0 \le \theta \le \pi$) is the angle between the directions of $\mathbf{A}$ and $\mathbf{B}$. It is easy to establish that, given any three vectors $\mathbf{A}$, $\mathbf{B}$ and $\mathbf{C}$, and any scalar α,

$$\begin{aligned}
&\text{(a)}\;\; \mathbf{A}\cdot\mathbf{B} \;=\; \mathbf{B}\cdot\mathbf{A}\;,\\
&\text{(b)}\;\; \alpha(\mathbf{A}\cdot\mathbf{B}) \;=\; (\alpha\mathbf{A})\cdot\mathbf{B} \;=\; \mathbf{A}\cdot(\alpha\mathbf{B})\;,\\
&\text{(c)}\;\; \mathbf{A}\cdot(\mathbf{B}+\mathbf{C}) \;=\; \mathbf{A}\cdot\mathbf{B}+\mathbf{A}\cdot\mathbf{C}\;.
\end{aligned} \tag{1.9}$$

It is clear from the definition of the dot product in (1.8) that two vectors $\mathbf{A}$ and $\mathbf{B}$ are perpendicular to each other, or *orthogonal*, if $\mathbf{A}\cdot\mathbf{B} = 0$. Also, the magnitude A of a vector $\mathbf{A}$ satisfies $A = \sqrt{\mathbf{A}\cdot\mathbf{A}}$. If $A = 1$, the vector $\mathbf{A}$ is called a *unit* vector.

The *cross product* (also known as *vector product*) of two vectors $\mathbf{A}$ and $\mathbf{B}$, denoted by $\mathbf{A}\times\mathbf{B}$, is a vector whose magnitude is equal to $AB|\sin\theta|$, whose

*The literal meaning of the Latin word *vector* is 'carrier,' and the position vector, which can be envisioned as "carrying" the particle from one configuration to another, is the prototypical vector.

direction is perpendicular to the plane defined by $\mathbf{A}$ and $\mathbf{B}$, and whose sense is determined by the right-hand rule as that of vector $\mathbf{C}$ in Fig. 1.8. Again, A,

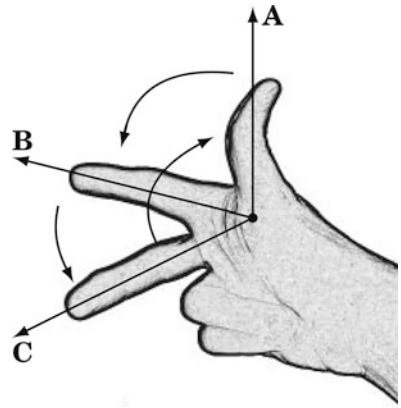

Figure 1.8. Illustration of the right-hand rule: the three vectors $\mathbf{A},\mathbf{B},\mathbf{C}$ form a right-hand triad if they are arranged in the order indicated by the curved arrows, that is, $(\mathbf{A},\mathbf{B},\mathbf{C})$, $(\mathbf{B},\mathbf{C},\mathbf{A})$ or $(\mathbf{C},\mathbf{A},\mathbf{B})$.

B are the magnitudes of $\mathbf{A}$ and $\mathbf{B}$ respectively, and θ $(0 \le \theta \le \pi)$ is the angle between the lines of $\mathbf{A}$ and $\mathbf{B}$. The preceding definition of the cross product readily implies that, given any three vectors $\mathbf{A}$, $\mathbf{B}$ and $\mathbf{C}$, and any scalar α,

$$\begin{aligned} &\text{(a)}\ \ \mathbf{A}\times\mathbf{B} = -\mathbf{B}\times\mathbf{A}\,, \\ &\text{(b)}\ \ \alpha(\mathbf{A}\times\mathbf{B}) = (\alpha\mathbf{A})\times\mathbf{B} = \mathbf{A}\times(\alpha\mathbf{B})\,, \\ &\text{(c)}\ \ \mathbf{A}\times(\mathbf{B}+\mathbf{C}) = \mathbf{A}\times\mathbf{B}+\mathbf{A}\times\mathbf{C}\,. \end{aligned} \tag{1.10}$$

Two vectors $\mathbf{A}$ and $\mathbf{B}$ of non-zero magnitude are termed *parallel* if $\mathbf{A}\times\mathbf{B}=\mathbf{0}$.

1.2.2 Cartesian Components

Vector-algebraic operations are easily executed by resolving all vectors into their components in a (rectangular) *Cartesian coordinate system*. We do this by defining three unit vectors $\mathbf{i}$, $\mathbf{j}$, $\mathbf{k}$ along three mutually orthogonal directions, such that the ordered triad $\{\mathbf{i},\mathbf{j},\mathbf{k}\}$ satisfies the right-hand rule. This clearly means that

$$\mathbf{i}\cdot\mathbf{i} = \mathbf{j}\cdot\mathbf{j} = \mathbf{k}\cdot\mathbf{k} = 1\,, \tag{1.11}$$

$$\mathbf{i}\cdot\mathbf{j} = \mathbf{j}\cdot\mathbf{k} = \mathbf{k}\cdot\mathbf{i} = 0\,, \tag{1.12}$$

and

$$\mathbf{i}\times\mathbf{j} = \mathbf{k}\quad,\quad \mathbf{j}\times\mathbf{k} = \mathbf{i}\quad,\quad \mathbf{k}\times\mathbf{i} = \mathbf{j}\,. \tag{1.13}$$

The directions of $\mathbf{i}$, $\mathbf{j}$, $\mathbf{k}$ define three mutually orthogonal axes x, y, and z, as in Fig. 1.9. The unit vectors $\mathbf{i}$, $\mathbf{j}$, $\mathbf{k}$ form a *basis* for all three-dimensional

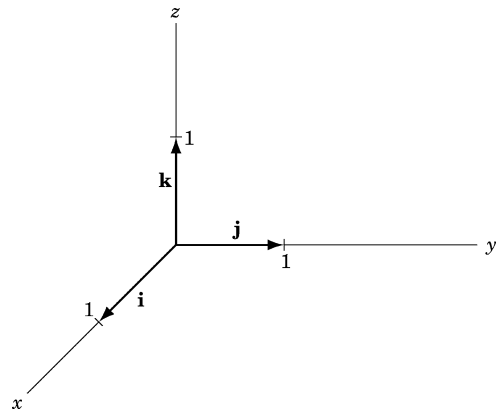

Figure 1.9. Cartesian coordinate system and basis vectors

vectors, in the sense that any vector $\mathbf{A}$ can be uniquely resolved into three vectors $\mathbf{A}_x$, $\mathbf{A}_y$ and $\mathbf{A}_z$ along the axes x, y and z, such that

$$\mathbf{A} = \mathbf{A}_x + \mathbf{A}_y + \mathbf{A}_z \,, \tag{1.14}$$

where

$$\mathbf{A}_x = (\mathbf{A}\cdot\mathbf{i})\mathbf{i} \quad , \quad \mathbf{A}_y = (\mathbf{A}\cdot\mathbf{j})\mathbf{j} \quad , \quad \mathbf{A}_z = (\mathbf{A}\cdot\mathbf{k})\mathbf{k} \,. \tag{1.15}$$

The *Cartesian components* (A_x, A_y, A_z) of $\mathbf{A}$ on the x, y and z axes are defined as

$$A_x = \mathbf{A}\cdot\mathbf{i} \quad , \quad A_y = \mathbf{A}\cdot\mathbf{j} \quad , \quad A_z = \mathbf{A}\cdot\mathbf{k} \,, \tag{1.16}$$

and are equal in absolute value to the magnitudes of the vectors $\mathbf{A}_x$, $\mathbf{A}_y$ and $\mathbf{A}_z$, respectively. With the help of (1.15) and (1.16), it follows from (1.14) that

$$\mathbf{A} = A_x\mathbf{i} + A_y\mathbf{j} + A_z\mathbf{k} \,, \tag{1.17}$$

as can also be seen from Fig. 1.10.

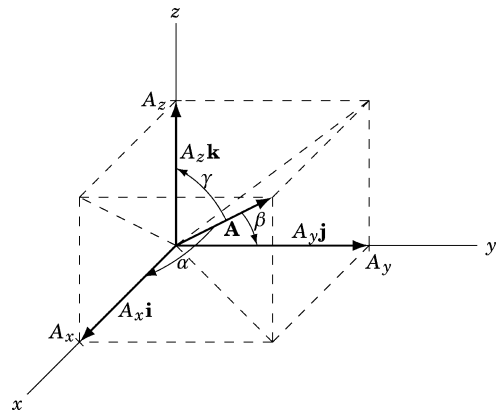

Figure 1.10. Cartesian components of a vector

For some mathematical purposes it is convenient to arrange the Cartesian components of a vector, say $\mathbf{A}$, in a column matrix: $\left\{ \begin{array}{c} A_x \\ A_y \\ A_z \end{array} \right\}$.

Taking into account the Cartesian coordinate representation of $\mathbf{A}$ in (1.17), it is a simple matter to express the scalar multiplication of $\mathbf{A}$ by α using components as

$$\alpha\mathbf{A} \;=\; \alpha(A_x\mathbf{i}+A_y\mathbf{j}+A_z\mathbf{k}) \;=\; (\alpha A_x)\mathbf{i}+(\alpha A_y)\mathbf{j}+(\alpha A_z)\mathbf{k}\;. \tag{1.18}$$

Likewise, the addition of $\mathbf{A}$ and $\mathbf{B}$ can be represented using components as

$$\begin{aligned}\mathbf{A}+\mathbf{B} &= (A_x\mathbf{i}+A_y\mathbf{j}+A_z\mathbf{k})+(B_x\mathbf{i}+B_y\mathbf{j}+B_z\mathbf{k}) \\ &= (A_x+B_x)\mathbf{i}+(A_y+B_y)\mathbf{j}+(A_z+B_z)\mathbf{k}\;.\end{aligned} \tag{1.19}$$

The dot product of two vectors $\mathbf{A}$ and $\mathbf{B}$ can be written in terms of their components as

$$\begin{aligned}\mathbf{A}\cdot\mathbf{B} &= (A_x\mathbf{i}+A_y\mathbf{j}+A_z\mathbf{k})\cdot(B_x\mathbf{i}+B_y\mathbf{j}+B_z\mathbf{k}) \\ &= A_xB_x+A_yB_y+A_zB_z\;,\end{aligned} \tag{1.20}$$

where we make use of (1.11), (1.12) and the properties (1.9) of the dot product. Using Cartesian components and taking into account (1.20), we find the magnitude of a vector $\mathbf{A}$ to be

$$A \;=\; \sqrt{\mathbf{A}\cdot\mathbf{A}} \;=\; \sqrt{A_x^2+A_y^2+A_z^2}\;. \tag{1.21}$$

Example 1.2.1: Calculation of dot product.
Find the dot product between the two vectors $\mathbf{A} = 30\mathbf{i} - 40\mathbf{j}$ and $\mathbf{B} = 56\mathbf{i} + 33\mathbf{j}$ using (a) Eq. (1.8) and (b) Eq. (1.20).

(a) The angle θ between $\mathbf{A}$ and $\mathbf{B}$ is equal to $\tan^{-1}(-40/30) - \tan^{-1}(33/56)$, so that $\mathbf{A}\cdot\mathbf{B} = \sqrt{30^2+40^2}\sqrt{56^2+33^2}\cos[\tan^{-1}(-40/30) - \tan^{-1}(33/56)] = 360$.

(b) $\mathbf{A}\cdot\mathbf{B} = 30\cdot 56 + (-40)\cdot 33 = 360$.

The direction of a vector $\mathbf{A}$ relative to the ordered triad $\{\mathbf{i},\mathbf{j},\mathbf{k}\}$ is characterized by the *direction cosines*

$$\cos\alpha \;=\; \frac{A_x}{A} \quad,\quad \cos\beta \;=\; \frac{A_y}{A} \quad,\quad \cos\gamma \;=\; \frac{A_z}{A}\;. \tag{1.22}$$

Comparing this result with Eq. (1.8), we see that (α,β,γ) are the angles between the axis of the vector $\mathbf{A}$ and the x-, y-, and z-axes, respectively, as seen in Fig. 1.10. Eqs. (1.21) and (1.22) immediately lead to the condition

$$\cos^2\alpha+\cos^2\beta+\cos^2\gamma \;=\; 1\;. \tag{1.23}$$

It follows from Eq. (1.23) that only two of the angles (α, β, γ) are independent. In other words, it takes just two angles to specify the direction of a vector in space. An alternative set of two angles doing just that consists of the *spherical angles* (ϕ, θ) shown in Fig. 1.11, such that

$$A_x = A\sin\phi\cos\theta \quad , \quad A_y = A\sin\phi\sin\theta \quad , \quad A_z = A\cos\phi \, . \tag{1.24}$$

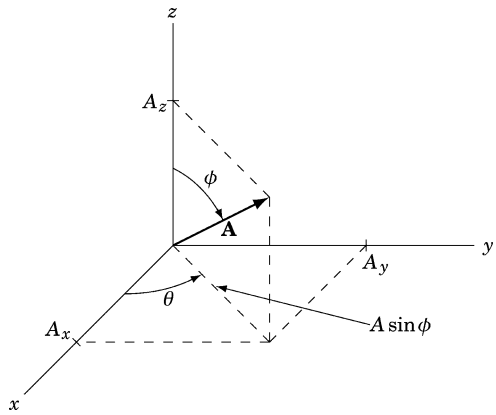

Figure 1.11. Spherical angles

The cross product $\mathbf{A}\times\mathbf{B}$ can be expressed in Cartesian components as

$$\begin{aligned}\mathbf{A}\times\mathbf{B} &= (A_x\mathbf{i}+A_y\mathbf{j}+A_z\mathbf{k})\times(B_x\mathbf{i}+B_y\mathbf{j}+B_z\mathbf{k}) \\ &= (A_yB_z-A_zB_y)\mathbf{i}+(A_zB_x-A_xB_z)\mathbf{j}+(A_xB_y-A_yB_x)\mathbf{k} \, .\end{aligned} \tag{1.25}$$

In this derivation, we made use of (1.13) and the properties (1.10) of the cross product. An alternative representation of the cross product using a symbolic matrix determinant is often employed in the form

$$\mathbf{A}\times\mathbf{B} = \begin{vmatrix} \mathbf{i} & \mathbf{j} & \mathbf{k} \\ A_x & A_y & A_z \\ B_x & B_y & B_z \end{vmatrix} \, . \tag{1.26}$$

Focusing on (1.25), we readily see that the cross product can be obtained by symbolically applying the well-known formula for the determinant of a 3×3 matrix to the right-hand side of (1.26).

Example 1.2.2: Calculation of cross product.
Find the cross product $\mathbf{A}\times\mathbf{B}$ of the two vectors of Example 1.2.1 using (a) the original definition of Sect. 1.2.1 and (b) Eq. (1.26).
(a) Since $\mathbf{A}$ and $\mathbf{B}$ are respectively in the fourth and first quadrant of the xy-plane, it follows from the right-hand rule that the direction of $\mathbf{A}\times\mathbf{B}$ that of the positive z-axis, while its magnitude is $\sqrt{30^2+40^2}\sqrt{56^2+33^2}\sin[\tan^{-1}(33/56)-$

$\tan^{-1}(-40/30)] = 3230$. Hence $\mathbf{A} \times \mathbf{B} = 3230\mathbf{k}$.
(b)

$$\begin{vmatrix} \mathbf{i} & \mathbf{j} & \mathbf{k} \\ 30 & -40 & 0 \\ 56 & 33 & 0 \end{vmatrix} = \mathbf{k}[30 \cdot 33 - (-40) \cdot 56] = 3230\mathbf{k}.$$

The *scalar triple product* of three vectors $\mathbf{A},\mathbf{B},\mathbf{C}$ (in that order) is defined as the dot product between $\mathbf{A}$ and $\mathbf{B} \times \mathbf{C}$. It follows from Eq. (1.26) that this product is given by

$$\mathbf{A} \cdot (\mathbf{B} \times \mathbf{C}) = \mathbf{A} \cdot \begin{vmatrix} \mathbf{i} & \mathbf{j} & \mathbf{k} \\ B_x & B_y & B_z \\ C_x & C_y & C_z \end{vmatrix} = \begin{vmatrix} A_x & A_y & A_z \\ B_x & B_y & B_z \\ C_x & C_y & C_z \end{vmatrix}. \tag{1.27}$$

It is easy to show that

$$\begin{aligned} \mathbf{A} \cdot (\mathbf{B} \times \mathbf{C}) &= \mathbf{B} \cdot (\mathbf{C} \times \mathbf{A}) = \mathbf{C} \cdot (\mathbf{A} \times \mathbf{B}) \\ &= (\mathbf{A} \times \mathbf{B}) \cdot \mathbf{C} \quad \text{etc.} \end{aligned} \tag{1.28}$$

From the last equality we can see that the order of dot and cross in a scalar triple product can be interchanged. Moreover, the value of the scalar triple product is the same for any even permutation of the order of the three vectors, while an odd permutation gives the negative of that value.

The *vector triple product* of three vectors is a vector of the form $\mathbf{A} \times (\mathbf{B} \times \mathbf{C})$. It can be shown that

$$\mathbf{A} \times (\mathbf{B} \times \mathbf{C}) = (\mathbf{A} \cdot \mathbf{C})\mathbf{B} - (\mathbf{A} \cdot \mathbf{B})\mathbf{C}\,. \tag{1.29}$$

Exercises

1.2-1. Find the length of vector $\mathbf{A} = 2\mathbf{i}+\mathbf{j}-3\mathbf{k}$ and its direction cosines relative to the triad $\{\mathbf{i},\mathbf{j},\mathbf{k}\}$.

1.2-2. Let $\mathbf{A} = \mathbf{i}-2\mathbf{j}-2\mathbf{k}$. Find the magnitude and the spherical angles of $\mathbf{A}$.

1.2-3. Let $\mathbf{A} = 3\mathbf{i}-2\mathbf{j}+\mathbf{k}$ and $\mathbf{B} = -\mathbf{i}+3\mathbf{j}-5\mathbf{k}$. Determine the vectors $\mathbf{A}+\mathbf{B}$ and $\mathbf{A}-\mathbf{B}$. Also, find the dot-product of $\mathbf{A}$ and $\mathbf{B}$ and the angle θ $(0 \le \theta \le \pi)$ between them.

1.2-4. Verify that the vectors $\mathbf{A} = 2\mathbf{i}+\mathbf{j}+\mathbf{k}$ and $\mathbf{B} = \mathbf{i}-\mathbf{j}-\mathbf{k}$ are orthogonal. Also, find a unit vector $\mathbf{C}$ which is orthogonal to both $\mathbf{A}$ and $\mathbf{B}$.

1.2-5. Let $\mathbf{A} = \mathbf{i}+3\mathbf{j}-2\mathbf{k}$ and $\mathbf{B} = -2\mathbf{i}+3\mathbf{k}$. Determine the cross product of $\mathbf{A}$ and $\mathbf{B}$ and the angle θ $(0 \le \theta \le \pi)$ between them.

1.2-6. Find the area of the parallelogram formed by the vectors $\mathbf{A} = 2\mathbf{i}+\mathbf{j}-4\mathbf{k}$ and $\mathbf{B} = -\mathbf{i}-\mathbf{j}+3\mathbf{k}$.

1.2-7. Find the volume of the parallelepiped formed by the vectors $\mathbf{A} = 2\mathbf{i}+\mathbf{j}-4\mathbf{k}$, $\mathbf{B} = -\mathbf{i}-\mathbf{j}+3\mathbf{k}$ and $\mathbf{C} = \mathbf{i}+\mathbf{j}+\mathbf{k}$.

1.2-8. Resolve the vector $\mathbf{A} = \mathbf{i}-3\mathbf{j}+5\mathbf{k}$ along the axes formed by the vectors $\mathbf{i}+\mathbf{j}$, $\mathbf{j}+\mathbf{k}$ and $\mathbf{k}+\mathbf{i}$. Confirm that the resulting three vectors $\mathbf{A}_1$, $\mathbf{A}_2$ and $\mathbf{A}_3$ sum up to $\mathbf{A}$.

1.2-9. Let the vector $\mathbf{A}$ be defined as $\mathbf{A} = 5\mathbf{i}+\mathbf{j}-3\mathbf{k}$. Resolve $\mathbf{A}$ into two vectors $\mathbf{A}_1$ and $\mathbf{A}_2$, where $\mathbf{A}_1$ is along the axis formed by $\mathbf{i}+\mathbf{j}+\mathbf{k}$.

1.2-10. Find a unit vector that is perpendicular to $\mathbf{i}-\mathbf{j}+\mathbf{k}$ and makes an angle $\pi/3$ with $\mathbf{i}+2\mathbf{j}-3\mathbf{k}$.

1.2-11. Use vector algebra to verify the *sine law*: given two vectors $\mathbf{A} = A_x\mathbf{i}+A_y\mathbf{j}$ and $\mathbf{B} = B_x\mathbf{i}+B_y\mathbf{j}$ that lie on the plane formed by $\mathbf{i}$ and $\mathbf{j}$ and their difference $\mathbf{C} = \mathbf{B}-\mathbf{A}$,

$$\frac{A}{\sin(\theta_{BC})} = \frac{B}{\sin(\theta_{CA})} = \frac{C}{\sin(\theta_{AB})}, \tag{1.30}$$

where A denotes the length of a vector $\mathbf{A}$ and θ_{AB}, $(0 \le \theta_{AB} \le \pi)$ the angle between vectors $\mathbf{A}$, $\mathbf{B}$, etc.. Draw a sketch showing all three vectors and angles involved in the preceding law.

1.2-12. Use vector algebra to verify the *cosine law*: given two vectors $\mathbf{A} = A_x\mathbf{i}+A_y\mathbf{j}$ and $\mathbf{B} = B_x\mathbf{i}+B_y\mathbf{j}$ that lie on the plane formed by $\mathbf{i}$ and $\mathbf{j}$ and their difference $\mathbf{C} = \mathbf{B}-\mathbf{A}$,

$$C^2 = A^2+B^2-2AB\cos(\theta_{AB}), \tag{1.31}$$

where A denotes the length of a vector $\mathbf{A}$, etc., and θ_{AB}, $(0 \le \theta_{AB} \le \pi)$ the angle between vectors $\mathbf{A}$, $\mathbf{B}$. Draw a sketch showing all three vectors and the angle involved in the preceding law.

1.3 Forces

1.3.1 The Physical Nature of Forces

As we noted in Sect. 1.1, forces represent interactions between bodies. A force acting on a body is typically represented by a vector at a point of the body. What we strictly mean here is that the force acts *at a point of the region occupied by the body*, but we often identify a body with the region occupied by it, except that portions of space containing zero or negligible mass can be included in or excluded from the region without affecting the identification.

Forces between bodies are ultimately the result of interactions at the molecular, atomic or subatomic level. Such interactions may be generally classified as short-range and long-range. Short-range interactions give rise to *contact forces*. These forces are generated by pushing, pulling and/or rubbing of material particles along the surface on which the bodies come to contact (or near contact), and are regarded as distributed over this contact surface. When this surface is very small in comparison with the total surface bounding each body, then these contact forces may be regarded as acting at a single point on each body's surface.

Long-range interactions include electrostatic, magnetostatic and gravitational forces, and as such they are generally experienced by all parts of a body, including its interior. The resulting forces are therefore called *body forces*.

1.3.2 The Mathematical Nature of Forces

Forces are vectorial in nature, as they are endowed with both magnitude and direction. Consequently, vector algebra is a useful tool for describing forces. For example, the effect of pulling a solid object using a rope can be represented by a force acting at the point where the rope is attached to the body, when the area of attachment is idealized as a point. Also, the direction of the force vector coincides with the direction of the rope.

We will define the *line of action* of a force as the line having the direction of the force and passing through its point of application. Oftentimes, it is of interest to determine the cumulative effect of all forces acting on a body. To simplify this problem, suppose that two forces $\mathbf{F}_1$ and $\mathbf{F}_2$ act simultaneously at the same point P of a body, as in Fig. 1.12. The *resultant* $\mathbf{R}$ of $\mathbf{F}_1$ and $\mathbf{F}_2$ can be graphically determined using the parallelogram rule. Alternatively, we may resort to vector addition relative to a fixed Cartesian coordinate system centered at the point of interest P. In this case, first resolve each of the two forces into their components along the axes x, y and z, with basis vectors $\mathbf{i}$, $\mathbf{j}$ and $\mathbf{k}$. This leads to

$$\mathbf{F}_1 = F_{1x}\mathbf{i} + F_{1y}\mathbf{j} + F_{1z}\mathbf{k} \quad , \quad \mathbf{F}_2 = F_{2x}\mathbf{i} + F_{2y}\mathbf{j} + F_{2z}\mathbf{k} \, . \tag{1.32}$$

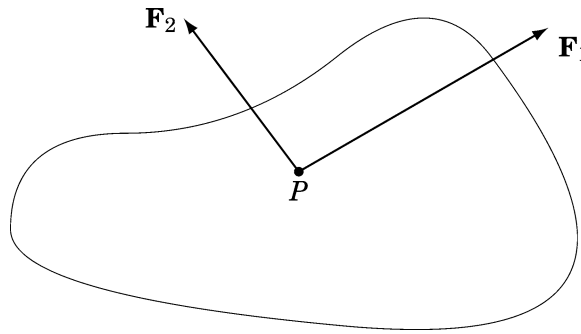

Figure 1.12. Two forces acting at the same point of a body

Vector addition may then be employed to determine the resultant $\mathbf{R}$ as

$$\begin{aligned}\mathbf{R} &= \mathbf{F}_1 + \mathbf{F}_2 \\ &= (F_{1x}\mathbf{i} + F_{1y}\mathbf{j} + F_{1z}\mathbf{k}) + (F_{2x}\mathbf{i} + F_{2y}\mathbf{j} + F_{2z}\mathbf{k}) \\ &= (F_{1x} + F_{2x})\mathbf{i} + (F_{1y} + F_{2y})\mathbf{j} + (F_{1z} + F_{2z})\mathbf{k}\,.\end{aligned} \tag{1.33}$$

Example 1.3.1: Calculation of the resultant of two forces.
Let the plane of Fig. 1.12 be the xy-plane, with the x-axis horizontal and the y-axis vertical. Suppose that the magnitudes of $\mathbf{F}_1$ and $\mathbf{F}_2$ are 150.0 N and 100.0 N, respectively, and that they subtend angles of 30.0° and 126.87°, respectively, with the x-axis. Find the magnitude and direction of the resultant $\mathbf{R}$ using: (a) the parallelogram rule and (b) Cartesian components.

(a) Since the angle between the force vectors is 96.87°, the magnitude of $\mathbf{R}$ is given by

$$\begin{aligned}R &= \sqrt{150.0^2 + 100.0^2 + 2\cdot 150.0\cdot 100.0\cos 96.87^\circ}\,\text{N} \\ &= 170.0\,\text{N}\,,\end{aligned}$$

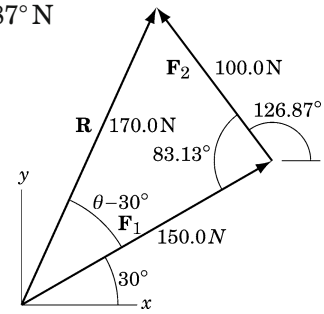

where we use the cosine law of Exercise **1.2-12**. The angle θ with the horizontal axis can be found by appealing to the sine law of Exercise **1.2-11**, for example $170.0/\sin 83.13^\circ = 100.0/\sin(\theta - 30^\circ)$, from which

$$\theta = 30^\circ + \sin^{-1}(100.0\sin 83.13^\circ/170.0) = 65.73^\circ.$$

(b) In Cartesian components we have

$$\mathbf{F}_1 = (129.9\mathbf{i} + 75.0\mathbf{j})\,\text{N} \quad , \quad \mathbf{F}_2 = (-60.0\mathbf{i} + 80.0\mathbf{j})\,\text{N}\,,$$

so that $\mathbf{R} = (69.9\mathbf{i} + 155.0\mathbf{j})$ N. Hence, the magnitude of $\mathbf{R}$ is $R = \sqrt{69.6^2 + 155.0^2} = 170.0$ N, and the angle θ with the horizontal axis is $\tan^{-1}(155.0/69.9) = 65.73^\circ$.

The resultant of three forces $\mathbf{F}_1$, $\mathbf{F}_2$, $\mathbf{F}_3$ acting at the same point may again be determined either graphically or algebraically. In either case, it is important to note that the order in which the forces are summed is immaterial, namely

$$\mathbf{R} = (\mathbf{F}_1+\mathbf{F}_2)+\mathbf{F}_3 = \mathbf{F}_1+(\mathbf{F}_2+\mathbf{F}_3) = (\mathbf{F}_3+\mathbf{F}_1)+\mathbf{F}_2 . \tag{1.34}$$

The same observation applies to the resultant of n forces $\mathbf{F}_1, \mathbf{F}_2, \ldots, \mathbf{F}_n$ acting at the same point.

The resultant $\mathbf{R}$ of two or more forces can be defined even when these act at different points of a body, as in Fig. 1.13. But if the resultant is itself to be

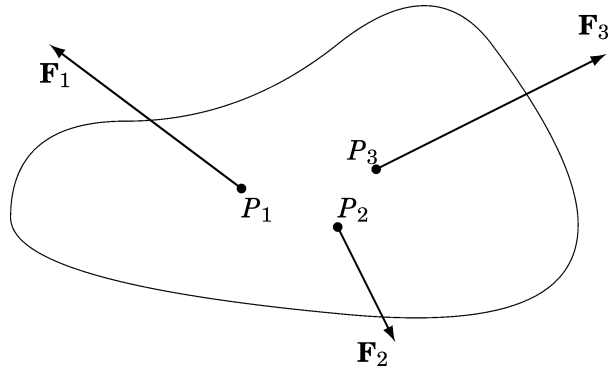

Figure 1.13. Three forces acting at different points of a body

interpreted as a force, the question arises: at what point is this force acting? This question will be answered in Sects. 1.4 and 1.5.

If two forces $\mathbf{F}_1$ and $\mathbf{F}_2$ acting on a body are *equal and opposite*, as in Fig. 1.14, then their resultant $\mathbf{R}$ is equal to zero,

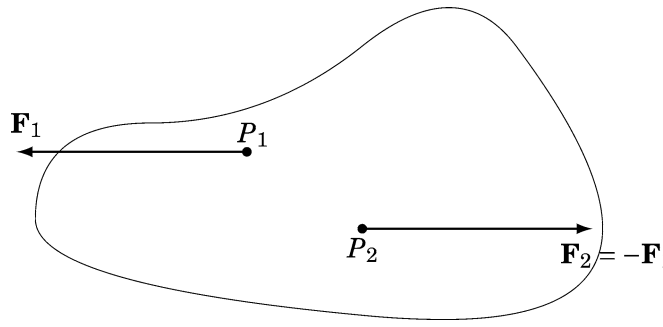

Figure 1.14. Two equal and opposite forces acting at different points of a body

When the lines of action of the forces acting on a body lie in the same

plane, then the forces are known as *coplanar*, and their resultant is necessarily coplanar with them. For instance, assume that $\mathbf{F}_1$ and $\mathbf{F}_2$ act in the plane defined by the x- and y-axes (the xy-plane). This means that these two forces can be resolved into their components as

$$\mathbf{F}_1 = F_{1x}\mathbf{i}+F_{1y}\mathbf{j} \quad , \quad \mathbf{F}_2 = F_{2x}\mathbf{i}+F_{2y}\mathbf{j} \, , \tag{1.35}$$

hence their resultant $\mathbf{R}$ is

$$\mathbf{R} = \mathbf{F}_1+\mathbf{F}_2 = (F_{1x}\mathbf{i}+F_{1y}\mathbf{j})+(F_{2x}\mathbf{i}+F_{2y}\mathbf{j}) = (F_{1x}+F_{2x})\mathbf{i}+(F_{1y}+F_{2y})\mathbf{j} \, , \tag{1.36}$$

therefore it also lies in the xy-plane. The same conclusion may be immediately drawn for the case of more than two coplanar forces.

Forces whose lines of action intersect at one point are called *concurrent*. On the other hand, forces whose points of application and directions are on the same line are known as *collinear*, and the resultant of two or more such forces is necessarily collinear with them.

1.3.3 Distributed Forces

In reality, forces are rarely applied at isolated points. Instead, they are (in the case of body forces) distributed over the volume of the body, or (in the case of contact forces) over some or all of its bounding surface. In the case of a cutting edge or the like, the distribution may be regarded as being over a line. Distributed forces are illustrated in Fig. 1.15.

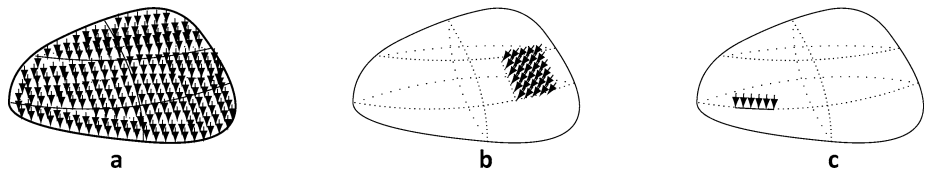

Figure 1.15. Illustration of distributed forces: (**a**) volume, (**b**) surface, (**c**) line

In the neighborhood of any point where a distributed force is applied, the local value of the force per unit volume, area or length, as the case may be, is called its *intensity*. For the force of gravity, the magnitude of its intensity (per unit volume) is known as *specific gravity* or *specific weight* (it is equal to the mass density times g). For a contact force that is a push, the intensity (per unit area) is called the *pressure*.

For some purposes, it is possible to replace a distributed force by a single force (called a *concentrated force*) acting at a representative point. The representative point for gravitational force is the *center of gravity*, where the body's total weight may be regarded as being concentrated. Similarly, the

pressure between two bodies in contact along some surface may be replaced by its resultant acting at a point that is the *center of pressure* of the contact surface. The determination of such representative points will be discussed in Sect. 1.5.

Exercises

1.3-1. Determine the direction cosines of a force $\mathbf{F}$ which is normal to the plane $x + y + 2z = 1$.

1.3-2. Let forces $\mathbf{F}_1 = (10\mathbf{i} + 2\mathbf{j} - \mathbf{k})$ N and $\mathbf{F}_2 = (-2\mathbf{i} + 3\mathbf{j} + 4\mathbf{k})$ N apply to a point O of a body. Find the resultant $\mathbf{R}$ of these forces.

1.3-3. Consider a two-dimensional body which occupies a unit square region in the (x, y) plane and carries point forces at each of the four vertices. If three of these forces are $\mathbf{F}_1 = (2\mathbf{i} + 3\mathbf{j})$ N, $\mathbf{F}_2 = (-3\mathbf{i} - \mathbf{j})$ N and $\mathbf{F}_3 = (\mathbf{i} + 7\mathbf{j})$ N, find the fourth force $\mathbf{F}_4$ if it is known that the resultant of all four forces is equal to zero.

1.3-4. The resultant $\mathbf{R}$ of two planar forces acting at a point O has direction cosines $(\frac{3}{5}, \frac{4}{5})$. If one of the two forces is $\mathbf{F}_1 = (2\mathbf{i} + 5\mathbf{j})$ N and the other force $\mathbf{F}_2$ has magnitude equal to $\sqrt{2}$ N, find $\mathbf{F}_2$ and $\mathbf{R}$.

1.3-5. Find the magnitude of a force $\mathbf{F}_2$ which lies along the axis $x + 2y = 0$, such that the resultant of $\mathbf{F}_1 = (2\mathbf{i} - 3\mathbf{j})$ N and $\mathbf{F}_2$ be collinear to $\mathbf{F} = (4\mathbf{i} + 5\mathbf{j})$ N.

1.3-6. Show that any two equal and opposite forces are coplanar.

1.3-7. Show that if the resultant of n forces acting at the same point is zero, then the resultant of any $n - 1$ of these forces is collinear to the remaining force.

1.3-8. Let a force $\mathbf{F}_1 = (3\mathbf{i} + \mathbf{j} + \mathbf{k})$ N act at a point O of a body with coordinates $(0, 0, 0)$ relative to a given Cartesian coordinate system (x, y, z). Determine a force $\mathbf{F}_2$ of unit magnitude which acts at another point P of the body with coordinates $(1, -2, 3)$, such that $\mathbf{F}_1$ and $\mathbf{F}_2$ are coplanar and perpendicular to each other.

1.3-9. Let a pressure force of linearly varying magnitude $3x$ Newton per unit length act on a line segment that extends from $x = 0$ to $x = a$. Find the resultant pressure force acting on the line segment.

1.3-10. Suppose that a sphere of radius R is immersed in a gravitational field whose intensity is $(\mathbf{i} + \mathbf{j})$ kN per unit volume. Find the resultant gravitational force acting on the sphere.

1.4 Moments

Consider a force $\mathbf{F}$ acting on a body at a point P, the line of action of $\mathbf{F}$ being in the xy-plane, as shown in Fig. 1.16. Now take a point O that does not

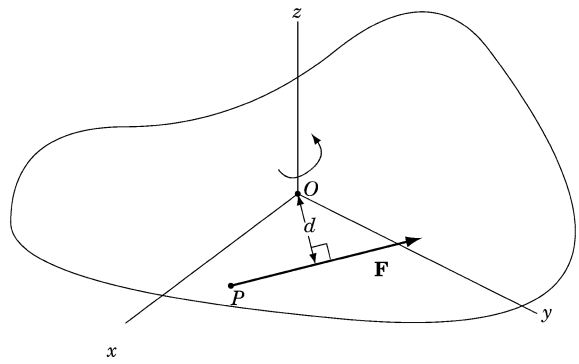

Figure 1.16. A force $\mathbf{F}$ in the xy-plane

lie along the line of action of $\mathbf{F}$ and assume, without loss of generality, that the z-axis passes through O, so that the x-, y-, and z-axes form a Cartesian coordinate system with right-hand basis $\{\mathbf{i},\mathbf{j},\mathbf{k}\}$. In this case, the *moment* of the force $\mathbf{F}$ about the point O quantifies the tendency of the force to rotate the body about the z-axis, as in Fig. 1.16, with the direction of rotation shown by the curved arrow.

It is important to understand that the moment of a force is vectorial in nature, because, just like the force itself, it is endowed with a magnitude and a direction. In particular, the magnitude of the moment is proportional to the magnitude of the force (the larger the force, the greater the tendency of rotation) and to the distance of the point O from the line of action of the force, called the *lever arm* or *moment arm* of the force (the longer the lever arm, the greater the tendency of rotation). Hence, the magnitude M_O of the moment of $\mathbf{F}$ about O is

$$M_O = Fd\,, \tag{1.37}$$

where F is the magnitude of $\mathbf{F}$ and d is the distance of the point O from the line of action of $\mathbf{F}$ (see Fig. 1.16. Using a wrench to rotate a bolt provides a simple intuitive means of appreciating how the magnitude of the applied moment can be affected by the magnitude and/or the lever arm of the applied force.

Example 1.4.1: Calculation of moment: geometric method.
Let the force shown in Fig. 1.16 be given by $\mathbf{F} = (-20\mathbf{i} + 15\mathbf{j})$ N, and let the point at which it acts have coordinates $(4,1)$ m. We wish to find the magnitude of the moment M_O. To do that we must first find the distance d from the origin O

to the line of action of the force. Since the line of action has the slope $-3/4$ and passes through the point $(-4,1)$, it is given by $(y-1)/(x-4) = -3/4$ (with distances in meters). Any line perpendicular to it has the slope $4/3$, and if this line passes through the origin then it satisfies $y/x = 4/3$. We thus have the simultaneous linear equations

$$\begin{aligned} 3(x-4)+4(y-1) &= 0\,, \\ 4x-3y &= 0\,, \end{aligned}$$

whose solution is easily found to be $x = 1.92$ m and $y = 2.56$ m, so that $d = \sqrt{x^2+y^2} = 3.2$ m, and $M_O = \sqrt{20^2+15^2}\ \text{N}\cdot 3.2\ \text{m} = 80\ \text{N}\cdot\text{m}$.

To understand the direction (or, equivalently, the orientation and sense) of a moment, consider first the moments produced by the same force $\mathbf{F}$ about the same point O, but relative to two mutually perpendicular axes, as shown in Fig. 1.17. It is clear from the figure that the two moments are identical in

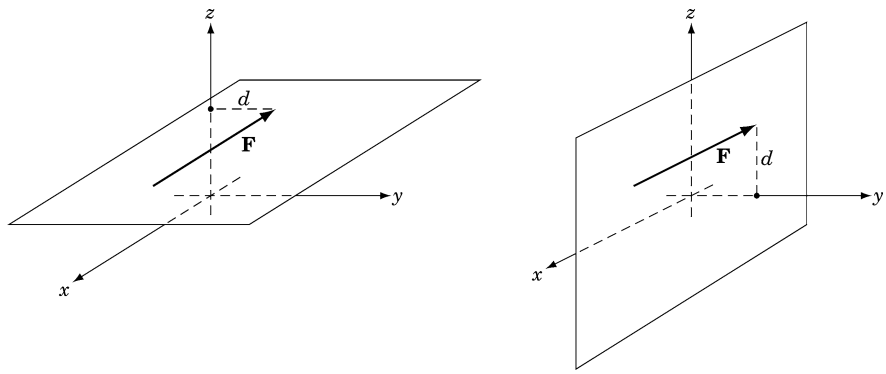

Figure 1.17. Moment of $\mathbf{F}$ about O relative to two mutually perpendicular axes z and y

magnitude, but quantify rotational tendencies about different axes, hence the moment about O possesses an orientation (namely, the orientation of the axis relative to which the moment tends to produce a rotation of the body). Next, the existence of a sense in the moment about a point O can be motivated by considering the moments produced separately by two forces $\mathbf{F}$ and $-\mathbf{F}$ that share the same line of action, as seen in Fig. 1.18. Clearly, both moments have the same magnitude and orientation, but opposite senses. The right-hand rule can be adopted to define the sense of a moment. To this end, let the fingers of the right hand be curled following the rotation induced by $\mathbf{F}$. Then, the thumb determines the sense of the moment vector.

Returning to Fig. 1.16, it is clear that we may write the moment of $\mathbf{F}$ about O vectorially as

$$\mathbf{M}_O = Fd\mathbf{k}\,, \tag{1.38}$$

where $\mathbf{M}_O$ is attached to point O. It is now easy to show that the preceding

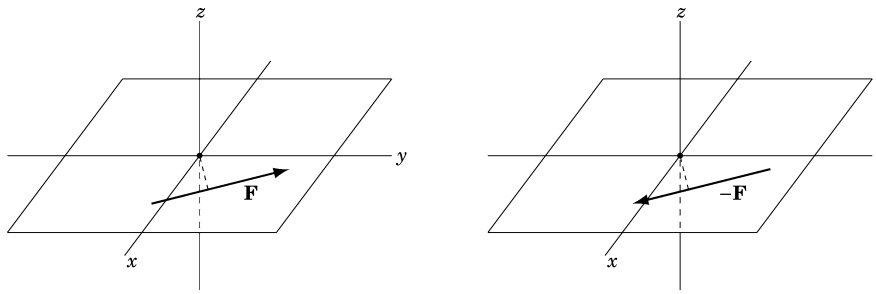

Figure 1.18. Moments of forces $\mathbf{F}$ and $-\mathbf{F}$ about O relative to the z-axis

formula may be also written as

$$\mathbf{M}_O = \mathbf{r} \times \mathbf{F} , \tag{1.39}$$

where $\mathbf{r}$ is the position vector drawn from O to a point on the line of action of $\mathbf{F}$. Indeed, with reference to Fig. 1.19, recall that the magnitude of the vector $\mathbf{r} \times \mathbf{F}$ is

$$rF \sin\theta = F(r \sin\theta) = Fd , \tag{1.40}$$

where r is the magnitude of the position vector $\mathbf{r}$. Also, the orientation of $\mathbf{r} \times \mathbf{F}$ is along $\mathbf{k}$, since

$$\mathbf{r} \times \mathbf{F} = (r_x \mathbf{i} + r_y \mathbf{j}) \times (F_x \mathbf{i} + F_y \mathbf{j}) = (r_x F_y - r_y F_x)\mathbf{k} . \tag{1.41}$$

Finally, for the force $\mathbf{F}$ shown in Fig. 1.19, the sense of $\mathbf{r} \times \mathbf{F}$ is along $+\mathbf{k}$ since $r_x F_y - r_y F_x > 0$.

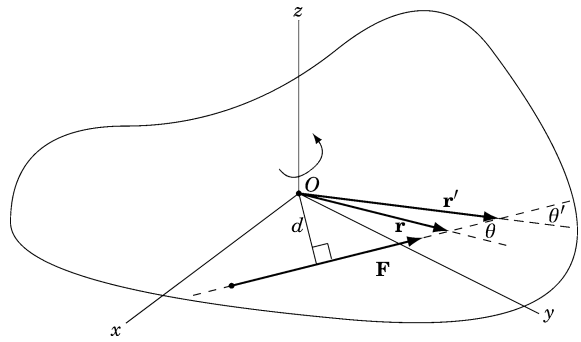

Figure 1.19. Moment of $\mathbf{F}$ about point O

Example 1.4.2: Calculation of moment: vectorial method.
To determine the moment of Example 1.4.1 by means of Eq. 1.39, we note that $\mathbf{r} = (-4\mathbf{i} + 1\mathbf{j})\text{m}$ and therefore

$$\mathbf{M}_0 \;=\; (4\mathbf{i} + 1\mathbf{j})\,\text{m} \times (-20\mathbf{i} + 15\mathbf{j})\,\text{N} = 80\mathbf{k}\ \text{N·m}\ .$$

We observe here that the formula (1.39) holds true when drawing a position vector from O to *any* point on the line of action of $\mathbf{F}$. This is easily confirmed by taking a vector $\mathbf{r}'$ from O to any point on the line action and noting that

$$r'F\sin\theta' \;=\; d\ . \tag{1.42}$$

This property of moments is referred to as the *principle of transmissibility*. Its practical meaning is that, as far as the determination of moments is concerned, a force can be viewed as a "floating" vector along its line of action.

The formula (1.39) may be likewise employed to determine the moment of any three-dimensional force about a point O, namely

$$\begin{aligned}\mathbf{M}_O \;&= \mathbf{r}\times\mathbf{F}\ ,\\ &= (r_x\mathbf{i} + r_y\mathbf{j} + r_z\mathbf{k})\times(F_x\mathbf{i} + F_y\mathbf{j} + F_z\mathbf{k})\\ &= (r_yF_z - r_zF_y)\mathbf{i} + (r_zF_x - r_xF_z)\mathbf{j} + (r_xF_y - r_yF_x)\mathbf{k}\ ,\end{aligned} \tag{1.43}$$

where, again, the vector $\mathbf{M}_O$ originates at point O. Likewise, we may determine the *resultant moment* about O of n forces $\mathbf{F}_1$, $\mathbf{F}_2$, …, $\mathbf{F}_n$ acting at the same point as

$$\begin{aligned}\mathbf{M}_O \;&= \mathbf{r}\times(\mathbf{F}_1 + \mathbf{F}_2 + \ldots + \mathbf{F}_n)\ ,\\ &= \mathbf{r}\times\mathbf{F}_1 + \mathbf{r}\times\mathbf{F}_2 + \ldots + \mathbf{r}\times\mathbf{F}_n\ .\end{aligned} \tag{1.44}$$

The preceding equation demonstrates that the moment about a point O of the resultant of a set of forces acting at another point P (see Fig. 1.20a) is equal to the sum of the moments of all the constituent forces about the point O. This result is known as *Varignon's theorem*[*].

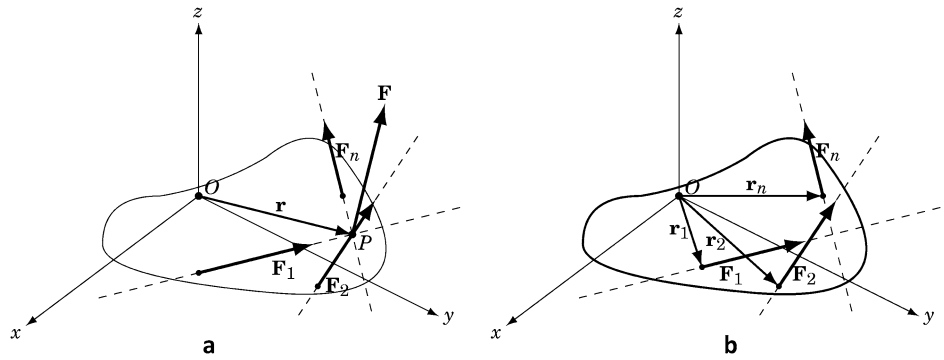

Figure 1.20. Moment of a set of forces: (**a**) concurrent (Varignon's theorem), (**b**) non-concurrent

[*]Pierre Varignon (1654-1722) was a French mathematician.

The resultant moment about a point O of n forces $\mathbf{F}_1, \mathbf{F}_2, \ldots, \mathbf{F}_n$ that are not necessarily concurrent, as in Figure 1.20b, is given by

$$\mathbf{M}_O = \mathbf{r}_1 \times \mathbf{F}_1 + \mathbf{r}_2 \times \mathbf{F}_2 + \ldots + \mathbf{r}_n \times \mathbf{F}_n \,, \tag{1.45}$$

where $\mathbf{r}_i$ denotes a vector originating at O and ending on a point lying on the line of action of $\mathbf{F}_i$.

In practical problems, it is often important to deduce the moment $\mathbf{M}_a$ of a force about a given axis a which passes through a point O, where this axis is not necessarily perpendicular to the plane of $\mathbf{F}$ and O (see Fig. 1.21). This

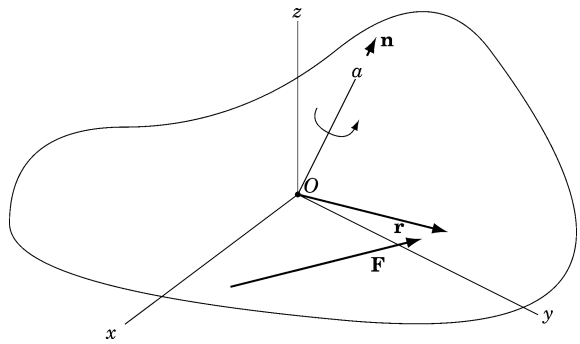

Figure 1.21. Moment of $\mathbf{F}$ about an axis a

can be easily accomplished by first computing the moment $\mathbf{M}_O$ using (1.43) and then projecting $\mathbf{M}_O$ along the axis a. In particular, let $\mathbf{n}$ be a unit vector along the a axis. Using vector algebra, the projection of $\mathbf{M}_O$ along a is

$$\begin{aligned} \mathbf{M}_a &= (\mathbf{M}_O \cdot \mathbf{n})\mathbf{n} \\ &= [(\mathbf{r} \times \mathbf{F}) \cdot \mathbf{n}]\mathbf{n} \end{aligned} \tag{1.46}$$

or, using components and recalling (1.26) and (1.27),

$$\mathbf{M}_a = \left(\begin{vmatrix} \mathbf{i} & \mathbf{j} & \mathbf{k} \\ r_x & r_y & r_z \\ F_x & F_y & F_z \end{vmatrix} \cdot \mathbf{n} \right) \mathbf{n} = \begin{vmatrix} n_x & n_y & n_z \\ r_x & r_y & r_z \\ F_x & F_y & F_z \end{vmatrix} \mathbf{n} \,. \tag{1.47}$$

1.4.1 Force Couple

A moment can be also produced by a *force couple*. This is a set of two equal and opposite forces lying on two (necessarily parallel) lines that are apart by a distance d, as in Fig. 1.22.

The resultant moment of these two forces about any point O (not necessarily on the plane of the two forces) is

$$\mathbf{M}_O = \mathbf{r}_1 \times \mathbf{F} + \mathbf{r}_2 \times (-\mathbf{F}) = (\mathbf{r}_1 - \mathbf{r}_2) \times \mathbf{F} \,, \tag{1.48}$$

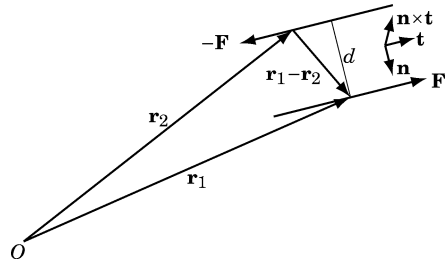

Figure 1.22. A force couple

where $\mathbf{r}_1$, $\mathbf{r}_2$ are the position vectors of any points on the lines of action of the two forces drawn from O. Denoting by $\mathbf{n}$ a unit vector in the plane of the two forces, normal to both forces and directed from $-\mathbf{F}$ to $\mathbf{F}$, and by $\mathbf{t}$ another unit vector along the line of action of the two forces, we may resolve the vector $\mathbf{r}_1-\mathbf{r}_2$ into its component vectors along $\mathbf{n}$ and $\mathbf{t}$ according to

$$\mathbf{r}_1-\mathbf{r}_2 = [(\mathbf{r}_1-\mathbf{r}_2)\cdot\mathbf{n}]\mathbf{n}+[(\mathbf{r}_1-\mathbf{r}_2)\cdot\mathbf{t}]\mathbf{t} \tag{1.49}$$

and also recognize that the distance d between the two forces can be expressed as

$$d = (\mathbf{r}_1-\mathbf{r}_2)\cdot\mathbf{n}\,. \tag{1.50}$$

Subsequently, recalling (1.48), (1.49) and (1.50), write

$$\begin{aligned}\mathbf{M}_O &= (\mathbf{r}_1-\mathbf{r}_2)\times\mathbf{F}\\ &= \big\{\big[(\mathbf{r}_1-\mathbf{r}_2)\cdot\mathbf{n}\big]\,\mathbf{n}+\big[(\mathbf{r}_1-\mathbf{r}_2)\cdot\mathbf{t}\big]\,\mathbf{t}\big\}\times\mathbf{F}\\ &= \big\{\big[(\mathbf{r}_1-\mathbf{r}_2)\cdot\mathbf{n}\big]\,\mathbf{n}\big\}\times\mathbf{F}\\ &= d\,\mathbf{n}\times\mathbf{F}\\ &= d\,\mathbf{n}\times(F\mathbf{t})\\ &= Fd\,\mathbf{n}\times\mathbf{t}\,,\end{aligned} \tag{1.51}$$

since $\mathbf{t}\times\mathbf{F}=\mathbf{0}$ due to the parallelism between $\mathbf{F}$ and $\mathbf{t}$. We conclude from (1.51) that the force couple is a moment whose magnitude is equal to the magnitude of the forces times the distance between their lines of action. Its orientation is normal to the plane of the two forces and its sense is determined by the right-hand rule, with the sense of the vector $\mathbf{n}\times\mathbf{t}$ in (1.51) shown in Fig. 1.22.

It is also clear from Fig. 1.22 that the vector difference $\mathbf{r}_1-\mathbf{r}_2$ is independent of the point O from which the vectors $\mathbf{r}_1$ and $\mathbf{r}_2$ are drawn. Consequently, the moment produced by a force couple (such a moment is usually called simply a *couple*) has the same vectorial value about any point, and hence does not need to have a specified point of application. Such a vector is called a *free vector*, in contrast to such vectors as a force or the moment of a force, which generally require the specification of a point of application.

Example 1.4.3: Moment of force couple.
We wish to determine the moment produced by the forces $\mathbf{F} = (4\mathbf{i} + 1\mathbf{j})$ lb and $-\mathbf{F}$ acting at the points given by the vectors $\mathbf{r}_1 = 40\mathbf{i} + 30\mathbf{j}$ and $\mathbf{r}_2 = 28\mathbf{i} + 42\mathbf{j}$ (in inches), respectively.

Using Eq. 1.48 (but writing $\mathbf{M}$ rather than $\mathbf{M}_O$, in view of the preceding discussion), we find

$$\mathbf{M} = [(40-28)\mathbf{i} + (30-42)\mathbf{j}]\text{in} \times (4\mathbf{i} + 1\mathbf{j})\text{lb} = 60\mathbf{k}\ \text{lb·in}\ .$$

If a force couple is applied to a body, then it may be regarded as an *applied moment* (or *couple*),[†] and if it is necessary to specify a point of application, then this can be taken as the point midway between the points of application of the two forces. In fact, a moment can be thought of as being concentrated and applied *at a point* if we envision the magnitude of the forces growing to infinity and the distance between their lines of action shrinking to zero, with their product remaining constant, as shown in Fig. 1.23.

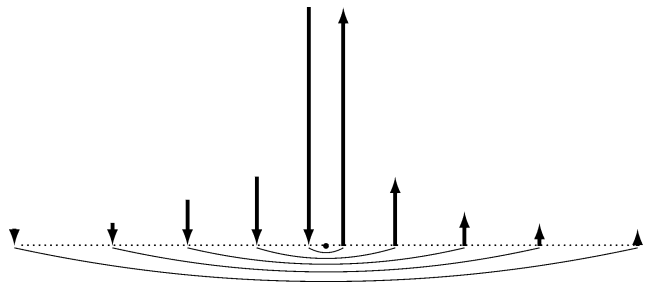

Figure 1.23. Force couples converging to a concentrated moment

A concentrated moment is typically designated by a double-headed arrow, as shown in Fig. 1.24a, except that when its axis is perpendicular to the figure it is designated by a curved arrow, as in Fig. 1.24b.

Figure 1.24. Designations of concentrated moments

Sometimes a moment can be applied by means of several couples working in concert, as for example two couples in the case of a Phillips screwdriver (Fig. 1.25a) and three couples in the case of a hexagonal wrench or nut driver (Fig. 1.25b).

[†]It is sometimes also called a *torque*, but in solid mechanics *torque* has a more specific meaning that will be defined in the next chapter.

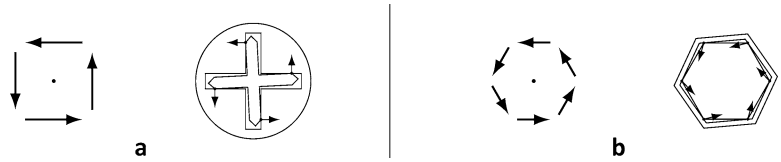

Figure 1.25. Moment applied by means of two or three couples: (**a**) Phillips screwdriver, (**b**) hexagonal wrench

Exercises

1.4-1. Find the moment of the force $\mathbf{F} = (3\mathbf{i} - \mathbf{j} + 2\mathbf{k})$ N acting at a point P with Cartesian coordinates $(1,-5,3)$ about a point O with Cartesian coordinates $(0,0,0)$.

1.4-2. Consider a rectangular region with vertices A, B, C and D having Cartesian coordinates $(0,0)$, $(4,0)$, $(4,1)$ and $(0,1)$ m, respectively. Suppose that a force $\mathbf{F} = (5\mathbf{i} + 5\mathbf{j})$ kN acts at point C. Find the moments of this force about all four vertices of the region.

1.4-3. Find the moment M_a of the force $\mathbf{F} = (6\mathbf{i} - 2\mathbf{j} + \mathbf{k})$ N acting at a point with Cartesian coordinates $(1,1,-1)$ m with respect to the axis a defined by the line with directional cosines $\frac{1}{3}(1,2,2)$ that passes through the point with Cartesian coordinates $(0,3,4)$ m.

1.4-4. Consider a rigid seesaw of total length 4 m which is in a horizontal position and which balances on a support at its midpoint O. Let a vertical force $\mathbf{F}_1 = -500\mathbf{j}$ N act at the tip of its left half. Determine the vertical force $\mathbf{F}_2$ required to act at the midpoint of the right half of the seesaw if the moment at the support point O is to vanish. How would the answer change if the seesaw assumes an inclined configuration with angle θ relative to the horizontal line?

1.4-5. Consider the coplanar forces $\mathbf{F}_1 = 10\mathbf{i}$ N and $\mathbf{F}_2 = 5\mathbf{j}$ N, whose lines of action are $y = 1$ m and $x = 1$ m, respectively. Find the locus of all points on the xy-plane about which the resultant moment of the two forces is equal to zero.

1.4-6. Let $\mathbf{F} = (3\mathbf{i} + 4\mathbf{j} - 2\mathbf{k})$ N be a force acting at a point with Cartesian coordinates (a,b,c) in meters. Determine a, b, c, such that the moment of $\mathbf{F}$ about the origin $(0,0,0)$ be equal to $8(\mathbf{i} + \mathbf{j} + \mathbf{k})$ Nm.

1.4-7. Suppose that a uniform pressure equal to $-2\mathbf{j}$ N/m acts on a line segment defined by $x = 0$ and $x = a$ in meters. Determine the moment due to the pressure about the points with coordinates $x = 0, a/2$ and a in meters.

1.4-8. If a force $\mathbf{F} = (-\mathbf{i} + 2\mathbf{j} - 3\mathbf{k})$ N acts at the point P with Cartesian coordinates $(5,-1,1)$ m, find an axis a passing through the origin $(0,0,0)$ such that moment of the force about is zero, provided the axis a makes the same angle with the x- and z-axes.

1.4-9. Show that if the moment of a force $\mathbf{F}$ about a point P which is not on its line of action is zero, then the force itself is zero.

1.4-10. Show that the moment M_a of a force $\mathbf{F}$ about an axis a may be computed by taking the projection along the axis of the moment of $\mathbf{F}$ about *any* point O of the axis.

1.4-11. Let a circular region of radius r be subject to a boundary force of constant magnitude t per unit length which is always tangential to the surface and has clockwise sense. Determine the resultant of this boundary force as well as the resultant moment about the center of the circular region.

1.5 Statically Equivalent Force Systems

1.5.1 Force Systems and Static Equivalence

We will define a *force system* as a set of forces and/or moments applied to a body, together with their points of application. Two force systems acting on a given body are called *statically equivalent* if they have the same resultant force and the same resultant moment about any given point.

The aforementioned principle of transmissibility gives us the simplest example of equivalent force systems: if a force system comprises a single force, then force systems equivalent to it are obtained by moving the point of application along the line of action of the force. Equally simple is also the static equivalence of a force couple to a moment, as discussed in Sect. 1.4. If a force system comprises only a moment or a force couple, then statically equivalent force systems are obtained by translating the moment or the force couple anywhere in the body.

It can easily be seen that statically equivalent force systems are not equivalent in every sense, especially if the body is deformable. A force applied as a push to, say, a lump of clay, as shown in Fig. 1.26a, produces different local effects from the same force applied as a pull in Fig. 1.26b.

Figure 1.26. Different local effects produced by statically equivalent forces

We examine next the equivalence between two force systems comprising the same force but with different lines of action. Consider, again, a solid body with a force $\mathbf{F}$ acting on it at a point P. We have already established that the moment $\mathbf{M}_O$ of $\mathbf{F}$ about another point O of the body is defined by

$$\mathbf{M}_O = \mathbf{r}_{OP} \times \mathbf{F} , \tag{1.52}$$

according to (1.39), where $\mathbf{r}_{OP}$ is the position vector of point P relative to point O, as in Fig. 1.27a. Now, let the same solid body be subject to a different force system consisting of the force $\mathbf{F}$ acting at the point O *and* the moment $\mathbf{M}_O$, as in Fig. 1.27b. Clearly, both force systems have the same resultant force $\mathbf{F}$. In addition, both force systems yield the same resultant moment about any other point Q. Indeed, the resultant moment of the first system about Q is

$$\mathbf{M}_Q^{(1)} = \mathbf{r}_{QP} \times \mathbf{F} , \tag{1.53}$$

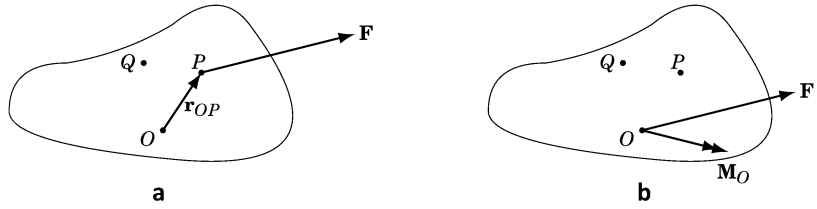

Figure 1.27. Two equivalent force systems acting on a solid body

while for the second system it is

$$\begin{aligned}\mathbf{M}_Q^{(2)} &= \mathbf{r}_{QO}\times\mathbf{F}+\mathbf{M}_O\\ &= \mathbf{r}_{QO}\times\mathbf{F}+\mathbf{r}_{OP}\times\mathbf{F}\\ &= (\mathbf{r}_{QO}+\mathbf{r}_{OP})\times\mathbf{F}\\ &= \mathbf{r}_{QP}\times\mathbf{F}\\ &= \mathbf{M}_Q^{(1)}\,.\end{aligned} \tag{1.54}$$

Another way to deduce the preceding force equivalence is to start with the force system of Fig. 1.27a and add a pair of equal and opposite forces $\mathbf{F}$ and $-\mathbf{F}$ at point O (see Fig. 1.28). The resulting force system is obviously statically equivalent to the original system and also identical to the force system in Fig. 1.27b with the moment $\mathbf{M}_O$ being replaced by a statically equivalent force couple.

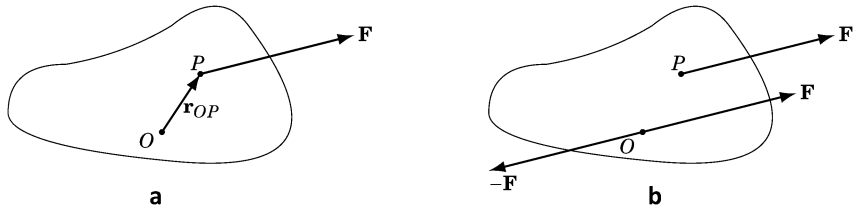

Figure 1.28. An alternative pair of equivalent force systems acting on the solid body of Fig. 1.27

The concept of force equivalence enables the unambiguous identification of the line of action for the resultant $\mathbf{R}$ of the forces $\mathbf{F}_1$, $\mathbf{F}_2$, …, $\mathbf{F}_n$ acting on different points of a solid body. To this end, let $\mathbf{r}_1$, $\mathbf{r}_2$, …, $\mathbf{r}_n$ be the position vectors of points on the line of action of each of the preceding forces, respectively, drawn from a point O, as in Fig. 1.29a. Then, the moment of these forces about the point O can be readily obtained as

$$\mathbf{M}_O \;=\; \sum_{i=1}^{n}(\mathbf{r}_i\times\mathbf{F}_i)\,. \tag{1.55}$$

Now, an equivalent force system consists of the (generally non-zero) resultant

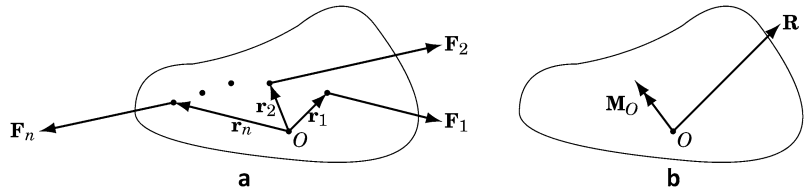

Figure 1.29. An equivalent force system to a set of forces $\mathbf{F}_1$, $\mathbf{F}_2$, ..., $\mathbf{F}_n$ acting on a solid body

$\mathbf{R} = \sum_{i=1}^{n} \mathbf{F}_i$ of the n forces with its line of action passing through O and the moment $\mathbf{M}_O$, as in Fig. 1.29b.

It is instructive to explore whether there exists a statically equivalent force system with a non-zero resultant force for which the resultant moment vanishes altogether. With reference to Fig. 1.29, such a force system is statically equivalent to a resultant force $\mathbf{R}$ and a resultant moment $\mathbf{M}_O$ acting at a point O. For this force system to be statically equivalent to the resultant force $\mathbf{R}$ alone, the line of action of this force should pass through a point P, such that

$$\mathbf{r}_{PO} \times \mathbf{R} + \mathbf{M}_O = \mathbf{0}\,, \tag{1.56}$$

where $\mathbf{r}_{PO}$ is the position vector of point O relative to P. Let us try to solve Eq. (1.56) for $\mathbf{r}_{PO}$ by assuming, with no loss of generality, that the direction of $\mathbf{R}$ is parallel to the z-axis, that is, $\mathbf{R} = R\mathbf{k}$ with $R \neq 0$. If we let $\mathbf{r}_{PO} = x\mathbf{i} + y\mathbf{j} + z\mathbf{k}$, then Eq. (1.56) is expressed in components as

$$yR + M_{Ox} = 0 \quad , \quad -xR + M_{Oy} = 0 \quad , \quad M_{Oz} = 0\,, \tag{1.57}$$

Therefore, a solution (x, y, z) exists if, and only if, the resultant moment vector $\mathbf{M}_O$ is perpendicular to the resultant force $\mathbf{R}$. If $\mathbf{M}_O$ has a component parallel to $\mathbf{R}$ then this component cannot be eliminated. But, in any case, z, which gives the position of O along the line of action of the force, is indeterminate, meaning that *any* point on the line of action of the resultant force may be considered as the point of application of this force.

As a consequence of the preceding discussion, we see that any force system is statically equivalent to one consisting of a single force and a moment parallel to the force. Such a system resembles the action exerted by a screwdriver or a nut driver, and has historically been called a *wrench*, a term that in Britain formerly included something equivalent to a nut driver.[‡]

When all the forces are coplanar, the resultant moment is necessarily perpendicular to the plane of the forces, and consequently an equivalent force with no moment can be found. In the special case of two coplanar forces $\mathbf{F}_1$, $\mathbf{F}_2$ with intersecting lines of action, it is easy to show that such an equivalent

[‡]What in North America is called a wrench is generally known as a *spanner* in the British Isles.

force system consists of a resultant force $\mathbf{F}_1 + \mathbf{F}_2$, its line of action passing through the intersection of the lines of action of the two constituent forces.

Example 1.5.1: *Equivalent force system to two coplanar forces with intersecting lines of action.*
Consider two coplanar forces $\mathbf{F}_1$ and $\mathbf{F}_2$, whose lines of action intersect at point O, as in Fig. 1.30a. An equivalent force system comprises the resultant

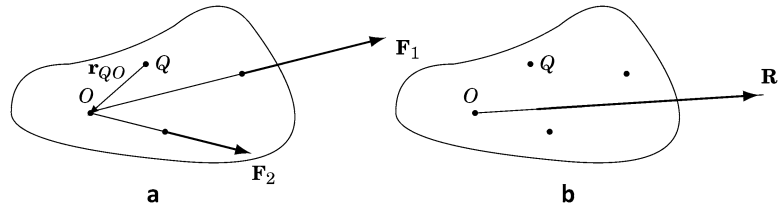

Figure 1.30. Equivalent force system to two coplanar forces with intersecting lines of action

$\mathbf{R} = \mathbf{F}_1 + \mathbf{F}_2$ with its line of action passing through O (see Fig. 1.30b). Indeed, in this case the moment of $\mathbf{R}$ about any point, say Q, is equal to the sum of the moments of $\mathbf{F}_1$ and $\mathbf{F}_2$ about the same point, since the lever arms for all three moments can be drawn to the intersection point O, and

$$\mathbf{r}_{QO} \times \mathbf{R} \;=\; \mathbf{r}_{QO} \times (\mathbf{F}_1 + \mathbf{F}_2) \;=\; \mathbf{r}_{QO} \times \mathbf{F}_1 + \mathbf{r}_{QO} \times \mathbf{F}_2 \,.$$

1.5.2 Center of Gravity, Mass and Volume

An important application of the concept of force equivalence is the determination of a body's *center of gravity*, that is, the point at which the body's weight may be assumed to act as though it were a concentrated force.

We begin by assuming that the body is made up of a finite number (say N) of particles, the mass of the i-th particle being m_i and its position vector $\mathbf{r}_i = x_i\mathbf{i} + y_i\mathbf{j} + z_i\mathbf{k}$ with respect to an origin O. We define the z-axis as being positive upward, and, without loss of generality, we assume that the force of gravity $\mathbf{F}_i$ on particle i acts along the z-axis with opposite sense to that of the axis, namely $\mathbf{F}_i = -m_i g\mathbf{k}$, as in Fig. 1.31. The resultant is clearly

$$\mathbf{R} \;=\; \sum_{i=1}^{N} \mathbf{F}_i \;=\; -Mg\mathbf{k}\,, \tag{1.58}$$

where $M = \sum_{i=1}^{N} m_i$ is the total mass of the body and Mg its weight.

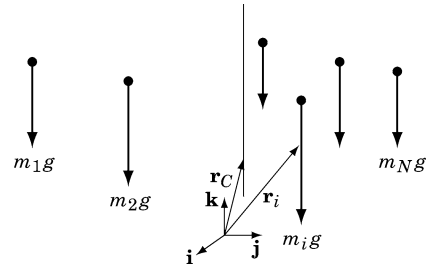

Figure 1.31. Center of gravity for a finite system of particles

Let C be a point such that the force system consisting of the particle weights is equivalent to $\mathbf{R}$ acting at C.[§] The resultant moment of the particle weights about C must be zero, that is,

$$\sum_{i=1}^{N}(\mathbf{r}_i - \mathbf{r}_C)\times(-m_ig)\mathbf{k} = \mathbf{0} \tag{1.59}$$

or, in components,

$$g\sum_{i=1}^{N} m_i(x_i - x_C) = 0 \quad , \quad g\sum_{i=1}^{N} m_i(y_i - y_C) = 0\,, \tag{1.60}$$

from which it follows that

$$x_C = \frac{1}{M}\sum_{i=1}^{N} m_ix_i \quad , \quad y_C = \frac{1}{M}\sum_{i=1}^{N} m_iy_i\,. \tag{1.61}$$

Note that, at this point, z_C is indeterminate. That is, the calculation has given us, consistent with the principle of transmissibility, only the line of action of $\mathbf{R}$ and not a specific point at which it acts.

Suppose, however, that the body is rotated by 90° about the x-axis. Equivalently, we can imagine that the direction of the force of gravity undergoes an equal and opposite rotation, so that it is now directed along the y-axis, and therefore $\mathbf{F}_i = m_ig\mathbf{j}$. The condition of zero moment about C is now obtained by replacing $\mathbf{k}$ with $\mathbf{j}$ in Eq. (1.59), and, by the same procedure that we have just followed we obtain, in addition to the first of Eqs. (1.61),

$$z_C = \frac{1}{M}\sum_{i=1}^{N} m_iz_i\,. \tag{1.62}$$

[§]The same procedure would, of course, apply to any other set of forces that are parallel but not necessarily coplanar.

Eqs. (1.61) and (1.62) uniquely determine the position vector $\mathbf{r}_C$ of the center of gravity uniquely. Note that, since g drops out of the equations, the body's center of gravity is also its *center of mass*.

If the body is a continuum, then the summation over particles is replaced by integration over the volume. Let ρ be the *mass density*, namely the mass per unit volume, defined at a point as

$$\rho = \lim_{V \to 0} \frac{M(\mathscr{R})}{V} , \tag{1.63}$$

where V is the volume of a region $\mathscr{R}$ containing the point P and $M(\mathscr{R})$ is the mass contained in $\mathscr{R}$. Accordingly, the mass contained in an infinitesimal volume element dV located at a point with position vector $\mathbf{r}$ relative to a fixed point O is ρdV, and the total mass of the body is $M = \int_{\mathscr{R}} \rho dV$. In direct analogy to the preceding analysis of the particle system, the position vector $\mathbf{r}_C$ of the center of gravity (or mass) satisfies

$$\int_{\mathscr{R}} (\mathbf{r} - \mathbf{r}_c) \times (-g\rho\, dV)\mathbf{k} = \mathbf{0} . \tag{1.64}$$

Eq. (1.64) and its rotated counterpart as in the earlier case of the particle system imply that

$$x_C = \frac{1}{M}\int_{\mathscr{R}} \rho x\, dV \quad , \quad y_C = \frac{1}{M}\int_{\mathscr{R}} \rho y\, dV \quad , \quad z_C = \frac{1}{M}\int_{\mathscr{R}} \rho z\, dV . \tag{1.65}$$

If, moreover, the density ρ is constant, then it too drops out of the equations and the center of mass is just the *centroid* (or *center of volume*), its coordinates given by

$$x_C = \frac{1}{V}\int_{\mathscr{R}} x\, dV \quad , \quad y_C = \frac{1}{V}\int_{\mathscr{R}} y\, dV \quad , \quad z_C = \frac{1}{V}\int_{\mathscr{R}} z\, dV . \tag{1.66}$$

For bodies with sufficient symmetry (or antisymmetry) to possess a clearly defined geometric center[¶], this center necessarily coincides with the centroid. An intuitive way to see this, at least for a body with three mutually perpendicular planes of symmetry, is to put the origin at the center of symmetry and define the axes so that the coordinate planes are the planes of symmetry. Now, for every volume element with a given value of x, there is a mirror image, across the yz-plane, with an equal and opposite value, so that $\int_{\mathscr{R}} x\, dV = 0$. Similarly, $\int_{\mathscr{R}} y\, dV = \int_{\mathscr{R}} z\, dV = 0$, so that $x_C = y_C = z_C = 0$, that is, the centroid coincides with the center of symmetry.

Obvious examples of such bodies are ellipsoids (including spheres), right cylinders whose base is a plane figure that in turn has a clearly defined center

[¶]The center may be defined as the intersection of any two lines of symmetry (or antisymmetry, as for example in a rhomboid) in two-dimensional figures, or of any three planes of symmetry (or antisymmetry) in three-dimensional figures.

(such as ellipses or regular polygons), or sufficiently symmetric combinations of such bodies, like the one in Fig. 1.32a. For a body that is made up of several symmetric bodies but lacks sufficient symmetry as a whole (as in Fig. 1.32b), the center of mass can be obtained by treating these bodies (subbodies) as particles located at their respective centers, as shown in Fig. 1.32c.

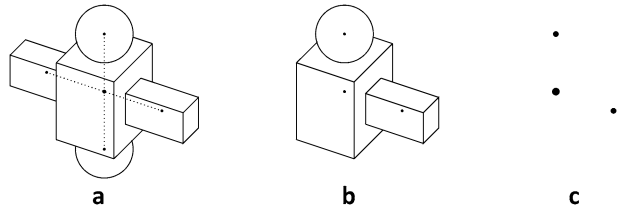

Figure 1.32. Bodies made up symmetric subbodies

Now consider a right cylinder or prism with generators parallel to the z-axis, shown in Fig. 1.33a, whose base is an irregular figure of area A in the xy-plane, as shown in Fig. 1.33c. By symmetry, the z-coordinate of the center of volume is that of the *middle plane* of the body, shown in Fig. 1.33b. Its x-

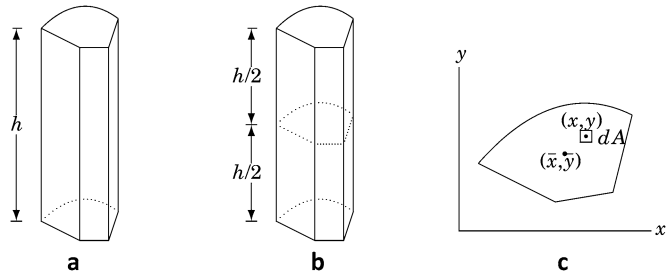

Figure 1.33. Right cylinder with irregular base

and y-coordinates are those of the centroid of the area, and are given by

$$\bar{x} = \frac{1}{A}\int_{\mathscr{A}} x\,dA \quad , \quad \bar{y} = \frac{1}{A}\int_{\mathscr{A}} y\,dA \; , \tag{1.67}$$

where $\mathscr{A}$ denotes the two-dimensional cross-sectional region shown in Fig. 1.33.

Once again, if the figure is a composite of symmetric figures with areas $A_1, A_2, \ldots$ and easily determined centers with coordinates $(\bar{x}_1, \bar{y}_1), (\bar{x}_2, \bar{y}_2), \ldots$, then the centroid is located at

$$\bar{x} = \frac{1}{A}\sum_i \bar{x}_i A_i \quad , \quad \bar{y} = \frac{1}{A}\sum_i \bar{y}_i A_i \; . \tag{1.68}$$

It is also evident that if a plane figure of area A is a part of a contact surface and is subject to a *uniform* pressure p, then the pressure distribution is equivalent to a force pA, perpendicular to the area, acting at the centroid of the area. The same would be true of a frictional force of intensity f.

Example 1.5.2: Centroid of a triangle.
Consider a triangle like the one shown in Fig. 1.34a, with one vertex located on the y-axis and the opposite side (of length b) parallel to it at a distance h. The area of the triangle is $A = bh/2$. The area of a strip of width dx spanning the triangle at x is, by similar triangles, $(x/h)b\,dx$. It follows from the first of Eqs. (1.67) that

$$\bar{x} = \frac{2}{bh}\int_0^h x(x/h)b\,dx = \frac{2}{h^2}\int_0^h x^2 dx = 2h/3\,.$$

The centroid is consequently located on a line parallel to the vertical side, one-

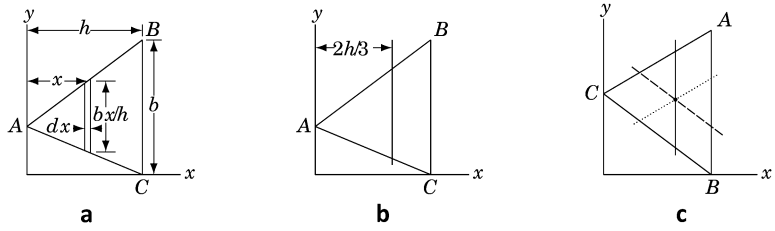

Figure 1.34. Centroid of a triangle

third of the distance from this side to the opposite vertex, shown in Fig. 1.34b. In order to fully determine the location of the centroid, we need only find another such line that intersects the first one, and we can do this by rotating the triangle so that another side is parallel to the y-axis and performing the same analysis. The result is shown in Fig. 1.34c, where the dashed line is the one obtained in Fig. 1.34b, and the dotted line is the one that would have been obtained if the side AC had been made vertical.

Example 1.5.3: Centroid of a semicircle.
Consider the semicircle of radius c shown in Figure 1.35a. We know from sym-

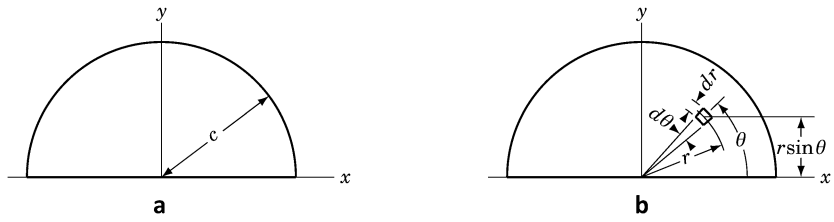

Figure 1.35. Centroid of a semicircle

metry that the centroid must lie on the y-axis and therefore need only determine its y-coordinate $\bar{y}$. We consider the infinitesimal area element shown in Figure 1.35b, occupying the region defined in polar coordinates by $(r-dr/2, r+dr/2)(\theta - d\theta/2, \theta + d\theta/2)$. Its area is $r\,d\theta\,dr$, and its y-coordinate (that is, its moment arm about the x-axis) is $r\sin\theta$. Since the area of the semicircle is $\pi c^2/2$, it follows that

$$\bar{y} = \frac{\int_0^c \int_0^\pi (r\sin\theta) r\,d\theta\,dr}{\pi c^2/2} = \frac{2}{\pi c^2}\int_0^c r^2\,dr \int_0^\pi \sin\theta\,d\theta = \frac{2}{\pi c^2}\cdot\frac{c^3}{3}\cdot 2 = \frac{4c}{3\pi}\,.$$

Exercises

1.5-1. Show that any two force couples with the same resultant moment $\mathbf{M}$ are equivalent force systems.

1.5-2. Show that a force system consisting of two equal forces $\mathbf{F}$ with lines of action that are apart by a distance d is equivalent to a force system consisting of a single force $2\mathbf{F}$ whose line of action is located at distances $d/2$ from the lines of actions of the two forces $\mathbf{F}$.

1.5-3. Find the line of action of the equivalent force system to a pair of parallel forces $\mathbf{F}_1$ and $\mathbf{F}_2$ ($\mathbf{F}_1 \cdot \mathbf{F}_2 > 0$) whose lines of actions are apart by a distance d.

1.5-4. Repeat the previous exercise assuming that $\mathbf{F}_1 \cdot \mathbf{F}_2 < 0$.

1.5-5. A force system consist of forces $\mathbf{F}_1 = 2\mathbf{i} + 3\mathbf{j} - \mathbf{k}$, $\mathbf{F}_2 = 2\mathbf{i} + 5\mathbf{k}$ and $\mathbf{F}_3 = \mathbf{i} + \mathbf{j} + \mathbf{k}$ acting at points with rectangular Cartesian coordinates $(0,0,0)$, $(0,0,1)$ and $(0,1,1)$. Find the equivalent force system for which the resultant of the three forces passes through the point with rectangular Cartesian coordinates $(1,1,1)$.

1.5-6. Let $\mathbf{F}_1 = F_{1x}\mathbf{i} + F_{1y}\mathbf{j}$ and $\mathbf{F}_2 = F_{2x}\mathbf{i} + F_{2y}\mathbf{j}$ be two non-zero coplanar forces acting at points $(0,0)$ and $(1,0)$, respectively. Find the line of action of their resultant for which the corresponding equivalent force system has zero moment.

1.5-7. Find the coordinates of the centroid of a trapezoid, as in the figure below.

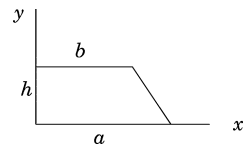

1.5-8. Find the y-coordinate of the centroid of the region bounded by two semicircles with radii b and c, as in the figure below.

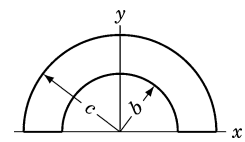

1.5-9. Find the coordinates of the centroid of the composite region shown in the figure below.

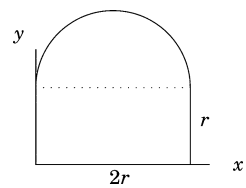

1.5-10. Find the coordinates of the centroid of the rectangular region with a hole centered at $(2r, 2r)$, as shown in the figure below.

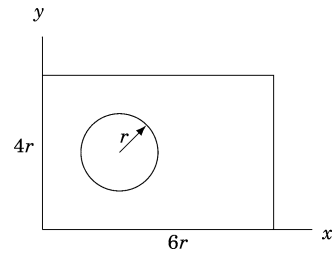

1.5-11. Find the centroid of the composite region shown in the figure below. Take $a = 2$ cm, $b = 9$ cm, and $c = 2$ cm.

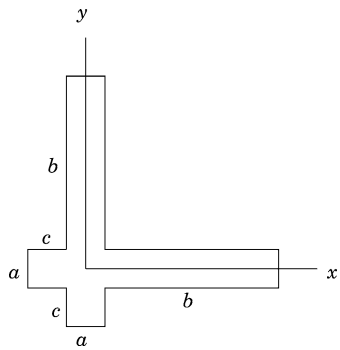

1.5-12. Use the representative data in the table below to determine the center of mass of the human body. Assume that the mass is uniformly distributed in each part.

Body part	head	neck	thorax	pelvis	thigh
Mass	4	1	20	10	8
Height	20	5	44	12	41

Body part	calf	foot	upper arm	forearm	hand
Mass	3.5	0.8	1.5	1.2	0.5
Height	41	6	30	26	15

(mass in kg, height in cm)

Chapter 2

Equilibrium

2.1 Equilibrium of Particle Systems

2.1.1 Introduction

It is well known that, in accordance with Newton's laws of motion, the effect of forces on bodies is to produce accelerated motion. For a body to remain at rest, then, it is necessary for the system of forces acting on it to be statically equivalent to the absence of forces. In this case, we say that the body is in equilibrium.

We will begin the study of equilibrium by focusing on a single particle. Then, we will proceed to consider systems of such particles, eventually going to the limit of such a system becoming a continuous body. The concept of work, both *actual* and *virtual*, will be introduced along the way.

By way of background, we recall the three laws of motion postulated by Sir Isaac Newton in his monumental work first published in 1687 under the title *Philosophiae Naturalis Principia Mathematica*, usually referred to simply as *Principia* (Fig. 2.1). As we will establish shortly, Newton's laws are sufficient to describe the motion of particles, but need to be generalized to describe the motion of more general bodies.

Newton's First Law states that every particle remains in a state of rest or motion with constant velocity unless an external force acts on it. *Newton's Second Law* states that a particle of mass m acted upon by a total external force $\mathbf{F}$ undergoes change in its velocity $\mathbf{v}$ according to

$$\mathbf{F} = \frac{d}{dt}(m\mathbf{v}) \,. \tag{2.1}$$

Assuming, in addition, that the mass m is constant, it follows from (2.1) that

$$\mathbf{F} = m\mathbf{a} \,, \tag{2.2}$$

© Springer International Publishing Switzerland 2017

J. Lubliner, P. Papadopoulos, *Introduction to Solid Mechanics*,
DOI 10.1007/978-3-319-18878-2_2

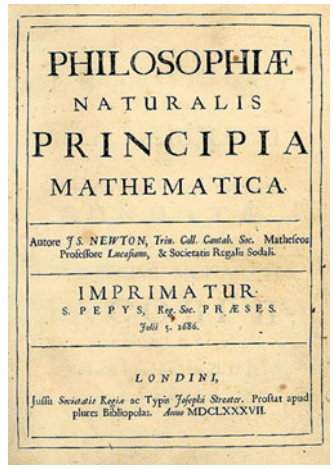
PHILOSOPHIÆ
NATURALIS
PRINCIPIA
MATHEMATICA
Autore J.S. NEWTON, Trin. Coll. Cantab. Soc. Matheseos Professore Lucasiano, & Societatis Regalis Sodali.
IMPRIMATUR
S. PEPYS, Reg. Soc. PRÆSES.
Julii 5. 1686.
LONDINI,
Juſſu Societatis Regiæ ac Typis Josephi Streater. Proſtat apud plures Bibliopolas. Anno MDCLXXXVII.

Figure 2.1. Title page of the *Principia*

where $\mathbf{a}$ is the acceleration of the particle. Eq. (2.2) implies that a particle is at rest or moving at a uniform velocity if the resultant force on it is zero. This shows that the First Law may be regarded as a special case of the Second Law, as long as the mass of the particle is constant. *Newton's Third Law* states that the force $\mathbf{F}_{ij}$ acting on particle i due to its interaction with particle j is equal and opposite to the force $\mathbf{F}_{ji}$ acting on particle j due to its interaction with particle i, namely

$$\mathbf{F}_{ij} = -\mathbf{F}_{ji} \,. \tag{2.3}$$

Newton's Third Law is often referred to as the *action-reaction law*.

2.1.2 Particle Systems

Let us now consider a discrete system of N particles, each labeled with a subscript i ($i = 1,\ldots,N$). Let the resultant force on the i-th particle be denoted $\mathbf{F}_i$. This force can be thought of as the vector sum of the forces exerted on this particle by each of the other particles in the system, $\mathbf{F}_{ij}$ ($j \neq i$), and the *external force* $\mathbf{F}_{i\mathrm{e}}$, as in Fig. 2.2. The external force $\mathbf{F}_{i\mathrm{e}}$ is defined as the resultant of all forces acting on the particle i due to its interaction with all entities other than the other particles in the system. The preceding statement is expressed in mathematical terms as

$$\mathbf{F}_i = \mathbf{F}_{i\mathrm{e}} + \sum_{j\neq i} \mathbf{F}_{ij} \,, \tag{2.4}$$

where

$$\sum_{j\neq i} = \sum_{j=1}^{i-1} + \sum_{j=i+1}^{N} \,, \tag{2.5}$$

with the understanding that, when $i = 1$ (or $i = N$), the first (or second) term on the right-hand side of (2.5) vanishes. If a particle i is in equilibrium, so that $\mathbf{F}_i = \mathbf{0}$, then Eq. (2.4) implies that

$$\mathbf{F}_{ie} + \sum_{j \neq i} \mathbf{F}_{ij} = \mathbf{0} \,. \tag{2.6}$$

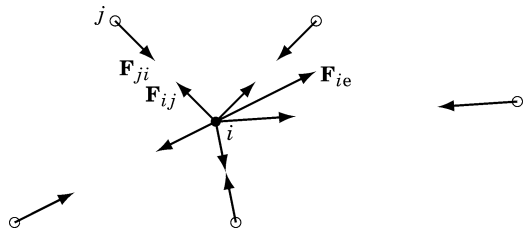

Figure 2.2. Forces on particle i belonging to a system of particles

If *each* particle i is in equilibrium, then, of course, the sum of the resultant forces acting on the whole system of particles is zero, namely

$$\sum_{i=1}^{N} \mathbf{F}_i = \mathbf{0} \,. \tag{2.7}$$

Appealing to (2.4), this sum is given by

$$\sum_{i=1}^{N} \mathbf{F}_i = \sum_{i=1}^{N} \mathbf{F}_{ie} + \sum_{i=1}^{N} \sum_{j \neq i} \mathbf{F}_{ij} \,. \tag{2.8}$$

But the double-sum term in (2.8) can be expressed with the aid of (2.5) as

$$\sum_{i=1}^{N} \sum_{j \neq i} \mathbf{F}_{ij} = \sum_{i=1}^{N} \sum_{j=1}^{i-1} \mathbf{F}_{ij} + \sum_{i=1}^{N} \sum_{j=i+1}^{N} \mathbf{F}_{ij} \,. \tag{2.9}$$

Further, the second double sum on the right-hand side of (2.9) can be rewritten, by interchanging the indices i and j, as $\sum_{j=1}^{N} \sum_{i=j+1}^{N} \mathbf{F}_{ji}$ or, equivalently, as $\sum_{i=1}^{N} \sum_{j=1}^{i-1} \mathbf{F}_{ji}$, since either way it represents the summation over all particle pairs (i, j) such that $i > j$. Consequently, Eq. (2.9) may be rewritten as

$$\sum_{i=1}^{N} \sum_{j \neq i} \mathbf{F}_{ij} = \sum_{i=1}^{N} \sum_{j=1}^{i-1} (\mathbf{F}_{ij} + \mathbf{F}_{ji}) \,. \tag{2.10}$$

In view of Newton's Third Law, as stated in Eq. (2.3), it follows that each term in parenthesis on the right-hand side of (2.10) vanishes, hence $\sum_{i=1}^{N} \sum_{j \neq i} \mathbf{F}_{ij} = \mathbf{0}$. This, in turn, implies that Eq. (2.8) reduces to

$$\sum_{i=1}^{N} \mathbf{F}_i = \sum_{i=1}^{N} \mathbf{F}_{ie} \,. \tag{2.11}$$

Finally, then, a necessary condition for a system of particles to be in equilibrium is deduced from (2.7) and (2.11) as

$$\sum_{i=1}^{N} \mathbf{F}_{i\mathrm{e}} = \mathbf{0}\,, \tag{2.12}$$

that is, the vector sum of the *external* forces on the system is zero.

Another property of forces due to the interaction between two particles is that they are typically directed along the line joining the particles, that is, they are *central*[*] (see Fig. 2.3). Now, if the position vector of particle i (with respect to an arbitrary origin O) is $\mathbf{r}_i$, then the vector from particle i to particle j is $\mathbf{r}_j - \mathbf{r}_i$, and since the cross-product of two parallel vectors is zero, it follows that $(\mathbf{r}_j - \mathbf{r}_i) \times \mathbf{F}_{ij} = \mathbf{0}$, as in Fig. 2.3. Now, Eq. (2.4) implies that

$$\sum_{i=1}^{N} \mathbf{r}_i \times \mathbf{F}_i = \sum_{i=1}^{N} \mathbf{r}_i \times \mathbf{F}_{i\mathrm{e}} + \sum_{i=1}^{N} \sum_{j \neq i} \mathbf{r}_i \times \mathbf{F}_{ij}\,. \tag{2.13}$$

Using a simple manipulation, as earlier, the double sum on the right-hand

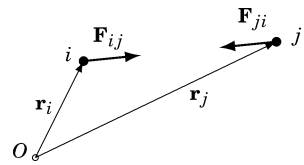

Figure 2.3. Central forces acting on particles i and j

side of (2.13) can again be rewritten as $\sum_{i=1}^{N} \sum_{j=1}^{i-1} (\mathbf{r}_i - \mathbf{r}_j) \times \mathbf{F}_{ij} = \mathbf{0}$, as in Exercise 2.1-3. Consequently, another necessary condition for the equilibrium of a particle system is that

$$\sum_{i=1}^{N} \mathbf{r}_i \times \mathbf{F}_{i\mathrm{e}} = \mathbf{0}\,, \tag{2.14}$$

namely that the vector sum of the moments of the external forces on the system is zero.

As already stated, Eqs. (2.12) and (2.14) are *necessary* conditions for the system of particles to be in equilibrium. It is important to recognize here that for a system of particles to be in equilibrium, every subset of particles from the system must also be in equilibrium. If all such subsystems are in equilibrium, then the whole system is also in equilibrium. Therefore, a *sufficient* condition for the system of N particles to be in equilibrium is that Eqs. (2.12) and (2.14) hold for all subsystems comprising M particles ($M < N$) from the original

[*]Non-central forces are encountered in electromagnetism and in certain complex particle interactions which involve more than two particles at a time.

system. For each particle i that belongs to such a subsystem, it should be understood that all forces acting on it due to its interaction with the $N-M$ particles that do not belong to the system must be treated as external forces. By the same token, interaction forces between particles in the subsystem are *internal forces* to the subsystem. Therefore, the distinction between internal and external forces depends crucially on the definition of the system under consideration.

Let us now consider a particle i that occupies a point defined by the vector $\mathbf{r}_i$ drawn to it from a fixed point O. If the particle changes its its position such that it now occupies a new point given by vector $\mathbf{r}'_i$, then the displacement vector

$$\mathbf{u} \;=\; \mathbf{r}'_i - \mathbf{r}_i \tag{2.15}$$

is the change in position (or placement) of the particle, as in Fig. 2.4.

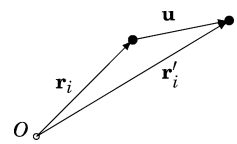

Figure 2.4. Displacement of a particle j

A particle system is *rigid* if the distances between all pairs (i,j) of particles remain unchanged. This means, in mathematical terms, that

$$(\mathbf{r}_i - \mathbf{r}_j)\cdot(\mathbf{r}_i - \mathbf{r}_j) \;=\; (\mathbf{r}'_i - \mathbf{r}'_j)\cdot(\mathbf{r}'_i - \mathbf{r}'_j)\,, \tag{2.16}$$

where particles i, j occupy points corresponding to vectors $\mathbf{r}_i$, $\mathbf{r}_j$ and $\mathbf{r}'_i$, $\mathbf{r}'_j$ at two instances. Invoking (2.15), the condition (2.16) may be restated as

$$(\mathbf{r}_i - \mathbf{r}_j)\cdot(\mathbf{r}_i - \mathbf{r}_j) \;=\; [(\mathbf{r}_i + \mathbf{u}_i) - (\mathbf{r}_j + \mathbf{u}_j)]\cdot[(\mathbf{r}_i + \mathbf{u}_i) - (\mathbf{r}_j + \mathbf{u}_j)]\,. \tag{2.17}$$

In a later section, it will be argued how the equilibrium equations (2.12) and (2.14) for rigid particle systems can be used to derive corresponding equilibrium equations for rigid bodies.

2.1.3 An Extension to Continuous Bodies

In reality, any physical body is ultimately a system of particles (atoms or molecules), though these are not necessarily governed by classical Newtonian mechanics. In practice, however, it is convenient to treat bodies as if they were continua, allowing the use of integral and differential calculus in place of algebraic operations over huge numbers of particles. In this case, the results we have just derived for particle systems are applicable to continuous bodies

by merely attaching the labels i ($i = 1,\ldots,N$) to those points of the body at which forces are applied. We let $\mathbf{F}_i$ now denote the *external force* acting there (see Fig. 2.5); then Eqs. (2.12) and (2.14) reduce respectively to

$$\sum_{i=1}^{N} \mathbf{F}_i \;=\; \mathbf{0} \tag{2.18}$$

and

$$\sum_{i=1}^{N} \mathbf{r}_i \times \mathbf{F}_i \;=\; \mathbf{0}\,. \tag{2.19}$$

Eqs. (2.19) may be appropriately modified if concentrated couples act on the body.

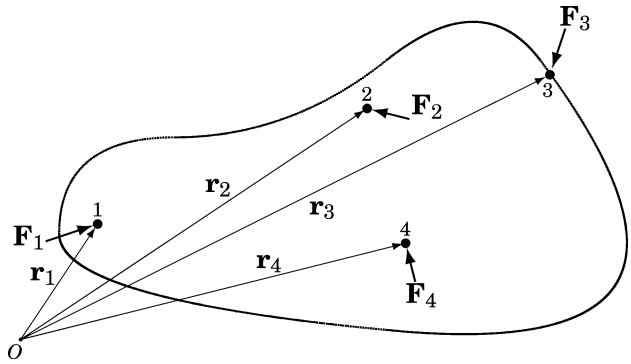

Figure 2.5. Discrete forces on a continuous body

In the case of forces that are not applied at discrete points but are distributed over volume (such as gravity) or area (such as pressure), the sums can be replaced by integrals, and, once the resultant of such a force distribution is found, it can be applied (instead of the distributed force) as a discrete force at an appropriate point of the body, as discussed in Sect. 1.5. Thus, for example, the gravitational force that is distributed throughout the body can be replaced by the body's weight acting at the center of mass. Similarly, any combination of discrete forces can be replaced by its resultant. Such a replacement does not affect the equilibrium of the body.

Eqs. (2.18) and (2.19) are often referred to as the equilibrium form of *Euler's laws*, because Euler[†] was the first to recognize the independence of force and moment equilibrium in continuous bodies. As we discussed in the preceding subsection, they are necessary and sufficient for the equilibrium of a body if they are satisfied for every part of the body.

[†]Leonhard Euler (1707-1783) was a Swiss mathematician and physicist.

Figure 2.6. Leonhard Euler

2.1.4 Work and Power

If the point of application of a force $\mathbf{F}$ (whether acting on a particle or a point of a continuous body) moves from an initial position given by $\mathbf{r}$ to one given by $\mathbf{r}+d\mathbf{r}$ (where $d\mathbf{r}$ is an infinitesimal displacement), then the *infinitesimal work* done by the force is $dW = \mathbf{F}\cdot d\mathbf{r}$. If the final position of the point is $\mathbf{r}'$, then the *work* done by the force is

$$W = \int_{\mathbf{r}}^{\mathbf{r}'} \mathbf{F}\cdot d\mathbf{r}\,, \tag{2.20}$$

as shown in Fig. 2.7. Generally, the force $\mathbf{F}$ need not remain constant through-

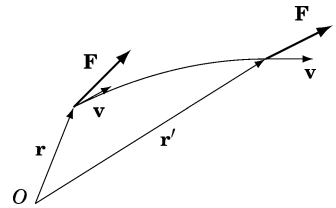

Figure 2.7. Work done by a force acting on a point

out the displacement of the point, but if it does, then the work in Eq. (2.20) is just $\mathbf{F}\cdot(\mathbf{r}'-\mathbf{r})$. Work, as defined here, is also called *actual work* in order to distinguish it from *virtual work*, to be defined shortly.

If the point of application of the force $\mathbf{F}$ is moving with velocity $\mathbf{v}$, then the infinitesimal displacement $d\mathbf{r}$ during a time increment dt is $\mathbf{v}dt$, and the infinitesimal work done is $dW = \mathbf{F}\cdot\mathbf{v}dt$. The rate of work, or *power*, is therefore

$$\Pi = \frac{dW}{dt} = \mathbf{F}\cdot\mathbf{v}\,. \tag{2.21}$$

If the force and velocity vectors are parallel, with components F and v, respectively, along their common axis, then the power is just Fv.

The definition of power in (2.21) is frequently used to identify a force (or force-like) quantity and a displacement (or displacement-like) quantity as *conjugate*. In this sense, a force is conjugate to the displacement of the point on which it acts. If the body's motion is limited to rotation about an axis, then, in the course of a rotation by an infinitesimal angle $d\theta$, the displacement of any point in the body has the scalar value $r\,d\theta$ (where r is the distance of the point from the axis of rotation), while its direction is perpendicular to both the axis and the line from the point to the axis, as shown in Fig. 2.8. Now, if a force $\mathbf{F}$ is acting at the point, then the component of the force that is parallel to that displacement, multiplied by r, is just the moment M of the force about the axis. Consequently, $dW = M\,d\theta$ and, if the angular velocity (in radians per unit time) is $\omega = d\theta/dt$, then the power is $M\omega$. In this case, we say that the moment M is conjugate to the angle of rotation θ. To obtain this result

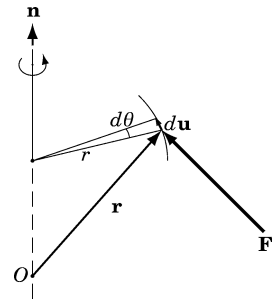

Figure 2.8. Force at a point in a body rotating about an axis

in terms of vectors, we let $\mathbf{n}$ be the unit vector along the axis such that the rotation about it follows the right-hand rule. If $\mathbf{r}$ is the radius vector to a given point from a point O on the axis, then the velocity of motion of the given point is $\mathbf{v} = \omega\mathbf{n} \times \mathbf{r}$, and the power is accordingly

$$\Pi \;=\; \mathbf{F}\cdot\mathbf{v} \;=\; \mathbf{F}\cdot\omega\mathbf{n}\times\mathbf{r} \;=\; \mathbf{n}\cdot(\mathbf{r}\times\mathbf{F})\omega \;=\; M\omega\,, \tag{2.22}$$

where $M = \mathbf{n}\cdot(\mathbf{r}\times\mathbf{F})$ is the component parallel to the axis of the moment vector (about O) of the force $\mathbf{F}$.

2.1.5 Virtual Work

Another way of expressing the equilibrium of a particle system—and by extension of any body—is by means of the *principle of virtual work*, which is introduced in this section.

Consider a system of particles that are subject to *constraints* in the sense that they are not free to displace arbitrarily, either with respect to one another

(*internal constraints*) or with respect to a fixed base (*external constraints*). Simple examples are shown in Fig. 2.9. Specifically, Fig. 2.9a shows an in-

Figure 2.9. Simple constraints: (**a**) internal, (**b**) external

ternal constraint in the form of a rigid link connecting two particles, so that their movement must be such that the distance between them remains constant and equal to d. (That is, they form a rigid particle system, as previously defined.) Fig. 2.9b shows the contours of a surface on which the particle must remain as it moves, representing an external constraint.

A displacement of the i-th particle that does not violate the constraints is called a *virtual*[‡] *displacement*; it may be written as $\mathbf{r}_i^* - \mathbf{r}_i$, where $\mathbf{r}_i$ is the current position vector and $\mathbf{r}_i^*$ is any other position vector that does not violate the constraints. If, for every particle, $\mathbf{r}_i^*$ is *close* to $\mathbf{r}_i$, then the virtual displacement may be regarded as infinitesimal and is usually denoted $\delta\mathbf{r}_i$. It follows from its definition that the δ operator is distributive: we can write $\delta(\mathbf{r}_i - \mathbf{r}_j)$ for $\delta\mathbf{r}_i - \delta\mathbf{r}_j$, since $(\mathbf{r}_i^* - \mathbf{r}_i) - (\mathbf{r}_j^* - \mathbf{r}_j) = (\mathbf{r}_i^* - \mathbf{r}_j^*) - (\mathbf{r}_i - \mathbf{r}_j)$.

As we argued above, a particle system is in equilibrium if and only if every subsystem thereof is in equilibrium, and therefore, if and only if each particle is in equilibrium. Thus, if the total force acting on the i-th particle is given by Eq. (2.4), and the particle is in equilibrium, then Eq. (2.6) implies that the *virtual work* on the particle (that is, the work done on it in the course of a virtual displacement), denoted δW_i, is also zero:

$$\delta W_i \;=\; \mathbf{F}_i \cdot \delta\mathbf{r}_i \;=\; \left(\mathbf{F}_{i\mathrm{e}} + \sum_{j\neq i} \mathbf{F}_{ij}\right) \cdot \delta\mathbf{r}_i \;=\; 0\,. \tag{2.23}$$

The total virtual work on the particle system is $\delta W = \sum_{i=1}^{N} \mathbf{F}_i \cdot \delta\mathbf{r}_i$ and is also zero, that is,

$$\delta W \;=\; \sum_{i}^{N} \left[\left(\mathbf{F}_{i\mathrm{e}} + \sum_{j\neq i} \mathbf{F}_{ij}\right) \cdot \delta\mathbf{r}_i \right] \;=\; 0\,. \tag{2.24}$$

The double sum involving the $\mathbf{F}_{ij}$ can now be manipulated similarly to what was done in the derivation of Eqs. (2.12) and (2.14) and can accordingly be

[‡]The word *virtual* here means "possible," and a virtual displacement is thus a possible displacement but not necessarily the actual one.

rewritten as

$$\sum_{i=1}^{N}\sum_{j=1}^{i-1}\mathbf{F}_{ij}\cdot\delta(\mathbf{r}_i-\mathbf{r}_j)\,. \tag{2.25}$$

The virtual work on the particle system can be therefore expressed as

$$\delta W \;=\; \delta W_{\text{ext}}+\delta W^{*}_{\text{int}}\,, \tag{2.26}$$

where the *external virtual work* is

$$\delta W_{\text{ext}} \;=\; \sum_{i}^{N}\mathbf{F}_{i\text{e}}\cdot\delta\mathbf{r}_i \tag{2.27}$$

and the *internal virtual work* is

$$\delta W^{*}_{\text{int}} \;=\; \sum_{i=1}^{N}\sum_{j=1}^{i-1}\mathbf{F}_{ij}\cdot\delta(\mathbf{r}_i-\mathbf{r}_j)\,. \tag{2.28}$$

The reason for the asterisk in the designation $\delta W^{*}_{\text{int}}$ is that in solid mechanics the convention is to define the internal virtual work as

$$\delta W_{\text{int}} \;=\; \sum_{i=1}^{N}\sum_{j=1}^{i-1}\mathbf{F}_{ji}\cdot\delta(\mathbf{r}_i-\mathbf{r}_j)\,, \tag{2.29}$$

that is (since $\mathbf{F}_{ji}=-\mathbf{F}_{ij}$), $\delta W_{\text{int}}=-\delta W^{*}_{\text{int}}$, and therefore the principle of virtual work takes the form

$$\delta W_{\text{ext}} \;=\; \delta W_{\text{int}}\,, \tag{2.30}$$

which will be used in later chapters. Eq. (2.30) states that for a system of particles that is in equilibrium, the virtual work done by the external forces equals the virtual work done by the internal forces.

For continuous bodies, in view of the extension discussed in Subsection 2.1.3, the equation for the external virtual work is

$$\delta W_{\text{ext}} \;=\; \sum_{i}\mathbf{F}_i\cdot\delta\mathbf{r}_i\,. \tag{2.31}$$

The internal virtual work δW_{int} depends on internal forces in the continuous body (to be discussed in Chap. 4) and will be treated in Chap. 5.

Example 2.1.1: Rigid particle system.
The rigidity of a particle system, as we have defined it earlier in this section, implies that $|\mathbf{r}_i-\mathbf{r}_j|$, for any pair of particles i and j, does not change. In other words, it is an internal constraint requiring that the virtual displacements satisfy $(\mathbf{r}_i-\mathbf{r}_j)\cdot\delta(\mathbf{r}_i-\mathbf{r}_j)=\mathbf{0}$. But since the interparticle forces $\mathbf{F}_{ij}$ are parallel to $\mathbf{r}_i-\mathbf{r}_j$, it follows that each member of the double sum in Eq. (2.28) must be zero, and hence in a rigid system the internal virtual work is identically zero. Consequently, for a rigid particle system in equilibrium,

$$\delta W \;=\; \delta W_{\text{ext}} \;=\; 0\,.$$

The preceding equation applies to any rigid body in equilibrium, with the external virtual work defined as in (2.31).

It is often convenient to specify the configuration of a body by means of a minimal set variables q_k that are not necessarily Cartesian coordinates; such variables are called *generalized coordinates* and may include, in particular, angles of rotation. The position of any particle is then given as $\mathbf{r}_i = \mathbf{r}_i(q_k)$. The notion of virtual displacement can be extended to these generalized coordinates, and if the similarly defined δq_k are likewise assumed to be infinitesimal, then the chain rule of differential calculus may be used to find the $\delta \mathbf{r}_i$, and the right-hand side of Eq. (2.31) becomes

$$\sum_i \mathbf{F}_i \cdot \sum_k \frac{\partial \mathbf{r}_i}{\partial q_k} \delta q_k = \sum_k \left(\sum_i \mathbf{F}_i \cdot \frac{\partial \mathbf{r}_i}{\partial q_k} \right) \delta q_k = \sum_k Q_k \delta q_k \,, \tag{2.32}$$

where Q_k is known as the *generalized force* conjugate to the generalized coordinate q_k. Thus, if a generalized coordinate represents a displacement (rotation), then the corresponding generalized force is the conjugate force (moment).

Exercises

2.1-1. Three particles are located on the vertices of an equilateral triangle. If $\mathbf{F}_{1e}$ is of known magnitude F and is directed along the line from particle 1 to particle 2, while $\mathbf{F}_{2e}$ is of unknown magnitude and its direction is perpendicular to that line, find $\mathbf{F}_{3e}$ (showing its direction on a sketch) so that equilibrium is satisfied.

2.1-2. If in the preceding exercise the force $\mathbf{F}_{2e}$ were directed along the line from particle 2 to particle 3, would the problem have a solution? Explain your answer.

2.1-3. Consider a system of four particles located at the vertices of a rectangle with sides $2a$ and a, as in the figure. Assume that the each particle i is subject to a central attractive force $F_{ij} = kd_{ij}$ due to the presence of particle $j(\neq i)$, where d_{ij} is the distance of the two particles and k is a constant. Sketch all forces acting on the four particles and determine the total external force F_{ie} acting on each particle in order for the system to be in equilibrium.

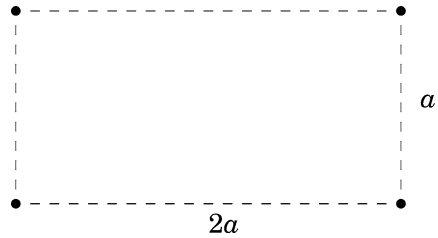

2.1-4. If a system of N particles is subject to central forces $\mathbf{F}_{ij}$ between each pair (i, j) of particles, show that

$$\sum_{i=1}^{N} \sum_{j=1}^{i-1} (\mathbf{r}_i - \mathbf{r}_j) \times \mathbf{F}_{ij} = \mathbf{0} .$$

2.1-5. Consider two particles i and j separated by distance r and define the function

$$U(r) = 4c \left[\left(\frac{a}{r} \right)^{12} - \left(\frac{a}{r} \right)^{6} \right] ,$$

where a and c are positive constants. Suppose that the equal-and-opposite forces developed between the two particles can be derived from the function $U(r)$, such that $\mathbf{F}_{ij} = \dfrac{\partial U}{\partial r} \mathbf{e}_{ij}$, where $\mathbf{e}_{ij}$ is a unit vector pointing from i to j. Plot the scalar value F_{ij} of $\mathbf{F}_{ij}$ as a function of r for nominal values $a = c = 1$ and comment on the dependence of F_{ij} on the value of r. Can you attach physical meaning to each of the two power terms in the definition of $U(r)$?

2.1-6. Consider the system of three particles shown in the figure. Each particle i is subjected to external forces F_i, $i = 1,2,3$. In addition, all particles are subjected to interaction forces. For instance, particle 1 is subjected to a force F_{12} due to its interaction with particle 2, etc., where interaction forces satisfy the condition $F_{ij} = F_{ji}$, $i \neq j$, $i,j = 1,2,3$.

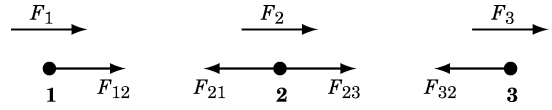

(a) If all the external forces are zero, show that the *system* of particles is always in equilibrium.

(b) If all the external forces are zero, what are the necessary and sufficient conditions for *each* particle to be in equilibrium?

(c) In the general case when the external forces are non-zero, express the interaction forces in terms of the external forces.

2.1-7. A person weighing 80 kg takes an elevator up 25 stories. If each story is 5 m height, determine the work (in J) done by the gravity force during this ride.

2.1-8. A particle traverses a semicircle of radius 5 ft, starting from the point shown in the figure. Define an angle θ that may be used to define the position of the particle on the semicircle. If there is a constant force $\mathbf{F} = 4\mathbf{i} + 3\mathbf{j}$ acting on the particle throughout its motion, plot the work done by the force as a function θ.

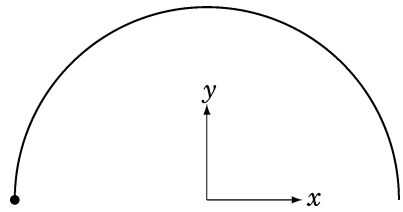

2.1-9. Assume, for simplicity, that the orbit of the earth around the sun is planar and ellipsoidal, with major axes of length 147 million km and 152 million km. Employing *Newton's law of universal gravitation*, the central force acting on the earth by the sun has magnitude

$$F = G\frac{m_s m_e}{d^2},$$

where $G = 6.6710^{-11}$ N(m/kg)^2 is the gravitational constant, $m_e = 5.9710^{24}$ kg is the mass of the earth, $m_s = 1.9910^{30}$ kg is the mass of the sun, and d is the distance between the centers of the two objects.

Estimate the work done by the sun's gravity force on the earth during one-quarter of the full trajectory, starting with the earth in the closest distance to the sun. Treat both objects as particles.

2.1-10. Consider the seesaw shown in the figure on the left below, assumed to be in equilibrium in the horizontal position. With the virtual displacement caused by the small rotation about the fulcrum shown in the figure on the right, use the principle of virtual work (treating the angle $\delta\theta$ as infinitesimal) to determine the equilibrium relation between F_1 and F_2.

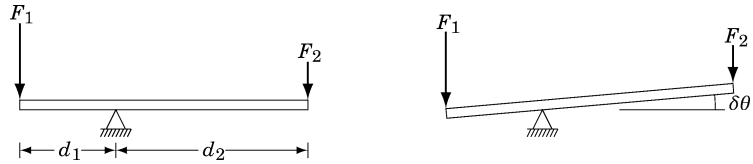

2.2 Equilibrium of Rigid Bodies in Two Dimensions

2.2.1 Introduction

When we refer to rigid bodies in solid mechanics, it is with the understanding that no real bodies are perfectly rigid. Indeed, the application of forces invariably causes some deformation, that is, changes in the distances between material points, which lead to changes in the shape and/or volume of the body). The deformation of a body will, in general, be different under various statically equivalent force systems, as exemplified in Fig. 1.26.

In many situations, however, the changes in overall geometry resulting from the deformation can be neglected. The body can then be, for the purposes of statics, idealized as rigid. These are the situations that will be studied in the remainder of this chapter, as well as in the following chapter.

2.2.2 Planar Force Systems

A system of forces $\mathbf{F}_i$ $(i = 1,2,\ldots,N)$ is called *planar* if the lines of action of all the forces lie in the same plane (that is, if all the forces are coplanar with one another). We consider here such a force system acting on a rigid body and we assume, without loss of generality, that the plane of the forces is the xy-plane. In this case, both the force vectors $\mathbf{F}_i$ and the position vectors $\mathbf{r}_i$ drawn from any point O in the xy-plane to any point on the line of action of any of the forces will have non-vanishing components only along the x- and y-axes, namely

$$\mathbf{F}_i = F_{ix}\mathbf{i} + F_{iy}\mathbf{j} \quad , \quad \mathbf{r}_i = x_i\mathbf{i} + y_i\mathbf{j} \, . \tag{2.33}$$

This means that the moment of the force $\mathbf{F}_i$ about the point O is

$$\mathbf{r}_i \times \mathbf{F}_i = (x_i F_{iy} - y_i F_{ix})\mathbf{k} = M_{iO}\mathbf{k} \, . \tag{2.34}$$

It is clear from (2.34) that the moment of $\mathbf{F}_i$ may have only one non-vanishing component, namely the one along the z-axis. Consequently, the six component equations constituted by Eqs. (2.18) and (2.19) reduce to only three:

$$\sum_{i=1}^{N} F_{ix} = 0 \quad , \quad \sum_{i=1}^{N} F_{iy} = 0 \quad , \quad \sum_{i=1}^{N} M_{iO} = 0 \, . \tag{2.35}$$

Note that the force equilibrium equations $(2.35)_{1,2}$ do not need to be written relative to the x- and y-axes, but may instead be written relative to any two axes, say a and b, as in Fig. 2.10a. This is, of course, because the vanishing of the components of $\mathbf{F}_i$ relative to any two axes in the xy-plane is equivalent to the vanishing of the vector $\mathbf{F}_i$ itself. Thus, Eqs. (2.35) may be written equivalently as

$$\sum_{i=1}^{N} F_{ia} = 0 \quad , \quad \sum_{i=1}^{N} F_{ib} = 0 \quad , \quad \sum_{i=1}^{N} M_{iO} = 0 \, . \tag{2.36}$$

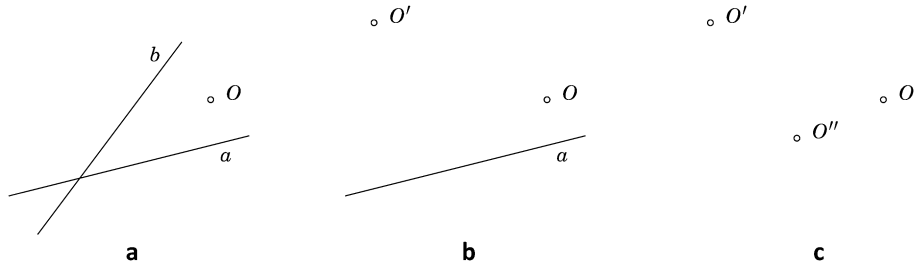

Figure 2.10. Three equivalent ways of writing the equilibrium equations in two dimensions

Another way of expressing planar force equilibrium is by means of the system of equations

$$\sum_{i=1}^{N} F_{ia} = 0 \quad , \quad \sum_{i=1}^{N} M_{iO} = 0 \quad , \quad \sum_{i=1}^{N} M_{iO'} = 0 \, , \tag{2.37}$$

which means that the component of the resultant force along any axis a is zero and the moments about two points O and O' in the xy-plane are also zero (see Fig. 2.10b). If the line OO' is not perpendicular to the a-axis, then we may establish the equivalence of Eqs. (2.36) and Eqs. (2.37) by showing that Eqs. (2.36) imply Eqs. (2.37), and vice-versa. To show the first, we assume that Eqs. (2.36) hold, implying that the force system is defined by a zero resultant force and zero moment about point O. Such a system clearly produces a zero moment about any other point (such as O') in the xy-plane, so that Eqs. (2.37) are satisfied. Conversely, if Eqs. (2.37) are assumed to hold, then Eq. $(2.37)_1$ immediately implies that the resultant force (if any) must be perpendicular to the a-axis. Eqs. $(2.37)_{2,3}$ further imply that the line of action of this resultant must pass through points O and O'. However, since OO' is assumed not to be perpendicular to the a-axis, this is possible only if the resultant force is zero, showing that (2.36) are satisfied. The sets of Eqs. (2.36) and (2.37) are consequently equivalent.

Yet another alternative set of equilibrium equations in two dimensions may be expressed as

$$\sum_{i=1}^{N} M_{iO} = 0 \quad , \quad \sum_{i=1}^{N} M_{iO'} = 0 \quad , \quad \sum_{i=1}^{N} M_{iO''} = 0 \, , \tag{2.38}$$

where the points O, O' and O'' are not on the same line, as shown in Fig. 2.10c. Again, arguing the equivalence of the sets of equations (2.36) and (2.38) entails establishing that the two sets imply each other. The derivation of (2.38) from (2.36) is trivial, as previously. That Eqs. (2.38) imply Eqs. (2.36) is established as follows: Eqs. $(2.38)_{1,2}$ imply that the line of action of the resultant force is defined by the points O and O', as argued earlier. However, since

O'' is not on the line defined by O and O', Eq. $(2.38)_3$ is only possible if the resultant force is equal to zero. Therefore, the equilibrium equations (2.36) and (2.38) are also equivalent.

The equilibrium equations are often written without any explicit reference to the points of application of the forces or moments; thus, for example, we write Eqs. (2.35) more succinctly as

$$\sum F_x = 0 \quad , \quad \sum F_y = 0 \quad , \quad \sum M_O = 0 \, . \tag{2.39}$$

Example 2.2.1: Square block with four forces.
Consider a unit square block subject to the four forces of equal magnitude F depicted in Fig. 2.11a.

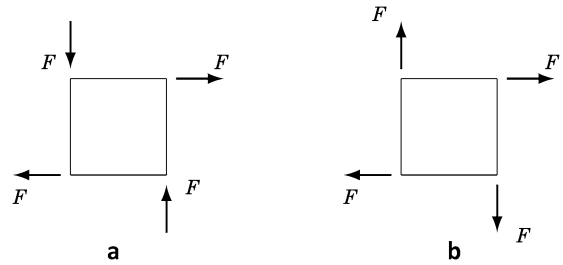

Figure 2.11. Unit square block under the influence of four forces

That this block is in equilibrium may be established by taking the sum of forces in the horizontal and vertical direction, as well as the sum of moments about any of the four vertices, according to (2.35) or (2.36). Alternatively, we may sum the forces in the horizontal direction, and also sum the moments about the top-left and bottom-right points (but not the top-left and top-right or the bottom-left and bottom-right points!), as stipulated by (2.37). Likewise, equilibrium may be established by taking moments about any three of the four vertices of the block, which corresponds to (2.38). Other points than the vertices may be used as well for taking moments. However, given that two of the four forces in this example pass from each of the vertices, the calculation of moments is simplified by taking moments about vertices.

The block in Fig. 2.11b is in force equilibrium, but not in moment equilibrium. This is easily inferred by noting that the two couples generated by the pairs of horizontal and vertical forces have the same sense. The same conclusion is reached by taking moments about any of the vertices. Interestingly, if the size of the block shrinks to zero (which is tantamount to the block becoming a particle), moment equilibrium plays no role in the equilibrium of the body. This is consistent with the observation in Sect. 2.1.3 about the independence of force and moment equilibrium in continuous bodies but not in particles.

2.2.3 Two-Force and Three-Force Bodies

A simple case of a planar force system occurs when there are only two non-zero forces $\mathbf{F}_1$ and $\mathbf{F}_2$ acting on a rigid body. Such a *two-force body* is shown in Fig. 2.12a. For force equilibrium, the two forces must be equal and opposite, and therefore parallel, but for moment equilibrium they must be collinear, since otherwise they would form a couple. In mathematical terms, if $\mathbf{F}_1$ and $\mathbf{F}_2$ are the two forces, then force equilibrium requires that

$$\mathbf{F}_1 + \mathbf{F}_2 = \mathbf{0}\,, \tag{2.40}$$

while moment equilibrium relative to any point O on the plane requires that

$$\mathbf{r}_1 \times \mathbf{F}_1 + \mathbf{r}_2 \times \mathbf{F}_2 = \mathbf{0}\,, \tag{2.41}$$

where $\mathbf{r}_1$, $\mathbf{r}_2$ are respectively drawn to the lines of action of $\mathbf{F}_1$ and $\mathbf{F}_2$ from any point. Eqs. (2.40) and (2.41) guarantee that the forces $\mathbf{F}_1$ and $\mathbf{F}_2$ are equal and opposite to each other, as well as collinear. Indeed, (2.40) directly implies that the forces are equal and opposite, therefore (2.41) necessitates that they form a zero force couple, hence they are also collinear.

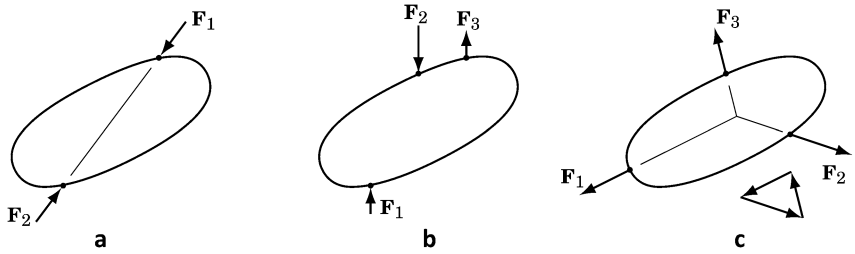

Figure 2.12. Two-force and three-force bodies: (**a**) two forces, (**b**) three parallel forces, (**c**) three concurrent forces

Almost as simple is the case of a *three-force body*, such as those shown in Fig. 2.12bc. Here, each of the three non-zero forces must be equal and opposite to the resultant of the other two, since force equilibrium and property (1.6)(b) (page 15) imply that

$$(\mathbf{F}_1 + \mathbf{F}_2) + \mathbf{F}_3 = (\mathbf{F}_2 + \mathbf{F}_3) + \mathbf{F}_1 = (\mathbf{F}_3 + \mathbf{F}_1) + \mathbf{F}_2 = \mathbf{0}\,. \tag{2.42}$$

Furthermore, each of the forces must be collinear with the resultant of the other two, since (2.42), property (1.10)(c) (page 17) and moment equilibrium about any point implies that

$$\begin{aligned} \mathbf{r}_1 \times \mathbf{F}_1 + \mathbf{r}_2 \times \mathbf{F}_2 + \mathbf{r}_3 \times \mathbf{F}_3 &= \mathbf{r}_1 \times \mathbf{F}_1 + \mathbf{r}_2 \times \mathbf{F}_2 + \mathbf{r}_3 \times (-\mathbf{F}_1 - \mathbf{F}_2) \\ &= (\mathbf{r}_1 - \mathbf{r}_3) \times \mathbf{F}_1 + (\mathbf{r}_2 - \mathbf{r}_3) \times \mathbf{F}_2 = \mathbf{0}\,. \end{aligned} \tag{2.43}$$

This means that the moment of any two of the forces (here, $\mathbf{F}_1$ and $\mathbf{F}_2$) about any point on the line of action of the third (here, $\mathbf{F}_3$) is equal to zero. If two of the forces are parallel, then the third must also parallel to them, as shown in Fig. 2.12b. On the other hand, if two of the forces are concurrent, then the third must be concurrent with them (otherwise, it would form a couple with the resultant of the first two), as shown in Fig. 2.12c, with the triangular force polygon shown on the side. The parallel case may, in fact, be regarded as the limit of the concurrent case as the point of concurrency recedes to infinity.

2.2.4 Degrees of Freedom and Constraints

Fixing the position of a rigid body in a plane requires the specification of three independent geometric quantities. These could be, for example, the x- and y-coordinates of one point (say 1) and either the x- or the y-coordinate of another point (say 2), as in Fig. 2.13a. The first two quantities obviously specify the position of point 1. Then, the third quantity fixes the position of point 2, since, due to rigidity, the distance d_{12} between these two points remains constant and equal to $\sqrt{(x_2-x_1)^2+(y_2-y_1)^2}$, so that y_2 can be derived if x_2 is given, and vice versa.

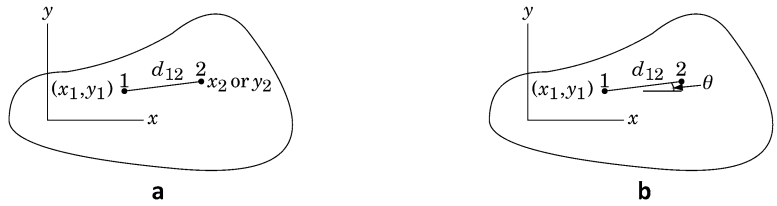

Figure 2.13. Fixing the position of a rigid body in a plane

Alternatively, the third quantity can be the angle subtended by a line between the points, as in Fig. 2.13b. If this angle (with respect to the x-axis) is θ, then $x_2 = x_1 + d_{12}\cos\theta$ and $y_2 = y_1 + d_{12}\sin\theta$. The position of any other point (say 3) is now also fixed due to triangulation, because the constancy of its distances d_{13} and d_{23} from points 1 and 2 is sufficient to fix it in place.

A rigid body confined to planar motion can therefore be said to have three *degrees of freedom* (abbreviated as *dof*), and to completely fix it in space three independent *external constraints* are necessary. That is, the body has to be connected to a fixed frame* by means of external *supports* that prevent changes in three independent kinematic quantities. Supports exert forces or moments (depending on whether what is prevented is a translation or a rotation) on the body; such forces and moments are called *reactions*. These are

*By a *fixed frame* we mean a combination of rigid bodies whose position in space remains unchanged.

conjugate (as defined in Sect. 2.1) to the translations or rotations that they prevent.

One possibility for the rigid body to be fixed is by three external supports, each of which prevents translation in one direction. Examples of such 1-dof supports are shown in Fig. 2.14.

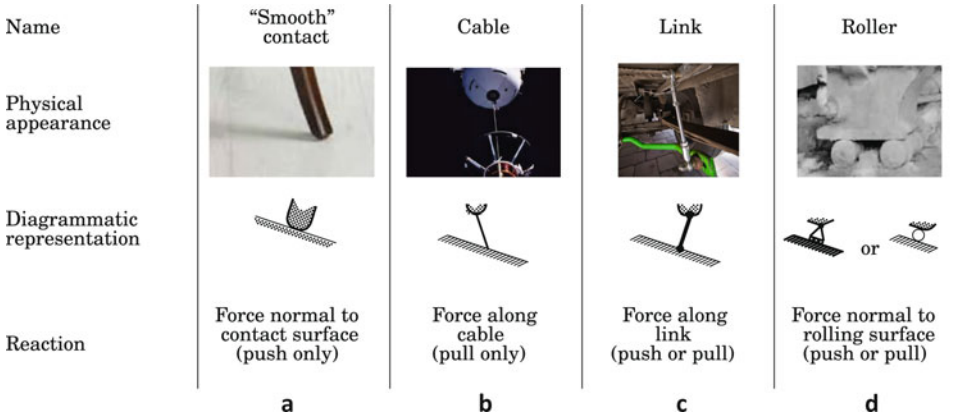

Figure 2.14. 1-dof constraints

Note that the cable and link of Figs. 2.14b and 2.14c, respectively, are assumed to be weightless, so that they act as two-force bodies. Note further that the roller support of Fig. 2.14d, while shown as though it rolled on only one surface (and therefore could exert only a push force), is conventionally assumed to act as if it rolled between two parallel surfaces and therefore the reaction force can be a push or a pull.

A set of external supports that prevents all rigid motion in the plane is *proper*, otherwise it is *improper*. Examples of proper and improper supports are shown in Fig. 2.16(a-c) and 2.16(d-f), respectively. A set of three 1-dof supports is proper if the lines of action of the reaction forces are not concurrent, as in Fig. 2.16b. If the lines of action are concurrent, then the supports are improper, because, in this case, rotation about the point of concurrency is, at least initially, not prevented (this is the case with the body shown in Fig. 2.16e). The same conclusion applies to the case of the three parallel reaction forces in Fig. 2.16d, since now translation perpendicular to the reactions is not prevented. Similarly, the vertical translation of the body in Fig. 2.16f is unrestrained, as neither of the two supports is resisting such motion.

Another possibility of fixing a rigid body in the plane is a combination of a 1-dof support with a 2-dof support, which may prevent either translation in all directions (such as a "rough"[†] contact support, Fig. 2.15a, or a *pin* or *hinge*

[†]The reason for the quotes around "rough" is explained in Sect. 2.2.5. This constraint is effective only if the normal component of the contact force is a push.

support, Fig. 2.15b); or else one translation component and rotation (*guided* support, Fig. 2.15d, where the previous remarks on the two-way nature of the roller force apply as well). Fig. 2.16b,c illustrates two examples of bodies that are held in place by such a combination of supports.

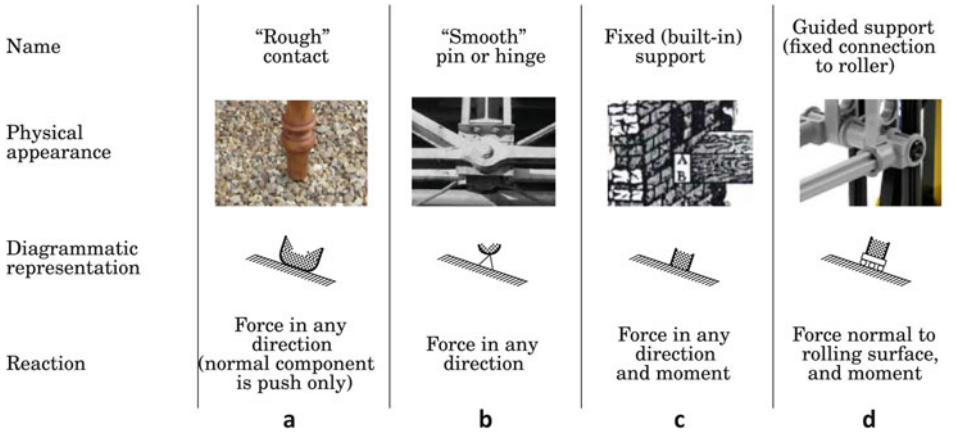

Figure 2.15. Two-dimensional 2-dof and 3-dof constraints

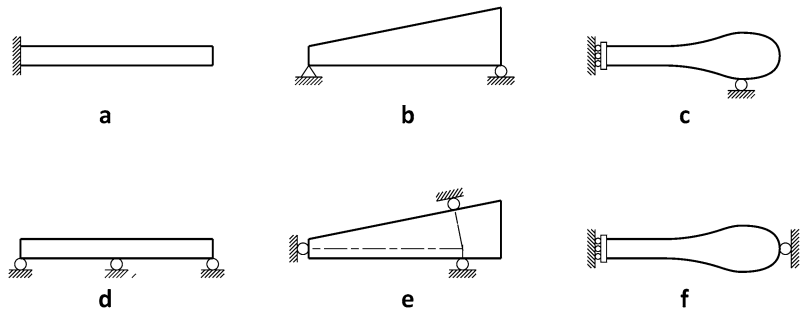

Figure 2.16. Properly (**a**–**c**) and improperly (**d**–**f**) constrained rigid bodies in two dimensions

Yet another possibility is a single support (called a *fixed* or *built-in* support) that prevents translation (in any direction) and rotation at one point; it is shown in Fig. 2.15c and used in properly supporting the body in Fig. 2.16a.

A body held in place by a fixed support, as in Fig. 2.16a, is said to be *cantilevered*. A body supported by a hinge and a roller, as in Fig. 2.16b, is generally known as *simply supported*. If the roller is moved inward from the end, then such a body is said to have an *overhang*, as in Fig. 2.17a, but if the overhang composes most of the body's span then it is also thought of as cantilevered, as in Fig. 2.17b.

Figure 2.17. Simply supported bodies with overhang

A system consisting of a body with the *minimum* number of proper supports is called *statically determinate*, meaning that the three equilibrium equations (2.35) (or any of their equivalents) suffice to find all the unknown reactions. It is easy to see that the systems in Fig. 2.16a–c are statically determinate.

A body may, of course, be held in place by more than the minimum supports necessary for proper constraint, in which case not only are the supports are proper, but the body is also *overconstrained*. Here, in general, the three equilibrium equations are not sufficient to determine the (four or more) unknown reactions. In this case, the system is said to be *statically indeterminate*. Examples of overconstrained bodies are shown in Fig. 2.18.

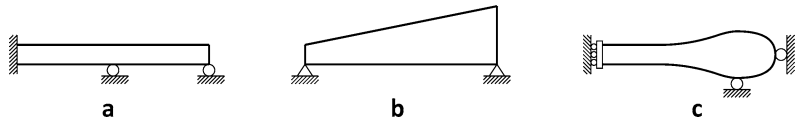

Figure 2.18. Examples of overconstrained bodies

Conversely, a body can be *underconstrained* if it does not have sufficient external supports for proper constraint, or else if, while properly constrained in the exterior, it has one or more *internal degrees of freedom*, such as might be represented by an internal hinge, that allow all or part of it to move, as in Fig. 2.19. In the latter case, the body is referred to as a *mechanism*.

Figure 2.19. Examples of mechanisms

A body that is overconstrained may be transformed into a statically determinate system by means of internal degrees of freedom, as, for example, the *three-hinged* (or *three-pinned*) *arch* shown in Fig. 2.20a. The analysis of such

systems will be undertaken in Sect. 2.4. However, if in the arch of Fig. 2.20a either one of the support hinges were replaced by a roller, the arch would become a mechanism and collapse (say, under its own weight), as in Fig. 2.20b.

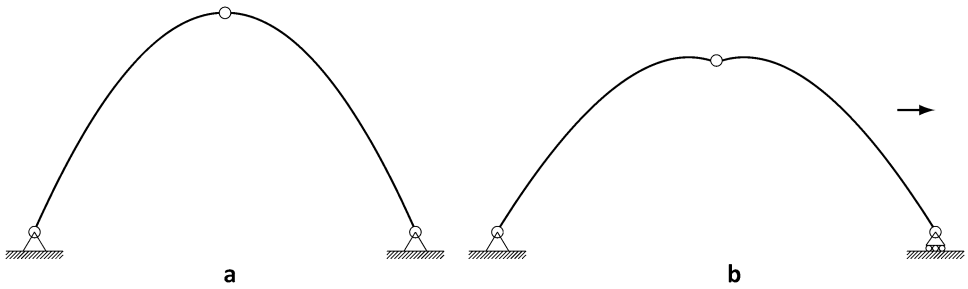

Figure 2.20. Three-hinged (three-pinned) arch: (**a**) statically determinate, (**b**) collapsing

It is also possible for a body to be overconstrained with respect to some degree(s) of freedom (and hence statically indeterminate) and underconstrained with respect to others. A simple example is seen in Fig. 2.21, where the body is overconstrained with respect to vertical translation with four reaction forces to be determined by two equilibrium equations, while being clearly underconstrained (actually, unconstrained) with respect to horizontal translation.

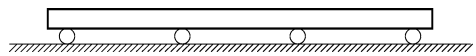

Figure 2.21. Example of a body that is both overconstrained and underconstrained

2.2.5 Friction

Contacts or connections are commonly referred to as "smooth" and "rough," indicating, respectively, the absence and presence of *friction*. Friction is the resistance to motion that is generated when one body slides or tends to slide past another under the influence of some external loading. We consider here only *dry friction*, that is friction between solids, as distinct from *wet* or *fluid friction*, which occurs between layers of fluid or between a solid and a fluid. We put the conventional terms "smooth" and "rough" in quotation marks because, in reality, friction increases both when the surfaces are very rough *and* when they are very smooth. The reason is that, generally, on very rough surfaces the asperities (small bumps in the surface) interfere with the sliding

motion and tend to lock the surfaces in place. With very smooth surfaces, on the other hand, the effective area of contact is larger, tending to increase friction. Very smooth surfaces are also more sensitive to chemical forces that develop between them and may resist the sliding motion (such forces increase as the distance between particles from the two surfaces becomes smaller). But the use of the terms *rough* and *smooth*, while frowned on by tribologists[‡] for the reasons just discussed, is still conventional among engineers.

In the case of contact with friction, as in Fig. 2.15a, the tangential part T of the contact force is the *frictional* force, which resists sliding between the surfaces in contact. Its direction, on each surface, is consequently opposed to the direction of potential sliding motion, as in Fig. 2.22.

In accordance with *Coulomb's law*[§]—also known as the *Amontons-Coulomb law*[¶]—the magnitude of the frictional force at rest cannot exceed that of the normal component (which can only be a push, as shown in Fig. 2.22), denoted N, multiplied by a certain positive number known as the *coef-*

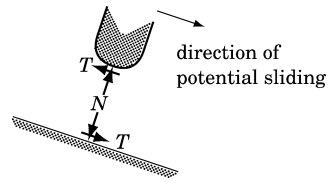

Figure 2.22. Contact forces in Coulomb's law

ficient of static friction, denoted μ_s. The value of this coefficient depends on the physical characteristics of the two surfaces in contact. Coulomb's law is expressed mathematically as

$$T \leq \mu_s N \, . \tag{2.44}$$

It is important to emphasize here that Coulomb's law specifies only the maximum possible friction force (equal to $\mu_s N$). Frictional forces of smaller magnitude are entirely possible and may apply to the body when it is in equilibriumIn this case, the frictional force cannot be determined from Coulomb's law. Rather, it may be calculated from the equilibrium equations.

Once static friction is overcome and the contacting surfaces are in relative motion, the tangential force resisting the motion is equal to $\mu_k N$, where the positive scalar μ_k is the so-called *coefficient of kinetic friction*, usually smaller than μ_s. If the body is in equilibrium with this force, then the motion will proceed at constant speed. Otherwise acceleration will occur.

[‡] *Tribology* is the discipline concerned with the study of friction, lubrication and wear.

[§] Charles-Augustin de Coulomb (1736–1806) was a French physicist.

[¶] Guillaume Amontons (1663–1705) was a French scientist who formulated the law of friction well before Coulomb, though the principle was already known to Leonardo da Vinci (1452–1519).

If friction is present in a hinge or pin support, there is resistance to rotation resulting in a moment reaction, and, so long as the friction is not overcome, the support will act like a fixed (built-in) one.

Some representative values of the coefficients of static and kinetic friction are given in Table 2.1. These values depend crucially on the conditions of experiments from which they were estimated and should be considered as coarsely approximate.

interface	μ_s	μ_k
aluminum-steel	0.60	0.45
copper-steel	0.55	0.35
glass-glass	0.90	0.40
wood-wood	0.60	0.50
rubber-concrete	1.0	0.80
ice-ice	0.10	0.030

Table 2.1. Typical values of the static and kinetic coefficients of dry friction for selected material interfaces

2.2.6 Free-Body Diagrams

Of the forces appearing in the equilibrium equations for a rigid body, some are specified at the outset; these forces (and, possibly, couples) are known as *loads*. The support reactions (also forces and/or couples), on the other hand, are not known to begin with, and it is their determination that constitutes the solution of the equilibrium equations. The remainder of this section will deal with the determination of the reactions in statically determinate rigid bodies under planar force systems.

The procedure consists of four steps. The first is the drawing of a schematic diagram showing a sketch of the body, its supports, and the loads acting on it. In the next step, the supports are replaced by their reactions, resulting in another diagram known as a *free-body diagram*. The drawing of a correct free-body diagram is a crucial step in solving a wide array of problems in solid mechanics. (Free-body diagrams will be discussed in greater generality in Sect. 2.4.)

The next step is the formulation of three independent equilibrium equations, each containing one or more of the reactions. Finally, these equations are solved for the reactions.

In practice, we observe the following conventions:

1. When the number of points at which loads and reactions are present is small, it is more common to designate them by letters $A, B, C, \ldots$ than by numbers.

2. The letter designating a point, when equipped with a subscript such as x or y, is also used to designate the component of a force reaction at the point.

3. The assumed sense of a reaction component need not coincide with the positive direction of the corresponding coordinate, especially if intuition indicates that it will be the opposite. If the initial guess is wrong, the value of the component will turn out to be negative, which is entirely acceptable.

Lastly, the equilibrium equations are solved for the unknown forces and/or moments.

The following examples will illustrate these usages.

Example 2.2.2: Particles connected by a spring.
We consider, first, the case of an elastic spring connecting two particles, as in Fig. 2.23a. Suppose that the spring is stretched by equal and opposite forces **F**, as in Fig. 2.23b, and examine the three elements of the system, namely the two particles and the spring itself, assuming that the system is in equilibrium. It is important to note that what constitutes an internal or external force depends crucially on the particular element under consideration. For instance, both forces on each of the two particles are external to them, while only one of them (the applied force **F**) is external to the full spring-particle system, as shown in Fig. 2.23c. Another critical observation is that drawing the forces on individual elements of a system entails the application of the action-reaction law discussed in Sect. 2.1.

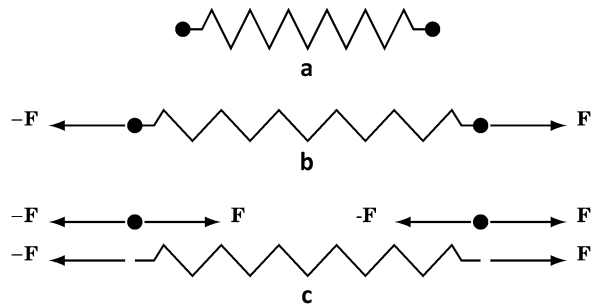

Figure 2.23. Spring connecting two masses: (**a**) spring with two masses under no force, (**b**) free-body diagram of mass-spring-mass system, (**c**) free-body diagrams of the three elements of the system

Example 2.2.3: Three-hinged arch.
For the three-hinged arch of Fig. 2.20a, however it may be loaded, each of the two hinge supports has two reactions and therefore the three global equilibrium

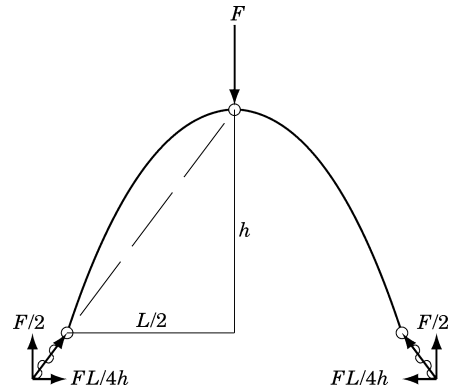

Figure 2.24. Support reactions on an apex-loaded three-hinged arch

equations are not sufficient to determine them. But since the pin joint at the apex is frictionless, only a force—and no moment—can be transmitted there, so that if the arch is sectioned at the pin (this is an example of the *method of sections*, which will be discussed in Sect. 2.4), the resultant moment about the pin *on each member* must be zero. This requirement provides an additional equilibrium equation.

In the simplest case where the arch is symmetric and the only load is a downward force F acting at the pin, this equilibrium is equivalent to each member being a two-force body, so that the support reactions must be directed toward the pin. By symmetry, the vertical components of the reactions are $F/2$, and therefore the (equal and opposite) horizontal components must, by similar triangles as seen in Fig. 2.24, have the value $FL/4h$ if L is the *span* and h is the *rise* of the arch.

In the more general case where forces act on each of the two members comprising the arch, one may directly resort to sectioning the arch and writing the equilibrium equations for each of the members. For instance, consider again the three-pin arch of Figure 2.20a, where the left member is now subjected to a horizontal force F_1 at a height h_1 from the left pin, while the right member is subjected to a vertical F_2 at a distance $L/4$ from the right pin, as in Figure 2.25a. In this case, we may write the horizontal and vertical force equilibrium equations for the left member, seen in Figure 2.25b, as

$$A_x + C_x + F_1 = 0 \quad , \quad A_y + C_y = 0 \, ,$$

and the moment equilibrium about the left pin at A as

$$-C_x h + C_y L/2 - F_1 h_1 = 0 \, .$$

The corresponding equations for the right member, seen in Figure 2.25c, may analogously be written as

$$B_x - C_x = 0 \quad , \quad B_y - C_y - F_2 = 0$$

and

$$C_x h + C_y L/2 + F_2 L/4 = 0 \, ,$$

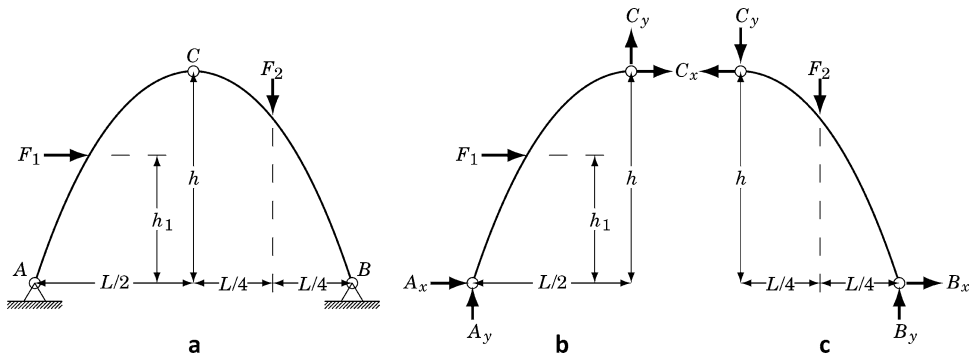

Figure 2.25. Analysis of an asymmetrically loaded three-hinged arch: (**a**) loading, (**b–c**) free-body diagrams of left and right members

where, in the last equations, moments are taken about the pin at B. The preceding six equations can be easily solved for the six unknowns A_x, A_y, B_x, B_y, C_x and C_y. It is important to observe in this example that the forces acting on the two members due to the pin at C are equal and opposite, which is an immediate consequence of Newton's Third Law.

Example 2.2.4: Flat contact with frictional sliding.
To appreciate the meaning of the inequality (2.44) governing friction, we consider a rigid body of weight W which is in flat contact with a rigid foundation and is pulled by a force F passing through its center of gravity, as in Fig. 2.26a, with the free-body diagram shown in Fig. 2.26b. When the frictional force is be-

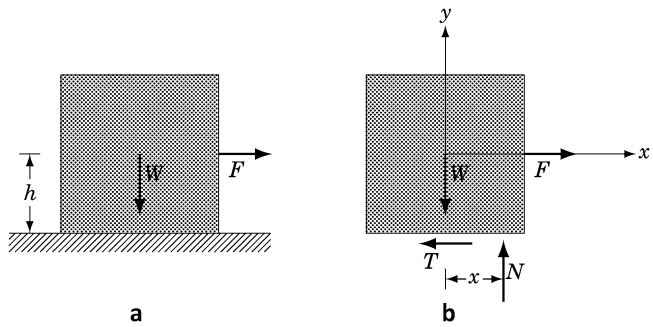

Figure 2.26. Flat contact between a rigid body and a foundation: (**a**) schematic diagram, (**b**) free-body diagram

low the maximum value $\mu_s N$ stipulated by inequality (2.44), the body remains in equilibrium. In this case, the equilibrium equations (2.35) lead to

$$F = T \quad , \quad W = N \quad , \quad \bar{x} = \frac{F}{N} h \, ,$$

that is, the frictional force T is equal and opposite to the pull force F, the weight of the body is balanced by the resultant reaction N normal to the bottom surface

of the body, and the reaction N is acting at a point with coordinate $\bar{x}$, such that (W,N) form a force couple that balances the force couple of (F,T). (It is assumed that the point of action of N is within the contact area, that is, that $\bar{x} < a$; otherwise the body will tip.)

In the limiting case of impending sliding, the pulling force F becomes equal to the maximum frictional force $T_{max} = \mu_s N$, so that Coulomb's law holds as an equality:

$$F = T_{max} = \mu_s N \, .$$

Now, the resultant $\mathbf{R}_s$ of the normal and tangential reactions on the frictional interface forms an angle ϕ_s with the normal to the foundation, such that

$$\tan\phi_s = \frac{T}{N} = \frac{\mu_s N}{N} = \mu_s \, .$$

The angle $\phi_s = \tan^{-1}\mu_s$ is referred to as the *angle of static friction*.

Once sliding begins, the frictional force becomes equal to $\mu_k N$ and the resultant reaction forms an *angle of kinetic friction* equal to $\phi_k = \tan^{-1}\mu_k$.

Example 2.2.5: Ladder.
Another example involving the just-discussed concept of friction is that of a person standing on a ladder, assumed to be in "smooth" contact with the wall and in "rough" contact with the ground, as shown schematically in Fig. 2.27a.

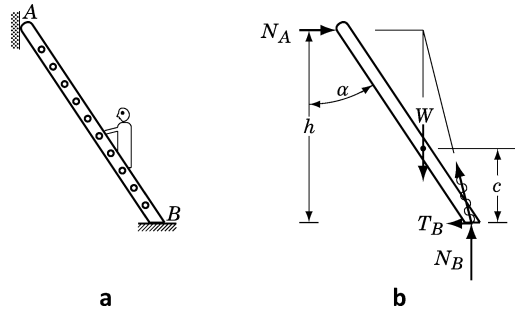

Figure 2.27. Person on a ladder: (**a**) schematic diagram, (**b**) free-body diagram

In the free-body diagram of Fig. 2.27b, W is the resultant of the weights of the person and the ladder. (The diagram also shows the concurrency of this resultant with those of the two contact forces.) It can be readily seen that the force system acting on the body consists of two equal and opposite vertical forces, $N_B = W$, and two equal and opposite horizontal forces, $N_A = T_B$. For moment equilibrium, then,

$$Wc\tan\alpha = T_B h \, ,$$

and therefore

$$T_B = W\frac{c}{h}\tan\alpha \, .$$

Since, however, $T_B \le \mu_s N_B = \mu_s W$, it follows that, for stability,

$$\frac{c}{h}\tan\alpha \le \mu_s \, .$$

Example 2.2.6: Lever.
Let us consider next the hinged rod shown in Fig. 2.28. Here, a force F is applied

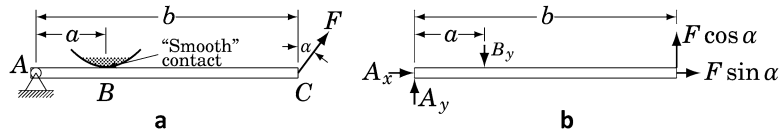

Figure 2.28. Hinged lever: (**a**) schematic diagram, (**b**) free-body diagram

at one end C of a rigid bar that is hinged at the other end A, with the intention of transmitting a larger force to a rigid body (potentially so as to lift it) in "smooth" contact with the bar at point B.

The equilibrium equations (2.35) applied to the forces shown in the free-body diagram (note that B_y is assumed to be downward, as expected on physical grounds, and not necessarily in accord with the usual convention for positive and negative forces) are

$$A_x + F\sin\alpha = 0 \quad , \quad A_y - B_y + F\cos\alpha = 0 \quad , \quad -aB_y + bF\cos\alpha = 0 \, ,$$

where the third equation represents moment equilibrium about point A. Note that this equation can be solved directly for B_y (while the first equation yields A_x); once B_y is determined it can be inserted into the second equation to determine A_y. On the other hand, the second and third equation can be combined linearly (by multiplying the former by a and subtracting it from the latter) to yield

$$-aA_y + (b-a)F\cos\alpha = 0 \, ,$$

but this is none other than moment equilibrium about B, illustrating the replacement of one of the force equilibrium equations (here, the force equilibrium equation in the y-direction) by another moment equilibrium equation, as previously discussed in Sect. 2.2.2. We now have three equations, each of which contains one and only one unknown reaction.

Figure 2.29. Practical lever problem

In practice the problem may be framed differently: the weight of the body to be lifted may be specified (say W) and what is to be determined is the magnitude of the lifting force F, which may be applied over a pulley, as shown in Fig. 2.29. It will be shown later that a force applied by means of a weightless cable over a frictionless pulley remains constant in magnitude.

Example 2.2.7: Lever-based exercise machine.
In the exercise machine shown schematically in Fig. 2.30, the lever, balanced on the fulcrum A, is pressed down by the force F in order to raise the roller B supporting the weight stack which offers the resistance R. Since B can move

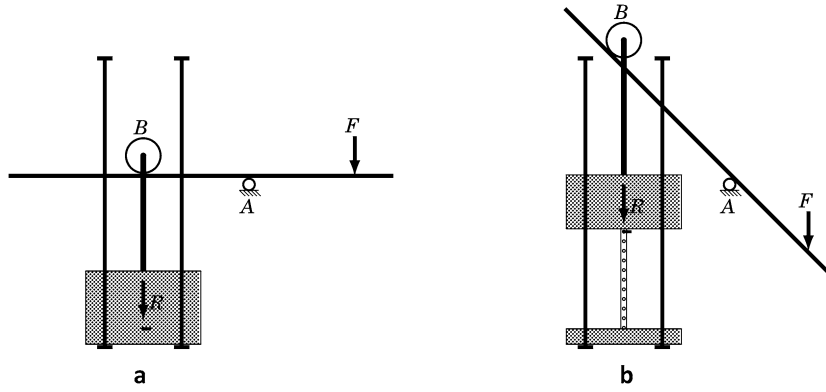

Figure 2.30. Lever-based exercise machine: (a) initial position, (b) position with weights raised

only vertically, the moment arm of the resisting force R remains constant, while that of the applied motive force F (necessarily downward) decreases, so that this force increases progressively through the movement.

Example 2.2.8: Pulley-based exercise machine.
In the machine shown schematically in Fig. 2.31a, used for leg extension and leg curl, the motive force F is applied normally (by means of a roller, or possibly a low-friction pad) to a crank attached rigidly (though with variable attachment points) to a wheel. As the wheel turns, it pulls a cable that is strung over some pulleys and raises the weight stack. In this machine, the moment arm of both the applied force F and the resisting force R remains constant through the movement.

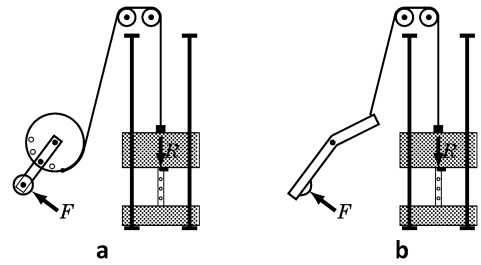

Figure 2.31. Pulley-based exercise machine

In the machine shown in Fig. 2.31b, a (possibly bent) hinged bar takes the place of the crank and wheel. Here, the moment arm of the resisting force is variable.

Example 2.2.9: Simply supported beam.
As was noted above, a body is called simply supported if the supports consist of one pin or hinge and one roller or "smooth" contact (the orientation of the contact surface being such that at equilibrium the force is a push). A straight bar that is intended to carry primarily transverse forces is called a *beam*. A simply supported beam, where the load F is the resultant of any loads that may be acting on the beam, is shown in Fig. 2.32a, with the free-body diagram shown in Fig. 2.32b.

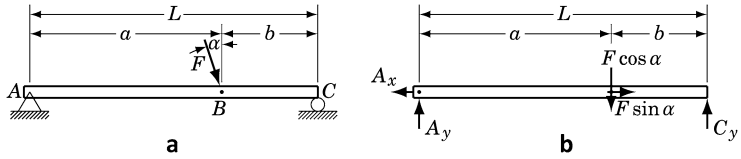

Figure 2.32. Simply supported beam: (**a**) schematic diagram, (**b**) free-body diagram

Equilibrium of forces in the x-direction immediately leads to $A_x = F\sin\alpha$. A_y and C_y can be solved from uncoupled equations if these represent moment equilibrium about C and A, respectively:

$$\sum M_C = bF\cos\alpha - LA_y = 0 \Rightarrow A_y = \frac{b}{L}F\cos\alpha$$

and

$$\sum M_A = -aF\cos\alpha + LC_y = 0 \Rightarrow C_y = \frac{a}{L}F\cos\alpha\,.$$

Equilibrium of forces in the y-direction can now be used as a check on the results:

$$A_y + C_y = \frac{a+b}{L}F\cos\alpha = F\cos\alpha\,,$$

since $a+b=L$.

It is important to point out that the use of the resultant in place of the actual loads acting on the beam is sufficient for the purpose of calculating support reactions, but not if one desires more information, as will be discussed in Sect. 2.4.

Exercises

2.2-1. Let forces $\mathbf{F}_1 = 2\mathbf{i} + \mathbf{j}$ and $\mathbf{F}_2 = -\mathbf{i} + 3\mathbf{j}$ act on a rigid body at points with coordinates $(2,0)$ and $(1,1)$, respectively. Find a third force $\mathbf{F}_3$ and its line of action such that the three-force system be in equilibrium.

2.2-2. Let forces $\mathbf{F}_1 = 2\mathbf{j}$ and $\mathbf{F}_2 = -5\mathbf{j}$ act on a rigid body at points with coordinates $(0,0)$ and $(1,-1)$. What is the line of action of a third force $\mathbf{F}_3$, such that the three forces be in equilibrium? How would your answer change if the rigid body is additionally subject to a moment $\mathbf{M} = 5\mathbf{k}$?

2.2-3. Consider a two-dimensional rigid body in the shape of a unit square whose vertices A, B, C, and D have coordinates $(0,0)$, $(1,0)$, $(1,1)$, and $(0,1)$, respectively. Suppose that there are forces acting only at the four vertices of the body, such that $\mathbf{F}_A = \mathbf{i} + \mathbf{j}$, $\mathbf{F}_B = \mathbf{i} + 4\mathbf{j}$, $\mathbf{F}_C = -2\mathbf{i} + F_{Cy}\mathbf{j}$ and $\mathbf{F}_D = F_{Dx}\mathbf{i} + F_{Dy}\mathbf{j}$. Determine the components F_{Cy}, F_{Dx} and F_{Dy}, such that the body remain in equilibrium. Obtain the solution three times using a suitable set of equilibrium equations in the form (2.35), (2.37), and (2.38).

2.2-4. Draw the free-body diagramfor the cantilevered body shown in the figure and use the equilibrium equations to find the reactions.

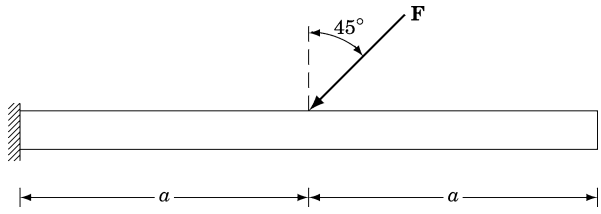

2.2-5. Draw the free-body diagram for the system shown in the figure, as well as for each of its three constituent parts (two cables and the box). Determine the forces on each cable assuming that the box weighs 600 kips.

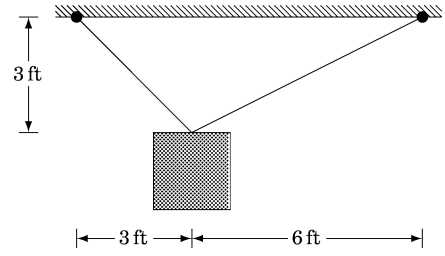

2.2-6. Let three rectangular objects of uniform density have width a and be stacked on top of each other as in the figure. If each object has weight W, find the maximum allowable offset b of the top object relative to the

bottom object before the system is unable to remain in an equilibrium state.

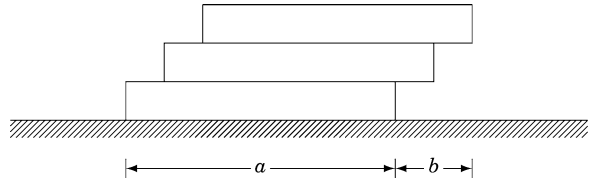

2.2-7. Find the solution to the problem in Exercise **2.2-6** for the case of n objects, where n is any positive integer.

2.2-8. A rectangular block with a mass of 100 kg is resting on an inclined surface, as in the figure. If the static coefficient of friction between the block and the surface is $\mu_s = 0.25$, find the magnitude F of the horizontal force needed to prevent its downward sliding. Also, find the magnitude F of the horizontal force needed to initiate an upward sliding of the block. If the kinetic coefficient of friction is $\mu_k = 0.2$, find the magnitude of the force F needed to sustain the upward sliding motion of the block under constant velocity.

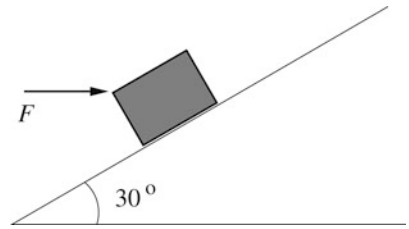

2.2-9. A homogeneous rigid rod of weight W and length L is in equilibrium on the frictional surface at point A and on the frictionless surface at point B, as shown in the figure.

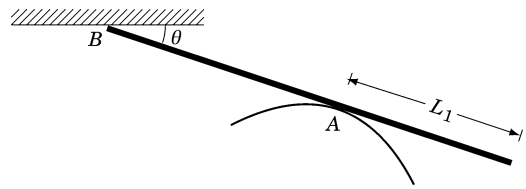

(a) Draw the free-body diagram of the rod.

(b) Find the reactions at points A and B. What should be the relation between the length L and the distance L_1 between the right end of the rod and point A to maintain equilibrium?

(c) If the static coefficient of friction between the rod and the surface at A is μ_s, what is the critical angle θ_{cr} at which the rod will start sliding?

2.2-10. The bar shown in the figure below is supported by a roller at point A and a rigid link at point B, and rests on a frictional surface at point C. The bar is subjected to the external force and moment shown in the figure, as well as to its own weight $W = 10\,\text{kN}$.

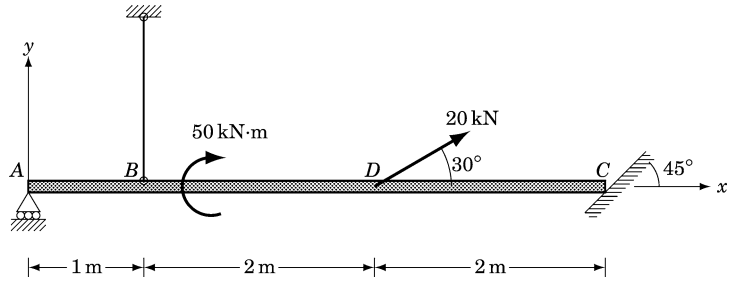

(a) Draw the free-body diagram of the bar showing all external forces.

(b) If friction is neglected, determine the magnitude of the force exerted on the bar by the rigid link element.

(c) If friction is included and sliding at point C is imminent, determine again the force exerted on the bar by the truss element. Assume that the static friction coefficient is $\mu_s = 0.5$.

2.2-11. Find the magnitude M of the maximum moment that may be applied on the cylinder of mass m and radius r shown in the figure without inducing sliding. Let the static coefficient of friction be μ_s on both frictional interfaces.

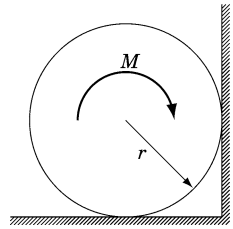

How would the answer to this problem change if the sense of the moment is reversed?

2.2-12. Consider a homogeneous square box of side L and weight W which is resting on a frictionless flat surface and is subjected to a horizontal form F acting midway on its right edge, as in the figure below. Suppose that the distribution of the normal reaction force on the box is quadratic and

of the form $p(x) = ax + bx^2$, where a and b are constants. Use equilibrium to determine the constants a and b.

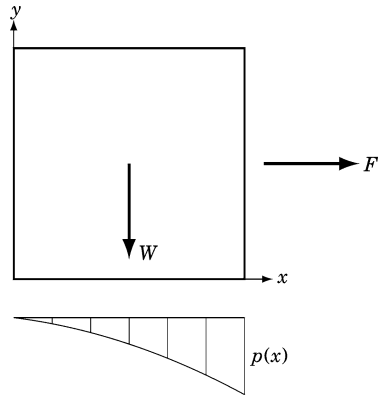

2.2-13. A homogeneous two-dimensional box of weight W is subject to a horizontal force F, as shown in the figure. The box is supported by a frictional surface with which the static coefficient of friction is $\mu_s = 0.25$.

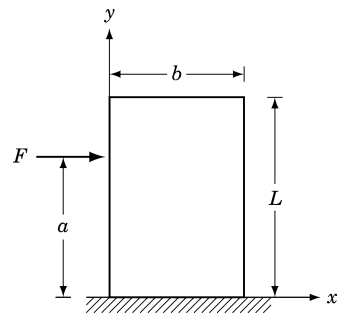

(a) If $F = 0.2W$, draw the free-body diagram of the box showing all external forces and reactions. Does the body slide for this value of F?

(b) Find the critical value F_c of the force F for which the box is at the onset of sliding.

(c) For $F = F_c$, find the horizontal coordinate x_c of the point at which the vertical reaction of the surface acts on the box to maintain equilibrium.

(d) Use the result of part (c) to determine a condition satisfied by the dimensions a and b, such that sliding of the box commences before tipping.

(e) What is the smallest value $F_{\min}$ of the horizontal force F that will tip the box, assuming that F may act at any point on the left edge of the box? What is the point at which the force acts in this case?

2.2-14. Find the reactions at points A and B in the three-hinged arch shown in the figure.

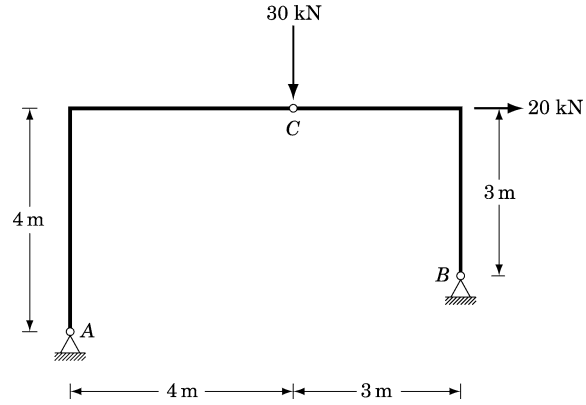

2.2-15. Find the force F_2 required to keep the system of pulleys in equilibrium under the influence of the force F_1.

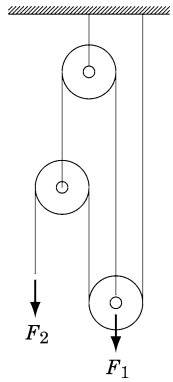

2.2-16. Show the degree of freedom allowed by the improper supports of Fig. 2.16d and Fig. 2.16e.

2.2-17. Explain why the support of Fig. 2.16f is improper.

2.2-18. An electric cord feeding a tool is bent about a rounded corner with friction by an angle θ, as shown in the figure below. If it is pulled from the tool end with a tension T, the tension on the plug end is reduced by the friction to a smaller value T', an effect known to electricians as *strain relief*. Find the ratio T'/T in terms of θ and the frictional coefficient μ.

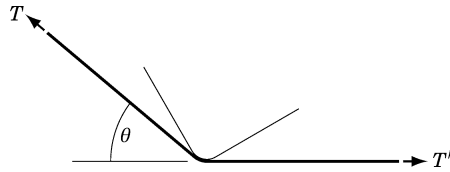

2.3 Equilibrium of Rigid Bodies in Three Dimensions

2.3.1 Three-Dimensional Force Systems

The equilibrium equations for a rigid body in three dimensions are given by Eqs. (2.18) and (2.19). Resolving all the vectors that appear in these equations with respect to a right-handed Cartesian basis $\{\mathbf{i},\mathbf{j},\mathbf{k}\}$ leads to

$$\sum_{i=1}^{N} F_{ix}\mathbf{i} + \sum_{i=1}^{N} F_{iy}\mathbf{j} + \sum_{i=1}^{N} F_{iz}\mathbf{k} = \mathbf{0} \tag{2.45}$$

and

$$\sum_{i=1}^{N} M_{Oix}\mathbf{i} + \sum_{i=1}^{N} M_{Oiy}\mathbf{j} + \sum_{i=1}^{N} M_{Oiz}\mathbf{k} = \mathbf{0}\,, \tag{2.46}$$

where

$$M_{Oix} = F_{iy}z_i - F_{iz}y_i \quad , \quad M_{Oiy} = F_{iz}x_i - F_{ix}z_i \quad , \quad M_{Oiz} = F_{ix}y_i - F_{iy}x_i \tag{2.47}$$

are the components of the moment $\mathbf{M}_{Oi}$ about a point O of the external force $\mathbf{F}_i$ acting at a point whose position vector relative to O has Cartesian coordinates (x_i, y_i, z_i). It follows from (2.45) and (2.46) that the six equilibrium equations may be expressed in component form as

$$\sum_{i=1}^{N} F_{ix} = 0 \quad , \quad \sum_{i=1}^{N} F_{iy} = 0 \quad , \quad \sum_{i=1}^{N} F_{iz} = 0 \tag{2.48}$$

and

$$\sum_{i=1}^{N} M_{Oix} = 0 \quad , \quad \sum_{i=1}^{N} M_{Oiy} = 0 \quad , \quad \sum_{i=1}^{N} M_{Oiz} = 0\,. \tag{2.49}$$

As in the two-dimensional case, there exist many equivalent sets of equilibrium equations alternative to the canonical equations (2.48) and (2.49). To derive one such set, we start with the five Eqs. $(2.48)_{1,2}$ and (2.49) and note that their enforcement reduces the statically equivalent force system to a force passing through point O and directed along the z-axis. Now, instead of considering the canonical sixth Eq. $(2.48)_3$, we may choose any point A that does not lie on the z-axis and take either

$$\sum_{i=1}^{N} M_{Aix} = 0 \tag{2.50}$$

(provided A does not lie in the xz-plane) or

$$\sum_{i=1}^{N} M_{Aiy} = 0 \tag{2.51}$$

(provided A does not lie in the yz-plane).

Example 2.3.1: Box subject to four forces.
Consider a rectangular box with sides of length a, b and c along the x-, y- and z-axes, respectively, and let it be subject to the four forces and an unspecified moment, shown in Fig. 2.33. Force equilibrium is readily established using Eqs. (2.48), since there are no forces acting along the x- or z-axes, while the forces along the y-axes trivially sum to zero. For moment equilibrium to hold, the x-, y- and z-moments about the origin should vanish, that is

$$\begin{aligned} -Fc - Fc - Fc + M_x &= 0 \\ M_y &= 0 \\ 3Fa - Fa - Fa + M_z &= 0\,. \end{aligned}$$

This implies that the box is in equilibrium if the applied moment is equal to $Fc\mathbf{i} - Fa\mathbf{k}$.

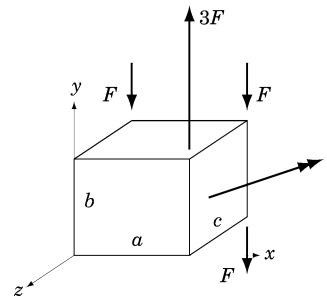

Figure 2.33. A box in equilibrium

2.3.2 Constraints in Three Dimensions

The analysis of the equilibrium of rigid bodies in three dimensions follows the same principles as in two dimensions. However, a three-dimensional rigid body has six degrees of freedom. This may be easily understood by fixing the position of any one particle in the body (three constraints) and noting that the body still possesses the freedom to rotate about any three mutually perpendicular axes, as shown in Fig. 2.34 for the case of a cube; eliminating this degree of freedom requires the specification of three additional constraints. Given the six degrees of freedom, there is a much greater variety of possible support constraints in three-dimensional rigid bodies.

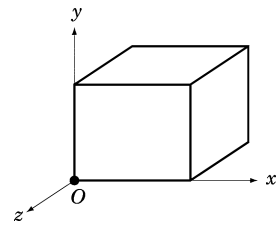

Figure 2.34. Cube with fixed vertex point O that may freely rotate about the x-, y-, and z-axes

Since a built-in support (as illustrated in Fig. 2.15c) prevents all rigid-body motion, in three dimensions it may be regarded as a 6-dof constraint. At the other extreme, the 1-dof constraints of Fig. 2.14 function as they do in two dimensions: they prevent translation in one direction only.

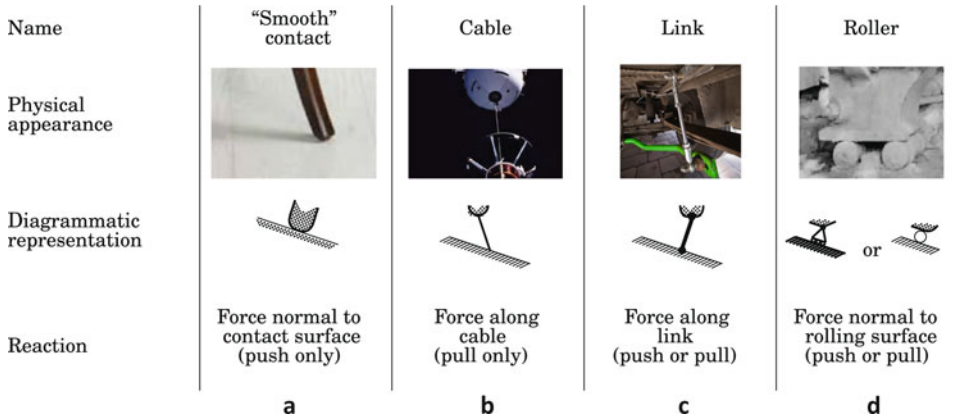

Figure 2.14. (reproduced)

An exception is the roller pictured in Fig. 2.14d. If the circle on the right represents a ball, or if the casters shown on the left can swivel, then the support does, in fact, provide a 1-dof constraint. But if the circle represents a cylinder or if the casters are somehow fixed to roll in one direction, and the surface is "rough," then the support (shown more explicitly in Fig. 2.36a) is a 2-dof constraint in that it also prevents translation parallel to the axis of the cylinder or caster. In that way it is equivalent to a support provided by two non-collinear links, as shown in Fig. 2.35a. (In Figs. 2.35a,b, any link can be replaced by a cable or a "smooth" contact, with the limitation that the force must be a pull or a push, respectively.)

A 3-dof constraint preventing all translation at a point (but allowing all rotation about it) is provided by three non-coplanar links as shown in Fig. 2.35b or, more simply, by the *ball-and-socket joint* of Fig. 2.35c. As can be seen, a perspective depiction is necessary in order to bring out the three-dimensional nature of the constraints.

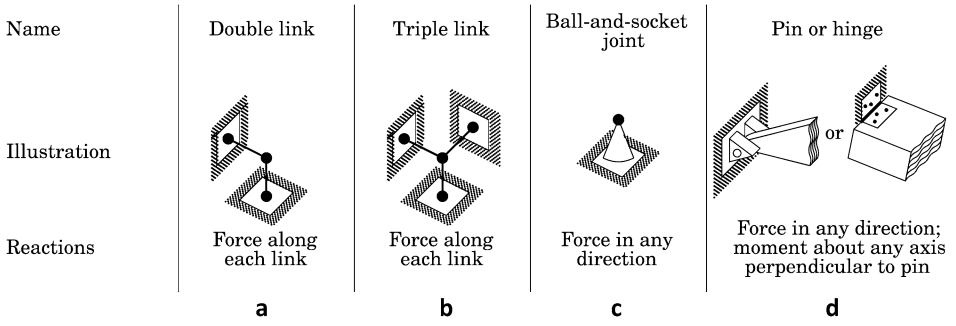

Figure 2.35. Some three-dimensional multi-dof constraints

The fixed collar-rod connection of Fig. 2.15c (page 71) is a 4-dof constraint, allowing translation along the rod and rotation about it. It can, however, be made into a 3-dof constraint by allowing rotation at the connection to the collar.

A pin joint or hinge in three dimensions, shown in Fig. 2.35d, is a 5-dof constraint: only rotation about the pin axis is allowed.

Some additional three-dimensional supports are shown in Fig. 2.36.

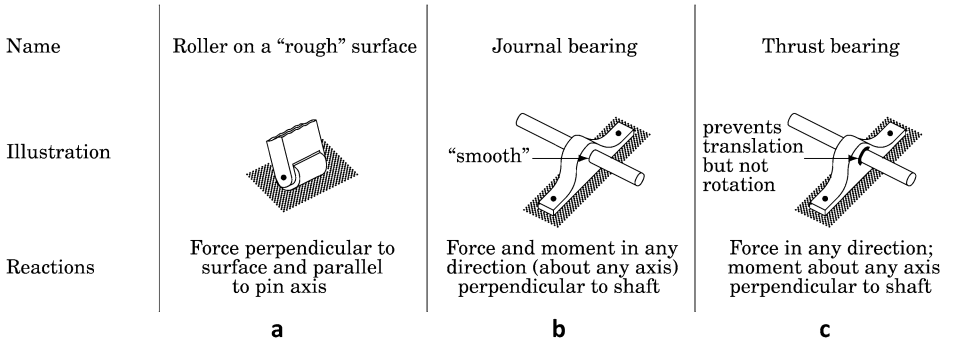

Figure 2.36. Additional three-dimensional multi-dof constraints

When combining supports to provide six constraints, care must be taken to make sure that they are proper. A pin can be combined with a single link (or the like) provided the reaction force there is not aligned with the pin axis.

By analogy with the two-dimensional case, if the supports exert forces only, then for static determinacy there must be six force reactions. These can be provided by combinations ranging from a triple link (or, *equivalently*, a ball-and-socket joint), a double link and a single link (or a similar 1-dof constraint) to six separate 1-dof constraints. For the supports to be proper, the following conditions are necessary:

(a) The reaction forces must not be parallel to one plane, otherwise nothing

prevents translation perpendicular to that plane.

(b) No more than three of the reaction forces can be concurrent. By contradiction, suppose that four of them are concurrent, say at point O, and the other two pass through points A and B, whose position vectors relative to O are $\mathbf{r}_A$ and $\mathbf{r}_B$, with the lines of action of the forces given by the unit vectors $\mathbf{n}_A$ and $\mathbf{n}_B$, respectively, as in Fig. 2.37. If the scalar values of the reaction forces at A and B are R_A and R_B, then the moment about O is $\mathbf{r}_A \times R_A\mathbf{n}_A + \mathbf{r}_B \times R_B\mathbf{n}_B$. Consider, now, an axis through point O that is parallel to the vector $(\mathbf{r}_A \times \mathbf{n}_A) \times (\mathbf{r}_B \times \mathbf{n}_B)$; the moment component about that axis is identically zero, and therefore the body is free to rotate about it.

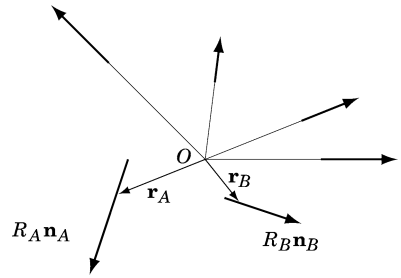

Figure 2.37. System of 6 reaction forces of which 4 are concurrent

(c) Since concurrent vectors become parallel as the point of concurrency recedes to infinity, it follows that, for the supports to be proper, no more than three of the reactions can be parallel. If, for example, a body rests on four supports all of which exert vertical forces, then the remaining two horizontal forces cannot prevent it from rotating about a vertical axis.

Examples of improperly constrained three-dimensional bodies are shown in Fig. 2.38.

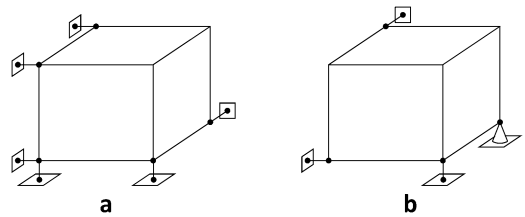

Figure 2.38. Improper combinations of single, double and triple links

Example 2.3.2: Box with improper supports.
There are two ways to establish that a set of supports on a body is improper. The first is to visually identify a rigid displacement (translation or rotation) that is not restrained by the supports. In the case of the box in Fig. 2.38a (reproduced again for clarity together with its free-body diagram in Fig. 2.39), we may note, by inspection, that a rotation about the x-axis is completely uninhibited by the supports, which is sufficient to render the supports improper.

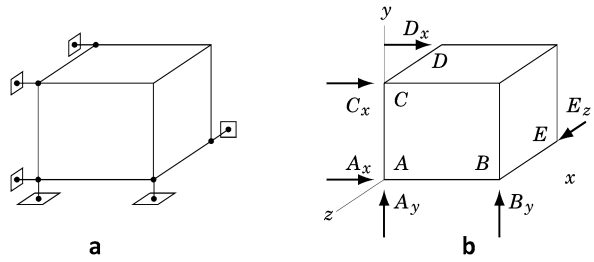

Figure 2.39. An analysis of a three-dimensional rigid body with improper supports

The second way to establish that the set of supports is improper is to draw a free-body diagram (although there are no external loads!) and examine the reaction forces. With reference to Fig. 2.39b, it is clear that there is at least one reaction in each of the three directions x, y, and z, which implies that all three translations are restrained. Likewise, at least one reaction contributes to the moment about the y- and z-axes (as well as all axes parallel to them). This, in turn, means that rotations about any axes parallel to the y- and z-axes are also restrained. However, this is not the case when it comes to moments about the x-axis. Indeed, no reactions contribute to this moment, since the A_x, A_y, B_y and E_z reactions intersect the x-axis and the C_x and D_x reactions are parallel to this axis. Therefore, any external load that results in a non-zero moment about the x-axis cannot be reacted upon by any of the supports, and would result in an uninhibited rotation of the body about the x-axis.

The following example illustrates the procedure followed in the solution of three-dimensional equilibrium problems.

Example 2.3.3: Cantilever assemblage of rigidly connected bars.
Let us consider the cantilevered assemblage of rigidly connected bars shown in Fig. 2.40. Let the respective mean lengths of bars AB, BC and CD be a, b and c, so that the coordinates of points A, B, C and D are $(0,0,c)$, $(a,0,c)$, (a,b,c) and $(a,b,0)$, respectively. In drawing a free-body diagrams, we simply replace the applied force F by its components and the fixed support D by the reactions acting there, as in Fig. 2.41.

The equations of force equilibrium yield $F_{Dx} = 0$, $F_{Dy} = F\cos\alpha$ and $F_{Dz} = -F\sin\alpha$. Equilibrium of moments about D can be expressed in vector form as

$$\mathbf{i}M_{Dx} + \mathbf{j}M_{Dy} + \mathbf{k}M_{Dz} + (-\mathbf{i}a - \mathbf{j}b + \mathbf{k}c) \times (-\mathbf{j}F\cos\alpha + \mathbf{k}F\sin\alpha) = 0\,, \qquad (2.52)$$

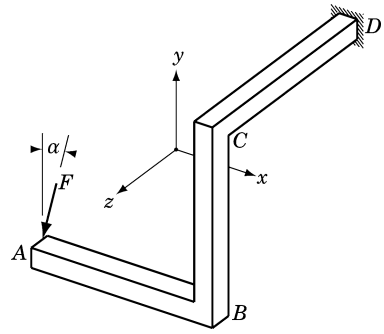

Figure 2.40. Three-dimensional bar assemblage

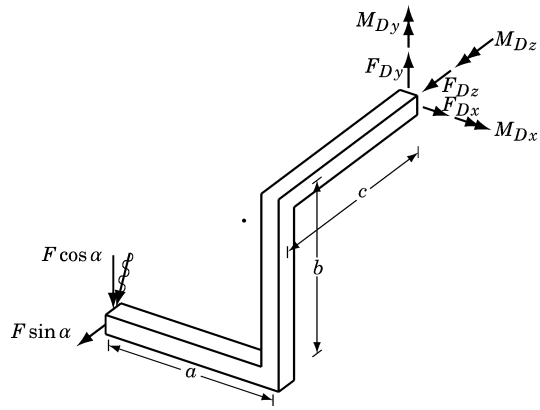

Figure 2.41. Free-body diagram for assemblage of Fig. 2.40

leading to

$$M_{Dx} = F(c\cos\alpha - b\sin\alpha) \quad , \quad M_{Dy} = Fa\sin\alpha \quad , \quad M_{Dz} = Fa\cos\alpha \; . \tag{2.53}$$

Exercises

2.3-1. Identify an equivalent system of equilibrium equations to (2.48) and (2.49) that include a single force equilibrium equation, say, $(2.48)_1$ and five moment equilibrium equations. Make sure to justify the equivalence of this system to (2.48) and (2.49).

2.3-2. For the improper combinations of constraints of Fig. 2.38b, find the degree(s) of freedom that are allowed using both geometric and mathematical arguments.

2.3-3. A system of four forces $\mathbf{F}_1$, $\mathbf{F}_2$, $\mathbf{F}_3$, $\mathbf{F}_4$ is acting on the rectangular parallelepiped of the figure below. Let the magnitudes of these forces be $F_1 = 5$ kN, $F_2 = 5\sqrt{2}$ kN, $F_3 = 8$ kN, and $F_4 = 5$ kN, respectively.

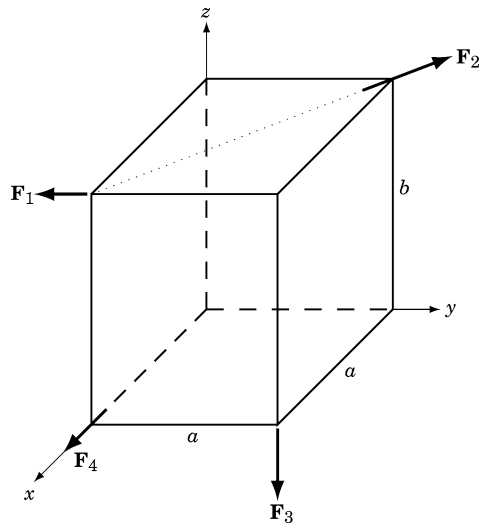

(a) Express each of the four forces in vector form.

(b) Find the resultant $\mathbf{R}$ of the four forces.

(c) Find the moment of $\mathbf{F}_2$ about the x-axis.

(d) What should be the relation between the lengths a and b so that the system of four forces be statically equivalent to a force that passes through point A?

2.3-4. Determine the reactions at the built-in support O of the three-dimensional rigid body depicted in the figure.

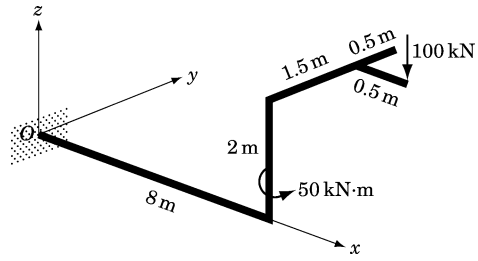

2.3-5. A rigid boom is kept in place by a ball-and-socket support at point O and by two rigid links, as in the figure (with the coordinates in meters). Determine the reactions at the ball-and-socket as well as the forces in the rigid links due to the force applied at the tip of the boom. For the given applied force, could the rigid links be replaced by cables?

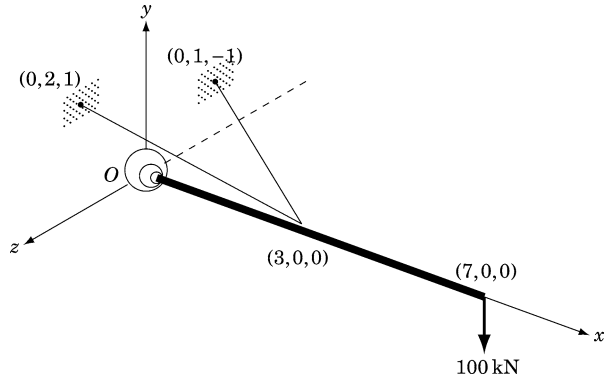

2.3-6. The two rods AC and BC are hinged together at C and are supported by the cable DE and the ball-and-socket joints at A and B. Rod BC is subjected to a force on the plane normal to the x-axis.

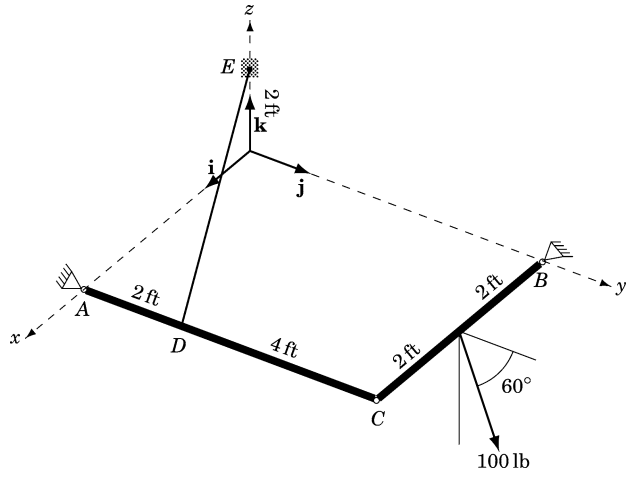

(a) Draw the free-body diagram of the system of the two rods.

(b) Using the free-body diagram of part (a), determine the tension T in the cable.
Hint: This can be accomplished by writing a single equilibrium equation.

2.3-7. The 1 m×1 m homogeneous square plate shown in the figure weighs 500 kN and is supported by a rigid link at A (midway on the edge of the plate), a ball-and-socket joint at B and a single journal bearing at D (assume that the bearing is equivalent to a double link along the x- and z-axis, and therefore generates no reaction moments). In addition, the plate is subject to a 100 kN force acting midway on the side BD and a moment of 200 kN·m, as shown in the figure.

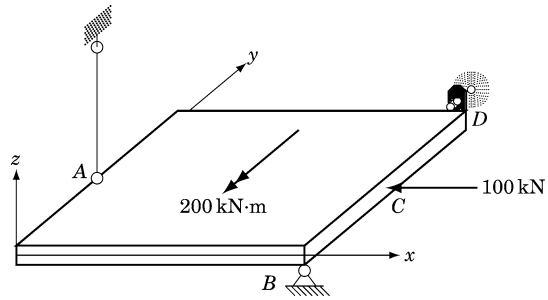

(a) Draw the free-body diagram of the plate.

(b) Using the free-body diagram of part (a), determine all reaction forces acting on the plate.

(c) For the given loading, is it possible to replace the rigid link of the system with an inextensible rope without upsetting equilibrium?

2.3-8. Stand against a "smooth" wall with your back straight, your legs together and your heels touching the wall. Now, keeping your back straight, attempt to lift one of your legs. What do you observe? Explain your observation using a sketch of your body with all resultant forces and reactions.

2.3-9. Stand against a "smooth" wall with your back straight, your legs together and one of your shoulders touching the wall so that your body is perpendicular to the wall. Now, keeping your back straight, attempt to lift forward your leg closest to the wall. What do you observe? Returning to the original position, attempt next to lift forward your leg furthest to the wall. What do you observe now? Explain your observations using a sketch of your body with all resultant forces and reactions for both cases.

2.4 Method of Sections

2.4.1 Introduction

The calculation of the support reactions on a rigid body in equilibrium is only one of the purposes of solving the equilibrium equations. In fact, it is not even the most important one. Far more important is the determination of whether the body can carry the loads imposed on it without failing in some way, and that knowledge can be obtained only if the *internal reactions*, that is, the forces and moments that one part of the body exerts on another, are known. If, for example, parts of the body are glued together, the forces transmitted by the glue must be known in order to determine whether it will hold. The same is true if the body is held together with fasteners (nails, bolts and the like) or through the cohesion of the material itself.

It is important to keep in mind is that the definition of any particular "body" is arbitrary: any portion of matter occupying a certain region in space may also be regarded as a body, and therefore any part of what had previously been defined as a body is in turn another body (which can be called a *subbody*). Furthermore (as was already discussed in Sect. 2.1 in reference to particles), a body is in equilibrium if, and only if, all of its subbodies are in equilibrium.

If the subbodies are imagined as parts into which the original body is divided, then the internal reaction components (force and moment) are conjugate to the imagined relative displacements (translation and rotation) between the parts, as illustrated in Fig. 2.42.

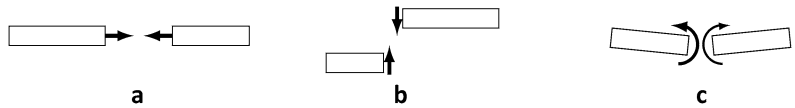

Figure 2.42. Internal reactions and imagined relative displacements of the subbodies

The determination of internal reactions by means of solving the equilibrium equations for subbodies (into which the body is divided by means of a surface drawn through it) is known as the *method of sections*[*]. As with the determination of support reactions, the first step in the method is the drawing of free-body diagrams. And, of course, no more unknown force or moment components can be determined by statics than the number of independent equilibrium equations. This means that, however the cohesive forces are distributed over the dividing surface, only their resultants can be found in this way. In order to determine such distributions, the deformability of the body

[*]This is the general definition, but "method of sections" is sometimes used in a restricted sense for a specific application of the method that will be discussed in Sect. 3.2.

must be taken into account, and this will be undertaken starting with Chapter 6.

Example 2.4.1: *Forces in a pulley.*
As our first case, we will analyze the forces on the pulley of Fig. 2.29 (page 80). The cut will be made through the cable on both sides of the pulley, and between the pulley and the pin, resulting in the free-body diagram shown in Fig. 2.43. Here T is the tension in the cable to the left of the pulley while P is the push

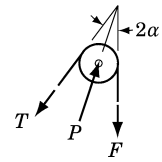

Figure 2.43. Free-body diagram of a pulley

exerted on the pulley by the frictionless pin. Since the free body is a three-force body, the line of action of this push must meet those of the cable tensions and, since it acts through the center of the pulley, it bisects the angle between then. If this angle is 2α, then equilibrium of forces perpendicular to the line of action of P requires that $F\sin\alpha = T\sin\alpha$ and therefore $T = F$, proving that in a weightless cable going around a frictionless pulley the tension is the same on both sides of the pulley. The remaining force equilibrium equation leads to

$$P = 2F\cos\alpha\ .$$

2.4.2 Slender Bodies

In the case of long slender bodies (usually, but not necessarily, straight) with a well-defined axis, it is generally convenient to define the components of the internal reaction in relation to the axis, as shown in Fig. 2.44, where the body axis is chosen to coincide with the x-axis. The component of the force along the

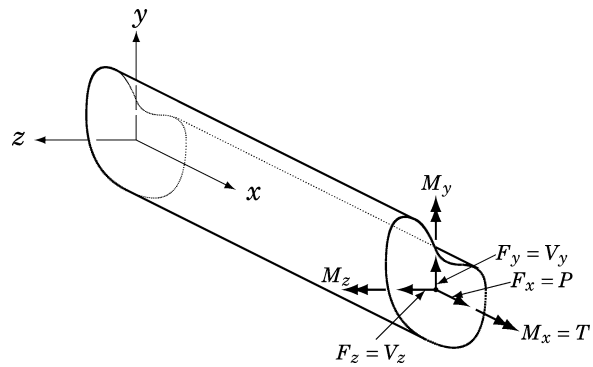

Figure 2.44. Internal reactions in a slender body

axis is called, naturally enough, the *axial force* and will be denoted P, which stand for "push" or "pull." The axial component of the moment, which tends to twist the body about the axis, is called the *torsional moment*, *twisting moment* or *torque*, and will be denoted T.[†] The force component transverse to the axis is called the *shear force* and usually denoted V, while the transverse moment is *bending moment*, denoted M. Both the shear force and the bending moment can be further decomposed into components along the two axes perpendicular to the body axis. Note that, while we have here defined $V_y = F_y$, so that its positive direction is the positive y-direction when it is acting on a cut facing the positive x-axis (and vice versa), as shown in the figure, there is another convention, common among structural engineers, with the opposite definition, namely $V_y = -F_y$.

For the other internal reactions, the common sign conventions, regardless of any choice of coordinate system, are as follows (shown in Fig. 2.45):

(a) Axial force: positive when in tension (each subbody pulls on the other), negative when in compression.

(b) Torque: positive according to the right-hand rule around an axis pointing outward from the cut.

(c) Bending moment: positive when causing bending that is convex upward.

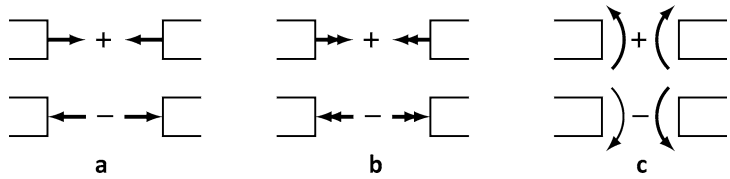

Figure 2.45. Sign conventions for (**a**) axial force, (**b**) torque, (**c**) bending moment

If the loading on a slender body includes forces or moments that are transverse (perpendicular to the axis), resulting in bending moments and shear forces, then, as we already mentioned in Sect. 2.2 (page 82) in a two-dimensional context, it is common to refer to the member as a *beam*. If the body carries only a torsional moment then it is usually called a *shaft*. Columns, posts and struts are designed primarily to carry compressive axial force. A slender body carrying an axial force that is either compressive or tensile is generally known simply as a *bar*.

If the loading on a slender body is planar (say in the xy-plane) then the only internal reactions are $F_x = P$, $F_y = V$ and $M_z = M$. The bending moment is usually depicted by means of a curved arrow having the sense of the moment, as shown in Fig. 2.46.

[†]The symbol T is also used, depending on the context, to denote the tension in a cable or the tangential force at a frictional interface.

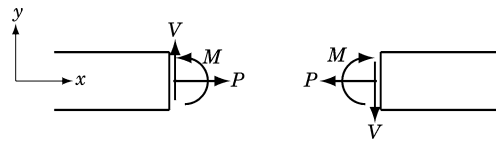

Figure 2.46. Internal reactions in a slender body under planar loading

Example 2.4.2: Internal reactions in a beam.
We consider, as an example, the beam loaded as shown in Fig. 2.32 (page 82). We divide it into two sections (subbodies) by means of a transverse cut at a distance x from the left end. The corresponding pairs of free-body diagrams are shown in Fig. 2.47. Note that the internal reactions P, V and M are shown as functions of

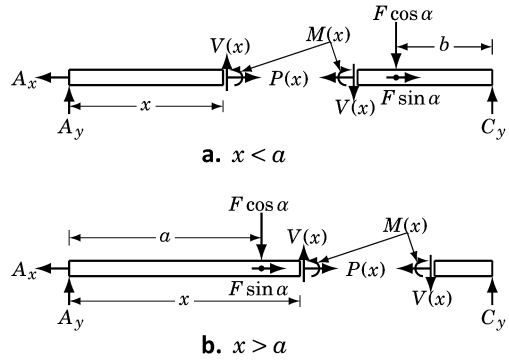

Figure 2.47. Free-body diagrams of sections of the beam of Fig. 2.32.

x, since their values depend on the location of the cut. For each of the two cases, $x < a$ and $x > a$, these values can be found by solving the equilibrium equations for either of the two subbodies. Furthermore, the support reactions appearing in the subbody chosen must be determined beforehand from the equilibrium of the whole body. This is not always the case: if the beam is cantilevered, then a subbody that includes the free end has no unknowns other than the internal reactions.

Looking at the left-hand section of Fig. 2.47a, we find that, for force equilibrium, $P(x) = A_x$ and $V(x) = -A_y$, while moment equilibrium about the point $(x,0)$ yields $M(x) = A_y x$. Inserting the previously derived values of A_x and A_y, we find that, for $x < a$,

$$P(x) = F\sin\alpha\,, \quad V(x) = -\frac{b}{L}F\cos\alpha\,, \quad M(x) = \frac{bx}{L}F\cos\alpha \quad (x<a)\,,$$

and the same result will be found for the right-hand section. Similarly, for $x > a$, we find from either section of Fig. 2.47b that

$$P(x) = 0\,, \quad V(x) = \frac{a}{L}F\cos\alpha\,, \quad M(x) = \frac{a(L-x)}{L}F\cos\alpha \quad (x>a)\,.$$

In later chapters, we will introduce the common practice of plotting the values of P, V and M against x, producing what are known respectively as the *axial-force*, *shear-force* (or simply *shear*) and *bending-moment* (or simply *moment*) *diagrams*.

As was pointed out in the discussion of Sect. 2.2, any other loading of the beam that is statically equivalent to that of Fig. 2.32 will produce the same support reactions. This is not true, however, of the internal reactions.

Example 2.4.3: Internal reactions in a beam under a uniformly distributed load.
We now suppose that the loading is transverse only (i.e. $\alpha = 0$, so that $P(x) = 0$) but that, rather than being concentrated at $x = a$, it is uniformly distributed over the beam, with an intensity (force per unit length) of F/L. The equivalent

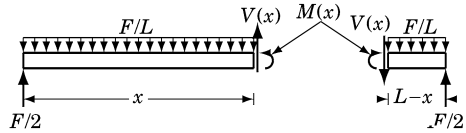

a. Original loading

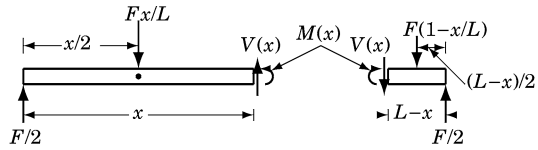

b. Statically equivalent loading

Figure 2.48. Free-body diagrams for a uniformly loaded simply supported beam

concentrated force would then be at $x = L/2 = a = b$, and the end reactions (vertical only) are $A_y = C_y = F/2$. If we now cut the beam at x, we obtain the free-body diagrams shown in Fig. 2.48a, which can be replaced for the purpose of equilibrium analysis *of the sections* by those of Fig. 2.48b.

Once again, the equilibrium of either the right-hand or the left-hand portion can be used to determine the internal reactions, namely,

$$V(x) = F\left(-\frac{1}{2} + \frac{x}{L}\right) \quad , \quad M(x) = \frac{F}{2}x(L-x)\,.$$

We note, in particular, that the maximum bending moment (which occurs at $x = L/2$) is $FL/8$. For the corresponding problem with the load F concentrated at $x = L/2$ (the special case of Fig. 2.32 with $\alpha = 0$ and $a = b = L/2$) the maximum bending moment is $FL/4$.

As we can see from the examples, in straight slender bodies the internal axial force is determined only by the axial loads, while the transverse loading determines the shear force and bending moment. Similarly, the internal torque is determined only by the torque loads. The three types of slender

bodies—bars carrying axial loads, shafts carrying torque and beams carrying transverse loads—will be studied separately, and the corresponding internal force and moment diagrams will be studied in greater depth in conjunction with the deformation of such bodies, once the relations between force and deformation are introduced in Chap. 6. Special consideration must be given to bars subject to an axial force that is compressive: if such bars are slender enough, then they are liable to buckle when the load reaches a critical value. The phenomenon of buckling will be studied on its own in Chap. 10.

This simple categorization of slender bodies does not work if they are curved or bent, like the members of the three-pinned arch of Fig. 2.20 (page 73) or of the three-dimensional assemblage of Fig. 2.40 (page 94).

Example 2.4.4: Internal reactions in a three-pinned arch.
To determine the internal reactions in the arch, we make a cut through the left-hand member at a point whose coordinates (with the left support as origin) are x, y and where the slope is $dy/dx = \tan\theta$, as shown in Fig. 2.49. We can

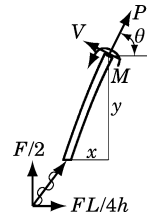

Figure 2.49. Free-body diagram of a portion of an apex-loaded three-hinged arch

solve directly for the internal forces (the axial force P and the shear force V) by considering force equilibrium not in the x- and y-directions but in the tangential and normal directions at x, y, yielding

$$P = -\frac{F}{2}\left(\sin\theta + \frac{L}{2h}\cos\theta\right) \quad , \quad V = -\frac{F}{2}\left(\cos\theta - \frac{L}{2h}\sin\theta\right) .$$

Note that the axial force is entirely compressive, a characteristic of arch action. (Of course, if the load were upward, the axial force would be tensile.)

Moment equilibrium leads to

$$M = \frac{F}{2}\left(x - \frac{Ly}{2h}\right) .$$

At the apex, where $x = L/2$ and $y = h$, the moment vanishes as it should.

In the special case where the arch is a triangle so that the members are straight, we have $y/x = 2h/L = \tan\theta$. Consequently, $V = M = 0$, and $P = -(F/2)\sqrt{1+(L/2h)^2}$.

Example 2.4.5: Internal reactions in a three-dimensional assemblage. For the internal reactions in the assemblage of Fig. 2.40 (page 94), we perform cuts in each of its three members. Since the assemblage is cantilevered, if we analyze the equilibrium of subbodies that include the free end then there is no need to know the reactions shown in Fig. 2.41. The corresponding free-body diagrams are shown in Fig. 2.50. Note that the diagrams omit, for the sake of clarity, those internal reaction components that are zero by inspection, namely, P and T in bar AB, and V_x in the other two bars. Note also that the assumed positive directions of the internal reactions in bar CD point in the negative x-, y- and z-directions, since the cut faces the negative z-direction.

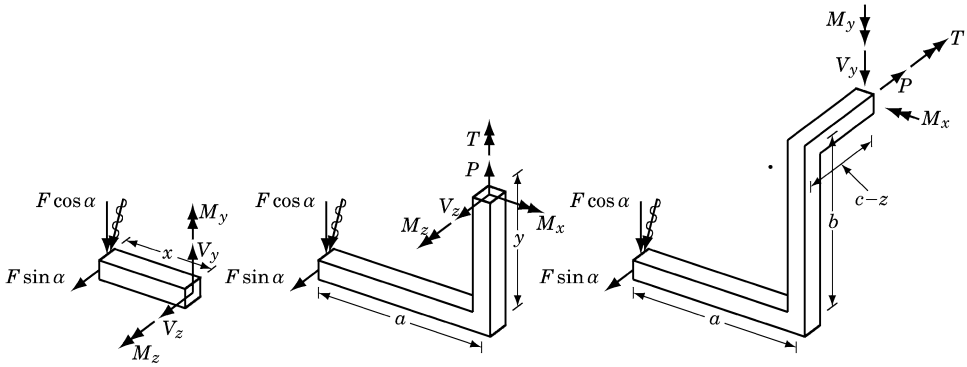

a. Bar AB **b.** Bar BC **c.** Bar CD

Figure 2.50. Free-body diagrams for the bars of Fig. 2.40

In bar AB, the nontrivial equilibrium equations are four in number, and yield the following results:

$$\begin{aligned} \textstyle\sum F_y = 0 \quad &\Rightarrow \quad V_y = F\cos\alpha \\ \textstyle\sum F_z = 0 \quad &\Rightarrow \quad V_z = -F\sin\alpha \\ \textstyle\sum M_y = 0 \quad &\Rightarrow \quad M_y = -(F\sin\alpha)x \\ \textstyle\sum M_z = 0 \quad &\Rightarrow \quad M_z = -(F\cos\alpha)x\ . \end{aligned}$$

In bar BC, we find

$$\begin{aligned} \textstyle\sum F_y = 0 \quad &\Rightarrow \quad P = F\cos\alpha \\ \textstyle\sum F_z = 0 \quad &\Rightarrow \quad V_z = -F\sin\alpha \\ \textstyle\sum M_x = 0 \quad &\Rightarrow \quad M_x = (F\sin\alpha)y \\ \textstyle\sum M_y = 0 \quad &\Rightarrow \quad T = -(F\sin\alpha)a \\ \textstyle\sum M_z = 0 \quad &\Rightarrow \quad M_z = -(F\cos\alpha)a\ . \end{aligned}$$

Note that as absolute forces and moments, these reactions are continuous across the joint B, except that their internal functions may change: the shear force V_y in AB becomes the axial force P in BC, while the bending moment M_y becomes the torque T.

Finally, in bar CD

$$\begin{aligned}
\sum F_y &= 0 \quad \Rightarrow \quad V_y = -F\cos\alpha \\
\sum F_z &= 0 \quad \Rightarrow \quad P = F\sin\alpha \\
\sum M_x &= 0 \quad \Rightarrow \quad M_x = -(F\sin\alpha)b + (F\cos\alpha)(c-z) \\
\sum M_y &= 0 \quad \Rightarrow \quad M_y = (F\sin\alpha)a \\
\sum M_z &= 0 \quad \Rightarrow \quad T = -(F\cos\alpha)a
\end{aligned}$$

Exercises

2.4-1. In the ladder of Example 2.2.5 (page 79), find the internal reactions at a section of the ladder halfway between A and the rung on which the person is standing.

2.4-2. Find the internal reactions on the transverse section located at $a/2$ from the built-in end of the body in Exercise **2.2-4** (page 83).

2.4-3. Find the internal reactions at the hinge C in Exercise **2.3-6** (page 96).

2.4-4. Find the internal reactions on the transverse section located midway between points C and D of the bar in Exercise **2.2-10** (page 85).

2.4-5. Find the internal reactions at the point with coordinates (5,0,0) in Exercise **2.3-5** (page 96).

2.4-6. In the pulley of Example 2.4.1 (page 99), suppose that there is friction between the pulley and the pin, the kinetic coefficient of friction being μ_k. If the radii of the pulley and the pin are R and r, respectively, find the relation between the cable tension T and the force F representing a weight that is (a) raised, (b) lowered.

2.4-7. In the assemblage of Fig. 2.40 (page 94), suppose that the force F applied at A is not as shown but is instead an axial pull on bar AB. Find the internal reactions in the bars.

2.4-8. Suppose that the three-hinged arch of Example 2.2.3 (page 76) has the shape of a parabola given by $y = h[1-(2x/L)^2]$, the origin being halfway between the supports. Find the internal reactions at the sections where (a) $x = L/4$ and (b) $y = h/2$.

Chapter 3

Articulated Assemblages of Rigid Members

3.1 Method of Joints

3.1.1 Introduction

In this chapter, we will study the equilibrium of assemblages of rigid bodies that are connected to one another with frictionless joints (also called *articulations*). The joints allow the rigid bodies to rotate but not translate relative to their neighbors. These bodies, called *members*; in fact, they are typically, though not necessarily, straight bars. The joints connect members to one another in the same way that the hinge and ball-and-socket supports studied in the last chapter connect bodies to a fixed base (allowing *absolute* rotation but not translation); consequently, they transmit only forces and not moments. Some of the members may, of course, be also connected to a fixed base so as to fix the configuration of the assemblage as a whole.

If a member has only two joints, and if it assumed that forces are applied only at the joints, then the member is necessarily a two-force body. The pair of equal and opposite, and collinear, forces acting on the member is called its *member force*; by the method of sections, these are the same as the resultants of the internal reactions on opposite sides of an imaginary cut through the member at any point between the joints, as illustrated in Fig. 3.1. If, further-

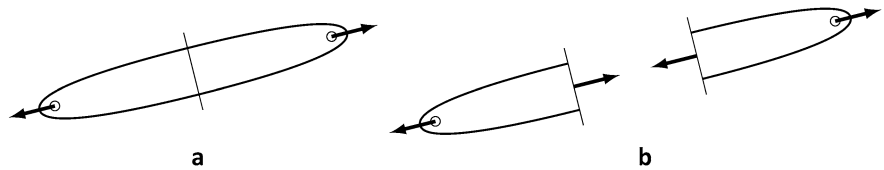

Figure 3.1. Member force and internal reaction

© Springer International Publishing Switzerland 2017
J. Lubliner, P. Papadopoulos, *Introduction to Solid Mechanics*,
DOI 10.1007/978-3-319-18878-2_3

more, the member is a straight bar, then the internal reaction resultant is an axial force, and the member force can be identified with it (it is treated as a singular "force" though in fact it represents a pair of forces) in accordance with the sign convention discussed in Sect. 2.4. If the member is curved or bent, then the method of sections can be applied to the member in order to analyze the internal forces and moments in it.

An articulated assemblage of rigid members is a special case of a *structure*, that is, a set of connected members designed to support and/or transfer forces. Depending on the combination of members and joints, such an assemblage can itself be rigid or flexible, as in Fig. 3.2. In the latter case (Fig.

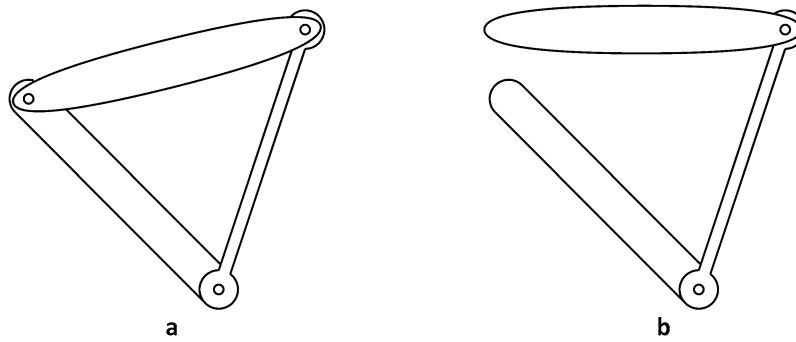

Figure 3.2. Three-member assemblages of articulated bodies: (**a**) rigid, (**b**) flexible

3.2b), the assemblage has one or more internal degrees of freedom and is a *mechanism* as defined in Sect. 2.2 (page 72).

Rigid assemblages of a type known as *trusses* will be studied in Sects. 3.2 and 3.3. Trusses are assemblages of two-force straight-bar members. When not all the forces are applied at the joints, then at least one of the members must be a multiforce body. Assemblages of this kind, called *frames* if rigid and *machines* if endowed with internal degrees of freedom, will be studied in Sect. 3.4. Flexible assemblages in the form of *chains* (becoming *cables* in the limit of infinitesimally short chain links) will be studied in Sect. 3.5.

The simplest articulated assemblage of straight bars in two dimensions that is a rigid body is a triangle with three bars and three joints (shown in Fig. 3.5a). Analogously, in three dimensions it is a tetrahedron with six bars and four joints. Like any other rigid body, such an assemblage has three and six degrees of freedom, respectively, in two and three dimensions, and consequently requires, in order to be fixed in space, at least three (six) independent constraints forming a proper set of supports.

3.1.2 Equilibrium of a joint

In an assemblage subject to external constraints, the unknowns are the constraint forces (reactions) and the member forces. In the just-discussed minimal assemblages, the numbers of these unknowns are six and twelve, respectively. Let us now apply the method of sections to such an assemblage by considering sections that encompass one and only one joint (called *one-joint sections*, as shown in Fig. 3.3a). When we consider sections of the bar up to the pin (Fig. 3.3b) and take into account (in accordance with Newton's Third Law) the equal and opposite nature of the forces between the pin and each bar, we see that the equilibrium of such a section is equivalent to that of the pin itself (Fig. 3.3c). When the latter point of view is taken, this subset of the method of sections becomes the *method of joints*.

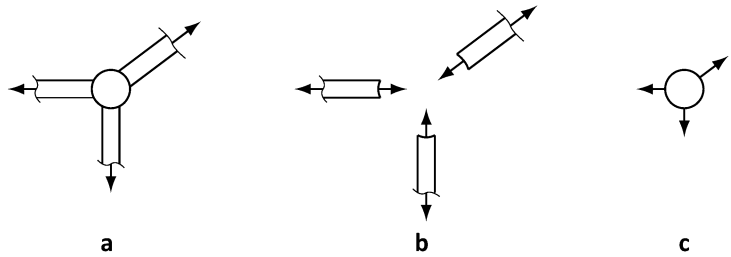

Figure 3.3. Equilibrium of a joint: (**a**) one-joint section, (**b**) bar sections, (**c**) forces on the pin

Since all the forces at a joint are necessarily concurrent, it follows that moment equilibrium is satisfied identically and the only equations available for the determination of unknown forces are those of force equilibrium, numbering two and three in two and three dimensions, respectively. If the joint forms part of a rigid assemblage, then the directions of all forces are known. Thus, if exactly two (in two dimensions) or three (in three dimensions) forces are unknown, they can be directly determined from the equilibrium of a single joint as illustrated in the following example.

Example 3.1.1: Weight supported by two bars.
For the assemblage shown (along with the free-body diagram) in Fig. 3.4, the

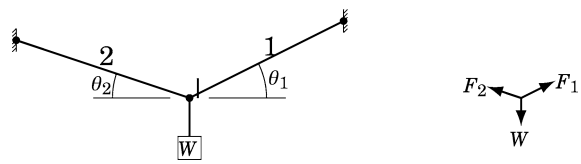

Figure 3.4. Example 3.1.1

equilibrium equations of the joint are

$$F_1 \cos\theta_1 - F_2 \cos\theta_2 = 0 ,$$
$$F_1 \sin\theta_1 + F_2 \sin\theta_2 = W ,$$

and the solution (when the trigonometric identity $\sin(\theta_1+\theta_2) = \sin\theta_1\cos\theta_2 + \sin\theta_2\cos\theta_1$ is used) is easily found to be

$$F_1 = W\frac{\cos\theta_2}{\sin(\theta_1+\theta_2)} \quad , \quad F_2 = W\frac{\cos\theta_1}{\sin(\theta_1+\theta_2)} .$$

3.1.3 Static determinacy of articulated assemblages

It should be clear that the equilibrium of all the one-joint sections (or, equivalently, of all the joints) is necessary and sufficient for the equilibrium of the assemblage, since any other section (including the whole assemblage) is a composite of two or more one-joint sections. Now, by the hypothesis of all the forces acting at the joints, the only equilibrium equations at each joint are those of the forces (since all the moments are identically zero) and their number is consequently two in two dimensions or three in three dimensions. For the simplest assemblage (triangle or tetrahedron), the total number is therefore six or twelve, and if there are no more constraints than necessary, this number is just sufficient to determine both the reactions and the member forces. The assemblage is then *statically determinate* (or *isostatic*) in a broader sense than that discussed in Sect. 2.2, where the determination of the external reactions was the only concern. Systems that are statically determinate in the latter, more limited, sense will from now on be called *externally statically determinate*.

More complex bar assemblages that remain isostatic can be formed by adding triangles—two bars and one joint at a time—in two dimensions, as illustrated in Fig. 3.5. The analogous construction in three dimensions, to be

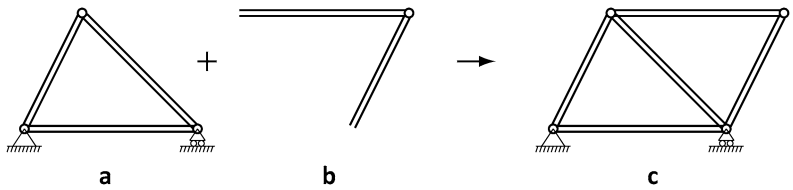

Figure 3.5. Adding bars to a simple structure

discussed in Sect. 3.3, involves adding tetrahedra by means of three bars and one joint at a time.

The assemblage will become statically indeterminate (or *hyperstatic*), in the broader sense discussed here, if it is given *either* more constraints *or* more bars than necessary, as shown in Fig. 3.6 (a and b, respectively). (Note that

the assemblage of Fig. 3.6b is externally statically determinate but not isostatic.) On the other hand, the structure of Fig. 3.6a can be made statically determinate by removing the bar between the supports, as in Fig. 3.6c. Here

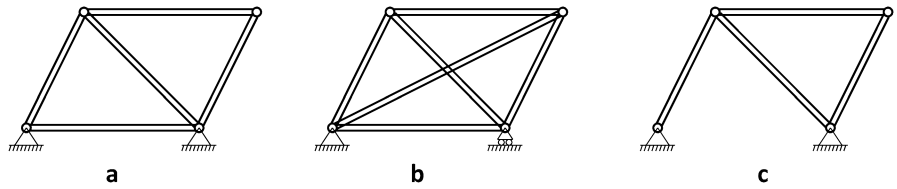

Figure 3.6. Statically indeterminate simple structures (a,b) and statically determinate structure (c)

the external reactions number four, but the equilibrium of the upper right-hand joint provides an additional equilibrium equation that is independent of the three global ones. (This case is similar to that of the three-pinned arch, page 73.)

In general, if the number of constraints, members and joints is r, n and j, respectively, then the necessary condition for static determinacy is

$$r + n = 2j \qquad \text{(two dimensions)} \tag{3.1}$$

or

$$r + n = 3j \qquad \text{(three dimensions)}\,. \tag{3.2}$$

This condition states that the number of unknowns (both internal forces and/or moments and support reactions) is equal to the number of equilibrium equations that may be employed for their determination. If the number on the left-hand side of Eq. (3.1) or (3.2) is greater than that on the right-hand side, then the assemblage is necessarily statically indeterminate, and the positive difference $r + n - 2j$ ($r + n - 3j$ in three dimensions) is the *degree of static indeterminacy* or *redundancy*, since one or more bars *or* constraints are not necessary for fixity and hence are redundant.

Example 3.1.2: Determination of the degree of static determinacy.
We will use Eq. (3.1) to determine the degree of static indeterminacy of the two-dimensional structures of Fig. 3.6.

$$\begin{aligned}
&\text{a}: \quad r = 4,\ j = 4,\ n = 5 \quad \Rightarrow \quad r + n - 2j = 1\\
&\text{b}: \quad r = 3,\ j = 4,\ n = 6 \quad \Rightarrow \quad r + n - 2j = 1\\
&\text{c}: \quad r = 4,\ j = 4,\ n = 4 \quad \Rightarrow \quad r + n - 2j = 0.
\end{aligned}$$

Thus the structures of Fig. 3.6a–b are statically indeterminate to the first degree, and that of Fig. 3.6c is statically determinate.

If, on the other hand, the right-hand side of Eq. (3.1) or (3.2) is greater than the left-hand side, then the assemblage has one or more degrees of freedom, their number being $2j-r-n$ ($3j-r-n$ in three dimensions). The assemblage is then called *hypostatic* or *statically underdeterminate* or, yet again, a mechanism. If, for example, the roller support of Fig. 3.5a is removed, then the degree of freedom is that of rotation about the hinge. If, instead, the hinge is replaced by a roller, then the assemblage can rotate about the intersection of the perpendiculars of the roller surfaces, or translate if these surfaces are parallel (as in the picture). These are *rigid-body degrees of freedom*. But if the bar between the supports is removed, then the assemblage becomes flexible, and the degree of freedom is one of deformation.

An articulated structure may, however, be statically indeterminate even when Eq. (3.1) is satisfied, if it is improperly constrained, as discussed in Sect. 2.2 (see Fig. 2.16, page 71) or if it simultaneously overconstrained internally (more bars than needed) and underconstrained externally. This would be the case, for example, of the assemblage of Fig. 3.6b if the hinge on the left were replaced by a roller. We now have four joints ($j = 4$), six bars ($n = 6$) and two constraints ($r = 2$), so that Eq. (3.1) is satisfied, but the assemblage is now free to translate horizontally.

It follows that Eqs. (3.1) and (3.2) are necessary but not sufficient for static determinacy. They are, however, sufficient if the structure is externally statically determinate (in which case it is also internally, and hence totally, statically determinate), or vice versa.

Exercises

3.1-1. A weight of 100 lb is suspended by three wires whose direction-cosine triads (see Eq. 1.22, page 19) relative to the point of suspension (with the z-axis positive upward) are, respectively, (1) $(\sqrt{1/2}, 0, \sqrt{1/2})$, (2) $(-1/4, 1/4, \sqrt{1/2})$, and (3) $(-1/4, -1/4, \sqrt{1/2})$). Using the three-dimensional force equilibrium equations for the joint, determine the forces F_1, F_2 and F_3.

3.1-2. Find the forces F_1 and F_2 in Example 3.1.1 when $\theta_1 = 30°$, $\theta_2 = 20°$, and $W = 100$ kN.

3.1-3. Find the forces F_1 and F_2 in Example 3.1.1 when $\theta_1 = \theta_2 = 45°$ and $W = 100$ lb.

3.1-4. Explain what happens in Example 3.1.1 when (a) $\theta_1 + \theta_2 = 0°$, (b) $\theta_1 + \theta_2 = 180°$.

3.1-5. Using the method of joints, determine the internal forces in the members of the three-pinned arch shown in the figure below.

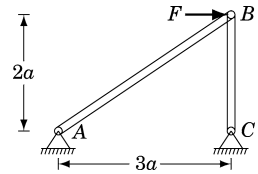

3.1-6. Using the method of joints, determine the internal forces in the members of the three-pinned arch shown in the figure below.

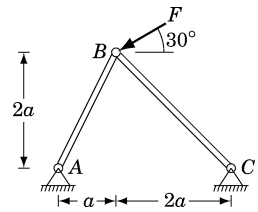

3.1-7. Use Eq. (3.1) to find the degree of static indeterminacy of the assemblage in the following figure.

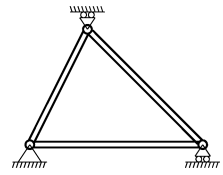

3.1-8. Use Eq. (3.1) to find the degree of static indeterminacy of the assemblages in the following figure.

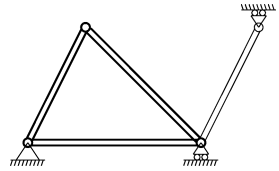

3.1-9. Verify that the assemblage shown in the figure (obtained by removing the interior bar from the structure of Fig. 3.5a and known as a *four-bar linkage*) is statically underdeterminate with one degree of freedom. Sketch this degree of freedom by showing another possible configuration of the assemblage.

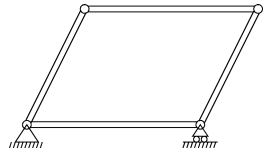

3.1-10. Show that if an additional support is provided to the assemblage of the preceding problem, as shown in the following figure, then the assemblage is statically determinate even though the external reactions number four. (Hint: compare with the structure of Fig. 3.6c.)

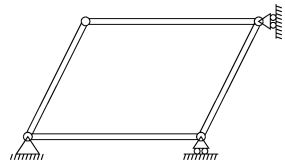

3.2 Two-Dimensional Trusses

3.2.1 Introduction

The structures of Figs. 3.5c and 3.6c are simple examples of statically determinate trusses, formed by adding triangles to a simply supported triangle and to a straight-legged three-pinned arch, respectively. They can be extended by increasing the number of triangles, not necessarily externally as illustrated in Fig. 3.5, but also internally: if a pin is inserted in the bar forming one side of a triangle and another bar is attached to it and to the pin at the opposite vertex, the result is the addition of one joint and two bars and thus the creation of an additional triangle, as shown in Fig. 3.7, where the added pins and bars are drawn with broken lines.

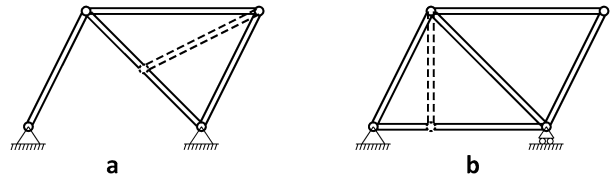

Figure 3.7. Truss extension by internal addition of triangles

While the joints are usually treated as pin joints, other kinds of connections are often used in practice, such as bolting or welding the ends of the members to a common plate (called a *gusset plate*), as shown in Fig. 3.8. Although such joints are in fact relatively rigid, the error resulting from treating them as pin joints turns out to be slight if the center lines of the connecting members are concurrent.

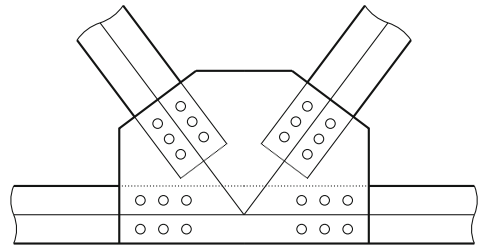

Figure 3.8. Joint with a gusset plate

3.2.2 Types of Trusses

The arch-based truss of Fig. 3.7a, with no bars connecting the supports directly, is also called an *open truss*, and is most likely to be found as a cantilevered one, like the one shown in Fig. 3.9. (In this figure and subsequent

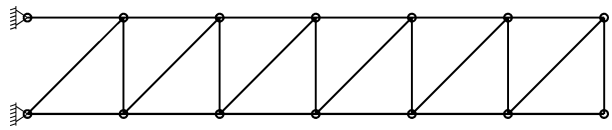

Figure 3.9. Cantilevered truss

ones the members are depicted by simple lines.)

In the simply supported truss of Fig. 3.7b, there is a line of bars going directly from one support to the other; these bars constitute the *bottom chord* of the truss. The *top chord* is constituted by the array of exterior members along the top of the truss, whether straight or not. The interior members connecting them, vertical and diagonal, constitute the *web*.

Trusses supporting roofs or bridges are normally simply supported, with the supports usually placed as far apart as possible, as shown in Fig. 3.10. The

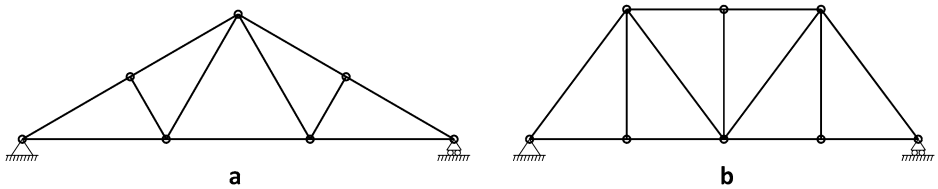

Figure 3.10. Simply supported trusses

truss of Fig. 3.10a is a *pitched* truss of a type that would be used to support a symmetric pitched roof. The truss of Fig. 3.10b is a typical bridge truss and is called a *flat* truss, even if the end panels are pitched. (The particular truss shown, with the interior diagonals sloping down toward the center, is known as a *Pratt*[*] truss.)

Consider, now, a truss similar to that of Fig. 3.10a but with the interior diagonals sloping up toward the center, and with additional horizontal and vertical members in the end panels, so that it is completely flat, as shown in Fig. 3.11; such a truss is known as a *Howe*[†] truss. If the loads are applied only at the bottom joints, as shown in the figure, then the method of joints applied to the endmost upper joints yields the result that the additional members

[*]Thomas Willis Pratt (1812-1875) was an American engineer.
[†]William Howe (1803-1852) was an American bridge builder.

carry no force; by definition, they are then *zero-force members*, and may consequently be dispensed with.

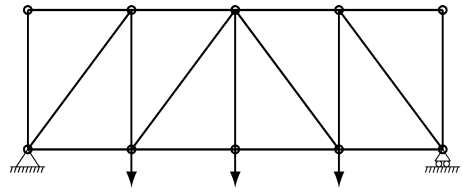

Figure 3.11. Truss with zero-force members

A zero-force member is also present in any three-bar joint, subject to no external, force where two truss members are collinear, as in Fig. 3.12. Here, the non-collinear member bears no force, as easily determined from force equilibrium in the direction perpendicular to the collinear members.

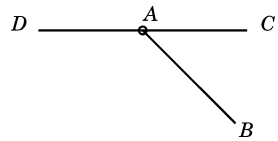

Figure 3.12. Joint A with zero-force member AB

3.2.3 Truss Analysis by the Method of Joints

As we discussed in the preceding section, in a statically determinate truss, with Eq. (3.1) satisfied, the $2j$ joint equilibrium equations are just enough to determine the n bar forces and the r support reactions. These equations must, in general, be solved simultaneously. The actual solution, if the joints number more than a few, can be carried out with the help of a computer program. This requires writing the equilibrium equations for all joints, casting them as a system of linear algebraic equations in matrix form, and, finally, solving the system. But, in view of the work needed to set up the matrix and solve the system, it may be more convenient to proceed joint by joint, where there are only two equations to be solved at a time. This is especially easy if there is one unsupported joint where only two bars meet, because in that case the two joint equilibrium equations immediately yield the two bar forces. The trusses of Fig. 3.10, by contrast, have no unsupported two-bar joint, and therefore, if the joint-by-joint procedure is to be followed, at least one reaction must be determined from the equilibrium of the whole truss before the method of joints can be used.

If the weight of truss members is to be included with the external forces and the weight is uniformly distributed along each bar, then equilibrium implies that the bar contributes half of its weight to each of its two joints, as shown in Fig. 3.13.

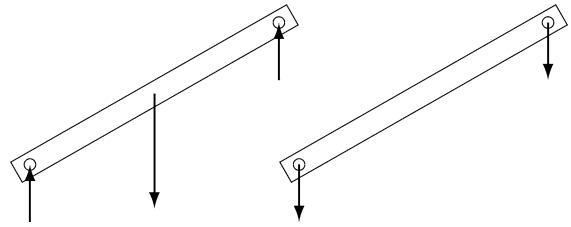

Figure 3.13. Distribution of truss-bar weight to its joints

Some examples of the application of the method of joints to trusses will now be presented.

Example 3.2.1: Cantilevered truss.
Consider a cantilever truss like that of Fig. 3.9, but with only two panels, loaded as shown in Fig. 3.14a, with the free-body diagram shown in Fig. 3.14b. The

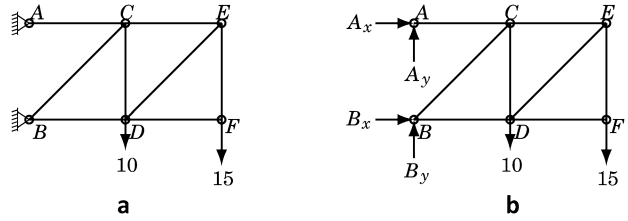

Figure 3.14. Short cantilevered truss

panels are assumed to be square (so that the diagonals are at 45°), and no dimensions or units are given.

Note that joint F meets the criteria specified above, and its force equilibrium immediately yields the result that the force in bar DF is 0 (the bar is thus a zero-force member), while in bar EF it is 15 (tension). With this information we can now proceed to joint E, where the only unknown forces are now those in bars CE and DE. The free-body diagram of this joint is shown in Fig. 3.15b, and the equilibrium equations are

$$\sum F_x = 0 = -P_{CE} - P_{DE}/\sqrt{2}$$

and

$$\sum F_y = 0 = -15 - P_{DE}/\sqrt{2}\,,$$

from which in follows that $P_{DE} = -15\sqrt{2} = -21.1$ (the minus sign means that the bar is in compression) and $P_{CE} = +15$ (tension).

Knowing P_{DE} and P_{DF} we can proceed to analyze joint D, where the still unknown forces are now P_{BD} and P_{CD}, and the free-body diagram is shown in Fig. 3.15c. The equilibrium equations are

$$\sum F_x = 0 = -P_{BD} + (-15\sqrt{2})/\sqrt{2}$$

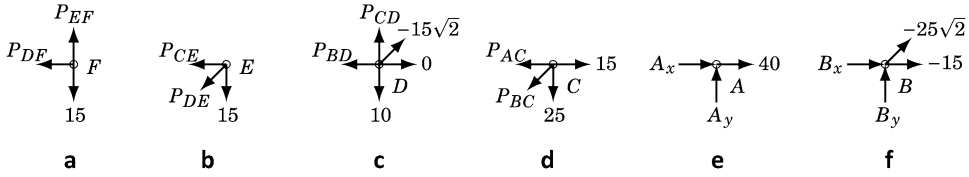

Figure 3.15. Free-body diagrams of the joints of the truss of Fig. 3.14

and

$$\sum F_y = 0 = P_{CD} - 10 + (-15\sqrt{2})/\sqrt{2}\,.$$

Hence $P_{BD} = -15$ (compression) and $P_{CD} = +25$ (tension).

The remaining unknown bar forces are P_{AC} and P_{BC}, and they are obtained from the equilibrium of joint C, as shown in Fig. 3.15d. From the equations

$$\sum F_x = 0 = -P_{AC} - P_{BC}/\sqrt{2} + 15$$

and

$$\sum F_y = 0 = -P_{BC}/\sqrt{2} - 25\,,$$

we obtain $P_{AC} = 40$ (tension) and $P_{BC} = -25\sqrt{2} = -35.4$ (compression).

With all the bar forces determined, the equilibrium equations for joints A and B, with free-body diagrams shown in Fig. 3.15e–f, give the reactions there. At A we have, obviously, $A_x = -40$ (that is, the support pulls the truss to the left) and $A_y = 0$, while at B we have $B_x = 40$ and $B_y = 25$.

The complete force diagram of the truss, showing the member forces and the external forces (loads and reactions), is shown if Fig. 3.16, in which C and T stand for compression and tension, respectively.

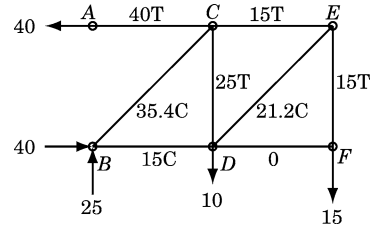

Figure 3.16. Force diagram of the truss of Fig. 3.14

It is easy to see that force equilibrium for the truss as a whole is satisfied: $\sum F_x = 40 - 40 = 0$ and $\sum F_y = 25 - 10 - 15 = 0$. For moment equilibrium, let us take moments about B; then, if the width or height of each square panel is a, $\sum M_B = 40a - 10a - 25(2a) = 0$. Global equilibrium therefore serves as a check on the calculations.

Example 3.2.2: A roof truss.
Suppose that the roof truss of Fig. 3.10a has the loads and dimensions shown in

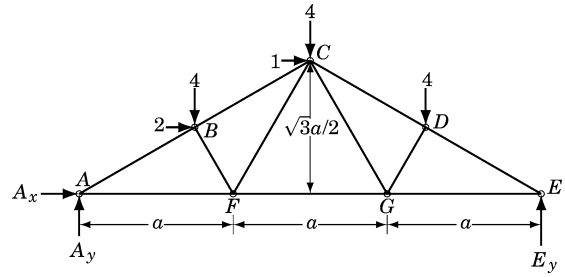

Figure 3.17. Loads, reactions and dimensions on the roof truss of Fig. 3.10a

Fig. 3.17, with the support reactions also shown. The vertical loads represent the weight of the roof, as transmitted to the truss joints by purlins, while the horizontal loads represent the force of wind, assumed in this case to be blowing from left to right.

In order to begin the application of the method of joints at E, we need the reaction E_y. This is easily determined by moment equilibrium about A:

$$\sum M_A = E_y(3a) - 4(9a/4) - 4(3a/2) - r(3a/4) - 1(\sqrt{3}a/2) - 2(\sqrt{3}a/4) = 0\,,$$

resulting in $E_y = 6.58$. With this information we can now perform joint equilibrium at E to yield $P_{DE} = -13.15$[‡] and $P_{EG} = 11.39$. With the former result we go to joint D. But here, instead of taking horizontal and vertical force equilibrium, we can instead do so with respect to the axes x' (along the chord CDE) and y' (along GD; along these axes the load at D has the respective components $+2.00$ and -3.46, and consequently $P_{CD} = -11.15$ and $P_{DG} = -3.46$. Note that this last result was obtained independently of the forces in the adjacent members, as happens whenever one of three bars meeting at a joint is perpendicular to the other two (a similar situation happens at B).

Knowing P_{DG} and P_{EG}, we can proceed to joint G. For vertical force equilibrium, the vertical components of P_{EG} and P_{CG} must be equal and opposite, but since both of these bars form a $60°$ angle with the horizontal, their resultants must be likewise, and consequently $P_{CG} = +3.46$. Horizontal force equilibrium now gives $P_{FG} = +7.93$.

Next, we go to C, where the equilibrium equations are

$$\sum F_x = 1 - (\sqrt{3}/2)P_{BC} - (1/2)P_{CF} - (\sqrt{3}/2)11.15 - (1/2)3.46 = 0$$

and

$$\sum F_y = -4 - (1/2)P_{BC} - (\sqrt{3}/2)P_{CF} + (1/2)11.15 + (\sqrt{3}/2)3.46 = 0\,,$$

yielding $P_{BC} = -10.58$ and $P_{CF} = +4.46$.

At this point, knowing P_{BC}, P_{CF} and P_{FG}, we have the choice of proceeding to B and F in either order. But of the four equilibrium equations at these joints only three are necessary, since there only three remaining unknown bar forces: P_{BF}, P_{AB} and P_{BF}; the fourth equation is consequently redundant, but may be used as a check on the calculations thus far. The reason is that we used a global

[‡]To keep algebraic operations consistent, we write all numbers to two decimal places.

equilibrium equation (which is a linear combination of the joint equations) at the outset, and therefore the full set joint equations is no longer a set of independent equations.

If, then, we first go to F, we find, in the same way as at G, that $P_{BF} = -4.46$ and $P_{AF} = +12.39$. At B, equilibrium of forces along BF confirms the former result, while equilibrium along ABC yields $P_{AB} = -10.85$. Finally, equilibrium at A gives the reactions $A_x = -3$ and $A_y = 5.42$. It is easy to see that results, together with the previously derived E_y, satisfy force equilibrium for the truss as a whole.

If we had chosen, instead, to begin the procedure at A, it would have been necessary to use two global equilibrium equations in order to determine the reactions there, and therefore two of the joint equations would have been redundant: one of the four equations at D and G, and horizontal force equilibrium at E.

3.2.4 Truss Analysis by the Method of Sections

The method of sections, discussed in Sect. 2.4, is a way of determining internal force resultants by sectioning the body into two parts and ensuring that each part is in equilibrium. For slender members under two-dimensional loading, as we saw, the three equilibrium equations furnish the axial and shear forces and the bending moment.

When the method of sections is applied to trusses, then a cut that goes through a number of bars allows for the determination of up to three unknown bar forces. The method is especially useful when it is desired to determine the forces in just one or a few members, even more so if the member or members are toward the interior of the truss.

In the particular case of a cut such that all the unknown forces, except the one in the desired member, are concurrent, the desired member force can be determined by moment equilibrium about the point of concurrency.

In general, identifying the cut necessary to deduce the force of a given member requires a combination of visual interpretation skills and experience. In contrast, the method of joints is entirely formulaic, hence procedurally straightforward.

By way of example, we will apply the method of sections to the same roof truss that we analyzed by the method of joints in Example 3.2.2.

Example 3.2.3: Roof truss of Example 3.2.2.
In the just-discussed truss shown in Fig. 3.17, it is possible to determine the force in member DE on its own by means of the cut shown in Fig. 3.18a, where, as can be seen, the unknown forces are A_x, A_y, P_{EG} and P_{DE}. But only the last-named force has a nonzero moment about A. By extending the force along its line of action to E and resolving it into horizontal and vertical components, this moment can be found to be $-(P_{DE}/2)(3a)$. Thus, for the section, moment

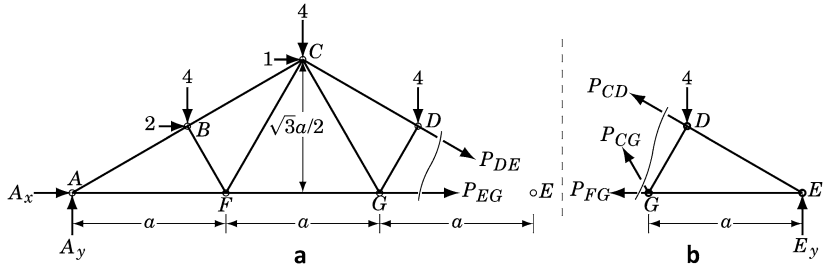

Figure 3.18. Method of sections for the forces in members DE and CG in the truss of Fig. 3.17

equilibrium about A requires that

$$-(P_{DE}/2)(3a) - 4(9a/4) - 4(3a/2) - 4(3a/4) - 1(\sqrt{3}a/2) - 2(\sqrt{3}a/4) \;=\; 0\,,$$

from which $P_{DE} = 13.15$, as before. P_{EG}, on the other hand, cannot be determined without knowing the reaction A_x, unless we take the section to the right of the cut, in which case we are back to the method of joints.

In the section shown in Fig. 3.18b, the force P_{CG} can similarly be determined independently of other forces by means of moment equilibrium about E:

$$\sum M_E \;=\; -(\sqrt{3}/2)P_{CG}(a) + 4(3a/4) = 0\,,$$

so that $P_{CG} = 3.46$ as before. The determination of the other member forces, however, requires the reaction E_y to be calculated beforehand. P_{CD} can then determined from moment equilibrium about G, and P_{FG} from moment equilibrium about C. The possibility of determining all three member forces by moment equilibrium, independently of one another, is due to the fact that no two of them are parallel.

Whether the method of joints or the method of sections will be used for any particular truss problem depends on the nature of the problem and the computing power available. If solving a large number of simultaneous algebraic equations does not present much difficulty, then setting up all the joint equilibrium equations is a straightforward procedure, with the overall equilibrium equations providing a check on the results. If the solution is to be done by hand, then experience will be the guide.

Exercises

3.2-1. Consider the tower truss shown in the figure below.

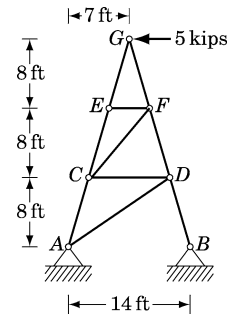

(a) Use the method of joints to determine all the bar forces starting from the top joint G. Identify zero-force members, if any.

(b) Recalculate all the bar forces by starting with the determination of the external reactions and proceeding from the base of the structure to the top.

3.2-2. Consider the truss shown in the figure below.

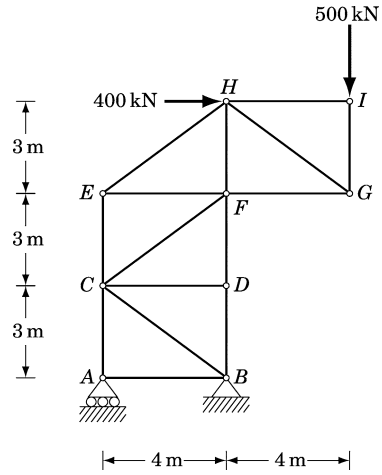

(a) Use the method of joints to determine all the bar forces starting from the top right joint I. Identify zero-force members, if any.

(b) Recalculate all the bar forces by starting with the determination of the external reactions and proceeding from the base of the structure to the top.

3.2-3. Determine the maximum value of the force F in the truss shown below if the allowable tensile force in any bar element is $P_t = 1000kN$ and the

allowable compressive force is $P_c = 800kN$. Which is (are) the critical bar(s) in deducing this maximum value?

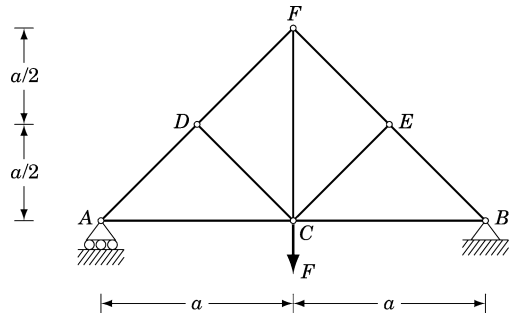

3.2-4. Use the method of sections to determine the bar forces P_{AC}, P_{AD} and P_{BD} of the tower truss of Exercise **3.2-1**.

3.2-5. A three-paneled cantilevered truss is used to support a vertical load W, as shown in the figure below. Assuming square panels, use the method of sections to determine the three bar forces of the leftmost panel in terms of W.

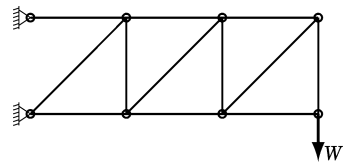

3.2-6. Use the method of sections to show that, in the truss of the figure above, all the vertical members carry a tensile force equal to W. What can you say about the diagonal members?

3.2-7. Use the method of joints to determine the bar forces in the horizontal members of the truss of the preceding exercise.

3.2-8. The truss in the figure below consists of two equilateral triangles ABC and DEF which share the same center of area and are connected by bars AD, BE, and CF. Use the method of sections to determine the forces P_{AD}, P_{BE} and P_{CF}.

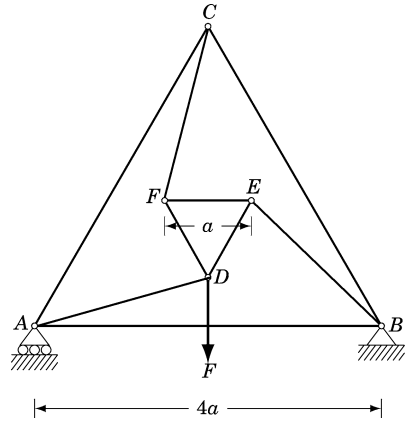

3.2-9. For the truss shown below, identify by inspection any zero-force members. Subsequently, use the method of sections to determine the forces P_{CB}, P_{CG} and P_{BG}.

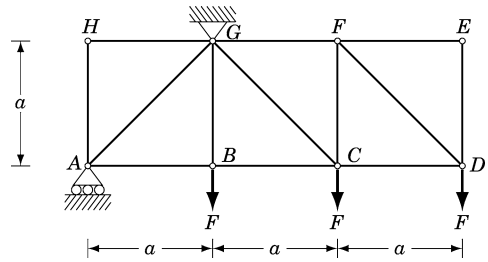

3.2-10. In the hexagonal truss shown in the figure below all truss bars have length 2 m.

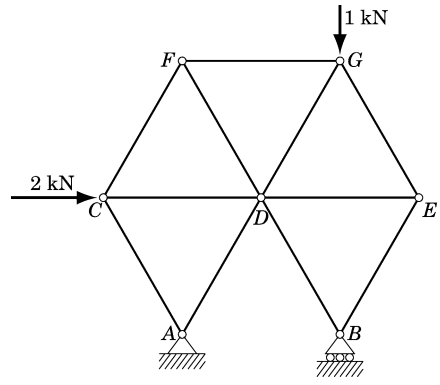

(a) Draw the free-body diagram of the truss.

(b) Show that the truss is statically determinate.

(c) Determine the external reactions at points A and B.

(d) Determine the forces in members DE, FG, BD and BE and state explicitly if they are in tension or compression.

3.2-11. Consider a planar truss bridge and let a vehicle of weight W be placed on it, as shown in the figure.

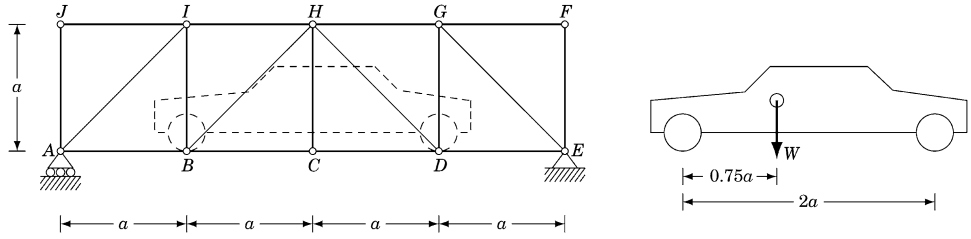

(a) Identify all zero-force members of the truss structure.

(b) Determine the external reactions at points A and E due to the weight for the vehicle.

(c) Determine the forces of members CD and IH due to the weight of the vehicle.

(d) Assume that the vehicle moves horizontally by a distance a to the left of its depicted position. How does the answer to part (c) change in this case?

3.3 Three-Dimensional Trusses

3.3.1 Introduction

Three-dimensional trusses (or *space trusses*) are a subclass of a class of structures known as space frames or space structures. They are called trusses, in principle, if all the joints are ball-and-socket (by analogy to the pin joints in plane trusses), but this not always followed in practice. Furthermore, as in the case of plane trusses, bolted or welded connections may be approximated as ball-and-socket joints if the centerlines of the joined members intersect at a point.

The analysis of all but the simplest of space trusses, while not different in principle from that of planar ones, becomes very involved analytically as the geometry becomes complicated, and is outside the scope of this book. The treatment in this section is for purposes of illustration only.

3.3.2 Simple Space Trusses

A *simple space truss* is one that is built up (by analogy with the discussion in Sect. 3.2) by adding tetrahedra (three bars and one new joint at a time) to an initial tetrahedron that may be closed or open, resulting in trusses that are the three-dimensional analogues of those of Figs. 3.5c and 3.6c, respectively. An open initial tetrahedron is essentially a tripod; it consists of three bars, each attached to the foundation with a ball-and-socket joint, as shown in Fig. 3.19a. Here $n = 3$, $j = 4$ and $r = 9$, so that Eq. 3.2 (page 111) is satisfied. A closed initial tetrahedron is made up of six bars connected to one another with four joints, three of which are attached to the base in such a way that the total number of constraints is six and they are proper, as shown in Fig. 3.19b; thus $n = 6$, $j = 4$, and $r = 6$, and Eq. 3.2 is likewise satisfied. In Fig. 3.19c, on the other hand, the supports are improper (the proof is left to an exercise).

Example 3.3.1: Towerlike simple space truss.
The construction of a rectangular towerlike structure by the successive addition of four tetrahedra to the initial one of Fig. 3.19b is shown in Fig. 3.20a–d. In each picture the added bars are indicated with thick lines. In picture a, the new joint E is connected to the initial structure by means of bars BE, CE and DE, forming the tetrahedron $BCDE$, and so on. Picture e shows a modification of the structure of Fig. 3.20d, in which the ground-level joint H has been anchored to the base, so that the connection at C has been changed in order to keep the structure statically determinate.

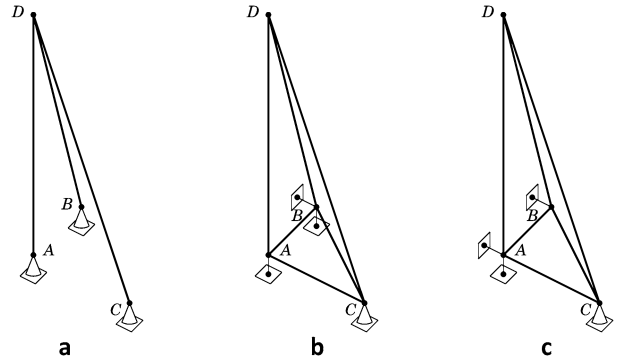

Figure 3.19. Initial tetrahedra: (**a**) open, (**b**) closed with proper constraints, (**c**) closed with improper constraints

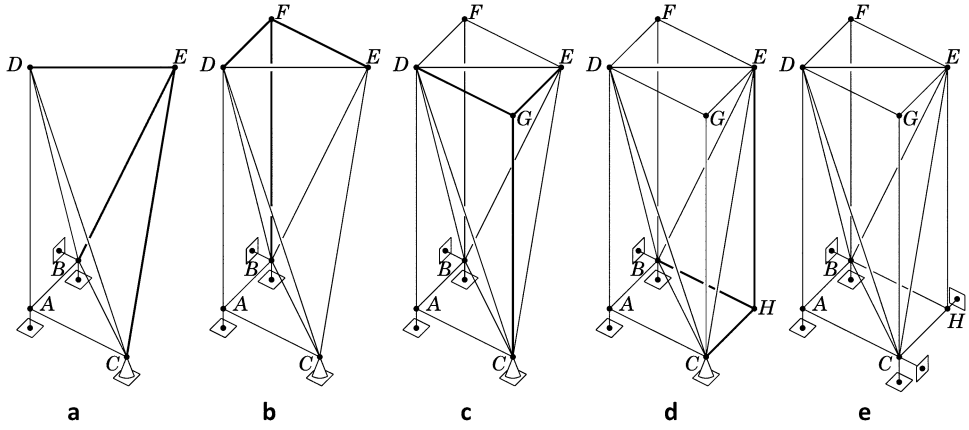

Figure 3.20. Construction of a towerlike simple space truss

3.3.3 Parallel Plane Trusses

When plane (two-dimensional) trusses are used to support roofs or bridges, at least two of them will normally be required. In the case of roof supports, three-dimensional stability is usually achieved by the diaphragm action* of the roof and the wall structures carrying the trusses. When two plane trusses support the bridge, however, the bridge deck may not be sufficient for such stability, and the trusses may need to be interconnected to form a three-dimensional structure.

Example 3.3.2: Two parallel trusses.
We consider two parallel and identical simply supported plane trusses, which are to be joined by transverse bars into a statically determinate three-dimensional truss.

*This refers to the relative rigidity of a planar structure in its own plane.

Let the number of joints and of bars in each of the two-dimensional trusses be j_0 and n_0, respectively. Then, by Eq. 3.1, $n_0 = 2j_0 - 3$. Let the supports be modified so that the constraints on the combined assemblage are proper but their number remains six. If the number of additional bars is n', then the total number of bars is $2n_0 + n' = 4j_0 - 6 + n'$, and since the total number of joints is now $2j_0$, Eq. 3.2 is satisfied if $n' = 2j_0$. This can be achieved if a bar perpendicular to the trusses is inserted between each pair of matching joints and, in addition, a bar is placed along one diagonal of some of the resulting rectangles. A possible arrangement

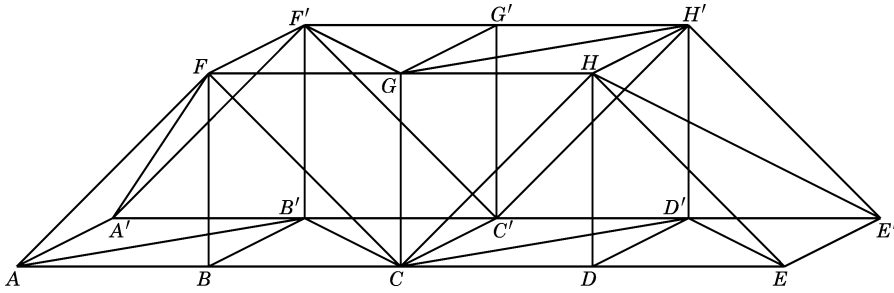

Figure 3.21. Two parallel trusses joined by bars to make a three-dimensional truss

of transverse bars for two Pratt trusses, each composed of six right triangles made by thirteen bars and eight joints, is shown in Fig. 3.21. Here the diagonal bars are placed in the eight external rectangles. If, however, such a truss is to support a bridge, then bars $A'F$ and $E'H$ (or any other diagonal bars joining lower and upper joints) would impede traffic, and their removal would require two additional internal constraints, such as braces at G and G' preventing the rotation of bars CG and $C'G'$ relative to bar GG', as shown in Fig. 3.22. An actual example of such a truss is shown in Fig. 3.23.

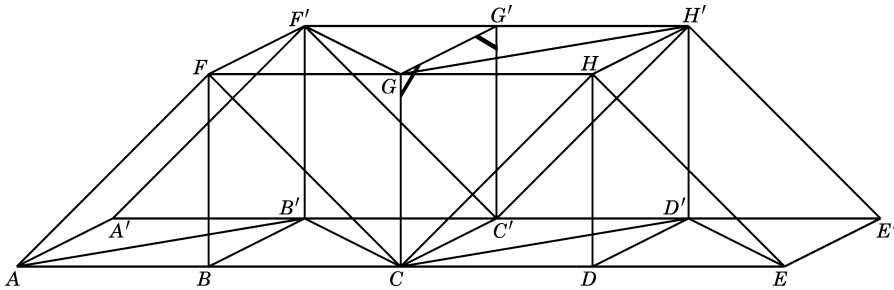

Figure 3.22. Modification of the three-dimensional truss of Fig. 3.21 by means of braces at G and G'

Figure 3.23. A single-track railroad bridge, converted to pedestrian use, in Walnut Creek, California (USA)

3.3.4 Telescope "Tubes"

In large telescopes, the tube that is characteristic of small-scale telescopes (like the Hevelius[†] telescope shown in Fig. 3.24a) is typically replaced by a three-dimensional truss in order to save weight. Fairly typical is the rather simple *Serrurier truss*, an example of which (the Shane Telescope of the Lick Observatory on Mount Hamilton near San Jose, California) is shown in Fig. 3.24b.

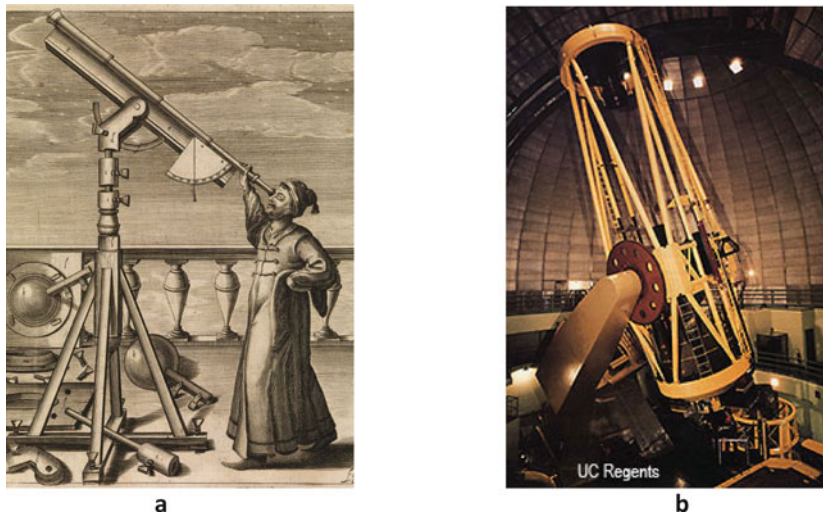

Figure 3.24. Telescope "tubes"

[†]Johannes Hevelius (1611–1687) was a Polish astronomer

In the telescopes of the Keck Observatory (on Mauna Kea in Hawaii), whose primary mirrors are hexagonal rather than of the usual circular shape, the "tube" truss is somewhat more complicated, as shown in Fig. 3.25. The figure also shows the small hexagonal assembly of simple trusses, seen near the top, that supports the secondary mirror.

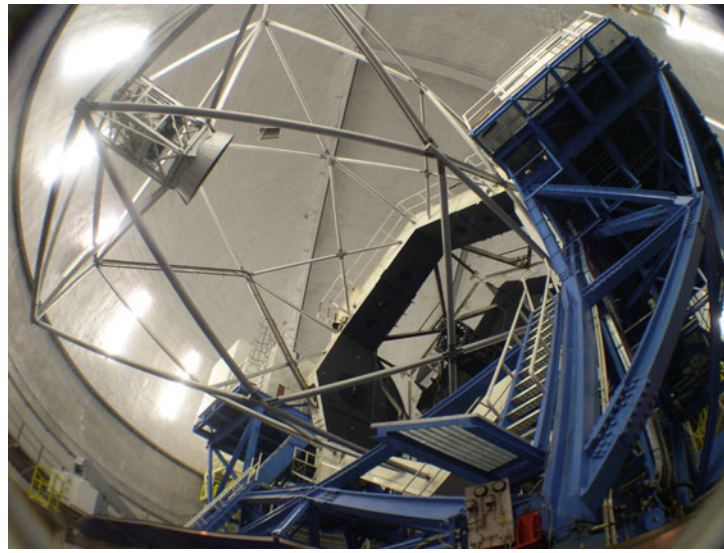

Figure 3.25. "Tube" of the Keck Observatory telescope

Exercises

3.3-1. Show that the supports of Fig. 3.19b provide a proper set of constraints (in the sense that no rotation of the figure is possible), while the constraints of Fig. 3.19c are improper.

3.3-2. In a tetrahedral truss like that of Fig. 3.19b, let the dimensions be $\overline{AB} = \overline{AC} = a$ and $\overline{AD} = 2a$, with AB, AC and AD mutually perpendicular. If a force F parallel to member AB (directed from A to B) acts at joint D, find the support reactions at A, B and C.

3.3-3. An assemblage of bars in the shape of a cube is assumed to be properly supported. How many diagonal bars are necessary for static determinacy? Sketch a possible arrangement.

3.3-4. A space structure in the shape of a pyramid is shown in the figure below. Find a proper set of supports that will make the structure statically determinate.

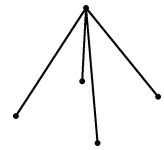

3.3-5. Find a combination of additional bars that will make the structure of Exercise **3.3-4** internally statically determinate (that is, isostatic with a proper set of external supports). Sketch a possible arrangement of bars and supports, and discuss in terms of tetrahedron addition.

3.3-6. A space structure in the shape of a two-tiered pyramid is shown in the figure below. Find a proper set of supports that will make the structure statically determinate.

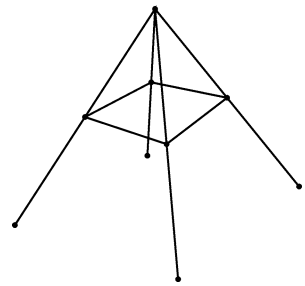

3.3-7. Find a combination of additional bars that will make the structure of Exercise **3.3-6** internally statically determinate (that is, isostatic with a proper set of external supports). Sketch a possible arrangement.

3.3-8. If, in the preceding exercise, it is desired to avoid horizontal bars at ground level, find a combination of additional bars *and* external support that will make the structure statically determinate.

3.3-9. Two parallel plane trusses having the form shown in the figure below are joined to form a three-dimensional truss. Find the number of additional bars needed for static determinacy, and sketch a possible arrangement.

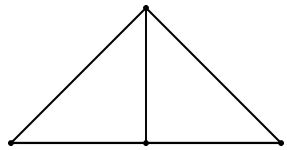

3.3-10. If, in the space truss of the preceding exercise, it is desired to keep the "traffic" space clear (as discussed in Example 3.3.2), find the minimum number of corner braces that would be necessary.

3.3-11. Two parallel plane trusses having the form shown in the figure below are joined to form a three-dimensional truss. Find the number of additional bars needed for static determinacy, and sketch a possible arrangement. Discuss the difference, if any, between this result and that of Exercise **3.3-3**.

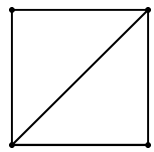

3.3-12. If, in the space truss of the preceding exercise, it is desired to keep the "traffic" space clear (as discussed in Example 3.3.2), find the minimum number of corner braces that would be necessary.

3.4 Frames and Machines

3.4.1 Introduction

Articulated systems whose members are not all two-force members (that is, at least one of them is a *multiforce member*) are known as *frames* or *machines*, depending on how they are used. Frames are typically stationary and are intended to support loads, while machines (as the term is used in the context of solid mechanics) include moving parts and are intended to change the effect of loads, in direction, magnitude or both.

The objective here is to determine all the forces that act on each member of a frame or machine using only the equilibrium equations, if this is possible. The approach is straightforward: we will draw free-body diagrams of the complete structure and/or individual members of it, and subsequently we will write the equilibrium equations and solve them to determine the forces on each member.

3.4.2 Frames

Frames are commonly encountered in a wide array of engineering systems, including prominently building systems. Some representative examples follow.

Example 3.4.1: Three-pinned arch.
A simple example of a frame is a straight-legged three-pinned arch with forces at the midpoints of the members, as shown in Fig. 3.26a. Just as would have

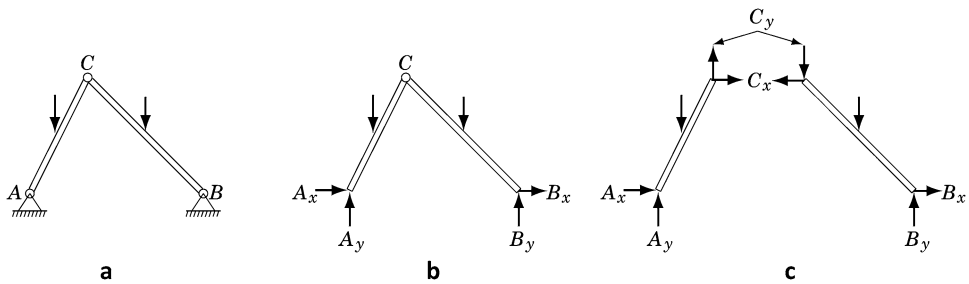

Figure 3.26. Straight-legged three-pinned arch loaded at the midpoints of the members

been the case if the arch had been loaded at the pin, a free-body diagram of the whole structure (Fig. 3.26b) yields only three equilibrium equations for the four unknown reactions A_x, A_y, B_x and B_y. Cutting the arch at the pin C, as in Fig. 3.26c, produces two additional unknown force components, namely C_x and C_y, raising the total to six, but the equilibrium of each member gives us three equations, for a total of six.

Example 3.4.2: Built-in signpost.
Another simple frame is the braced, built-in signpost shown in Fig. 3.27a. Unlike the previous example, this frame is stable when it is released from the

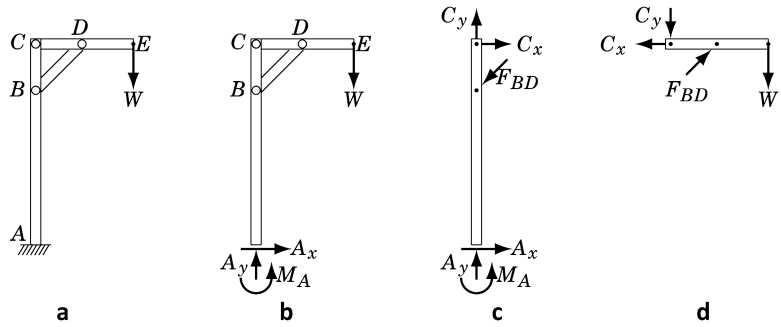

Figure 3.27. Braced built-in signpost

supports, and consequently the support reactions can be determined from the free-body diagram of the whole frame, shown in Fig. 3.27b. But the members ABC and CDE are multiforce members, and in order to determine the forces acting on the members the frame must be decomposed at the pins, with the free-body diagrams of these members shown in Figs. 3.27c and 3.27d, respectively. Since member BD is a two-force member, the direction of its member force F_{BD} is known, and consequently the additional unknowns are three in number: the x- and y-components of the pin force at C and the member force F_{BD}. Any two of the three free-body diagrams of Figs. 3.27b–d can be combined to yield the necessary six equilibrium equations, but it is easiest to use those of b and d, since the former can be used to give the support reactions and the latter the internal reactions, independently of each other. The free-body diagram of c can then be used as a check on the results.

Suppose, for example, that the height of the post ABC is h, while the length of the segments BC, CD and DE is $0.3h$. Applying the equilibrium equations $\sum F_x = 0$, $\sum F_y = 0$ and $\sum M_{(A)} = 0$ to the free-body diagram of Fig. 3.27b immediately yields the results

$$A_x = 0 \quad , \quad A_y = W \quad , \quad M_A = 0.6Wh \, . \tag{3.3}$$

When these results are inserted into the equilibrium equations for the free-body diagram of Fig. 3.27c, we obtain

$$C_x - F_{BD}/\sqrt{2} = 0 \quad , \quad C_y + W = 0 \quad , \quad 0.6Wh + (F_{BD}/\sqrt{2})(0.7h) - C_x h = 0 \, . \tag{3.4}$$

For the free-body diagram of Fig. 3.27d, the equilibrium equations (with the moments taken about C) are

$$F_{BD}/\sqrt{2} - C_x = 0 \quad , \quad -C_y - W = 0 \quad , \quad (F_{BD}/\sqrt{2})(0.3h) - 0.6Wh = 0 \, . \tag{3.5}$$

In these two sets of equations, the first and second equations are obviously equivalent, and the third equation of the first set becomes equivalent to that of the second set when the substitution $C_x = F_{BD}/\sqrt{2}$ is made in the former. The results are $C_x = 2W$, $C_y = -W$ and $F_{BD} = 2\sqrt{2}W$.

Example 3.4.3: Stepladder.
As yet another example, let us consider the hinged stepladder shown in Fig. 3.28a. Such a ladder becomes a frame when the spreader is fully extended, as in Fig. 3.28b, and may consequently be treated as a two-force member.

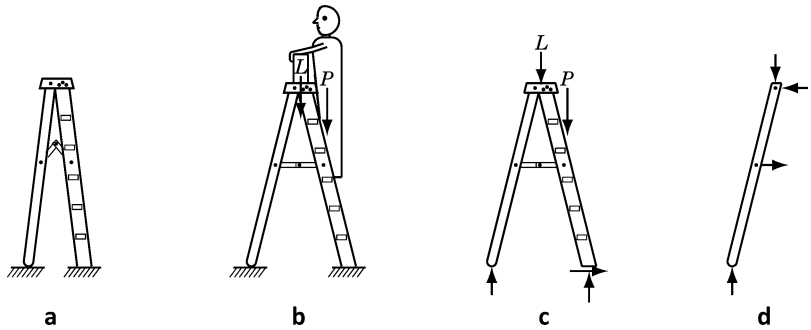

Figure 3.28. Stepladder

The support leg is assumed to be in frictionless contact with the ground and to be hinged to the top platform, which is rigidly attached to the step leg. The ground contact of the step leg has friction. The platform carries a load L (a tool box, a paint bucket or the like), and a person of weight P stands on the third step. The ladder as a whole is statically determinate, with the free-body diagram shown in Fig. 3.28c. When the vertical ground reaction under the support leg is determined, the free-body diagram of this leg, shown in Fig. 3.28d, allows the determination of the spreader tension and the force transmitted by the platform hinge. Details are left to Exercise **3.4-5**.

3.4.3 Machines

Machines are like frames in that they include one or more multiforce member, but unlike them they are not rigid but have one or more internal degrees of freedom. Moreover, instead of carrying loads that are transmitted to external supports, a machine transmits applied forces to the object (known as the *workpiece* or sometimes as the *work*) that it operates on. The operation may be clamping (pliers, tongs, clamp), cutting (shears, scissors), lifting (jack), turning (adjustable wrench), compressing (vise) and the like. In each case, we examine the equilibrium of the device in a particular configuration with regard to the workpiece.

Example 3.4.4: Pliers.

In Fig. 3.29a we see a pair of pliers whose jaws are clamping a cylindrical workpiece, with a transverse pair of forces of magnitude P applied symmetrically to the handles. Because of symmetry, the forces Q transmitted to the work (shown

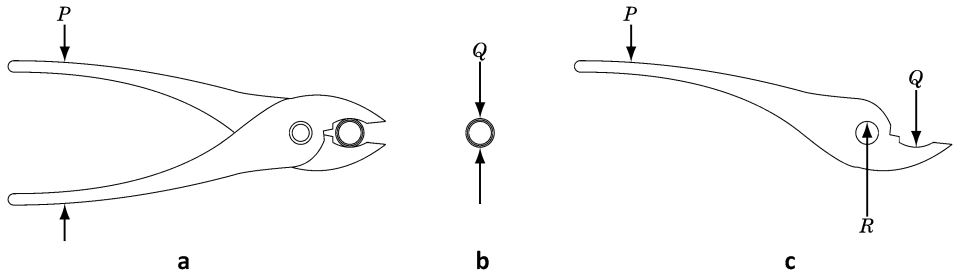

Figure 3.29. Straight pliers

in Fig. 3.29b) are also transverse, as are the forces R transmitted to the pin. The free-body diagram for one half of the pliers is shown in Fig. 3.29c, and that for the other half would simply be its mirror image. The problem is thus equivalent to that of a seesaw or of a lever with transverse forces only.

The symmetry does not hold in the case of slip-joint pliers, shown in Fig. 3.30. The analysis will be left to an exercise.

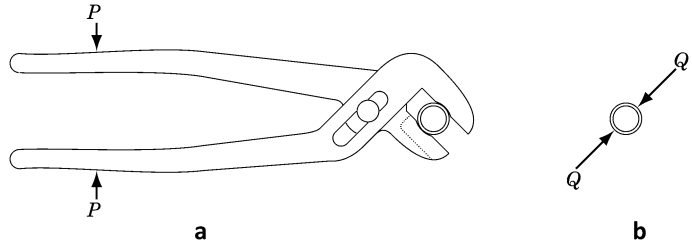

Figure 3.30. Slip-joint pliers

Example 3.4.5: Toggle vise.
Vises and similar clamping devices typically use screw mechanisms, which

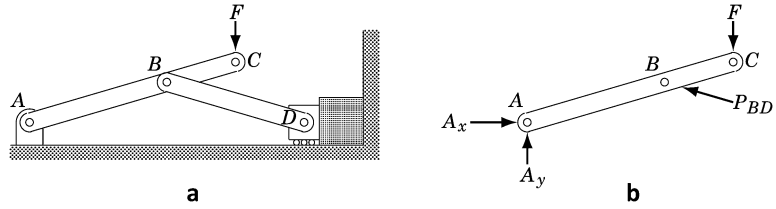

Figure 3.31. Toggle vise

derive their clamping force through friction, and whose analysis is outside the scope of this book. A vise based on a *toggle* mechanism is shown in Fig. 3.31a, with the free-body diagram of the multiforce member ABC in Fig. 3.31b. For a given applied load F, the compressive force P_{BD} in the two-force member BD can be determined by moment equilibrium about A, and the clamping force is its horizontal component.

Example 3.4.6: Modeling of leg extension. The human musculoskeletal system is, like most biological structures, a very complex mechanical system. (Or, rather, a *mechanochemical* system, since the internal forces may be generated by chemical reactions, such as those leading to muscle contraction.) Some of its subsystems can, however, be approximately modeled as fairly simple machines. One example is the mechanism of knee extension (straightening of the leg from a flexed position). The knee is essentially a hinge joint, and the patella (kneecap) acts like a pulley, with the quadriceps and patellar tendons together acting like a cable sliding over it. The contraction of the quadriceps muscle provides the tension T. The patellar tendon is attached to the tuberosity of the tibia, as shown in Fig. 3.32a, where the force F is provided by an exercise machine like that in Fig. 2.31 (page 81). The weight of the lower leg is not included here, but it is (labeled W) in the free-body diagram of the lower leg shown in Fig. 3.32b, R being the reaction at the knee joint; the angle α is known as the *Q angle*. An anatomical drawing of the joint is shown in Fig. 3.32c.

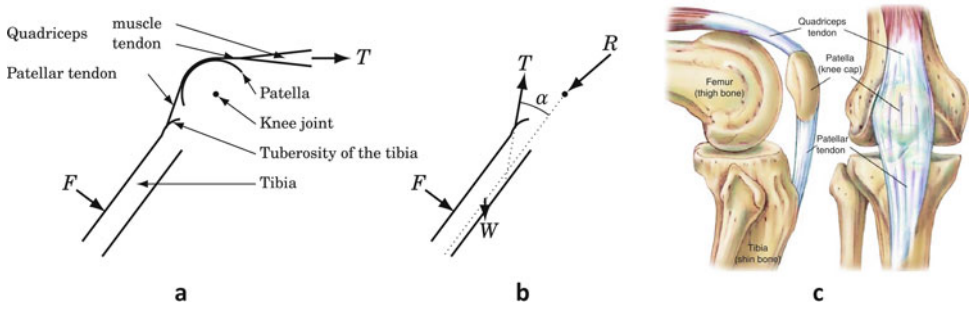

Figure 3.32. Leg extension: (**a**) simple mechanical model, (**b**) free-body diagram of lower leg, (**c**) the knee joint

Exercises

3.4-1. Determine all forces acting on each of the two members of the three-pinned structure shown in the figure below.

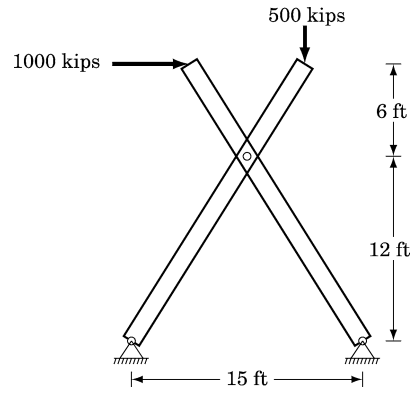

3.4-2. Determine all forces acting on each of the two members of the three-pinned structure shown in the figure below.

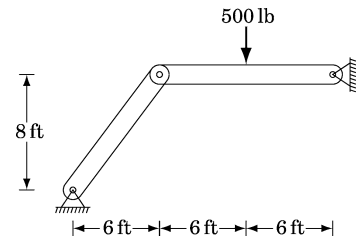

3.4-3. Determine all forces acting on each of the three members of the structure shown in the figure below.

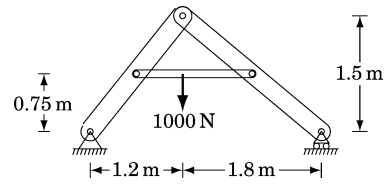

3.4-4. In the structure of the preceding exercise, the load is moved so that it is halfway between the pins supporting the horizontal bar. Determine all forces acting on the members.

3.4-5. Determine all forces acting on each of the three members of a stepladder (as discussed in Example 3.4.3) when it is in the extended configuration, as in the figure below. Assume that $L = 200$ N, $P = 1000$ N and that P

applies at the point halfway up the step leg. You may ignore the weight of the ladder.

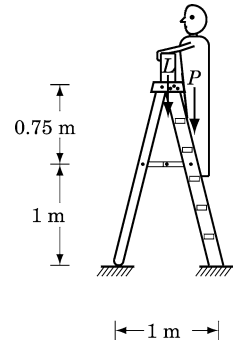

3.4-6. Two tubes of weight 100 kips each are suspended by wires and a third tube rests on top of them as shown in the figure, with the contact assumed frictionless. What is the maximum allowable weight of the top tube if equilibrium is to be maintained?

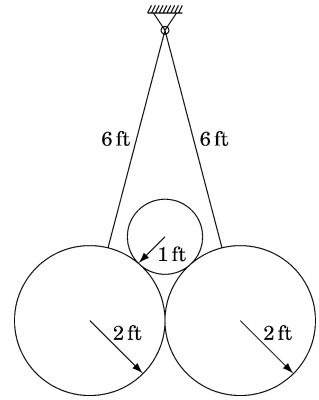

3.4-7. For the slip-joint pliers shown in the figure below determine the force Q exerted on the cylindrical workpiece in terms of the force P applied at the handles.

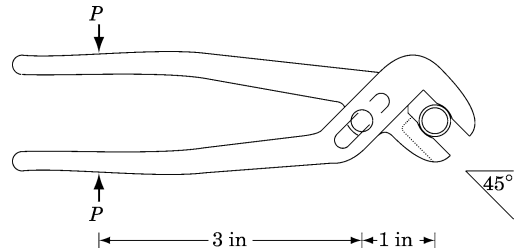

3.4-8. In the toggle vise illustrated in Fig. 3.31a, assume that the dimensions are $\overline{AB} = \overline{BD} = 1.0$ m, $\overline{BC} = 0.5$ m, and the height of the triangle ABD

is 0.28 m. Determine the force F required to produce a clamping force of 1 kN.

3.4-9. Assume that, in the free-body diagram of Fig. 3.32b, the longitudinal axis of the tibia intersects the lines of action of the quadriceps tension T and of the lower-leg weight W at points that are, respectively, at one-half and three-quarters of the distance from the knee joint to the line of action to the applied force F. If the lower leg is inclined at 45°, find expressions for T and R in terms of F, W and α.

3.4-10. A traditional brake used on a horse-drawn carriage is shown in perspective in the photograph on the left of the figure below, and in two dimensions in the sketch on the right. When the coachman pushes the

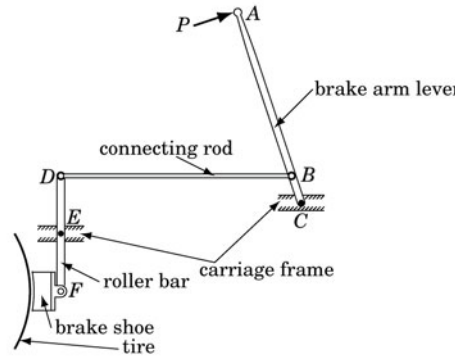

brake arm lever ABC, the pushing force P is transmitted through the connecting rod BD, the roller bar DEF and the brake shoe as a normal force N acting on the tire, with the resulting friction slowing the motion. (Note in the photograph that a ratchet allows the force to be maintained after the coachman lets go of the brake arm lever.) Find the relation between N and P if the dimensions are (in centimeters) $\overline{AB} = 90$, $\overline{BC} = 15$, $\overline{BD} = 120$, $\overline{DE} = \overline{EF} = 30$, and the brake arm lever is at 18° from the vertical while the connecting rod and the roller bar are horizontal and vertical, respectively.

3.5 Chains and Cables

3.5.1 Introduction

While the machines discussed in Sect. 3.4.3 have internal degrees of freedom, a machine is analyzed in a particular configuration in which it is assumed to be in equilibrium. There are, however, flexible structures in which the configuration is *imposed* by the equilibrium conditions under a given loading, and the determination of this configuration is an essential part of solving the overall problem.

In this section, we will discuss the simplest type of such a structure, namely, a *chain*, consisting of rigid two-force members (called *links*) connected end-to-end with pin joints, each joint connecting only two members. In the limit as the links become infinitely short and their number grows to infinity, the chain becomes a *cable*, and, as is usual in such limiting cases, the algebraic equations governing the problem turn into a differential equation.

Chains and cables are the first examples of nonlinear systems encountered in this book. As we will argue later in this section, the nonlinearity of these systems is purely geometric and stems from the fact that their equilibrium configurations involve large rotations (in the case of chains) and large changes in slope (for cables).

3.5.2 Simple Chain: Kinematics

Let us look at the simple assemblage of Fig. 3.5a, shown again as Fig. 3.33a. The assemblage can be made flexible, with one degree of freedom, by remov-

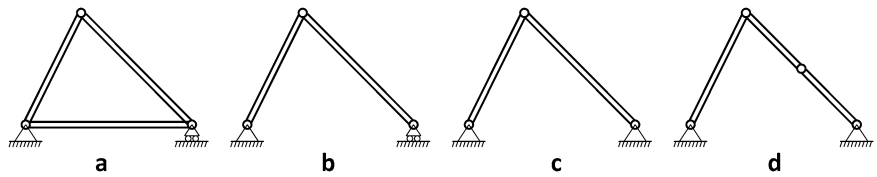

Figure 3.33. Rigid and flexible bar assemblages

ing the bottom bar, as in Fig. 3.33b (making it like the mechanism of Fig. 2.19a or 2.20). It can be made rigid again by replacing the roller joint on the right with a hinge, as in Fig. 3.33c. This assemblage can, in turn, be made flexible again by inserting a hinge in one of the bars. Now, as can be seen from Fig. 3.33d, the assemblage has three members ($n = 3$) and four joints ($j = 4$), while the number of constraints remains four ($r = 4$), so that $2j - n - r = 1$. In other words, there are eight independent equilibrium equations for the seven force unknowns (three member forces and four reaction components), hence

the system has one internal degree of freedom.

This assemblage can be thought of as a three-bar linkage, but here it will be called a *simple chain*. The fact that it has one internal degree of freedom is illustrated in Fig. 3.34, where some of its possible configurations are shown.

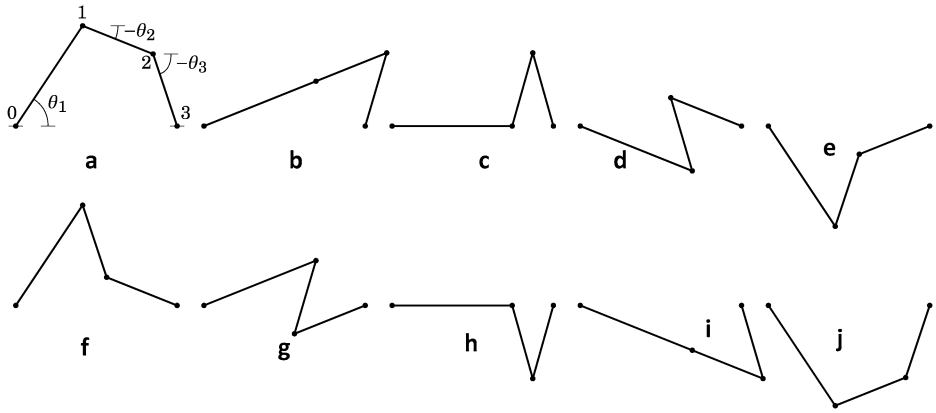

Figure 3.34. Possible configurations of the assemblage of Fig. 3.33d

It will be convenient to use a number (rather than a letter) designation for the joints, from 0 to 3 going from left ro right, with the members accordingly designated 01, 12 and 23; thus the angle θ_i is measured counterclockwise from the horizontal to the link between joints $i-1$ and i, as shown in Fig. 3.34a. It is clear that of the three angles θ_i $(i = 1,2,3)$ only one can be specified arbitrarily, though in this particular example, since links 12 and 23 are initially collinear, for a given value of θ_1 there are two sets of values of θ_2 and θ_3, depending on whether joint 2 is nudged outward (as in Figs. 3.34a–e) or inward (as in Figs. 3.34f–j). Note also that each configuration in the lower row is the mirror image of one in the upper row.

The angles are related by the two *compatibility conditions*

$$l_{01}\cos\theta_1 + l_{12}\cos\theta_2 + l_{23}\cos\theta_3 \;=\; L \tag{3.6}$$

and

$$l_{01}\sin_1 + l_{12}\sin\theta_2 + l_{23}\sin\theta_3 \;=\; 0\,, \tag{3.7}$$

where l_{ij} $(i,j = 0,1,2)$ is the length of link ij and L is the *span* of the system, that is, the distance between the left and right supports (which are assumed to lie on the same level). The term "compatibility" is meant to emphasize that the relative placement of the links should be geometrically compatible with the position of the supports of the chain.

3.5.3 Simple Chain: Equilibrium

The angles θ_i define the shape of the simple chain and are unknowns in addition to the forces. For the simple chain of Fig. 3.33d, the total number of unknowns is now ten (four external reactions, three bar forces, three angles), as is the number of independent equations (eight equilibrium equations— two at each of four joints—and two compatibility equations). All these equations are nonlinear in the angles θ_i (as they involve trigonometric functions), thus rendering the chain a nonlinear structure.

Suppose that the chain is in the configuration of Fig. 3.34a and that downward vertical forces (say weights), denoted F_1 and F_2, act at joints 1 and 2, respectively, with the free-body diagram shown in Fig. 3.35. When the

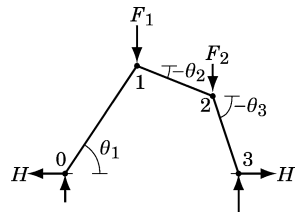

Figure 3.35. Free-body diagram of the assemblage of Fig. 3.33d, assumed in the configuration of Fig. 3.34a, under point forces at the joints

method of joints is applied to them, it becomes immediately apparent from the equilibrium of the horizontal forces that the horizontal components of all the member forces must be equal (they are also equal to the horizontal components of the support reactions). Let this value be denoted H (positive if tensile, negative if compressive). The member force in this link is thus $H\sec\theta_i$, and its vertical component is accordingly $H\tan\theta_i$. To begin with, then, the system can be regarded as one with the four unknowns H, θ_1, θ_2 and θ_3. From the equilibrium of vertical forces at joints 1 and 2 it follows that

$$F_1 = H(\tan\theta_2 - \tan\theta_1) \tag{3.8}$$

and

$$F_2 = H(\tan\theta_3 - \tan\theta_2)\,. \tag{3.9}$$

The four unknowns can be determined by solving the four equations (3.6–3.9) simultaneously. Note that if $(H, \theta_1, \theta_2, \theta_3)$ is a solution of the problem, then so is $(-H, -\theta_1, -\theta_2, -\theta_3)$. The two equilibrium configurations are consequently mirror images of each other, with the members in compression in one (the "arch"configuration, as in Fig. 3.34a) and in tension in the other (the "cable" configuration, as in Fig. 3.34j).

Example 3.5.1: Equilibrium of a simple chain.
Suppose that, in the simple chain of Figure 3.35, the link lengths are $l_{01} = 2.0$

m and $l_{12} = l_{23} = 1.4$ m, the span is $L = 3.0$ m, and the loads are $F_1 = 40$ kN and $F_2 = 30$ kN. Eqs. (3.6)–(3.9) are nonlinear and must, in general, be solved by some numerical method. But it is found by trial and error that, if we assume $\theta_1 = 59°$, $\theta_2 = -20°$ and $\theta_3 = -62°$, then the left-hand sides of Eqs. (3.6) and (3.7) are respectively 3.003 m and -0.0006 m. Eqs. (3.8) and (3.9) then yield $H = -19.72$ kN and $H = -19.78$ kN, respectively. These results are well within our criteria of accuracy.

In reality, the equilibrium of the "cable" configuration is stable while that of the "arch" configuration is unstable. Why? Because, given an ever so slight disturbance, in the latter configuration the assemblage will spontaneously "snap through" (go through a sequence of nonequilibrium configurations) into the former— as illustrated in Fig. 3.36a—but not vice versa, because to do so would require that work be done in raising the weights. Another way of

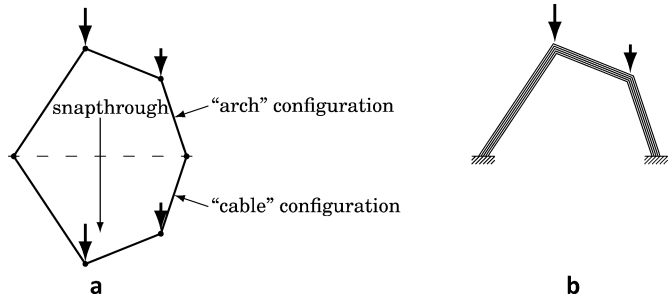

Figure 3.36. (**a**) "Arch" and "cable" configurations of the assemblage of Fig. 3.33d; (**b**) rigid arch based on this assemblage

expressing the condition is that a configuration with the weights in the higher position has a higher potential energy than the one with the weights in the lower position.

The concept of stability of equilibrium will be taken up again in Chap. 10. For now, only flexible assemblages that are stable (i.e. with the members in tension) will be studied. This does not mean, however, that the "arch" solutions are useless. Making one or more of the joints rigid (that is, preventing rotation about it) changes the assemblage from flexible to rigid (statically determinate or indeterminate), but if the geometry and loading are unchanged, then the equilibrium equations remain the same and so do the member forces. A rigid arch based on the assemblage of Fig. 3.33d is shown in Fig. 3.36b.

3.5.4 Cables and Chains

If the links in a simple chain are short and their number is large, then the kind of assemblage that we are discussing is called a *chain*, without the qualification "simple." In the limit as the links become infinitely short, the chain becomes a *cable* and its equilibrium is analyzed by differential calculus rather

than algebra. Cable analysis is usually applied to chains if the links are short enough.

We assume here that chains and cables are inextensible (unlike, say, bungee cords), yet flexible (unlike *simple* chains) in the sense of offering no resistance to bending. This means that if a chain or cable acts as a two-force member, then it must be taut (stretched), and the force can only be tensile.

3.5.5 Cables with Concentrated Loads

If a cable supports concentrated transverse loads, as in Fig. 3.37a, then each portion of the cable between loads and/or supports is a straight two-force member carrying a tension T_i ($i = 0, 1, \ldots$).

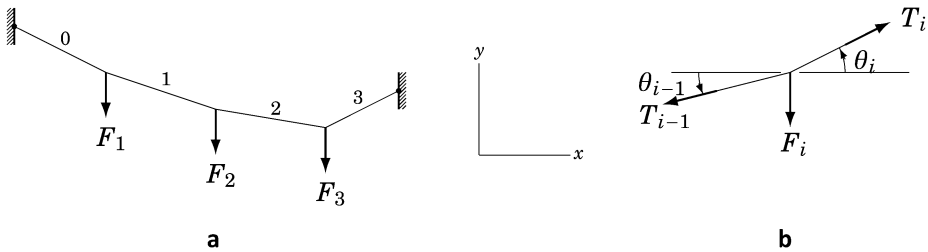

Figure 3.37. (**a**) Cable with concentrated loads. (**b**) Free-body diagram of cable section with concentrated load F_i.

A free-body diagram of the i-th load-carrying point is shown in Fig. 3.37b. Note that θ is assumed to be $\tan^{-1} dy/dx$. Equilibrium of forces in the x-direction yields

$$T_i \cos\theta_i \;=\; T_{i-1} \cos\theta_{i-1} \,, \tag{3.10}$$

that is

$$T_i \cos\theta_i \;=\; H \;=\; \text{constant} \,, \tag{3.11}$$

where H is the horizontal component of the tension in every segment of the cable. Consequently,

$$T_i \;=\; H \sec\theta_i \quad , \quad i = 0, 1, \ldots \,. \tag{3.12}$$

Equilibrium of forces in the y-direction yields

$$T_i \sin\theta_i - T_{i-1} \sin\theta_{i-1} \;=\; H(\tan\theta_i - \tan\theta_{i-1}) \;=\; F_i \,. \tag{3.13}$$

If there are n points with concentrated loads (therefore $n+1$ straight segments), then there are n such equations for the $n+2$ unknowns $\theta_0, \ldots, \theta_n$ and

H. Consequently, two additional compatibility conditions about the cable geometry must be given in order to determine the geometry and forces of the cable. One such condition is typically the location of one support relative to the other. The other may be the total length of cable or the vertical coordinate of the lowest point on the cable relative to one of the supports (the *sag* of the cable).

It should be emphasized that the cable of Fig. 3.37a is externally statically indeterminate, since it is supported by two pins. However, the external reactions at the two pins are fully determined upon finding the internal forces. Indeed, a free-body diagram of the joint at each pin includes the known internal force due to the first or last cable segment and the two unknown reactions. As is the case with all statically indeterminate structures, the internal and reaction forces are determined by using both the equilibrium equations and conditions of geometric compatibility.

3.5.6 Cables with Distributed Loads

If the load distribution is continuous, the load intensity per unit *horizontal* length (positive downward) being w (in general a function of position), then a free-body diagram of the infinitesimal segment located between the points whose x-coordinates are x and $x+dx$, respectively, is shown in Fig. 3.38. Equilibrium of forces in the x-direction is given by

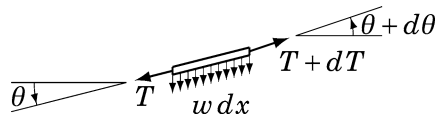

Figure 3.38. Free-body diagram of cable section with distributed load

$$(T+dT)\cos(\theta+d\theta) \;=\; T\cos\theta\;. \tag{3.14}$$

Upon expanding the left-hand side of (3.14), we find that

$$(T+dT)(\cos\theta\cos d\theta-\sin\theta\sin d\theta) \;=\; T\cos\theta\;. \tag{3.15}$$

Ignoring the term involving second-order differentials and recalling that $\sin d\theta \doteq d\theta$ and $\cos d\theta \doteq 1$, Eq. (3.15) reduces to

$$dT\cos\theta - T\sin\theta d\theta \;=\; d(T\cos\theta) \;=\; 0\;, \tag{3.16}$$

or

$$T \;=\; H\sec\theta\;, \tag{3.17}$$

which is analogous to (3.12). Equilibrium of forces in the y-direction is given by

$$(T+dT)\sin(\theta+d\theta)-T\sin\theta \;=\; w\,dx\;. \tag{3.18}$$

Following again the procedure used to derive (3.16) and taking into account (3.17), Eq. (3.18) simplifies to

$$d(T\sin\theta) \;= H\,d\tan\theta \;=\; w\,dx\;, \tag{3.19}$$

which is analogous to (3.13). Since $\dfrac{dy}{dx}=\tan\theta$, Eq. (3.19) may be rewritten as

$$H\frac{d^2y}{dx^2} \;=\; w\;. \tag{3.20}$$

It follows that any portion of a cable that is unloaded ($w=0$) is necessarily straight. A cable subject to discrete point loads only is consequently indistinguishable, as regards equilibrium analysis, from an assemblage of rigid bars with pin joints at the load points.

Eq. (3.20) is a second-order differential equation for the y-coordinate of points on the cable as a function of the x-coordinate. Its general solution has two constants of integration, which are determined by specifying the coordinates of the two supports. An additional geometric condition, such as the sag or the length of the cable, is then needed to determine H.

Example 3.5.2: Parabolic cable.
If the load is uniformly distributed with respect to the horizontal line, then $w=$ constant, and the general solution of Eq. (3.20) is

$$y \;=\; \frac{wx^2}{2H}+ax+b\;, \tag{3.21}$$

where a and b are constants to be determined from boundary conditions. This equation describes a parabola.

If the vertical position of the lowest point on the cable (the vertex of the parabola) is known, then it is convenient to choose this point as the origin of the coordinate system, as in Fig. 3.39, so that

$$y \;=\; \frac{wx^2}{2H}\;. \tag{3.22}$$

Note that H, and the horizontal distances l_A and l_B from the origin to the two boundary points A and B, are unknown. However,

$$y_A \;=\; \frac{wl_A^2}{2H}\quad,\quad y_B \;=\; \frac{wl_B^2}{2H}\quad,\quad l_A+l_B \;=\; L\;. \tag{3.23}$$

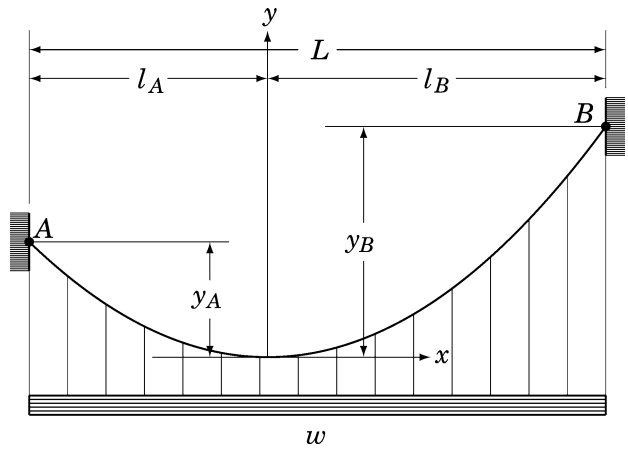

Figure 3.39. Parabolic cable with coordinate system originating at the vertex of the parabola

It follows that the span L (which is known) is

$$L = \sqrt{\frac{2H}{w}}(\sqrt{y_A} + \sqrt{y_B}) , \tag{3.24}$$

from which H can be obtained, and

$$l_A = \frac{\sqrt{y_A}}{\sqrt{y_A} + \sqrt{y_B}} L \quad , \quad l_B = \frac{\sqrt{y_B}}{\sqrt{y_A} + \sqrt{y_B}} L . \tag{3.25}$$

The tension at any point can be obtained from equation (3.17). Since Eq. $(3.19)_2$ yields

$$\tan\theta = \frac{dy}{dx} = \frac{wx}{H} \tag{3.26}$$

and $\sec\theta = \sqrt{1+\tan^2\theta}$, it follows that

$$T = H\sqrt{1+(wx/H)^2} = \sqrt{H^2+(wx)^2} . \tag{3.27}$$

Note that the maximum tension $T_{\max}$ occurs at the point on the cable where the slope is steepest, i.e., at the higher support point, while the minimum tension $T_{\min}$ occurs at the vertex and is equal to H.

Example 3.5.3: Catenary cable.
If the load is uniformly distributed with respect to the arc length s of the cable and is of intensity μ (for example the weight per unit length of the cable or chain itself), then if the load per unit horizontal length is w, an element of arc length ds (and horizontal projection dx) carries a load equal to $\mu ds = w dx$, so that $w = \mu ds/dx = \mu\sec\theta = \mu\sqrt{1+(dy/dx)^2}$. Eq. (3.20) therefore becomes

$$\frac{1}{\sqrt{1+(dy/dx)^2}} \frac{d^2y}{dx^2} = \frac{\mu}{H} . \tag{3.28}$$

We now define a new variable z, such that $dy/dx = \sinh z$. It follows that $d^2y/dx^2 = (\cosh z)dz/dx$, and since $\sqrt{1+\sinh^2 z} = \cosh z$, Eq. (3.28) reduces to

$$\frac{dz}{dx} = \frac{\mu}{H} . \tag{3.29}$$

If the origin is once again taken at the lowest point on the cable, where $dy/dx = 0$ (hence, also $z = 0$), then $z = \mu x/H$ and therefore $dy/dx = \sinh(\mu x/H)$, which can be integrated to yield

$$y = \frac{H}{\mu}\left(\cosh\frac{\mu x}{H} - 1\right) , \tag{3.30}$$

satisfying the boundary condition $y = 0$ at $x = 0$. The curve described by Eq. (3.30) is known as a *catenary*, from the Latin word *catena* meaning 'chain'.

It follows from the discussion of an arch based on the equilibrium configuration of a chain (page 145) that an arch in the shape of a parabola will be in equilibrium under a load that is uniformly distributed with respect to the horizontal line, and a catenary arch will be in equilibrium under a load that is uniformly distributed with respect to arc length. The former design may be used to support a bridge that is much heavier than the arch, while the latter may be used for a free-standing arch carrying only its own weight, as illustrated in Fig. 3.40.

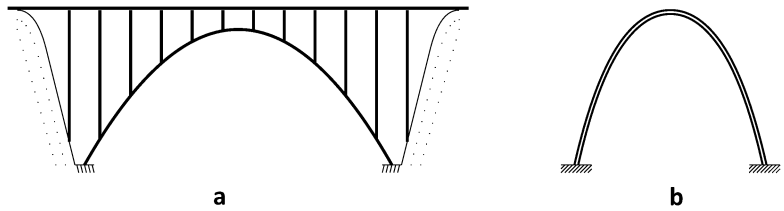

Figure 3.40. Arches based on cable configurations: (**a**) parabolic, (**b**) catenary

Exercises

3.5-1. Consider a chain made of four equal links. Write the compatibility equations, and show that the chain has two degrees of freedom by showing that, when the inclinations of two of the links are specified, there are only two possible positions for the other two. Sketch some such configurations.

3.5-2. A chain made of three equal links of length l has a span of $L = 2.5l$, has its supports at the same level, and is subject to forces applied at the joints (labeled from left to right) such that $F_1 = F$ and $F_2 = 1.5F$. Derive the equations that would determine the configuration of the chain.

3.5-3. Consider a chain made of three members with lengths $l_{01} = l_{12} = l_{23} = l$, as in the figure. What should be the ratio F_1/F_2 of the forces acting on the pins that would keep the member 1-2 horizontal? For this case, determine the angles θ_1 and θ_3.

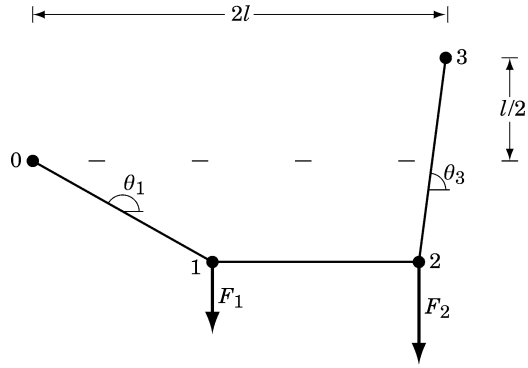

3.5-4. A chain made of four equal links of length l has a span of $L = 3l$, has its supports at the same level, and is subject to forces applied at the joints (labeled from left to right) such that $F_1 = F$, $F_2 = 2F$, and $F_3 = 1.5F$. Derive the equations that would determine the configuration of the chain.

3.5-5. A cable spanning 4 m, with the supports at the same level, carries a single load of mass 100 kg at a point whose horizontal distance from the left-hand support is 1.5 m. If the sag is 0.8 m, determine the tension in each segment of the cable.

3.5-6. A cable spanning 300 ft supports a load of 30 lb/ft uniformly distributed with respect to the horizontal and is suspended from the two fixed points located as shown. Determine the maximum and minimum tensions $T_{\max}$ and $T_{\min}$ $(= H)$ in the cable.

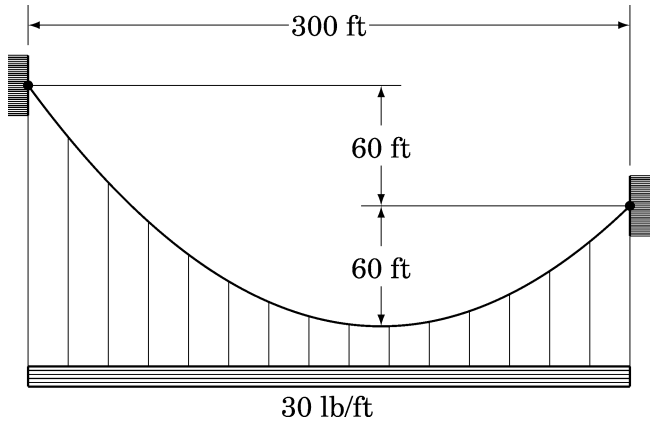

3.5-7. Consider a cable which supports its own weight and has mass of 10 kg per meter of its length. Suppose that the cable is suspended between two points which are located 250 m apart and are at the same height. Also, suppose that the sag of the cable is 50 m. Determine the maximum and minimum tension in the cable, as well as the total length of the cable.
Note: You may use a numerical or graphical method to obtain one or more of the required answers in this problem.

3.5-8. The balloon shown in the figure is held in place by a 200-ft cord that weighs 1.2 lb/ft. In addition, it is known that the cord makes an angle of 60^o with the horizontal at point A and that the tension in the cord at point A is 100 lb.

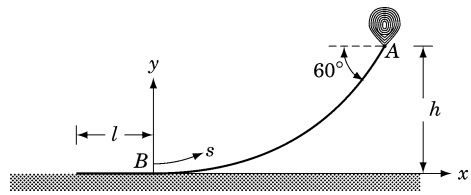

(a) Determine the length l of the cord that lies on the ground.

(b) Determine the height h of the point A.

Hint: Establish the coordinate system of the cord at point B, as in the figure.

3.5-9. Consider a cable that is pinned at its two end points A and B, as shown in the figure. Let the cable be subjected to a load w per unit horizontal length and suppose that it can support a maximum tensile force T_b = 1000 lb before it breaks.

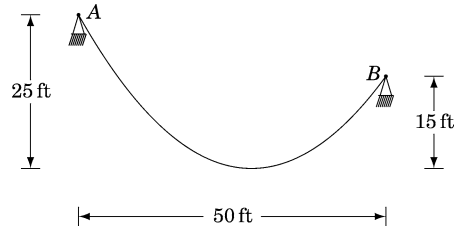

(a) Determine the maximum value $w_{\max}$ of the load w that the cable can support before breaking.

(b) If the load is equal to $w_{\max}$, what is the tension at a point located halfway between the lowest point of the cable and point B?

3.5-10. If a parabolic cable is symmetric, with $y_A = y_B = y_m$ and $l_A = l_B = L/2$, then its shape can be described by the formula $y = y_m(2x/L)^2$. If the cable is, in fact, a catenary, find the percent error in applying the parabolic formula at the quarter points ($x = \pm L/4$) when the sag-span ratio y_m/L is (a) 0.1, (b) 0.2, (c) 0.3.

3.5-11. For symmetric cables as defined in the preceding exercise, plot y_m/L against wH/L for a parabolic cable and against $\mu H/L$ for a catenary cable, up to $y_m/L = 0.5$.

3.5-12. A competition tennis net stretches 33 ft and is 42 in high at the two end posts. The nets hangs on a cable (assumed here to be inextensible) which passes through pulleys at the top of the end posts and is secured vertically on the ground, as shown in the figure. The weight of the tennis net (including the cable) is approximately 0.33 lb/ft.

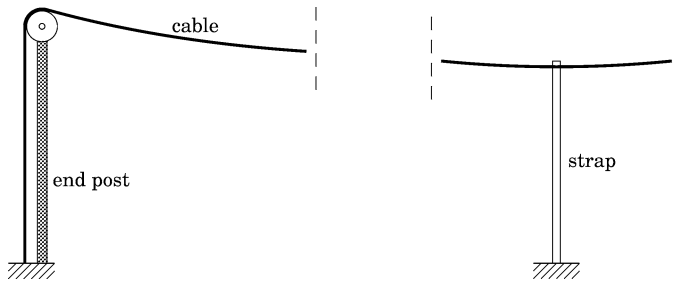

The cable is stretched to tension T_0, at which its height at the center reaches 36 in. At this stage, a vertical strap, which is passed around the cable at the center of the net, starts developing a tensile force F which keeps the cable from increasing its height at the center with an increase of the tension force T. Determine and plot the force F as a function of T.

3.5-13. Suppose that the parabolic arch of Fig. 3.40a has a span of 160 m and a height of 70 m. If the weight of the bridge can be represented as a uniformly distributed load of 30 kN/m, and if the arch is assumed to act like an inverted cable, find (a) the horizontal thrust and (b) the magnitude of the support reactions.

3.5-14. The catenary arch of Fig. 3.40b has a square cross-section of 2 ft by 2 ft and is made of a material with a specific weight of 160 lb/ft^3. If the span is 100 ft and the height is 80 ft, and if the arch is assumed to act like an inverted cable, find (a) the horizontal thrust and (b) the magnitude of the support reactions.

Chapter 4

Stress

4.1 Normal Stress, Saint-Venant's Principle

4.1.1 Introduction

Experience shows that when a straight bar (or wire, cable, rubber band or the like) is subjected to a tensile axial force, it stretches and, as the force is increased, eventually breaks. Depending on the material of which the bar is made, the bar may or may not undergo a considerable amount of permanent elongation, with relatively little resistance, before it breaks. The onset of this elongation is known as *yielding*, and a material that allows it is called *ductile*. These properties will be discussed further in Chap. 11.

The force required to break a bar (its ultimate force) is a property of the bar, in the sense that when a number of identical specimens (that is, bars made of the same material and having the same geometry) are pulled independently until they break, the spread among the values of the ultimate force is slight. The same is true of the force required to initiate yielding. If the bar is a member of a structure whose dimensions are required to remain more or less constant, then yielding may be regarded as a form of failure.

If, now, several (say n) identical bars are assembled in parallel and pulled together, the total force required to break the assemblage will be essentially n times the ultimate force for a single bar. But a single bar can also be regarded as made up of a number of parallel elements (fibers), and if such fibers are thought of as having the same cross-section, then it follows that the force required to break a bar is proportional to its cross-sectional area. In other words, it is the *force per unit area* (called *stress*) required to break a bar that is a property of the material. Just like force, stress is a mathematical idealization (as opposed to a directly observable quantity). Stress is intended to quantify the interaction between the constituent parts of the body when subject to external loading, analogously to the interparticle forces discussed

© Springer International Publishing Switzerland 2017

J. Lubliner, P. Papadopoulos, *Introduction to Solid Mechanics*,
DOI 10.1007/978-3-319-18878-2_4

in Sect. 2.1.

The tensile stress at any stage of loading is denoted σ, while the maximum stress attained before fracture is called the *ultimate tensile strength* and will be denoted σ_U^{t}. Again, if the material is ductile then it also has a *yield stress*, denoted σ_Y. Of course, when a bar elongates under tensile loading, then it

Figure 4.1. Narrowing of a bar as it elongates under an applied tensile force

typically also narrows, as seen schematically in Fig. 4.1, and therefore its cross-sectional area A does not remain constant. When the stress is defined on the basis of the actual (variable) area then it is called the *true stress*; when it is defined relative to the initial cross-sectional area A_0 then it is called the *nominal stress* or *engineering stress*. As long as the deformation is slight, the distinction can be practically ignored, and this will be done in this book unless explicitly stated otherwise.

When the axial force is compressive rather than tensile, then the maximum compressive stress attained before fracture or rupture is the *ultimate compressive strength*.

4.1.2 Definition of Normal Stress

Compressive and tensile stresses constitute *normal stress* because the force vector from which they are calculated is normal (perpendicular) to the area on which it acts. While, in the preceding discussion, this stress was obtained by simply dividing the force by the area, this procedure gives us only the *average* stress. We will now discuss normal stress in greater generality.

Consider a member of a frame, machine, or other structure, such that, on a planar cross-section of area A, the resultant force is normal to the cross-section. We do not assume that the member has a well-defined axis, or, if it does, that the cross-section is necessarily perpendicular to it. This normal force, shown in Fig. 4.2, is therefore not necessarily the same as the previously discussed axial force P, and will instead be denoted N. It is the resultant of the normal components of the forces sustained by all the parallel fibers normal to the cross-section.

Consider next a small region of area ΔA in the cross-section, centered at a point C. Let r be a characteristic linear dimension of this region, such that the area ΔA vanishes as r approaches zero (that is, $\lim_{r\to 0} \Delta A = 0$). Also, let ΔN be the total normal force acting on the small region, as shown in Fig. 4.3. The

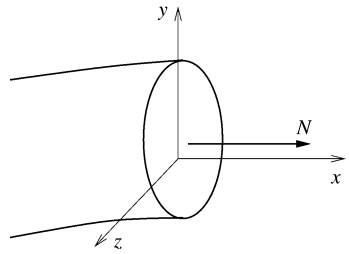

Figure 4.2. Cross-section with resultant normal force N

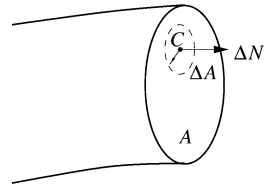

Figure 4.3. Force ΔN acting on a small region of area ΔA centered at point C on the cross-section

normal stress σ at point C on the cross-section is defined as

$$\sigma = \lim_{r \to 0} \frac{\Delta N}{\Delta A} . \tag{4.1}$$

Clearly, σ may be viewed as the force per unit area acting on the small circular region as it shrinks to a point. If ΔN is a pull force, then σ is a *tensile stress*. Conversely, if ΔN is a push force, then σ is a *compressive stress*. If the previous limiting process is followed at every point of the cross-section, we obtain a *normal stress field* $\sigma(y,z)$, where, without loss of generality, the cross-section is assumed to be in the (y,z)-plane. This means that the resultant normal force N is related to the normal stress by

$$N = \int_A \sigma(y,z)\, dA , \tag{4.2}$$

as seen in Fig. 4.4.

The *average normal stress* on the cross-section is defined as

$$\overline{\sigma} = \frac{N}{A} . \tag{4.3}$$

If the normal stress field acting on the cross-section happens to be *uniform* (that is, independent of position in the cross-section), then $\sigma(y,z) = \sigma = \text{const.}$. In this special case,

$$N = \int_A \sigma(y,z)\, dA = \int_A \sigma\, dA = \sigma \int_A dA = \sigma A , \tag{4.4}$$

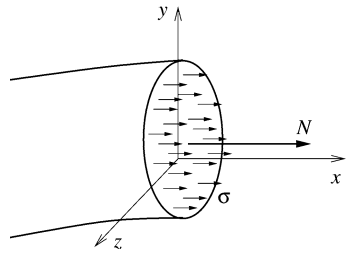

Figure 4.4. Normal stress field $\sigma(y,z)$ and its resultant N

therefore, by virtue of Eq. (4.3), $\sigma = \overline{\sigma}$. In addition, the resultant normal force N necessarily acts at the centroid of the cross-section. To show this, we assume that N acts at a point on the cross-section with coordinates (y_R, z_R). For the resultant normal force N and the uniform stress field σ to be statically equivalent, the two force systems must generate the same moment relative to the origin O of the coordinate system. This means that

$$(y_R\mathbf{j} + z_R\mathbf{k}) \times N\mathbf{i} = \int_A (y\mathbf{j} + z\mathbf{k}) \times \sigma\mathbf{i}\, dA \,, \tag{4.5}$$

which, with the aid of (4.4), implies that

$$y_R = \frac{1}{A}\int_A y\, dA \quad , \quad z_R = \frac{1}{A}\int_A z\, dA \,. \tag{4.6}$$

If the stress in *non-uniform*, then the point of action (that is, the intersection of the line of action with the cross-section) of the resultant force N may be determined as described in Sect. 1.5.2.

Since stress is defined as force per area, its units are clearly those of force per length squared. As already discussed in Sect. 1.1.2 (page 6), when US customary units are used, stress may be expressed in pounds per square foot (psf) or pounds per square inch (psi). The former unit is commonly used for pressure in fluids, but it is too small for stress in solids. In fact, the hard solids normally used in engineering applications typically undergo working stresses of the order of thousands of pounds (kilopounds or kips) per square inch, denoted ksi. Likewise, the pascal (Pa), which is the fundamental SI unit of stress, is also a very small unit for conventional solids, where stress is typically measured in megapascals (MPa).

4.1.3 Saint-Venant's Principle

An axial force can be applied to an end of a bar in different ways, ranging from concentrated at the centroid (Fig. 4.5a) to distributed across the area normal to the axis of the bar (Fig. 4.5b). While at the right end all the fibers are being pulled together and can be assumed to carry the same stress, at the left end

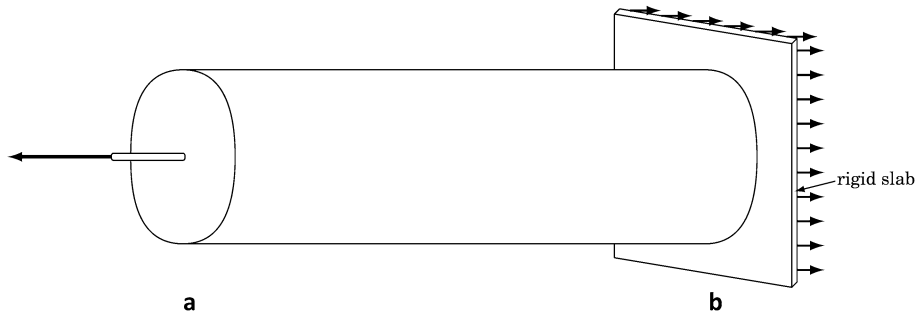

Figure 4.5. Different ways of applying an axial force

only the fibers in the middle are being pulled and the others are essentially free of stress. It turns out, however, that within a distance of one or two diameters from the left end the distribution of stress becomes more or less uniform; the influence of the way in which the force is applied is consequently an *end effect*, and if the bar is sufficiently slender then most of it will be under uniformly distributed stress.

This result is a special case of *Saint-Venant's principle*.* This principle asserts that, given two different but statically equivalent loadings over a small portion of a body, their effects are significantly different only in the immediate vicinity of the loading. Although Saint-Venant's principle can be rigorously shown to hold for only a small class of problems in solid mechanics, it is invoked widely in engineering practice.

4.1.4 Uniaxial, Biaxial and Triaxial Stress

If a body is loaded such that normal stress is acting on a cross-section and is zero on all planes perpendicular to this cross-section, then it is said to be in a state of *uniaxial stress*. This is the stress state that is usually assumed in bars under axial force.

A body is said to be in a state of *biaxial stress* if normal stresses are acting on cross-sections which are perpendicular to two orthogonal axes, as, for example, in the stretching of the plate shown in Fig. 4.6. If the two stresses are equal, then the state of stress is called *equibiaxial*.

A *triaxial stress* state occurs in a body when normal stresses are acting on cross-sections which are perpendicular to a triad of mutually orthogonal axes. This would be the case, for example, when a cube is subject to uniform normal stresses acting on each pair of opposite faces. If all three stresses are equal, then the body is in a state of *equitriaxial stress* or, as is more commonly said, *hydrostatic stress*, since it corresponds to the state of stress of a fluid at rest.

*Barré de Saint-Venant (1797-1886) was a French engineer.

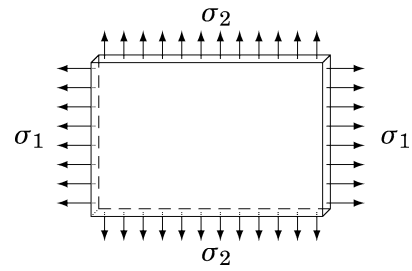

Figure 4.6. Biaxial stretching of a plate

Exercises

4.1-1. The bar with the cross-section shown in the figure, with all dimensions in centimeters, is subject to a uniform tensile stress of 200 MPa. Find the resultant normal force and the point at which it acts in the cross-section.

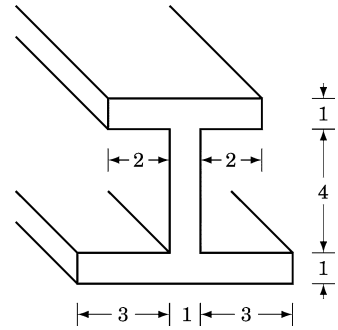

4.1-2. A weightlifter weighs 100 kg and lifts another 200 kg. If each of the weightlifter's shoes rests on the floor covering an area of 250 cm^2, find the average compressive stress (in MPa) below each foot of the weightlifter.

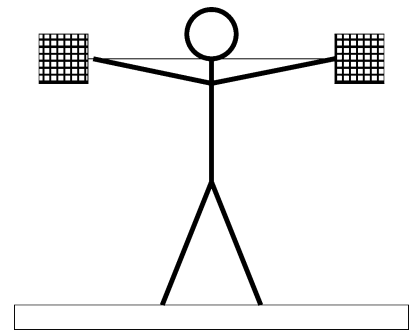

4.1-3. Consider a block with a square cross-section of side length 0.5 m, which is subject to compressive forces of 200 N, as in the figure. Determine

the mean compressive stress acting on the inclined plane shown in the figure.

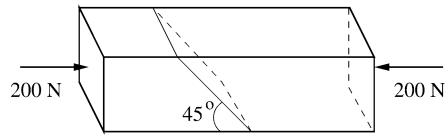

4.1-4. The cross-section of a square bar occupies, in the yz-plane, the region bounded by the lines $y = \pm c$, $z = \pm c$. If the resultant normal force N acts at $y = c/3$, $z = 0$, and if the normal stress σ_x is assumed to vary linearly with y, find its distribution and the ratio of the maximum stress $\sigma_{\max}$ to the average stress $\overline{\sigma}$.

4.1-5. The normal stress on a bar of circular cross-section with radius c is assumed to be given by $\sigma_x(r) = \sigma_{\max}[1-(r/c)^2]$. Find the resultant normal force and the ratio of the maximum stress $\sigma_{\max}$ to the average stress $\overline{\sigma}$.

4.1-6. A rectangular plate occupies the region bounded by the planes $x = \mp a/2$, $y = \pm b/2$, $z = \pm t/2$. If the plate is in a state of uniform equibiaxial stress $\sigma_x = \sigma_y = \sigma$, find the resultant normal forces N_x and N_y on each of the edges (narrow faces) of the plate.

4.1-7. A rectangular plate occupies the region bounded by the planes $x = \mp a/2$, $y = \pm b/2$, $z = \pm t/2$, with $a = 500$ mm, $b = 300$ mm, and $c = 10$ mm. If the resultant normal force on each edge (narrow face) is 600 N and if the state of stress in the plate is assumed uniform, find the stresses σ_x and σ_y.

4.1-8. A circular plate is in a state of uniform equibiaxial stress $\sigma_x = \sigma_y = \sigma$. By considering the equilibrium of the small element shown shaded in the figure below, find the shear stress on the edge of the plate as a function of θ.

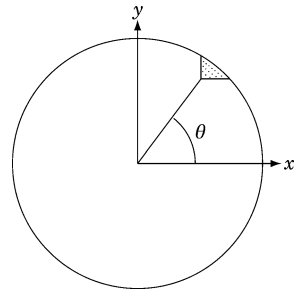

4.1-9. Repeat the preceding exercise for a state of biaxial stress with $\sigma_x = \sigma$, $\sigma_y = \frac{1}{2}\sigma$.

4.2 Shear Stress

4.2.1 Introduction

As we saw in Chap. 2, in a two-force body the two equal and opposite forces must be collinear, and, therefore, when acting at the two ends of a straight bar they must be axial. If a pair of equal and opposite transverse forces is applied to a rod, then a moment reaction is necessary for equilibrium, as seen in Fig. 4.7. At any cross-section of the rod the internal force system consists

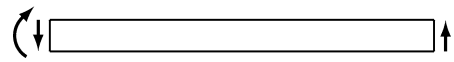

Figure 4.7. Transverse force applied to a rod

of a shear force and a bending moment. As will be argued in Chap. 8, the moment gives rise to a nonuniform distribution of normal stress, while the shear force produces a *shear stress*, denoted τ (see Fig. 2.46, page 101). If, however, instead of a rod we have a short connecting member, such as a rivet or bolt, then the bending moment will be small and its effect can, as a first approximation, be neglected.

We can understand the difference between the effect of shearing on such a short connector and a long or slender one such as a nail by observing what happens when a flat object is attached to a wall by one or the other. When the shearing force is great enough, the bolt will shear across, as in Fig. 4.8a, but the nail (assuming that it is, as usual, made of a ductile metal) will bend and eventually slide out, as in Fig. 4.8b.

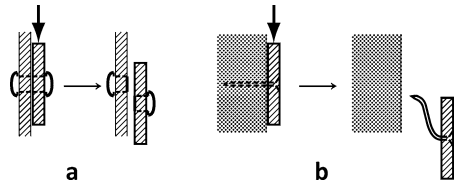

Figure 4.8. Effect of shearing force on a connector: (**a**) short connector (rivet), (**b**) long connector (nail)

A short connector, then, will fail in shear if the transverse force is of sufficient magnitude, and, as in the case of axial force, the strength is proportional to the area. Therefore, the measure of the *shear strength* of the material is the shear force required for failure (whether this is defined as fracture or yielding) divided by the cross-sectional area.

In general, there is no reason to suppose that the distribution of the local shear stress before failure is uniform. In fact, as we will learn in the course of studying the bending of beams, it *cannot* be uniform. At failure, however, it

must be close to uniform, since shear failure occurs when all the fibers break or yield in shear. The *ultimate shear strength* (defined analogously to ultimate tensile and compressive strength) will be denoted τ_U, while the yield stress in shear will analogously be denoted τ_Y.

4.2.2 Definition of Shear Stress

By analogy with Sect. 4.1, we consider a member of a frame or a machine which is subject only to a resultant shear force $\mathbf{V}$ acting on the planar cross-section $\mathscr{A}$ of area A, as in Fig. 4.9. The shear force is represented here as a vector to reflect the fact that, while it is always in the plane of the cross-section, its direction is not given at the outset (unlike the case of normal force, whose direction is fixed). As with normal force, the shear force $\mathbf{V}$ is the

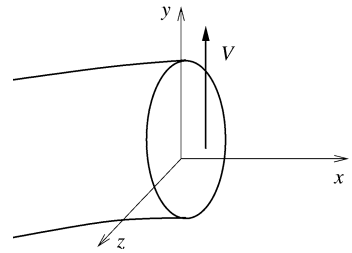

Figure 4.9. Cross-section with resultant shear force $\mathbf{V}$

resultant of distributed forces per unit area which all act at different points of the cross-section, although (in contrast to normal stresses) these forces do not necessarily have the same direction as $\mathbf{V}$, as shown in Fig. 4.10.

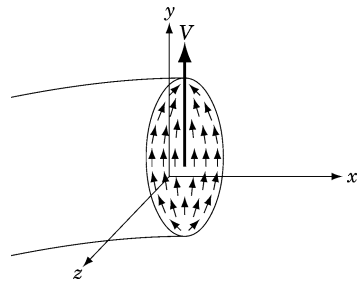

Figure 4.10. Stresses on a cross-section with resultant shear force $\mathbf{V}$

Repeating the argument of Sect. 4.1, the *shear stress* $\boldsymbol{\tau}$ at a point C of the cross-section is defined as

$$\boldsymbol{\tau} = \lim_{r \to 0} \frac{\Delta \mathbf{V}}{\Delta A} , \tag{4.7}$$

where the shear force $\Delta\mathbf{V}$ is acting on a small region of area ΔA (and characteristic linear dimension r) in the cross-section, centered at a point C, as in

Fig. 4.11. Note that the direction of the force $\Delta\mathbf{V}$ (and hence also of the shear stress $\boldsymbol{\tau}$) may vary from point to point, while still lying in the plane of the cross-section. A *shear stress field* $\boldsymbol{\tau}(y,z)$ can be deduced from the preceding

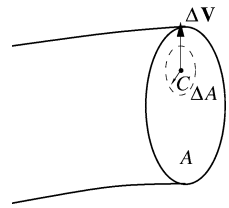

Figure 4.11. Force $\Delta\mathbf{V}$ acting on circular region of area ΔA centered at point C on the cross-section

limiting analysis, such that the resultant shear force $\mathbf{V}$ is related to the shear stress by

$$\mathbf{V} = \int_{\mathscr{A}} \boldsymbol{\tau}(y,z)\,dA\ . \tag{4.8}$$

.

As we already noted, there is no reason for the distribution of the local shear stress to be uniform. The *average shear stress* acting on the cross-section can now be defined as the vectorial analogue of Eq. (4.3), that is,

$$\bar{\boldsymbol{\tau}} = \frac{\mathbf{V}}{A}\ . \tag{4.9}$$

Example 4.2.1: Variable shear stress over a rectangular cross-section. We consider a rectangular bar whose axis lies along the x-axis and whose cross-section occupies the region in the yz-plane defined by $-h/2 < y < h/2$, $-b/2 < z < b/2$. Let the shear stress be oriented along the y-axis over the cross-section and be given by $\tau = \tau_1[1-(2y/h)^2]$. We wish to find the resultant shear force and the average shear stress.
Eq. (4.8) takes the form

$$\begin{aligned}\mathbf{V} &= \int_{-b/2}^{b/2}\int_{-h/2}^{h/2}\{\mathbf{j}\tau_1[1-(2y/h)^2]\}\,dy\,dz \\ &= \mathbf{j}\tau_1\int_{-h/2}^{h/2}[1-(2y/h)^2]dy\cdot\int_{-b/2}^{b/2}dz \\ &= \frac{2}{3}bh\mathbf{j}\tau_1\ ,\end{aligned}$$

since

$$\int_{-h/2}^{h/2}[1-(2y/h)^2]dy = 2h/3\ .$$

The average shear stress is now equal to

$$\bar{\boldsymbol{\tau}} = \frac{\frac{2}{3}bh}{bh}\mathbf{j}\tau_1 = \frac{2}{3}\tau_1\mathbf{j}\,.$$

4.2.3 Single and Double Shear

Connectors such as pins, rivets or bolts can be used in various ways to join plates that may be subject to forces tending to slide them apart. Two of these ways, known respectively as *single shear* and *double shear*, are illustrated in Fig. 4.12.

Figure 4.12. Single and double shear: (**a**) single shear, (**b**) double shear

It can be seen in Fig. 4.12a that the forces in single shear are not exactly in moment equilibrium. What this means regarding the plates is that they will bend a little so that the forces become collinear, as seen in Fig. 4.13. As regards the connector (which undergoes a slight tilt), the couple formed

Figure 4.13. Bending of plates in single shear

by the two non-collinear forces must be balanced by couples acting between the shank and the heads (or the head and the nut, if the connector is a bolt). These couples must in turn be balanced by forces acting on the heads, but since the plate can exert only a compressive force, a tensile force is formed between the shank and the heads as well. The free-body diagrams are shown in Fig. 4.14. The additional forces shown in the figure cannot be determined by statics alone (though they can be estimated), and their effect, like that of the couples, is usually neglected.

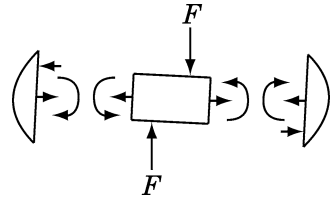

Figure 4.14. Couples on a connector in single shear

It can be deduced from the preceding discussion that a simple pin, with at most one head, may not be a good connector in single shear. In particular, the tilting of the connector seen in Fig. 4.14 shows that the force F is not strictly perpendicular to the shank but has a tangential component that tends to produce sliding between it and the plate, and in the absence of a head or nut or cotter (split) pin, or sufficient friction, the plates may separate. Clearly, there is no such issue with the double shear connector of Fig. 4.12b.

Example 4.2.2: Clevis fastener.
A *clevis fastener*, shown in Fig. 4.15, is a classic example of a connector using double shear. The clevis itself is the U-shaped element that may be either a an

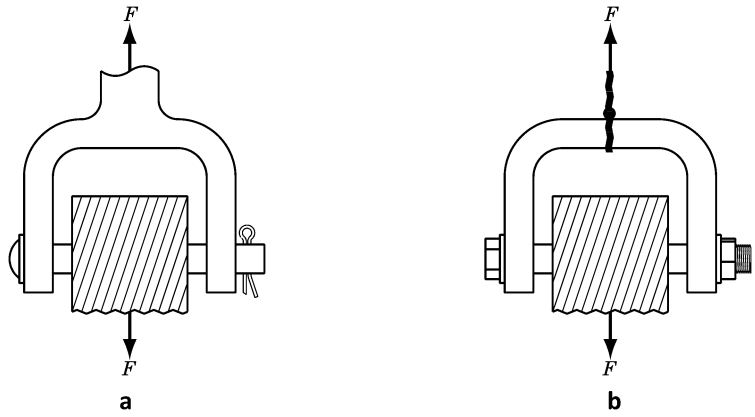

Figure 4.15. Clevis fastener: (**a**) clevis as an integral part of rod, with clevis pin; (**b**) clevis as a separate unit, with clevis bolt

integral part of the rod carrying the axial force F, as in Fig. 4.15a, or a separate unit, as in Fig. 4.15b; and the shear force may be carried either by a pin (*clevis pin*) secured with a cotter pin, as in Fig. 4.15a, or a bolt, as in Fig. 4.15b.

If the cross-sectional area of the pin or bolt is A, then the average shear stress there is, of course, $F/2A$.

Exercises

4.2-1. Consider a block with a square cross-section of side length 0.5 m, which is subject to compressive forces of 200 N, as in the figure. Determine the average shear stress acting on the inclined plane shown in the figure.

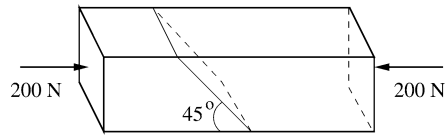

4.2-2. A circular plate is in a state of uniform equibiaxial stress $\sigma_x = \sigma_y = \sigma$. By considering the equilibrium of the small element shown shaded in the figure below, find the shear stress on the edge of the plate as a function of θ.

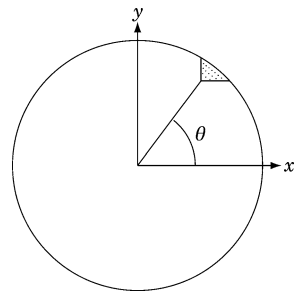

4.2-3. Do the preceding exercise for a state of biaxial stress with $\sigma_x = \sigma$, $\sigma_y = \frac{1}{2}\sigma$.

4.2-4. If the force F transmitted by a rivet in single shear (as in Fig. 4.12a) is 1.5 kips and the rivet diameter is 0.5 in, find the average shear stress.

4.2-5. If the force F transmitted by a rivet in double shear (as in Fig. 4.12b) is 10 kN and the rivet diameter is 10 mm, find the average shear stress.

4.2-6. Consider a rivet of 15-mm diameter connecting two plates as in Fig. 4.12a. If the average shear stress in the rivet is not to exceed 150 MPa, find the maximum value of the force F.

4.2-7. Consider a rivet of 0.625-in diameter connecting three plates as in Fig. 4.12b. If the average shear stress in the rivet is not to exceed 20 ksi, find the maximum value of the force F.

4.2-8. Assume that, for a rivet in double shear as in Fig. 4.12b, the forces shown are the only ones acting on the rivet shank. If the shank length is l, estimate the bending moment M acting on the shank at the middle of its span.

4.2-9. Let the tensile forces shown in Fig. 4.14 as acting between the heads and the shank of the rivet be denoted T. Estimate T in terms of F by assuming that the distance between the lines of action of the forces F is one half the shank length l, and that of the normal forces acting on each head is three quarters of the shank diameter d. Determine the resulting average axial stress σ in the shank.

4.3 Simple Stress States, Stress-Based Design

4.3.1 Introduction

By and large, it is not possible to determine by statics alone the distribution of stress corresponding to a given resultant force or moment. The best we can determine in such a case is average values of stress. But there are a few exceptional cases in which it can be argued that the stress will not deviate significantly from the average. We will refer to such cases as *simple stress states*, though a more accurate description would be *locally statically determinate* states.

One such case is the by now familiar straight bar carrying an axial force, where, since all the fibers elongate more or less together, it can be inferred that they carry the same stress if the material is homogeneous, as illustrated in Fig. 4.16.

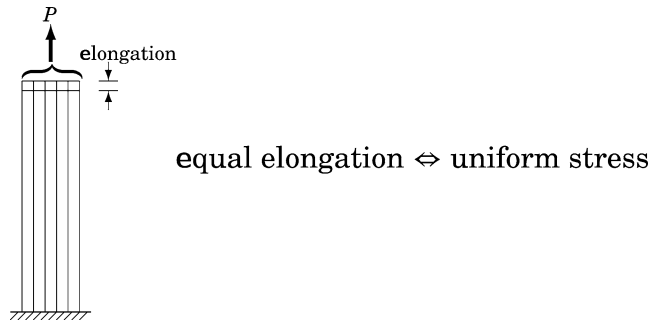

Figure 4.16. Uniformity of stress in a bar

Other cases involve hollow bodies such as shells and tubes. In some such bodies it may be possible, for certain kinds of loading, to determine, by statics alone, an *average* stress across the wall thickness. If, now, this thickness is quite small in comparison with the overall dimensions (that is, if the body is *thin-walled*), then it can be argued that there is simply *not enough room* for the stress to diverge significantly from the average, yielding once more a stress state that may be regarded as simple in the sense of the preceding definition. We will give here two examples of such bodies, limited to cases with circular symmetry about an axis: a shell under internal pressure and a tube subject to a twisting moment.

4.3.2 Thin-Walled Pressure Vessels

Closed, pressurized thin-walled shells of revolution, usually called *pressure vessels*, can be regarded to a close approximation as being in a state of biaxial stress, as discussed in Sect. 4.1. What is meant by *thin-walled* is, specifically, that the wall thickness, say t, is considerably smaller than the mean radius,

say r, that is, the ratio t/r can be neglected next to unity ($t/r \ll 1$ or $t \ll r$). If this condition is met, then the approximate equilibrium equations can be treated as though they were exact.

We will limit the discussion here to the two simplest shapes, namely, a spherical shell and a cylindrical one with hemispherical caps.

Example 4.3.1: Spherical shell.

Because of spherical symmetry, any element of the shell that is small enough to be regarded as nearly flat is very nearly under equibiaxial stress; it will be shown that the compressive stress due to the internal pressure p is negligible alongside the tensile stress in the skin, which will be denoted σ; the thinness of the skin also allows us to neglect any variation in stress through the thickness.

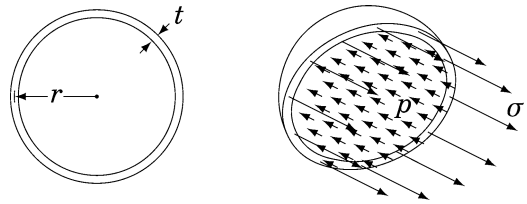

Figure 4.17. Geometry and equilibrium of a pressurized spherical shell

The equilibrium between the stress σ and the internal pressure p (more generally, the difference between the internal and external pressures) is obtained by dividing the shell into two halves, one of which is shown in Fig 4.17, and ensuring that each half, *including the gas contained in the hemisphere*, is in equilibrium. The pressure acts over the inner circle, whose area $\pi(r-t/2)^2$ may be approximated by πr^2 if $t \ll r$. The stress acts over the area between the two circles, $\pi[(r+t/2)^2-(r-t/2)^2] = 2\pi rt$. Equilibrium therefore requires that

$$\sigma \cdot 2\pi rt \;=\; p \cdot \pi r^2 \;, \tag{4.10}$$

or

$$\sigma \;=\; \frac{pr}{2t} \;. \tag{4.11}$$

Since $r \gg t$, the neglect of the compressive stress due to the pressure is justified.

Example 4.3.2: Cylindrical shell.

In a cylindrical shell there is no reason for the longitudinal stress σ_l to be the same as the circumferential stress σ_c (also called *hoop stress*). The former can be obtained by means of a free-body diagram analogous to that for the sphere, Fig. 4.18a, and consequently

$$\sigma_l \;=\; \frac{pr}{2t} \;. \tag{4.12}$$

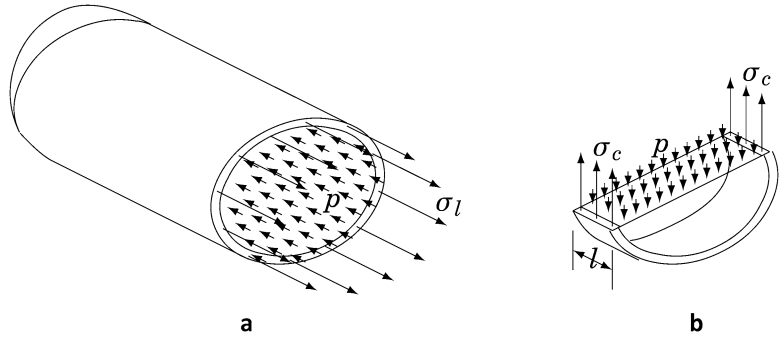

Figure 4.18. Equilibrium of a pressurized cylindrical shell

To determine the circumferential stress we slice a segment of the shell, of length l, and use half of it, including the gas, as our free body, as shown in Fig. 4.18b. The pressures acting over the semicircular areas, in the longitudinal direction, cancel each other and are not shown. The pressure acting over the rectangular area $(2r-t)l$, approximated as $2rl$, are balanced by the circumferential stress acting over the solid area $2tl$. Consequently,

$$\sigma_c = \frac{pr}{t} . \tag{4.13}$$

The analysis of thin-walled shells of revolution of other shapes and with loadings other than a uniform pressure is similar in principle, though more complicated in detail.

4.3.3 Torque on a thin-walled circular tube

An essentially uniform state of shear stress can be produced, at least in theory, by applying a torque (a moment about the longitudinal axis) to a thin-walled (in the sense defined above, page 169) circular tube. This loading tends to twist the tube, and will be discussed in more detail when the topic of torsion is taken up in Chapter 7. For now, it is sufficient to observe that in the free-body diagram of Fig. 4.19 the stresses on the cut surface must be such that their resultant is equal to the applied torque. If there are any normal stresses on the cut, their distribution must be such that their resultant force and moment are zero; and any such distribution, other than identically zero stress, would violate circular symmetry. The same circular symmetry requires that the distribution of shear stress be uniform around the circumference, and the thinness of the wall can be expected to prevent much variation in the stress from inside to outside.

It is easy to see that if the thickness of the tube is t and its mean radius is r, then a small sector subtending an angle $d\theta$ has an area of $tr\,d\theta$, and if the shear stress is τ, then the force acting on the element is $\tau tr\,d\theta$. The moment arm being approximately r, the moment about the axis is $\tau tr^2 d\theta$. The total

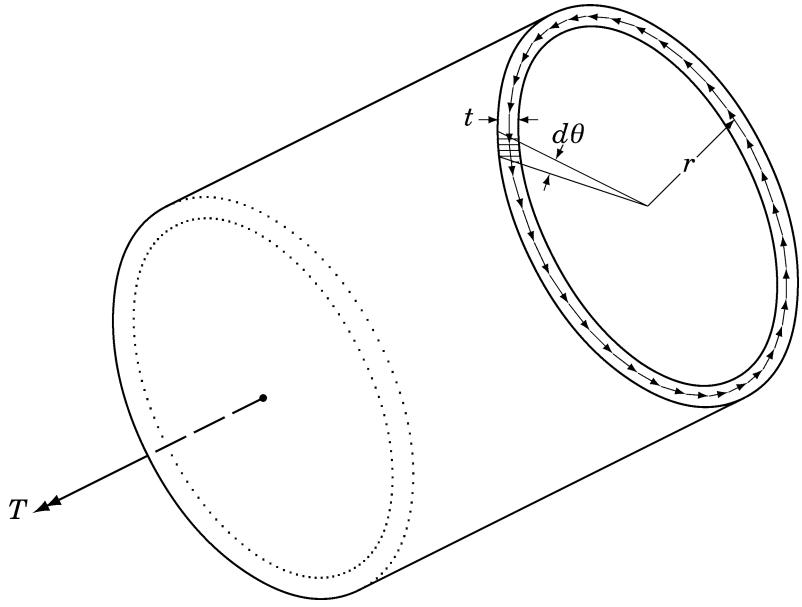

Figure 4.19. Shear stress in a thin-walled circular tube subject to a torque

moment about the axis, or torque T, is therefore

$$T = \oint \tau t r^2 d\theta = 2\pi\tau t r^2 , \tag{4.14}$$

so that

$$\tau = \frac{T}{2\pi r^2 t} . \tag{4.15}$$

In principle, then, it is possible to measure the shear strength of a material by twisting a thin-walled circular tube until it fails in shear. In practice, however, such a tube may crumple before it fails in shear, unless precautions are taken to prevent crumpling.

4.3.4 The Concept of Design

The word "design" can be used with many different meanings. To quote a few from Merriam-Webster's Collegiate Dictionary, 11th edition: "a mental project or scheme in which means to an end are laid down"; "a preliminary sketch or outline showing the main features of something to be executed"; "an underlying scheme that governs functioning, developing, or unfolding"; "a plan or protocol for carrying out or accomplishing something (as a scientific experiment), also: the process of preparing this"; "the arrangement of elements or details in a product or work of art".

In the context of solid mechanics, the use of the term is rather restricted. It typically means the selection of the cross-sectional dimensions of structural or machine members for which the overall "arrangement of elements or

details" has already been prepared. The criteria for the selection are also provided by mechanics, and chief among them is strength: the member must not fail (however mechanical failure is defined) when the loads that the structure or machine is intended to carry (the *design loads*) are applied to it.

In this section our analysis will be limited to situations in which the stress state can be treated as simple. In later chapters, situations where the stress varies over the cross-section will be considered, once we have learned to analyze such stress states.

4.3.5 Safety Factor, Allowable Stress

Engineering practice typically requires that the structure or machine remain safe at loads higher than the design loads, just in case the original estimate of these loads is in error. For this reason the expected loads are multiplied by a number s greater than one, called the *safety factor*, before the member forces are calculated. Engineering codes may specify different safety factors for different kinds of loads. In buildings, for example, a distinction is made between *dead loads* (typically the weight of the building mass itself and permanent additions) and *live loads*, which may be quite variable (for example, wind forces and the weight of building occupants) and are relatively unpredictable, so that a higher safety factor may be applied to the latter than to the former. Different modes of failure may also necessitate different safety factors, depending on the variability of the corresponding failure test results.

For now, we will limit our discussion to failure governed by the attainment of a critical stress (to be denoted σ_{cr} or τ_{cr}) in the member. Since in *statically determinate* systems the member forces are proportional to the loads (provided all the loads themselves vary proportionally), the stresses (defined simply as force per unit area) will be so likewise. In this case, the safety factor is used as a *load factor* augmenting the design load F to sF to reach a state of failure. However, the safety factor can then be used in a different way, namely, as a *stress factor*. In this case, if, say, a tension member is said to fail under the yield stress σ_Y when the load is given by a force sF, then under the design load the stress in the member is σ_Y/s. The member can consequently be "designed" so that the stress does not exceed this value—called the *allowable stress*, σ_{all}—under the design load.

As will be shown in Chap. 11, in statically indeterminate systems the equivalence between load factor and stress factor does not hold, and the use of one or the other may lead to different results. The key to the difference is the *redundancy* present in statically indeterminate systems, with the effect that the failure of a single member or connection does not imply the failure of the whole system.

4.3.6 Design of Axial-Force Members

In a straight bar of uniform cross-sectional area A, subject to forces only at the ends, the internal axial force P and the axial stress $\sigma = P/A$ are constant (within the limits allowed by Saint-Venant's principle). The requirement that this stress not exceed (in magnitude) the allowable stress σ_{all} implies that if P is the magnitude of the axial force under the design loads, then

$$P/A \leq \sigma_{\text{all}} . \tag{4.16}$$

Equivalently, if $P_{\text{cr}} = \sigma_{\text{cr}} A$ is the magnitude of the axial force at failure (where the critical stress σ_{cr} may be the yield stress, the fracture stress or the ultimate strength), then

$$sP \leq P_{\text{cr}} , \tag{4.17}$$

so that the same inequality holds, with $\sigma_{\text{all}} = \sigma_{\text{cr}}/s$. Inverting the inequality gives an expression for the smallest required cross-sectional area:

$$A \geq A_{\text{min}} = \frac{P}{\sigma_{\text{all}}} . \tag{4.18}$$

If the axial force varies along the length (as in a cable or arch, or in a bar with variable axial loading), then the maximum axial force P_{max} must be determined, and the criterion (4.18) becomes

$$A \geq \frac{P_{\text{max}}}{\sigma_{\text{all}}} . \tag{4.19}$$

If, on the other hand, the cross-sectional area varies while the axial force is constant, then

$$A_{\text{min}} \geq \frac{P}{\sigma_{\text{all}}} . \tag{4.20}$$

When both the axial force and the cross-sectional area vary, the stress must be determined as a function of position, and its maximum value must be set so as not to exceed the allowable stress. It is possible (though not always practical) to design a member subject to a varying axial force with an area variation such that the stress is constant.

For compression members, once the required area has been determined, it is necessary to check whether buckling will occur. This, however, is influenced not only by the area but by the shape of the cross-section, as will be discussed in Chap. 10.

Critical stresses and allowable stresses for an array of engineering materials are found in Appendix B: Table B-5 (SI, page 519) and Table B-6 (US, page 520). It will be noted that, depending on the type of material, the critical stress is either an ultimate strength (denoted σ_U or τ_U) or a yield stress (denoted σ_Y or τ_Y), as discussed in Sect. 4.1 (page 155). In the case of ultimate

normal stresses, the superscripts ^{t} and ^{c} refer to tension and compression, respectively. Where no allowable stress is shown, the safety factor depends on the application (it is usually higher in machines, due to the dynamic loads, than in structures under static loading).

4.3.7 Design of Shear Connectors

As we noted in Sect. 4.2, the distribution of shear stress in a shear connector is, in general, nonuniform. But it can be reasonably argued that, whatever the distribution may be, it will be similar in connectors of a given type that differ only in cross-sectional area. Consequently, it can be argued that the failure force is, as with axial-force members, proportional to the area, and when such a force is determined experimentally for a given connector, then the allowable shear stress τ_{all} obtained by dividing the force by the area and the safety factor is valid for other connectors of the same type and made from the same material. Consequently, the minimum required cross-sectional area for a given transverse force F is given by

$$A_{\text{min}} = \frac{F}{\tau_{\text{all}}}. \tag{4.21}$$

It should be noted that τ_{all} may have different values in single and double shear.

4.3.8 Bearing Stress

Another potential mode of failure in a shear connection may be crushing due to the compressive stress between the plate and the connector. The actual distribution of stress on the curved contact surface may be difficult to determine, but a nominal *bearing stress* σ_b may be defined by dividing the contact force F (or $F/2$ in the outer plates in double shear, as in Fig. 4.12) by the *projected* plane area, as shown in Fig. 4.20. Here t is the plate thickness and d is the diameter of the rivet or bolt, so that the projected area is $A = td$. If, as is often the case, the bolt material is stronger than the plate material, then the bearing stress may be critical in determining the required thickness of the plate.

Another example of design based on bearing stress is illustrated in Fig. 4.21, where a compressive load P carried by a steel column is transmitted to a concrete pier through a steel base plate. The area A of the base plate is determined by the requirement that the nominal bearing stress P/A not exceed the allowable bearing stress of the concrete.

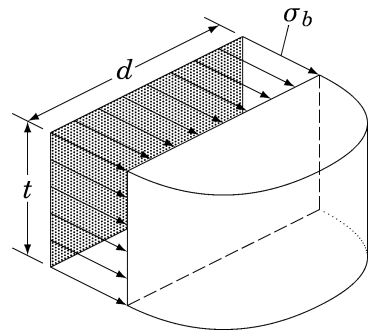

Figure 4.20. Projected area for bearing stress

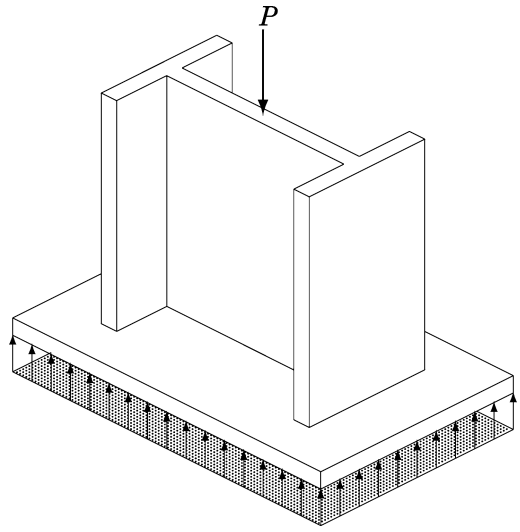

Figure 4.21. Column base plate

4.3.9 Adhesive Shear Stress

An alternative to solid shear connectors such as rivets, bolts or pins is provided by some kind of adhesive spread over the contact surface. If the joint is to transmit a force F and the allowable shear stress of the adhesive—a property of the adhesive material—is τ_{all}, then the required contact area is given by Eq. (4.21), just as for connectors.

Example 4.3.3: Rod embedded in a solid matrix.
We suppose that a rod of diameter d is embedded in a preexisting hole in a solid matrix to a depth h, with adhesive coating the cylindrical contact surface. The contact area is then πhd, and the minimum embedding depth is $h_{\min} = F/\pi d\tau_{\text{all}}$.

The situation is different if the hole is not preexisting but is created by driving,

say, a nail or a stake into the matrix, or, equivalently, if it is preexisting but smaller than what is driven into it. The expansion of the (relatively soft) matrix material produces a compressive stress between it and the rod*, and the shear stress that resists extraction is due to friction governed by Coulomb's law as discussed in Sect. 2.2. The compressive stress, however, cannot be determined by elementary methods.

*In the case of a cork forced into a bottle it is the compression of the relatively soft cork that produces the stress.

Exercises

4.3-1. Calculate the tensile stress in a rubber balloon that is inflated with a pressure of 500 kPa to a radius of 12 cm and a thickness of 1 mm.

4.3-2. A spherical pressure vessel of 26-in diameter is inflated with a pressure of 150 psi. Find the minimum thickness required if the tensile stress in any direction is not to exceed 10 ksi.

4.3-3. A cylindrical pressure vessel of 6-in diameter is made of 10-gauge sheet aluminum, with a thickness of 0.1091 in. If the maximum tensile stress is not to exceed 15 ksi, find the maximum pressure.

4.3-4. If an inflatable rubber tire is modeled as a cylindrical pressure vessel, find the largest allowable diameter if the pressure is 750 kPa, the thickness is 0.9 mm and the maximum tensile stress is not to exceed 25 MPa.

4.3-5. If a force of 100 lb is applied through a wrench of length 14.5 in to a length of iron pipe with an outside diameter of 1.315 in and a wall thickness of 0.065 in, find the resulting average shear stress.

4.3-6. Find the minimum wall thickness required for a thin-walled tube of radius 5 cm to carry a torque of 2.5 kN·m if the shear stress is not to exceed 90 MPa.

4.3-7. The weight of the homogeneous block shown in the figure is supported by two rigid links AC and BD. If the allowable tensile stress for each link is 10 MPa, find the cross sectional area of each link, such that the average tensile stress in each link is 20% below the allowable value.

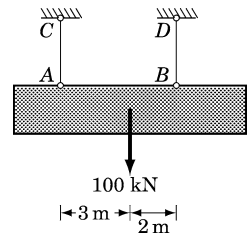

4.3-8. Consider a small structure which rests on a square concrete foundation and suppose that an earthquake applies to it an equivalent load of 800 kips, as in the figure. Also, assume that the structure is bolted on the foundation with bolts whose cross-section is 0.5 in^2 and whose allowable stress is 20 ksi. If the earthquake load is resisted equally by each of the bolts on the two sides of the foundation parallel to its direction, find the maximum spacing of the bolts such that the average shear stress does not exceed the allowable value.

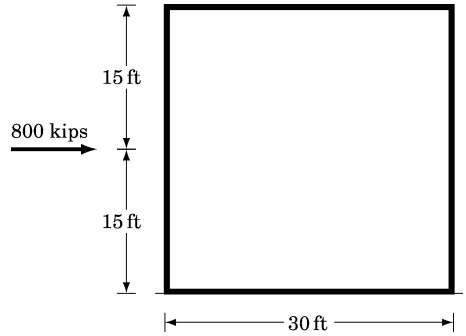

4.3-9. In exercise machines of the type illustrated in Fig. 2.31 (page 81), the lifted weights are supported by a pin inserted into a perforated rod rigidly attached to the topmost weight. If the allowable stress in double shear is 12 ksi, find the minimum diameter required for the pin to support a weight stack of 500 lb.

4.3-10. A dowel of 10-mm diameter, made of wood with an ultimate tensile strength of 60 MPa, is embedded in a hole and bonded with a glue whose shear strength is 25 MPa. Find the depth of the hole required if the force needed to extract the dowel is the same as that needed to break it in tension.

4.4 General State of Stress

4.4.1 Introduction

In Sects. 4.1 and 4.2 we defined normal stress and shear stress, respectively, associated with the corresponding force resultants. While Figs. 4.2–4.4 and 4.9–4.10 show axes labeled xyz, with the x-axis normal to the cross-section, we did not make any explicit reference to these axes in defining the respective stresses.

We are now ready to consider the possibility that the resultant force $\mathbf{R}$ on the cross-section may have both normal and shear components, as may every partial force $\Delta\mathbf{R}$ acting on a small element of area ΔA. We can thus write

$$\Delta\mathbf{R} = \mathbf{i}\Delta N + \Delta\mathbf{V} \tag{4.22}$$

and, by combining Eqs. (4.1) and (4.7),

$$\lim_{r\to 0}\frac{\Delta\mathbf{R}}{\Delta A} = \mathbf{i}\sigma + \boldsymbol{\tau}\,, \tag{4.23}$$

where we recall that both $\Delta\mathbf{V}$ and $\boldsymbol{\tau}$ are vectors in the yz-plane. It must be borne in mind, however, that the choice of the x-axis as being normal to the cross-section is arbitrary, and this choice should be reflected in the notation. Consequently, the normal stress will be written as σ_x, while the y- and z-components of $\boldsymbol{\tau}$ are τ_{yx} and τ_{zx}, respectively. Note that the first of the two subscripts in the shear stress components refers to the direction of the vector $\boldsymbol{\tau}$, and the second refers to the direction normal to the cross-section. The stresses acting on a cross-sectional area element ΔA are shown in Fig. 4.22. Also note that the area element ΔA shown in the figure is rectangular rather

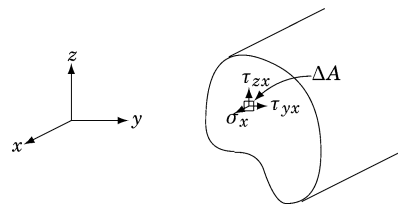

Figure 4.22. Stresses on a cross-sectional area element

than, as before, circular. In fact the shape of the element does not matter, provided r is a representative dimension such that the element shrinks to a point as $r \to 0$.

Note further that, in accordance with the subscript convention for the shear stresses, the normal stress could be denoted τ_{xx}. Indeed, a consistent double-subscript notation using the same basic symbol (τ or σ) for both normal and shear stresses is not unusual in the literature of solid mechanics. We

will not use this notation, because in virtually all the cases that we will study there is no more than one normal stress and/or one shear stress, and with the σ and τ notations the subscripts can often be dispensed with altogether.

Note, finally, that the directions of the stresses as shown in Fig. 4.22 are the positive directions of their respective axes when they are on a "positive" cut (that is, one facing the positive x-axis). Clearly, those directions will be opposite on the opposite cut (the one facing the negative x-axis).

4.4.2 Stresses on a Volume Element

Once we have moved from a body with a well-defined axis to one of arbitrary shape, no one Cartesian axis is more significant than any other, and we can define the stresses on an area element facing the y- or z-axis in the same way as above. These stresses are shown on the positive faces of the cuboidal volume element shown in Fig. 4.23. Also note that the normal stresses in Fig. 4.23 are positive (tensile) when they have the sense of the positive axes x, y, and z when acting on planes whose outward normals point toward the positive x, y and z axes *or* when they have the sense of the negative axes x, y, and z when acting on planes whose outward normals point toward the negative x, y and z axes. The same convention applies to the shear stresses. The cuboidal

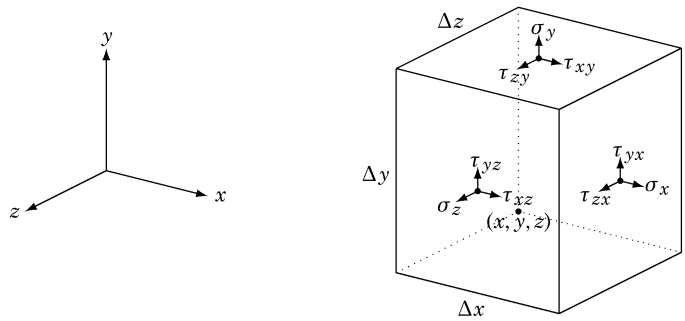

Figure 4.23. Stresses on a three-dimensional volume element

element is assumed small enough for the variation of the stresses through its extent to be neglected. Consequently, the resultants of the stresses can be assumed to act at the midpoints of the faces, as shown in the figure. Furthermore, if there are no forces acting in the interior of the element, the stresses on the (hidden) negative faces can be assumed to be equal and opposite to those shown, and therefore the element is in force equilibrium.

Moment equilibrium, as well as force equilibrium when the stresses are variable, will be considered in the next section.

4.4.3 State of Stress, Stress Tensor

Knowledge of the stresses on three mutually perpendicular planes at a point in a body determines the *state of stress* at the point, in the same sense that knowing the Cartesian components of a vector with respect to axes x, y, z means knowing the vector. The stresses σ_x, $\tau_{xy}, \ldots \sigma_z$, which can be conveniently arranged in matrix form as

$$\begin{bmatrix} \sigma_x & \tau_{xy} & \tau_{xz} \\ \tau_{yx} & \sigma_y & \tau_{yz} \\ \tau_{zx} & \tau_{zy} & \sigma_z \end{bmatrix}, \tag{4.24}$$

are called the components of stress with respect to the axes x, y, z. In Sect. 4.6 it will be shown that when these components are known then those with respect to any other set of axes (say x', y', z') can be easily calculated.

The quantity of which the stresses shown in Eq. (4.24) are the components is known as the *stress tensor*. What makes a quantity represented by an array like that of Eq. (4.24) a tensor* is the fact that when the square matrix multiplies a column matrix whose elements are the components of a vector (as defined in Sect. 1.2†), the elements of the resulting column matrix are the components (with respect to the same coordinate system) of another vector. That is, if $\{u\}$ and $\{v\}$ are column matrices representing respectively the vectors $\mathbf{u}$ and $\mathbf{v}$ with respect to a given coordinate system, and if $[A]$ is a square matrix such that

$$\{v\} = [A]\{u\}, \tag{4.25}$$

then the matrix $[A]$ represents a tensor with respect to the same coordinate system.

To observe the tensorial nature of the stress components we consider first, for simplicity, the two-dimensional case in which all the stress components in which one of the subscripts is z, that is, those on the plane of constant value of z, namely σ_z, τ_{zx} and τ_{zy}, as well as the shear components τ_{xz} and τ_{yz} that are directed along the z-axis, are zero. It follows that the matrix representation of the stress components in (4.24) reduces to

$$\begin{bmatrix} \sigma_x & \tau_{xy} \\ \tau_{yx} & \sigma_y \end{bmatrix}. \tag{4.26}$$

We now consider an infinitesimal body (assumed to be a subbody of some larger body) in the shape of a right-triangle wedge, shown in Fig. 4.24, where the legs of the triangle are parallel to x- and y-axes and the orientation of the hypotenuse is defined by the outward unit normal vector $\mathbf{n}$, with components $n_x = \cos\theta$ and $n_y = \sin\theta$, as shown in Fig. 4.24. We assume that the wedge is

*More precisely, a *second-rank* or (in British usage) *second-order* tensor

†In linear algebra, any column matrix can be called a vector.

of unit thickness in the direction perpendicular to the figure, and the area of the inclined plane is dA. Let now the resultant force on the inclined plane be written as $\mathbf{f}dA$. The quantity $\mathbf{f}$ is called the *traction vector* (or *stress vector*) on the infinitesimal inclined plane.[‡] The force equilibrium equations of the

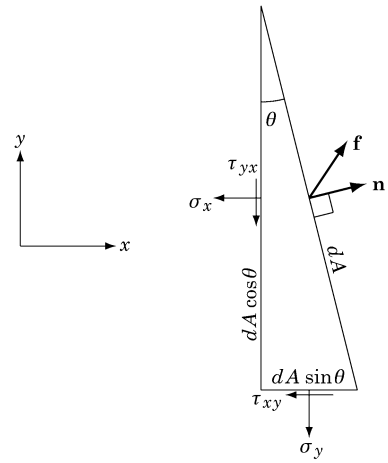

Figure 4.24. Traction on a wedge

wedge with the respect to the axes x, y are obtained by setting equal to zero the algebraic sums of the x- and y-components of the tractions on the three sides of the wedge shown in Fig. 4.24 multiplied by their respective areas. If any body force were present, its resultant would be proportional to the volume of the wedge, but since the wedge is assumed infinitesimally small, the volume is an infinitesimal of higher order than the area[§] and hence the contribution of the body force can be neglected alongside the surface forces. Consequently, the force equilibrium equations of the wedge take the form

$$f_x dA = \sigma_x dA\cos\theta + \tau_{xy} dA\sin\theta \quad , \quad f_y dA = \tau_{yx} dA\cos\theta + \sigma_y dA\sin\theta \; . \tag{4.27}$$

Dividing both sides of the equations in (4.27) by dA and recalling the definition of the components n_x and n_y leads to

$$f_x = \sigma_x n_x + \tau_{xy} n_y \quad , \quad f_y = \tau_{yx} n_x + \sigma_y n_y \; . \tag{4.28}$$

The preceding equation may be expressed in matrix form as

$$\left\{ \begin{array}{c} f_x \\ f_y \end{array} \right\} = \left[\begin{array}{cc} \sigma_x & \tau_{xy} \\ \tau_{yx} & \sigma_y \end{array} \right] \left\{ \begin{array}{c} n_x \\ n_y \end{array} \right\} \; . \tag{4.29}$$

[‡]While the components of the traction vector have the dimensions of stress (force per unit area), they are not technically stress components, since there is no reference in them to the axes defined by the inclined plane.

[§]The volume is of the order of the cube and the area is of the order of the square of a typical dimension.

It follows from our definition that the matrix (4.26) represents a two-dimensional tensor, since, when multiplied by the components of the outward unit vector normal to the include surface, it produces the components of the traction vector on the same surface.

Example 4.4.1: Calculation of traction from stress.
Suppose that the angle θ in Fig. 4.24 is 22.6°, so that $\mathbf{n} = (12\mathbf{i} + 5\mathbf{j})/13$, and let the stress matrix (4.26) be given by

$$\begin{bmatrix} 55 & -39 \\ -39 & 77 \end{bmatrix} \text{MPa}.$$

The traction components are, by Eq. (4.28),

$$f_x = [55(12/13) + (-39)(5/13)]\,\text{MPa} = 35.8\,\text{MPa},$$
$$f_y = [(-39)(12/13) + 77(5/13)]\,\text{MPa} = -6.4\,\text{MPa}.$$

The traction vector can also be resolved with respect to axes that are normal and tangential to the inclined face of the wedge, in which case they do in fact constitute stresses (normal and shear, respectively). The unit normal vector $\mathbf{n}$ is given above, while the unit tangential vector is $\mathbf{t} = (-5\mathbf{i} + 12\mathbf{j})/13$. The corresponding traction components are therefore

$$f_n = \mathbf{f}\cdot\mathbf{n} = (35.8\mathbf{i} - 6.4\mathbf{j})\cdot(12\mathbf{i} + 5\mathbf{j})/13\,\text{MPa} = 30.6\,\text{MPa},$$
$$f_t = \mathbf{f}\cdot\mathbf{t} = (35.8\mathbf{i} - 6.4\mathbf{j})\cdot(-5\mathbf{i} + 12\mathbf{j})/13\,\text{MPa} = -19.7\,\text{MPa}.$$

The determination of stress components with respect to different axes will be studied generally in Sect. 4.6.

The preceding result can be extended to the three-dimensional stress case if, instead of a two-dimensional wedge, we consider a tetrahedron with an inclined face of area dA defined by the unit outward normal vector $\mathbf{n}$ with components n_x, n_y, n_z, and with the other three faces perpendicular to the x-, y- and z-axes respectively, as in Fig. 4.25.

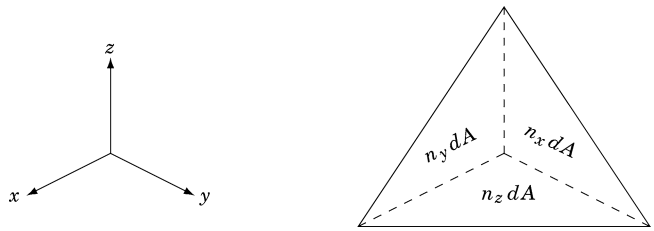

Figure 4.25. Tetrahedron with three edges aligned with the orthogonal axes x, y, z, and with inclined face of area dA and outward unit normal $\mathbf{n}$

Figure 4.26. Augustin-Louis Cauchy

This is known as the *Cauchy*[¶] *tetrahedron*. Now, the mutually perpendicular faces of the tetrahedron have areas $n_x dA$, $n_y dA$ and $n_z dA$. Repeating the procedure just discussed for the two-dimensional case leads to expressions for the three-dimensional components of the traction vector in the form

$$\begin{aligned} f_x &= \sigma_x n_x + \tau_{xy} n_y + \tau_{xz} n_z \,, \\ f_y &= \tau_{yx} n_x + \sigma_y n_y + \tau_{yz} n_z \,, \\ f_z &= \tau_{zx} n_x + \tau_{zy} n_y + \sigma_z n_z \end{aligned} \tag{4.30}$$

or, in matrix form,

$$\left\{ \begin{array}{c} f_x \\ f_y \\ f_z \end{array} \right\} = \left[\begin{array}{ccc} \sigma_x & \tau_{xy} & \tau_{xz} \\ \tau_{yx} & \sigma_y & \tau_{yz} \\ \tau_{zx} & \tau_{zy} & \sigma_z \end{array} \right] \left\{ \begin{array}{c} n_x \\ n_y \\ n_z \end{array} \right\} . \tag{4.31}$$

As in the two-dimensional case discussed in Example 4.4.1, the traction vector may be resolved with respect to the normal direction of the inclined plane, so that the normal component of the traction is $f_n = \mathbf{f} \cdot \mathbf{n}$, which is also the normal stress σ. The vector difference between the total traction vector $\mathbf{f}$ and the vector $f_n \mathbf{n}$ is therefore the shear-stress vector $\boldsymbol{\tau}$ discussed in Sect. 4.2, that is,

$$\boldsymbol{\tau} = \mathbf{f} - (\mathbf{f} \cdot \mathbf{n}) \mathbf{n} \,. \tag{4.32}$$

[¶]Baron Augustin-Louis Cauchy (1789–1857) was a French mathematician (Fig. 4.26) and, arguably, one of the most influential figures in the development of solid mechanics as a scientifically based discipline.

Exercises

4.4-1. For a two-dimensional state of stress with components $\sigma_x = 15$, $\tau_{xy} = 11$, $\sigma_y = -8$ and $\tau_{yx} = 11$ (all in ksi), find the traction vector on the inclined plane of the wedge of Fig. 4.24 if $\theta = 30°$.

4.4-2. For the data of the preceding exercise, find the traction components with respect to the normal and tangential axes of the inclined plane.

4.4-3. For a two-dimensional state of stress with components $\sigma_x = -90$, $\tau_{xy} = -75$, $\sigma_y = -150$ and $\tau_{yx} = -75$ (all in MPa), find the traction vector on the inclined plane of the wedge shown below.

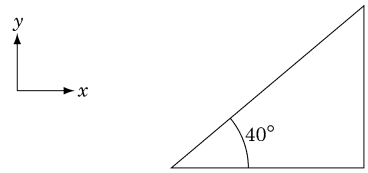

4.4-4. For the data of the preceding exercise, find the traction components with respect to the normal and tangential axes of the inclined plane.

4.4-5. A circular plate is in a state of uniform two-dimensional stress stress, with the components as in Eq. (4.26). By considering the equilibrium of the small element shown shaded in the figure below, find the normal and tangential traction components (and hence the normal and shear stresses) on the edge of the plate as a function of θ.

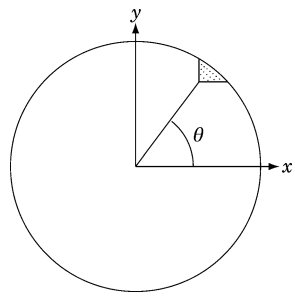

4.4-6. For a three-dimensional state of stress with components $\sigma_x = 55$, $\tau_{xy} = -30$, $\tau_{xz} = 0$, $\tau_{yx} = -30$, $\sigma_y = 40$, $\tau_{yz} = 25$, $\tau_{zx} = 0$, $\tau_{zy} = 25$ and $\sigma_z = -60$ (all in MPa), find the traction vector on an inclined plane with $\mathbf{n} = (1/\sqrt{3})(\mathbf{i} - \mathbf{j} - \mathbf{k})$.

4.4-7. Using Eq. (1.29) (page 21) for the vector triple product, show that Eq. (4.32) may be written as

$$\boldsymbol{\tau} = \mathbf{n} \times (\mathbf{f} \times \mathbf{n}) \ .$$

4.4-8. Using the result of Exercise **4.4-7**, find the shear-stress vector $\boldsymbol{\tau}$ on the inclined plane for the data of Exercise **4.4-6**.

4.4-9. For the two-dimensional case, with $\mathbf{n} = \mathbf{i}\cos\theta + \mathbf{j}\sin\theta$ and with the traction given by Eq. (4.28), use the result of Exercise **4.4-7** to determine the shear stress on the inclined plane in terms of σ_x, τ_{xy}, τ_{yx}, σ_y and θ.

4.5 Local Equilibrium Equations

4.5.1 Introduction

The local equilibrium equations for a three-dimensional continuum are obtained as described in Sect. 2.3 by considering a finite-sized volume element of the body and taking the limit as its size goes to zero. In particular, we take this element to be a rectangular parallelepiped with one corner at a point with coordinates $(\bar{x},\bar{y},\bar{z})$ and the other corners at $(\bar{x}+\Delta x,\bar{y},\bar{z})$, $(\bar{x},\bar{y}+\Delta y,\bar{z})$, …, $(\bar{x}+\Delta x,\bar{y}+\Delta y,\bar{z}+\Delta z)$, as shown in Fig. 4.27.

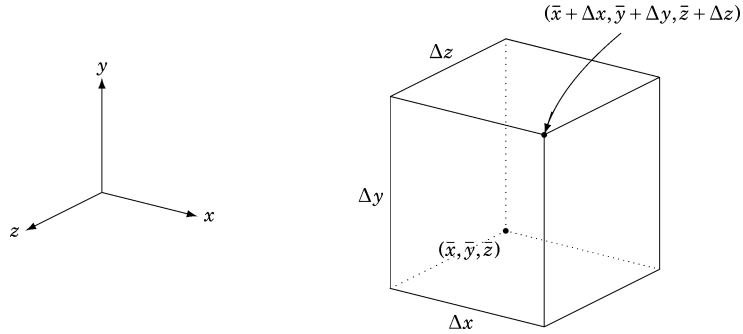

Figure 4.27. A rectangular parallelepiped with one corner at $(\bar{x},\bar{y},\bar{z})$.

4.5.2 Equilibrium Equations in Plane Stress

We suppose, to begin with, that the body is in a state of *plane stress* in the xy-plane, meaning that the stress tensor is represented by the two-dimensional matrix (4.26) and, moreover, the nonvanishing stress components σ_x, σ_y, τ_{xy} and τ_{yx} depend only on x and y. It is also assumed that the *body force* $\mathbf{b}$ (with dimensions of force per unit volume) has only the components b_x and b_y, and that these are also independent of z. In that case, the element of Fig. 4.23 need only be viewed in two dimensions, as in Fig. 4.28, with the stress and body-force components as shown. Note that the axes have been rotated so that the xy-plane, rather than the yz-plane, is now the plane of the paper.

Employing a Taylor series expansion around $x=\bar{x}$, the stress σ_x at a point $(\bar{x}+\Delta x,y)$ on the face with coordinates $x=\bar{x}+\Delta x$ is related to the stress at a point $(\bar{x},y)$ on the opposite face $x=\bar{x}$ and its derivatives according to

$$\sigma_x(\bar{x}+\Delta x,y) \;=\; \sigma_x(\bar{x},y) \;+\; \frac{\partial\sigma_x}{\partial x}(\bar{x},y)\Delta x \;+\; \frac{1}{2!}\frac{\partial^2\sigma_x}{\partial x^2}(\bar{x},y)\Delta x^2 \;+\; \ldots\,. \qquad (4.33)$$

Taking now the limit as Δx becomes infinitesimally small (and denoted by dx), all the terms of the expansion in (4.33) involving quadratic and higher

powers of Δx become negligible compared to the first two terms on the right-hand side, hence

$$\sigma_x(\bar{x}+dx,y) \;=\; \sigma_x(\bar{x},y) \;+\frac{\partial\sigma_x}{\partial x}(\bar{x},y)dx\;. \tag{4.34}$$

Corresponding formulae apply for σ_y, τ_{xy} and τ_{yx}, and the resulting stresses are shown in Fig. 4.28. We obtain the forces acting on the element by mul-

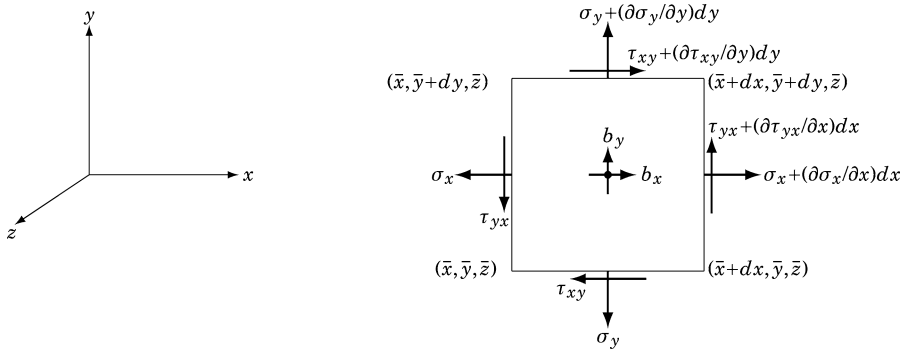

Figure 4.28. Free-body diagram for an infinitesimal rectangular parallelepiped in the state of plane stress

tiplying all the stresses by their respective areas and the body-force components by the volume $dxdydz$. Summing all the forces acting in the x-direction and setting the sum equal to zero for equilibrium, we find that

$$\left[\sigma_x+\frac{\partial\sigma_x}{\partial x}dx\right](dydz)+\left[\tau_{xy}+\frac{\partial\tau_{xy}}{\partial y}dy\right](dxdz)+b_x(dxdydz)$$
$$-\sigma_x(dydz)-\tau_{xy}(dxdz) \;=\; 0\;,$$

which, upon simplifying and noting that $dxdydz \neq 0$, leads to

$$\frac{\partial\sigma_x}{\partial x}+\frac{\partial\tau_{xy}}{\partial y}+b_x \;=\; 0\;. \tag{4.35}$$

Performing a similar operation with the forces in the y-direction leads to

$$\frac{\partial\sigma_y}{\partial y}+\frac{\partial\tau_{yx}}{\partial x}+b_y \;=\; 0\;. \tag{4.36}$$

We now consider moment equilibrium. Since the element is infinitesimal, it can be assumed that the normal stresses and the body forces are essentially constant, so that their lines of action go through the center of the element, and only the shear stresses cause a moment about this point. Since the resultant force is zero, moments can be taken about any point, and we can choose, for simplicity, the point $(\bar{x}+dx,\bar{y}+dy,\bar{z})$. The moment about this point is then simply

$$\tau_{yx}(dydz)dx-\tau_{xy}(dxdz)dy \;=\; 0\;, \tag{4.37}$$

from which it follows that

$$\tau_{yx} = \tau_{xy} \, . \tag{4.38}$$

Eq. (4.38) implies that, when in equilibrium, both shear stresses associated with neighboring edges should point toward (or away from) the common edge, as in Fig. 4.29a. Otherwise, the body would spin, which is the case in Fig. 4.29b. Eqs. (4.42) collectively imply that the matrix of stress components in Eq. (4.24) is symmetric.

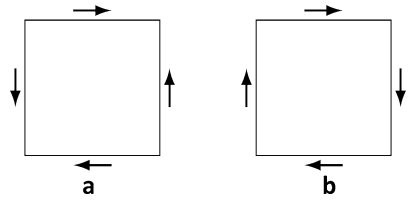

Figure 4.29. Cross-section in equilibrium (**a**) or inequilibrium (**b**) depending on the sense of the shear stresses acting on its edges

4.5.3 Extension to Three Dimensions

The extension of the preceding results to three dimensions is straightforward; we draw a cuboidal box, as seen in Fig. 4.30,* in which we include the body-force component b_z in the interior and appropriate values of the stress components σ_z, τ_{zx}, τ_{zy}, τ_{xz} and τ_{yz} on the corresponding sides. (To minimize

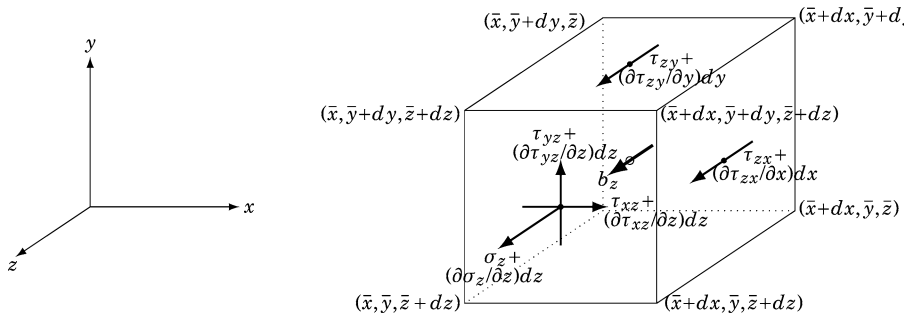

Figure 4.30. Three-dimensional extension of Fig. 4.28

clutter, only the terms not shown in Fig. 4.28 are indicated, and only those acting on the positive sides of the cuboid.) The resulting three-dimensional equilibrium equations are

$$\frac{\partial\sigma_x}{\partial x} + \frac{\partial\tau_{xy}}{\partial y} + \frac{\partial\tau_{xz}}{\partial z} + b_x = 0 \, , \tag{4.39}$$

*Note, if comparing with Fig. 4.23, that the directions of the axes are different.

$$\frac{\partial \sigma_y}{\partial y} + \frac{\partial \tau_{yx}}{\partial x} + \frac{\partial \tau_{yz}}{\partial z} + b_y = 0 \,, \tag{4.40}$$

$$\frac{\partial \sigma_z}{\partial z} + \frac{\partial \tau_{zy}}{\partial y} + \frac{\partial \tau_{zx}}{\partial x} + b_z = 0 \,, \tag{4.41}$$

$$\tau_{yx} = \tau_{xy} \quad , \quad \tau_{zy} = \tau_{yz} \quad , \quad \tau_{xz} = \tau_{zx} \,. \tag{4.42}$$

Eqs. (4.39-4.42) need to be solved when analyzing general three-dimensional solid bodies in equilibrium. These comprise a system of three coupled partial differential equations in Eqs. (4.39)–(4.41), known as *Cauchy's equations* for equilibrium, subject to three algebraic conditions in Eqs. (4.42). With the exception of a few simple, yet important, cases, the solution of Eqs. (4.39-4.42) is obtained using numerical methods.

Example 4.5.1: Compression under gravity.
We consider a body bounded above by the plane $z = 0$ (with z positive upward), with a pressure p_0 acting on this plane and the weight of the body (of density ρ) in its interior. The body force is accordingly $\mathbf{b} = -\rho g \mathbf{k}$, and if no shear stresses are assumed to exist, then Eqs. (4.39-4.42) take the form

$$\frac{\partial \sigma_x}{\partial x} = 0 \quad , \quad \frac{\partial \sigma_y}{\partial y} = 0 \quad , \quad \frac{\partial \sigma_z}{\partial z} - \rho g = 0 \,.$$

The third equation is satisfied, along with the boundary condition at $z = 0$, by $\sigma_z = -p_0 + \rho g z$. The satisfaction of the other equations depends on the material. If it is a fluid then, by *Pascal's law*[†], $\sigma_x = \sigma_y = \sigma_z$. If it is a solid cylinder (not necessarily circular) with generators parallel to the z-axis, then a possible solution is given by $\sigma_x = \sigma_y = 0$.

4.5.4 Simple Shear

If, in the absence of body force, it is possible to find a coordinate system x, y, z such that, in a given portion of a body, the only nonvanishing stress component is one of the shear stresses (say $\tau_{xz} = \tau_{zx} = \tau$), then every point of this portion is in equilibrium if τ is independent of x and z, since Eqs. (4.39-4.42) are then satisfied. The stress state of such a portion of a body is known as *simple shear*.

Example 4.5.2: Local equilibrium of a tube in torsion.
We examine a small, almost-rectangular element of the tube of Fig. 4.19, shown in Fig. 4.31 along with the local coordinate system chosen to define the stress components. If the element is small enough it can be assumed as being in plane stress.[‡] Unlike the tube of Fig. 4.19, however, in Fig. 4.31 we show the possible variation of the shear stress through the thickness. Since this variation is with the respect to the y-direction, it does not affect the equilibrium of the element.

[†]Blaise Pascal (1623–1662) was a French philosopher, physicist and mathematician, for whom the pascal is named.

[‡]This assumption would not be valid if other stress components were involved.

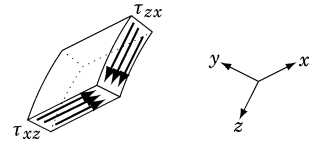

Figure 4.31. Example 4.5.2

4.5.5 Stress Functions

Many problems in solid mechanics can be reduced to finding a scalar function of x, y, z (called a *stress function*) with the property that all the stress components can be generated from it in such a way that the equilibrium equations are satisfied. An example is shown below, and other examples will be considered in exercises.

Of course, since nearly all problems in solid mechanics involve stress states that are *not* simple (in the sense of Sect. 4.3), that is, locally statically determinate, the fact that the stress field derived from a given stress function satisfies equilibrium does not mean that it is unique. As with finite-degree-of-freedom systems, the complete solution of such problems requires the satisfaction of both equilibrium and geometric compatibility, mediated by material properties.

Example 4.5.3: The Prandtl[§] stress function.

We consider a prismatic[¶] rod with the z-axis as its longitudinal axis and with a cross-section $\mathscr{A}$ (of area A) in the xy-plane. If it is assumed that all stresses except $\tau_{yz}(=\tau_{zy})$ and $\tau_{zx}(=\tau_{xz})$ are zero, then, if a differentiable function $\chi(x,y)$ can be found such that

$$\tau_{yz} = -\frac{\partial \chi}{\partial x} \quad , \quad \tau_{xz} = \frac{\partial \chi}{\partial y} \, , \tag{4.43}$$

it is easy to see that all the equilibrium equations (4.39–4.42) are satisfied with zero body force. It also follows from Eqs. (4.43) that the shear-stress vector $\boldsymbol{\tau}$ $(= \tau_{xz}\mathbf{i} + \tau_{yz}\mathbf{j})$ is perpendicular to $(\partial\chi/\partial x)\mathbf{i} + (\partial\chi/\partial y)\mathbf{j}$. Consequently, if χ is represented by a surface, then at any point the direction of the shear stress is along the contour and its numerical value is that of the slope.

If, moreover, the function χ is such that it is constant along the boundary of $\mathscr{A}$, then it can be shown that (a) the shear stress at the boundary is tangential to it (so that the boundary is free of traction) and (b) the force resultant of the stress distribution is zero. The first follows from the preceding discussion of the

[§]Ludwig Prandtl (1875–1953) was a German engineering scientist.

[¶]In engineering, *prismatic* (when describing a straight slender body) is commonly used for what in mathematical language is *cylindrical*—that is, having a uniform cross-section—in order to avoid the implication of a *circular* cylinder.

direction of the shear-stress vector. To show the second, we note that, say, the y-component of the shear force (the only possible force resultant) is given by

$$V_y = \int_{\mathscr{A}} \tau_{yz}\, dA = -\int_{\mathscr{A}} \frac{\partial \chi}{\partial x} dx\, dy.$$

If the integration with respect to x is carried out first, it goes (if there is no hole to be crossed) from one point on the boundary, say 1, to another, say 2, with the same value of y, as seen in Fig. 4.32a. The result of this partial integration is $-\chi_2 + \chi_1$, but this is zero if χ is constant on the boundary.

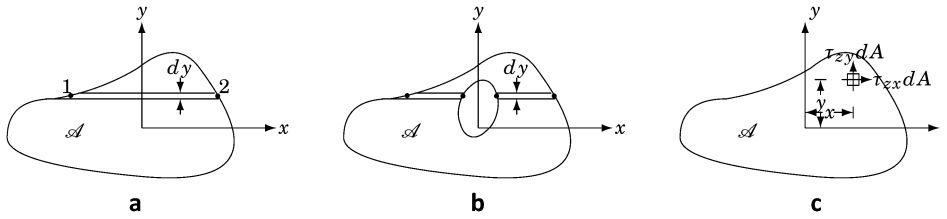

Figure 4.32. Example 4.5.3: integration over $\mathscr{A}$ (**a**) without and (**b**) with a hole; (**c**) moment of stress field

If the cross-section $\mathscr{A}$ contains a hole, as in Fig. 4.32b, then χ is assumed constant along the boundary of the hole, though not necessarily with the same value as on the outer boundary. The preceding results remain valid, the proof being left to an exercise.

The only resultant of the stress field is, therefore a torque T $(= M_z)$, given (as can be seen from Fig. 4.32c) by

$$T = \int_{\mathscr{A}} (x\tau_{yz} - y\tau_{xz})\, dA = -\int_{\mathscr{A}} \left(x\frac{\partial \chi}{\partial x} + y\frac{\partial \chi}{\partial y} \right) dA\ .$$

Now, the integrand in the third member of this equation can be written as $\partial(x\chi)/\partial x + \partial(y\chi)/\partial y - 2\chi$. If the cross-section has no holes, and χ is defined such that its constant value on the boundary is zero, then the area integrals of the first two terms in the last expression are also zero, leaving

$$T = 2\int_{\mathscr{A}} \chi\, dA\ . \tag{4.44}$$

Exercises

4.5-1. In a two-dimensional region the shear stress is given by $\tau_{xy} = Ax^2 + By^2$, where A and B are constants. Assuming zero body force and using Eq. (4.38), find the simplest expressions for σ_x and σ_y so that the two-dimensional equilibrium equations (4.35–4.36) are satisfied.

4.5-2. In a two-dimensional region bounded by $y = \pm c$, $\sigma_x = Axy$, where A is a constant. Assuming zero body force and using Eq. (4.38), solve the equilibrium equations (4.35–4.36) for τ_{xy} and σ_y such that $\tau_{xy} = 0$ and $\sigma_y = 0$ at $y = \pm c$.

4.5-3. Find the simplest stress field satisfying the equilibrium equations (4.39)–(4.42) if the body force is given by $\mathbf{b} = -\rho g \mathbf{k}$ (e.g., if the body force is due to gravity along the negative $\mathbf{k}$-axis with gravitational constant g).

4.5-4. Derive equation $(4.42)_1$ by taking moments of all forces about the point with coordinates $(\bar{x} + dx/2, \bar{y} + dy/2, \bar{z})$ without invoking force equilibrium. State clearly any assumptions made in deducing $(4.42)_1$ in this case.

4.5-5. Suppose that, in a two-dimensional region, a function $\Phi(x, y)$ exists such that $\sigma_x = \partial^2\Phi/\partial y^2$ and $\sigma_y = \partial^2\Phi/\partial x^2$. Find an expression for τ_{xy} in terms of $\Phi(x, y)$ so that the equilibrium equations equations (4.35) and (4.36) are satisfied with zero body force.

4.5-6. Suppose that, in a three-dimensional region, a function $\psi(x, y, z)$ exists such that $\tau_{yz} = \partial^2\psi/\partial x\partial z$, $\tau_{zx} = \partial^2\psi/\partial y\partial z$, and $\tau_{xy} = -\partial^2\psi/\partial z^2$. Find expressions for σ_x, σ_y and σ_z in terms of $\psi(x, y)$ so that the equilibrium equations (4.39–4.42) are satisfied with zero body force.

4.5-7. If, in Example 4.5.5, the cross-section contains a hole, show that the results for the shear stress at the boundary and the vanishing of the shear force remain valid.

4.6 Stress Transformation, Principal Stresses, Mohr's Circle

4.6.1 Transformation of Stress Components

Let, for a given state of plane stress, the stress components with respect to a set of Cartesian axes x, y be as shown in Fig. 4.33a. It is important to appreciate that these components are specific to the choice of the axes x, y, which has been made here in an arbitrary manner. This motivates our quest to determine the corresponding stress components with respect to another set of axes x', y', rotated by an angle θ from the first set, as shown in Fig. 4.33b. (Recall that, in view of Eq. $(4.42)_1$, $\tau_{yx} = \tau_{xy}$ and $\tau_{y'x'} = \tau_{x'y'}$.)

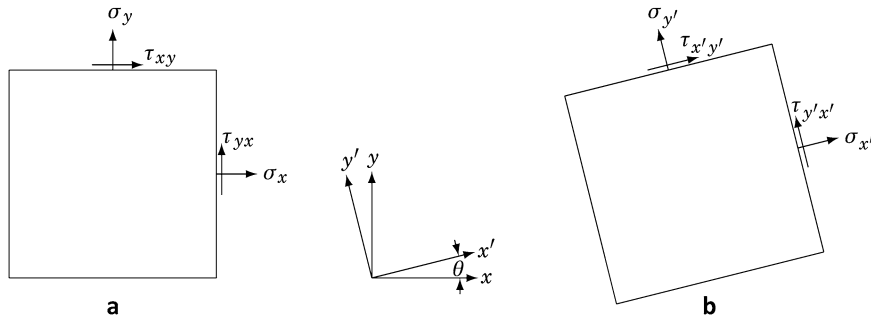

Figure 4.33. Stress components with respect to different sets of axes (only the stresses on the positive faces are shown): (**a**) original axes, (**b**) rotated axes

The relation between the two sets of stress components can be calculated from the equilibrium of a wedge like that of Fig. 4.24 (page 183, with body force ignored as we discussed there) but with the normal vector $\mathbf{n}$ now defining the x'-axis, as in Fig. 4.34. An alternative notation for the stress components $\sigma_{x'}$ and $\tau_{x'y'}$, namely σ_θ and τ_θ, respectively, is also shown in the figure. This notation makes the dependence on the angle of rotation θ explicit. If the wedge were such that the hypotenuse is perpendicular to the y'-axis then this angle would be greater by another 90°; it follows that if $\sigma_{x'} = \sigma_\theta$, then $\sigma_{y'} = \sigma_{\theta+\pi/2}$, as in Fig. 4.34.

The stress components σ_θ and τ_θ are evidently the components of the traction vector $\mathbf{f}$ with the respect to the x'- and y'-axes, respectively; that is, since $\mathbf{n} = \mathbf{i}' = \mathbf{i}\cos\theta + \mathbf{j}\sin\theta$ and $\mathbf{j}' = -\mathbf{i}\sin\theta + \mathbf{j}\cos\theta$,

$$\sigma_\theta = \mathbf{f}\cdot(\mathbf{i}\cos\theta + \mathbf{j}\sin\theta) \quad , \quad \tau_\theta = \mathbf{f}\cdot(-\mathbf{i}\sin\theta + \mathbf{j}\cos\theta)\,. \tag{4.45}$$

Combining these equations with Eq. (4.28) yields

$$\sigma_\theta = \sigma_x\cos^2\theta + 2\tau_{xy}\cos\theta\sin\theta + \sigma_y\sin^2\theta \tag{4.46}$$

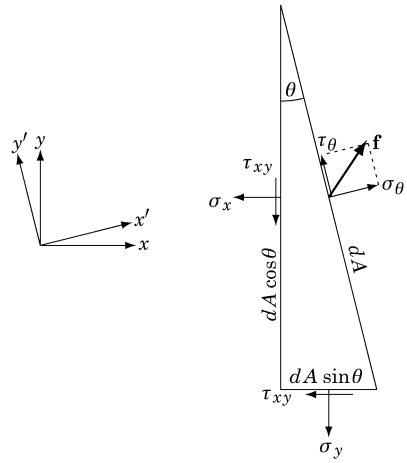

Figure 4.34. Stresses on a wedge

and

$$\tau_\theta = (\sigma_y - \sigma_x)\cos\theta\sin\theta + \tau_{xy}(\cos^2\theta - \sin^2\theta)\,. \tag{4.47}$$

With $\sigma_{y'}$ determined by replacing θ with $\theta + \pi/2$ in Eq. (4.46), an expression for the transformed stresses may be written in matrix form as follows:

$$\begin{bmatrix} \sigma_{x'} & \tau_{x'y'} \\ \tau_{x'y'} & \sigma_{y'} \end{bmatrix} = \begin{bmatrix} \cos\theta & \sin\theta \\ -\sin\theta & \cos\theta \end{bmatrix} \begin{bmatrix} \sigma_x & \tau_{xy} \\ \tau_{xy} & \sigma_y \end{bmatrix} \begin{bmatrix} \cos\theta & -\sin\theta \\ \sin\theta & \cos\theta \end{bmatrix}. \tag{4.48}$$

Eqs. (4.46) and (4.47) may be rewritten in yet another way by using the trigonometric identities $\cos^2\theta + \sin^2\theta = 1$, $\cos 2\theta = \cos^2\theta - \sin^2\theta$ and $\sin 2\theta = 2\sin\theta\cos\theta$, from which it follows that

$$\cos^2\theta = \frac{1+\cos 2\theta}{2} \quad , \quad \sin^2\theta = \frac{1-\cos 2\theta}{2} \quad , \quad \sin\theta\cos\theta = \frac{\sin 2\theta}{2}\,. \tag{4.49}$$

Consequently,

$$\sigma_\theta = \frac{\sigma_x + \sigma_y}{2} + \frac{\sigma_x - \sigma_y}{2}\cos 2\theta + \tau_{xy}\sin 2\theta \tag{4.50}$$

and

$$\tau_\theta = -\frac{\sigma_x - \sigma_y}{2}\sin 2\theta + \tau_{xy}\cos 2\theta\,. \tag{4.51}$$

Eqs. (4.50) and (4.51) clearly show how the normal and shear stresses on a given surface element vary with the orientation of the surface. It should not be surprising that this variation is periodic with period π, since a rotation of 180° brings us to the face opposite the original one, and the stresses across opposite faces must be equal.

Example 4.6.1: Calculation of transformed stresses.
Suppose that $\sigma_x = 40$ MPa, $\sigma_y = -20$ MPa, and $\tau_{xy} = 25$ MPa. We wish to calculate $\sigma_{x'}$, $\sigma_{y'}$, and $\tau_{x'y'}$ for $\theta = 30°$ using Eqs. (4.50) and (4.51).
Since $\sigma_{x'} = \sigma_\theta$ and $\sigma_{y'} = \sigma_{\theta+\pi/2}$, we find, by Eq. (4.50), that

$$\sigma_{x'} = \left(\frac{40-20}{2} + \frac{40+20}{2}\cos 60° + 25\sin 60°\right)\text{MPa} = 46.65 \text{ MPa},$$
$$\sigma_{y'} = \left(\frac{40-20}{2} + \frac{40+20}{2}\cos 240° + 25\sin 240°\right)\text{MPa} = -26.65 \text{ MPa},$$

while, by Eq. (4.51),

$$\tau_{x'y'} = \left(-\frac{40+20}{2}\sin 60° + 25\cos 60°\right)\text{MPa} = -13.48 \text{ MPa}.$$

The transformation of stress components from one set of coordinates to another is not limited to the case where either set is Cartesian, as will be seen in the following example.

Example 4.6.2: Stress components in polar coordinates.
An infinitesimal area element in polar coordinates, along with the stresses acting on it if the stress is uniform, is shown in Fig. 4.35a. (Note that the meaning of σ_θ here is not the same as in the preceding discussion; it is the circumferential normal stress (or hoop stress) discussed in Example 4.3.2, page 170.) Wedges for

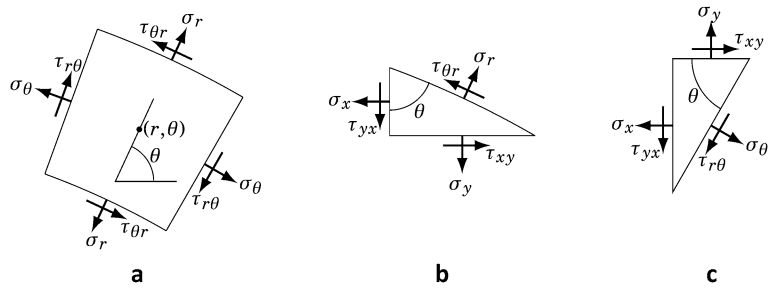

Figure 4.35. (a) Stresses on an infinitesimal area in polar coordinates in a uniform stress state (b)–(c) Wedges for the determination of stress components

the determination of these stress components can be formed from the element as shown in Fig. 4.35b–c. Since the area is infinitesimal, the curvature of the hypotenuse in Fig. 4.35b and the fact that the inclination of the one in Fig. 4.35c can be ignored, and we find accordingly

$$\begin{aligned} \sigma_r &= \sigma_x\cos^2\theta + 2\tau_{xy}\cos\theta\sin\theta + \sigma_y\sin^2\theta, \\ \sigma_\theta &= \sigma_x\sin^2\theta - 2\tau_{xy}\cos\theta\sin\theta + \sigma_y\cos^2\theta, \\ \tau_{r\theta} &= \tau_{\theta r} = (\sigma_y - \sigma_x)\cos\theta\sin\theta + \tau_{xy}(\cos^2\theta - \sin^2\theta). \end{aligned} \tag{4.52}$$

If the stress is variable, however, then the non-rectangular nature of the element must be taken into account in deriving the equilibrium equations. With the coordinates of the points A, B, C and D in Fig. 4.36 being respectively

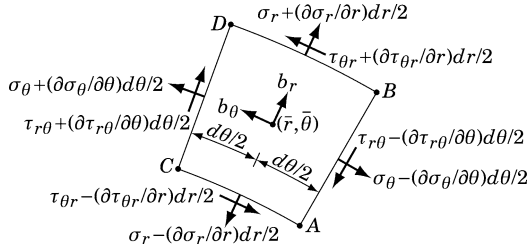

Figure 4.36. Stresses on an infinitesimal area in polar coordinates in a state of variable stress

$(\bar{r}-dr/2,\bar{\theta}-d\theta/2)$, $(\bar{r}+dr/2,\bar{\theta}-d\theta/2)$, $(\bar{r}+dr/2,\bar{\theta}-d\theta/2)$ and $(\bar{r}+dr/2,\bar{\theta}+d\theta/2)$, We see that, when the equilibrium equations of the volume element are written with respect to the radial and circumferential directions at the center of the element ($\Sigma F_r = 0$, $\Sigma F_\theta = 0$), account must be taken of the fact that (a) the areas of the faces containing the arcs AC and BD are, respectively, $(r-dr/2)d\theta\,dz$ and $(r+dr/2)d\theta\,dz$, and (b) the faces AB and CD are inclined by an angle $d\theta/2$ with respect to the radial direction. With $\cos(d\theta/2)$ and $\sin(d\theta/2)$ approximated by 1 and $d\theta/2$, respectively, and with only the terms of the first degree in dr and $d\theta$ retained, the local equilibrium equations in polar coordinates turn out to be

$$\begin{aligned} &\frac{\partial\sigma_r}{\partial r}+\frac{\sigma_r-\sigma_\theta}{r}+\frac{1}{r}\frac{\partial\tau_{r\theta}}{\partial\theta}+b_r=0\,,\\ &\frac{\partial\tau_{r\theta}}{\partial r}+\frac{2\tau_{r\theta}}{r}+\frac{1}{r}\frac{\partial\sigma_\theta}{\partial\theta}+b_\theta=0\,. \end{aligned} \tag{4.53}$$

4.6.2 Principal Stresses

For both the normal stress and the shear stress, there are orientations that make their values maximum or minimum, and these can be determined by differentiating the right-hand sides of Eqs. (4.50) and (4.51) with respect to θ and setting the derivatives equal to zero. Calculating maximum values of normal and shear stresses is important in stress-based design, since these values often determine material failure.

Starting from Eq. (4.50), we may find a maximum or minimum normal stress by setting

$$\frac{d\sigma_\theta}{d\theta} = 2\left(-\frac{\sigma_x-\sigma_y}{2}\sin 2\theta+\tau_{xy}\cos 2\theta\right) = 0\,. \tag{4.54}$$

The quantity inside the parentheses in Eq. (4.54) is just the right-hand side of Eq. (4.51), that is, it equals the value of τ_θ, so that the normal stress attains its maximum and minimum values precisely on those surfaces on which the shear stress is zero, namely, those whose orientations are given by values of θ, denoted θ_p, that satisfy

$$\frac{\sigma_x-\sigma_y}{2}\sin 2\theta_p = \tau_{xy}\cos 2\theta_p \tag{4.55}$$

or, provided $(\sigma_x - \sigma_y)$ and τ_{xy} are not both zero (an important special case that will be discussed below),

$$\tan 2\theta_p = \frac{2\tau_{xy}}{\sigma_x - \sigma_y} . \tag{4.56}$$

Because the tangent function has periodicity π, it follows that $\tan 2(\theta + \pi/2) = \tan 2\theta$, so that if an angle θ_p has been found that satisfies Eq. (4.56), then $\theta_p \pm \pi/2$ does so likewise. In any 180° range of surface orientations, there are consequently two mutually perpendicular ones, given by, say θ_{p1} and θ_{p2}, on which the normal stress is respectively (algebraically) maximum and minimum. The normal axes of these surfaces are called the *principal axes of stress*, and the corresponding values of the normal stress, $\sigma_{\theta_{p1}}$ and $\sigma_{\theta_{p2}}$, are called the *principal stresses*. They are usually denoted simply σ_1 and σ_2, and are illustrated in Fig. 4.37.

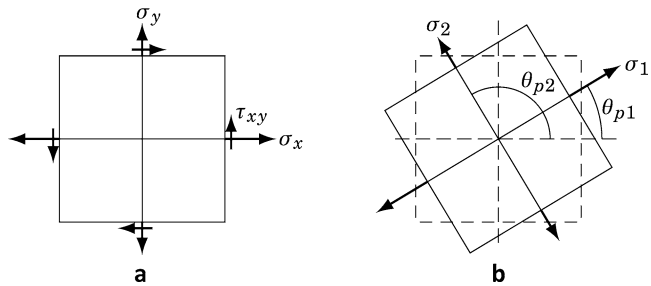

Figure 4.37. Principal stresses: (**a**) element along original axes, (**b**) element along principal axes

The special case $\sigma_x = \sigma_y$, with $\tau_{xy} \neq 0$, means that $\tan 2\theta_{p1,2} = \infty$, so that $2\theta_{p1,2} = \pm\pi/2$ (or $\pm 3\pi/2$), and therefore the principal axes are at 45° to the original axes. If, on the other hand, $\sigma_x = \sigma_y$ and $\tau_{xy} = 0$, then *any* value of θ satisfies Eq. (4.55). In other words, all axes are principal axes; the shear stress is zero on all rotated surface elements, and the normal stresses have the same value on all of them, as is also clear from Eqs. (4.50) and (4.51).

In order to determine the principal stresses in the general case, we need to derive expressions for $\cos 2\theta_p$ and $\sin 2\theta_p$ from Eq. (4.56). For each value of the tangent, there are two pairs of values of the cosine and the sine:

$$\cos 2\theta_{p1,2} = \pm \frac{1}{\sqrt{1 + \tan^2 2\theta_p}} \quad , \quad \sin 2\theta_{p1,2} = \pm \frac{\tan 2\theta_p}{\sqrt{1 + \tan^2 2\theta_p}} , \tag{4.57}$$

with θ_p given by Eq. (4.56). Letting

$$r = \sqrt{\left(\frac{\sigma_x - \sigma_y}{2}\right)^2 + \tau_{xy}^2} , \tag{4.58}$$

it follows from (4.56) and (4.57) that

$$\cos 2\theta_{p1,2} = \pm\frac{\sigma_x - \sigma_y}{2r} \quad , \quad \sin 2\theta_{p1,2} = \pm\frac{\tau_{xy}}{r} \, . \tag{4.59}$$

Inserting these values into Eq. (4.50) and recalling the definition of r in (4.58) results in

$$\sigma_{1,2} = \frac{\sigma_x + \sigma_y}{2} \pm \sqrt{\left(\frac{\sigma_x - \sigma_y}{2}\right)^2 + \tau_{xy}^2} \, . \tag{4.60}$$

Note that, by this result, σ_1 is the algebraically larger of the principal stresses, so that $r = (\sigma_1 - \sigma_2)/2$. However, this particular numbering of the principal stresses is not always applied, so that, more generally, $r = |\sigma_1 - \sigma_2|/2$. Also note that

$$\sigma_1 + \sigma_2 = \sigma_x + \sigma_y \, , \tag{4.61}$$

but since the initial choice of axes x and y is arbitrary, the result holds when these axes are replaced by any rotated axes x' and y'. In other words, the sum of the normal stresses on two perpendicular faces is independent of their orientation.

Example 4.6.3: Calculation of principal stresses and directions.
We wish to find the principal stresses and directions for the stress state of Example 4.6.1, using both the original and the transformed stress components. With the original stress components, we find first that

$$r = \sqrt{30^2 + 25^2}\ \text{MPa} = 39.05\ \text{MPa} \, .$$

With the positive roots in Eqs. (4.59), and limiting ourselves to positive values of the angles, we find that Eq. $(4.59)_1$ is satisfied when θ_{p1} is 19.9° or 160.1°, and $(4.59)_2$ when θ_{p1} is 19.9° or 70.1°; consequently (since both equations must be satisfied), $\theta_{p1} = 19.9°$. Similarly, $\theta_{p2} = 109.9°$. Now, by Eq. (4.60),

$$\sigma_1 = (10{+}39.05)\ \text{MPa} = 49.05\ \text{MPa} \quad , \quad \sigma_2 = (10{-}39.05)\ \text{MPa} = -29.05\ \text{MPa} \, .$$

With the transformed stress components calculated in Example 4.6.1, we have

$$r = \sqrt{[(46.65 + 26.65)/2]^2 + 13.48^2}\ \text{MPa} = 39.05\ \text{MPa}$$

as before, and, since $\sigma_{x'} + \sigma_{y'} = 20$ MPa, the results for the principal stresses are the same. For the principal directions we find $\theta_{p1} = -10.1°$ and $\theta_{p2} = 79.9°$, which differ from the previously found angles by 30°, as they should.

It is possible to express the stress components σ_x, σ_y and τ_{xy} in terms of the principal stresses σ_1, σ_2 and the angle θ_{p1}, just as Eqs. (4.58)–(4.60) give the latter set of variables in terms of the former. To this end, we start by noting from Eqs. (4.59) that

$$\frac{\sigma_x - \sigma_y}{2} = r\cos 2\theta_{p1} \quad , \quad \tau_{xy} = r\sin 2\theta_{p1} \, . \tag{4.62}$$

When these expressions are substituted in Eqs. (4.50)–(4.51) and combined with the trigonometric identities $\cos(\alpha-\beta) = \cos\alpha\cos\beta + \sin\alpha\sin\beta$ and $\sin(\alpha-\beta) = \sin\alpha\cos\beta - \cos\alpha\sin\beta$, the result is

$$\sigma_\theta = \frac{\sigma_x+\sigma_y}{2} + r\cos 2(\theta_{p1}-\theta) \quad , \quad \tau_\theta = r\sin 2(\theta_{p1}-\theta)\,. \tag{4.63}$$

By combining these equations with Eq. (4.61) and setting $\theta = 0$ (which yields σ_x and τ_{xy}) and $\theta = \pi/2$ (which yields σ_y and $-\tau_{xy}$), we obtain

$$\begin{aligned} \sigma_x &= \frac{\sigma_1+\sigma_2}{2} + \frac{\sigma_1-\sigma_2}{2}\cos 2\theta_{p1}\,, \\ \sigma_y &= \frac{\sigma_1+\sigma_2}{2} - \frac{\sigma_1-\sigma_2}{2}\cos 2\theta_{p1}\,, \\ \tau_{xy} &= \frac{\sigma_1-\sigma_2}{2}\sin 2\theta_{p1}\,. \end{aligned} \tag{4.64}$$

We conclude from the preceding analysis that it takes *three* scalars to completely specify a state of plane stress, in the same way that it takes *two* numbers to specify a two-dimensional vector (such as force or velocity), whether these be two Cartesian components or the magnitude and an angle specifying the direction.

Note that, by Eqs. (4.61) and $(4.64)_{1,2}$, $(\sigma_1+\sigma_2)/2$ is the average of the normal stresses on any two mutually perpendicular faces parallel to the z-axis, and by Eq. $(4.63)_1$ it is also the average over all orientations in the xy-plane. This quantity is referred to as the *mean in-plane stress*.

An alternative approach for deducing the principal stresses and principal axes of stress is based on observing with reference to Fig. 4.24 that a unit normal vector $\mathbf{n}$ to an inclined plane indicates a principal axis if the shear stress on this plane vanishes, or equivalently that $\mathbf{f}$ is purely normal, that is, $\mathbf{f} = \sigma\mathbf{n}$, where σ is the normal stress on the plane. Recalling Eqs. (4.28), this implies that

$$\sigma_x n_x + \tau_{xy} n_y = \sigma n_x \quad , \quad \tau_{xy} n_x + \sigma_y n_y = \sigma n_y \tag{4.65}$$

or, equivalently, that

$$(\sigma_x-\sigma)n_x + \tau_{xy} n_y = 0 \quad , \quad \tau_{xy} n_x + (\sigma_y-\sigma)n_y = 0\,. \tag{4.66}$$

For these equations to yield a (non-zero) solution for n_x and n_y, it is necessary that the two lines described by (4.66) in the $n_x n_y$-plane be coincident, namely that

$$\frac{\sigma_x-\sigma}{\tau_{xy}} = \frac{\tau_{xy}}{\sigma_y-\sigma}\,, \tag{4.67}$$

therefore

$$(\sigma_x-\sigma)(\sigma_y-\sigma) - \tau_{xy}^2 = 0\,, \tag{4.68}$$

where we note that the left-hand side is the determinant of Eqs. (4.66). This can be rewritten as the quadratic equation in σ,

$$\sigma^2 - (\sigma_x + \sigma_y)\sigma + \sigma_x\sigma_y - \tau_{xy}^2 = 0 , \tag{4.69}$$

whose roots are precisely the principal stresses $\sigma_{1,2}$ derived previously in Eqs. (4.58) and (4.60).

Once the principal stresses are determined, each of their values can be introduced into *either one* of Eqs. (4.66) in order to determine the ratio $n_y/n_x = \tan\theta_{p1,2}$, which gives the direction of the corresponding principal axis. In this manner, one may obtain two mutually orthogonal unit vectors $\mathbf{n}_{1,2}$ that define the principal axes.

Example 4.6.4: Algebraic calculation of principal directions.
If the values of the stress components σ_x, σ_y and τ_{xy} given in Example 4.6.1 are introduced into Eq. (4.69), it follows trivially that the roots of this equation are just the principal stresses found in Example 4.6.3. We now introduce these principal stresses into Eq. $(4.66)_1$, and find that, for $\sigma = \sigma_1$, $n_y/n_x = -(40-49.05)/25 = 0.362 = \tan 19.9°$, and, for $\sigma = \sigma_2$, $n_y/n_x = -(40+29.05)/25 = -2.762 = \tan 109.9°$. The same results are found with Eq. $(4.66)_2$.

It is easy to extend this method of obtaining the principal stresses and principal axes of stress to general three-dimensional stress states. Indeed, with reference to the Cauchy tetrahedron of Fig. 4.25, the condition that the traction vector $\mathbf{f}$ is parallel to the unit vector $\mathbf{n}$ translates to the three-dimensional counterpart of Eqs. (4.65) in the form

$$\begin{aligned} (\sigma_x - \sigma)n_x + \tau_{xy}n_y + \tau_{xz}n_z &= 0 , \\ \tau_{xy}n_x + (\sigma_y - \sigma)n_y + \tau_{yz}n_z &= 0 , \\ \tau_{xz}n_x + \tau_{yz}n_y + (\sigma_z - \sigma)n_z &= 0 . \end{aligned} \tag{4.70}$$

Setting the determinant of this system to zero yields a cubic equation of the form

$$\sigma^3 - I_1\sigma^2 + I_2\sigma - I_3 = 0 , \tag{4.71}$$

where I_1, I_2 and I_3 are known as the *principal invariants* of the matrix in (4.24) that contains the stress components, and are given by

$$\begin{aligned} I_1 &= \sigma_x + \sigma_y + \sigma_z \\ I_2 &= \sigma_x\sigma_y + \sigma_y\sigma_z + \sigma_z\sigma_x - \tau_{xy}^2 - \tau_{yz}^2 - \tau_{xz}^2 \\ I_3 &= \sigma_x\sigma_y\sigma_z + 2\tau_{xy}\tau_{yz}\tau_{xz} - \tau_{xy}^2\sigma_z - \tau_{yz}^2\sigma_x - \tau_{xz}^2\sigma_y . \end{aligned} \tag{4.72}$$

These three scalars are called "invariants" because it can be shown that their values are independent of the axes in which the stress components are defined, in the same way that the magnitude of a vector (defined by the square

root of the sum of the squares of the components) is independent of such axes. The components of a triad of mutually perpendicular unit vectors $\mathbf{n}_1$, $\mathbf{n}_2$, $\mathbf{n}_3$ can be deduced from (4.70) in an analogous manner to that of the two-dimensional case discussed earlier.

When expressing the components of stress relative to the principal axes of stress, the matrix representation becomes diagonal, namely

$$\begin{bmatrix} \sigma_1 & 0 & 0 \\ 0 & \sigma_2 & 0 \\ 0 & 0 & \sigma_3 \end{bmatrix} , \tag{4.73}$$

and the invariants may be expressed as

$$I_1 = \sigma_1+\sigma_2+\sigma_3 \quad , \quad I_2 = \sigma_1\sigma_2+\sigma_2\sigma_3+\sigma_3\sigma_1 \quad , \quad I_3 = \sigma_1\sigma_2\sigma_3 \, . \tag{4.74}$$

The algebraic problem of finding principal stresses is a special case of a general class of problems known as linear eigenvalue problems. In this context, the principal stresses are the *eigenvalues* and the vectors defining the principal axes are the *eigenvectors* of the matrix of the stress components.

Similarly to the definition of the mean in-plane stress above, we can define the *mean stress* in general as the average of the normal stresses on any three mutually perpendicular planes, that is

$$\bar{\sigma} = \frac{1}{3}(\sigma_x+\sigma_y+\sigma_z) = \frac{1}{3}(\sigma_1+\sigma_2+\sigma_3) = \frac{1}{3}I_1 \, . \tag{4.75}$$

This can also be shown to be the average normal stress over all angular orientations in three dimensions. A three-dimensional stress state represented by

$$\begin{bmatrix} \bar{\sigma} & 0 & 0 \\ 0 & \bar{\sigma} & 0 \\ 0 & 0 & \bar{\sigma} \end{bmatrix} \tag{4.76}$$

(the representation being the same in any coordinate system) is known as *hydrostatic*, since it is the only stress state possible in a fluid at rest under a *pressure* $p = -\bar{\sigma}$, in accordance with Pascal's law.

4.6.3 Maximum In-Plane Shear Stress

We now seek to determine the orientations that yield maximum shear stress in the xy-plane, given a state of plane stress in the same plane. To this end, we differentiate Eq. (4.51) with respect to θ and set the result equal to zero, leading to the equation

$$\tan 2\theta_s = -\frac{\sigma_x-\sigma_y}{2\tau_{xy}} \, . \tag{4.77}$$

Note that the right-hand side of this equation is the negative reciprocal of that of Eq. (4.56). Since $\tan\theta\tan(\theta+\pi/2) = -1$, this means that the values of $2\theta_s$

differ from those of $2\theta_p$ by a right angle, and hence the corresponding values $\theta_{s1,2}$ differ from $\theta_{p1,2}$ by $\pi/4$. That is, the surfaces on which the in-plane shear stress is maximum or minimum are at 45° to the principal surfaces.

It follows from (4.77) that

$$\cos 2\theta_{s1,2} = \pm\frac{\tau_{xy}}{r} \quad , \quad \sin 2\theta_{s1,2} = \mp\frac{\sigma_x - \sigma_y}{2r} \, . \tag{4.78}$$

Inserting again these values into Eq. (4.50) and recalling the definition of r in (4.58) leads to

$$\tau_{\theta_s} = \pm r \quad , \quad \sigma_{\theta_s} = \frac{\sigma_x + \sigma_y}{2} \, . \tag{4.79}$$

Thus, r is the numerical maximum of the shear stress acting on planes parallel to the z-axis, though, as will be shown later, the maximum in-plane shear stress is not necessarily the maximum shear stress acting on *all* planes at a point in a three-dimensional body. Note that the normal stress at maximum in-plane shear stress is generally not zero, as seen in $(4.79)_2$. Rather, it is equal to the average normal stress over all the orientations θ ranging from $\theta = 0$ to $\theta = \pi$, a result that can be readily established by taking the average of σ_θ in (4.50). It is thus equal to the previously defined mean in-plane stress.

Eqs. (4.79) can be rewritten in terms of the principal stresses, by using Eqs. (4.58) and (4.60), as follows:

$$\tau_{\theta_s} = \pm\frac{\sigma_1 - \sigma_2}{2} \quad , \quad \sigma_{\theta_s} = \frac{\sigma_1 + \sigma_2}{2} \, . \tag{4.80}$$

The relation between the maximum-in-plane-shear axes and the principal axes is shown in Figure 4.38.

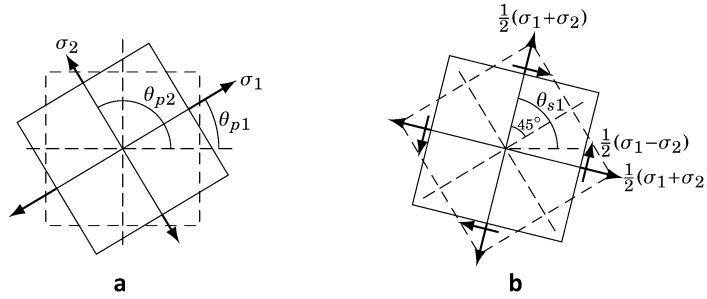

Figure 4.38. Maximum in-plane shear: (**a**) element along principal axes (from Fig. 4.37b), (**b**) element along maximum-in-plane-shear axes

It is important to emphasize here that the algebraic sign of the shear stress is of no particular significance. In fact, if a given observer sees a shear stress as positive, then an observer facing the same stress while rotated by a 90° angle will see it as negative. Whether a normal stress is tensile or compressive is, on the other hand, independent of the observer.

4.6.4 Mohr's Circle for Stress

There exists a graphical method for visualizing the transformation of stresses and for determining the maximum and minimum values of the normal and shear stress components in plane stress. To introduce this method, we begin by restating Eqs. (4.50) and (4.51) as

$$\sigma_\theta - \frac{\sigma_x + \sigma_y}{2} = \frac{\sigma_x - \sigma_y}{2}\cos 2\theta + \tau_{xy}\sin 2\theta \tag{4.81}$$

and

$$\tau_\theta = -\frac{\sigma_x - \sigma_y}{2}\sin 2\theta + \tau_{xy}\cos 2\theta \ . \tag{4.82}$$

Next, we square both of the preceding equations and add them to find that

$$\left(\sigma_\theta - \frac{\sigma_x + \sigma_y}{2}\right)^2 + \tau_\theta^2 = \left(\frac{\sigma_x - \sigma_y}{2}\right)^2 + \tau_{xy}^2 = r^2 \ , \tag{4.83}$$

which is the equation of a circle in the $(\sigma_\theta \tau_\theta)$-plane centered at the point $\left(\frac{\sigma_x + \sigma_y}{2}, 0\right)$ and having radius r, as defined in (4.58). This is known as *Mohr's*[*] *circle*, and is shown in Fig. 4.39.

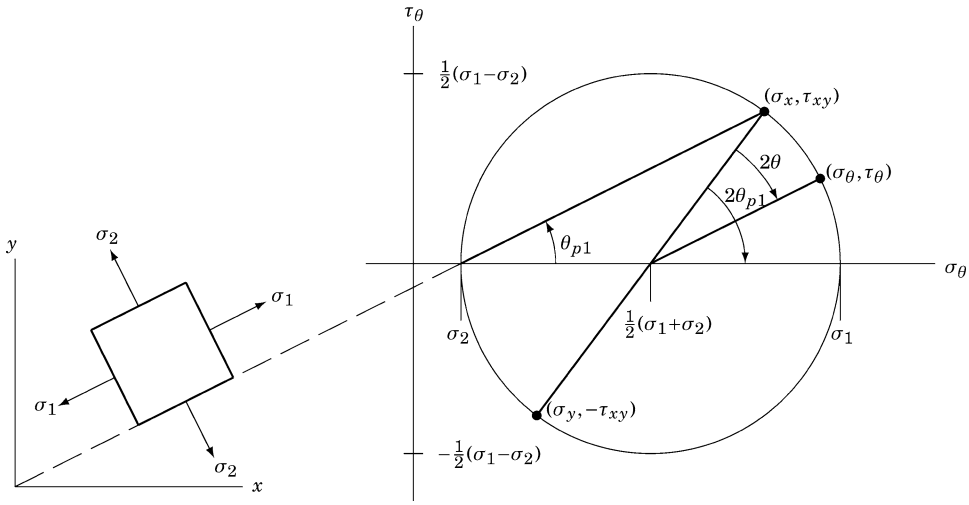

Figure 4.39. Mohr's circle for stress

Note that a *counterclockwise* rotation of the axes by an angle θ of the plane corresponds to a *clockwise* motion by an angle 2θ on Mohr's circle. To argue this point, assume that an infinitesimal counterclockwise rotation $d\theta$

[*]Christian Otto Mohr (1835-1918) was a German civil engineer (Fig. 4.40).

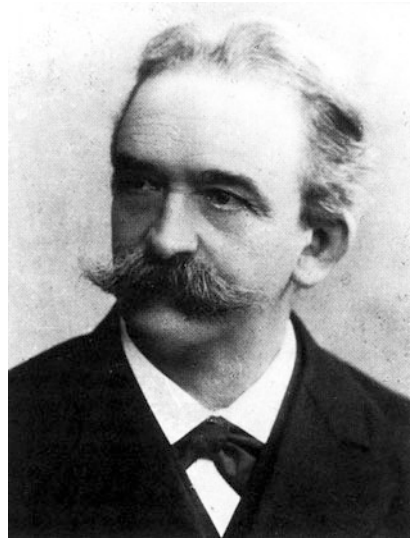

Figure 4.40. Christian Otto Mohr

is introduced in the physical domain. Since $d\theta$ is infinitesimal, $\sin 2d\theta \doteq 2d\theta$ and $\cos 2d\theta \doteq 1$. Recalling Eq. (4.50), due to this small counterclockwise rotation,

$$\sigma_\theta \doteq \frac{\sigma_x+\sigma_y}{2}+\frac{\sigma_x-\sigma_y}{2}+\tau_{xy}2d\theta = \sigma_x+2\tau_{xy}d\theta > \sigma_x \tag{4.84}$$

if $\tau_{xy}>0$, which implies that the stress point A of Fig. 4.41 moves clockwise.

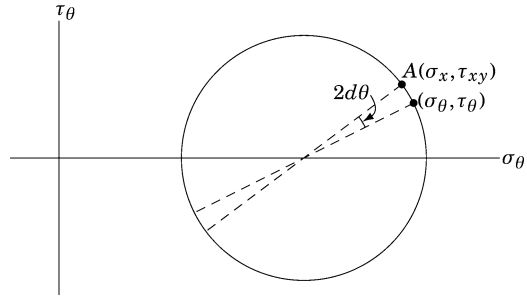

Figure 4.41. Sense of motion on the Mohr's circle for counterclockwise rotation of the infinitesimal element

It is clear from Eq. (4.60) that the intercepts of the circle with the σ_θ-axis are $(\sigma_1,0)$ and $(\sigma_2,0)$, consistent with the result that σ_1 and σ_2 are the maximum and minimum values of σ_θ. Similarly, the radius $r=\frac{1}{2}(\sigma_1-\sigma_2)$ is seen to be the numerical maximum of τ_θ.

In order to construct the Mohr's circle when the original stress components σ_x, σ_y and τ_{xy} are given, we note that the points (σ_x, τ_{xy}) and $(\sigma_y, -\tau_{xy})$ correspond respectively to $\theta = 0$ and $\theta = \pm\pi$, that is, they are diametrically opposite. When we plot these two points and draw a straight line between them, this line is a diameter of the circle, and its intersection with the σ_θ-axis is the center of the circle, $(\frac{1}{2}(\sigma_x + \sigma_y), 0)$. The circle can now be drawn.

It is clear that the triangle formed by connecting the center of the circle with the points (σ_x, τ_{xy}) and $(\sigma_2, 0)$, is isosceles, since two of the sides are equal to the radius. The angle between these sides is the complement of the angle $2\theta_{p1}$ subtended by the radial line to (σ_x, τ_{xy}). But it is also the complement of the sum of the other two angles of the isosceles triangle, which are equal to each other and therefore to θ_{p1}. Consequently, the line from $(\sigma_2, 0)$ to (σ_x, τ_{xy}) is parallel to the first principal axis, and the rectangular element whose faces are along the principal directions can be formed as shown in the left-hand portion of Fig. 4.39.

A similar construction can be made to get the element on whose faces the shear stress is maximum, by drawing an isosceles triangle connecting the center with (σ_x, τ_{xy}) and $(\frac{1}{2}(\sigma_x + \sigma_y), \pm r)$. This is left to an exercise.

Consider next the case of triaxial stress, as defined in Sect. 4.1. Clearly, here all three normal stresses are principal stresses. Without loss of generality, let $\sigma_1 \geq \sigma_2 \geq \sigma_3$ and draw on the same axes the Mohr's circles corresponding to the stress on the xy-, yz- and zx-planes, see Fig. 4.42. In this case, the numerical maximum shear stress is $(\sigma_1 - \sigma_3)/2$. For the special case $\sigma_3 = 0$, (which corresponds to a state of plane stress in the xy-plane), the numerical maximum shear stress is $\tau_{xz\max} = \sigma_1/2$. This is greater than the numerical maximum shear in the (x, y)-plane, which, in this case, is equal to $\tau_{xy\max} = (\sigma_1 - \sigma_2)/2$. In contrast, if $\sigma_2 = 0$ (which represents a state of plane stress in the xz-plane), then the numerical maximum shear is indeed the numerical maximum shear in the xz-plane, namely $\tau_{xz\max} = (\sigma_1 - \sigma_3)/2$.

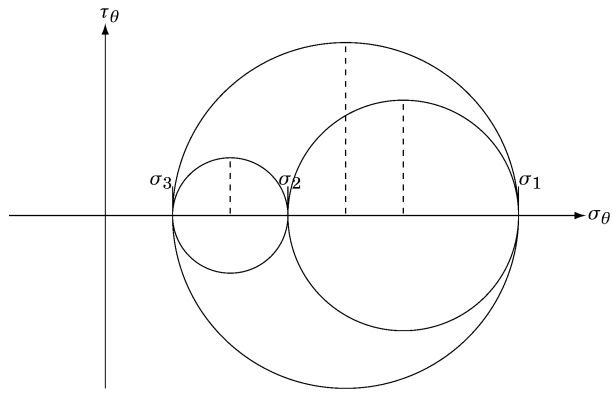

Figure 4.42. Mohr's circles for a state of triaxial stress

Example 4.6.5: Simple shear and pure shear.
For a state of simple shear as defined in Sect. 4.5, with $\tau_{xz} = \tau_{zx}$ $(= \tau)$ as the only nonzero stress components, Eq. (4.71) reduces to $\sigma^3 - \tau^2\sigma = 0$, so that the matrix of principal stresses and the Mohr's circles are as shown in Fig. 4.43a and 4.43b, respectively. A rectangular element in the plane of the first and third

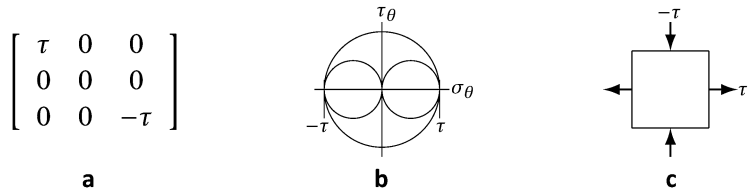

Figure 4.43. Example 4.6.5

principal axes, with sides parallel to these axes, experiences the stresses shown in Fig. 4.43c. When a state of stress is so described it is often called *pure shear*, though it is of course equivalent to simple shear with respect to axes at 45° to the principal axes. In fact, any state of stress for which the principal axes are found to be of the form $\sigma_1 = -\sigma_3$ and $\sigma_2 = 0$ is similarly equivalent to simple shear.

When the principal stresses are numbered independently of their values, then the numerical maximum shear stress is given by

$$\tau_{\max} = \frac{1}{2}\max(|\sigma_1 - \sigma_2|, |\sigma_1 - \sigma_3|, |\sigma_2 - \sigma_3|)\,. \tag{4.85}$$

4.6.5 Octahedral Stresses

It is clear that any state of stress may be represented as one of triaxial stress if the reference axes x, y, z are made to coincide with the principal axes; the stress tensor is then represented by the diagonal matrix (4.73). It is instructive to consider the stresses on those planes whose normal directions equidistant from the principal directions, that is, the planes whose unit normal vectors are given by

$$\mathbf{n} = \frac{1}{\sqrt{3}}(\pm\mathbf{i} \pm \mathbf{j} \pm \mathbf{k}). \tag{4.86}$$

There are eight such vectors, one for each choice of algebraic sign inside the parentheses of Eq. (4.86), corresponding to the eight octants of a three-dimensional Cartesian coordinate system. If we observe a set of planes, one for each such normal vector, such that their distances from the origin are the same, then these planes are seen to intersect forming a tetrahedron, as seen in Fig. 4.44. The planes are accordingly known as the *octahedral planes*. With the stress tensor given by (4.73), Eq. (4.31) for the traction yields the *octahedral traction*

$$\mathbf{f}_{\text{oct}} = \frac{1}{\sqrt{3}}(\pm\sigma_1\mathbf{i} \pm \sigma_2\mathbf{j} \pm \sigma_3\mathbf{k})\,. \tag{4.87}$$

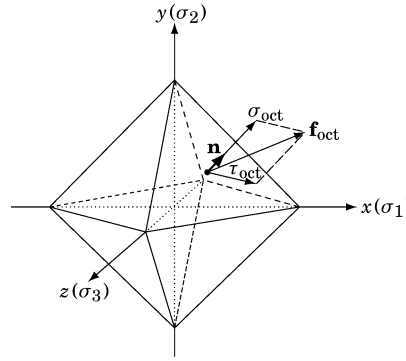

Figure 4.44. Octahedral stresses

The octahedral normal stress is just $\sigma_{oct} = \mathbf{n} \cdot \mathbf{f}_{oct}$ and, with $\mathbf{n}$ given by Eq. (4.86), becomes

$$\sigma_{oct} = \frac{1}{3}(\sigma_1 + \sigma_2 + \sigma_3) , \tag{4.88}$$

that is, it is equal to the mean stress $\bar{\sigma}$.

The shear stress in an octahedral plane is a vector than can be obtained from Eq. (4.32), but if we are interested only its magnitude, we can obtain it by applying the Pythagorean theorem. If this magnitude is called the *octahedral shear stress* and denoted τ_{oct}, its square is accordingly given by

$$\begin{aligned} \tau_{oct}^2 &= |\mathbf{f}_{oct}|^2 - \sigma_{oct}^2 = \frac{\sigma_1^2 + \sigma_2^2 + \sigma_3^2}{3} - \left(\frac{\sigma_1 + \sigma_2 + \sigma_3}{3}\right)^2 \\ &= \frac{2}{9}(\sigma_1^2 + \sigma_2^2 + \sigma_3^2 - \sigma_2\sigma_3 - \sigma_1\sigma_3 - \sigma_1\sigma_2) \\ &= \frac{1}{9}[(\sigma_2 - \sigma_3)^2 + (\sigma_1 - \sigma_3)^2 + (\sigma_1 - \sigma_2)^2] . \end{aligned} \tag{4.89}$$

For a state of pure shear as discussed in Example 4.6.5, the octahedral shear stress is $\tau_{oct} = \sqrt{2/3}\tau$.

Exercises

4.6-1. Determine the stresses $\sigma_{x'}$ and $\tau_{x'y'}$ acting on the inclined plane shown in the figure.

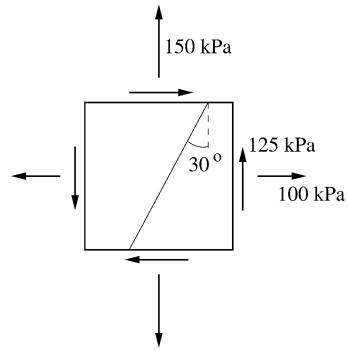

4.6-2. The stress σ_θ assumes values 10, 0 and -20 MPa when acting on planes whose outward normals form angles $\theta = \pi/6, \pi/3$ and $2\pi/3$ with an axis x, as in the figure. Determine the stresses σ_x, σ_y and τ_{xy}.

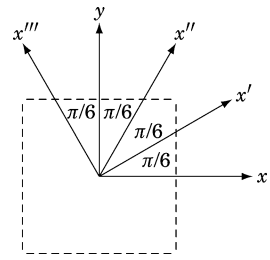

4.6-3. Show that $\sigma_x + \sigma_y = \sigma_{x'} + \sigma_{y'}$ for any angle θ relating the axes x and y to the rotated axes x' and y'.

4.6-4. Derive Eqs. (4.53) on the basis of the discussion leading up to them.

4.6-5. Find the principal stresses and the principal axes of stress for the infinitesimal box shown in the figure, using the formulae (4.56) and (4.60). Repeat the derivation using the alternative approach involving the solution of Eq. (4.68).

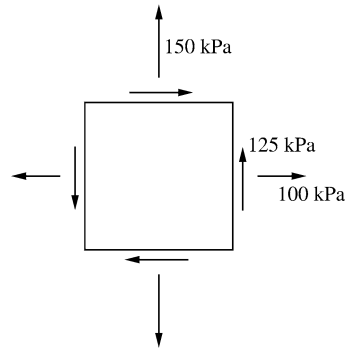

4.6-6. For the state in the preceding exercise, find the maximum shear stress and the associated normal stress. In addition, find the angle by which the box needs to be rotated from its original orientation to attain the state of maximum shear stress.

4.6-7. A material is able to sustain maximum normal stress of 100 MPa and maximum shear stress of 75 MPa. Suppose that a point of this material is stressed as in the figure. Find the maximum allowable value of p.

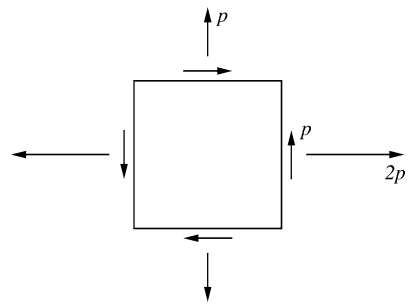

4.6-8. Draw an infinitesimal element on whose faces the shear stress is maximum, by starting with an isosceles triangle connecting the center with (σ_x, τ_{xy}) and $(\frac{1}{2}(\sigma_x + \sigma_y), \pm r)$ in the Mohr's circle, and repeating the procedure described in the text for the maximum normal stress case.

4.6-9. Solve Exercises **4.6-5** and **4.6-6** graphically using the Mohr's circle.

4.6-10. Suppose that there exist two orientations of the infinitesimal element in a state of plane stress for which the normal and shear stresses $(\sigma_\theta, \tau_\theta)$ attain values $(100, 75)$ kPa and $(120, 60)$ kPa. Construct the Mohr's circle by determining its center and radius. Then, calculate the maximum/minimum normal stress, the maximum in-plane shear stress and the maximum shear stress.

4.6-11. Consider a point O in a solid body in the state of plane stress on the (x, y) plane. The figure below shows the stress components acting at O along planes 1 and 2.

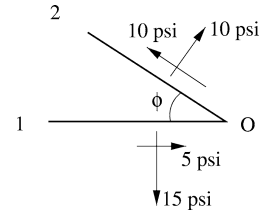

(a) Determine the angle ϕ between the two planes.
Hint: You may want to draw a Mohr's circle.

(b) Find the principal stresses σ_1 and σ_2 and the angles formed between the principal directions and the plane 1.

(c) Find the maximum in-plane shear stress and the normal stress on the planes of maximum in-plane shear stress.

4.6-12. Assume that a point in a solid body is in the state of plane stress and that its total stress is obtained from the superposition of the two loading states (denoted I and II) shown in the figure below. Also, let the coordinate system (x', y') employed to characterize State II is obtained from the coordinate system (x, y) employed to characterize State I by a counter-clockwise rotation of $\pi/6$.

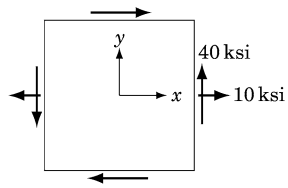

State I

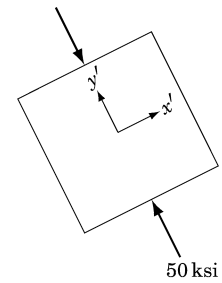

State II

(a) Find the components of the total stress (i.e., the stress due to the superposition of States I and II) in the (x, y)-system.

(b) For the total stress state (I+II) found in part (a), determine the maximum in-plane shear and the orientation of the plane on which it occurs relative to the (x, y)-axes.

(c) For the total stress state (I+II) found in part (a), determine the principal stresses and the orientations of the planes on which they act relative to the (x, y)-axes.

4.6-13. Show that the maximum shear stress given by Eq. (4.85) can also be expressed as

$$\tau_{\max} = \frac{1}{4}(|\sigma_1 - \sigma_2| + |\sigma_1 - \sigma_3| + |\sigma_2 - \sigma_3|) \, .$$

4.6-14. For a state of stress such that $\sigma_1 = 2\sigma_2$ $(= \sigma)$ and $\sigma_3 = 0$, find the mean stress, the maximum shear stress and the octahedral shear stress.

4.6-15. For a state of stress such that $\sigma_1 = \sigma_2$ $(= \sigma)$ and $\sigma_3 = 2\sigma$, find the mean stress, the maximum shear stress and the octahedral shear stress.

4.6-16. Suppose that the axes of the rectangular Cartesian coordinate system (x, y, z) align with the principal stresses $(\sigma_1, \sigma_2, \sigma_3)$ of the stress at a given point. Show that the components (f_x, f_y, f_z) of the traction vector on any plane passing through this point satisfy the equation

$$\frac{f_x^2}{\sigma_1^2} + \frac{f_y^2}{\sigma_2^2} + \frac{f_z^2}{\sigma_3^2} = 1 \, .$$

This is the equation of an ellipsoid termed the *Lamé stress ellipsoid*. What is the physical meaning of a typical point on this ellipsoid?

Chapter 5

Deformation and Strain

5.1 Longitudinal Strain

5.1.1 Definition

As already discussed with broad strokes in Sect. 1.1, *deformation* is the change in the distances between material points, which, in turn, leads to changes in shape and/or size of the body. All real materials undergo some deformation under the influence of forces. To quantify the deformation of a solid body relative to some reference configuration, it is important to introduce the notions of stretch and strain.

The deformation that is easiest to observe is the stretching of a bar made of a single material when a tensile force is applied to it. Suppose that a force pulling on a bar of initial length L stretches it by an amount ΔL, as in Fig. 5.1. The (relative) *stretch* λ of the bar is defined as

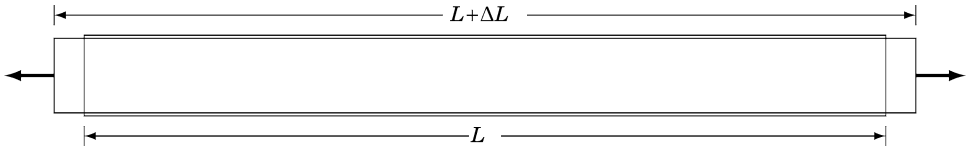

Figure 5.1. Elongation of a bar under an applied tensile force

$$\lambda = \frac{L+\Delta L}{L} = 1+\frac{\Delta L}{L}\,. \tag{5.1}$$

Clearly, the (relative) stretch is always a positive number, which attains values greater than 1 when the bar is elongated and less than 1 when the bar is shortened. If, on the other hand, the bar is rigid, then the stretch must be always equal to 1.

The bar in Fig. 5.1 may also be regarded as composed of two identical bars of length $L/2$ in series, with the same force pulling on each of them, as

© Springer International Publishing Switzerland 2017

J. Lubliner, P. Papadopoulos, *Introduction to Solid Mechanics*,
DOI 10.1007/978-3-319-18878-2_5

in Fig. 5.2. Since the half-bars are identical, each one stretches by an amount $\Delta L/2$.

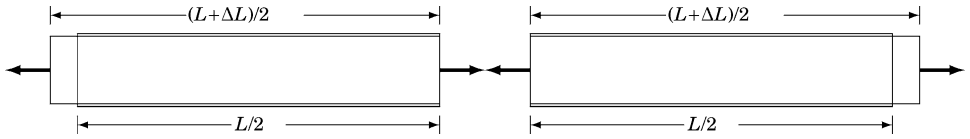

Figure 5.2. Bar in tension regarded as two half-bars in series

The original bar can also be subdivided into any other combination of bars in series, and it can similarly be argued that the elongation ΔL of each one is proportional to its length. It follows that the elongation per unit length, $\Delta L/L$, is independent of the length of the bar. This quantity is known as *longitudinal strain* and is usually denoted ε, that is,

$$\varepsilon = \frac{\Delta L}{L} . \tag{5.2}$$

When the bar lengthens, the longitudinal strain is clearly positive, while when it shortens the same strain is negative. Also, zero strain is experienced if the bar remains rigid. It follows from (5.1) and (5.2) that, in this case, the stretch and longitudinal strain are related by $\lambda = 1 + \varepsilon$. The longitudinal strain defined by Eq. (5.2) is more specifically referred to as *conventional strain* or *engineering strain*.

The definition of longitudinal strain is not unique. For instance, an alternative strain measure ϵ may be defined as the ratio of the elongation ΔL divided by the *final* length $L' = L + \Delta L$, namely

$$\epsilon = \frac{\Delta L}{L + \Delta L} = \frac{\varepsilon}{1 + \varepsilon} . \tag{5.3}$$

The difference between the preceding two definitions of strain is slight as long as the elongation ΔL remains very small compared to the initial length L or, equivalently, if the strain ε is very small compared to unity:

$$|\varepsilon| \ll 1 . \tag{5.4}$$

Longitudinal strains that satisfy inequality (5.4) are called *infinitesimal*; otherwise, they are referred to as *finite*. Infinitesimal strains are characteristic of bodies that are stiff under the influence of typical forces and can, for the purposes of statics, be treated as rigid because any changes in geometry are too slight to affect the equilibrium equations significantly.

Yet another important definition of longitudinal strain, which is particularly useful when the elongation ΔL is not very small in comparison with the initial length L, can be derived by supposing that the force is applied in infinitesimal increments that, in turn, produce infinitesimal changes $d\ell$ in the

length of the bar. For each such force increment, the corresponding increment of strain is $d\varepsilon = d\ell/\ell$, where ℓ is the *current* length. A measure of the total strain is then defined as the sum of these strain increments, expressed by the integral

$$\varepsilon_\ell \;=\; \int_L^{L+\Delta L} \frac{d\ell}{\ell} \;=\; \ln\left(1+\frac{\Delta L}{L}\right) = \ln(1+\varepsilon)\;. \tag{5.5}$$

Because the formula takes the form of a logarithm, this strain is usually called the *logarithmic strain*, motivating the notation ε_ℓ. It is also known as *true strain*.

Example 5.1.1: Values of different strain measures.
We will calculate the values of ϵ and ε_ℓ when $\varepsilon = 0.05$, 0.10 and 0.25.
For $\varepsilon = 0.05$, $\epsilon = 0.05/1.05 = 0.0476$ and $\varepsilon_\ell = \ln 1.05 = 0.0488$.
For $\varepsilon = 0.10$, $\epsilon = 0.10/1.10 = 0.0909$ and $\varepsilon_\ell = \ln 1.10 = 0.0953$.
For $\varepsilon = 0.25$, $\epsilon = 0.25/1.25 = 0.20$ and $\varepsilon_\ell = \ln 1.25 = 0.223$.

As can be readily seen from Eqs. (5.1)–(5.3) and (5.5), the quantities λ, ε, ϵ and ε_ℓ are dimensionless. Strain is often denominated using percentages: a longitudinal strain of 0.3%, for example, implies an elongation of 3 units in a bar of initial length of 1000 units. Alternatively, strain may be expressed simply as a decimal fraction, but such a fraction will often have at least three zeros after the decimal point and therefore this notation is not very convenient. Strains can also be expressed in whole numbers, to engineering accuracy, if the basic unit is a *millionth*, that is, if it is written as $N \times 10^{-6}$ where N is (approximately) an integer. This unit is called a *microstrain*.*

In practice, solids such as glass, hard plastic or cast iron, may sustain strains of the order of a few tens of a percent before failure. Other metals and alloys, depending on their composition, can survive higher strains, up to a few percent. Rubber is a typical example of a material that may undergo finite strain (up to tens of percent or more) without breaking.

5.1.2 Practical Strain Measurement

All three measures of strain discussed earlier in this section can be easily calculated when the elongation ΔL is large enough to be measured. However,

*Some authors write this in the form of a millionth of a unit of length divided by the same unit of length, for example μm/m ("micrometer per meter") or μin/in ("microinch per inch"). Apart from unwarranted redundancy, there is nothing wrong with this way of expressing strain, but there is a tendency to neglect the "per meter" or "per inch" that can lead to misinterpretation. If we were to cancel the "m" or "in" in the fractional representation we would be left with μ, and that would be all right if this symbol were not still being used (especially in astronomy and the semiconductor industry) to denote the micron, an old name for micrometer (μm), perhaps in order to avoid confusion between this last term (stressed on the third syllable) and *micrometer*, stressed on the second syllable and denoting a measuring instrument. (No such confusion occurs when British or Canadian spelling is used, because the metric unit is then written *micrometre*.)

since hard solids undergo strains of the order of a few thousandths before they fail, this means that in a specimen of, say, 10 cm length, the elongation at failure will be well under a millimeter and therefore difficult to measure. What is more, if the bar is in any way not uniform along its length, Eqs. (5.2), (5.3) and (5.5) define only the *average strain* along the length, while the *local* strain varies. In order to measure local strain, we must determine the change in length of a short line segment drawn locally. A more precise definition of local strain will be given later in this section.

Fortunately, physicists have discovered coupling between longitudinal deformation and various electrical properties of solids (such as conductance in wires), and engineers have developed electromechanical devices that take advantage of this coupling and that, when they are attached to a body being deformed and are properly calibrated, give strain as their output. Such devices are known as *strain ga(u)ges*.

In the remainder of this book, unless explicitly stated otherwise, all strain calculations will employ engineering strain.

5.1.3 Local Longitudinal Strain

We consider, first, a body in its reference state, and focus on two material points A and B, as in Fig. 5.3a. We then let the body deform under the in-

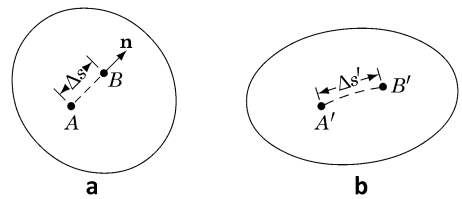

Figure 5.3. A body with two material points in its reference configuration (**a**) and deformed configuration (**b**)

fluence of some (at this stage unspecified) external force. The material points that in the reference state were positioned along the line segment AB now occupy the curved segment $A'B'$ (Fig. 5.3b). If the segments AB and $A'B'$ have lengths Δs and $\Delta s'$, respectively, then the average longitudinal engineering strain for this segment is defined as

$$\bar{\varepsilon}_{AB} = \frac{\Delta s' - \Delta s}{\Delta s} . \tag{5.6}$$

Considering, next, the limit as point B approaches point A along the direction of the unit vector $\mathbf{n}$ pointing from A to B, we define the *local longitudinal strain* at A in the direction $\mathbf{n}$ as

$$\varepsilon_n = \lim_{\substack{B \to A \\ \text{along } \mathbf{n}}} \frac{\Delta s' - \Delta s}{\Delta s} = \frac{ds' - ds}{ds} = \frac{ds'}{ds} - 1 . \tag{5.7}$$

Similarly, the *local stretch* at A in the direction $\mathbf{n}$ is

$$\lambda_n = \lim_{\substack{B\to A \\ \text{along } \mathbf{n}}} \frac{\Delta s'}{\Delta s} = \frac{ds'}{ds} . \tag{5.8}$$

A more useful definition of local longitudinal strain can be achieved by introducing the concept of *displacement*. To this end, we consider a bar whose axis lies along, say, the x-axis, and assume that in the course of elongation its cross-sections remain plane. The distance by which a cross-section originally located at a point with coordinate x has moved is called its *axial displacement* and is denoted $u(x)$, as seen in Fig. 5.4. In the same way, the cross-section

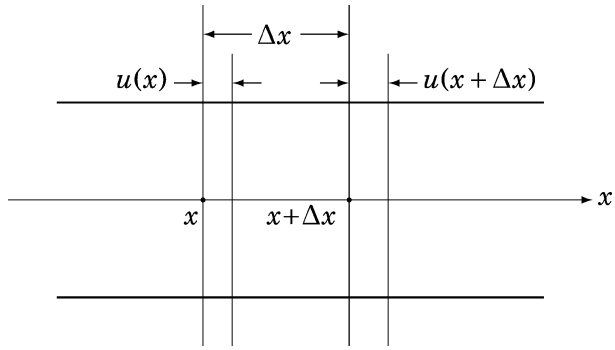

Figure 5.4. Axial displacement

that was originally located at some point with coordinate $x+\Delta x$ undergoes displacement $u(x+\Delta x)$. Now, if we use the segment $(x, x+\Delta x)$ as the gauge length for defining longitudinal strain, then its new length is

$$[x+\Delta x+u(x+\Delta x)]-[x+u(x)] = \Delta x+u(x+\Delta x)-u(x) \tag{5.9}$$

and its elongation is therefore just $u(x+\Delta x)-u(x)$. Applying the definition (5.6), we find that the average longitudinal engineering strain of the segment is

$$\bar{\varepsilon} = \frac{u(x+\Delta x)-u(x)}{\Delta x} \tag{5.10}$$

and in the limit as Δx goes to zero this reduces to the local longitudinal strain at x, given by

$$\varepsilon_x = \lim_{\Delta x\to 0} \frac{u(x+\Delta x)-u(x)}{\Delta x} \tag{5.11}$$

or, in accordance with the fundamental definition of the derivative of the function $u(x)$,

$$\varepsilon_x = \frac{du}{dx} . \tag{5.12}$$

The reason for introducing the subscript x in the definition (5.12) is to indicate that the x-axis was chosen as the reference axis.

When Eq. (5.12) is integrated over the length of the bar (say, from 0 to L), we find

$$\int_0^L \varepsilon_x \, dx \;=\; u(L) - u(0) \;=\; \Delta L \;. \tag{5.13}$$

It follows that Eq. (5.2) also gives the average value of the longitudinal strain over the length.

5.1.4 Virtual Displacement, Virtual Strain and Virtual Work (Longitudinal)

In order to apply the principle of virtual work , discussed in Sect. 2.1, to continuous bodies, we may begin with the case of a fiber of cross-sectional area ΔA, which is located along the x-axis and is subject to tension. Next, we let particles i and j be identified with points whose initial positions are at x and $x + \Delta x$, respectively, so that the *variable* position vectors of the two particles are

$$\mathbf{r}_i \;=\; [x + u(x)]\mathbf{i} \quad , \quad \mathbf{r}_j \;=\; [x + \Delta x + u(x + \Delta x)]\mathbf{i} \;. \tag{5.14}$$

Therefore, the virtual relative change of position, which is given by

$$\delta(\mathbf{r}_j - \mathbf{r}_i) \;=\; \delta[u(x + \Delta x) - u(x)]\mathbf{i} \;, \tag{5.15}$$

may also be expressed, if Δx is sufficiently small, as

$$\delta(\mathbf{r}_j - \mathbf{r}_i) \;=\; \delta\varepsilon_x \Delta x \mathbf{i} \;, \tag{5.16}$$

thus defining the longitudinal *virtual strain* $\delta\varepsilon_x$.

If the fiber is subject to a tensile stress σ_x, and if the segment between i and j is regarded as a link transmitting the internal force between the two "particles," then $\mathbf{F}_{ij} = (\sigma_x \Delta A)\mathbf{i} = -\mathbf{F}_{ji}$ (since the tension pulls particle i in the positive, and particle j in the negative, x-direction). Thus the contribution of the two particles to the internal virtual work, as defined by Eq. (2.29), is $\sigma_x \delta\varepsilon_x (\Delta A \Delta x)$. But $\Delta A \Delta x$ is just the volume of the element between i and j, and we may accordingly define the internal virtual work per unit volume, associated with longitudinal strain, by

$$\delta W^0_{\text{int}} \;=\; \sigma_x \delta\varepsilon_x \;. \tag{5.17}$$

If the fiber belongs to a bar of cross-section $\mathscr{A}$ with area A, then the corresponding internal virtual work per unit length is obtained by integrating δW^0_{int} over the area to obtain

$$\delta W'_{\text{int}} \;=\; \int_{\mathscr{A}} \sigma_x \delta\varepsilon_x \, dA \;. \tag{5.18}$$

If, lastly, the axis of the bar occupies the interval $0 < x < L$, then the total internal virtual work is

$$\delta W_{\text{int}} = \int_0^L \delta W'_{\text{int}} dx \,. \tag{5.19}$$

When δ is replaced by d in Eqs. (5.17–5.19), these equations give the actual work done when the longitudinal strain changes from ε_x to $\varepsilon_x + d\varepsilon_x$.

Exercises

5.1-1. Consider a bar of initial length $L = 10$ in and plot the average longitudinal strains defined in (5.2), (5.3), (5.5) for elongations ΔL ranging continuously from 0 to 2 in. Comment on the differences between these strains in terms of the value of ΔL. What is the maximum value of the average stretch λ of the bar for which the aforementioned three measures of strain differ by no more than 1% from each other?

5.1-2. Find the values of the engineering strain corresponding to (a) $\varepsilon_\ell = \pm 0.05$, (b) $\varepsilon_\ell = \pm 0.10$, (c) $\varepsilon_\ell = \pm 0.20$.

5.1-3. Consider a bar which, in the reference state, occupies the region between points with coordinates $x = 0$ and $x = 1$ m. Assume that, owing to external loading, the local engineering strain of the bar is $\varepsilon(x) = 0.001(x^2 + x + 1)$, with x in meters. Find the total elongation and the average stretch of the bar.

5.1-4. A bar of initial length L is fixed at $x = 0$, and its longitudinal displacement is given by $u(x) = [2(x/L)^3 - (x/L)^2]\Delta L$. Plot the strain as a function of x/L in terms of $\Delta L/L$.

5.1-5. Two bar in series, of length 20 in and 15 in, respectively, are each in a state of uniform strain with values of 0.0023 and 0.0018, respectively. Find the total elongation of the compound bar.

5.1-6. Consider a square region of unit side that undergoes deformation, as in the figure. If the deformed positions A', B', C', and D' of the corner points A, B, C, and D are $(-0.125, 0)$, $(1.125, -0.125)$, $(1.125, 1.125)$ and $(0.25, 1)$, respectively, determine the average longitudinal strain along the segments AB, BC, and BD.

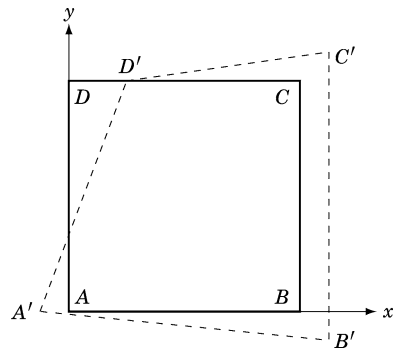

5.1-7. A bar of variable cross-sectional area $A(x)$ is subject to an axial force P. If the stress σ_x is assumed to be uniform over every cross-section, show that the total internal virtual work is equal to $P\delta\Delta L$.

5.1-8. Show that, if the length of a bar subject to an axial force P changes from L to $L + dL$, the actual work done is $P\,dL$.

5.2 Shear Strain

5.2.1 Basic Concepts

Just as it is empirically obvious that a tensile force applied to a bar produces an elongation, so it is clear that when shear forces are applied to a rectangular

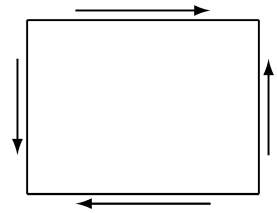

Figure 5.5. Shear forces on a rectangular block

block, in the form of two equal and opposite couples (for equilibrium) as shown in Fig. 5.5, then the result will be a distortion which can take one of the forms in Fig. 5.6.

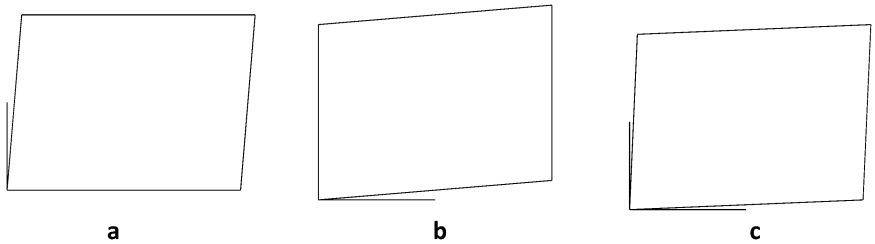

Figure 5.6. Distortion of a rectangular block

It is important to observe that the shapes of the three parallelograms shown in Fig. 5.6 are the same to within a rigid rotation. It can be said more generally that the application of forces to a body, or—locally—of stress to a small portion of a body, results in a combination of deformation and rotation. At this point, we must emphasize that in order for the "infinitesimal" approximation to apply (so that changes in geometry can be neglected in equilibrium calculations), not only the strains but also the angles of rotation (in radians) must be very small compared to unity. This will be discussed in Sect. 5.3.

The deformation of the rectangular block, then, is evidenced by the fact that it is no longer rectangular, and the change in the included angle (from a right angle) may be used as the measure of *shear strain*. Since the shear forces shown in Fig. 5.5 are in accord with what we have defined as positive shear stress, the distortion shown in Fig. 5.6 corresponds to positive shear strain. If, then, the included angles (in radians) of the lower left and upper right corners are $\pi/2-\gamma$, and those of the other two corners are $\pi/2+\gamma$, then

γ is the conventional value of the shear strain. As in the case of longitudinal strain, we will generally assume that the shear strain is infinitesimal, that is, $|\gamma| \ll 1$.

5.2.2 Local Shear Strain

Consider a deformable solid and take a point A in its reference configuration. From that point, draw two perpendicular line elements ending at points B and C. Upon undergoing deformation, the line elements AB and AC become curved elements $A'B'$ and $A'C'$, as seen in Fig. 5.7. Let $\mathbf{n}$ and $\mathbf{t}$ be unit vectors

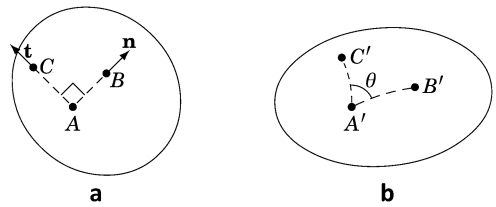

Figure 5.7. A body with two perpendicular material line elements in its reference configuration (**a**) and their deformed counterparts (**b**)

in the direction of AB and AC, respectively, hence $\mathbf{n} \cdot \mathbf{t} = 0$. The *engineering shear strain* γ_{nt} at point A associated with perpendicular directions $\mathbf{n}$ and $\mathbf{t}$ is defined as

$$\gamma_{nt} = \frac{\pi}{2} - \lim_{\substack{B \to A \\ \text{along } \mathbf{n} \\ C \to A \\ \text{along } \mathbf{t}}} \theta \,, \tag{5.20}$$

where θ is the angle formed by the tangent lines to the curved line elements $A'B'$ and $A'C'$ at point A'. In other words, γ_{nt} at point A is equal to the difference from $\frac{\pi}{2}$ of the angle formed between $A'B'$ and $A'C'$ as these two line elements shrink to infinitesimal length. Clearly, γ_{nt} is dimensionless and $\gamma_{nt} = 0$ in rigid displacement. Also, since γ_{nt} is the change in the angle between the two vectors $\mathbf{n}$ and $\mathbf{t}$, it could just as well have been designated γ_{tn}, that is,

$$\gamma_{nt} = \gamma_{tn} \tag{5.21}$$

always holds true.

The local shear strain at a point is determined by considering two perpendicular line segments intersecting at the point and measuring their change of direction after the application of shear force. This may be accomplished by finding the angles α and β by which the two line segments rotate toward each other, as shown in Fig. 5.8.

It is important to note, however, that the shear strain depends on the directions of the reference lines AB and AC. Consider, for example, a square that has been distorted into a rhombus, as shown in Fig. 5.9. There is clearly

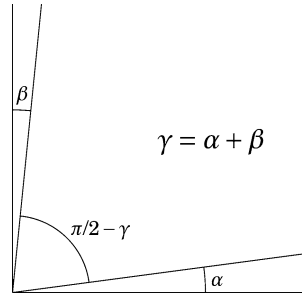

Figure 5.8. Definition of shear strain

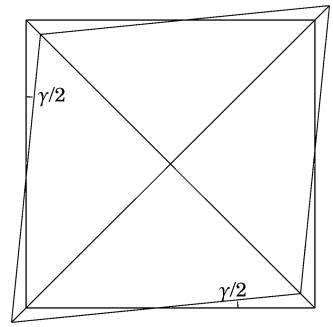

Figure 5.9. Dependence of shear strain on reference axes

a shear strain γ if the reference lines are chosen as parallel to the sides of the square. If, on the other hand, they are taken as parallel to the diagonals, then there is no shear strain. In general, if the reference lines are parallel to axes labeled x and y, then the shear strain is denoted γ_{xy}.

Example 5.2.1: Calculation of shear strain.
A square with sides of length 100 μm, with its lower left-hand corner at (0,0), is deformed so that its corners are now at (3,2), (104.5,3.5), (105.5,107) and (4,105.5).
The shear strain is

$$\gamma = \frac{3.5-2}{100} + \frac{4-3}{100} = 0.035.$$

5.2.3 Rotation

Note that if the angles α and β of Fig. 5.8 are such that $\beta = -\alpha$, as in Fig. 5.10a, then clearly $\gamma = 0$, and the element undergoes a rigid rotation of angle α. More generally, when $\beta \neq -\alpha$, then the angle of rotation of the line that was originally halfway between the x- and y-axes (that is, the lower-left-to-upper-right diagonal if the element is a square) is $\frac{1}{2}(\alpha - \beta)$, as shown is Fig. 5.10b.

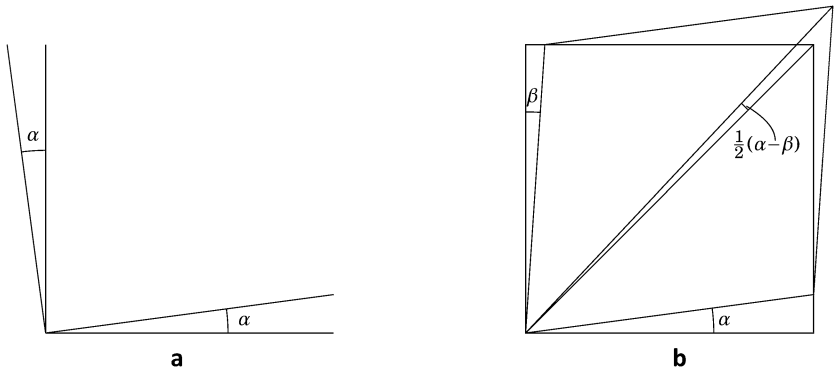

Figure 5.10. Rotation: (**a**) rigid rotation, (**b**) rotation of diagonal line

(The proof is left to an exercise.) This angle is clearly the average of the rotations of the sides along the x- and y-axes, and can also be shown to be the average rotation of the element.

5.2.4 Virtual Work in Shear

As we mentioned in Sect. 2.1 (page 58), the work done by a moment M in the course of an infinitesimal rotation $d\theta$ is $dW = M\,d\theta$, and the corresponding virtual work is $\delta W = M\,\delta\theta$. Let us now consider the rectangular block shown in Fig. 5.11a, its thickness perpendicular to the page being c, with the angles α and β undergoing virtual changes $\delta\alpha$ and $\delta\beta$, respectively, as shown in Fig. 5.11b. Note that the angles α and β shown in Fig. 5.11b are greatly exagger-

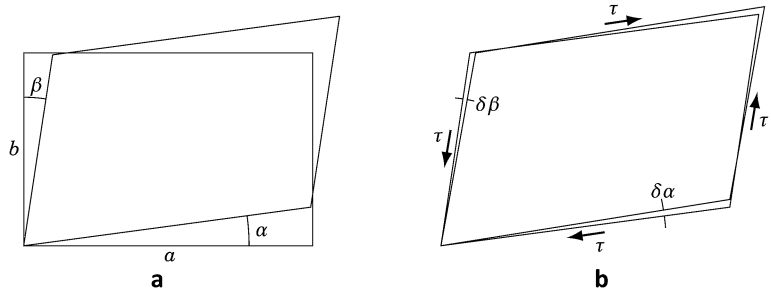

Figure 5.11. Virtual work in shear: (**a**) original and deformed configurations, (**b**) virtual deformation. Both deformations are intentionally exaggerated for illustrative purposes.

ated and, in reality, they are assumed infinitesimal. Thus, the moment arm of the shear stresses τ acting on the originally vertical sides is a, and therefore these stresses form a counterclockwise couple of forces τbc yielding the counterclockwise moment τabc acting on the counterclockwise virtual rotation $\delta\alpha$. Similarly, the shear stresses on the originally horizontal sides form the clockwise moment τabc acting on the clockwise virtual rotation $\delta\beta$. The

total internal virtual work in two-dimensional shear is therefore

$$\delta W_{\text{int}} = \tau abc\,\delta\gamma\,, \tag{5.22}$$

and, since the volume of the block is abc, the internal virtual work per unit volume is

$$\delta W^0_{\text{int}} = \tau\,\delta\gamma\,. \tag{5.23}$$

Again, if the shear strain changes by an actual infinitesimal increment $d\gamma$, the actual work increment per unit volume is $\tau\,d\gamma$.

Exercises

5.2-1. Determine the engineering shear strain (as defined in Fig. 5.8) at points A and B of the solid body of Exercise **5.1-6** (page 222).

5.2-2. Determine the engineering shear strain (as defined in Fig. 5.8) at points C and D of the solid body of Exercise **5.1-6** (page 222).

5.2-3. Suppose that a thin-walled circular tube like that of Fig. 4.19, of length L, is twisted so that one end is rotated by an angle ϕ with respect to the other end. Isolating a small element of the tube, and assuming the twist to be uniform along the length, find the engineering shear strain in the tube.

5.2-4. Assuming all angles to be infinitesimal, show that if the undeformed element of Fig. 5.10b is a square, the lower-left-to-upper-right diagonal rotates by an angle $\frac{1}{2}(\alpha - \beta)$. (*Hint:* You may use the relation $d \tan^{-1} s/ds = 1/(1+s^2)$.)

5.2-5. Determine the angles of rotations of the diagonals $\overline{AC}$ and $\overline{BD}$ of the solid body of Exercise **5.1-6** (page 222).

5.3 Displacement, General State of Strain

5.3.1 Displacement

The definition of the longitudinal strain in terms of the axial displacement of the cross-section of a bar, Eq. (5.12), will now be generalized to three-dimensional displacements in bodies of arbitrary shape.

We recall from Sect. 1.1 that if a body is displaced from one position to another, then we call the displacement *rigid* if, for any two particles that occupy points A and B in the original position and A' and B' in the displaced position, the distance between them remains unchanged. Otherwise, the body is said to undergo deformation.

Now suppose that the particles that occupy points A and B have coordinates (x,y,z) and $(x+\Delta x, y+\Delta y, z+\Delta z)$, respectively, relative to a fixed Cartesian coordinate system with basis $\{\mathbf{i},\mathbf{j},\mathbf{k}\}$. The distance between A and B is then given by $\Delta r = \sqrt{(\Delta x)^2+(\Delta y)^2+(\Delta z)^2}$, and the unit vector $\mathbf{n}$, shown in Fig. 5.12 as indicating the direction from A to B, may be defined by $n_x = \Delta x/\Delta r$, $n_y = \Delta y/\Delta r$, $n_z = \Delta z/\Delta r$.

If the coordinates of A' and B' are (x',y',z') and $(x'+\Delta x', y'+\Delta y', z'+\Delta z')$, respectively, then we define the *displacement vector* for the particle that occupies A (and, after deformation, A') as $\mathbf{u} = u\mathbf{i}+v\mathbf{j}+w\mathbf{k}$ with components

$$\begin{aligned} u(x,y,z) &= x'-x, \\ v(x,y,z) &= y'-y, \\ w(x,y,z) &= z'-z\,, \end{aligned} \tag{5.24}$$

as in Fig. 5.12. The dependence of $\mathbf{u}$ on the position of the point A in a given region translates into writing its components as functions of (x,y,z), as in Eq. (5.24), and referring to it as a *displacement field*. Likewise, the

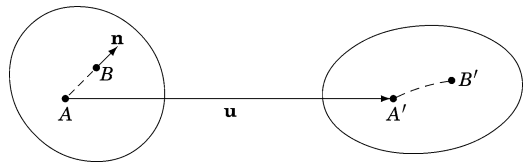

Figure 5.12. A body, with two material points shown, in its reference state (left) and deformed state (right)

displacement of the particle that occupies point B (and, after deformation, B') has components

$$\begin{aligned} u(x+\Delta x, y+\Delta y, z+\Delta z) &= (x'+\Delta x')-(x+\Delta x) = u(x,y,z)+(\Delta x'-\Delta x)\,, \\ v(x+\Delta x, y+\Delta y, z+\Delta z) &= (y'+\Delta y')-(y+\Delta y) = v(x,y,z)+(\Delta y'-\Delta y)\,, \\ w(x+\Delta x, y+\Delta y, z+\Delta z) &= (z'+\Delta z')-(z+\Delta z) = w(x,y,z)+(\Delta z'-\Delta z)\,. \end{aligned} \tag{5.25}$$

We now assume that the distance between the points A and B (and, likewise, A' and B') becomes infinitesimal, and we use differentials (dx, dy, dz) instead of differences $(\Delta x, \Delta y, \Delta z)$. It follows that Δr becomes $dr = \sqrt{(dx)^2 + (dy)^2 + (dz)^2}$ and, also, $n_x = dx/dr$, $n_y = dy/dr$, $n_z = dz/dr$. Since the differentials are assumed infinitesimal, it follows that, by taking the total differentials of Eqs. (5.24) and using the definition of the components of the normal vector, we obtain

$$\begin{aligned} dx' &= dx + \frac{\partial u}{\partial x}dx + \frac{\partial u}{\partial y}dy + \frac{\partial u}{\partial z}dz = dr\left(n_x + n_x\frac{\partial u}{\partial x} + n_y\frac{\partial u}{\partial y} + n_z\frac{\partial u}{\partial z}\right) \\ dy' &= dy + \frac{\partial v}{\partial x}dx + \frac{\partial v}{\partial y}dy + \frac{\partial v}{\partial z}dz = dr\left(n_y + n_x\frac{\partial v}{\partial x} + n_y\frac{\partial v}{\partial y} + n_z\frac{\partial v}{\partial z}\right) \\ dz' &= dz + \frac{\partial w}{\partial x}dx + \frac{\partial w}{\partial y}dy + \frac{\partial w}{\partial z}dz = dr\left(n_z + n_x\frac{\partial w}{\partial x} + n_y\frac{\partial w}{\partial y} + n_z\frac{\partial w}{\partial z}\right). \end{aligned} \tag{5.26}$$

Next, we recall that $dr' = \sqrt{(dx')^2 + (dy')^2 + (dz')^2}$, and substitute here the expressions for dx', dy' and dz' from (5.26) by assuming that all partial derivatives $\partial u/\partial x$, $\partial v/\partial x$ etc. are *small compared to unity* (that is, $|\partial u/\partial x| \ll 1$ etc.). When these quantities are regarded as infinitesimal, their squares and products can be neglected, and

$$\begin{aligned} dr' \doteq \Bigg\{1 + 2\Bigg[n_x^2\frac{\partial u}{\partial x} + n_x n_y\left(\frac{\partial u}{\partial y} + \frac{\partial v}{\partial x}\right) + n_x n_z\left(\frac{\partial u}{\partial z} + \frac{\partial w}{\partial x}\right) \\ + n_y^2\frac{\partial v}{\partial y} + n_y n_z\left(\frac{\partial v}{\partial z} + \frac{\partial w}{\partial y}\right) + n_z^2\frac{\partial w}{\partial z}\Bigg]\Bigg\}^{1/2} dr\,. \end{aligned} \tag{5.27}$$

Furthermore, since the quantity in square brackets is small compared to unity, we may further use the approximation $\sqrt{1+2\zeta} \doteq 1 + \zeta$* for $|\zeta| \ll 1$, and finally obtain the result for the longitudinal strain at the point of interest along the direction defined by $\mathbf{n}$, by analogy with the uniaxial definition, as

$$\begin{aligned} \varepsilon_n &= \frac{dr' - dr}{dr} \\ &= n_x^2\frac{\partial u}{\partial x} + n_x n_y\left(\frac{\partial u}{\partial y} + \frac{\partial v}{\partial x}\right) + n_x n_z\left(\frac{\partial u}{\partial z} + \frac{\partial w}{\partial x}\right) + n_y^2\frac{\partial v}{\partial y} + n_y n_z\left(\frac{\partial v}{\partial z} + \frac{\partial w}{\partial y}\right) + n_z^2\frac{\partial w}{\partial z}\,. \end{aligned} \tag{5.28}$$

Clearly, if $\mathbf{n}$ is aligned with the x-axis (or, equivalently, the y-axis or z-axis), then the above equation takes the simple form $\varepsilon_x = \partial u/\partial x$ and, analogously, $\varepsilon_y = \partial v/\partial y$ and $\varepsilon_z = \partial w/\partial z$. In summary, these expressions define the three longitudinal (or normal) strains along the x-, y-, and z-axes, namely,

$$\varepsilon_x = \frac{\partial u}{\partial x}\quad,\quad \varepsilon_y = \frac{\partial v}{\partial y}\quad,\quad \varepsilon_z = \frac{\partial w}{\partial z}\,. \tag{5.29}$$

*This is derived by taking the square-root of the algebraic identity $(1+\zeta)^2 = 1 + 2\zeta + \zeta^2$, and ignoring the second-order term ζ^2.

If we limit ourselves to the general two-dimensional state of deformation in, say, the (x, y)-plane (in which case $w = 0$), referred to as *plane strain*, with $n_x = \cos\theta$ and $n_y = \sin\theta$, the longitudinal (or normal) strain along $\mathbf{n}$, with the aid of Eqs. $(5.29)_{1,2}$, reduces to

$$\begin{aligned} \varepsilon_n &= \frac{\partial u}{\partial x}\cos^2\theta + \left(\frac{\partial u}{\partial y} + \frac{\partial v}{\partial x}\right)\cos\theta\sin\theta + \frac{\partial v}{\partial y}\sin^2\theta \\ &= \varepsilon_x\cos^2\theta + \left(\frac{\partial u}{\partial y} + \frac{\partial v}{\partial x}\right)\cos\theta\sin\theta + \varepsilon_y\sin^2\theta \ . \end{aligned} \tag{5.30}$$

It should be clear that the definition of ε_x in Eq. $(5.29)_1$ is just the generalization of the definition of uniaxial strain, $\varepsilon = du/dx$, introduced in Sect. 5.1, as are $\varepsilon_y = \partial v/\partial y$ and $\varepsilon_z = \partial w/\partial z$; these are the *longitudinal* or *normal* strain components, analogous to the normal stress components.

The quantity which appears in parentheses in Eqs. $(5.30)_{2,3}$ is the *engineering shear strain* γ_{xy}, namely,

$$\gamma_{xy} = \frac{\partial u}{\partial y} + \frac{\partial v}{\partial x} \ . \tag{5.31}$$

The geometric interpretation of the two partial derivative terms in Eq. (5.31) can be seen in Fig. 5.13, which is a more detailed version of Fig. 5.8. Since

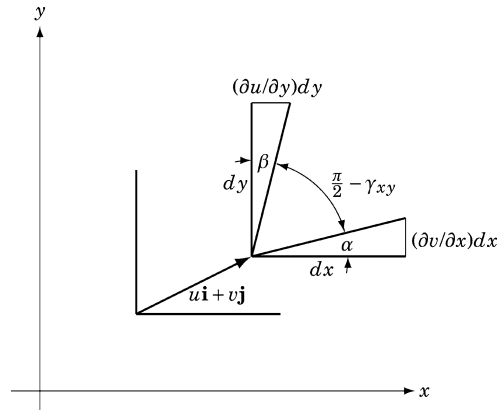

Figure 5.13. Geometric meaning of shear strain

$\partial u/\partial y$ and $\partial v/\partial x$ are infinitesimal, it follows from Fig. 5.13 that $\alpha = \partial v/\partial x$ and $\beta = \partial u/\partial y$ (in radians). This, in turn, implies that for two perpendicular line elements that are initially parallel to the x- and y-axes, respectively, $\gamma_{xy} = \alpha + \beta$ is the amount (in radians) by which the angle between them changes from a right angle.

With the preceding definitions of strain in place, one may rewrite (5.30) as

$$\varepsilon_n = \varepsilon_x\cos^2\theta + \gamma_{xy}\cos\theta\sin\theta + \varepsilon_y\sin^2\theta \ . \tag{5.32}$$

The extension to three dimensions is straightforward, with the shear strains γ_{yz} and γ_{zx} defined as

$$\gamma_{yz} = \frac{\partial v}{\partial z} + \frac{\partial w}{\partial y} \quad , \quad \gamma_{zx} = \frac{\partial w}{\partial x} + \frac{\partial u}{\partial z} \, . \tag{5.33}$$

Note that, in view of Eq. (5.21), the engineering shear strains are symmetric in their two indices, that is

$$\gamma_{xy} = \gamma_{yx} \quad , \quad \gamma_{yz} = \gamma_{zy} \quad , \quad \gamma_{zx} = \gamma_{xz} \, . \tag{5.34}$$

It can be easily shown that, for Eqs. $(5.29)_{1,2}$ and (5.31) to be valid simultaneously—that is, for the longitudinal and shear strains to be *compatible* with one another—they must satisfy the *compatibility condition* given by

$$\frac{\partial^2 \varepsilon_x}{\partial y^2} + \frac{\partial^2 \varepsilon_y}{\partial x^2} = \frac{\partial^2 \gamma_{xy}}{\partial x \partial y} \tag{5.35}$$

(the derivation is left to an exercise). In plane strain this equation is a necessary and sufficient condition for strain compatibility. In general, however, this equation and its yz and zx analogues are necessary but not sufficient.

In complete analogy to stress, the components of strain can be arranged in a matrix representing a second-rank tensor (the *strain tensor*). However, for mathematical reasons that will be explained in the next section, the shear strains used in the tensorial representation are half of the respective engineering strains, that is

$$\varepsilon_{xy} = \frac{1}{2}\gamma_{xy} \quad , \quad \varepsilon_{yz} = \frac{1}{2}\gamma_{yz} \quad , \quad \varepsilon_{zx} = \frac{1}{2}\gamma_{zx} \, . \tag{5.36}$$

The matrix of the components of the strain tensor thus takes the form

$$[\varepsilon] = \begin{bmatrix} \varepsilon_x & \varepsilon_{xy} & \varepsilon_{xz} \\ \varepsilon_{yx} & \varepsilon_y & \varepsilon_{yz} \\ \varepsilon_{zx} & \varepsilon_{zy} & \varepsilon_z \end{bmatrix} \, . \tag{5.37}$$

Note that this matrix is symmetric, given the conditions of Eqs. (5.34) and (5.36).

Example 5.3.1: Derivation of strain components from displacement.
It should be obvious from Eqs. (5.29), (5.31) and (5.33) that the strain field is uniform (that is, the strain components are independent of position) if and only if the displacement components are linear functions of the coordinates.
Suppose, then, that

$$u = a_0 + a_1 x + a_2 y + a_3 z \quad , \quad v = b_0 + b_1 x + b_2 y + b_3 z \quad , \quad w = c_0 + c_1 x + c_2 y + c_3 z \, .$$

It follows that the strain matrix (5.37) is given by

$$[\varepsilon] = \begin{bmatrix} a_1 & \frac{1}{2}(a_2 + b_1) & \frac{1}{2}(a_3 + c_1) \\ \frac{1}{2}(a_2 + b_1) & b_2 & \frac{1}{2}(b_3 + c_2) \\ \frac{1}{2}(a_3 + c_1) & \frac{1}{2}(b_3 + c_2) & c_3 \end{bmatrix} \, .$$

5.3.2 Displacement Gradient and Rotation

The strain matrix (5.37) does not obey a relation of the form of Eq. (4.25) (page 182), and the tensorial nature of strain will be shown through another property in Sect. 5.4. If, however, the partial derivatives of the displacements are placed in a square matrix, say $[D]$,

$$[D] = \begin{bmatrix} \partial u/\partial x & \partial u/\partial y & \partial u/\partial z \\ \partial v/\partial x & \partial v/\partial y & \partial v/\partial z \\ \partial w/\partial x & \partial w/\partial y & \partial w/\partial z \end{bmatrix}, \tag{5.38}$$

then this matrix clearly does obey Eq. (4.25), since the relation between the vectors $d\mathbf{u} = \mathbf{i}du + \mathbf{j}dv + \mathbf{k}dw$ and $d\mathbf{r} = \mathbf{i}dx + \mathbf{j}dy + \mathbf{k}dz$ can be written in matrix form as

$$\begin{Bmatrix} du \\ dv \\ dw \end{Bmatrix} = [D] \begin{Bmatrix} dx \\ dy \\ dz \end{Bmatrix}. \tag{5.39}$$

Consequently, $[D]$ represents a second-rank tensor known as the *displacement gradient*.

The matrix $[D]$ (or, for that matter, any square matrix) may be additively decomposed into its *symmetric* and *antisymmetric* parts according to the identity

$$[D] = \underbrace{\frac{1}{2}([D] + [D]^T)}_{\text{symmetric}} + \underbrace{\frac{1}{2}([D] - [D]^T)}_{\text{antisymmetric}}, \tag{5.40}$$

where $[D]^T$ denotes the transpose of $[D]$. It follows from Eqs. (5.29), (5.31) and (5.33) that the strain matrix is equal to the symmetric part of the displacement-gradient matrix $[D]$.

The antisymmetric part of $[D]$ may be expressed, with the aid of Eqs. (5.38) and (5.40), as

$$[\omega] = \begin{bmatrix} 0 & -\omega_z & \omega_y \\ \omega_z & 0 & -\omega_x \\ -\omega_y & \omega_x & 0 \end{bmatrix}, \tag{5.41}$$

where, by definition,

$$\omega_x = \frac{1}{2}\left(\frac{\partial w}{\partial y} - \frac{\partial v}{\partial z}\right), \quad \omega_y = \frac{1}{2}\left(\frac{\partial u}{\partial z} - \frac{\partial w}{\partial x}\right), \quad \omega_z = \frac{1}{2}\left(\frac{\partial v}{\partial x} - \frac{\partial u}{\partial y}\right). \tag{5.42}$$

We note, referring to Fig. 5.13, that $\omega_z = \frac{1}{2}(\alpha - \beta)$ and is, as we discussed in Sect. 5.2 (page 227), the average angle of rotation in the xy-plane, that is, about the z-axis. Similarly, ω_x and ω_y are the average angles of rotation about the x- and y-axes, respectively. For this reason the matrix $[\omega]$ contains the components of what is known as the (infinitesimal) *rotation tensor*.

In summary, Eq. (5.40), when coupled with the definitions in (5.37) and (5.41), may be rewritten as

$$[D] \;=\; [\varepsilon] + [\omega]\,, \tag{5.43}$$

that is, it is equal to the sum of the strain and rotation tensors. Since the components of both of these tensors are infinitesimal, the tensors themselves are also typically referred to as such.

When there is no deformation but only a rigid rotation, that is, when $[\varepsilon] = 0$ and therefore $[D] = [\omega]$ as given by Eq. (5.41), then it can be shown that the relation (5.39) between $d\mathbf{u}$ and $d\mathbf{r}$ may be written as

$$d\mathbf{u} \;=\; \boldsymbol{\omega} \times d\mathbf{r}\,, \tag{5.44}$$

where $\boldsymbol{\omega} = \omega_x\mathbf{i} + \omega_y\mathbf{j} + \omega_x\mathbf{k}$ is known as the (infinitesimal) *rotation vector*.[†] The proof is left to an exercise.

Example 5.3.2: Derivation of the rotation vector from displacements. Applying Eqs. (5.42) to the displacement field of Example 5.3.1 yields the rotation vector

$$\boldsymbol{\omega} \;=\; \tfrac{1}{2}[(c_2 - b_3)\mathbf{i} + (a_3 - c_1)\mathbf{j} + (b_1 - a_2)\mathbf{k}]\,.$$

5.3.3 Internal Virtual Work (General Case)

With the shear strains defined in terms of displacement, as in Eq. (5.31), we can define virtual strain in shear similarly to our definition of virtual longitudinal strain in Sect. 5.1, obtaining a result equivalent to that derived geometrically in Sect. 5.2 (page 224). We consider a narrow strip (of cross-sectional area ΔA in the yz-plane, the x-axis being the longitudinal axis) in a state of simple shear in the xy-plane such that, with reference to Fig. 5.13, $\beta = 0$, so that the only relevant displacement component is v. Now, for representative particles i at x and j at $x + \Delta x$,

$$\delta(\mathbf{r}_j - \mathbf{r}_i) \;=\; [\delta v(x + \Delta x) - \delta v(x)]\mathbf{j} \;=\; [\delta(\partial v/\partial x)\Delta x]\mathbf{j}\,, \tag{5.45}$$

but in this case $\partial v/\partial x = \gamma_{xy}$. With a positive shear stress τ_{xy} acting according to the usual sign convention, $\mathbf{F}_{ij} = \tau_{xy}\Delta A\mathbf{j} = -\mathbf{F}_{ji}$, and therefore the internal virtual work per unit volume is

$$\delta W^0_{\text{int}} \;=\; \tau_{xy}\delta\gamma_{xy} \quad \text{(shear in } xy\text{-plane)}\,, \tag{5.46}$$

which is identical (except for subscripts) to Eq. (5.23). It is not difficult to extend this derivation to the more general case shown in Fig. 5.13, and also

[†]Note that the same symbol, $\boldsymbol{\omega}$, is used for it as for the angular velocity defined in Sect. 2.1 (page 58).

to shear strain in the other two planes. It is interesting to note here that the above expression may be also written, with the aid of Eq. (5.36), as

$$\delta W^0_{\text{int}} = \tau_{xy}\delta\varepsilon_{xy} + \tau_{yx}\delta\varepsilon_{yx} \tag{5.47}$$

by merely exploiting the symmetry of stresses and strains. From this we conclude that the shear stress τ_{xy} is conjugate (in the sense discussed in Sect. 2.1.4) to the strain ε_{xy} and, likewise, τ_{yx} is conjugate to ε_{yx}.

The results can be further extended to general three-dimensional strain, with the internal virtual work given by the sum of the contributions of all the normal stresses and shear stresses, as exemplified by Eqs. (5.17) and (5.46), respectively:

$$\delta W^0_{\text{int}} = \sigma_x\delta\varepsilon_x + \sigma_y\delta\varepsilon_y + \sigma_z\delta\varepsilon_z + \tau_{yz}\delta\gamma_{yz} + \tau_{xz}\delta\gamma_{xz} + \tau_{xy}\delta\gamma_{xy}\ . \tag{5.48}$$

Exercises

5.3-1. Show that, if ε_x and ε_y are given by Eq. (5.29)$_{1,2}$ and γ_{xy} is given by Eq. (5.31), then they must satisfy Eq. (5.35).

5.3-2. Consider a body which in its undeformed state occupies a rectangular domain, as in the figure. Assume that the body deforms in such a way that the horizontal displacement u for any point is given by $u(x,y) = 0.01xy$ in meters, while the vertical displacement $v = 0$.

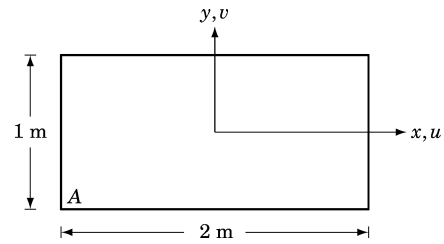

(a) Sketch the deformed shape of the body (you may wish to magnify the displacement in your sketch).

(b) Determine the strain components ε_x, ε_y and ε_{xy} for any point with coordinates x and y.

(c) Compute the engineering shear strain γ_{xy} at point A using (5.20) and compare it to its counterpart computed from part (b). Are they exactly equal? If yes (or no), why (or why not)?

5.3-3. Consider a square block in the state of plane strain in the (x,y)-plane, as in the figure. Let the $x-$ and $y-$components (u,v) of the displacement be given (in millimeters) by

$$\begin{aligned} u(x,y) &= 0.01x + 0.05y \\ v(x,y) &= -0.03x + 0.02y \end{aligned}$$

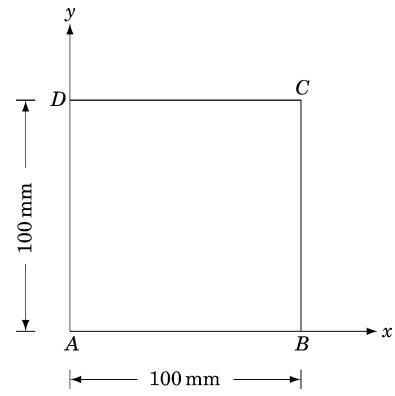

(a) Determine the normal strains ε_x, ε_y and the shear strain γ_{xy} in the block.

(b) Find the length of the line element AB in the deformed state of the block.

(c) Find the angle between line elements AC and BD in the deformed state of the block.

5.3-4. For the block of Exercise **5.3-3**, find the longitudinal strains along the diagonals AC and BD.

5.3-5. Find the average rotation angle ω_z in the block of Problem **5.3-3**. Show that it is the average of the rotation angles of the sides along the x- and y-axes.

5.3-6. Derive Eq. (5.44).

5.3-7. With the *del* (or *nabla*) operator defined as $\nabla = \mathbf{i}\dfrac{\partial}{\partial x} + \mathbf{j}\dfrac{\partial}{\partial y} + \mathbf{k}\dfrac{\partial}{\partial z}$, write Eq. (5.42) in vector notation.

5.3-8. For the three-dimensional displacement field given by

$$\begin{aligned} u(x,y,z) &= (3.2x + 2.3y - 1.6z)10^{-3}\,, \\ v(x,y,z) &= (1.5x - 2.4y - 2.7z)10^{-3}\,, \\ w(x,y,z) &= (2.5x + 2.7y - 2.5z)10^{-3}\,, \end{aligned}$$

determine (a) the strain component matrix $[\varepsilon]$ and (b) the rotation vector $\boldsymbol{\omega}$, as well as (c) the magnitude of the rotation in degrees of arc.

5.4 Strain Transformation, Principal Strains

5.4.1 Basic Concepts

For the strain tensor defined in Sect. 5.3 we do not have an equation of the form (4.25). We will establish the tensorial nature of strain, instead, by showing that its components transform from one set of axes to another in exactly the same way as those of stress.

Eq. (5.28) immediately furnishes the expression for the transformation of the longitudinal strain components in two dimensions from xy-axes to $x'y'$-axes. The latter are rotated with respect to the former by an angle θ if we simply reinterpret ε_n as $\varepsilon_{x'}$. As in the case of stresses, we get $\varepsilon_{y'}$ by replacing θ with $\theta + \pi/2$.

More formally, we can derive the transformation equations by expressing Eqs. $(5.29)_{1,2}$ and (5.31) in terms of displacement components u', v' with respect to the rotated axes x', y', that is, $\varepsilon_{x'} = \partial u'/\partial x'$ etc.

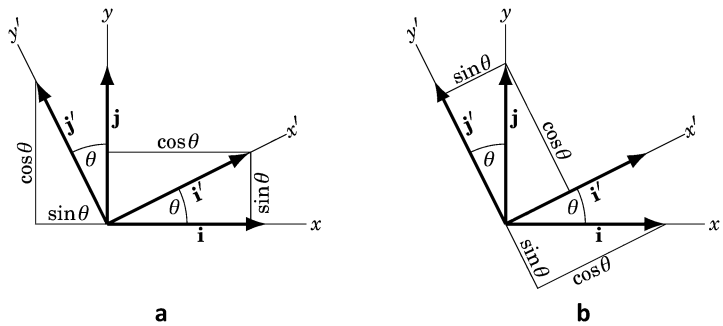

Figure 5.14. Relation between unit vectors along original and rotated axes

From Fig. 5.14a we obtain the relation between the unit vectors ($\mathbf{i}'$,$\mathbf{j}'$) and ($\mathbf{i}$,$\mathbf{j}$) as

$$\mathbf{i}' = \mathbf{i}\cos\theta + \mathbf{j}\sin\theta\ ,\quad \mathbf{j}' = \mathbf{j}\cos\theta - \mathbf{i}\sin\theta\ . \tag{5.49}$$

If the two-dimensional displacement vector is $\mathbf{u} = u\mathbf{i} + v\mathbf{j}$, then $u' = \mathbf{u}\cdot\mathbf{i}'$ and $v' = \mathbf{u}\cdot\mathbf{j}'$, that is,

$$u' = u\cos\theta + v\sin\theta\ ,\quad v' = -u\sin\theta + v\cos\theta\ . \tag{5.50}$$

In fact, Eqs. (5.50) govern the transformation of the components of any two-dimensional vector from those with respect to the original axes to those with respect to the rotated axes.

The inverse of Eqs. (5.50) may be obtained either directly from Fig. 5.14b or by solving these equations for u and v (or even more simply by replacing θ with $-\theta$ and interchanging the primed and non-primed components). It follows that the coordinates x, y (since they are the components of the position

vector $\mathbf{r}$) can be expressed in terms of x', y' by

$$x = x'\cos\theta - y'\sin\theta\ ,\quad y = x'\sin\theta + y'\cos\theta\ . \tag{5.51}$$

In order to find the partial derivatives $\partial u'/\partial x'$ etc., we need to use the chain rule for partial derivatives, for example,

$$\frac{\partial u'}{\partial x'} = \frac{\partial u'}{\partial x}\frac{\partial x}{\partial x'} + \frac{\partial u'}{\partial y}\frac{\partial y}{\partial x'}\ , \tag{5.52}$$

in order to obtain $\partial x/\partial x'$ and $\partial y/\partial x'$ from Eqs. (5.51). Consequently,

$$\varepsilon_{x'} = \frac{\partial u'}{\partial x'} = \left(\frac{\partial u}{\partial x}\cos\theta + \frac{\partial v}{\partial x}\sin\theta\right)\cos\theta + \left(\frac{\partial u}{\partial y}\cos\theta + \frac{\partial v}{\partial y}\sin\theta\right)\sin\theta\ , \tag{5.53}$$

which reduces to the right-hand side of Eq. (5.28), and, lastly,

$$\begin{aligned}\varepsilon_{x'} &= \varepsilon_x\cos^2\theta + \varepsilon_y\sin^2\theta + \gamma_{xy}\sin\theta\cos\theta,\\ \varepsilon_{y'} &= \varepsilon_y\cos^2\theta + \varepsilon_x\sin^2\theta - \gamma_{xy}\sin\theta\cos\theta\ .\end{aligned} \tag{5.54}$$

It can be easily seen from Eq. (5.54) that $\varepsilon_{x'} + \varepsilon_{y'} = \varepsilon_x + \varepsilon_y$.

Following the same methodology, we find that $\gamma_{x'y'}$ transforms according to

$$\gamma_{x'y'} = -2(\varepsilon_x - \varepsilon_y)\sin\theta\cos\theta + \gamma_{xy}(\cos^2\theta - \sin^2\theta)\ . \tag{5.55}$$

The derivation of the preceding formula is left to an exercise.

With the help of Eqs. (4.49), Eqs. (5.54)–(5.55) can also be written as

$$\begin{aligned}\varepsilon_{x'} &= \frac{\varepsilon_x + \varepsilon_y}{2} + \frac{\varepsilon_x - \varepsilon_y}{2}\cos 2\theta + \frac{\gamma_{xy}}{2}\sin 2\theta\ ,\\ \varepsilon_{y'} &= \frac{\varepsilon_x + \varepsilon_y}{2} - \frac{\varepsilon_x - \varepsilon_y}{2}\cos 2\theta - \frac{\gamma_{xy}}{2}\sin 2\theta\ ,\\ \gamma_{x'y'} &= \gamma_{xy}\cos 2\theta - (\varepsilon_x - \varepsilon_y)\sin 2\theta\ .\end{aligned} \tag{5.56}$$

Example 5.4.1: Strain components in polar coordinates.
If, considering the element shown Fig. 4.35a (page 197), we denote the longitudinal strains in the radial and circumferential directions, respectively, as ε_r and ε_θ, and the engineering shear strain as $\gamma_{r\theta}$, then it follows from the tensorial nature of strain that these components are related to the Cartesian ones by equations analogous to (4.52), namely,

$$\begin{aligned}\varepsilon_r &= \varepsilon_x\cos^2\theta + \gamma_{xy}\cos\theta\sin\theta + \varepsilon_y\sin^2\theta\ ,\\ \varepsilon_\theta &= \varepsilon_x\sin^2\theta - \gamma_{xy}\cos\theta\sin\theta + \varepsilon_y\cos^2\theta\ ,\\ \gamma_{r\theta} &= 2(\varepsilon_y - \varepsilon_x)\cos\theta\sin\theta + \gamma_{xy}(\cos^2\theta - \sin^2\theta)\ .\end{aligned} \tag{5.57}$$

The relations between the polar components of strain and those of displacement are not as simple as the ones for Cartesian components. If the polar displacement components are denoted u_r and u_θ, then the Cartesian ones are given by

$$u = u_r\cos\theta - u_\theta\sin\theta\quad ,\quad v = u_\theta\cos\theta + u_r\sin\theta\ . \tag{5.58}$$

If these are used in Eqs. (5.29)$_{1,2}$ and (5.31), along with the chain rule for partial differentiation between Cartesian and polar coordinates, and then inserted in Eqs. (5.57), the result (after some lengthy though straightforward manipulation) is

$$\varepsilon_r = \frac{\partial u_r}{\partial r} \quad , \quad \varepsilon_\theta = \frac{u_r}{r} + \frac{1}{r}\frac{\partial u_\theta}{\partial \theta} \quad , \quad \gamma_{r\theta} = \frac{\partial u_\theta}{\partial r} + \frac{1}{r}\frac{\partial u_r}{\partial \theta} - \frac{u_\theta}{r} \, . \tag{5.59}$$

This result may also be obtained by a direct analysis of the deformation of the element. A simple instance of such an analysis is left to an exercise.

5.4.2 Strain-Gauge Rosettes

If, by analogy with the notation of Sect. 4.6.1 (page 195) for stress, we write ε_θ (not to be confused with ε_θ in Eqs. (5.57) and (5.59)) for $\varepsilon_{x'}$, then the relation between the longitudinal strain along any line in the xy-plane forming an angle θ with the x-axis and the components ε_x, ε_y and γ_{xy} is

$$\varepsilon_\theta = \varepsilon_x \cos^2\theta + \varepsilon_y \sin^2\theta + \gamma_{xy} \sin\theta \cos\theta \, . \tag{5.60}$$

As we mentioned in Sect. 5.1, longitudinal strain can be measured by means of a strain gauge. Consequently, if in the neighborhood of a point on the surface of a body three gauges can be placed at three different angles (say $\theta_1, \theta_2, \theta_3$) to the x-axis, and Eq. (5.60) is written for each of them, then the resulting set of three equations,

$$\begin{aligned} \varepsilon_{\theta_1} &= \varepsilon_x \cos^2\theta_1 + \varepsilon_y \sin^2\theta_1 + \gamma_{xy} \sin\theta_1 \cos\theta_1 \, , \\ \varepsilon_{\theta_2} &= \varepsilon_x \cos^2\theta_2 + \varepsilon_y \sin^2\theta_2 + \gamma_{xy} \sin\theta_2 \cos\theta_2 \, , \\ \varepsilon_{\theta_3} &= \varepsilon_x \cos^2\theta_3 + \varepsilon_y \sin^2\theta_3 + \gamma_{xy} \sin\theta_3 \cos\theta_3 \, , \end{aligned} \tag{5.61}$$

can be solved for ε_x, ε_y and γ_{xy} and so the two-dimensional state of strain can be determined.

A combination of strain gauges used in this way is known as a *strain-gauge rosette*. One such rosette is the *rectangular* or 45° rosette (see Fig. 5.15a for possible configurations), in which $\theta_1 = 0$, $\theta_2 = \pi/4$ and $\theta_3 = \pi/2$. The second of Eqs. (5.61) can then be solved for γ_{xy} in terms of ε_x ($= \varepsilon_0$), ε_y ($= \varepsilon_{\pi/2}$) and $\varepsilon_{\pi/4}$ as

$$\gamma_{xy} = 2\varepsilon_{\pi/4} - \varepsilon_x - \varepsilon_y \, , \tag{5.62}$$

since $\sin(\pi/4) = \cos(\pi/4) = 1/\sqrt{2}$.

Another combination, known as the *delta* or equiangular rosette (with possible configurations shown in Fig. 5.15b), has $\theta_1 = 0$, $\theta_2 = \pi/3$ and $\theta_3 = -\pi/3$ (or, equivalently, $2\pi/3$). The second and third of Eqs. (5.61) become

$$\varepsilon_{\pm\pi/3} = \frac{1}{4}\varepsilon_x \pm \frac{\sqrt{3}}{4}\gamma_{xy} + \frac{3}{4}\varepsilon_y \, . \tag{5.63}$$

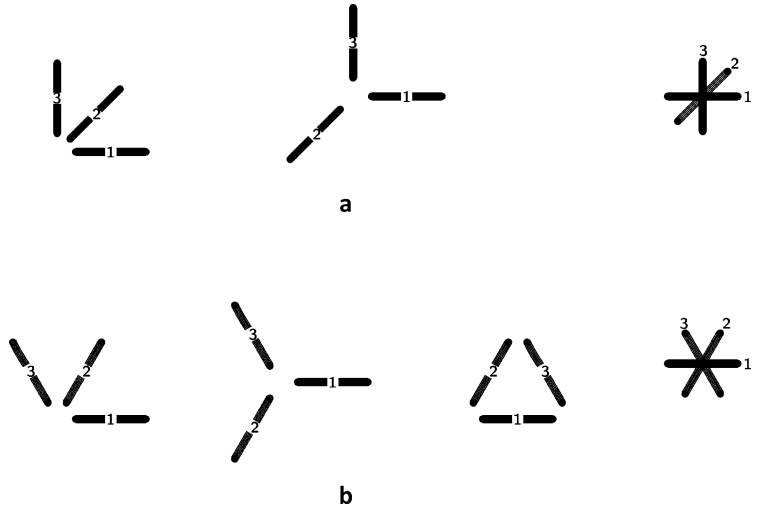

Figure 5.15. Geometrically different but functionally equivalent configurations of (**a**) rectangular and (**b**) delta rosettes

Adding these two equations leads to

$$\varepsilon_y = \frac{2}{3}(\varepsilon_{\pi/3} + \varepsilon_{-\pi/3}) - \frac{1}{3}\varepsilon_x \,, \tag{5.64}$$

where, again, $\varepsilon_x = \varepsilon_0$, while subtracting the second of Eqs. (5.63) from the third yields

$$\gamma_{xy} = \frac{2}{\sqrt{3}}(\varepsilon_{\pi/3} - \varepsilon_{-\pi/3}) \,. \tag{5.65}$$

Example 5.4.2: Strain-gauge rosette measurement.

We suppose that the readouts of a delta rosette are $\varepsilon_0 = 386$, $\varepsilon_{\pi/3} = -347$ and $\varepsilon_{-\pi/3} = 291$, with units in microstrain. From the above equations we obtain (to three significant digits)

$$\varepsilon_x = 386 \quad , \quad \varepsilon_y = -166 \quad , \quad \gamma_{xy} = -737 \,. \tag{5.66}$$

Strain-gauge rosettes can be configured in various ways that are geometrically different but functionally equivalent, as shown in Fig. 5.15.

5.4.3 Principal Strains

The principal strains ε_i $(i = 1,2,3)$ can be derived by exactly the same method as the principal stresses, discussed in Sect. 4.6, provided one remembers to

use the shear strains ε_{xy}, etc., as opposed to the corresponding engineering shear strains γ_{xy}, etc. This includes expressing the transformation equations in terms of 2θ as in Eqs. (4.50)–(4.51).

The physical meanings of the principal strains are analogous to those of the principal stresses: they represent the stationary values (maximum, minimum and [in three dimensions] saddle point) of the longitudinal strain along all possible directions through a point. The principal axes of strain are also those that, taken pairwise, undergo no shearing. The directions of maximum shear strain, likewise, are at 45° to the principal axes.

If, by analogy with the definition of r for stress (Eq. (4.58), page 199), we define for the case of plane strain

$$s = \frac{1}{2}\sqrt{(\varepsilon_x - \varepsilon_y)^2 + \gamma_{xy}^2}\,, \tag{5.67}$$

then

$$\tan 2\theta_p = \frac{\gamma_{xy}}{\varepsilon_x - \varepsilon_y}\,, \quad \cos 2\theta_{p1,2} = \pm\frac{\varepsilon_x - \varepsilon_y}{2s}\,, \quad \sin 2\theta_{p1,2} = \pm\frac{\gamma_{xy}}{2s}\,. \tag{5.68}$$

By analogy with Eq. (4.60) we thus obtain

$$\varepsilon_{1,2} = \frac{\varepsilon_x + \varepsilon_y}{2} \pm s\,. \tag{5.69}$$

Example 5.4.3: Principal strains and directions.

For the data of Example 5.4.2, we find

$$s = \tfrac{1}{2}\sqrt{(386+166)^2 + 737^2} = 460\,, \tag{5.70}$$

and therefore $\varepsilon_{p1,2} = \frac{1}{2}(386-166) \pm 460 = 570, -350$. The direction of the principal axis for the algebraically larger principal strain is given $\theta_{p1} = \frac{1}{2}\cos^{-1}[(386+166)/2\times 460] = \frac{1}{2}\sin^{-1}[(-737/2\times 460] = -26.6°$.

In the same way that r was found to be the value of the maximum in-plane shear stress, so $2s$ is the value of the maximum in-plane shear strain.

Mohr's Circle for Strain

Mohr's circles for strain can be drawn analogously with those for stress, with ε_θ and $\frac{1}{2}\gamma_\theta$ as abscissa and ordinate, respectively. If ε_x, ε_y and γ_{xy} are known or have been calculated from strain-gauge-rosette results, then a Mohr's circle for strain in the xy-plane can be constructed in the same way as for stress.

By analogy with Eqs. (4.63) for stress, we can write

$$\varepsilon_\theta = \varepsilon_m + s\cos 2(\theta_{p1} - \theta) \quad , \quad \gamma_\theta = 2s\sin 2(\theta_{p1} - \theta)\,, \tag{5.71}$$

where $\varepsilon_m = \frac{1}{2}(\varepsilon_x + \varepsilon_y) = \frac{1}{2}(\varepsilon_1 + \varepsilon_2)$ is the mean in-plane strain for the (x,y)-plane. By analogy with Eq. (4.79), the maximum in-plane engineering shear strain is given by

$$\gamma_{\theta_s} = \pm 2s. \tag{5.72}$$

With the help of Eq. $(5.71)_1$ we can get the principal strains and directions directly from the strain-gauge readouts, without first converting to components in a particular set of axes. Let these readouts be written as

$$\varepsilon_{\theta_i} = \varepsilon_m + s\cos 2(\theta_{p1} - \theta_i)\,, \quad i = 1,2,3\,, \tag{5.73}$$

and rewritten as

$$\varepsilon_{\theta_i} = \varepsilon_m + (\cos 2\theta_i)s\cos 2\theta_{p1} + (\sin 2\theta_i)s\sin 2\theta_{p1}\,, \quad i = 1,2,3\,. \tag{5.74}$$

We now have a set of three linear equations for the three unknowns ε_m, $s\cos 2\theta_{p1}$ and $s\sin 2\theta_{p2}$. Solving for them gives all the information necessary to produce the Mohr's circle and the directions of the principal axes of strain.

Example 5.4.4: Mohr's circle for strain.

Starting with the readouts in Example 5.4.2, we find that Eqs. (5.74) now read

$$\begin{aligned} \varepsilon_m + s\cos 2\theta_{p1} &= 386\,, \\ \varepsilon_m - \frac{1}{2}s\cos 2\theta_{p1} + \frac{\sqrt{3}}{2}s\sin 2\theta_{p1} &= -347\,, \\ \varepsilon_m - \frac{1}{2}s\cos 2\theta_{p1} - \frac{\sqrt{3}}{2}s\sin 2\theta_{p1} &= 291\,. \end{aligned} \tag{5.75}$$

Adding the three equations leads to $\varepsilon_m = (386 - 347 + 291)/3 = 110$; the first equation then yields $s\cos 2\theta_{p1} = 386 - 110 = 276$. Lastly, subtracting the third equation from the second yield $s\sin 2\theta_{p1} = (-347 - 291)/\sqrt{3} = -368$. We now find $s = \sqrt{276^2 + 368^2} = 460$ and therefore (to the usual precision) $\varepsilon_{p1,2} = 110 \pm 460 = 570, -350$, while $\theta_{p1} = \frac{1}{2}\cos^{-1}(276/460) = \frac{1}{2}\sin^{-1}(-368/460) = -26.6°$, as we found before.

The results are shown in Fig. 5.16.

5.4.4 Area and Volume Strain

The mean in-plane strain ε_m discussed in the preceding subsection has a nice physical interpretation. If an infinitesimal rectangular element in the xy-plane, of sides dx by dy, undergoes deformation in the (x,y)-plane, the lengths of the sides will change to $(1+\varepsilon_x)dx$ and $(1+\varepsilon_y)dy$, respectively, so that the area will change from $dA = dxdy$ to $dA' = (1+\varepsilon_x)(1+\varepsilon_y)dA$. We can define the *area strain* by analogy with longitudinal strain as

$$\varepsilon_{\mathrm{A}} = \frac{dA' - dA}{dA} = (1+\varepsilon_x)(1+\varepsilon_y) - 1 \doteq \varepsilon_x + \varepsilon_y = 2\varepsilon_m\,, \tag{5.76}$$

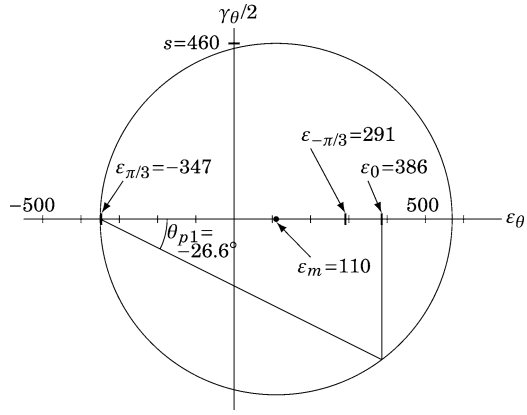

Figure 5.16. Example of a Mohr's circle for strain

the approximation being valid when the strains are infinitesimal.

We can similarly define the volume strain, usually called *volumetric strain*, by considering an infinitesimal rectangular box of sides dx, dy and dz. When the box is deformed, the volume will change from $dV = dx\,dy\,dz$ to $dV' = (1+\varepsilon_x)(1+\varepsilon_y)(1+\varepsilon_z)dV_0$, and the volumetric strain, if infinitesimal, is

$$\varepsilon_{\mathrm{V}} \;=\; \frac{dV' - dV}{dV} \;\doteq\; \varepsilon_x + \varepsilon_y + \varepsilon_z \;. \tag{5.77}$$

Deformation consisting only of volume change (that is, such that $\varepsilon_1 = \varepsilon_2 = \varepsilon_3 = \frac{1}{3}\varepsilon_{\mathrm{V}}$) is known as *dilation* or *dilatation*. (Some writers use *dilatation* as another term for the volumetric strain.) Conversely, deformation with $\varepsilon_{\mathrm{V}} = 0$, involving change of shape at constant volume, is known as *distortion*, as, for example, when a strain tensor consists only of shear components. A material that can undergo only distortion and not dilatation is called *incompressible*; dense rubber comes fairly close to being such a material.

Exercises

5.4-1. Use the chain rule to derive the transformation equation for $\gamma_{x'y'}$ in terms of ε_x, ε_y and γ_{xy} by analogy with the result for $\varepsilon_{x'}$.

5.4-2. For strains given by $\varepsilon_x = 450$, $\varepsilon_y = -300$ and $\gamma_{xy} = 850$ (with units in microstrain), find the components $\varepsilon_{x'}$, $\varepsilon_{y'}$ and $\gamma_{x'y'}$ when $\theta = 40°$.

5.4-3. For strains given by $\varepsilon_x = -0.0008$, $\varepsilon_y = 0.0012$ and $\gamma_{xy} = -0.0015$, find the components $\varepsilon_{x'}$, $\varepsilon_{y'}$ and $\gamma_{x'y'}$ when $\theta = 60°$.

5.4-4. Show *graphically* why, when the displacements in polar coordinates are such that $u_\theta = 0$, the circumferential displacement ε_θ is not in general zero.

5.4-5. Given a displacement field such that $u_\theta = 0$ and u_r is independent of θ, find the dependence of u_r on r such that the area strain ε_A is identically zero.

5.4-6. Consider a material point in plane strain and let the strain readouts from a delta rosette be $\varepsilon_{\theta_1} = 0.001$, $\varepsilon_{\theta_2} = -0.002$, and $\varepsilon_{\theta_3} = 0.004$, where $\theta_1 = 0^o$, $\theta_2 = 60^o$, and $\theta_3 = 120^o$, where all angles are taken counterclockwise relative to the x-axis. Determine the strain components $\varepsilon_{x'}$, $\varepsilon_{y'}$, $\varepsilon_{x'y'}$, if the x'-axis is obtained by a counterclockwise rotation of 30^o from the x-axis.

5.4-7. Consider a material point in plane strain with strain components $\varepsilon_x = -0.005$, $\varepsilon_y = 0.001$, and $\gamma_{xy} = 0.006$. Find the principal strains and associated directions. Also, find the maximum/minimum in-plane engineering shear strains and directions, as well as the average normal strain.

5.4-8. Show that the average of the area strains on three mutually perpendicular planes equals one-half the volume strain.

5.4-9. An unconstrained solid in the shape of a right circular cylinder expands uniformly as a result of heating, resulting in a volume strain of 0.009. Find the longitudinal strain ε_z and the polar components of in-plane strain.

Chapter 6

Elasticity

6.1 Springs and Hooke's Law (Axial and Shear)

6.1.1 Springs

A *spring* is any device in which the application of a load produces a conjugate displacement that increases with, although it is not always strictly proportional to, the load. If the load is a force and the displacement is a translation then the spring is called *translational*; if it is moment and rotation, then the spring is *rotational* (more commonly called a torsion spring). Typically springs are simple coil-like (spiral or helical) or bar-like objects, but it is often useful to think of complex assemblages as springs as well.

With this more general view in mind, it is convenient to use the term *generalized displacement* when either a translation or a rotation is meant, in order to avoid confusion with *displacement* as formally defined in the preceding chapter (Sect. 5.3, page 230). The conjugate force or moment can then be referred to as the corresponding *generalized force*, consistent with the definition in Sect. 2.1 (page 61) in connection with generalized coordinates. (In fact, generalized displacements are often used as the generalized coordinates of a system that can somehow be modeled as an assemblage of springs.) In the remainder of this section, however, the qualifier "generalized" is implicit.

Examples of translational springs include the traditional helical or coil spring shown schematically in Fig. 6.1a; a bar under axial force to be studied in Sect. 6.3, illustrated in Fig. 6.1b; and an end-loaded cantilever beam (whose load-deflection relation will be studied in Sect. 8.4), shown in Fig. 6.1c. Rotational springs include the conventional torsion bar (to be studied in Sect. 7.1) of Fig. 6.1d, and a cantilever subject to an end moment, Fig. 6.1e.

If the proportionality between load and displacement is exact at every stage of loading or unloading, as in Fig. 6.2a, then the spring is called *linear* or *linearly elastic*, and the ratio between load and displacement is called

© Springer International Publishing Switzerland 2017

J. Lubliner, P. Papadopoulos, *Introduction to Solid Mechanics*,
DOI 10.1007/978-3-319-18878-2_6

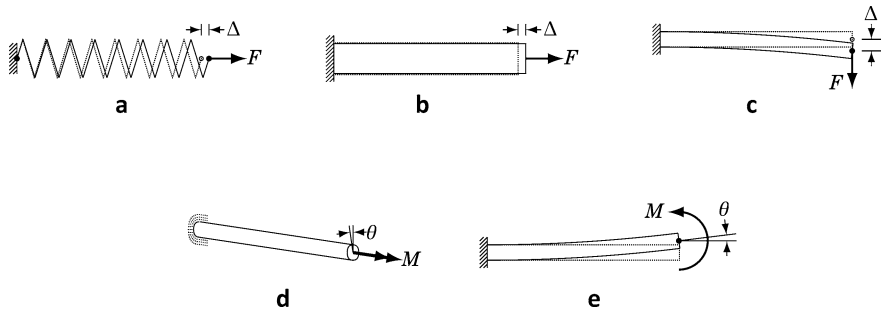

Figure 6.1. Examples of springs: a–c translational springs, d–e rotational springs

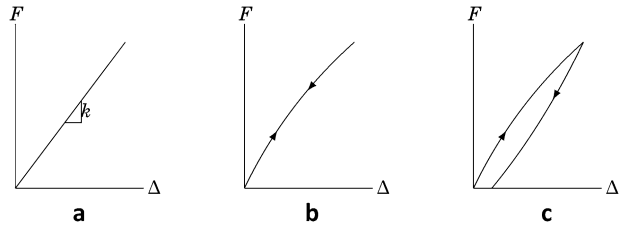

Figure 6.2. Load-displacement diagrams for a spring: (**a**) linearly elastic; (**b**) nonlinearly elastic; (**c**) inelastic

the *spring constant*, usually denoted simply k for a translational spring and something different (here we will use $\bar{k}$) for a rotational spring. If F denotes the force and Δ the displacement of the spring, then the relation

$$F = k\Delta\,, \tag{6.1}$$

is known as *Hooke's law*.* Hooke became interested in springs as part of his quest to design a watch whose performance would be regulated by the precisely repeatable oscillation of a spring mechanism. Such a precision watch would be used, in conjunction with solar observation, to estimate longitude by commercial and military seamen, a problem of great import during Hooke's time. Motivated by this application, Hooke conducted experiments on the displacement of springs, as seen in Fig. 6.3.

The linear spring is the prototype of a material behavior in general bodies called *linear elasticity*, which will be introduced in this chapter and applied to special bodies in the next four chapters.

If a spring is not linear, then it may be *nonlinearly elastic*, as in Fig. 6.2b, or *inelastic*, as in Fig. 6.2c. What the load-displacement diagrams a and b

*Robert Hooke (1635–1703) was an English all-around scientist, perhaps the first professional research scientist in history (as curator of experiments of the Royal Society). He also originated the concept of arches as inverted cables, discussed in Sect. 3.5.

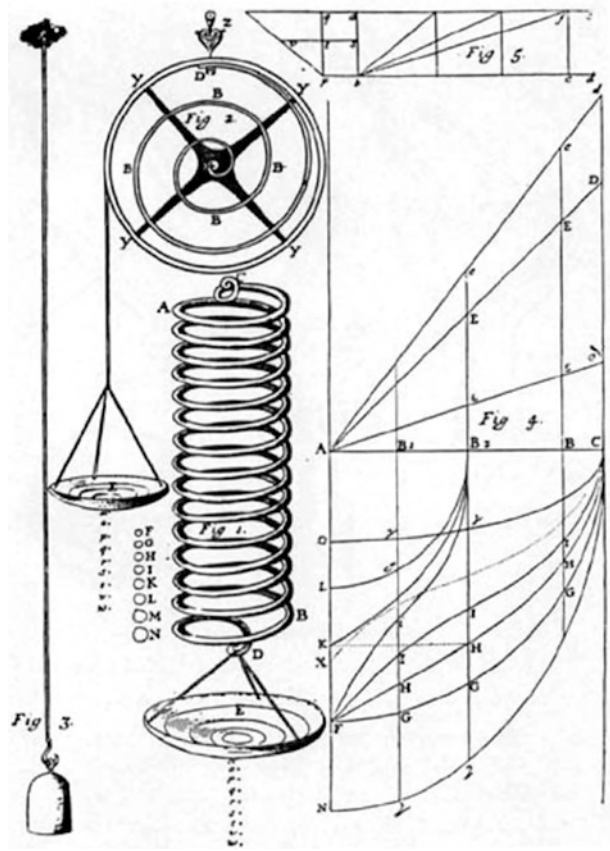

Figure 6.3. Plate from Hooke's lecture depicting a spring-pulley system and its force-displacement response

have in common, and what is in fact a defining feature of elasticity, is the one-to-one relation between load and displacement (the arrows in Fig. 6.2b show that the same relation holds whether the loading is increasing or decreasing). For an inelastic body, on the other hand, not only will the load-displacement relation be different in loading and unloading, but it may depend on the rate of loading (in which case the behavior is called *rate-dependent*, while otherwise it is *rate-independent*). What is more, upon unloading the displacement does not, in general, return to zero, although for some materials it may do so after some time has passed. Inelastic behavior will be discussed in Chap. 11. Nonlinearly elastic behavior occurs primarily in materials, such as rubber or soft biological tissue, which are capable of undergoing large deformation. Virtually all solids have a range within which the response is, or may be reasonably approximated as, linearly elastic.

Example 6.1.1: Estimating the spring constant from experimental data.

When the experimental load-displacement data for a spring are not exactly proportional but it is still desired to treat the spring as linear, some form of approximation (such as least squares) can be used to estimate the spring constant. Suppose, for example, that the points are as shown in Fig. 6.4. The method of

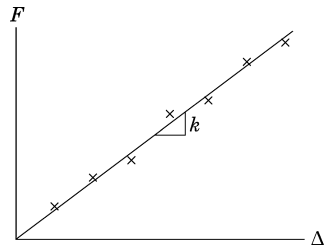

Figure 6.4. Spring constant by least squares

least squares implies that the best value of k is given by

$$k = \frac{\sum_i F_i \Delta_i}{\sum_i \Delta_i^2} , \tag{6.2}$$

and is equal to the slope of the line shown in the figure.

6.1.2 Hooke's Law: Uniaxial

As we discussed in Sect. 4.1, the strength of a material (as distinct from that of a body made of the given material) is measured by stress. In the same way, the elasticity of the material is measured by the relation between stress and strain. Consider, for example, the axially loaded bar of Fig. 6.1b, and assume that it is linearly elastic. As we discussed in Sect. 5.1 (see Fig. 5.2, page 216), what describes the local deformation is the average longitudinal strain $\varepsilon = \Delta L/L_0$. By the same token, if both the cross-sectional area and the force were doubled (from A to $2A$ and from F to $2F$), so that the average normal stress $\bar{\sigma} = F/A = 2F/2A$ would be the same, the bar would be equivalent to two of the original bars in parallel and would elongate by the same amount. It follows that the linear elasticity of the *material* in uniaxial loading is given by a linear relation between σ and ε,

$$\sigma = E\varepsilon . \tag{6.3}$$

Eq. (6.3) represents the *uniaxial* Hooke's law, and the coefficient E is known as the modulus of elasticity, elastic modulus, or, most commonly, *Young's modulus*[†] of the material.

[†]Thomas Young (1773–1829) was a British all-around scientist, although his definition of the modulus elasticity used units of force not stress, and the concept of what is called Young's modulus was used before him by the Italian scientist and architect Giordano Riccati (1709–1790).

Because so much of the theory and practice of solid mechanics is based on linear elasticity, its concepts are often applied to materials that are not actually linearly elastic, and then an approximate value of Young's modulus must be estimated, as we will discuss in the following example.

Example 6.1.2: Estimating the elastic modulus from experimental data. If the experimental data resulting from a tension or compression test on a material specimen are plotted as a stress-strain diagram and all the points lie on a straight line, then the slope of this line is the Young's modulus. If the points do not lie on a straight line, then, if it desired to treat the material as linearly elastic, an approximate value of the modulus must be estimated for the range in which the material is expected to be used. Considering, for example, the

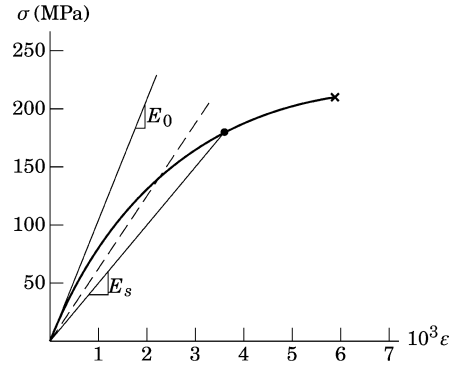

Figure 6.5. Tensile tress-strain diagram for gray cast iron

data for gray cast iron shown as a continuous curve in Fig. 6.5, we see that the stress-strain relation is nonlinear practically from the outset. For small stresses (in relation to the ultimate tensile strength indicated by the cross), the initial tangent modulus E_0 can be used. Over a larger range of stresses, say up to the point indicated by the bullet, the secant modulus E_s would be too low for most stress in the range, and therefore some intermediate value between E_0 and E_s, such as the slope of the dotted line, must be used. Stress-strain diagrams will be discussed in depth in Sect. 11.1.

The extent to which a nonlinearly elastic material, capable of large strains, can be approximately treated as a linearly elastic one can be seen from the following example.

Example 6.1.3: Elasticity with large strains.
The elasticity of rubber (or, more generally, of materials known as *elastomers*) is not due, as in hard solids, to the resistance of the interatomic bonds but to the thermal motion of long, flexible chainlike molecules whose orientation changes under the influence of applied stress. A commonly accepted theory leads to the following relation, in a state of uniaxial stress, between the true stress σ_t (de-

fined in Sect. 4.1, p. 156) and the stretch λ (defined by Eq. (5.1), p. 215):

$$\sigma_t = \frac{E}{3}\left(\lambda^2 - \lambda^{-1}\right), \tag{6.4}$$

where E is the Young's modulus at very small strains. We note that at a conventional strain of 60%, that is, $\lambda = 1.6$, the true stress equals $E \cdot 0.645$, so that it differs from what would have been its linearly elastic value (namely, $E \cdot 0.6$) by 7.5%.

Because rubber is virtually incompressible, under a stretch λ the cross-sectional area becomes A_0/λ, and consequently the engineering stress σ_e equals σ_t/λ. As can be seen from Fig. 6.6, the engineering stress-strain relation—and hence the force-elongation relation—deviates from linearity considerably more than that between true stress and conventional strain.

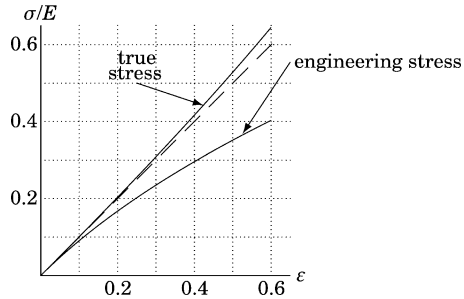

Figure 6.6. Stress-strain curves for rubber

Clearly, the larger the Young's modulus in a linearly elastic material, the larger the stress that develops due to a given strain; the material is accordingly said to be "stiffer." In the opposite case it is said to be more compliant (or, somewhat imprecisely, *softer*). Approximate values of Young's modulus for an array of materials are given in Appendix B, Table B-5 (SI, page 519) and Table B-6 (US, page 520).

As with the load-displacement relation in springs, most solids exhibit a linear uniaxial stress-strain relation only for a certain range of strains. This range depends on the material and may vary from approximately 0.1% for metals to more than 50% for rubber.

Example 6.1.4: Elongation of a steel wire.
A weight of 5 kg_f is suspended by a wire of length 25 cm and cross-sectional area 2.5 mm^2. We wish to find the elongation of the wire.
The force, by Eq. (1.1) (page 6), is 49 N, and the stress is therefore (49/2.5) N/mm^2 = 19.6 MPa. Using Eq. (6.3) and E = 200 GPa from Table B-5, we find the strain to be $\varepsilon = (19.6/200) \times 10^{-3} = 98 \times 10^{-6}$. By Eq. (5.2) (page 216) the elongation is therefore $\Delta L = 98 \times 10^{-6} \times 0.25$ m = 24.5 μm.

Example 6.1.5: Shortening of a concrete column.
A 10-ft concrete column of circular cross-section with diameter 16 in in carries a compressive load of 50 k. We wish to find the shortening of the column, disregarding the effect of its own weight.
The compressive stress is $\sigma = 50\ \text{k}/(\pi \cdot 8^2 \text{in}^2) = 0.25$ ksi. The compressive strain is $0.25/3000 = 83 \times 10^{-6}$, and the shortening is accordingly $83 \times 10^{-6} \times 120$ in = 0.01 in.

6.1.3 Hooke's Law in Shear

For a material element in a state of simple shear (as in the twisting of a thin-walled tube discussed in Sect. 4.2), a relation analogous to (6.3) in the linearly elastic regime exists between the shear stress τ and the corresponding shear strain γ, namely,

$$\tau = G\gamma\,, \tag{6.5}$$

where G is known as the *shear modulus*. For most solids the value of G is a little less than one-half (but no less than one-third) that of E; the relationship between G and E will be further discussed in the next section.

Example 6.1.6: Shearing of a narrow rectangular block.
Except for the torsion of a thin-walled tube discussed in Sect. 4.3 (page 171), it is generally difficult to produce a state of simple shear stress in real bodies. In the case of the rectangular block shown in Fig. 6.7a, the application of the shear force F produces a clockwise couple with the tangential reaction along the base, which must be balanced by the normal forces shown there. (Note that

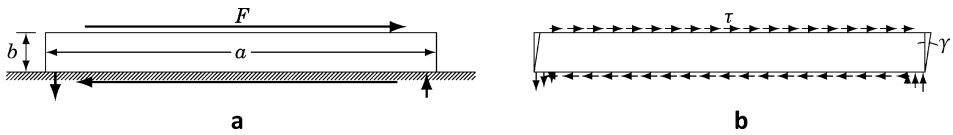

Figure 6.7. Shearing of a narrow rectangular block: (**a**) forces, (**b**) approximate stress distribution and deformation

the tensile force shown on the left side of the base is necessary to prevent the block from rotating about the lower right-hand corner.) Furthermore, the shear force cannot be distributed uniformly since, the vertical edges of the block being free, the shear stress must be zero at the corners. If, however, the block is sufficiently narrow ($b \ll a$), these end effects can be neglected, and in accordance with Saint-Venant's principle we can assume, approximately, a uniform shear stress $\tau = F/ac$ (where c is the thickness of the block perpendicular to the page) over most of the block. Consequently, the angular change seen in Fig. 6.7b is, approximately (in radians), $\gamma = F/acG$

Exercises

6.1-1. A spring is tested by incrementally hanging 1-kg weights from it and measuring the resulting displacements, with the following results:

Force (kg_f)	1	2	3	4	5
Displ. (mm)	15.0	28.2	44.1	59.7	76.4

Plot the results and find the straight line that would, in your view, best represent the spring if it is to be approximated as a linear one. Explain your choice, and calculate the spring constant to three significant figures in kN/m.

6.1-2. A tensile test on rubber yields the results, for engineering stress and strain, shown in the figure below.

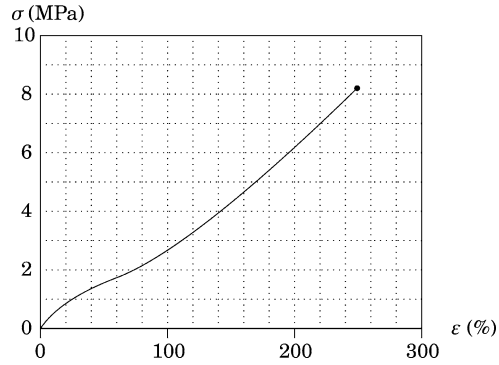

If the rubber is to be approximated as linearly elastic, estimate the values of E to be used (**a**) over the full range of strain, (**b**) over the range up to 50%, (**c**) over the range up to 20%.

6.1-3. A compression test on concrete yields the data points shown in the figure below. If the concrete is to be treated as linearly elastic in the range of stresses up to 45% of the maximum stress attained, estimate the value of E to be used.

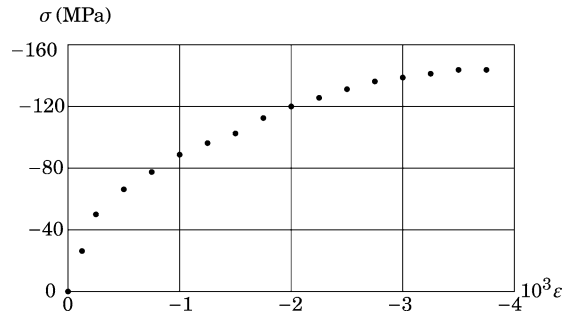

6.1-4. Find the tensile force necessary to stretch a 4-ft length of steel wire, of cross-sectional area $0.02\,\text{in}^2$, by 1/32 in.

6.1-5. A cubic block of rubber, 50 cm on each side, is placed between two rigid slabs as shown in the figure below. Assuming the rubber to be in a state of uniaxial stress when the force F is applied, find the value of F needed to compress the block by 5 cm. Assume $E = 0.05$ GPa.

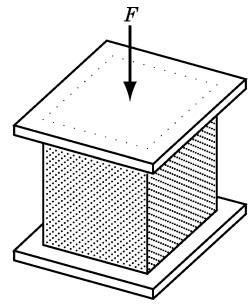

6.1-6. A rigid bar is suspended by two wires 0.1 m long, each of cross-sectional area $A = 5\ \text{mm}^2$, and made of a material with Young's modulus $E = 100$ GPa. If the bar is subjected to a vertical load $F = 150$ kN, as in the figure, find the angle by which the bar will rotate under the influence of F.

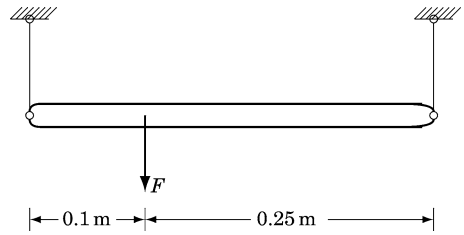

6.1-7. The shaft of the London Monument, shown in the figure on the right, is a hollow circular stone column, 120 ft tall, of outer diameter 15 ft and inner diameter 13 ft. If the superstructure weighs 300 k and the Young's modulus of the stone is 7,500 ksi, find the resulting shortening of the column.

6.1-8. A rigid plank 12 ft long is supported at its ends by two wooden posts, each 10 ft tall and of square cross-section, one $3.5\,\text{in} \times 3.5\,\text{in}$ ("four-by-four") and the other $5.5\,\text{in} \times 5.5\,\text{in}$ ("six-by-six"). If the plank is initially level, find its slope after a uniformly distributed load of 500 lb/ft is placed on it.

6.1-9. A square rubber tile, 1 cm thick, is subject to the shear forces shown in the figure. Assuming that they are uniformly distributed along the

edges, find the magnitude of F necessary to change the included angles by 5°. Use the value of $E = 0.06$ GPa and assume $G = E/3$.

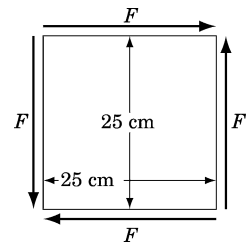

6.1-10. Assuming that $b \ll a$ in Example 6.1.6, estimate the magnitude of the maximum normal stress at the bottom ends of the block in terms of the nominal shear stress $\tau = F/ac$ by assuming that the normal stress has a linear distribution, starting from zero at a distance b from the end.

6.2 Generalized Hooke's Law

6.2.1 Introduction

In this section we extend Hooke's law to general states of stress and strain, as described in Sect.s 4.4 and 5.3, respectively. The most general such extension is a linear relation between the stress matrix given by Eq. (4.24) and the strain matrix given by Eq. (5.37), and this is what will be developed here. The *theory of linear elasticity* based on this relation is of fundamental importance in engineering.*

6.2.2 Isotropy

Isotropy with respect to a given material property (e.g., the stress-strain response) means that the property is independent of the orientation (that is, it is unaffected by any rotation) of a given material element. A material endowed with isotropy is called *isotropic* (with respect to the given property). A material that is not isotropic with respect to a given material property is known as *anisotropic*.

Isotropy with respect to the stress-strain response can be elucidated by means of the simple thought experiment illustrated in Fig. 6.8. Suppose that

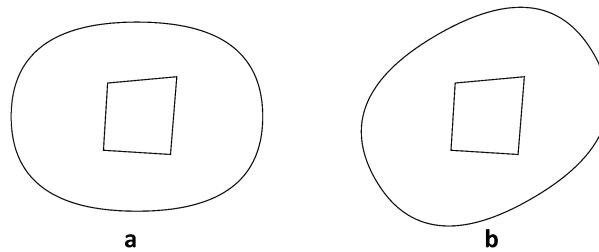

Figure 6.8. Illustration of isotropy in the stress-strain response: a given deformation (visualized by a polygon) applied to a material element in configuration **a** and another arbitrarily rotated configuration **b** produces the same stresses

a small material element is subjected to a given deformation (illustrated by the polygon in Fig. 6.8a) and develops some stress. Alternatively, let the material element be first rotated by some arbitrary angle (as in Fig. 6.8b) and then subjected to the *same* deformation as before. If the material is isotropic, then the stress will be the same in both cases.

*Remarkably enough, some of the early work in the theory was motivated not by an interest in solids *per se* but by the belief that light is propagated through a medium, called *ether*, with properties similar to those of elastic solids.

6.2.3 Poisson's Ratio

We begin by considering a body undergoing deformation and isolating a volume element like that of Fig. 4.23. Taking the size of the box to be very small (or, in the limit, infinitesimal), it is reasonable to assume that the strain is uniform (that is, independent of position) inside the box. Also, we know from experience (see Fig. 4.1, page 156) that when a slender body is pulled along its major axis, the material contracts in the directions perpendicular to this axis. If the longitudinal strain component along the axis is tensile and equal to $\varepsilon_{\text{long}} > 0$, and if, owing to isotropy, the contraction along any transverse direction is represented by the lateral strain $\varepsilon_{\text{lat}} < 0$, then the ratio

$$\nu = -\frac{\varepsilon_{\text{lat}}}{\varepsilon_{\text{long}}} \tag{6.6}$$

is a material parameter known as the *Poisson's ratio*[†]. This number characterizes the severity of the lateral contraction experienced by the material when subjected to uniaxial elongation. Clearly, $\nu = 0$ means no lateral contraction, while the higher the value of ν, the larger the effected lateral contraction. Negative values of ν are rarely encountered; materials that have them are called *auxetic*.

6.2.4 The Principle of Superposition

The *principle of superposition* allows the additivity of effects (here, strains) in the presence of multiple causes (here, stresses). Invoking this principle, we may express the total strain experienced by a body as the sum of all strains due to the individual components of stress present in the body.

Use of the principle of superposition is justified when: (a) the differential equations of equilibrium are linear in the stresses, (b) the relations between strain and displacement are linear, and (c) the relations between stress and strain are linear. Condition (a) is satisfied by the equilibrium equations (4.39-4.42). To see this, we may take two sets of stresses and body forces,

$$(\sigma_x^{(1)}, \sigma_y^{(1)}, \sigma_z^{(1)}, \tau_{xy}^{(1)}, \tau_{yz}^{(1)}, \tau_{zx}^{(1)}, b_x^{(1)}, b_y^{(1)}, b_z^{(1)}) \tag{6.7}$$

and

$$(\sigma_x^{(2)}, \sigma_y^{(2)}, \sigma_z^{(2)}, \tau_{xy}^{(2)}, \tau_{yz}^{(2)}, \tau_{zx}^{(2)}, b_x^{(2)}, b_y^{(2)}, b_z^{(2)}) \,, \tag{6.8}$$

that satisfy the equilibrium equations (4.39–4.42), and confirm that the linear combination of the two sets,

$$\begin{aligned} &c_1(\sigma_x^{(1)}, \sigma_y^{(1)}, \sigma_z^{(1)}, \tau_{xy}^{(1)}, \tau_{yz}^{(1)}, \tau_{zx}^{(1)}, b_x^{(1)}, b_y^{(1)}, b_z^{(1)}) \\ &\qquad + c_2(\sigma_x^{(2)}, \sigma_y^{(2)}, \sigma_z^{(2)}, \tau_{xy}^{(2)}, \tau_{yz}^{(2)}, \tau_{zx}^{(2)}, b_x^{(2)}, b_y^{(2)}, b_z^{(2)}) \,, \end{aligned} \tag{6.9}$$

[†]Siméon Poisson (1781–1840) was a French mathematician, astronomer, and physicist.

for any c_1, c_2, satisfies the equilibrium equations. Condition (b) is similarly verified by choosing two displacements $(u^{(1)}, v^{(1)}, w^{(1)})$ and $(u^{(2)}, v^{(2)}, w^{(2)})$, and noting, with the aid of (5.29), (5.31) and (5.33), that, when summed, the displacements yield the sum of the individual strains $(\varepsilon_x^{(1)}, \varepsilon_y^{(1)}, \varepsilon_z^{(1)}, \gamma_{xy}^{(1)}, \gamma_{yz}^{(1)}, \gamma_{zx}^{(1)})$ and $(\varepsilon_x^{(2)}, \varepsilon_y^{(2)}, \varepsilon_z^{(2)}, \gamma_{xy}^{(2)}, \gamma_{yz}^{(2)}, \gamma_{zx}^{(2)})$. Finally, condition (c) is readily deduced from (6.3) and (6.5).

6.2.5 Isotropic Linear Elasticity

We will now attempt to generalize the previous stress-strain relations to the case in which all components of strain may be non-zero in the volume element. To do so, we will invoke the principle of superposition and the isotropy of the material.

We assume that the normal stress components σ_x, σ_y and σ_z act at every point in the infinitesimal box. As a consequence of Eqs. (6.3) and (6.6), the stress σ_x alone would produce the strains

$$\varepsilon_x = \frac{\sigma_x}{E} \quad , \quad \varepsilon_y = -\nu\frac{\sigma_x}{E} \quad , \quad \varepsilon_z = -\nu\frac{\sigma_x}{E} \, . \tag{6.10}$$

Likewise, the stresses σ_y and σ_z acting separately would produce the strains

$$\varepsilon_x = -\nu\frac{\sigma_y}{E} \quad , \quad \varepsilon_y = \frac{\sigma_y}{E} \quad , \quad \varepsilon_z = -\nu\frac{\sigma_y}{E} \tag{6.11}$$

and

$$\varepsilon_x = -\nu\frac{\sigma_z}{E} \quad , \quad \varepsilon_y = -\nu\frac{\sigma_z}{E} \quad , \quad \varepsilon_z = \frac{\sigma_z}{E} \, , \tag{6.12}$$

respectively. Note that isotropy is responsible for the dependence of all the axial strains on the *same* material parameters E and ν in (6.10–6.12). The principle of superposition implies that the resultant longitudinal strains due to the combined action of the three normal stresses σ_x, σ_y and σ_z are

$$\begin{aligned} \varepsilon_x &= \frac{1}{E}(\sigma_x - \nu\sigma_y - \nu\sigma_z) \, , \\ \varepsilon_y &= \frac{1}{E}(\sigma_y - \nu\sigma_z - \nu\sigma_x) \, , \\ \varepsilon_z &= \frac{1}{E}(\sigma_z - \nu\sigma_x - \nu\sigma_y) \, . \end{aligned} \tag{6.13}$$

In addition, recalling (6.5), the relation between shear stresses and strains is

$$\begin{aligned} \gamma_{xy} &= \frac{1}{G}\tau_{xy} \, , \\ \gamma_{yz} &= \frac{1}{G}\tau_{yz} \, , \\ \gamma_{zx} &= \frac{1}{G}\tau_{zx} \, , \end{aligned} \tag{6.14}$$

where isotropy again allows us to conclude that the same material parameter G applies to all three shear directions.

The formulae (6.13) and (6.14) may be readily inverted (as long as $\nu \neq -1$ or 0.5) in order to relate stresses to strains according to

$$\begin{aligned}
\sigma_x &= \frac{E}{(1+\nu)(1-2\nu)}\left[(1-\nu)\varepsilon_x + \nu\varepsilon_y + \nu\varepsilon_z\right] , \\
\sigma_y &= \frac{E}{(1+\nu)(1-2\nu)}\left[(1-\nu)\varepsilon_y + \nu\varepsilon_z + \nu\varepsilon_x\right] , \\
\sigma_z &= \frac{E}{(1+\nu)(1-2\nu)}\left[(1-\nu)\varepsilon_z + \nu\varepsilon_x + \nu\varepsilon_y\right] ,
\end{aligned} \tag{6.15}$$

and

$$\begin{aligned}
\tau_{xy} &= G\gamma_{xy} , \\
\tau_{yz} &= G\gamma_{yz} , \\
\tau_{zx} &= G\gamma_{zx} .
\end{aligned} \tag{6.16}$$

Upon examining (6.13) and (6.14), or, equivalently, (6.15) and (6.16), it becomes clear that the effects of normal and shear stresses are uncoupled in the sense that normal stresses result in longitudinal strains and shear stresses in shear strains.

A body made of a material that has the same properties (whether elastic or not) at every point is called *homogeneous*.

Two important special cases will be described in the following examples.

Example 6.2.1: Hooke's law in plane stress.
In the special case where $\sigma_z = \tau_{yz} = \tau_{zx} = 0$, as in (4.26) (page 182), Eqs. (6.13) and (6.14) reduce to

$$\begin{aligned}
\varepsilon_x &= \frac{1}{E}(\sigma_x - \nu\sigma_y) , \\
\varepsilon_y &= \frac{1}{E}(\sigma_y - \nu\sigma_x) , \\
\varepsilon_z &= -\frac{\nu}{E}(\sigma_x + \sigma_y) , \\
\gamma_{xy} &= \frac{1}{G}\tau_{xy} \quad , \quad \gamma_{xz} = \gamma_{yz} = 0 .
\end{aligned} \tag{6.17}$$

The derivation of the equation for the stresses in terms of the strains is left to an exercise.

Example 6.2.2: Hooke's law in plane strain.

If $\varepsilon_z = \gamma_{xz} = \gamma_{yz} = 0$, Eqs. (6.15) and (6.16) reduce to

$$\begin{aligned} \sigma_x &= \frac{E}{(1+\nu)(1-2\nu)}\left[(1-\nu)\varepsilon_x + \nu\varepsilon_y\right] , \\ \sigma_y &= \frac{E}{(1+\nu)(1-2\nu)}\left[(1-\nu)\varepsilon_y + \nu\varepsilon_x\right] , \\ \sigma_z &= \frac{E}{(1+\nu)(1-2\nu)}(\nu\varepsilon_x + \nu\varepsilon_y) , \\ \tau_{xy} &= G\gamma_{xy} \quad , \quad \tau_{xz} = \tau_{yz} = 0 . \end{aligned} \tag{6.18}$$

6.2.6 Relation Among E, ν and G

It is easy to show that only two of the three material parameters E, ν, and G that appear in the strain-stress relations (6.13) and (6.14) are independent, while the third can be written in terms of the other two. To this end, consider

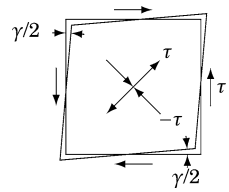

Figure 6.9. Relation among E, ν and G

the infinitesimal box of Fig. 6.9 (based on Fig. 5.9, page 226) with uniform shear stress τ, for which (6.5) implies that the shear strain γ is given by

$$\gamma = \frac{\tau}{G} . \tag{6.19}$$

It follows from Eqs. (4.60) and (5.69), respectively, that the principal stresses are $\sigma_{1,2} = \pm\tau$ and the corresponding principal strains are $\varepsilon_{1,2} = \pm\gamma/2$. We therefore see from Eqs. (6.13) that

$$\frac{\gamma}{2} = \frac{1}{E}\left[(\tau - \nu(-\tau)\right] = \frac{1+\nu}{E}\tau . \tag{6.20}$$

A comparison of Eqs. (6.19) and (6.20) leads to the conclusion that

$$G = \frac{E}{2(1+\nu)} . \tag{6.21}$$

6.2.7 Lamé Formulation of the Stress-Strain Relations

Given the relation (6.21), and with the definition

$$\lambda = \frac{\nu E}{(1+\nu)(1-2\nu)} , \tag{6.22}$$

Eqs. (6.15) may be rewritten as

$$\begin{aligned} \sigma_x &= \lambda(\varepsilon_x+\varepsilon_y+\varepsilon_z)+2G\varepsilon_x \,, \\ \sigma_y &= \lambda(\varepsilon_x+\varepsilon_y+\varepsilon_z)+2G\varepsilon_y \,, \\ \sigma_z &= \lambda(\varepsilon_x+\varepsilon_y+\varepsilon_z)+2G\varepsilon_z \,. \end{aligned} \tag{6.23}$$

These equations, together with (6.16), constitute the Lamé formulation[‡] of isotropic linear elasticity, with λ and G known as the *Lamé coefficients*. In most presentations of this formulation the shear modulus is denoted μ rather than G.

6.2.8 Bulk Modulus

Recalling the definition (5.77) (page 245) of the volumetric strain ε_{V}, we can use Eqs. (6.13) to relate it to the stress by

$$\varepsilon_{\mathrm{V}} = \frac{1-2\nu}{E}(\sigma_x+\sigma_y+\sigma_z) \,. \tag{6.24}$$

Given the definition (4.75) (page 203) of the mean stress, Eq. (6.24) can be rewritten as

$$\bar{\sigma} = K\varepsilon_{\mathrm{V}} \,, \tag{6.25}$$

where the material parameter K, defined as

$$K = \frac{E}{3(1-2\nu)} \,, \tag{6.26}$$

is the *bulk modulus*, which characterizes the resistance of the material to volume change when subject to hydrostatic loading (see page 203).

Eq. (6.26) shows that the bulk modulus becomes infinite in the limit as ν approaches 0.5. In this limit, the material becomes incompressible (as defined in Sect. 5.4, page 245). Given that, with rare exceptions, ν is nonnegative, it follows that, typically, $0 \le \nu \le 0.5$, and consequently, by Eq. (6.21), that $E/3 \le G \le E/2$, as already suggested in Sect. 6.1.

Example 6.2.3: Calculation of shear and bulk moduli from tension test. We suppose that a tension test on a steel specimen yields $E = 202$ MPa, and measurement of the lateral strain yields $\nu = 0.315$.
For the shear and bulk moduli, respectively, we find

$$G = \frac{202}{2\cdot 1.315}\,\mathrm{MPa} = 76.8\,\mathrm{MPa} \quad , \quad K = \frac{202}{1-2\cdot 0.315}\,\mathrm{MPa} = 546\,\mathrm{MPa} \,.$$

[‡]Gabriel Lamé (1795–1870) was a French mathematician.

6.2.9 Deviatoric Hooke's Law

The extent to which a state of stress differs from a hydrostatic one, represented by the matrix (4.76) (page 203), is given by the *deviatoric* stress (also called *stress deviator*, defined by subtracting the mean stress $\bar{\sigma}$ from the normal stress components. That is, it is represented (in a given coordinate system) by the matrix

$$[\sigma'] = \begin{bmatrix} \sigma'_x & \tau_{xy} & \tau_{xz} \\ \tau_{xy} & \sigma'_y & \tau_{yz} \\ \tau_{xz} & \tau_{yz} & \sigma'_z \end{bmatrix} , \tag{6.27}$$

where

$$\sigma'_x = \sigma_x - \bar{\sigma} = \sigma_x - \frac{1}{3}(\sigma_x + \sigma_y + \sigma_z) = \frac{1}{3}(2\sigma_x - \sigma_y - \sigma_z) , \tag{6.28}$$

and similarly

$$\sigma'_y = \frac{1}{3}(2\sigma_y - \sigma_x - \sigma_z) \quad , \quad \sigma'_z = \frac{1}{3}(2\sigma_z - \sigma_x - \sigma_y) . \tag{6.29}$$

It follows from (6.28) and (6.29) that

$$\sigma'_x + \sigma'_y + \sigma'_z = 0 , \tag{6.30}$$

or, that the trace (that is, the sum of the major diagonal terms) of the matrix of deviatoric stress in (6.27) vanishes.

The principal deviatoric stresses σ'_1, σ'_2, σ'_3 are defined similarly (they correspond to the case where the xyz-axes coincide with the principal axes). It is obvious that the first invariant of the deviatoric stress I'_1, analogous to I_1 for the actual stress (Eq. $(4.72)_1$, page 202), vanishes identically. The second invariant I'_2, analogous to I_2, can be shown to be given by

$$I'_2 = -J_2 , \tag{6.31}$$

where

$$J_2 = \frac{1}{6}[(\sigma_1 - \sigma_2)^2 + (\sigma_2 - \sigma_3)^2 + (\sigma_1 - \sigma_3)^2] . \tag{6.32}$$

(Note, by comparing with Eq. (4.89) for the octahedral shear stress, that $J_2 = (3/2)\tau^2_{\text{oct}}$.) Using Eq. $(4.72)_2$ for I_2, with the normal stresses $\sigma_x, \sigma_y, \sigma_z$ replaced by their deviators $\sigma'_x, \sigma'_y, \sigma'_z$ as defined by Eqs. (6.28–6.29), J_2 can also be expressed in the form

$$J_2 = \frac{1}{6}[(\sigma_x - \sigma_y)^2 + (\sigma_y - \sigma_z)^2 + (\sigma_x - \sigma_x)^2] + \tau^2_{xy} + \tau^2_{yz} + \tau^2_{xz} . \tag{6.33}$$

The derivation is left to an exercise.

The deviatoric strain is defined similarly by subtracting $\frac{1}{3}\varepsilon_V$ from the longitudinal strain components, so that

$$\varepsilon'_x = \frac{1}{3}(2\varepsilon_x - \varepsilon_y - \varepsilon_z) \quad , \quad \varepsilon'_y = \frac{1}{3}(2\varepsilon_y - \varepsilon_x - \varepsilon_z) \quad , \quad \varepsilon'_z = \frac{1}{3}(2\varepsilon_z - \varepsilon_x - \varepsilon_y) \, . \tag{6.34}$$

Note that the deviatoric strain represents distortion, as defined in Sect. 5.4 (page 245), and any deformation described by infinitesimal strains can be expressed as a superposition of dilatation and distortion.

Now, if we substitute $\sigma_x = \sigma'_x + \bar{\sigma}$, $\varepsilon_x = \varepsilon'_x + \frac{1}{3}\varepsilon_V$, etc., in Eqs. (6.13), we find that the first of these equations becomes

$$\varepsilon'_x + \frac{1}{3}\varepsilon_V = \frac{1}{E}[\sigma'_x - \nu\sigma'_y - \nu\sigma'_z + (1-2\nu)\bar{\sigma}] \, . \tag{6.35}$$

But, in view of Eqs. (6.25) and (6.26), the terms involving ε_V and $\bar{\sigma}$ cancel each other. Since, furthermore, $\sigma'_x + \sigma'_y + \sigma'_x = 0$, we also have

$$\sigma'_x - \nu\sigma'_y - \nu\sigma'_z = (1+\nu)\sigma'_x \, , \tag{6.36}$$

so that, with the help of Eq. (6.21),

$$\varepsilon'_x = \frac{1+\nu}{E}\sigma'_x = \frac{1}{2G}\sigma'_x \, . \tag{6.37}$$

We thus find that, in an isotropic linearly elastic solid, the relation between deviatoric stress and strain is governed entirely by the shear modulus, with the component matrices related simply by

$$\begin{bmatrix} \sigma'_x & \tau_{xy} & \tau_{xz} \\ \tau_{xy} & \sigma'_y & \tau_{yz} \\ \tau_{xz} & \tau_{yz} & \sigma'_z \end{bmatrix} = 2G \begin{bmatrix} \varepsilon'_x & \frac{1}{2}\gamma_{xy} & \frac{1}{2}\gamma_{xz} \\ \frac{1}{2}\gamma_{xy} & \varepsilon'_y & \frac{1}{2}\gamma_{yz} \\ \frac{1}{2}\gamma_{xz} & \frac{1}{2}\gamma_{yz} & \varepsilon'_z \end{bmatrix} , \tag{6.38}$$

in the same way that relation between the mean stress and the volumetric strain is governed by the bulk modulus, as given by Eq. (6.25).

6.2.10 Column-Matrix Notation for Stress and Strain

If we wished to express the linear equations relating stress and strain, either Eqs. (6.13–6.14) or Eqs. (6.15–6.16), as relations between the stress tensor represented by the matrix (4.24) and the strain tensor represented by the matrix (5.37), then we would have to imagine the coefficients as occupying a four-dimensional box (representing a *fourth-rank tensor*). To avoid the difficulty of such a representation, a convention has been established to represent stress and strain by 6×1 column matrices, denoted $\{\sigma\}$ and $\{\varepsilon\}$, respectively, as

$$\{\sigma\} = \begin{Bmatrix} \sigma_x \\ \sigma_y \\ \sigma_z \\ \tau_{yz} \\ \tau_{zx} \\ \tau_{xy} \end{Bmatrix} \tag{6.39}$$

and

$$\{\varepsilon\} = \left\{ \begin{array}{c} \varepsilon_x \\ \varepsilon_y \\ \varepsilon_z \\ \gamma_{yz} \\ \gamma_{zx} \\ \gamma_{xy} \end{array} \right\} . \tag{6.40}$$

With this notation it easy to see that the internal virtual work per unit volume given by Eq. (5.48) (page 236) can be simply expressed, using matrix multiplication, as

$$\delta W^0_{\text{int}} = \{\sigma\}^T \delta\{\varepsilon\} , \tag{6.41}$$

where the superscript ^{T} denotes the transposition of a matrix, which in the case of a column matrix means its conversion into a row matrix (which may also be written as $\langle\sigma\rangle$). The right-hand side of Eq. (6.41) is thus a 1×1 matrix, equivalent to a scalar.

Eqs. (6.15–6.16) can now be written in the compact form

$$\{\sigma\} = [C]\{\varepsilon\} , \tag{6.42}$$

where $[C]$ is the *elasticity matrix* given by

$$[C] = \frac{E}{1+\nu} \left[\begin{array}{cccccc} \frac{1-\nu}{1-2\nu} & \frac{\nu}{1-2\nu} & \frac{\nu}{1-2\nu} & 0 & 0 & 0 \\ \frac{\nu}{1-2\nu} & \frac{1-\nu}{1-2\nu} & \frac{\nu}{1-2\nu} & 0 & 0 & 0 \\ \frac{\nu}{1-2\nu} & \frac{\nu}{1-2\nu} & \frac{1-\nu}{1-2\nu} & 0 & 0 & 0 \\ 0 & 0 & 0 & \frac{1}{2} & 0 & 0 \\ 0 & 0 & 0 & 0 & \frac{1}{2} & 0 \\ 0 & 0 & 0 & 0 & 0 & \frac{1}{2} \end{array} \right] \tag{6.43}$$

where we make use of the identity (6.21). For isotropic linearly elastic bodies the internal virtual work per unit volume is therefore

$$\delta W^0_{\text{int}} = \{\varepsilon\}^T [C] \delta\{\varepsilon\} , \tag{6.44}$$

with $[C]$ given as above.

Since the matrix representation of Eqs. (6.13–6.14) is the inverse of Eq. (6.42), these will be written as

$$\{\varepsilon\} = [C]^{-1}\{\sigma\} , \tag{6.45}$$

where

$$[C]^{-1} = \frac{1}{E}\begin{bmatrix} 1 & -\nu & -\nu & 0 & 0 & 0 \\ -\nu & 1 & -\nu & 0 & 0 & 0 \\ -\nu & -\nu & 1 & 0 & 0 & 0 \\ 0 & 0 & 0 & 2(1+\nu) & 0 & 0 \\ 0 & 0 & 0 & 0 & 2(1+\nu) & 0 \\ 0 & 0 & 0 & 0 & 0 & 2(1+\nu) \end{bmatrix} \tag{6.46}$$

is known as *compliance matrix*, respectively, frequently also denoted $[S]$.

In situations where some of the stress or strain components are identically zero, the dimensions of the column matrices can be reduced. In problems of plane stress or plane strain, for example, we may write them as 3×1 matrices, namely,

$$\{\sigma\} = \begin{Bmatrix} \sigma_x \\ \sigma_y \\ \tau_{xy} \end{Bmatrix} \quad , \quad \{\varepsilon\} = \begin{Bmatrix} \varepsilon_x \\ \varepsilon_y \\ \gamma_{xy} \end{Bmatrix} . \tag{6.47}$$

The stiffness-tensor and compliance matrices are therefore 3×3, and Eqs. (6.17) and (6.18), with ε_z and σ_z disregarded (since they do not contribute to the virtual work), may be rewritten in the form

$$[C]^{-1} = \frac{1}{E}\begin{bmatrix} 1 & -\nu & 0 \\ -\nu & 1 & 0 \\ 0 & 0 & 2(1+\nu) \end{bmatrix} \qquad \text{(plane stress)} \tag{6.48}$$

and

$$[C] = \frac{E}{1+\nu}\begin{bmatrix} \dfrac{1-\nu}{1-2\nu} & \dfrac{\nu}{1-2\nu} & 0 \\ \dfrac{\nu}{1-2\nu} & \dfrac{1-\nu}{1-2\nu} & 0 \\ 0 & 0 & \dfrac{1}{2} \end{bmatrix} \qquad \text{(plane strain).} \tag{6.49}$$

If, however the out-of-plane strain or stress is of interest, then it must be obtained from the three-dimensional relations, and is given, respectively, by

$$\varepsilon_z = -\frac{\nu}{E}(\sigma_x + \sigma_y) \qquad \text{(plane stress)} \tag{6.50}$$

and

$$\sigma_z = \frac{\nu E}{(1+\nu)(1-2\nu)}(\varepsilon_x + \varepsilon_y) \qquad \text{(plane strain)} . \tag{6.51}$$

Example 6.2.4: Elastic deformation of a cylindrical pressure vessel. It is clear from the discussion of thin-walled pressure vessels in Sect. 4.3 (page 169) that a small element of the shell is very nearly in a state of plane stress, since the normal stress perpendicular to the shell (the radial stress σ_r) is of the order of the pressure p and is therefore much smaller than the in-plane

stresses, given by Eq. (4.11)–(4.13), when $r \gg t$. In a cylindrical shell the in-plane[§] strains are the longitudinal strain ε_l and the circumferential or hoop strain ε_c. The latter is the same as the strain component ε_θ in polar coordinates discussed in Example 5.4.1 (page 240) and is therefore given by Eq. $(5.59)_2$, which, because of axial symmetry (implying $u_\theta = 0$) reduces to $\varepsilon_\theta = u_r/r$. Since on the average u_r is just the change in radius Δr, we have

$$\Delta r = r\varepsilon_\theta = \frac{r}{E}(\sigma_c - \nu\sigma_l) = \frac{pr^2}{Et}\left(1 - \frac{\nu}{2}\right) . \tag{6.52}$$

The radial strain is, similarly, the thickness change $\Delta t/t$, and consequently

$$\Delta t = t\varepsilon_r = -\frac{\nu t}{E}(\sigma_c + \sigma_l) = -\frac{3\nu pr}{2E} . \tag{6.53}$$

6.2.11 Anisotropic Linear Elasticity

For the discussion of anisotropically elastic materials there exists a notation, known as the *Voigt*[¶] notation, in which the elements of the column matrices (6.39) and (6.40) are labeled $\sigma_1,\ldots,\sigma_6$ and $\varepsilon_1,\ldots,\varepsilon_6$, respectively, with the elements of the elasticity matrix $[C]$ accordingly designated $C_{11},\ldots,C_{66}$. Eqs. (6.42) and (6.45) can thus be rewritten as

$$\sigma_i = \sum_{j=1}^{6} C_{ij}\varepsilon_j , \qquad \varepsilon_j = \sum_{j=1}^{6} C_{ij}^{-1}\sigma_j . \tag{6.54}$$

In the isotropic case we can identify the elements of $[C]$ as follows: $C_{11} = C_{22} = C_{33} = (1-\nu)E/(1+\nu)(1-2\nu)$; $C_{12} = C_{21} = C_{13} = C_{31} = C_{23} = C_{32} = \nu E/(1+\nu)(1-2\nu)$; $C_{44} = C_{55} = C_{66} = G$; and all other $C_{ij} = 0$. The condition (6.21) can then be written as

$$C_{11} = C_{12} + 2C_{44} . \tag{6.55}$$

Some simple cases of anisotropic elasticity will now be discussed.

Example 6.2.5: Cubic symmetry.
Most solids can be classified as either amorphous or crystalline. Amorphous solids can generally be expected to behave isotropically, unless they are reinforced with fibers or the like. Crystalline solids do so when they are polycrystalline, that is, when they are made up of a great many small crystals (grains) that are oriented randomly relative to one another. In a single crystal, however, the elastic response depends on how the directions of stress and strain are oriented with respect to the crystal axes.

In many crystalline solids (most elemental metals and metal halides, for example) the crystal structure is cubic (simple, face-centered or body-centered, as illustrated in Fig. 6.10). In such a solid, if the axes x, y, z coincide with the crystal

[§] meaning, in this case, "in the tangent plane"

[¶] Woldemar Voigt (1850–1919) was a German physicist.

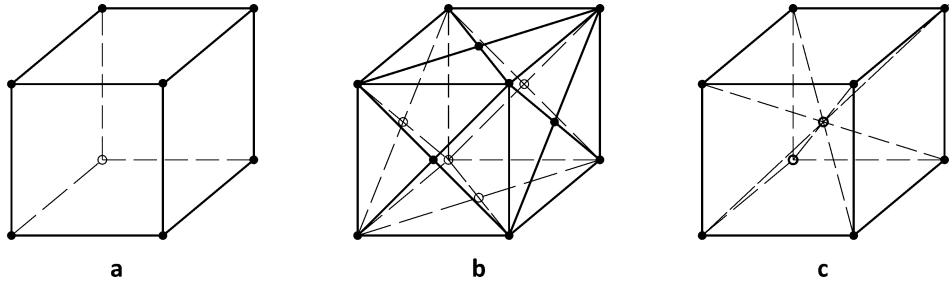

Figure 6.10. Cubic crystal structures: (**a**) simple, (**b**) face-centered, (**c**) body-centered

axes (an important proviso), then their order can be interchanged, and the equalities $C_{11} = C_{22} = C_{33}$, $C_{12} = C_{21} = C_{13} = C_{31} = C_{23} = C_{32}$ and $C_{44} = C_{55} = C_{66}$ hold as they do for isotropic solids. Moreover, by symmetry, a longitudinal strain along a crystal axis should not entail any shear stress, and a shear strain in the plane of any two crystal axes should not entail any normal stress, or any shear stress other than the conjugate one; hence the condition that all the other $C_{ij} = 0$ holds as well. Thus there are three independent elastic moduli, C_{11}, C_{12} and C_{44}, which in general do *not* satisfy Eq. (6.55). The extent to which this equation is not satisfied (for example, the value of $(C_{12} - 2C_{44})/C_{11} - 1$) may be taken as a measure of anisotropy. It so happens that this value is very nearly zero for tungsten, so that this metal may be regarded as isotropic in its monocrystalline form.

It will be noted that in both isotropic solids and those with cubic symmetry, the symmetry condition $C_{ij} = C_{ji}$ holds for all i, j. It will be shown in Sect. 6.5 that this condition holds for all linearly elastic solids.

Cubically symmetric crystals form a special case of materials known as *orthotropic*, characterized by the fact that, with respect to a special set of axes, the relations between stress and strain are similar form to Eqs. (6.13) and (6.14), but with different values of E, ν and G for each relation. That is, the compliance matrix $[C]^{-1}$ takes the form

$$[C]^{-1} = \begin{bmatrix} \frac{1}{E_x} & -\frac{\nu_{xy}}{E_x} & -\frac{\nu_{xz}}{E_x} & 0 & 0 & 0 \\ -\frac{\nu_{yx}}{E_y} & \frac{1}{E_y} & -\frac{\nu_{yz}}{E_y} & 0 & 0 & 0 \\ -\frac{\nu_{zx}}{E_z} & -\frac{\nu_{zy}}{E_z} & \frac{1}{E_z} & 0 & 0 & 0 \\ 0 & 0 & 0 & \frac{1}{G_{yz}} & 0 & 0 \\ 0 & 0 & 0 & 0 & \frac{1}{G_{zx}} & 0 \\ 0 & 0 & 0 & 0 & 0 & \frac{1}{G_{xy}} \end{bmatrix}. \tag{6.56}$$

An example of an orthotropic solid, whose anisotropy is due to its fibrous nature, is provided by wood. The direction of the fibers (or "grain") is normally that of the longitudinal axis of timber elements. If the timber is cut from a portion of the tree that is relatively far from the core, then the curvature of the growth rings may be neglected in a first approximation, and the axes that are tangential to the rings and normal to them (in the transverse plane), the latter being the radial axis, also form natural axes similar to the crystal axes of the preceding example. It is common to designate the longitudinal, tangential and radial axes by the indices L, T and R, respectively, as in Fig. 6.11. In Tables B-5 and B-6, the values of E given for wood are those of E_L,

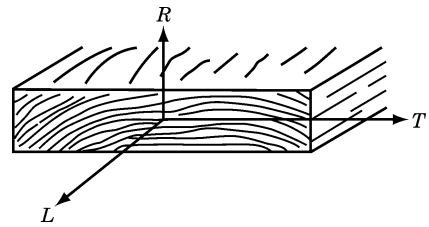

Figure 6.11. Axes of orthotropy in wood: L longitudinal, T tangential, R radial

while those for G and ν are ranges spanned by G_{TL} and G_{RL} and by ν_{TL} and ν_{RL}, respectively.

Another special case of orthotropy, known as *transverse isotropy*, occurs when the material properties are unchanged under any rotation about the longitudinal axis. If this axis is the x-axis then, in the matrix of Eq. (6.56), the values of the coefficients are unchanged under any interchange of y and z, and, in addition, a relation of the form (6.21) applies to the values of E, G and ν governing stresses in the transverse plane ($E_y = E_z$, $G_{yz} = G_{zy}$ and $\nu_{yz} = \nu_{zy}$). Transversely isotropic behavior is observed in unidirectional fiber-reinforced plastics, as well as in bone.

Exercises

6.2-1. Consider the deformable body of Exercise **5.3-3**, and assume that it is in a state of plane strain. Assume, further, that the body is homogeneous and is made of an isotropic linearly elastic material with $E = 100$ GPa and $\nu = 0.3$. In this case, determine all non-zero components of stress at the points with coordinates $(0,0)$ and $(0.5,0.25)$.

6.2-2. Consider a body in plane strain that is made of an isotropic linearly elastic material. Suppose that two experiments are carried out to determine the elastic constants for this material: the first is an equibiaxial strain experiment with $\varepsilon_x = \varepsilon_y = 0.005$, yielding the normal stresses $\sigma_x = \sigma_y = 10$ MPa, while the second is a shear strain experiment with $\gamma_{xy} = 0.002$, yielding the shear stress $\tau_{xy} = 1.5$ MPa. Use the data from these tests to estimate E, ν, G and K.

6.2-3. For a body in plane stress in the (x,y)-plane, show that

$$\sigma_x = \frac{E}{1-\nu^2}\left(\varepsilon_x + \nu\varepsilon_y\right),$$
$$\sigma_y = \frac{E}{1-\nu^2}\left(\varepsilon_y + \nu\varepsilon_x\right).$$

How is the out-of-plane strain ε_z related to the in-plane strains?

6.2-4. If an elasticity problem in plane strain has been solved for the in-plane stresses, strains and displacements in terms of E and ν, find the modified values of these constants (say E' and ν') in terms of which the same solution would be valid for the equivalent problem in plane stress.

6.2-5. A solid cylinder made of an isotropic linearly elastic solid is embedded in a rigid matrix with frictionless contact. If it is subject to a compressive axial force, find the relation between the axial normal stress and the longitudinal strain, as well as the compressive stress between the cylinder and the matrix.

6.2-6. Derive Eq. (6.33).

6.2-7. For the state of strain given in column-matrix form by

$$\{\varepsilon\} = \begin{Bmatrix} 6.3 \\ -5.2 \\ 7.9 \\ -6.0 \\ 0.0 \\ 11.2 \end{Bmatrix} \times 10^{-3},$$

find the corresponding stress matrix $\{\sigma\}$ if $E = 200$ GPa and $\nu = 0.29$.

6.2-8. Consider a rectangular block in the state of plane stress in the (x, y)-plane, as in the figure (with all dimensions in cm). Assume that the block is made of a homogeneous isotropic linearly elastic material with $E = 100$ GPa and $\nu = 0.25$, and let the components of stress in the block be given in MPa by

$$\begin{aligned} \sigma_x(x,y) &= 100x \\ \sigma_y(x,y) &= 0 \\ \tau_{xy}(x,y) &= -100x + 200y \ , \end{aligned}$$

where x and y are measured in cm.

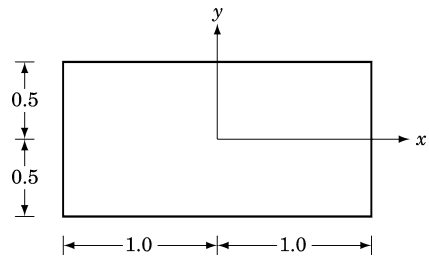

(a) Determine all the components of strain in the block, as a function of the coordinates x and y.

(b) Compute the total elongation of a material line in the block defined by $y = 0$.

(c) Compute the total elongation of a material line in the block defined by $x = 0.5$.

(d) Compute the change from $\pi/2$ of the angle formed by material lines with coordinates $x = 1$ cm and $y = 0.5$ cm.

(e) Compute the change from $\pi/2$ of the angle formed by material lines with coordinates $x + y = 0.5$ and $x - y = 0.5$.

6.2-9. For the strain matrix $\{\varepsilon\}$ given in Exercise **6.2-7**, find the corresponding deviatoric strain $\{\varepsilon\}'$.

6.2-10. For the state of stress given in column-matrix form by

$$\{\sigma\} = \begin{Bmatrix} -7.5 \\ 4.9 \\ 11.9 \\ 0.0 \\ 0.0 \\ -3.3 \end{Bmatrix} \times 10^3 \,\text{ksi} \ ,$$

find the corresponding strain matrix $\{\varepsilon\}$ if $E = 20{,}000$ ksi and $G = 7{,}500$ ksi.

6.2-11. For the stress matrix $\{\sigma\}$ given in Exercise **6.2-10**, find the corresponding deviatoric stress $\{\sigma\}'$.

6.2-12. Derive Eq. (6.55).

6.2-13. Derive the 3×3 matrix $[C]$ for plane stress.

6.2-14. Derive the 3×3 matrix $[C]^{-1}$ for plane strain.

6.2-15. A closed cylindrical shell made of steel ($E = 202\,\text{GPa}$, $\nu = 0.29$), of mean diameter 25 cm and thickness 1.5 mm, is filled with a gas under a pressure of 500 kPa. Find the resulting changes in the diameter and the thickness.

6.2-16. Calculate the number of independent elastic parameters for a transversely isotropic linearly elastic materials, taking the symmetry of $[C]$ into account.

6.3 Elongation of Axially Loaded Elastic Bars

6.3.1 Introduction

The elongation of axially loaded bars constitutes one of the basic applications of elasticity in engineering, along with the torsion of shafts under applied torque, the bending of beams under transverse forces (and, possibly, applied bending moments), and the buckling of columns under compressive axial loads. But in these last three applications it is necessary to determine the distribution of stress over the cross-section, and the results are highly dependent on its shape. These three topics will consequently be given chapters of their own in which the necessary theory is developed. This is not necessary for the axially loaded elastic bars, which are the subject of this section.

6.3.2 Elongation of a Uniform, Homogeneous Bar Under End Forces

In a bar of uniform cross-section that is subject to forces only at the ends, the axial force P is, as we know, constant along its length. The elastic behavior of such a bar, illustrated in Fig. 6.1b, was introduced in Sect. 6.1 as an example of a simple translational spring and in connection with the definition of Young's modulus, and was the subject of some exercises in that section. It will here be treated more fully. The study of bars subject to tensile loading can be traced at least as far back as to the observations of Galileo, as shown in Fig. 6.12.

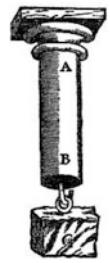

Figure 6.12. Illustration of a bar under tensile loading from Galileo's *Dialogues Concerning Two New Sciences* (1638).

For such a bar, it can be assumed that all the fibers (elements parallel to the axis) elongate by the same amount, as illustrated in Fig. 4.16 (page 169). This assumption is exact if the forces are transmitted through rigid plates attached to the ends, as in Fig. 4.5b (page 159). Consistent with this assumption, the longitudinal strain ε is uniform through the cross-section (designated $\mathscr{A}$), and therefore, if the bar is homogeneous and linearly elastic, with Young's modulus E, the axial stress is uniform and equal to $\sigma = E\varepsilon$.

Clearly, the uniform axial stress trivially satisfies the local equilibrium equations (4.39–4.41). For the external force P to be in equilibrium with the resultant of the stresses at any cross-section, as can be seen from the free-body

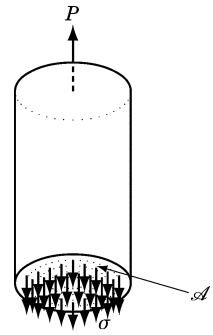

Figure 6.13. Internal equilibrium of an axially loaded bar

diagram shown in Figure 6.13, we have, in general,

$$P = \int_{\mathcal{A}} \sigma \, dA \,, \tag{6.57}$$

but with the stress being uniform* this is just

$$P = \sigma A = E\varepsilon A \,. \tag{6.58}$$

Given the definition of strain in Eq. (5.2), this becomes

$$P = \frac{EA}{L} \Delta L \,. \tag{6.59}$$

Since the applied force at either end equals P, it follows that the quantity EA/L is the ratio of applied force to elongation and is therefore equivalent to the spring constant discussed in Sect. 6.1. Therefore, Eq. (6.59) may be also written as

$$P = k\Delta L \,, \tag{6.60}$$

where $k = EA/L$. The spring constant k is also called the *axial stiffness* of the bar. The product EA is known as the *axial rigidity* of the cross-section.

As regards the line of action of the axial force P, it follows from the discussion in Sect. 1.5 that it must intersect each cross-section at its centroid. The line going through the centroids is consequently the axis of a homogeneous bar.

In a quasi-rigid articulated assemblage of axially loaded bars, such as a truss, the fact that the bars elongate requires them to rotate in order to remain connected at the joints, thus satisfying the requirement of compatibility

*By Saint-Venant's principle, the stress can be expected to be uniform under other attachment conditions as well, except near the ends.

similar to that of the chains in Sect. 3.5 (page 143). The difference is that the displacements are generally very small in comparison to the lengths of the bars, allowing the equations to be linearized, as will be discussed in the following example.

Example 6.3.1: Displacement in a simple plane truss.
Let u and v denote the horizontal and vertical components of the displacement of joint B of the simple truss (an apex-loaded asymmetric straight-legged three-pinned arch) whose geometry and loading are shown in Fig. 6.14, with the dashed and solid lines representing respectively the original and displaced configurations. (Since the vertical displacement is downward, its magnitude is shown as $-v$.) Let the original lengths of the left-hand and right-hand members be denoted L_1 and L_2, respectively, and their elongations ΔL_1 and ΔL_2.The magnitudes of the displacements shown in the figure are exaggerated, and in fact are supposed to be small enough that the angles α and β do not change significantly. By the Pythagorean theorem, then

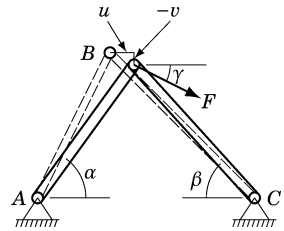

Figure 6.14. Example 6.3.1

$$\begin{aligned}(L_1+\Delta L_1)^2 &= (L_1\cos\alpha+u)^2+(L_1\sin\alpha+v)^2\,,\\ (L_2+\Delta L_2)^2 &= (L_2\cos\beta-u)^2+(L_2\sin\beta+v)^2\,.\end{aligned} \tag{6.61}$$

When the squared expressions are expanded, the quadratic terms in ΔL_1, ΔL_2, u and v can be dropped, and since $\cos^2\alpha+\sin^2\alpha=\cos^2\beta+\sin^2\beta=1$, the quadratic terms in L_1 and L_2 cancel, leaving

$$\Delta L_1 = u\cos\alpha+v\sin\alpha \quad , \quad \Delta L_2 = -u\cos\beta+v\sin\beta\,, \tag{6.62}$$

which can be solved for u and v as

$$u = \frac{\Delta L_1\sin\beta-\Delta L_2\sin\alpha}{\sin(\alpha+\beta)} \quad , \quad v = \frac{\Delta L_1\cos\beta+\Delta L_2\cos\alpha}{\sin(\alpha+\beta)}\,, \tag{6.63}$$

noting that the determinant of the coefficients of the right-hand side of Eqs. (6.62) is $\cos\alpha\sin\beta+\sin\alpha\cos\beta=\sin(\alpha+\beta)$. The elongations ΔL_1 and ΔL_2 are in turn expressed in terms of the respective bar forces P_1 and P_2 by elastic relations of the form (6.60), that is, $P_i=k_i\Delta L_i$ $(i=1,2)$, while the P_i are related to the load F by the equilibrium equations

$$-P_1\cos\alpha+P_2\cos\beta+F\cos\gamma = 0 \quad , \quad P_1\sin\alpha+P_2\sin\beta+F\sin\gamma = 0\,. \tag{6.64}$$

On substituting the elongations given by Eqs. (6.62) into the elastic relations, and the resulting expressions for the bar forces into the equilibrium equations

(6.64), we obtain

$$\begin{aligned}(k_1\cos^2\alpha + k_2\cos^2\beta)u + (k_1\sin\alpha\cos\alpha - k_2\sin\beta\cos\beta)v &= F\cos\gamma,\\ (k_1\sin\alpha\cos\alpha - k_2\sin\beta\cos\beta)u + (k_1\sin^2\alpha + k_2\sin^2\beta)v &= -F\sin\gamma\,.\end{aligned} \tag{6.65}$$

(Note that the off-diagonal coefficients are equal; this is not a coincidence, and the fact will be discussed in Sect. 6.5.) Alternatively, we may solve the equilibrium equations (6.64) for the P_i, and then substitute $\Delta L_i = P_i/k_i$ into Eqs. eq:3pinch6-displ to obtain the displacements u and v; the result will of course be equivalent to solving Eqs. (6.65). The two approaches represent, respectively, the displacement and force methods of elastic analysis, which will be discussed in Sect. 6.4.

Example 6.3.2: A problem involving large displacements.
The preceding example will now be revisited, assuming that the displacement of the pin B is not necessarily small relative to the size of the bars. To simplify the analysis, we consider the special case $\alpha = \beta = \pi/4$, $\gamma = -\pi/2$ and $k_1 = k_2 = k$. In this case Eqs. (6.65) would readily yield $u = 0$ and $v = F/k$. However, on departing from the assumption of small displacements, a more elaborate analysis is required. To this end, we start by noting that symmetry still implies $u = 0$. In addition, since the vertical displacement v may be large, let the force F (also vertical) must be applied on the deformed configuration, as shown in Fig. 6.15.

As can be seen from the geometry of the deformed truss, the angles $\alpha' = \beta'$

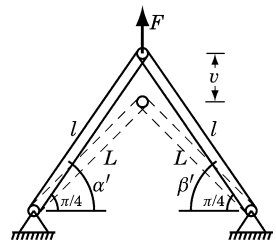

Figure 6.15. Example 6.3.2

satisfy

$$\tan\alpha' = \tan\beta' = \frac{L/\sqrt{2}+v}{L/\sqrt{2}}\,. \tag{6.66}$$

Therefore, vertical equilibrium of the joint B (expressed, again, on the basis of the geometry of the deformed configuration) implies that

$$F - P_1\sin\alpha' - P_2\sin\beta' = 0\,. \tag{6.67}$$

This may also be written as

$$F = 2P\sin\alpha'\,, \tag{6.68}$$

since, by symmetry, the forces P_1 and P_2 must be equal. Assuming, as in the previous example, that the relation between the force in the bars and the elongation is still linear,[†] we deduce that

$$P = k(l - L)\,. \tag{6.69}$$

[†]This assumption implies that the material is of the type discussed in Example 6.1.3 and that the linearity is based on the engineering stress-strain curve of Fig. 6.6.

Using, again, the geometry of the deformed truss, the length l of the deformed bars can be readily expressed as

$$l = \frac{L}{\sqrt{2}\cos\alpha'} . \tag{6.70}$$

With the aid of Eqs. (6.69) and (6.70), the equilibrium equation (6.68) becomes

$$F = 2kL\left[\frac{\tan\alpha'}{\sqrt{2}} - \sin\alpha'\right] . \tag{6.71}$$

Since (6.66) implies that

$$\sin\alpha' = \frac{L/\sqrt{2}+v}{\sqrt{(L/\sqrt{2}+v)^2+(L/\sqrt{2})^2}} , \tag{6.72}$$

the force F in Eq. (6.71) may be related to the displacement v by

$$F = 2kL\left[\frac{L/\sqrt{2}+v}{L} - \frac{L/\sqrt{2}+v}{\sqrt{(L/\sqrt{2}+v)^2+(L/\sqrt{2})^2}}\right] . \tag{6.73}$$

The force-displacement relation (6.71) is clearly non-linear in v and should be contrasted to $F = kv$ which we deduced earlier for the case of small displacements, that is, for $v \ll L$. In fact, it is instructive to verify that Eq. (6.73) indeed reduces to $F = kv$ in the latter case. To this end, we rewrite the rightmost term in Eq. (6.73) as

$$\begin{aligned}
\frac{L/\sqrt{2}+v}{\sqrt{(L/\sqrt{2}+v)^2+(L/\sqrt{2})^2}} &= \sqrt{\frac{(L/\sqrt{2}+v)^2}{(L/\sqrt{2}+v)^2+(L/\sqrt{2})^2}} \\
&= \sqrt{\frac{1}{2}+\frac{(L/\sqrt{2})v+v^2/2}{(L/\sqrt{2}+v)^2+(L/\sqrt{2})^2}} \\
&\doteq \sqrt{\frac{1}{2}+\frac{(L/\sqrt{2})v}{L^2}} \\
&= \sqrt{\frac{1}{2}\left(1+\frac{v}{L/\sqrt{2}}\right)} \\
&\doteq \frac{1}{\sqrt{2}}\left(1+\frac{v}{\sqrt{2}L}\right) .
\end{aligned} \tag{6.74}$$

In $(6.74)_3$, the condition $v \ll L$ implies that quadratic terms in v are neglected when added to linear linear terms in v and, likewise, linear terms in v are neglected when added to constant terms of order L. Also, in $(6.74)_5$ the approximation $\sqrt{1+2\zeta} \doteq 1+\zeta$ is employed (see also the footnote in Sect. 5.3, p. 231). Substituting (6.74) into Eq. 6.71 leads to

$$F = 2kL\left[\frac{L/\sqrt{2}+v}{L} - \frac{1}{\sqrt{2}} - \frac{v}{2L}\right] = kv , \tag{6.75}$$

which proves the desired reduction to the linear case.

6.3.3 Composite Bars

A bar is called *composite* if the Young's modulus E varies over the cross-section—if, for example, the cross-section presents more than one material.[‡] Suppose, to be specific, that the cross-section is made of two materials, 1 and 2 (as shown in Fig. 6.16a and illustrated in Fig. 6.16b), occupying regions $\mathscr{A}_1$ and $\mathscr{A}_2$, with respective cross-sectional areas A_1 and A_2 and Young's moduli E_1 and E_2. Assuming that the strain remains uniform on any given cross-

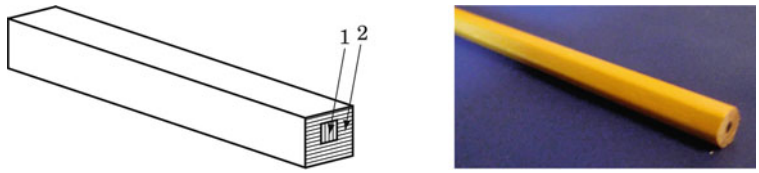

Figure 6.16. Composite bar: (**a**) schematic drawing, (**b**) illustration

section regardless of its varying material properties, the stresses in the two materials are $\sigma_1 = E_1\varepsilon$ and $\sigma_2 = E_2\varepsilon$. It follows that the forces transmitted through $\mathscr{A}_1$ and $\mathscr{A}_2$ are $P_1 = \sigma_1 A_1$ and $P_2 = \sigma_2 A_2$, and, consequently, the total axial force is

$$P \;=\; P_1 + P_2 \;=\; \frac{E_1A_1 + E_2A_2}{L}\Delta L \;. \tag{6.76}$$

The axial rigidity is therefore the sum of the rigidities E_1A_1 and E_2A_2 of the respective components. If these are, in turn, uniform over the length, then the axial stiffness or spring constant is the sum of the component spring constants, as befits spring elements acting in parallel.

The two partial axial forces P_1 and P_2 are also related to their resultant P as

$$P_1 \;=\; \frac{E_1A_1}{E_1A_1 + E_2A_2}P \quad , \quad P_2 \;=\; \frac{E_2A_2}{E_1A_1 + E_2A_2}P \;, \tag{6.77}$$

and act at the respective centroids of $\mathscr{A}_1$ and $\mathscr{A}_2$. Regarding P_1,

$$\begin{aligned} P_1 \;&= \sigma_1 A_1 \\ &= E_1\varepsilon A_1 \\ &= E_1A_1\frac{\Delta L}{L} \\ &= \frac{E_1A_1}{E_1A_1 + E_2A_2}P \;, \end{aligned} \tag{6.78}$$

where we used the uniaxial elastic stress-strain relation (6.3) (page 250), the definition of uniaxial strain (5.2) (page 216), and Eq. (6.76). The resultant

[‡]Such a bar is not to be confused with one that is made of a composite material but is homogeneous on a macroscopic scale.

consequently acts at a point along the line segment joining the two centroids, the location of this point (called the *effective centroid*) being such that if its distance from the centroid of $\mathscr{A}_1$ is d_1 and that from the centroid of $\mathscr{A}_2$ is d_2, then, for moment equilibrium, $P_1 d_1 = P_2 d_2$, as seen in Fig. 6.17. Consequently, if the distance between the centroids is $d = d_1 + d_2$, then

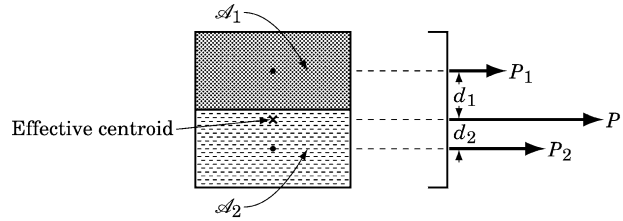

Figure 6.17. Effective centroid (black circles denote centroids of partial areas)

$$d_1 = \frac{E_2 A_2}{E_1 A_1 + E_2 A_2} d \quad , \quad d_2 = \frac{E_1 A_1}{E_1 A_1 + E_2 A_2} d \, . \tag{6.79}$$

In a composite elastic bar, the axis of the bar is therefore the line joining the *effective* centroids.

It is sometimes convenient to designate the *effective axial rigidity* of a composite bar as $\overline{EA}$, and write the force-elongation relation (6.76) as

$$P = \frac{\overline{EA}}{L} \Delta L \, . \tag{6.80}$$

It follows from Eq. (6.76) that $\overline{EA} = E_1 A_1 + E_2 A_2$.

6.3.4 Nonuniform Bars

Consider, now, a bar aligned with the x-axis, with one end at $x = 0$ and the other at $x = L$, and let the effective axial rigidity $\overline{EA}(x)$ be a function of x, provided that the variation is such that that the effective centroid of every cross-section lies exactly on the x-axis, as seen in Fig. 6.18.

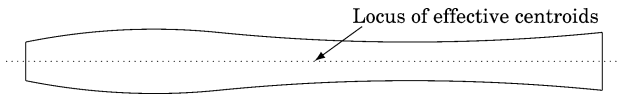

Figure 6.18. Nonuniform bar

The local relation between axial force and strain is

$$P = \overline{EA}(x) \varepsilon(x) \, . \tag{6.81}$$

Since, by Eq. (5.12), $\varepsilon(x) = du/dx$ and also $\Delta L = u(L) - u(0)$, it follows that

$$\Delta L = \int_0^L \varepsilon(x)dx = P\int_0^L \frac{1}{\overline{EA}(x)}dx \,. \tag{6.82}$$

The stiffness or spring constant k of the bar is therefore given by

$$\frac{1}{k} = \int_0^L \frac{1}{\overline{EA}(x)}dx \,. \tag{6.83}$$

The reciprocal $1/k$ of the axial stiffness is known as the *axial flexibility* of the bar.

If the bar consists of a number (say n) of uniform segments of length L_i and effective axial rigidity $\overline{EA}_i$ $(i = 1,\ldots,n)$, then Eq. (6.83) reduces to

$$\frac{1}{k} = \sum_{i=1}^{n} \frac{L_i}{\overline{EA}_i} = \sum_{i=1}^{n} \frac{1}{k_i} \,. \tag{6.84}$$

Since the bar segments are in series, it is the flexibilities that add.

6.3.5 Bars with Variable Internal Axial Force: Axial-Force Diagrams

We will consider, next, bars in which the internal axial force varies with position, as a result of the external axial forces not being applied only at the ends. Forces applied along the bar may be discrete or distributed along the length of the bar (or some segment thereof). An example of a distributed axial force is the weight of a vertical bar. Whether discrete or distributed, such forces must of course be applied in such a way that their line of action coincides with the axis of the bar.

We consider, again, a bar aligned with the x-axis. The variation of the axial force P acting on the cross-section at x, which can be represented graphically by an axial-force diagram, was already discussed in Sect. 2.4, and can be derived by the method of sections as shown in Fig. 6.19, where in each case the thick-lined rectangles represent the free bodies. In the case of discrete forces $F_0, F_1, F_2, \ldots$ applied at points $0, x_1, x_2, \ldots$, the method is illustrated in Fig. 6.19a. So, for example, for $x < x_1$, $P(x) = -F_0$; for $x_1 < x < x_2$, $P(x) = -F_0 - F_1$; and so on. The axial-force diagram then consists of a series of horizontal lines, as shown in Fig. 6.20a.

In the case of a distributed axial load such that the force per unit length is $p(x)$, the method of sections is applied to a slice of the bar contained between the sections at x and $x + dx$, as shown in Fig. 6.19b. For equilibrium,

$$p(x)dx + P(x + dx) - P(x) = 0 \,, \tag{6.85}$$

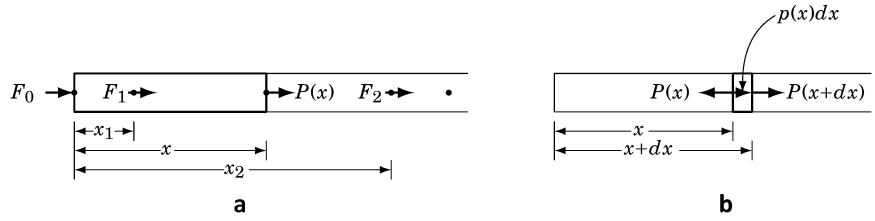

Figure 6.19. The method of sections applied to a bar under axial loads

and, since $P(x+dx) = P(x) + (dP/dx)dx$, this results in the differential equation

$$\frac{dP}{dx} = -p(x)\,. \tag{6.86}$$

Note that this equation can be alternatively obtained by integrating the local equilibrium equation (4.39) (page 190) over the cross-section $\mathscr{A}$ if the shear stresses are assumed to vanish[§] and if we define $p(x) = \int_{\mathscr{A}} b_x\, dA$, since $P = \int_{\mathscr{A}} \sigma_x\, dA$.

In the absence of discrete loads (other than at the ends), then,

$$P(x) = -F_0 - \int_0^x p(x')dx'. \tag{6.87}$$

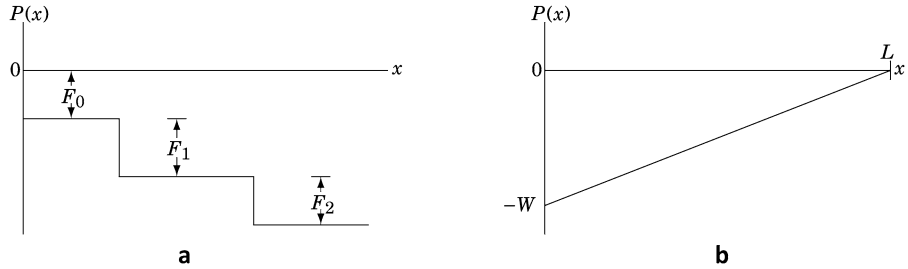

Figure 6.20. Examples of axial-force diagrams for discrete and distributed loads

Example 6.3.3: Internal axial force in a column bearing its own weight. We consider a column of height L and of uniform cross-section standing freely under its own weight W. If the x-axis is taken as positive upward from the base, then the base reaction is just $F_0 = W$. The distributed force is just the weight of the column per unit length, acting downward, that is, $p(x) = -W/L$. Eq. (6.87) then yields $P(x) = -W(1 - x/L)$, as shown in Fig. 6.20b.

[§]This assumption is not actually necessary if the bounding surface of the bar is traction-free.

There exists a method for expressing axial-force diagrams like the one of Fig. 6.20a, as well as those with other discontinuities (for example, those resulting from discontinuous distributed force), in closed form. The method is based on the use of the so-called *singularity functions*, described in Appendix A. The use of these functions will be discussed in detail in Chap. 8.

6.3.6 Bars with Variable Internal Axial Force: Stress and Elongation

We limit our discussion to bars that are homogeneous with Young's modulus E, and assume that the uniform distribution of axial stress over the cross-section holds in the case of variable axial force and variable cross-sectional area, except in the vicinity of sections where the axial force or the area changes abruptly. The value of the stress as a function of x is accordingly

$$\sigma(x) = \frac{P(x)}{A(x)} . \tag{6.88}$$

For the purpose of stress-based design, we must determine the point x where the stress in (6.88) attains its maximum value. In materials for which the allowable stress is different in tension and compression, the numerical maxima of both the positive and negative ranges of $\sigma(x)$ must be found.

If the bar is tapered, then the stress will not be strictly uniaxial, as can be seen from Fig. 6.21, since in the fibers near the traction-free edge the stress must be parallel to the edge. If, however the taper is slight, then the stress

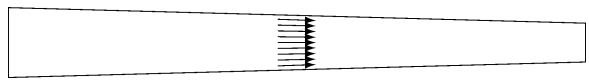

Figure 6.21. Stress in a tapered bar

can be assumed to be uniaxial to a good degree of approximation, and then Eqs. (6.3), (5.12) and (6.88) imply that

$$\frac{P(x)}{A(x)} = E\varepsilon(x) = E\frac{du(x)}{dx} \tag{6.89}$$

or

$$\frac{du(x)}{dx} = \frac{P(x)}{EA(x)} . \tag{6.90}$$

This equation may be integrated to yield

$$u(x) = u(0) + \int_0^x \frac{P(x')}{EA(x')}\,dx', \tag{6.91}$$

from which an *elongation diagram* can be drawn. The total elongation is

$$\Delta L = u(L) - u(0) = \int_0^L \frac{P(x)}{EA(x)}\,dx\,. \tag{6.92}$$

We can easily see that Eq. (6.92) reduces to (6.59) when P and A are independent of x.

Example 6.3.4: Shortening of a free-standing column.
We consider the shortening of a column under its own weight. By the principle of superposition, this may be added to the shortening due to any load that the column may carry.
(a) *Cylindrical column.* If the internal axial force varies as shown in Fig. 6.20b and if the column cross-section is constant, then

$$\Delta L = -\frac{W}{EA}\int_0^L \left(1-\frac{x}{L}\right)dx = -\frac{WL}{2EA}\,.$$

(b) *Conical column.* Suppose that the column has the shape of a truncated cone, with the radii at the top and bottom being a and b, respectively ($b > a$). Let x be measured vertically downward from the top, so that the radius at x is $r(x) = a + \alpha x$, where $\alpha = (b-a)/L$. If the specific weight is γ, then the axial force at x is the weight of the material above it, that is,

$$P(x) = -\pi\gamma\int_0^x (a+\alpha x')^2 = -\frac{\pi\gamma}{3\alpha}[(a+\alpha x)^3 - a^3]\,,$$

and the elongation is, by Eq. (6.92),

$$\Delta L = -\frac{\gamma}{3E\alpha}\int_0^L \left[(a+\alpha x) - \frac{a^3}{(a+\alpha x)^2}\right]dx = -\frac{\gamma}{3E\alpha^2}\left[\frac{b^2-a^2}{2} - a^3\left(\frac{1}{a}-\frac{1}{b}\right)\right]\,,$$

which, upon simplification and the substitution $\alpha = (b-a)/L$, reduces to

$$\Delta L = -\frac{(1+2a/b)\gamma L^2}{6E}\,.$$

It is easy to check that this result coincides with that of part (a) when $a = b$.

6.3.7 Virtual Work

Under the assumption—stated at the beginning of the section—of uniform longitudinal strain given by Eq. (5.12), the internal virtual work per unit length, given by Eq. (5.18), becomes $\delta W'_{\text{int}} = P\delta(du/dx)$, which (as a result of the distributive property of the δ operator) may be rewritten as $Pd(\delta u)/dx$. The total internal virtual work is accordingly

$$\delta W_{\text{int}} = \int_0^L P\frac{d(\delta u)}{dx}\,dx\,. \tag{6.93}$$

The external virtual work is the sum of that done by the distributed load p (which is $p\delta u$ per unit length) and that done by any end forces, F_0 and F_L, that may be applied. Thus

$$\delta W_{\text{ext}} = \int_0^L p\delta u dx + F_0\delta u(0) + F_L\delta u(L) . \tag{6.94}$$

Before equating the right-hand sides of (6.93) and (6.94), we transform the former by integration by parts to obtain

$$\delta W_{\text{int}} = P\delta u\Big|_0^L - \int_0^L \delta u \frac{dP}{dx} dx . \tag{6.95}$$

The principle of virtual work can now be expressed as

$$\delta W_{\text{ext}} - \delta W_{\text{int}} = \int_0^L \left(\frac{dP}{dx} + p\right) dx + \big[F_L - P(L)\big]\delta u(L) + \big[F_0 + P(0)\big]\delta u(0) = 0 . \tag{6.96}$$

The integral vanishes identically, for an arbitrary virtual displacement $\delta u(x)$, if and only if the equilibrium equation (6.86) is satisfied. At the ends, either the applied axial force is prescribed (i.e. $P(L) = F_L$ and/or $P(0) = -F_0$, corresponding to a free end) or the displacement is prescribed (not necessarily equal to zero), corresponding to a fixed end. We see that the differential equation of equilibrium *and* the boundary conditions follow from an application of the principle of virtual work.

Exercises

6.3-1. The two-bar structure is subject to a vertical force $F = 100$ kN at the hinge O, as in the figure. If each bar has Young's modulus $E = 100$ GPa and cross sectional area $A = 10$ mm^2, find the total displacement of the point O.

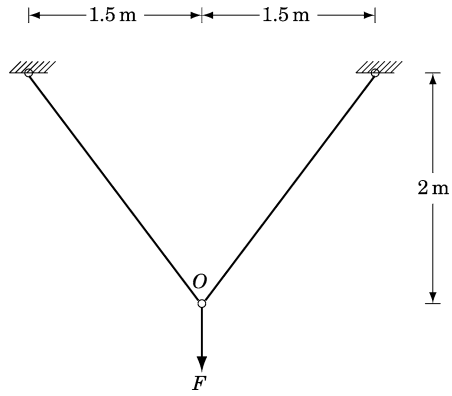

6.3-2. Taking into account the change in the geometry due to the displacement in Exercise **6.3-1**, calculate the forces in the two bars and compare the values with those calculated on the basis of the original geometry.

6.3-3. The boxed chandelier sketched in the figure below is suspended by four cables, of length 85 cm, making an angle of 75°with the vertical. If the weight of the chandelier is 28 kg$_f$ and the cables have $EA =$

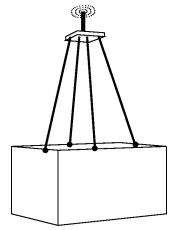

120 MN, calculate how much the chandelier drops after it is hung.

6.3-4. In the structure shown in the figure below, member AB is made of steel pipe with inner and outer diameters of 20 mm and 25 mm, respectively, and member BC is a solid steel rod of diameter 15 mm. Assuming $F = 50$ kN, $E = 202$ GPa and no buckling of the compression member, find the horizontal and vertical displacements of joint B.

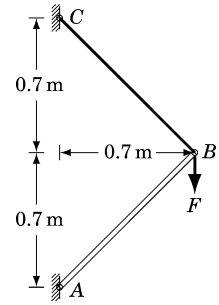

6.3-5. Consider a bar made of a homogeneous linearly elastic material with Young's modulus E with cross-section of constant area A and length L. Assume that the bar is separately subjected to either a concentrated force P or a distributed constant force p per unit length along its major axis, as in the figure.

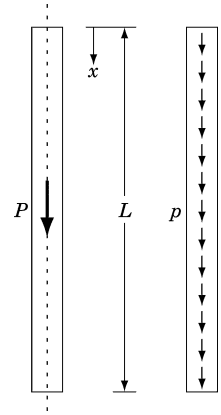

(a) What is the relation between P and p that would render the two force systems statically equivalent?

(b) Assume that the bar is held fixed at the top end and that the relation between P and p deduced in part (a) holds. At which point should P act such that the two force systems produce the same displacement of the bottom end?

(c) Repeat parts (a) and (b) assuming that the distributed force is linear in x and of the form $p(x) = ax$.

6.3-6. In the truss of Fig. 6.14, let the coordinates of joints A, B and C be, in meters, (0,0), (0.60, 1.20) and (1.80,0), respectively. Furthermore, let $EA = 150\,\text{MN}$ for both members, $F = 112\,\text{kN}$ and $\gamma = 26.56°$. Find the horizontal and vertical displacements of joint B.

6.3-7. Three elastic cords, of lengths 30 in, 26 in and 25 in, are hooked together and loaded as shown in the figure.

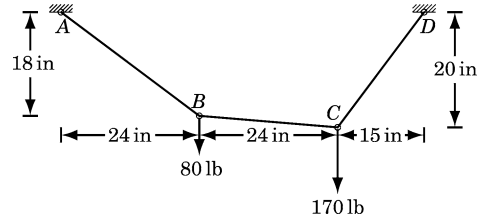

(a) Verify that the assemblage is in equilibrium as shown, using the method of Sect. 3.5.

(b) Assuming that the displacements are small enough not to affect the geometry and that the cords are linearly elastic with EA = 7.5 kip, find the horizontal and vertical displacements of points B and C.

6.3-8. A simply-supported bar is subject to axial forces shown in the figure. Draw the axial force diagram and, also, find the total elongation of the bar assuming that $E = 10^4$ ksi and $A = 0.1$ in^2.

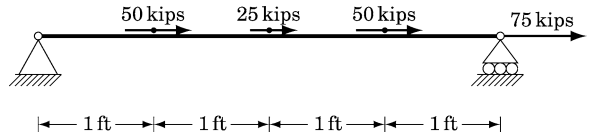

6.3-9. The 1-ft-long cantilever bar shown in the figure has a circular cross-section with variable radius $r = 1 + 0.25x$ (with x in inches) and Young's modulus $E = 5 \times 10^3$ ksi. For each of the two cases where it is built in (a) on the left and (b) on the right, draw the axial-force diagram and determine the total elongation of the bar due to the distributed load $p(x) = 10(x + 1)$ kips/in.

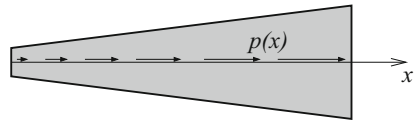

6.3-10. Find a number β, in terms of a and b, such that the result of part (b) of Example 6.3.4 may be written as $\Delta L = -\beta WL/EA$, and show that $\beta = \frac{1}{2}$ when the column is a circular cylinder ($a = b$), as in part (a).

6.3-11. An artwork consists of five aluminum disks, with weights shown in the figure, connected by 1-ft lengths of AWG[¶] No. 8 aluminum wire (diameter 0.1285 in). Treating the disks as rigid and assuming

[¶]American Wire Gage

$E = 10 \times 10^3$ ksi, determine the total elongation of the fixture and the maximum stress in the wire.

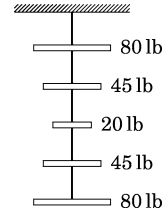

6.3-12. In the figure above, the discs above the bottom one are supported on the continuous 5-ft wire by clips. If the clips fail and all the disks fall to rest on the bottom one, what is the additional elongation? Use the wire properties given in the preceding exercise.

6.3-13. The obelisk of Queen Hapshetsut at Karnak, Egypt, has the shape of a slender truncated pyramid of square cross-section, surmounted by a small pyramid (*pyramidion*) at the top, as seen in the figure on the right. It is 97.5 ft high, 8.6 ft wide at the base, and 5.3 ft wide at the top. If the specific weight of the stone is 165 lb/ft^3 and its Young's modulus is 10.6 $\times 10^6$ psi, and if the pyramidion is ignored, determine the shortening of the obelisk under its own weight after it is erected.

6.4 Static Indeterminacy in Linearly Elastic Bodies

6.4.1 Introduction

As we discussed in Sect. 2.2, a system is statically indeterminate if the equilibrium equations are insufficient for the determination of all internal forces. To this end, in addition to equilibrium, the deformation of the system needs to be taken into consideration. In this section, we revisit static indeterminacy in the specific context of linearly elastic bodies.

Consider the compound elastic bar subject to a force F at the junction of the two components, as shown in Fig. 6.22. Since the bar is built-in at

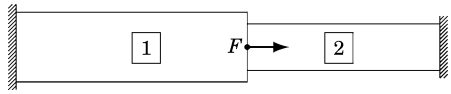

Figure 6.22. Compound bar built in at both ends

both ends, horizontal reactions develop at both ends, but only one equilibrium equation—that of horizontal force equilibrium—is nontrivial. The bar is consequently *statically indeterminate*.

Let the left-hand and right-hand segments of the bar be designated with the indices 1 and 2, respectively, with (P_1, P_2), $(\Delta L_1, \Delta L_2)$ and (k_1, k_2) denoting their respective internal axial forces, elongations and axial stiffnesses. The free-body diagram of the compound bar is shown in Fig. 6.23. (Note that, without introducing any restrictions, the axial forces P_1 and P_2 are here drawn as compressive, although the solution may ultimately dictate that one or both be tensile.)

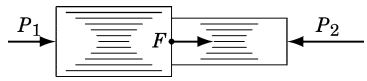

Figure 6.23. Free-body diagram of compound bar built in at both ends

The horizontal force equilibrium equation for the compound bar is

$$P_1 + F - P_2 = 0\,. \tag{6.97}$$

In addition, we have the constraint that the total elongation of the compound bar, which is the sum of the individual elongations ΔL_1 and ΔL_2, is zero. That is,

$$\Delta L_1 + \Delta L_2 = 0 \tag{6.98}$$

is the condition of compatibility between the internal deformation of the two component bars and the external constraint imposed by the built-in boundaries. Since the system is linearly elastic, the compatibility condition may be expressed with the aid of Eq. (6.60) in terms of the internal forces as

$$\frac{P_1}{k_1} + \frac{P_2}{k_2} = 0 \,, \tag{6.99}$$

and we now have two equations for the unknowns P_1 and P_2, that is, Eqs. (6.97) and (6.99). This approach for determining the internal forces exemplifies the *force method*.

Another way of solving the problem would be to treat the elongations ΔL_1 and ΔL_2 themselves as the unknowns, and to express the equilibrium equation in terms of them by substituting $P_1 = k_1 \Delta L_1$ and $P_2 = k_2 \Delta L_2$ in Eq. (6.97):

$$k_1 \Delta L_1 - k_2 \Delta L_2 + F = 0 \,. \tag{6.100}$$

We now have two equations for the unknowns ΔL_1 and ΔL_2, Eqs. (6.98) and (6.100). This approach represents what is known as the *displacement method*.

In a more systematic application of the displacement method, it is the displacement Δ (assumed here positive to the right) at the junction, conjugate to the force F, that is taken as the unknown variable. The compatibility conditions relate this displacement to the elongations of the component bars, namely,

$$\Delta L_1 = \Delta \quad , \quad \Delta L_2 = -\Delta \,. \tag{6.101}$$

The elastic relations (more generally, constitutive relations) then relate these elongations to the internal forces, resulting in

$$P_1 = k_1 \Delta \quad , \quad P_2 = -k_2 \Delta \,. \tag{6.102}$$

Finally, the equilibrium equation of the junction, $P_1 - P_2 = F$, is written in terms of the displacement Δ as

$$(k_1 + k_2)\Delta = F \,, \tag{6.103}$$

which determines Δ in terms of F in the form of a single equation, since the system has one degree of freedom. With Δ known, the internal forces and elongations are calculated from Eqs. (6.101) and (6.102).

With the force method, the unknown can be either P_1 or P_2 , and can be interpreted as either an internal force or a reaction. With the latter point of view, the corresponding constraint can be regarded as redundant (as discussed in Sect. 3.1, page 111). The reaction that is the unknown of the problem can then itself be called redundant. Suppose that it is the right-hand reaction, and let it be denoted X (assumed positive to the right). The equilibrium equations derived by the method of sections are

$$P_1 = F + X \quad , \quad P_2 = X \,, \tag{6.104}$$

and the elastic relations lead to

$$\Delta L_1 = \frac{F+X}{k_1} \quad , \quad \Delta L_2 = \frac{X}{k_2} \, . \tag{6.105}$$

Finally, the compatibility condition $\Delta L_1 + \Delta L_2 = 0$ takes the form

$$\frac{F}{k_1} + \left(\frac{1}{k_1} + \frac{1}{k_2} \right) X = 0 \, , \tag{6.106}$$

leading to

$$X = -\frac{k_2}{k_1 + k_2} F \, . \tag{6.107}$$

Once again, there is only one equation, since the degree of static indeterminacy (redundancy) is 1.

6.4.2 The Displacement Method: General

If a compound bar consists of more than two (say $n+1$) component bars, as in Fig. 6.24, then there would be n junctions and the system would have n degrees of freedom, the unknowns being the joint displacements Δ_i ($i = 1, \ldots, n$, with i designating the junction of bars i and $i+1$).

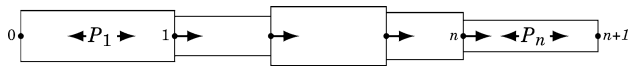

Figure 6.24. Compound bar with more than two component bars

The compatibility conditions are $\Delta L_i = \Delta_i - \Delta_{i-1}$ ($i = 1, \ldots, n+1$, with $\Delta_0 = \Delta_{n+1} = 0$), and the equilibrium equations are $P_i = F_i + P_{i+1}$ ($i = 1, \ldots, n$), where F_i is a load that may be acting at junction i. With the elastic relations $P_i = k_i \Delta L_i$, the equilibrium equations become

$$k_{i+1}\Delta_{i+1} - (k_i + k_{i+1})\Delta_i + k_i \Delta_{i-1} = -F_i \quad , \quad i = 1, \ldots, n \, . \tag{6.108}$$

The constants k_{i+1}, $-(k_i + k_{i+1})$, k_i multiplying the displacements Δ_{i+1}, Δ_i, Δ_{i-1} in Eq. (6.108) are referred to as *stiffness coefficients*.

With the force method, on the other hand, the solution is still one of a single equation, since the degree of force redundancy remains one, and in a case like this there is no reason to use the displacement method *unless a knowledge of the displacements is what is desired*. In the latter case, it would be natural to use the displacement method, independently of the degree of static indeterminacy of the system, and even in a statically determinate case, as was done in Example 6.3.1 (page 275).

But there also cases of systems that are highly redundant but narrowly constrained (that is, with few degrees of freedom), and in those cases the displacement method is advantageous even for the determination of internal forces, as in the following example.

Example 6.4.1: Asymmetric array of parallel bars or cables.
The planar array shown in Fig. 6.25 suspends a rigid block exerting a downward force F as shown. The independent variables determining the configuration (that is, the generalized coordinates discussed in Sect. 2.1) are the generalized displacements consisting of the downward translation Δ and the angle of rotation θ, assumed positive as shown. If x_i $(i = 1,\dots,n)$ is the x-coordinate of the

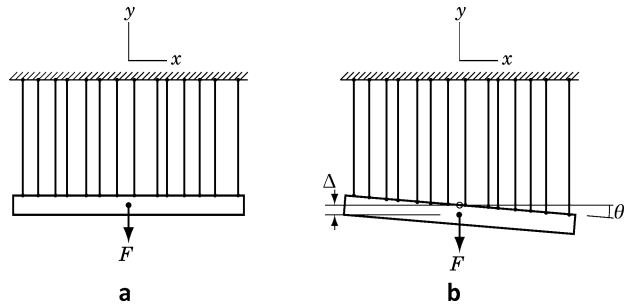

Figure 6.25. Example 6.4.1: (**a**) original configuration, (**b**) displaced configuration

i-th member (bar or cable), then its elongation, if θ is small, is $\Delta L_i = \Delta + x_i\theta$; these equations constitute the compatibility conditions. The force in each member is accordingly $P_i = k_i(\Delta + x_i\theta)$. The equilibrium equations are

$$\sum_i P_i = F \quad , \quad \sum_i x_i P_i = 0 \tag{6.109}$$

for force and moment equilibrium, respectively. Note that, since these are two in number, the degree of redundancy is $r = n - 2$. On defining

$$k = \sum_i k_i \quad , \quad k' = \sum_i k_i x_i \quad , \quad k'' = \sum_i k_i x_i^2 \, , \tag{6.110}$$

the equilibrium equations in terms of Δ and θ are

$$\begin{aligned} k\Delta + k'\theta &= F, \\ k'\Delta + k''\theta &= 0 \end{aligned} \tag{6.111}$$

(note once again that the off-diagonal coefficients are equal), and the solution is

$$\Delta = \frac{k''}{kk'' - k'^2}F \quad , \quad \theta = -\frac{k'}{kk'' - k'^2}F \, . \tag{6.112}$$

6.4.3 The Force Method: General

As we said above, in the force method the unknowns to be determined are the redundant forces or moments; these can be either external reactions or

internal force resultants. The usual procedure is to select the r constraints that are considered redundant (their choice is usually arbitrary) and then to imagine that they have been removed, so that the system is "reduced" to static determinacy. The redundant constraints may be either external or internal, and in the latter case it may be helpful to regard the reduced system as separated into two or more statically determinate subsystems.

The next step is to calculate the generalized displacements conjugate to the redundant generalized forces in the reduced system; these displacements (or rotations) are denoted Δ_{i0} $(i = 1,\ldots,r)$. Then the constraint forces (or moments) are imagined to be applied to the reduced system as though they were (unknown) loads X_i $(i = 1,\ldots,r)$; in the case of internal constraints these "loads" are applied as equal and opposite pairs acting on the corresponding subsystems at the point of separation. Next, for each X_j the resulting displacements conjugate to all the X_i (including $i = j$) are calculated; these are denoted Δ_{ij}. Lastly, the compatibility conditions are invoked. In the case of external constraints for which the constraint condition is $\Delta_i = 0$, the principle of superposition (based on the fact that all the governing equations are linear) leads to a system of r equations,

$$\sum_{j}^{r} \Delta_{ij} + \Delta_{i0} \;=\; 0\,, \quad i = 1,\ldots,r\,. \tag{6.113}$$

To show that these are indeed equations for the unknowns X_i, we give each X_j the value 1 (this procedure is sometimes called the method of virtual forces) and denote the corresponding values of Δ_{ij} as f_{ij} (these are called the *flexibility coefficients*), so that, in view of the linearity of the system, the actual Δ_{ij} is given by $f_{ij}X_j$, and therefore the preceding equation may be rewritten as

$$\sum_{j}^{r} f_{ij}X_j \;=\; -\Delta_{i0}\,, \quad i = 1,\ldots,r\,. \tag{6.114}$$

It will be found that the flexibility coefficients obey the symmetry condition $f_{ij} = f_{ji}$, just as do the stiffness coefficients in the displacement method.

When the redundant constraints are internal, then compatibility is enforced by making the relevant generalized displacements of the subsystems match at the points of separation, thus restoring the system to its connected configuration. The two approaches, of course, yield equivalent results, as will be illustrated in the following example.

Example 6.4.2: Rigid block suspended from four cables.
We will look at a specific case of Example 6.4.1 with $n = 4$ (so that $r = 2$), with the cables located and numbered as shown in Fig. 6.26a, so that $x_1 = -3$, $x_2 = 4$, $x_3 = -10$, $x_4 = 10$ (the units do not matter), and the cable stiffnesses by $k_1 = k_0/1.2$, $k_2 = k_0$, $k_3 = k_0/2$ and $k_4 = k_0/1.6$, where k_0 is a reference value of the stiffness.

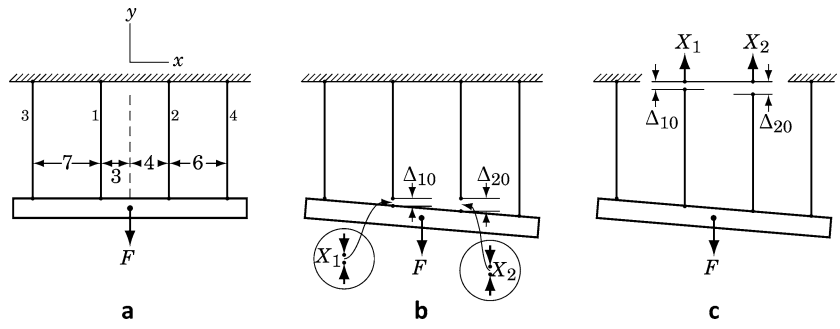

Figure 6.26. Example 6.4.2

For the redundant forces we choose, first, $X_1 = P_1$ and $X_2 = P_2$, and imagine the cuts to be at the points where the block is attached to the cables. The reduced system consists, as in Fig. 6.26b, of a block suspended from the two cables 3 and 4, and separately the two disconnected cables 1 and 2. Since the block subsystem is geometrically symmetric, it follows that $P_{30} = P_{40} = F/2$, and therefore $\Delta_{30} = (2/k_0)(F/2) = F/k_0$, $\Delta_{40} = (1.6/k_0)(F/2) = 0.8F/k_0$. The quantities Δ_{10} and Δ_{20} are found by linear interpolation as $0.93F/k_0$ and $0.86F/k_0$, respectively.

If we now apply an upward force X_1 at node 1 of the block suspended from the two end cables, the forces in those cables will be $P_{31} = -0.65X_1$ and $P_{41} = -0.35X_1$, respectively (the fact that they are compressive does not matter, since these are purely theoretical values), and the corresponding displacements will be $\Delta_{31} = -1.3X_1/k_0$, $\Delta_{41} = -0.56X_1/k_0$, and therefore, by linear interpolation, $\Delta_{11} = -1.041X_1/k_0$ and $\Delta_{21} = -0.782X_1/k_0$. Similarly, an upward force X_2 at node 2 produces the forces $P_{32} = -0.3X_2$ and $P_{42} = -0.7X_2$, with the corresponding displacements $\Delta_{32} = -0.6X_2/k_0$, $\Delta_{42} = -1.12X_2/k_0$, so that (again by linear interpolation) $\Delta_{12} = -0.782X_2/k_0$ and $\Delta_{22} = -0.964X_1/k_0$.

If, now, the forces X_1 and X_2 are applied to the cables 1 and 2, then the original system is restored when the stretches of these cables, X_1/k_1 and X_2/k_2 respectively, match the displacements of the nodes produced by F, X_1 and X_2 acting on the block:

$$\Delta_{10} + \Delta_{11} + \Delta_{12} = X_1/k_1 \quad , \quad \Delta_{20} + \Delta_{21} + \Delta_{22} = X_2/k_2 \, , \tag{6.115}$$

or, upon inserting numerical values and multiplying by k_0,

$$\begin{aligned} 0.930F - 1.041X_1 - 0.782X_2 &= 1.200X_1, \\ 0.860F - 0.782X_1 - 0.964X_2 &= 1.000X_2 \, . \end{aligned} \tag{6.116}$$

Note that, if the redundant cables had been cut at their points of suspension rather than at the block, as in Fig. 6.26c, then the terms on the right-hand sides of these equations, representing the elasticity of these cables, would have been included in Δ_{11} and Δ_{22} while the right-hand sides would have been zero (since the points of suspension do not displace), and the resulting equations would have been equivalent:

$$2.241X_1 + 0.782X_2 = 0.930F \quad , \quad 0.782X_1 + 1.964X_2 = 0.860F \, . \tag{6.117}$$

(Note the symmetry of the flexibility coefficients.) The solutions are $X_1 = P_1 = 0.3045F$, $X_2 = P_2 = 0.3166F$. P_3 and P_4 are found by equilibrium as $P_3 = 0.5F - 0.65X_1 - 0.3X_2 = 0.2071F$ and $P_4 = 0.5F - 0.35X_1 - 0.7X_2 = 0.1718F$.

6.4.4 Static Indeterminacy at the Continuum Level

With few exceptions, solid bodies in general are statically indeterminate at the continuum level in the sense that even when the internal force resultants can be determined by equilibrium, the stress distributions cannot. The exceptions are the cases that we called *simple stress states* in Sect. 4.3: thin-walled pressure vessels, the torsion of a thin-walled tube (such a tube need not be circular, as will be seen in Sect. 7.2)—in both of these cases it is the thin-walled property that allows the assumption—and the axially loaded homogeneous bar studied in Sect. 6.3.

Both the displacement method and the force method are used in studying specific problems of elastic continua. The difference is that the equations to be solved are not, as with finite-degree-of-freedom systems, algebraic, but differential (ordinary or partial, depending on the spatial dimensionality of the continuum).

The displacement method is based on formulating (by virtue of certain—possibly simplifying—assumptions regarding the geometry) a displacement field that obeys the constraints defining the problem but is otherwise unknown. The compatibility conditions are those relating strain and displacement as in Sect. 5.3. Next, the stress is related to the strain and thus expressed in terms of the displacement. The local equilibrium equations (Sect. 4.5) accordingly become differential equations for the displacement. In problems involving slender bodies the stress may be related to the internal force resultants by means of integration over the cross-section.

In applying the force method to continua, typically, a stress field that satisfies equilibrium is assumed to be generated from a stress function, as discussed in Sect. 4.5 (page 192), which is the unknown quantity of the problem. The strain is expressed in terms of the stress (and hence the stress function), and the compatibility of the strain field with the geometric constraints produces the equation to be solved. The number of problems in continuum elasticity that have been solved by this method is relatively small in comparison to those solved by the displacement method. This is especially true when approximate solutions, for the countless problems for which no exact solutions have been found, are included. The technique used most often, by far, for finding such approximate solutions is the *finite-element method*.

The finite-element method is based on dividing the region occupied by the body into a large number of small subregions, called *element domains*, forming a *finite-element mesh*. Such element domains are typically line segments (in one dimension), polygons (in two dimensions) or polyhedra (in three

dimensions), though curvilinear elements are possible when curvilinear (for example polar) coordinates are used, as in Fig. 6.27a. More typically, however, curved boundaries are approximated by straight-line segments, as in Fig. 6.27b.

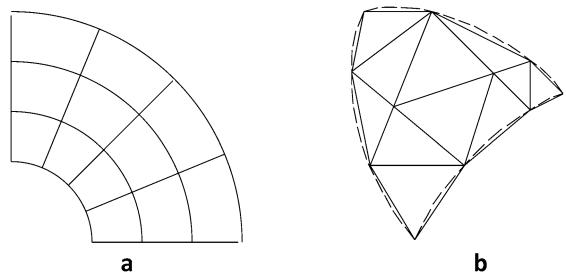

Figure 6.27. Some two-dimensional finite-element meshes: (**a**) curvilinear elements based on polar coordinates, (**b**) typical triangular mesh with straight-line approximation of curved boundary

Associated with each element domain are points known as *nodes*, which include at least the vertices of the polygons (or polyhedra), but may also include other points on the boundary of the element domain, and possibly in the interior as well. The non-interior nodes are, of course, shared with neighboring element domains. The approximation consists of assuming that within each element domain the displacement field is determined by the displacements (and possibly the rotations) at the nodes. The nodal generalized displacements thus constitute the generalized coordinates of the system. The overall displacement field comprises the displacement fields in each of the element domains. On the common boundaries between neighboring element domains, the displacement is typically defined by the (shared) boundary nodes, which enforces compatibility between the displacements of the two element domains. equilibrium is enforced by applying the principle of virtual work , which yields a set of algebraic equations for the nodal generalized displacements. For linearly elastic systems, however, it is possible to express this in the form of an energy principle, and the discussion will accordingly be continued in Sect. 6.5.

Exercises

6.4-1. A three-bar system is subject to a force F, as in the figure. If all three bars have the same axial rigidity EA, find the internal force in each each bar using: (a) the displacement method, and (b) the force method. In both methods, assume that the elongation of the bars is much smaller than their original lengths.

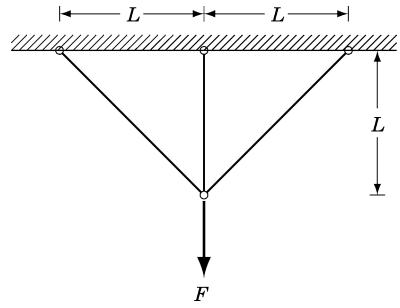

6.4-2. Solve the problem of Example 6.4.2 by the displacement method, and compare the results with those in the example.

6.4-3. A three-member truss structure is subject to a force F, as in the figure below. All three bars have the same length L and are made of the same linearly elastic material with Young's modulus E. Bars AD and BD have a constant cross-section of area A_1, while bar CD has a constant cross-section of area A_2.

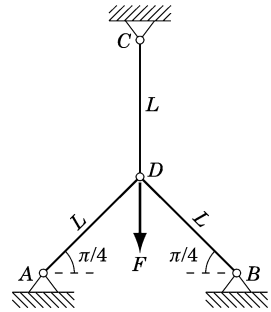

(a) Find the forces in each of the three bars in terms of F, A_1 and A_2.

(b) Find the ratio A_1/A_2 such that all three bars carry the same force in absolute value.

(c) Is it possible to find a ratio A_1/A_2 such that all three bars have the same average normal stress in absolute value?

6.4-4. A three-member truss structure is subject to a force F, as shown in the figure below. All three bars have the same length L and cross-sectional

area A, and are made of the same linearly elastic material with Young's modulus E. Using the force method, determine the bar forces by treating successively each of the bars AD, BD and CD as the redundant.

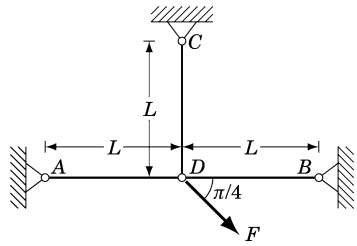

6.4-5. Solve the problem of the preceding exercise by the displacement method.

6.4-6. A rigid rectangular block of weight W is supported in a horizontal position by a symmetric array of five columns, with their centerlines equally spaced, as shown in the figure below. The columns are made of the same linearly elastic material, and their cross-sectional areas are such that $A_1 = 3A_3$ and $A_2 = 2A_3$. Neglecting the column weights, find the force in each column as a fraction of W.

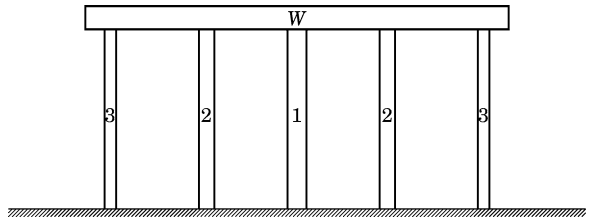

6.4-7. In the assemblage of Exercise **6.4-6**, it turns out that the columns have a combined weight of $0.45W$. Find the force in each column in terms of W.

6.4-8. In the assemblage of Exercise **6.4-6**, an additional concentrated load W is placed on the block directly above the right-hand column 2, as in the figure below. Find the force in each column in terms of W.

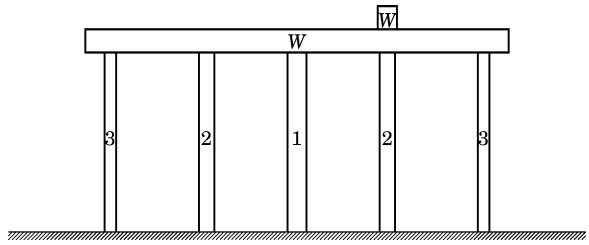

6.4-9. A conical column, as in Example 6.3.4(b), is rigidly attached at the top

so that it cannot shorten under its own weight. Find the reaction at the top in terms of the parameters given in the example.

6.4-10. A stepped column consists of three circular cylinders of the same linearly elastic material, as shown in the figure, with cross-sectional areas such that $A_3 = 3A_1$ and $A_2 = 2A_1$. If the column is rigidly attached at the top so that it cannot shorten under its weight, find the reaction at the top in terms of the total weight W of the column.

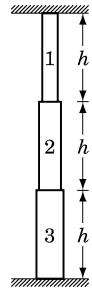

6.4-11. The three bars of the figure below have the same cross-sectional area A and are made of linearly elastic material with Young's modulus E. Suppose that the vertical bar is stretched by δ ($\delta \ll L$) to become connected at point B with the two inclined bars at the pin C.

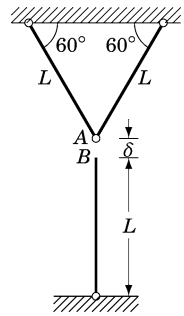

(a) Write the compatibility condition relating the vertical displacement of B and C after the two points are attached.

(b) Use the result of part (a) to determine the forces in the three bars in terms of E, A, δ and L.

6.5 Elastic Energy

6.5.1 Introduction

As we said in Sect. 1.1, every physical process—the acceleration of a car, the ringing of a bell, the contraction of a muscle—involves the conversion of work into energy, or vice versa, or of energy from one kind to another; these changes are governed by the first law of thermodynamics, which, in broad terms, asserts that energy can be converted between different forms but cannot be destroyed.

If, within a given physical process, there are two or more effects, each with an associated energy, then if the energy change associated with one effect is small compared to that associated with another, the former may often be neglected. In solid mechanics, the main forms of energy are kinetic (if motion occurs), gravitational, elastic (to be discussed below), and thermal. Friction, for example, leads to the conversion (or, as is frequently said, dissipation) of kinetic energy into heat, and if we idealize a process as frictionless it is because the dissipated energy is much smaller than other energy changes.

If, furthermore, the energy of one effect depends on variables corresponding to another, then the two effects are *coupled* and must be treated together. Otherwise, they are *uncoupled* and may be treated separately. This is what, on the one hand, makes possible the division of physical science into separate sciences (such as solid mechanics), and, on the other hand, necessitates the development of multiphysics disciplines such as mechanochemistry (which includes the study of muscular contraction).

6.5.2 Elastic Energy of Simple Springs

The work done by a generalized force (that is, a force F or moment M) acting on the conjugate generalized displacement (translation Δ or angle of rotation θ) is given by $\int_0^\Delta F\,d\Delta$ (or $\int_0^\theta M\,d\theta$), and is shown by the vertically shaded areas in the diagrams of Fig. 6.28.

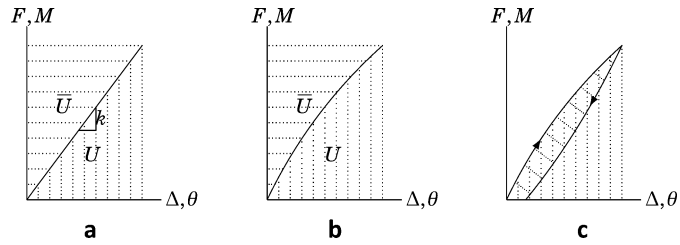

Figure 6.28. Energy for the load-displacement diagrams of Fig. 6.2

In the remainder of this section, for simplicity, only F and Δ will be used to denote generalized force and displacement, respectively, and the qualifier

"generalized" will often be omitted.

When the load is removed, in the case of the elastic springs represented in diagrams **a** (linear) and **b** (nonlinear) in Fig. 6.28, the work is done in reverse (since the load F remains positive while $d\Delta$ becomes negative), or equivalently, it is the spring that is doing the work on the agency applying the load. Consequently, the work done on an elastic spring is stored as potential energy—specifically, *elastic energy* or *strain energy*, denoted U—in the spring. In the inelastic spring of diagram c, on the other hand, only the area under the unloading curve represents the work that is done by the spring upon unloading, and the diagonally shaded area between the curves represents *dissipated work,* that is work that has been expended in loading but is not recovered by the spring upon unloading.

In the linear spring, the elastic energy is just the area of a triangle, that is, its value is $\int_0^\Delta F\,d\Delta' = \frac{1}{2}k\Delta^2$. It is also equal to the horizontally shaded area of the triangle to the left of the loading-unloading line, and to $\frac{1}{2}F^2/k$. In the nonlinearly elastic spring (diagram b), the vertically and horizontally shaded areas are different; the former is the strain energy $U = \int_0^\Delta F\,d\Delta$, while the latter is $F\Delta - \int_0^\Delta F\,d\Delta = \int_0^F \Delta\,dF$, and is called the *complementary energy* and denoted $\overline{U}$. While in a linear spring the two quantities have the same value at a given state, they are nonetheless conceptually distinct, in that U is a function of Δ and $\overline{U}$ is a function of F. Specifically,

$$U = \frac{k\Delta^2}{2} \quad , \quad \overline{U} = \frac{F^2}{2k} \, . \tag{6.118}$$

For a rotational spring the corresponding relations are

$$U = \frac{\bar{k}\theta^2}{2} \quad , \quad \overline{U} = \frac{M^2}{2\bar{k}} \, . \tag{6.119}$$

6.5.3 Linearly Elastic Systems with More Than One Degree of Freedom

A simple example of a system with two degrees of freedom is the compound linearly elastic bar shown in Fig. 6.29. A straightforward application of the

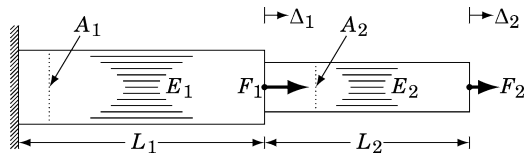

Figure 6.29. Compound bar with two degrees of freedom

method of sections shows that the internal axial force in the left-hand portion

is $F_1 + F_2$, while the one in the right-hand portion is F_2. If the respective elongations are Δ_1 and $\Delta_2 - \Delta_1$, then

$$\Delta_1 = \frac{F_1 + F_2}{k_1} \quad , \quad \Delta_2 - \Delta_1 = \frac{F_2}{k_2} \, , \tag{6.120}$$

where $k_1 = E_1 A_1 / L_1$ and $k_2 = E_2 A_2 / L_2$ are the spring constants of the respective portions. These equations can easily be solved either for Δ_1 and Δ_2 in terms of F_1 and F_2 or vice versa. The solutions can be written in the alternative forms

$$\Delta_i = \sum_{j=1}^{2} f_{ij} F_j \quad , \quad F_i = \sum_{j=1}^{2} k_{ij} \Delta_j \, , \tag{6.121}$$

where the flexibility coefficients f_{ij}, already introduced in the preceding section and making up the *flexibility matrix*

$$\begin{bmatrix} f_{11} & f_{12} \\ f_{21} & f_{22} \end{bmatrix} , \tag{6.122}$$

are given by

$$f_{11} = \frac{1}{k_1} \quad , \quad f_{12} = \frac{1}{k_1} \quad , \quad f_{21} = \frac{1}{k_1} \quad , \quad f_{22} = \frac{1}{k_1} + \frac{1}{k_2} \, . \tag{6.123}$$

Likewise, the stiffness coefficients k_{ij} making up the *stiffness matrix*

$$\begin{bmatrix} k_{11} & k_{12} \\ k_{21} & k_{22} \end{bmatrix} , \tag{6.124}$$

which is the inverse of the flexibility matrix, are given by

$$k_{11} = k_1 + k_2 \quad , \quad k_{12} = -k_2 \quad , \quad k_{21} = -k_2 \quad , \quad k_{22} = k_2 \, . \tag{6.125}$$

Note that $f_{12} = f_{21}$ and $k_{12} = k_{21}$, that is, *the flexibility and stiffness matrices are symmetric*. This, as was already indicated in the preceding section, is not a coincidence, as will now be shown.

In order to determine the work done by the forces F_1 and F_2 in the course of producing the displacements Δ_1 and Δ_2, we suppose first that F_1 is applied first, producing the displacements $\Delta_{11} = f_{11} F_1$ and $\Delta_{21} = f_{21} F_1$ at points 1 and 2, respectively, and the work done is $\frac{1}{2} F_1 \Delta_{11}$, as in the simple spring. The force F_2 produces the additional displacements $\Delta_{12} = f_{12} F_2$ and $\Delta_{22} = f_{22} F_2$. The work done by F_2 is $\frac{1}{2} F_2 \Delta_{22}$, but the force F_1—which now remains constant—does the additional work $F_1 \Delta_{12}$, so that the total work done by the two forces is

$$W_{\text{tot}} = \tfrac{1}{2}(F_1 \Delta_{11} + F_2 \Delta_{22}) + F_1 \Delta_{12} \, . \tag{6.126}$$

If the order of application of the forces is reversed, it is easy to retrace the steps of the preceding analysis and conclude that the total work done is $W'_{\text{tot}} =$

$\frac{1}{2}(F_1\Delta_{11}+F_2\Delta_{22})+F_2\Delta_{21}$. But since in any elastic body the work is stored as elastic energy, and since the mechanical state (stress and displacement fields) of such a body depends only on the applied loads and/or displacements and not on the order in which they are applied,* it follows that

$$F_1\Delta_{12} \;=\; F_2\Delta_{21}\;, \tag{6.127}$$

or, in words, *the work done by a force on the displacement produced by another force is equal to the work done by the latter on the displacement produced by the former*. This result can be readily generalized to two *sets of forces*, and is known as the *Maxwell–Betti reciprocal theorem*.†

It follows immediately from Eq. (6.127) and from the definitions of Δ_{12} and Δ_{21} that $f_{12} = f_{21}$, and, consequently,‡ that $k_{12} = k_{21}$. The reciprocal theorem explains the symmetry relations that were found in the preceding section.

Note that the definitions of Δ_{12} and Δ_{21} imply that each side of Eq. (6.127) can be written as $W_{\text{tot}} = \frac{1}{2}(f_{12}+f_{21})F_1F_2$. The total work can therefore be expressed, with the aid of Eq. $(6.121)_1$, as $W_{\text{tot}} = \dfrac{1}{2}\displaystyle\sum_{i=1}^{2}\sum_{j=1}^{2} f_{ij}F_iF_j$. Since this is a function of the forces, it also constitutes the complementary energy $\overline{U}$ of the system, that is,

$$\overline{U} \;=\; \frac{1}{2}\sum_{i=1}^{2}\sum_{j=1}^{2} f_{ij}F_iF_j\;. \tag{6.128}$$

When rewritten in terms of the displacements, it is equal to the strain energy,

$$U \;=\; \frac{1}{2}\sum_{i=1}^{2}\sum_{j=1}^{2} k_{ij}\Delta_i\Delta_j\;. \tag{6.129}$$

Note further that, when the k_{ij} are expressed in terms of k_1 and k_2, U can also be written as

$$U \;=\; \frac{1}{2}k_1\Delta_1^2+\frac{1}{2}k_2(\Delta_2-\Delta_1)^2\;, \tag{6.130}$$

where the terms on the right-hand side represent the strain energy of each of the component bars. We may say more generally that the strain energy is an *additive* quantity, in that the total strain energy of a body is the sum of the strain energies of its parts. The same can be said of the complementary energy.

*This exclusive dependence of the state on the applied loads and/or displacements is often regarded as the defining property of an elastic body.

†James Clerk Maxwell (1831–1879) was a British physicist and Enrico Betti (1823–1892) was an Italian mathematician.

‡It is an elementary result in linear algebra that the inverse of a symmetric matrix is also symmetric.

The preceding results can be easily generalized to a system with any number of degrees of freedom (say N): we can pick any two of them, and apply the argument leading to Eq. (6.127) to the corresponding displacements and their conjugate forces. Thus,

$$F_i = \sum_{j=1}^{N} k_{ij}\Delta_j \quad , \quad \Delta_i = \sum_{j=1}^{N} f_{ij}F_j \, , \tag{6.131}$$

with

$$k_{ij} = k_{ji} \quad , \quad f_{ij} = f_{ji} \, , \tag{6.132}$$

and the strain energy U and complementary energy $\overline{U}$ are given by

$$U = \frac{1}{2}\sum_{i=1}^{N}\sum_{j=1}^{N} k_{ij}\Delta_i\Delta_j \quad , \quad \overline{U} = \frac{1}{2}\sum_{i=1}^{N}\sum_{j=1}^{N} f_{ij}F_iF_j \, . \tag{6.133}$$

6.5.4 Energy Principles

Conservation of Energy

As we noted above, the work W done on a linearly elastic system is stored as elastic energy U (that is, such a system is *conservative*), and in some cases (only for linearly elastic bodies) a simple statement of the *principle of conservation of energy* in the form

$$W = U \quad \text{or} \quad W = \overline{U} \tag{6.134}$$

can be used to calculate displacements. A typical case is the determination of the displacement conjugate to a single load carried by a statically determinate multi-member system. If the load is, say, F, then all the internal forces are proportional to F, and consequently the complementary energy of each member is proportional to F^2. When the member energies are added to yield the energy of the system, this too will be proportional to F^2 and may be written as $F^2/2k$, where k is the spring constant of the system when regarded as a simple spring.

Example 6.5.1: Displacement of a truss carrying a single load.
In the equilateral truss (with member length L) shown in Fig. 6.30, it will be assumed for simplicity that all member cross-sections are the same, so that they all have the same stiffness $k_0 = EA/L$, and the complementary energy of the truss is therefore

$$\overline{U} = \frac{1}{2k_0}\sum_{i=1}^{7} P_i^2 \, . \tag{6.135}$$

A static analysis by the method of joints leads to $P_1 = P_4 = P_7 = -F/\sqrt{3}$, $P_2 = P_6 = F/2$, $P_3 = P_5 = F/\sqrt{3}$, so that

$$\overline{U} = \frac{F^2}{2k_0}[5(1/\sqrt{3})^2 + 2(1/2)^2] = 2.167\frac{F^2}{2k_0} \, . \tag{6.136}$$

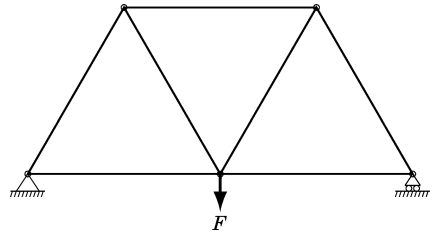

Figure 6.30. Example 6.5.1

The deflection of the load point is therefore $2.167 F/k_0$.

Castigliano's Theorems

The partial differentiation of the expressions (6.133) for U and $\overline{U}$ with respect to their respective variables yields, once the symmetry relations (6.132) have been taken into account,

$$\frac{\partial U}{\partial \Delta_i} = \sum_{j=1}^{N} k_{ij}\Delta_j \quad , \quad \frac{\partial \overline{U}}{\partial F_i} = \sum_{j=1}^{N} f_{ij}F_j \, . \tag{6.137}$$

As a consequence of Eqs. (6.131) it follows that

$$F_i = \frac{\partial U}{\partial \Delta_i} \quad , \quad \Delta_i = \frac{\partial \overline{U}}{\partial F_i} \, . \tag{6.138}$$

These results are known as *Castigliano's*[§] *first* and *second theorems*, respectively. They are often found expressed in terms of the *generalized forces* Q_i and *generalized coordinates* q_i discussed in Sect. 2.1 (page 61), that is,

$$Q_i = \frac{\partial U}{\partial q_i} \quad , \quad q_i = \frac{\partial \overline{U}}{\partial Q_i} \, . \tag{6.139}$$

Castigliano's first and second theorems can be used to derive the equations corresponding to the displacement and force methods, respectively, for the solutions of statically indeterminate problems. For the displacement method, the derivation is straightforward: once the strain energy is expressed as a function of the independent displacements Δ_i in the form of Eq. $(6.133)_1$, Eqs. $(6.138)_1$ immediately yield Eqs. $(6.131)_1$, which are just the required set of equations to be solved.

[§]Carlo Alberto Castigliano (1847–1884) was an Italian engineer and mathematician.

Example 6.5.2: Example 6.4.1 revisited using Castigliano's first theorem.
Here the strain energy of the i-th bar or cable is

$$U_i = \frac{1}{2}k_i(\Delta L_i)^2 \;=\; \frac{1}{2}k_i(\Delta + x_i\theta)^2,$$

and $U = \sum_i U_i$. The applied loads conjugate to Δ and θ are F and 0, respectively, so that

$$\begin{aligned} F \;&=\; \frac{1}{2}\frac{\partial}{\partial\Delta}\sum_{i=1}^{n} k_i(\Delta + x_i\theta)^2 = \sum_{i=1}^{n} k_i(\Delta + x_i\theta), \\ 0 \;&=\; \frac{1}{2}\frac{\partial}{\partial\theta}\sum_{i=1}^{n} k_i(\Delta + x_i\theta)^2 \;=\; \sum_{i=1}^{n} k_i x_i(\Delta + x_i\theta). \end{aligned}$$

When k, k' and k'' are defined as in Example 6.4.1, the equations are precisely the same.

The equations of the force method can likewise be derived from Castigliano's second theorem, but the derivation is a little more complicated, since the complementary energy has to be expressed in terms of both the prescribed loads and the unknown redundants. Rather than describe a general procedure, we illustrate the method by means of the same example.

Example 6.5.3: Example 6.4.1 revisited using Castigliano's second theorem.
The complementary energy of each cable is $\overline{U}_i = P_i^2/k_i$. From Example 6.4.2 we already know that, in the redundant cables, $P_1 = X_1$ and $P_2 = X_2$. For cables 3 and 4 we superpose the axial force due to the load (equal to $0.5F$ in each cable) with those due to the redundants (P_{31} and P_{32} in the former, P_{41} and P_{42} in the latter) to obtain

$$P_3 \;=\; 0.5F - 0.65X_1 - 0.3X_2 \quad , \quad P_4 \;=\; 0.5F - 0.35X_1 - 0.7X_2\,, \tag{6.140}$$

so that, upon substituting the values of the k_i,

$$\overline{U} \;=\; \frac{1.2}{2k_0}X_1^2 + \frac{1}{2k_0}X_2^2 + \frac{2}{2k_0}(0.5F - 0.65X_1 - 0.3X_2)^2 + \frac{1.6}{2k_0}(0.5F - 0.35X_1 - 0.7X_2)^2\,. \tag{6.141}$$

Thus,

$$\begin{aligned} k_0\frac{\partial\overline{U}}{\partial X_1} \;&=\; 1.2X_1 + 2(-0.65)(0.5F - 0.65X_1 - 0.3X_2) + 1.6(-0.35)(0.5F - 0.35X_1 \\ &\qquad -0.7X_2) \;=\; 2.241X_1 + 0.782X_2 - 0.930F, \\ k_0\frac{\partial\overline{U}}{\partial X_2} \;&=\; X_2 + 2(-0.3)(0.5F - 0.65X_1 - 0.3X_2) + 1.6(-0.7)(0.5F - 0.35X_1 \\ &\qquad -0.7X_2) \;=\; 0.782X_1 + 1.964X_2 - 0.860F\,, \end{aligned} \tag{6.142}$$

and setting the right-hand sides equal to zero yields precisely the same equations as those in Example 6.4.2.

Extremum Principles

Castigliano's first theorem can also be used to establish the special case in solid mechanics of the general physical *principle of minimum total potential energy*. According to this principle, if U is the internal potential energy (which in the case of elastic solids is just the strain energy) and V is the external potential energy, then in a stable equilibrium state the total potential energy $\Pi = U + V$ is minimum. In the case of mechanical systems subject to discrete loads F_i, the external potential energy is $V = -\sum_i F_i \Delta_i$. The potential energy as a function of the displacements is accordingly

$$\Pi(\Delta_1, \ldots, \Delta_n) = \frac{1}{2} \sum_{i=1}^{N} \sum_{j=1}^{N} k_{ij} \Delta_i \Delta_j - \sum_{i=1}^{N} F_i \Delta_i \,, \tag{6.143}$$

and, since the prescribed loads F_i are constants, Eqs. (6.131)$_1$ are equivalent to

$$\frac{\partial \Pi}{\partial \Delta_i} = 0 \,, \quad i = 1, \ldots, n \,. \tag{6.144}$$

Eqs. (6.144) are necessary (though not sufficient) conditions for the function Π to attain a minimum over all possible displacements Δ_i.

A useful application of the principle of minimum total potential energy is in the *approximate* solution of problems in elasticity. If the displacements are assumed to be determined by a smaller number of parameters (say A_i) and an approximation (say Π^*) to the total potential energy is accordingly determined as a function of the A_i, then the choice of these parameters that will make the *best approximation* (that is, that will come closest to satisfying equilibrium, energy being used as a measure of closeness) will be the one that minimizes Π^*. In other words, the A_i must satisfy

$$\frac{\partial \Pi^*}{\partial A_i} = 0 \tag{6.145}$$

in addition to the conditions for the corresponding value of Π^* to be a minimum.

The complementary version of this principle is essentially the same as Castigliano's second theorem applied to a system with constraints given by $\Delta_i = 0$ $(i = 1, \ldots, r)$. It can be generalized to the case of constraints with prescribed nonzero displacements $\overline{\Delta}_i$ by defining a "complementary potential energy" $\overline{\Pi} = \overline{U} - \sum_i X_i \overline{\Delta}_i$, and then compatibility is equivalent to an extremum (not necessarily minimum) of $\overline{\Pi}$.

Elastic Energy of a Continuum

In view of the additivity of energy, it follows that the elastic energy of a simple axially loaded bar is the sum of the energies of its constituent volume

elements. Considering a prismatic element of area ΔA and length Δx, and assuming uniform conditions, we find that the axial force acting on it is $\sigma_x \Delta A$ and its elongation is $\varepsilon_x \Delta x$, so that its energy is $\frac{1}{2}\sigma_x \varepsilon_x (\Delta A \Delta x)$, and since $\Delta A \Delta x$ is the volume element, the strain energy and complementary energy *per unit volume* are respectively

$$U^0 = \frac{1}{2} E \varepsilon_x^2 \quad , \quad \overline{U}^0 = \frac{\sigma_x^2}{2E} \tag{6.146}$$

by analogy with Eq. (6.118).

For a volume element in simple shear it follows from the definition of internal virtual work in shear, Eq. (5.46), that the strain energy and complementary per unit volume are given by

$$U^0 = \frac{1}{2} G \gamma_{xy}^2 \quad , \quad \overline{U}^0 = \frac{\tau_{xy}^2}{2G} \, . \tag{6.147}$$

Analogous expressions apply to the stress and strain components in an isotropic linearly elastic body. Therefore, the strain energy and complementary energy per unit volume U^0 and $\overline{U}^0$ can be obtained from the sum

$$\frac{1}{2}(\sigma_x \varepsilon_x + \sigma_y \varepsilon_y + \sigma_z \varepsilon_z + \tau_{yz}\gamma_{yz} + \tau_{xz}\gamma_{xz} + \tau_{xy}\gamma_{xy}) \tag{6.148}$$

by respectively expressing the stresses in terms of the strains, Eqs. (6.15) and (6.16), and the strains in terms of the stresses, Eqs. (6.13) and (6.14). The results are

$$\begin{aligned} U^0 = \frac{1}{2} \frac{E}{(1+\nu)(1-2\nu)} \Big[& (1-\nu)(\varepsilon_x^2 + \varepsilon_y^2 + \varepsilon_z^2) + 2\nu(\varepsilon_y \varepsilon_z + \varepsilon_z \varepsilon_x + \varepsilon_x \varepsilon_y) \\ & + \tfrac{1}{2}(1-2\nu)(\gamma_{yz}^2 + \gamma_{zx}^2 + \gamma_{xy}^2) \Big] \end{aligned} \tag{6.149}$$

and

$$\begin{aligned} \overline{U}^0 = \frac{1}{2E} \Big[& \sigma_x^2 + \sigma_y^2 + \sigma_z^2 - 2\nu(\sigma_y \sigma_z + \sigma_z \sigma_x + \sigma_x \sigma_y) \\ & + 2(1+\nu)(\tau_{yz}^2 + \tau_{zx}^2 + \tau_{xy}^2) \Big] . \end{aligned} \tag{6.150}$$

By analogy with Castigliano's theorems, the stress-strain relations can be written as

$$\sigma_x = \frac{\partial U^0}{\partial \varepsilon_x}, \ldots, \tau_{yz} = \frac{\partial U^0}{\partial \gamma_{yx}}, \ldots \, , \tag{6.151}$$

and

$$\varepsilon_x = \frac{\partial \overline{U}^0}{\partial \sigma_x}, \ldots, \gamma_{yz} = \frac{\partial \overline{U}^0}{\partial \tau_{yz}}, \ldots \, . \tag{6.152}$$

An exception must be made, however, for the validity of Eqs. (6.151) for the normal stresses when the material is incompressible, as defined in Sect. 6.2.

In that case, the normal stresses are indeterminate from (6.151) to within an additive constant that is common to all three. When solving for the stress in a body, this constant may be determined from the tractions applied at the boundary.

In terms of the matrix notation of Sect. 6.2.10 (page 264), Eqs. (6.149) and (6.150) can be written compactly as

$$U^0 = \tfrac{1}{2}\{\varepsilon\}^T[C]\{\varepsilon\} \quad , \quad \overline{U}^0 = \tfrac{1}{2}\{\sigma\}^T[C]^{-1}\{\sigma\} \, , \tag{6.153}$$

and Eqs. (6.151) and (6.152) as

$$\sigma_i = \frac{\partial U^0}{\partial \varepsilon_i} \quad , \quad \varepsilon_i = \frac{\partial \overline{U}^0}{\partial \sigma_i} \, , \quad i = 1, \ldots, 6 \, . \tag{6.154}$$

It follows from Eqs. $(6.54)_1$ (page 267) and $(6.154)_1$ that

$$\frac{\partial \sigma_i}{\partial \varepsilon_j} = C_{ij} = \frac{\partial^2 U^0}{\partial \varepsilon_i \partial \varepsilon_j} \, . \tag{6.155}$$

Since, as is well known, second partial derivatives are independent of the order of differentiation, it follows further that $C_{ij} = C_{ji}$ for all i, j, that is, the elasticity matrix $[C]$ is symmetric (in matrix notation, $[C] = [C]^T$), even when such symmetry is not imposed by the material structure (as we saw in the case of isotropic and cubically symmetric solids in Sect. 6.2). The same is necessarily true of the compliance matrix $[C]^{-1}$.

If the stress and strain components are decomposed into their hydrostatic and deviatoric parts, then we can show that, for an isotropic solid, the strain energy and complementary energy can be similarly decomposed. If, in Eq. (6.148), we write $\sigma_x = \overline{\sigma} + \sigma'_x$, $\varepsilon_x = \frac{1}{3}\varepsilon_V + \varepsilon'_x$, and similarly for the y- and z-components, then the sum of the first three terms in the expression in parentheses becomes

$$\begin{aligned} &\sigma_x\varepsilon_x + \sigma_y\varepsilon_y + \sigma_z\varepsilon_z \\ &\quad = (\overline{\sigma} + \sigma'_x)(\tfrac{1}{3}\varepsilon_V + \varepsilon'_x) + (\overline{\sigma} + \sigma'_y)(\tfrac{1}{3}\varepsilon_V + \varepsilon'_y) + (\overline{\sigma} + \sigma'_z)(\tfrac{1}{3}\varepsilon_V + \varepsilon'_z) \\ &\quad = \overline{\sigma}\varepsilon_V + \overline{\sigma}(\varepsilon'_x + \varepsilon'_y + \varepsilon'_z) + \tfrac{1}{3}(\sigma'_x + \sigma'_y + \sigma'_z)\varepsilon_V + (\sigma'_x\varepsilon'_x + \sigma'_y\varepsilon'_y + \sigma'_z\varepsilon'_z) \, . \end{aligned} \tag{6.156}$$

But the second and third terms in the last sum are identically zero because of the property of the deviatoric matrices shown in Eq. (6.30), from which it follows that

$$\sigma_x\varepsilon_x + \sigma_y\varepsilon_y + \sigma_z\varepsilon_z = \overline{\sigma}\varepsilon_V + (\sigma'_x\varepsilon'_x + \sigma'_y\varepsilon'_y + \sigma'_z\varepsilon'_z) \, . \tag{6.157}$$

We thus obtain, with the help of Eqs. (6.25) and (6.38),

$$U_0 = \frac{K}{2}\varepsilon_V^2 + \frac{G}{2}(2{\varepsilon'_x}^2 + 2{\varepsilon'_y}^2 + 2{\varepsilon'_z}^2 + \gamma_{yz}^2 + \gamma_{xz}^2 + \gamma_{xy}^2) \tag{6.158}$$

and

$$\overline{U}_0 = \frac{1}{2K}\bar{\sigma}^2 + \frac{1}{4G}(\sigma_x'^2 + \sigma_y'^2 + \sigma_z'^2 + 2\tau_{yz}^2 + 2\tau_{xz}^2 + 2\tau_{xy}^2) . \tag{6.159}$$

The decomposition of the energy is consistent with the principle that, in an isotropic linearly elastic solid, dilatation (involving hydrostatic stress and volumetric strain) and distortion (involving deviatoric stress and strain) are *uncoupled* effects, as discussed above (page 300).

The sum in parentheses in Eq. (6.159) is just twice the invariant J_2 defined by Eq. (6.32) (page 263), as can easily be ascertained by expressing the stress components in principal axes. The distortional complementary energy per unit volume is thus $J_2/2G$, equal to that in simple shear with $\tau = \sqrt{J_2}$.

Extremum Principles for Continua; the Finite-Element Method

The extremum principles discussed above for discrete systems apply to continua as well. The corresponding differential equations are generated from them by means of a mathematical method known as the *calculus of variations*.

Here, too, the principle of minimum potential energy is a powerful tool for finding approximate solutions, the already introduced finite-element method being perhaps the most prominent example of its application.

As we said in Sect. 6.4 (page 295), the displacement field within each finite element domain $\mathscr{R}_e$ is completely determined by the nodal (generalized) displacements, say Δ_i ($i = 1,\ldots,n$, where n is the total number of degrees of freedom of the nodes associated with the element). This displacement field is expressed in the form of linear combinations of low-order polynomial column-matrix-valued functions $\{N^e\}_i$ ($i = 1,\ldots,n$), called *element interpolation functions*, with the Δ_i as coefficients. It follows that the displacement field within each element domain can be expressed as

$$\{u\} = \sum_{i=1}^{n} \{N^e\}_i \Delta_i . \tag{6.160}$$

Since the strains are determined by the displacements through the strain-displacement relations (5.29), (5.31) and (5.33), they can likewise be so expressed, meaning that there exist column-matrix-valued functions $\{\phi^e\}_i$ ($i = 1,\ldots,n$) depending on the position of the nodes, such that, within the element domain,

$$\{\varepsilon\} = \sum_{i=1}^{n} \Delta_i \{\phi\}_i , \tag{6.161}$$

the summation being over the degrees of freedom associated with the element. Consequently, the total strain energy U_e stored in the element is, on the basis

of Eq. (6.153),

$$U^e = \frac{1}{2}\sum_{i=1}^{n}\sum_{j=1}^{n}\left(\int_{\mathscr{R}_e}\{\phi\}_i^T[C]\{\phi\}_j\,dV\right)\Delta_i\Delta_j\,. \tag{6.162}$$

The integrals inside the parentheses in Eq. (6.162) are denoted $k^e_{ij} = k^e_{ji}$; they are the *element stiffness coefficients*, and their symmetry follows from that of $[C]$. The total strain energy U of the system is given by the sum of the strain energies of all the elements, that is

$$U = \sum_e U^e\,. \tag{6.163}$$

Example 6.5.4: The T3 element.
It is common to designate polygonal elements as Tn or Qn if they are triangles or quadrilaterals, respectively, with n being the number of nodes. Some examples are shown in Fig. 6.31. The T3 is clearly the simplest two-dimensional finite el-

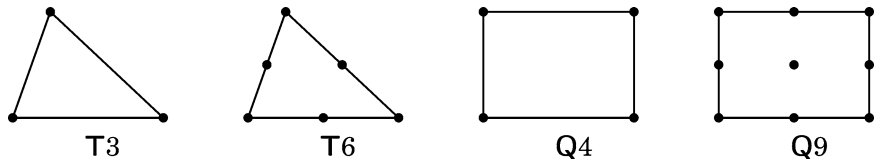

Figure 6.31. Some polygonal elements

ement; it has 6 degrees of freedom and is thus consistent with a linear variation of the displacements u and v across the element with position, given by

$$u(x,y) = A_1 + A_2x + A_3y \quad , \quad v(x,y) = B_1 + B_2x + B_3y\,,$$

so that the six constants $A_1,\ldots,B_3$ can be related to the nodal displacements $\Delta_1,\ldots,\Delta_6$. The strains in the element are therefore constant.
We will consider here a special case of such an element in the shape of a *right* triangle, with two adjacent ones shown in Fig. 6.32. The numbers in parenthe-

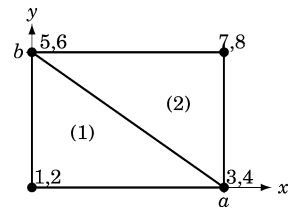

Figure 6.32. Adjacent right-triangle T3 elements

ses identify the elements, and the nodal indices are defined so that odd and even refer respectively to x- and y-displacements, so that Δ_1 is the x-displacement of the node at $(0,0)$ and so on. It is easy to see that, in element (1)

$$u(x,y) = \Delta_1 + (\Delta_3-\Delta_1)\frac{x}{a} + (\Delta_5-\Delta_1)\frac{y}{b} \quad , \quad v(x,y) = \Delta_2 + (\Delta_4-\Delta_2)\frac{x}{a} + (\Delta_6-\Delta_2)\frac{y}{b}\,.$$

(The corresponding expressions for element (2) are left to an exercise.) The $\{\phi\}_i$ for element (1) are therefore constant column matrices given by

$$\{\phi\}_1 = \begin{Bmatrix} -1/a \\ 0 \\ -1/b \end{Bmatrix}, \quad \{\phi\}_2 = \begin{Bmatrix} 0 \\ -1/b \\ -1/a \end{Bmatrix}, \quad \{\phi\}_3 = \begin{Bmatrix} 1/a \\ 0 \\ 0 \end{Bmatrix},$$

$$\{\phi\}_4 = \begin{Bmatrix} 0 \\ 0 \\ 1/a \end{Bmatrix}, \quad \{\phi\}_5 = \begin{Bmatrix} -1/a \\ 0 \\ -1/b \end{Bmatrix}, \quad \{\phi\}_6 = \begin{Bmatrix} 0 \\ 0 \\ 1/b \end{Bmatrix}.$$

If the thickness of the element (along the z-direction) is t then the k^e_{ij} are the products of the volume $abt/2$ and $\{\phi\}_i^T[C]\{\phi\}_j$. If the body is assumed to be in plane strain then $[C]$ is given by Eq. (6.49), and thus, for example,

$$\begin{aligned} k^{(1)}_{11} &= \frac{Eabt}{2(1+\nu)} \left\langle -\frac{1}{a} \quad 0 \quad -\frac{1}{b} \right\rangle \begin{bmatrix} \frac{1-\nu}{1-2\nu} & \frac{\nu}{1-2\nu} & 0 \\ \frac{\nu}{1-2\nu} & \frac{1-\nu}{1-2\nu} & 0 \\ 0 & 0 & \frac{1}{2} \end{bmatrix} \begin{Bmatrix} -\frac{1}{a} \\ 0 \\ -\frac{1}{b} \end{Bmatrix} \\ &= \frac{Et}{2(1+\nu)} \left[\frac{1-\nu}{1-2\nu} \frac{b}{a} + \frac{a}{2b} \right], \end{aligned}$$

and similarly for the other $k^{(1)}_{ij}$ $(i,j = 1,\ldots,6)$ and $k^{(2)}_{ij}$ $(i,j = 3,\ldots,8)$. It is obvious that, when the global stiffness matrix is assembled, $k_{ij} = 0$ for all pairs i,j such that one of them is 1 or 2 and the other is 7 or 8.

Exercises

6.5-1. Compute the total internal energy in the elastic compound bar of the figure due to the force $F = 100$ kips, where $E_1 = 10^4$ ksi, $E_2 = 5 \times 10^3$ ksi, and the sides of the square cross-sections have length $a_1 = 4$ in and $a_2 = 8$ in.

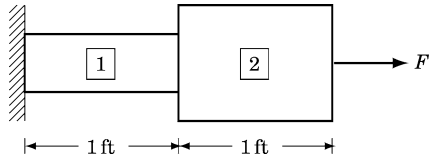

6.5-2. Assuming that the body of Exercise **5.3-2** (page 237) is of thickness 0.1 m (along the z-axis) and is in a state of plane stress, determine its total internal energy U if $E = 155$ GPa and $\nu = 0.33$.

6.5-3. For the block of Exercise **5.3-3** (page 238), in a state of plane strain, determine the internal energy U' per unit thickness along the z-axis if $E = 202$ GPa and $\nu = 0.29$.

6.5-4. For the two-bar truss of Exercise **6.3-1** (page 285), compute the total internal energy and the work done by the external force F, and use the fact that they are equal to determine the total displacement of point O.

6.5-5. For the structure of Exercise **6.3-4** (page 285), formulate the total internal energy U as a function of the horizontal and vertical displacements of point B, and calculate these displacements by Castigliano's first theorem (Eq. $(6.138)_1$).

6.5-6. For the structure of Exercise **6.3-4** (page 285), formulate the total complementary energy $\overline{U}$ as a function of the load F, and calculate the vertical displacement of point B by Castigliano's second theorem (Eq. $(6.138)_2$). How would you use this theorem to calculate the horizontal displacement as well?

6.5-7. For the bar of Exercise **6.3-8** (page 287), with the load-application points numbered $1,\ldots,4$ from left to right, formulate the total internal energy U as a function of the horizontal displacements $\Delta_1,\ldots,\Delta_4$, and calculate these displacements by Castigliano's first theorem (Eq. $(6.138)_1$).

6.5-8. For the bar of Exercise **6.3-8** (page 287), with the applied loads designated $F_1,\ldots,F_4$ from left to right, formulate the total complementary energy $\overline{U}$ as a function of these loads, and calculate the conjugate displacements $\Delta_1,\ldots,\Delta_4$ by Castigliano's second theorem (Eq. $(6.138)_2$).

6.5-9. Find the bar forces in Exercise **6.4-11** (page 299) using Castigliano's second theorem (Eq. $(6.138)_2$).

6.5-10. For an isotropic, linearly elastic solid, find the strain energy and complementary energy per unit volume for a state of plane stress in the xy-plane.

6.5-11. For an isotropic, linearly elastic solid, find the strain energy and complementary energy per unit volume for a state of plane strain in the xy-plane.

6.5-12. Show that the sum in parentheses in Eq. (6.159) is equal to J_2.

6.5-13. Find expressions for $u(x,y)$ and $v(x,y)$ in element (2) of Example 6.5.4 in terms of $\Delta_3,\ldots,\Delta_8$.

6.5-14. For a T3 element that is not a right triangle but has the dimensions shown in the figure below, find the matrices $\{\phi\}_i$ $(i=1,\ldots,6)$.

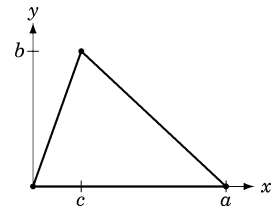

6.5-15. Find $k_{12}^{(1)}$ and $k_{22}^{(1)}$ for Example 6.5.4.

6.5-16. Find $k_{33}^{(1)}$ and $k_{33}^{(2)}$ for Example 6.5.4.

6.6 Thermoelastic Properties of Solids

6.6.1 Introduction

The relations between stress and strain that have been discussed in this chapter up to now have ignored the effect of temperature. It is, however, well known that the behavior of solids may be highly influenced by temperature, which, as discussed in Sect. 1.1 (page 7), is a measure of thermal energy, representing the vibration of atoms and the random motion of molecules.

One example is the dependence of the elastic moduli E and G on temperature. In most relatively stiff solids, these moduli decrease with temperature, that is, the material becomes more compliant as it is heated.* For rubberlike solids, on the other hand, the elastic moduli increase with temperature, as can be seen by hanging a weight from a rubber band—producing an initial stretch—and then heating it or cooling it, causing it to contract or stretch, respectively.

An even more important temperature effect on the behavior of solids is in the generation of thermal strains and stresses, which is discussed below.

6.6.2 Thermal Strain

Changes in the temperature of unconstrained solids lead to thermal expansion (or contraction), evidenced as *thermal strain* at constant (even zero) stress. In unconstrained isotropic solids, this strain is purely volumetric, as illustrated in Fig. 6.33. That is, the longitudinal strain components ε_x, ε_y and

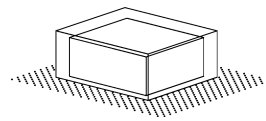

Figure 6.33. Thermal expansion of a rectangular block resting on a frictionless flat surface

ε_z all change by the same amount, which is proportional to the temperature change:

$$\varepsilon_x^{\mathrm{t}} = \varepsilon_y^{\mathrm{t}} = \varepsilon_z^{\mathrm{t}} = \alpha(T - T_0)\,. \tag{6.164}$$

Here the superscript "t" stands for "thermal", T denotes the current temperature with T_0 being a reference temperature (at which there is no thermal strain), and α is a material property known as *linear coefficient of thermal expansion*. (Clearly, the volumetric strain is $\varepsilon_{\mathrm{V}}^{\mathrm{t}} = 3\alpha(T - T_0)$.) Values of α for a range of materials materials are shown in Tables B-5 (SI, page 519) and B-6 (US, page 520).

*At the melting point, in particular, the shear modulus must decrease to zero, since a liquid, by definition, has no shear resistance at rest.

If the temperature change in the body is uniform and the body is free to expand, its deformation is a uniform volume change. If the temperature change varies through the body, then the strain-displacement relations (5.29), with the local values of $\alpha(T - T_0)$ on the left-hand sides, must be integrated to yield the displacement field resulting from the temperature change, as in the following example.

Example 6.6.1: Thermal deformation of a bar under a linearly varying temperature.
A bar of length L, initially at a uniform temperature T_0, is placed in environment where the temperature varies linearly from T_1 and one end (say $x = 0$) and T_2 at the other (say $x = L$), with $T_2 > T_1$. We wish to find the elongation of the bar.
The longitudinal thermal strain is

$$\varepsilon_x^t = \alpha[T_1 - T_0 + (T_2 - T_1)x/L] ,$$

and therefore, by Eq. (5.13),

$$\Delta L = \alpha[(T_1 - T_0)L + (T_2 - T_1)(L/2)] = \alpha\left(\frac{T_1 + T_2}{2} - T_0\right)L .$$

In a body subject to nonuniform heating or cooling, the temperature will in general vary in both space and time, the variation being governed by the *heat equation*. When the external heating conditions become constant in time, the temperature will eventually attain an equilibrium distribution, which in a homogeneous one-dimensional body such as a bar is linear (as in the preceding example), while in two dimensions it must satisfy the *Laplace equation*

$$\frac{\partial^2 T}{\partial x^2} + \frac{\partial^2 T}{\partial y^2} = 0 . \tag{6.165}$$

Note that this equation is satisfied by a temperature field of the form

$$T(x, y) = A_1 + A_2 x + A_3 y + A_4 xy , \tag{6.166}$$

and such a form can be used, for example, in a rectangular region along whose boundary the temperature varies linearly between the corners. In this case, the constants A_i, $i = 1, \ldots, 4$, are determined from the prescribed boundary temperatures.

When the body is under stress, whether initially or as a result of constraints that prevent free thermal expansion, we may, using the principle of superposition, add the thermal strains given by Eq. (6.164) to the elastic ones given by Eqs. (6.13) to produce the *thermoelastic* strain-stress-temperature

relations,

$$\begin{aligned}\varepsilon_x &= \frac{1}{E}(\sigma_x - \nu\sigma_y - \nu\sigma_z) + \alpha(T - T_0)\,,\\ \varepsilon_y &= \frac{1}{E}(\sigma_y - \nu\sigma_z - \nu\sigma_x) + \alpha(T - T_0)\,,\\ \varepsilon_z &= \frac{1}{E}(\sigma_z - \nu\sigma_x - \nu\sigma_y) + \alpha(T - T_0)\,.\end{aligned} \tag{6.167}$$

Eqs. (6.14) governing the shear strains, on the other hand, are not affected by the changes in temperature.

In anisotropic bodies the thermal strain is not, in general, purely volumetric. Indeed, one may envision an unconstrained body with a much higher coefficient of thermal expansion along, say, the x-axis than along the y-axis. In this case, an increase in temperature makes the body expand much more along the x- than the y-axis. The resulting deformation now consists of both volumetric and deviatoric parts.

6.6.3 Thermal Stress

If a body is statically determinate at both the structural and the continuum level, then the stresses are determined entirely by the external loads through the equilibrium equations. Therefore, in the absence of such loads, the stresses are zero, so that any deformation occurring in the body as a result of temperature change is purely thermal. If, however, there is static indeterminacy due to constraints that restrict deformation, then a temperature change may produce stresses even when there is no load. Such stresses are known as *thermal stresses*.

The simplest example is given by a uniform, homogeneous bar that is fixed at both ends. In such a bar $\varepsilon_x = 0$, and therefore, if the state of stress in the bar is assumed as uniaxial, Eq. $(6.167)_1$ yields

$$\sigma_x = -E\alpha(T - T_0)\,. \tag{6.168}$$

Note that the stress is compressive on heating and tensile on cooling. Recall that, as was mentioned in Sect. 2.4, slender members under a compressive axial force will buckle if the force is great enough; buckling due to heating is known as *thermal buckling*.

A slightly more complicated example will now be considered.

Example 6.6.2: Thermal stresses in a compound bar.
We consider a compound bar like that in Fig. 6.22, without the load F. Equilibrium requires the axial force P to be constant, and compatibility requires the total elongation $\Delta L = \Delta L_1 + \Delta L_2$ to be zero. Now the elongation of each component bar is the sum of the elastic elongation P/k_i and the thermal elongation

$\alpha_1(T-T_0)L_i$ $(i=1,2)$. Consequently,

$$P = -k(\alpha_1 L_1 + \alpha_2 L_2)(T-T_0)\,,$$

where $k = k_1k_2/(k_1+k_2)$. The stresses are given by P/A_1 and P/A_2.

A similar complication arises when the temperature varies along a uniform bar. Details are left to an exercise.

6.6.4 Thermoelastic Energy Relations

The thermoelastic relations between stress and strain can be written in terms of energy functions, as in Eqs. (6.151) and (6.152), provided the strain energy and complementary energy are appropriately generalized. When elastic energy is generalized to include dependence on temperature it is known as *free energy*, and the generalizations of strain energy and complementary energy are respectively known as the *Helmholtz*[†] and the *Gibbs*[‡] free energy.

If the Helmholtz and Gibbs free energies per unit volume are denoted Ψ^0 and Φ^0, respectively, then their forms for isotropic linearly thermoelastic solids may be obtained by adding the terms $-[E\alpha/(1-2\nu)](\varepsilon_x+\varepsilon_y+\varepsilon_z)(T-T_0)$ and $\alpha(\sigma_x+\sigma_y+\sigma_z)(T-T_0)$, in addition to terms depending on the temperature only[§], to the strain and complementary energies given by Eqs. (6.149) and (6.150), respectively. These lead to the thermoelastic stress-strain-temperature and strain-stress-temperature relations in the form

$$\sigma_x = \frac{\partial \Psi^0}{\partial \varepsilon_x}, \ldots \tag{6.169}$$

and

$$\varepsilon_x = \frac{\partial \Phi^0}{\partial \sigma_x}, \ldots\,. \tag{6.170}$$

[†]Hermann von Helmholtz (1821–1894) was a German physiologist and physicist.

[‡]Josiah Willard Gibbs (1839–1903) was an American physicist, chemist and mathematician.

[§]Such terms are necessary for the derivation of the specific heat.

Exercises

6.6-1. Explain why, in an isotropic material, no shear strain is produced by a temperature change.

6.6-2. A cylindrical rod made of an elastic material with Young's modulus E, Poisson's ratio ν and linear thermal-expansion coefficient α is confined in a rigid matrix so that it cannot expand laterally but is free to do so longitudinally. Given a temperature change ΔT, find the ratio between the longitudinal strain ε_l and ΔT.

6.6-3. A steel plate assumed to be in a state of plane stress (in the xy-plane) is constrained so that it cannot expand in its plane and is subjected to a temperature increase of 15°C. If $E = 200\,\text{GPa}$, $\nu = 0.3$ and $\alpha = 14 \cdot 10^{-6}/°\text{C}$, find the resulting state of stress.

6.6-4. Solve the problem of the preceding exercise with the change that the plate cannot expand in the x-direction but is free to expand in the y-direction.

6.6-5. Show that, for a uniform, homogeneous bar that is fixed at both ends and whose temperature changes from a uniform initial temperature T_0 to a varying temperature $T(x)$, Eq. (6.168) may be replaced by $\sigma_x = -E\alpha(\overline{T} - T_0)$, where $\overline{T}$ is the average temperature of the bar.

6.6-6. In the compound bar shown in the figure, segments 1 and 3 are aluminum cylinders ($E = 69\,\text{GPa}$, $\alpha = 22.2 \times 10^{-6}/°\text{K}$, diameter 10 cm) and segment 2 is a brass cylinder ($E = 102\,\text{GPa}$, $\alpha = 18.7 \times 10^{-6}/°\text{K}$, diameter 8 cm). If the bar is initially unstressed and then heated uniformly from 20°C to 40°C, determine (a) the displacements of the junctions 12 and 23, and (b) the axial stress in each segment.

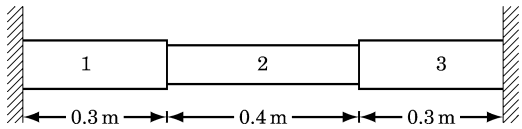

6.6-7. Solve the problem of the preceding exercise if the heating is not uniform but such that the final temperature varies linearly from 30°C at the left end to 50°C at the right end.

6.6-8. The circular bar of length L shown in the figure is constrained to just fit between two fixed supports at points A and B at a given temperature T. The bar is made of an elastic material with Young's modulus E and coefficient of thermal expansion α. Also, the cross-section of the bar has radius r_A at point A and r_B at point B. Suppose that the temperature of the bar increases uniformly to $T + \Delta T$.

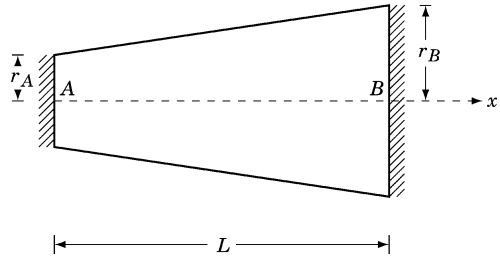

(a) Determine the resultant reactions at A and B in terms of E, α, ΔT, r_A and r_B.

(b) Use the result of part (a) to determine the location and magnitude of the maximum value of the average normal stress in the bar, in terms of E, α, ΔT, r_A and r_B.

6.6-9. A circular disk of thickness t rests in frictionless contact on a rigid plate. Another such plate is placed above it, the distance between the plates being (and remaining) $t + d$, as shown in the figure. The disk is then subjected to heating, the initial temperature being T_0.

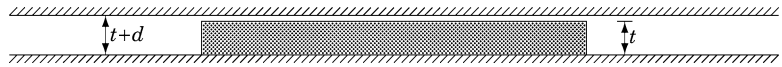

(a) Determine the temperature T_1 at which the disk just touches the upper plate, in terms of E, ν, α, t, d, and T_0.

(b) If the disk is heated further, determine the pressure developed between it and the plates for $T > T_1$.

(c) Assuming that the in-plane stresses remain zero, determine the in-plane longitudinal strains for $T > T_1$.

6.6-10. Consider a weightless rigid block supported by three parallel rods, each of uniform cross sectional area A, as shown in the following figure. The outer rods are symmetrically positioned with reference to the center rod, and are made of a linear elastic material with Young's modulus E_1 and linear coefficient of thermal expansion α_1. The center rod is made of a linear elastic material with Young's modulus E_2 and linear coefficient of thermal expansion α_2. When the system is at a uniform temperature T_0, all three rods are of equal length L_0 and are unstressed.

Assume now that the temperature of the system is increased to $T = T_0 + \Delta T$. Determine the displacement of the block and the stress in each rod under this thermal loading.

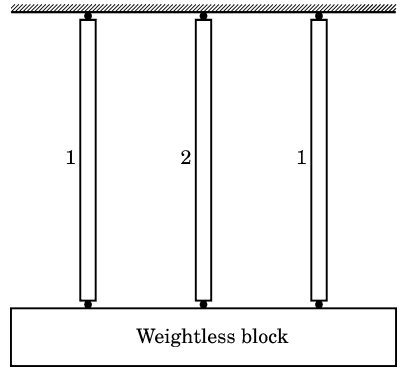

6.6-11. Suppose that a cube made of steel is fully and tightly enclosed in a rigid cavity, and is free of stress at room temperature. Calculate the stress in the cube when its temperature is raised by 20°C. Assume that the material properties of the cube are $E = 200\,\text{GPa}$, $\nu = 0.3$ and $\alpha = 12 \times 10^{-6}/^{\circ}\text{C}$.

6.6-12. The cylindrical bar of diameter $d = 0.1$ m shown in the figure is made of two parts with $E_1 = 20$ GPa, $\alpha_1 = 10^{-6}$ $1/^{o}$C and $E_2 = 50$ GPa, $\alpha_2 = 10^{-6}$ $1/^{o}$C. The bar is fixed on both ends and is initially free of stress. Subsequently, the bar is subjected to a force $F = 100$ kN at its midpoint and a temperature increase $\Delta T = 50°$C.

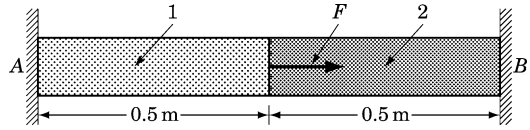

(a) Determine the reactions at A and B due to the combined effect of the applied force and the imposed temperature increase.

(b) Draw the axial force diagram for the bar.

(c) Find the total elongation of each of the two parts of the bar.

Chapter 7

Torsion

7.1 Torsion of elastic circular bars

7.1.1 Introduction

As we established in Sect. 4.3.3, the shear stress τ in a thin-walled circular tube of mean radius r subject to a torque T can be determined independently of the material properties and is given (at least far enough away from the ends, in accordance with Saint-Venant's principle) by Eq. (4.15),

$$\tau = \frac{T}{2\pi r^2 t} . \tag{7.1}$$

A circular shaft, whether hollow (that is, a thick-walled tube) or solid, may be treated as a large set of concentric thin-walled tubes, as shown (in cross-section) in Fig. 7.1. If the inner and outer radii of the shaft are b and c,

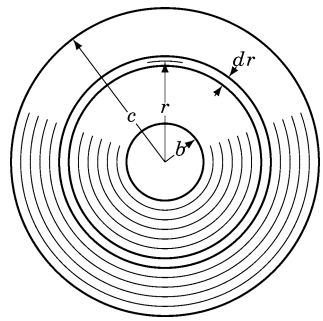

Figure 7.1. A circular shaft as a system of concentric thin-walled tubes

respectively (with the special case $b = 0$ representing a solid shaft), then a differential element of thickness dr at a mean radius r ($b < r < c$) may be

© Springer International Publishing Switzerland 2017

J. Lubliner, P. Papadopoulos, *Introduction to Solid Mechanics*,
DOI 10.1007/978-3-319-18878-2_7

regarded as a thin-walled tube carrying a torque dT, such that, in accord with Eq. (7.1),

$$dT = 2\pi\tau(r)r^2 dr \,, \tag{7.2}$$

where $\tau(r)$ is the average shear stress in the given differential element. The total torque is consequently given by

$$T = 2\pi \int_b^c \tau(r)r^2 dr \,. \tag{7.3}$$

That the tube is locally in equilibrium is discussed in Example 4.5.2 (page 191). What cannot be determined by equilibrium alone is the distribution $\tau(r)$ of the shear stress across the shaft; in fact, it can be shown that the number of possible distributions that are in equilibrium with an applied torque T is infinite. In other words, with the resultant torque known everywhere in the shaft, the system of concentric thin-walled tubes is *externally statically determinate* but *locally statically indeterminate*.

7.1.2 Twist of an elastic thin-walled tube

We now go back to the thin-walled tube of Sect. 4.3. Let the longitudinal axis of the tube coincide with the x-axis and occupy the interval $0 < x < L$, where L is the length of the tube. Consider a short annular element located between x and $x+dx$, and out of that element cut an almost-rectangular segment subtending the infinitesimal angle $d\theta$, as shown in Fig. 7.2a, with shear stresses acting on the cut planes as illustrated by the arrows. The shear stress cor-

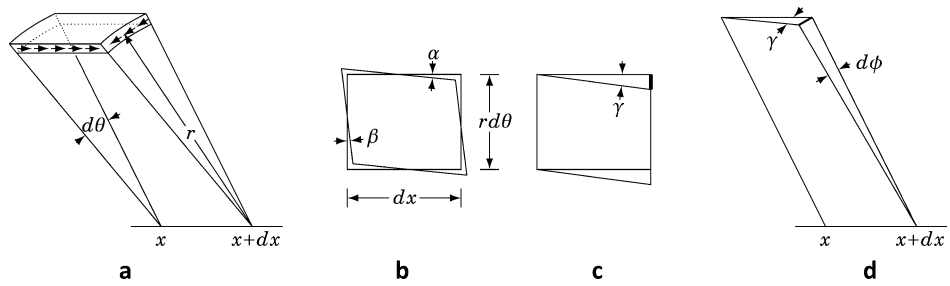

Figure 7.2. Shear strain in a twisted thin-walled circular tube

responds to a shear deformation (discussed in Sect. 5.2) shown in Fig. 7.2b, where the element is depicted in plane view (the slight curvature being disregarded). As in Fig. 5.8 (page 226), the shear strain γ is equal to the sum of the angles α and β. In the present case, α represents the deformation of the generators of the cylinder into helices, which, in turn, represents the *twisting* of the tube. More specifically, a member is said to twist if different cross-sections along its axis rotate relative to one another. The *angle of twist* of the section at x with respect to its initial position is denoted $\phi(x)$. If $\phi(x)$ is

constant, then there is no twist, only a rigid-body rotation. The angle of twist per unit length, ϕ' (or $d\phi/dx$), is called simply the *twist* of the tube.

The angle β represents *warping*, that is, the deformation of a previously plane cross-section into a curved one. In the case of a uniform circular tube, however, we can demonstrate by a simple symmetry argument that no such warping can take place, since any nontrivial warping pattern would violate circular symmetry,* which is assumed to hold after twisting (an assumption that is valid for small twists). Consequently, $\beta = 0$ and the actual deformed shape of the element is as shown in Fig. 7.2c. We now relate the shear angle γ to the differential twist $d\phi$ [$= \phi(x + dx) - \phi(x) = \phi' dx$] between the sections at x and at $x + dx$, illustrated in Fig. 7.2d. We accomplish this by showing that the length of the thick-lined line segment in Figs. 7.2c and 7.2d is given by both γdx and $r d\phi$ (this is another example of a compatibility condition), so that

$$\gamma = r\phi' . \tag{7.4}$$

Combining Eqs. (7.1) and (7.4) with the linearly elastic stress-strain relation (6.5) leads to the *torque-twist relation* for an elastic thin-walled circular tube:

$$T = 2\pi r^3 t G \phi' . \tag{7.5}$$

We note that if the relation between the shear stress τ and the shear strain γ were not linearly elastic, then the torque-twist relation would still have the same form as the uniaxial stress-strain relation, since in a thin-walled tube both the relation between stress and torque and that between strain and twist are linear, regardless of material properties.

7.1.3 Twist of a thick-walled or solid shaft

The preceding analysis may be applied to each of the concentric thin-walled tubes that make up the thick-walled tube shown in Fig. 7.1, provided we can show that all these concentric elements have the same twist ϕ. In order to show that this is the case, we use another symmetry argument and a proof by contradiction. Let there be an observer at each end of the shaft, with each of them facing the shaft and applying a counterclockwise torque, as shown in Fig. 7.3a. It stands to reason that, by symmetry, each observer should see the same deformation. Now suppose that, from the point of view of Observer 1, the outer elements twist more than the inner ones; then what was initially a diametric line will become curved as shown in Fig. 7.3b. Now, since all segments of the shaft undergo the same torque, the same deformation must appear at all cross-sections. But Observer 2 will see the cross-sections deform as in Fig. 7.3c, contradicting the symmetry. Consequently, diametric lines do not curve, meaning that all the concentric tubes undergo the same twist ϕ'. It

*In fact, it is *only* in the case of circular symmetry that no warping takes place.

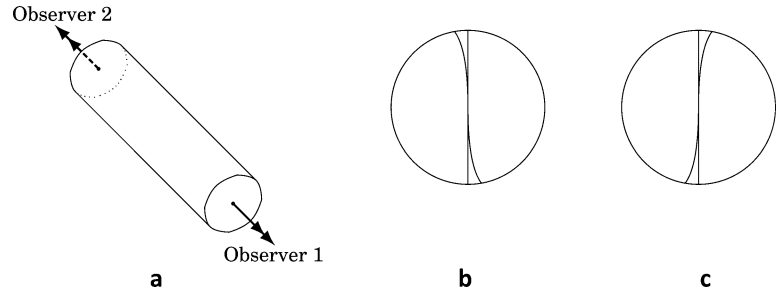

Figure 7.3. Symmetry argument showing that all concentric tubes undergo the same twist

follows that Eq. (7.4) for the shear strain applies at all r in the thick-walled tube, and therefore, appealing again to Eq. (6.5), we see that the shear stress as a function of r is

$$\tau(r) \;=\; G\phi' r \;. \tag{7.6}$$

Inserting this into Eq. (7.3) yields the torque-twist relation

$$T \;=\; 2\pi G\phi' \int_b^c r^3\, dr \;=\; G\frac{\pi(c^4-b^4)}{2}\phi' \;. \tag{7.7}$$

The special case $b = 0$ corresponds to the solid cylindrical shaft, for which

$$T \;=\; G\frac{\pi c^4}{2}\phi' \;. \tag{7.8}$$

The general theory of torsion of elastic shafts (which is not developed in this book, but is briefly discussed in Sect. 7.4) shows that for all homogeneous elastic shafts with shear modulus G, the torque-twist relation can be written in the form

$$T \;=\; GJ\phi' \;, \tag{7.9}$$

where the product GJ is known as the *torsional rigidity* of the shaft, and J is a quantity of dimension $[L]^4$ determined by the geometry of the cross-section. In the case of the circular shaft, J is also equal to $I_p = \int_{\mathscr{A}} r^2 dA = \int_{\mathscr{A}} (y^2+z^2) dA$, an integral that for a general area $\mathscr{A}$ in the yz-plane is known as the *polar second moment of area* (also called *polar moment of inertia*)[†]. But the identity $J = I_p$ holds only in the case of circular symmetry; otherwise, it can be shown that $J < I_p$.

Returning to circular shafts, if we now write

$$J \;=\; \frac{\pi(c^4-b^4)}{2} \;, \tag{7.10}$$

[†]Second moments of area ("moments of inertia") will be discussed further in Sect. 8.2.

then Eqs. (7.6) and (7.8) imply that the shear-stress distribution in a thick-walled tube or solid shaft under a torque T is given by

$$\tau(r) = \frac{Tr}{J} \tag{7.11}$$

and the maximum shear stress, which clearly occurs at $r = c$, is

$$\tau_{\max} = \frac{Tc}{J} . \tag{7.12}$$

Eq. (7.12) is used in the stress-based design of shafts in the same way that $\sigma = P/A$ is used in the stress-based design of axial bars, except that it is limited to the elastic range. In the special case of a solid circular shaft, with J given by Eq. (7.10) with $b = 0$, Eq. (7.12) reduces to

$$\tau_{\max} = \frac{2T}{\pi c^3} . \tag{7.13}$$

Example 7.1.1: Limiting case of thin-walled circular tubes in torsion.
In order to show that the result for thin-walled tubes, Eq. (7.5), is in fact a good approximation for an elastic tube when its thickness is small, we let $r = \frac{1}{2}(b+c)$ and $t = c - b$ and note that

$$c^4 - b^4 = (c-b)(b+c)(b^2+c^2) . \tag{7.14}$$

Now, $(c-b)(b+c) = 2tr$ and

$$b^2 + c^2 = (r - \tfrac{1}{2}t)^2 + (r + \tfrac{1}{2}t)^2 = 2r^2[1 + (t/2r)^2] . \tag{7.15}$$

Consequently, $J = 2\pi t r^3[1 + (t/2r)^2]$, so that the error in applying Eq. (7.5) is of the order of the square of the thickness-to-diameter ratio. If this ratio is, for example, 1/10, then the error is one percent.

The application of Eq. (7.12) to stress-based design is illustrated in the following example.

Example 7.1.2: Stress-based design of a hollow shaft.
A tube made of a high-strength aluminum alloy is to be used as a shaft to transmit a torque of 5.0 k·in. If the outer diameter is to be 1.2 in, we wish to find the largest value of the inner diameter (that is, the thinnest possible tube) such that the allowable shear stress of 20 ksi will not be exceeded. We can use Eq. (7.12) to determine the minimum value of J:

$$J_{\min} = \frac{Tc}{\tau_{\text{all}}} = \frac{5.0 \text{ kip}\cdot\text{in}\cdot 0.6 \text{ in}}{20 \text{kip}\cdot\text{in}^{-2}} = 0.15 \text{ in}^4 .$$

From Eq. (7.10) it follows that

$$b = \left(c^4 - \frac{2J}{\pi}\right)^{1/4} ,$$

and therefore $b_{\max} = [0.6^4 - (2\cdot 0.15/\pi)]^{1/4}$ in $= 0.43$ in. The maximum inner diameter is therefore 0.86 in, and the minimum thickness is 0.34 in.

7.1.4 Angle of Twist

For a shaft whose axis occupies an interval of length L along the x-axis (say $0 < x < L$), the total angle of twist is

$$\Delta\phi \;=\; \phi(L) - \phi(0) \;=\; \int_0^L \phi'(x)\,dx\;. \tag{7.16}$$

If $\phi' = T/GJ$ is constant, it follows from Eq. (7.9) that

$$T \;=\; \frac{GJ}{L}\Delta\phi\;. \tag{7.17}$$

The quantity GJ/L, representing the ratio of the applied torque to the twist, is known as the *torsional stiffness* . It is also the *torsional spring constant*, denoted $\bar{k}$ in Sect. 6.1, of a shaft when the shaft is used as a rotational spring, as in Fig. 6.1d (page 248).

Example 7.1.3: Calculation of angle of twist.
A solid circular steel shaft of diameter 18 mm and length 600 mm carries a torque of 80 N·m. We wish to find the total angle of twist.
Using $G = 75$ GPa, we find

$$\frac{GJ}{L} = \frac{\pi}{2\cdot 0.6\ \text{m}} 75\cdot 10^9\ \text{N}\cdot\text{m}^{-2}(9\cdot 10^{-3}\ \text{m})^4 = 1.29\cdot 10^3\ \text{N}\cdot\text{m}\;,$$

from which

$$\Delta\phi = \frac{80\ \text{N}\cdot\text{m}}{1.29\cdot 10^3\ \text{N}\cdot\text{m}} = 0.062\ \text{rad} = 3.6^\circ\;.$$

7.1.5 Composite shafts

If a shaft is made of more than one material, with different values of the shear modulus G, then the analysis of the preceding section is still applicable, provided the composite cross-section has circular symmetry. The only difference is that G in Eq. (7.6) is now a function of r, and the result for the total torque is, instead of Eq. (7.7),

$$T \;=\; 2\pi\phi' \int_b^c G(r) r^3\,dr\;. \tag{7.18}$$

Example 7.1.4: Torsion of a composite shaft. Suppose, for example, that the shaft is made up of a solid inner core of radius c_1 and shear modulus G_1, rigidly bonded to a shell with outer radius c_2 and shear modulus G_2. Eq. (7.18) then becomes

$$T \;=\; 2\pi\phi' \left(G_1 \int_0^{c_1} r^3\,dr + G_2 \int_{c_1}^{c_2} r^3\,dr \right) \;=\; (G_1 J_1 + G_2 J_2)\phi'\;, \tag{7.19}$$

where J_1 and J_2 are the respective values of J, given by Eq. (7.10), for the core and the shell. We see that the torsional rigidities are additive, as befits elements

acting in parallel. As regards the shear stress, Eq. (7.6) applies in each material region with the respective value of G, so that

$$\tau(r) = \begin{cases} G_1\phi' r, & 0 < r < c_1 \\ G_2\phi' r, & c_1 < r < c_2 \end{cases} . \tag{7.20}$$

With the help of Eq. (7.19), we find the respective maximum stresses as

$$\tau_{\max i} = \frac{TG_i c_i}{G_1 J_1 + G_2 J_2} , \quad i = 1,2 . \tag{7.21}$$

In designing such a shaft, each maximum stress must be limited to the allowable shear stress in the corresponding material.

By analogy with the effective axial rigidity discussed in Sect. 6.3 (page 279), we may define the *effective torsional rigidity* $\overline{GJ}$ for non-homogeneous elastic shafts, such that

$$T = \overline{GJ}\phi' . \tag{7.22}$$

7.1.6 Virtual Work and Elastic Energy in Torsion

Since every part of the shaft is assumed to be in a state of simple shear, the internal virtual work per unit volume is given, in accord with Eq. (5.46) (page 235), by $\tau\delta\gamma$, and per unit length,upon using Eq. (7.3), by

$$\delta W'_{\text{int}} = \int_{\mathscr{A}} \tau\delta\gamma\, dA = 2\pi\delta\phi' \int_b^c \tau r^2\, dr = T\delta\phi' , \tag{7.23}$$

Thus, the total internal virtual work is

$$\delta W_{\text{int}} = T\delta\Delta\phi , \tag{7.24}$$

which, of course, equals the external virtual work of the applied torque. The increment of actual work (per unit length), as the twist goes from ϕ' to $\phi'+d\phi'$ is $Td\phi'$, and the actual work, stored as elastic energy per unit length, is

$$U'_{\text{tor}} = \int_0^{\phi'} (GJ\psi)d\psi = \frac{GJ\phi'^2}{2} \tag{7.25}$$

(here ψ is a dummy variable). It follows that the total elastic energy is now equal to

$$U = \frac{GJ(\Delta\phi)^2}{2L} . \tag{7.26}$$

On comparing with Eq. $(6.119)_1$, the right-hand side of (7.26) may be written as $\frac{1}{2}\bar{k}(\Delta\phi)^2$, where $\bar{k} = GJ/L$ is the aforementioned torsional stiffness (or spring constant) of the shaft. The preceding results are completely analogous to those for axial bars and translational spring constants. We may accordingly also express the complementary energy per unit length in torsion as

$$\overline{U}'_{\text{tor}} = \frac{T^2}{2GJ} . \tag{7.27}$$

Torque and Angle-of-Twist Diagrams

Torque and angle-of-twist diagrams for shafts with variable internal torque are found in exactly the same way as axial-force and elongation diagrams, respectively, for bars with variable internal axial force (Sect. 6.3, page 281), as shown in the following example.

Example 7.1.5: Torque and angle-of-twist diagrams.
Consider a uniform circular shaft of radius c and length L with the left end ($x = 0$) fixed and the right end ($x = L$) free, subject to concentrated torques $-\overline{T}$ at $x = L/2$ and $2\overline{T}$ at $x = L$, as shown in Fig. 7.4a. Free-body diagrams taken with cuts

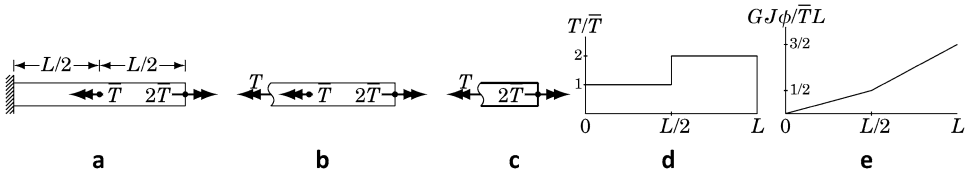

Figure 7.4. Construction of torque and angle-of-twist diagrams: (**a**) geometry and loading, (**b–c**) free-body diagrams, (**d**) torque diagram, (**e**) angle-of-twist diagram

at $0 < x < L/2$ and $L/2 < x < L$, shown in Fig. 7.4b and 7.4c, respectively, show that the respective internal torques there are $\overline{T}$ and $2\overline{T}$, resulting in the torque diagram shown in Fig. 7.4d. The angle-of-twist diagrams consequently have the respective slopes $\overline{T}/GJ$ and $2\overline{T}/GJ$, where $J = \pi c^4/2$, as seen in Fig. 7.4e.

7.1.7 Rotating Shaft

The angular velocity of a rotating body was discussed in Sect. 2.1 (page 58). But the rate of rotation is often expressed in terms of the *frequency* f in revolutions (or cycles) per unit time. Since one cycle equals 2π radians, it follows that $\omega = 2\pi f$ and $\Pi = 2\pi M f$ if ω is given in radians per second and the frequency in cycles per second, also known as *hertz* (Hz).[‡] The general expression for the power generated by a moment $\mathbf{M}$ on a rotating shaft is given by Eq. (2.22) (page 58). In the case of a shaft rotating about its axis with frequency f (or angular velocity ω), the power is given by $\Pi = T\omega = 2\pi T f$. If a shaft is to transmit this power from a motor running at the given speed, then the torque carried by the shaft is accordingly equal to $T = \Pi/\omega$ or

$$T = \frac{\Pi}{2\pi f} . \tag{7.28}$$

[‡]A factor of 60 is necessary when, as is often the case, the frequency is given in revolutions per minute (RPM) rather than per second.

Example 7.1.6: Stress-based design of a shaft for a given motor speed and power.
We wish to find the minimum diameter d of a sold circular steel shaft that is to transmit 40 kW of power at 15 Hz if the allowable shear stress is 100 MPa. Combining Eqs. (7.13) and (7.28) leads to

$$\tau_{\max} = \frac{\Pi}{\pi^2 c^3 f}$$

and therefore, if $\tau_{\max} \le \tau_{\text{all}}$,

$$d = 2c \ge 2\left(\frac{\Pi}{\pi^2 f \tau_{\text{all}}}\right)^{1/3} .$$

Now, since $1\,\text{W} = 1\,\text{J}\cdot\text{s}^{-1} = 1\,\text{N}\cdot\text{m}\cdot\text{s}^{-1}$, and since a hertz has the dimension s^{-1}, it follows that kW/Hz will be of dimensions $\text{kN}\cdot\text{m}$. When this dimension is divided by MPa = $10^3\text{kN}\cdot\text{m}^{-2}$, it becomes $10^{-3}\,\text{m}^3$. Hence

$$d_{\min} = 0.2\left(\frac{40}{\pi^2 \cdot 15 \cdot 100}\right)^{1/3} \text{m} = 28\ \text{mm} .$$

7.1.8 Closely Coiled Helical Springs

While the helical spring shown in Fig. 6.1a (page 248) is used as a translational spring, its internal response is primarily in torsion. When the spring is

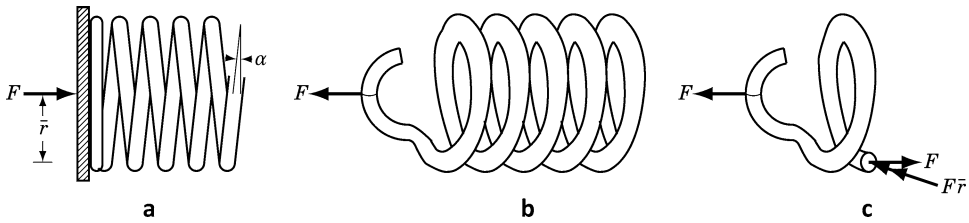

Figure 7.5. Closely coiled helical spring: (**a**) side view showing compressive force, (**b**) oblique view showing tensile force, (**c**) free-body diagram for an axial cut

used to transmit a compressive force, the turn of wire near the end is flattened to make it perpendicular to the axis of the helix, so that the force can be applied through a pressure plate or the like, as seen in a side view in Fig. 7.5a. For tension, a portion of wire near the end is bent into a hook whose furthest point is on the axis, as in Fig. 7.5b. Fig. 7.5c shows a free-body diagram for the subbody obtained by cutting the wire in an axial plane (that is, a longitudinal plane containing the helix axis). The internal resultant consists of a longitudinal force F and a moment $F\bar{r}$ perpendicular to the cut. Because the cut is at an angle α (the helix angle) with respect to the local transverse section of the bent wire, the internal force F has a shear component $F\cos\alpha$ and an axial component (with respect to the wire) $F\sin\alpha$. Similarly, the moment $F\bar{r}$ may

be resolved into a torque $F\bar{r}\cos\alpha$ and a bending moment $F\bar{r}\sin\alpha$. If, however, the helix angle α is small (in practice less than 10°), in which case the spring is referred to as *closely coiled*, then the effects of axial force and bending may be neglected. If, moreover, the wire diameter d is small compared to the helix radius $\bar{r}$ (the distance from the axis to the middle of the wire), then the effect of the shear force can also be neglected. We will show this by comparing the energy due to shear force with that due to torsion. While the distribution of shear stress due to the shear force cannot be determined by ordinary methods of analysis, its average value is $F/A = F/\pi(d/2)^2$, and consequently the order of magnitude of the complementary energy per unit length of wire, $\overline{U}'_{\text{sh}}$, is $F^2/2AG = 2F^2/\pi d^2 G$. The corresponding quantity due to torsion is, by Eq. (7.27),

$$\overline{U}'_{\text{tor}} = \frac{(F\bar{r})^2}{2G(d^4/32)} . \tag{7.29}$$

The ratio of $\overline{U}'_{\text{sh}}$ to $\overline{U}'_{\text{tor}}$ is therefore of order $(d/4\bar{r})^2$, so that the effect of shear force is negligible for thin-wired springs (as discussed in Sect. 6.5, page 300). For springs made of relatively thicker wire, correction factors have been derived. From Eq. (7.29) we may derive the total complementary energy by multiplying the right-hand side by the developed length of the wire. If the number of turns is N, then this length is $2N\pi\bar{r}\sec\alpha$, which may be replaced by $2N\pi\bar{r}$ if the spring is closely coiled. Consequently,

$$\overline{U} = \frac{F^2 64N\bar{r}^3}{2Gd^4} . \tag{7.30}$$

By comparison with Eq. $(6.118)_2$ (page 301), we immediately obtain the spring constant of a closely coiled thin-wired spring as

$$k = \frac{Gd^4}{64N\bar{r}^3} . \tag{7.31}$$

Exercises

7.1-1. A cylindrical tube of length 1 m, mean diameter 16 cm and thickness 2 cm is found to require a torque of 615 kN·m in order to twist it by one degree. Assuming the material to be linearly elastic and treating the tube as thin-walled, find the shear modulus G.

7.1-2. Solve the problem of the preceding exercise without treating the tube as thin-walled.

7.1-3. A pipe of outer and inner diameter 6 in and inner diameters 5 in is found to twist 0.132°/ft when subjected to a torque of 5 kip-ft. Assuming the material to be linearly elastic, find the shear modulus G.

7.1-4. Solve the problem of the preceding exercise by treating the pipe as a thin-walled tube.

7.1-5. For the homogeneous elastic solid shaft of radius 0.1 m, shown in the figure, draw the torque diagram and determine the angle of twist between its end points if $G = 100$ GPa. Also, determine the maximum shear stress and indicate the section of the shaft in which it occurs.

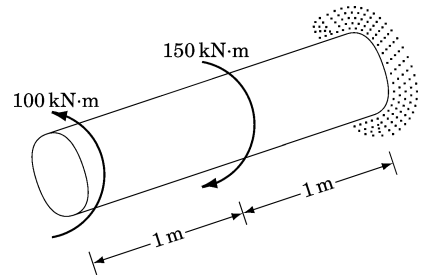

7.1-6. The thick-walled elastic shaft of the figure has inner radius of 0.05 m and outer radius of 0.1 m. The shaft is subjected to a distributed torque of 25 kN·m/m. Draw the torque diagram and determine the angle of twist between the end points of the shaft, assuming that $G = 50$ GPa. In addition, determine the distribution of the maximum shear stress along the axis of the shaft.

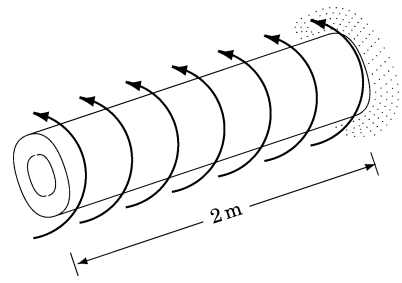

7.1-7. A solid steel shaft of 1.5-in diameter is encased in a brass tube with outer diameter 2 in.

(a) Assuming the shear modulus to be 10,600 ksi for steel and 5,400 ksi for brass, find the effective torsional rigidity $\overline{GJ}$ of the composite shaft.

(b) Assuming the allowable stress in shear to be 12 ksi in the steel and 7 ksi in the brass, find maximum allowable torque $T_{\max}$ that can be carried by the composite shaft.

7.1-8. A solid shaft of radius c, made of a metal with shear modulus G_1, is encased in a thin sleeve of thickness t, made of a plastic with shear modulus G_2. If t is small compared to c and G_2 is small compared to G_1, find the shear stress in the plastic when a torque T is applied to the composite shaft. Explain any approximating assumptions you make.

7.1-9. A hollow steel shaft, with an outer diameter of 2 in, is to transmit 70 hp (see page 7) of power at 18 Hz. If the allowable shear stress is 12 ksi, find the minimum wall thickness required.

7.1-10. Find that the lowest engine speed (in RPM) with which 35 kW of power can be transmitted by a solid brass shaft of diameter 1.5 cm if the allowable shear stress of 50 MPa is not to be exceeded.

7.1-11. For a closely coiled thin-wired helical spring, find the relation (a) between the maximum shear stress and the applied force, (b) between the maximum shear strain and the elongation.

7.1-12. For a spring made of 2-mm high-strength steel wire, with $\bar{r}$ = 12 mm and N = 15, find the spring constant k if G = 78 GPa, and the maximum force that can be transmitted if the shear stress is not to exceed 150 MPa.

7.2 Torsion of Non-Circular Thin-Walled Tubes

7.2.1 Shear Stress and Torque

As we discussed in Sect. 7.1, in a thin-walled circular tube subject to a torque T the shear stress is given by Eq. (7.1), independently of the material properties. If the tube is elastic, then the torque is related to the twist ϕ' as in Eq. (7.5).

If the cross-section of the thin-walled tube is not circular, or if the thickness is not uniform, the preceding results do not apply. In order to determine

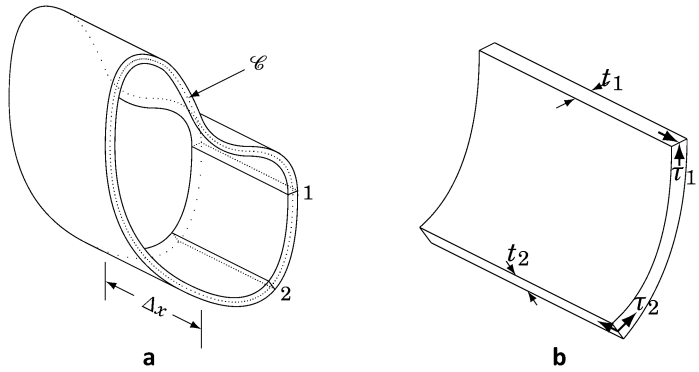

Figure 7.6. Torsion of a noncircular tube

the shear stress in such cases, we first cut out a slice of the tube, of thickness Δx, as shown in Fig. 7.6a, where the dotted curve $\mathscr{C}$ is the *mean curve* of the cross-section, and then we isolate the element bounded by the rectangles 1 and 2, as shown enlarged in Fig. 7.6b. If we assume, again, that the tube is thin enough so that we may neglect any variation in shear stress across the thickness, and if we let Δx go to the infinitesimal dx so that any variation in t along x may be neglected, then the equilibrium of forces in the x-direction (since there are no normal stresses) requires that

$$\tau_1 t_1 dx \;=\; \tau_2 t_2 dx \;. \tag{7.32}$$

Since the planes 1 and 2 are arbitrary, the product τt must be constant along the perimeter of the cross-section. This product is called *shear flow* and is designated q; it is a force per unit length. We may assume that in any small element of the cross-section the line of action of the shear flow is tangential to the mean curve, so that, on an infinitesimal element in which the length of the mean curve is ds, the force is $q\,ds$. Its moment arm about any fixed reference point O is r_t, the perpendicular distance between the local tangent to the mean curve and O, as in Fig. 7.7. The local contribution to the torque

is therefore $dT = qr_t\,ds$, and the total torque is

$$T = \oint qr_t\,ds = q\oint r_t\,ds\,, \tag{7.33}$$

the right-hand side of the equation resulting from the fact that q is constant.

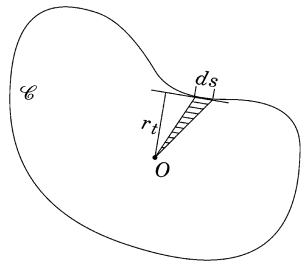

Figure 7.7. Geometry of thin-walled cross-section

As we can see from Fig. 7.7, the area of the cross-hatched triangle is $\frac{1}{2}r_t ds$. Consequently, the integral on the right-hand side of Eq. (7.33) is twice the area enclosed by the curve $\mathscr{C}$, which will be denoted $\overline{A}$, and therefore, upon using Eq. (7.33), we find that

$$T = 2\overline{A}q\,. \tag{7.34}$$

In view of the definition of q it follows that, at any point of the cross-section, the shear stress is given by

$$\tau = \frac{T}{2\overline{A}t}\,, \tag{7.35}$$

where t is the *local* thickness. Eq. (7.35) implies that

$$\tau_{\max} = \frac{T}{2\overline{A}t_{\min}}\,, \tag{7.36}$$

where $t_{\min}$ is the smallest thickness in the cross-section. This is especially important if the tube is made of parts with different thickness *and* different material properties.

It follows from the results derived here that the torsion of a thin-walled tube represents a *simple stress state* in the sense of Sect. 4.3, even if the tube is not circular, and Eq. (7.35) is just the generalization of Eq. (4.15) or (7.1) to the non-circular case.

7.2.2 Torque-Twist Relation

If the tube is made of a linearly elastic material, with shear modulus G, then a torque-twist relation can be derived as follows: the shear strain can be

expressed as $\gamma = \alpha + \beta$, where α and β represent the angle change due to twisting and warping, respectively, as in Fig. 7.2 (page 324). Now, if ds is, as above, a differential element of the curve $\mathscr{C}$, then βds is the infinitesimal increment in axial displacement, say du. Between any two points 1 and 2 on $\mathscr{C}$, consequently, $\int_1^2 \beta ds = u_2 - u_1$, but integrating all the way around $\mathscr{C}$ brings us back to point 1, and therefore $\oint_{\mathscr{C}} \beta ds = u_1 - u_1 = 0$, so that

$$\oint_{\mathscr{C}} \gamma ds = \oint_{\mathscr{C}} \alpha ds \,. \tag{7.37}$$

Now, in the same way that we derived $\alpha = r\phi'$ for a circular tube (Eq. (7.4), since in the circular tube $\gamma = \alpha$), we get $\alpha = r_t \phi'$, so that

$$\oint_{\mathscr{C}} \alpha ds = \oint_{\mathscr{C}} r_t \phi' ds = \phi' \oint_{\mathscr{C}} r_t ds = 2\bar{A}\phi' \,. \tag{7.38}$$

If we further let $\gamma = \tau/G$ with τ given by Eq. (7.35), we obtain

$$\oint_{\mathscr{C}} \gamma ds = \oint_{\mathscr{C}} \frac{\tau}{G} ds = \frac{T}{2\bar{A}G} \oint_{\mathscr{C}} \frac{ds}{t} \,. \tag{7.39}$$

Solving Eq. (7.39) for T and taking into account Eqs. (7.37) and (7.38), we arrive at

$$T = \frac{4\bar{A}^2}{\displaystyle\oint_{\mathscr{C}} \frac{ds}{t}} G\phi' \,. \tag{7.40}$$

In view of the definition of J in Sect. 7.1 (page 326), we may regard Eq. (7.40) as a special case of Eq. (7.9), with J given by

$$J = \frac{4\bar{A}^2}{\displaystyle\oint_{\mathscr{C}} \frac{ds}{t}} \,. \tag{7.41}$$

This result may be derived more quickly by equating the complementary energy per unit length, given by Eq. (7.27), with the area integral of the complementary per unit volume in simple shear, given by Eq.(6.147)$_2$ with τ_{xy} replaced by τ as given by Eq. (7.35). That is,

$$\frac{T^2}{2GJ} = \frac{1}{2G} \oint \left(\frac{T}{2\bar{A}t} \right)^2 t ds \,, \tag{7.42}$$

from which Eq. (7.41) follows immediately.

7.2.3 Examples

Some examples will now be considered. The first is an ordinary tube of non-circular cross-section.

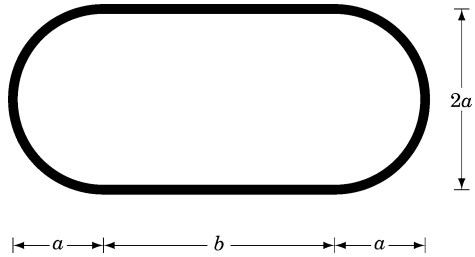

Figure 7.8. Cross-section of a thin-walled tube

Example 7.2.1: Torsion of a thin-walled tube. We consider the thin-walled tube with a cross-section shown in Fig. 7.8 and assume that the thickness is constant and equal to t.

If the cross-section is subjected to a torque T, then Eq. (7.35) implies that the shear stress is

$$\tau = \frac{T}{2(\pi a^2 + 2ab)t} .$$

In addition, the torsional rigidity of the cross-section can be deduced from (7.41) as

$$GJ = \frac{4G\bar{A}^2}{\oint_{\mathscr{C}} \frac{ds}{t}} = \frac{2G(\pi a^2 + 2ab)^2 t}{\pi a + b} .$$

A thin-walled tube that contains an internal partition is usually referred to in structural and aircraft engineering practice as *multicell*, an example of which will now be studied.

Example 7.2.2: Torsion of a two-cell airfoil. We consider the two-cell airfoil cross-section shown in Fig. 7.9a (though the the three-cell cross-section of Fig. 7.9b is more typical in practice). As with a single-cell cross-section, we begin by noting that the shear flow has different values in different branches of the cross-section. In particular, let the shear flow around the i-th cell ($i = 1, 2, \ldots$) be q_i (taken as positive when oriented counterclockwise). Repeating the equilibrium argument that led to (7.32), we deduce that the shear flow in the branch between cells 1 and 2 is $q_1 - q_2$. Another way of appreciating this point is to note that the shear flow in such a branch results from the superposition of the shear flows associated with the two cells.

If we will limit ourselves to the two-cell section of Fig. 7.9a and assume that the thickness is constant and equal to t in all branches, it follows that the shear stress in the three parts of the cross-section is

$$\tau_1 = \frac{q_1}{t} \quad , \quad \tau_2 = \frac{q_2}{t} \quad , \quad \tau_3 = \frac{q_1 - q_2}{t} , \tag{7.43}$$

where τ_1 and τ_2 are the shear stresses in the outer walls of cells 1 and 2, respectively, and τ_3 is that in the inner wall.

Figure 7.9. Cross-sections of multicell airfoils: (**a**) two-cell, (**b**) three-cell

We note next that the total torque equals the sum of the torques due to the shear flow around each of the two cells. In view of Eqs. (7.35) and (7.43), this implies that

$$T = 2\overline{A}_1 q_1 + 2\overline{A}_2 q_2 = 2\overline{A}_1 \tau_1 t + 2\overline{A}_2 \tau_2 t \,, \tag{7.44}$$

where $\overline{A}_1$, $\overline{A}_2$ are the areas enclosed by the dotted curves labeled $\mathscr{C}_1$ and $\mathscr{C}_2$ in Fig. 7.9a.

Lastly, it follows from applying Eqs. (7.38) and (7.39) to each of the curves $\mathscr{C}_1$ and $\mathscr{C}_2$ that

$$\oint_{\mathscr{C}_1} \tau ds = 2\overline{A}_1 G\phi' \quad , \quad \oint_{\mathscr{C}_2} \tau ds = 2\overline{A}_2 G\phi' \,, \tag{7.45}$$

where τ is given by (7.43) for each branch of the cross-section.

Eqs. $(7.44)_2$ and (7.45) may be solved for T, τ_1, τ_2 and ϕ' in terms of the given geometric and material properties of the cross-section.

Exercises

7.2-1. Show that for a hollow circular shaft with outer radius $c_o = c + t/2$ and inner radius $c_i = c - t/2$, the torque-twist relation can be approximated by equation (7.5) if $t \ll c$.

7.2-2. Show that Eq. (7.35) reduces to Eq. (7.1) for a thin-walled circular tube of uniform thickness.

7.2-3. Determine the torsional rigidity of a homogeneous elastic thin-walled shaft with shear modulus G whose cross-section is an equilateral triangle of side a, with constant thickness t.

7.2-4. Determine the torsional rigidity of a homogeneous elastic thin-walled shaft with shear modulus G whose cross-section is a right triangle with legs a and b and with constant thickness t.

7.2-5. Determine the torsional rigidity of a homogeneous elastic thin-walled shaft with shear modulus G whose cross-section is an ellipse with semi-axes a and b and with constant thickness t.

7.2-6. Determine the torsional rigidity of a homogeneous elastic thin-walled shaft with shear modulus G and having a rectangular cross-section of constant thickness t, as in the figure. Find the relation between the lengths a and b that would maximize the torsional rigidity for fixed perimeter of the cross-section.

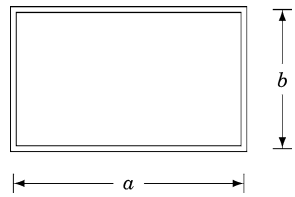

7.2-7. Consider an elastic thin-walled tube which is fixed on one end and free on the opposite end, as in the figure. The tube has a square cross-section of side a and thickness t, and is loaded by two torques T_1 and T_2.

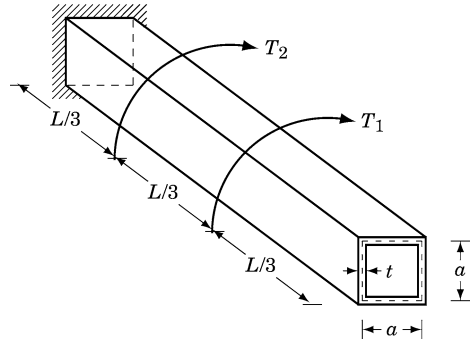

(a) Draw the torque diagram for the tube.

(b) Determine the value of the maximum shear stress in the tube.

(c) Determine the total twist of the tube due to the applied torques, assuming that the shear modulus is constant and equal to G.

7.2-8. Derive results analogous to those of Example 7.2.2 for the three-cell section of Fig. 7.9b.

7.2-9. Consider a shaft of symmetric rectangular two-cell cross-section as shown in the figure. How much (in percent) does the partition contribute to the torsional stiffness of the shaft?

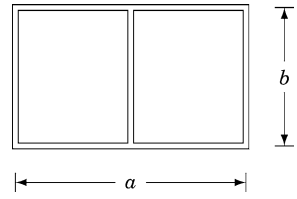

7.2-10. Consider a shaft of triangular two-cell cross-section as shown in the figure, with dimensions in centimeters and a uniform thickness of 1 cm. Calculate J, and compare with what the value would be without the partition.

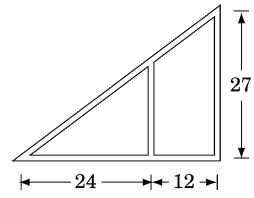

7.3 Compound Shafts

7.3.1 Compound Shafts

A *compound shaft* is usually taken to mean a shaft composed of several segments in series, with different values of GJ (or, more generally, $\overline{GJ}$). Here, we will generalize the definition somewhat to include all shafts in which $T/\overline{GJ}$ varies along the axis, whether due to the variation of $\overline{GJ}$, of T (though *uniform* shafts with variable internal torque have already been considered) or of both, and whether such variation is abrupt or continuous. In all such cases, the angle of twist at x (relative to $x = 0$) is found by integration of Eq. (7.22) to be

$$\phi(x) = \int_0^x \frac{T(x')}{\overline{GJ}(x')} dx' , \tag{7.46}$$

and the total angle of twist is of course $\phi(L)$.

If the variation in $\overline{GJ}$ or T is abrupt, then let the shaft be made up of a number (say n) of segments of length L_i ($i = 1,\ldots,n$), with $L = \sum_{i=1}^{n} L_i$, where in each segment both $\overline{GJ}$ and T are constant. It follows that within the i-th segment, the integrand of Eq. (7.46) has the value $T_i/\overline{GJ}_i$, and consequently

$$\phi(L) = \sum_{i=1}^{n} \frac{T_i L_i}{\overline{GJ}_i} . \tag{7.47}$$

In the special case of constant torque, we obtain the result that the rotational spring constant $\bar{k}$ of the shaft is given by

$$\frac{1}{\bar{k}} = \sum_{i=1}^{n} \frac{L_i}{\overline{GJ}_i} = \sum_{i=1}^{n} \frac{1}{\bar{k}_i} , \tag{7.48}$$

as would be expected for a system whose members are in series. Eq. (7.48) is completely analogous to Eq. (6.84) for axially loaded bars.

An example with continuous variation will now be considered.

Example 7.3.1: Tapered shaft.
One possible case of variable $\overline{GJ}$ occurs if the shaft is tapered, so that it is J that is variable. We assume that the shaft is slender enough for the theory of this chapter to apply as a reasonable approximation, and suppose that the shaft (of length L) is conical, with the radius c varying from c_1 (at $x = 0$) to c_2, with $c_2 > c_1$, so that $c(x) = c_1 + (c_2 - c_1)x/L$, and therefore $J(x) = (\pi/2)[c_1 + (c_2 - c_1)x/L]^4$, which can be rewritten as $J(x) = J_1[1 + (\lambda - 1)x/L]^4$, with $J_1 = \pi c_1^4/2$ and $\lambda = c_2/c_1$.
The maximum shear stress at any section is given by Eq. (7.12) with the local values of T, c and J. The angle of twist under a constant torque is

$$\phi(L) = \frac{T}{GJ_1} \int_0^L \frac{dx}{[1 + (\lambda - 1)x/L)^4} = \frac{TL}{GJ_1(\lambda - 1)} \int_1^\lambda \frac{d\xi}{\xi^4} = \frac{TL}{GJ_1} \frac{\lambda^2 + \lambda + 1}{3\lambda^3} .$$

Torque and Angle-of-Twist Diagrams

Torque diagrams for shafts with variable internal torque are found in exactly the same way as axial-force diagrams for bars with variable internal axial force (Sect. 6.3, page 281), using singularity functions (see Appendix A) if desired. Angle-of-twist diagrams are, by the same token, analogous to elongation diagrams.

Example 7.3.2: Compound shaft with two segments.
We consider a compound shaft analogous to the compound axially loaded bar of Fig. 6.29, but with torques $\overline{T}_1$ and $\overline{T}_2$ in place of the forces F_1 and F_2. In terms of singularity functions we may write the internal torque $T(x)$ as

$$T(x) = \overline{T}_1 + \overline{T}_2 - \overline{T}_1 H(x - L_1) ,$$

and consequently

$$\phi'(x) = \frac{\overline{T}_1 + \overline{T}_2}{\overline{GJ}_1} + \left(\frac{\overline{T}_2}{\overline{GJ}_2} - \frac{\overline{T}_1 + \overline{T}_2}{\overline{GJ}_1} \right) H(x - L_1) ,$$

so that

$$\phi(x) = \frac{\overline{T}_1 + \overline{T}_2}{\overline{GJ}_1} x + \left(\frac{\overline{T}_2}{\overline{GJ}_2} - \frac{\overline{T}_1 + \overline{T}_2}{\overline{GJ}_1} \right) \langle x - L_1 \rangle ,$$

and therefore,if $\phi(0) = 0$,

$$\phi(L_1 + L_2) = \frac{\overline{T}_1 + \overline{T}_2}{\overline{GJ}_1}(L_1 + L_2) + \left(\frac{\overline{T}_2}{\overline{GJ}_2} - \frac{\overline{T}_1 + \overline{T}_2}{\overline{GJ}_1} \right) L_2 = \frac{(\overline{T}_1 + \overline{T}_2) L_1}{\overline{GJ}_1} + \frac{\overline{T}_2 L_2}{\overline{GJ}_2} ,$$

as expected. The torque and angle-of-twist diagrams are shown in Fig. 7.10, where we write, for simplicity, $\bar{k}_i$ for $\overline{GJ}_i / L_i$.

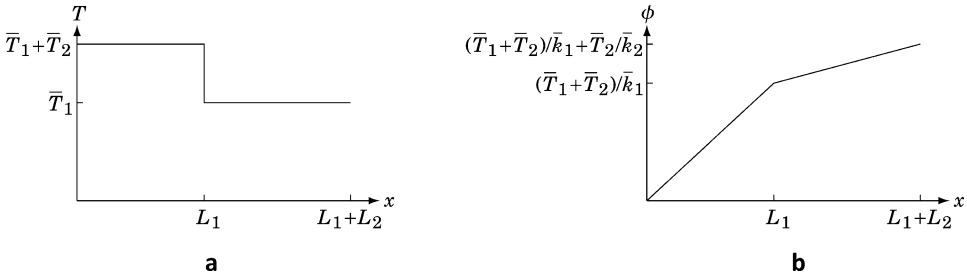

Figure 7.10. Torque diagram (**a**) and angle-of-twist diagram (**b**) for Example 7.3.2

7.3.2 Distributed Torque

Just as an axial force may be distributed along a bar, so a torque may be distributed along the length of a shaft, and the equilibrium equation is, by

analogy with Eq. (6.86),

$$\frac{dT}{dx} = -t(x)\,, \tag{7.49}$$

where $t(x)$ is the distributed torque per unit length, and may include concentrated torques with the help of singularity functions (Appendix A).

Example 7.3.3: Turning a shaft embedded in a material with friction. Suppose that a uniform circular shaft of radius r and length L is embedded in a matrix (of, say, soil or clay) exerting a uniform pressure p on its surface. If the coefficient of friction between the shaft and the embedding material is μ, then, when an attempt is made to turn the shaft, a frictional force per unit area of μp must be overcome, and this force will exert a torque per unit length equal to $t = \mu p(2\pi r)r = 2\pi\mu p r^2$. If a torque T_1 is applied to one end of the shaft while the other end is free, then the magnitude of T_1 necessary to overcome the friction is obtained by integrating Eq. (7.49), namely, $T_1 = 2\pi\mu p r^2 L$. The internal torque along the shaft is $T(x) = 2\pi\mu p r^2 x$, and the total angle of twist of the shaft just before it begins to turn is

$$\phi(L) = \frac{1}{GJ}\int_0^L T(x)\,dx = \frac{2\pi\mu p r^2}{GJ}\frac{L^2}{2} = \frac{\pi\mu p r^2 L^2}{GJ}\,.$$

7.3.3 Statically Indeterminate Shafts

Just like a bar under axial forces, a shaft is statically indeterminate if it is built-in at both ends, and the method of analysis is identical. Since the degree of static indeterminacy is one, the force method is the simplest to use, regardless of how many torques are applied along the length of the shaft (that is, of the number of degrees of freedom).

Example 7.3.4: Torsion of a doubly built-in shaft. A uniform shaft of length L, built-in at both ends, is subject to a torque of total magnitude $\overline{T}$ that is uniformly distributed along the interval $L/4 < x < L/2$, as shown in Fig. 7.11. If the torque at $x = 0$ is T_0, then the internal torque $T(x)$ is

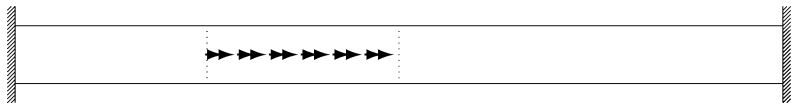

Figure 7.11. Example 7.3.4

$$T(x) = \begin{cases} T_0, & 0 < x < L/4 \\ T_0 - 4(x - L/4)\overline{T}/L, & L/4 < x < L/2 \\ T_0 - \overline{T}, & L/2 < x < L \end{cases}\,.$$

The compatibility condition $\phi(L) = 0$ is accordingly given (with the constant factor $1/GJ$ omitted) by

$$0 = \int_0^L T(x)\,dx = T_0 L - (4\overline{T}/L)\int_{L/4}^{L/2}(x - L/4)\,dx - \overline{T}L/2 = T_0 L - \overline{T}(L/8 + L/2)\,,$$

so that $T_0 = (5/8)\overline{T}$.

Exercises

7.3-1. Determine the magnitude of the force F (in kips) needed to generate a total angle of twist of 1 degree in the compound elastic circular shaft shown in the figure, if the shear modulus is $G = 4000$ ksi.

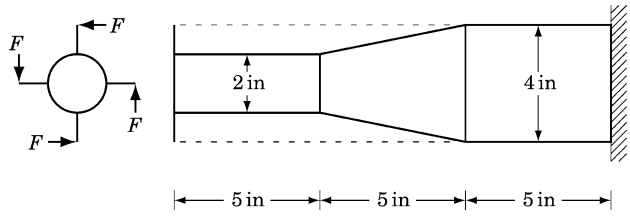

7.3-2. A solid steel shaft of length 50 cm and diameter 2 cm is rigidly attached to one end of a hollow brass shaft of length 30 cm and inner and outer diameters 3 and 4 cm, which is fixed at its other end, as shown in the figure. If $G = 73$ GPa for steel and 37.5 GPa for brass, find the rotational spring constant $\bar{k}$ of the compound shaft.

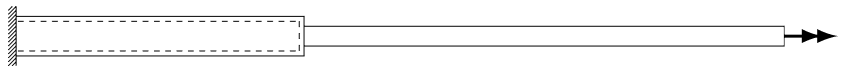

7.3-3. A solid steel shaft of length 50 cm and diameter 2 cm is rigidly attached to the bottom of a cylindrical brass container of depth 30 cm and inner and outer diameter 3 and 4 cm, whose rim is fixed, as shown in transverse section the figure. If $G = 73$ GPa for steel and 37.5 GPa for brass, find the rotational spring constant $\bar{k}$ of the assemblage.

7.3-4. In order to reduce the stiffness of a solid shaft of circular cross-section of length 40 in and diameter 2 in, a portion of it is replaced by a tube of the same outer diameter and thickness 0.08 in, made of the same material. How long does this portion need to be in order to reduce the stiffness by a factor of two?

7.3-5. A steel shaft of length 30 cm, built-in at one end, has the cross-section of Fig. 7.13a, each arm being of length 2.4 cm and thickness 1.6 mm. In order to make it easier to apply a torque, a 10-cm portion at the free end in encased in a plastic sleeve that can be regarded as a thin-walled tube of mean radius 2.5 cm and thickness 2 mm. If the shear modulus is 75 GPa for the steel and 1.3 GPa for the plastic, find the rotational spring constant $\bar{k}$ of the assemblage, and compare with what it would be without the sleeve.

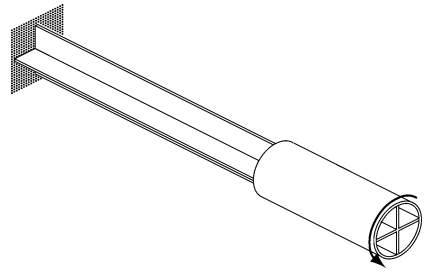

7.3-6. In the tapered shaft of Example 7.3.1, find the maximum shear stress over the entire length of the shaft.

7.3-7. Solve the problem of Example 7.3.2 without using singularity functions, and draw the torque and angle-of-twist diagrams.

7.3-8. Verify that the result for $\phi(L)$ in Example 7.3.3 is dimensionless.

7.3-9. Solve the problem of Example 7.3.4 using singularity functions, and draw the torque and angle-of-twist diagrams.

7.3-10. A compound shaft, whose left third $(0 < x < L/3)$ is a cylinder of radius c and whose right two-thirds $(L/3 < x < L)$ is a tube of outer radius c and inner radius $c/2$, is built-in at both ends and is subjected to a concentrated torque $\overline{T}$ at $x = L/3$. Draw the torque and angle-of-twist diagrams, and find the maximum shear stress.

7.4 Open Thin-Walled Sections

7.4.1 Introduction

A general theory of the torsion of elastic shafts may be based on the assumption that, if the axis of the shaft is taken to be the z-axis, then the displacement field in the plane of the cross-section $\mathscr{A}$ is that of a rigid rotation of the cross-section by the angle of twist ϕ. If this angle is sufficiently small then the displacements along the x- and y-axes are

$$u = -y\phi \quad , \quad v = x\phi \, . \tag{7.50}$$

The shear-strain components are therefore given, according to Eq. (5.33) (page 233), by

$$\gamma_{xz} = -y\phi' + \frac{\partial w}{\partial x} \quad , \quad \gamma_{yz} = x\phi' + \frac{\partial w}{\partial y} \, , \tag{7.51}$$

where ϕ' now stands for $d\phi/dz$ and w is the displacement along the z-axis. If the shear stresses are expressed in terms of the Prandtl stress function χ of Example 4.5.3 by Eqs. (4.43) (page 192) and related to the strains by Hooke's law, Eqs. $(6.16)_{2,3}$ (page 260), then

$$\frac{\partial \chi}{\partial y} = G\left(-y\phi' + \frac{\partial w}{\partial x}\right) \quad , \quad \frac{\partial \chi}{\partial x} = G\left(-x\phi' - \frac{\partial w}{\partial y}\right) \, . \tag{7.52}$$

The axial displacement w (which represents the warping of the cross-section) can be eliminated between the two equations in (7.52) by differentiating the first with respect to y and the second with respect to x, and adding the left-hand sides, resulting in

$$\frac{\partial^2 \chi}{\partial x^2} + \frac{\partial^2 \chi}{\partial y^2} = -2G\phi' \, . \tag{7.53}$$

The solution of this equation for χ represents, as we pointed out in Sect. 6.4 (page 295), the solution of the torsion problem by the force method.

It was noted by Prandtl that Eq. (7.53) happens to be, mathematically, the same as that governing the deflection of a homogeneous membrane (such as a soap film) subjected to a uniform pressure and with uniform surface tension, and with the same outline as that of the cross-section of the shaft. This coincidence (usually referred to as the *membrane analogy* or *soap-film analogy*) provides an experimental means of solving the problem. Analytical solutions have been found for very few cross-sections. For shafts of rectangular cross-section, a solution based on the displacement method (with the warping displacement w as the unknown) was developed by Saint-Venant. The theory is beyond the scope of this book, and will not be pursued here, except to show a qualitative picture of shear-stress distribution in Fig. 7.12, which is easily seen to be consistent with the discussion of the shear-stress vector following

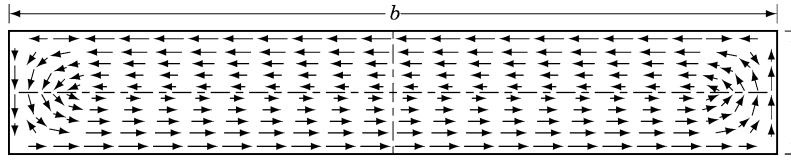

Figure 7.12. Shear-stress distribution in a shaft of rectangular cross-section

Eqs. (4.43) (page 192). We will, moreover, use only the results in the limit as the rectangle becomes very narrow, that is, $t \ll b$, where b and t are the lengths of the long and short sides of the rectangle, respectively (in practice this means that, more or less, $b/t > 15$).* The results are, first, that in the torsional rigidity GJ,

$$J = \frac{t^3 b}{3} \tag{7.54}$$

and, second, that the maximum shear stress, which occurs (antisymmetrically) on the outer edges at the midpoints of the long sides, is given by

$$\tau_{\max} = \frac{3T}{t^2 b} = \frac{Tt}{J} . \tag{7.55}$$

7.4.2 Assemblages of Thin-Walled Rectangular Shafts

Consider a shaft whose cross-section is a combination of narrow rectangles, whether in the form of an extruded shape, a flat plate that has been folded, or several flat plates that have been welded together (examples are shown in Fig. 7.13). When such a shaft is twisted as a unit, the elements making it up act in parallel, so that they undergo the same twist ϕ' while the torque is the sum of the torques acting on each element, so that

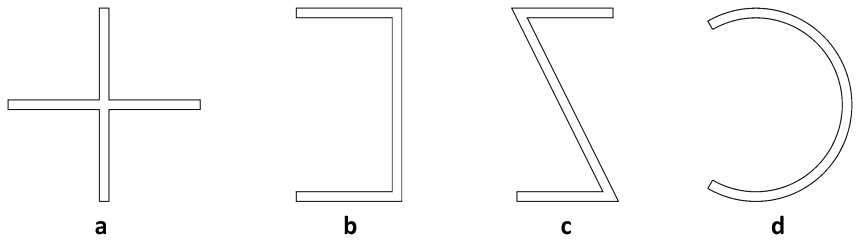

Figure 7.13. Examples of assemblages of thin-walled rectangular shafts

$$J = \sum_i J_i . \tag{7.56}$$

*For $b/t = 10$, for example, the number 3 in Eqs. (7.54) and (7.55) is actually 3.20.

Except in the vicinity of a joint between two elements, the stress distribution will not be greatly different from what it would be in a narrow rectangular shaft. This means that each J_i is given approximately by

$$J_i = \frac{t_i^3 b_i}{3} . \tag{7.57}$$

In each flat element, the maximum stress is given by

$$\tau_{i\max} = \frac{T_i t_i}{J_i} = \frac{T t_i}{J} , \tag{7.58}$$

since $T_i/J_i = G\phi' = T/J$. Consequently, if the elements have different thicknesses,

$$\tau_{\max} = \frac{T t_{\max}}{J} . \tag{7.59}$$

If all elements have the same thickness t, then Eqs. (7.54) and (7.55) apply, with $b = \sum_i b_i$.

Example 7.4.1: Comparison of open and closed thin-walled sections. The two sections shown in Fig. 7.14 can be thought of as resulting from two different ways of joining two equal channel sections like that of Fig. 7.13a. They consequently have the same overall dimensions and area, and, as will be shown in the next chapter, the same flexural strength and stiffness when they are used as beams bending in the xy-plane. When we compare their torsional properties,

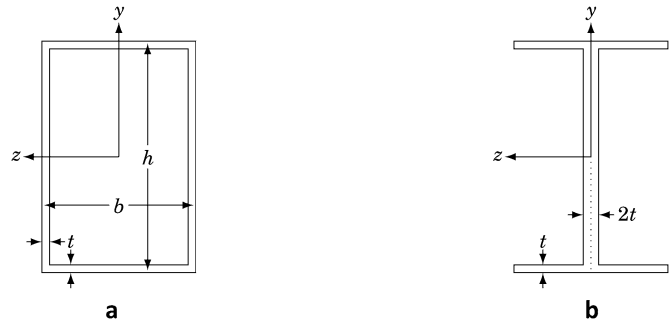

Figure 7.14. Example 7.4.1

we recall from Sect. 7.2 that for the rectangular tube (or box beam) of Fig. 7.14a the torsional strength ($T/\tau_{\max}$) is, by Eq. (7.36),

$$\frac{T}{\tau_{\max}} = 2bht ,$$

while the torsional rigidity ($T/\phi' = GJ$) is, by Eq. (7.40),

$$\frac{T}{\phi'} = G\frac{2b^2h^2t}{b+h} .$$

For the I-section of Fig. 7.14b we have

$$J = 2\frac{bt^3}{3} + \frac{h(2t)^3}{3} = \frac{(2b+8h)t^3}{3}$$

and therefore, by Eq. (7.59),

$$\frac{T}{\tau_{\max}} = \frac{J}{2t} = \frac{(b+4h)t^2}{3} .$$

7.4.3 Combinations of Open Thin-Walled and Other Sections

If open thin-walled sections are rigidly combined with other sections (solid or tubular), they may be regarded as acting in parallel just like the assemblages studied here, so that their torsional rigidities add, and the maximum stress in each subsection is found from the torque carried by it by the corresponding formula, as in the following example.

Example 7.4.2: Turbine rotor shaft.
A turbine rotor shaft may be modeled as in Fig. 7.15, with a number of blades (in this case 6) rigidly attached to a solid cylinder of the same material. If each

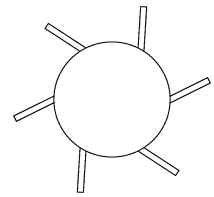

Figure 7.15. Example 7.4.2

blade is of thickness t and width b, and the radius of the cylinder is c, then the total torsional rigidity is given by GJ with

$$J = \frac{\pi c^4}{2} + 6 \cdot \frac{t^3 b}{3} = \frac{\pi c^4}{2} + 2t^3 b .$$

If the total torque is T, then the torques carried by the cylinder and each of the blades are respectively

$$T^{\text{cyl}} = \frac{\pi c^4}{\pi c^4 + 4t^3 b} T , \quad T^{\text{bl}} = \frac{(2/3)t^3 b}{\pi c^4 + 4t^3 b} T ,$$

and the maximum stresses are respectively

$$\tau_{\max}^{\text{cyl}} = \frac{4c}{\pi c^4 + 4t^3 b} T , \quad \tau_{\max}^{\text{bl}} = \frac{2t}{\pi c^4 + 4t^3 b} T .$$

Note that, in the preceding example, if b and c are of the same order of magnitude while t is considerably smaller, then the blades have little effect on the stiffness or strength of the combined shaft.

Exercises

7.4-1. Show that the results for circular shafts derived in Sect. 7.1 are equivalent to those that would be obtained from the Prandtl stress function $\chi(x,y) = (G\phi'/2)(c^2 - x^2 - y^2)$.

7.4-2. The function $\chi(x,y) = Cy[(y-h)^2 - \lambda^2 x^2]$ goes to zero on the lines $y = 0$ and $y = h \pm \lambda x$, forming an isosceles triangle of height h and base $2h/\lambda$.

(a) Find values of λ and C for which χ satisfies Eq. (7.53). What kind of triangle is this?

(b) Determine T and $\tau_{\max}$ for the values found in (a).

7.4-3. If each arm of the cross-shaped section shown in Fig. 7.13a is of length b and thickness t, find the torsional strength $T/\tau_{\max}$ and rigidity factor J of the shaft having this cross-section.

7.4-4. If each flange of the channel section shown in Fig. 7.13b is of length a and the web is of depth h, with the thickness t constant, find the torsional strength $T/\tau_{\max}$ and rigidity factor J of the shaft having this cross-section.

7.4-5. If the arc-shaped section shown in Fig. 7.13d is of radius r and thickness t, and subtends an angle of 240°, find the torsional strength $T/\tau_{\max}$ and rigidity factor J of the shaft having this cross-section.

7.4-6. A shaft of thin-walled semicircular cross-section, of radius 10 cm, thickness 6 mm and length 75 cm, made of a material with $G = 24.5$ GPa, is to be used as a rotational spring, as shown in the figure. Find the spring constant $\bar{k}$.

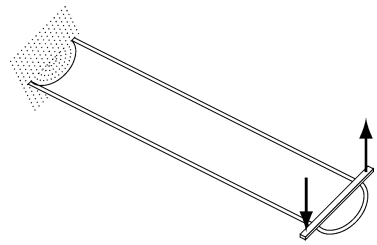

7.4-7. An extruded aluminum channel has the dimensions (in inches) shown in the figure. If $G = 3.75 \times 10^3$ ksi, find the torsional rigidity GJ of the section.

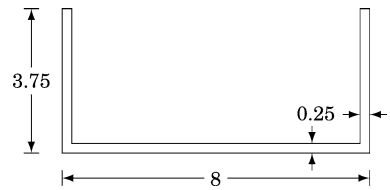

7.4-8. Compare the torsional strength and rigidity of a thin-walled circular tube of radius r and thickness t with what it would be if the tube were given a lengthwise slit.

7.4-9. Redo Example 7.4.2 when the solid cylinder is replaced with a thin-walled tube of the same thickness t as the blade, with c as the mean radius.

7.4-10. Suppose that, in Example 7.4.2, the cylinder is not solid but hollow, with inner and outer diameters of 35 mm and 50 mm. If the blades have b = 125 mm and t = 7.5 mm, and if τ_{all} = 50 MPa, determine the maximum power (in kW) that such a shaft can transmit at 50 Hz.

Chapter 8

Elastic Bending of Beams

8.1 Shear and Bending-Moment Diagrams

8.1.1 Introduction

The notion of shear-force (or shear) and bending-moment diagrams was introduced by means of some examples in Sect. 2.4. Knowledge of the distribution of shear force and bending moment in a beam is essential for the determination of the stresses and the deflection of the beam. For this reason, the calculation of these diagrams is developed here systematically on the basis of differential equations of equilibrium analogous to Eq. (6.86) for axial forces and to Eq. (7.49) for torques.

8.1.2 Method of Sections

Consider a beam spanning a portion of the x-axis and subject to a distributed transverse force of intensity $w(x)$* acting in the xy-plane, as shown in Fig. 8.1a. The force is assumed positive downward, and its distribution is not necessarily continuous (or, more generally, not described by a simple function over the whole span). Since there are no external forces acting in the direction parallel to the beam, the internal reactions, as defined by Fig. 2.46, are the shear force V and the bending moment M, with their values on the two faces of the section between x and $x+\Delta x$ depicted in Fig. 8.1b. By the convention already introduced in Sect. 2.4, the moment on the section at $x+\Delta x$ (which has an outward normal pointing toward the positive x-axis) is taken to be positive when, as a vector, it points toward the positive z-axis, that its, it tends to bend the beam so that it is concave upward. Likewise, the shear force at $x+\Delta x$ is positive when pointing along the positive y-axis, that is, upward.

*This w should not be confused with the same symbol used to denote displacement in the z-direction in Sect. 5.3.

© Springer International Publishing Switzerland 2017

J. Lubliner, P. Papadopoulos, *Introduction to Solid Mechanics*,
DOI 10.1007/978-3-319-18878-2_8

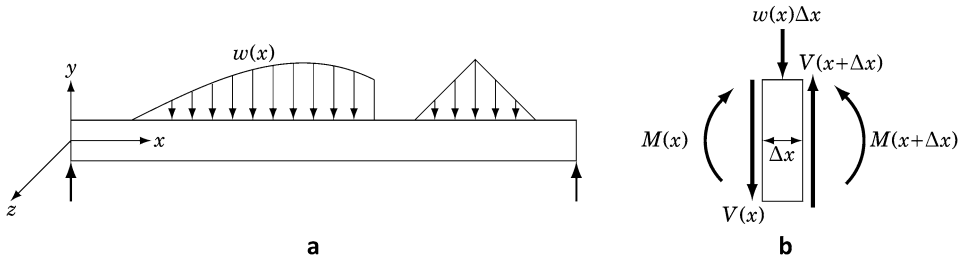

Figure 8.1. Beam under a distributed transverse force: (**a**) loading of the beam, (**b**) forces and moments on section $(x, x+\Delta x)$

The force equilibrium of the section in Fig. 8.1b reduces to $\sum F_y = 0$, and is given by

$$V(x+\Delta x) - V(x) - w(x)\Delta x \;=\; 0\,. \tag{8.1}$$

Dividing the left-hand side by Δx and taking the limit as $\Delta x \to 0$ we immediately obtain the differential equation of transverse force equilibrium,

$$\frac{dV}{dx} \;=\; w(x)\,, \tag{8.2}$$

analogous to Eq. (6.86) for axial force equilibrium and to Eq. (7.49) for torque equilibrium. For moment equilibrium, we balance the moments about an axis parallel to the z-axis and passing through the center of the section. We assume, for now, that the line of action of the resultant force $w(x)\Delta x$ passes through this midpoint. The moment equilibrium is then given by

$$M(x+\Delta x) - M(x) + [V(x+\Delta x) + V(x)]\frac{\Delta x}{2} \;=\; 0\,, \tag{8.3}$$

which, with the help of (8.1), becomes

$$M(x+\Delta x) - M(x) + V(x)\Delta x + w(x)\frac{(\Delta x)^2}{2} \;=\; 0\,. \tag{8.4}$$

When the left-hand side of this equation is divided by Δx and the limit as $\Delta x \to 0$ is taken, the term in $w(x)$ disappears (therefore it does not really matter if the line of action of $w(x)\Delta x$ passes exactly through the midpoint), and the limit is

$$\frac{dM}{dx} + V(x) \;=\; 0\,. \tag{8.5}$$

Eqs. (8.2) and (8.5) can be combined to yield

$$\frac{d^2M}{dx^2} \;=\; -w(x)\,. \tag{8.6}$$

The moment distribution $M(x)$ can therefore be obtained by twice integrating the load distribution $w(x)$, with the appropriate two boundary conditions used to determine the constants of integration.

Example 8.1.1: Simply supported beam with uniform load.
Let a beam of length L, spanning the interval $0 < x < L$, be simply supported (as defined in Sect. 2.2) and take the load to be uniformly distributed, that is, $w(x) = \overline{w}$, where $\overline{w}$ is a constant, as shown in Fig. 8.2a. Integrating Eq. (8.6) twice yields

$$M(x) = -\overline{w}\frac{x^2}{2} + Ax + B \,,$$

where A and B are constants of integration. (Note the resemblance of this result to the one for the deflection of a cable under a load that is uniformly distributed with respect to the horizontal, Sect. 3.5). The boundary conditions are $M(0) = M(L) = 0$, so that $B = 0$ and $A = \overline{w}L/2$. Consequently,

$$M(x) = \frac{\overline{w}}{2}x(L - x) \,.$$

The shear and bending-moment diagrams are shown in Fig. 8.2b and 8.2c. The

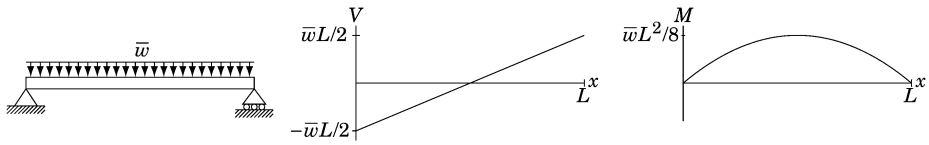

Figure 8.2. Simply supported beam under a uniformly distributed load: (**a**) loading, (**b**) shear diagram, (**c**) moment diagram

maximum bending moment occurs at $x = L/2$ and is given by

$$M_{\max} = \frac{\overline{w}L^2}{8} \,.$$

This equation is one of the most widely used formulas in structural engineering.

Example 8.1.2: Cantilever beam with uniform load.
Suppose that a beam of length L, spanning the interval $0 < x < L$, is a cantilever (see Fig. 2.16a), built in at $x = 0$, and carrying a uniformly distributed load of intensity $\overline{w}$, as illustrated in Fig. 8.3a. At the free end $x = L$, the boundary conditions are $V = 0$ (equivalent to $dM/dx = 0$) and $M = 0$. Consequently,

$$-\overline{w}L + A = 0 \,,$$

$$-\overline{w}\frac{L^2}{2} + AL + B = 0 \,.$$

It follows that $A = \overline{w}L$ and $B = -\overline{w}L^2/2$, so that

$$M(x) = -\frac{\overline{w}}{2}(x^2 - 2Lx + L^2) = -\frac{\overline{w}(L - x)^2}{2} \,.$$

The shear and bending-moment diagrams are shown in Fig. 8.3b and 8.3c, respectively. We see that in this case the numerically largest moment is at the built-in end and its magnitude is given by $|M|_{\max} = \overline{w}L^2/2$. In practice, it is common to write $M_{\max}$ for $|M|_{\max}$.

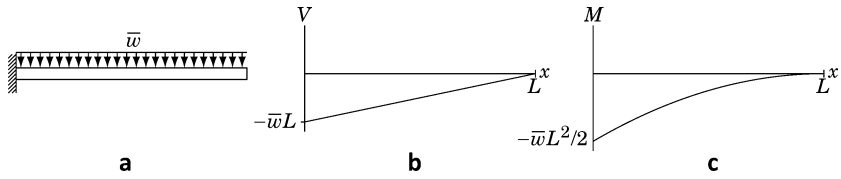

Figure 8.3. Cantilever beam under a uniformly distributed load: (**a**) loading, (**b**) shear diagram, (**c**) moment diagram

8.1.3 Concentrated Forces

Suppose that the beam carries a concentrated downward force F_1 at $x = x_1$. Here, again, the analogy between the moment diagram and the deflection of a cable, noted in Example 8.1.1, can be used. A free-body diagram of a thin slice of the beam containing $x = x_1$, shown in Fig. 8.4, leads to

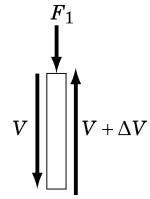

Figure 8.4. Force equilibrium of a thin section containing a concentrated load

$$\Delta V = F_1 \,, \tag{8.7}$$

that is, the value of the shear force changes by F_1, so that, in view of Eq. (8.5), the slope of the moment diagram changes by $-F_1$.

Example 8.1.3: Cantilever beam under a point load.
If a cantilever beam spans the domain $(0,L)$, as shown in Fig. 8.5a, it is clear that $V = M = 0$ in the segment $x > x_1$. Eq. (8.7) leads to $V = -F_1$, and hence $dM/dx = F_1$, for $x < x_1$. The condition $M = 0$ at $x = x_1$ yields $M(x) = F_1(x - x_1)$ in that range; the resulting moment diagram is shown in Fig. 8.5b. The special

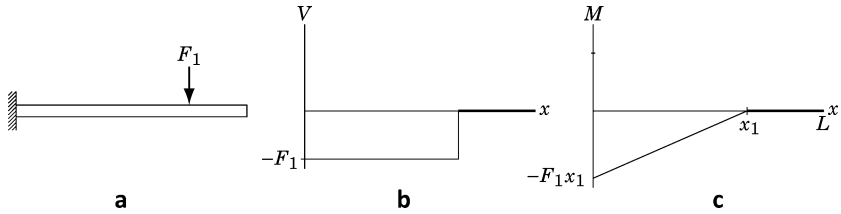

Figure 8.5. Cantilever beam under a single concentrated load: (**a**) loading, (**b**) shear diagram, (**c**) moment diagram

case of a cantilever carrying a concentrated force at is free end (tip) is obtained by letting $x_1 = L$.

Alternatively, a cantilever that carries (in addition to any other loading) a downward concentrated force F_1 at its free end may be analyzed more simply by not including this force in the loading but instead replacing the free-end condition $V = 0$ with $V(0) = F_1$ or $V(L) = -F_1$ if the free end is at $x = 0$ or $x = L$, respectively.

Example 8.1.4: Simply supported beam with point load.

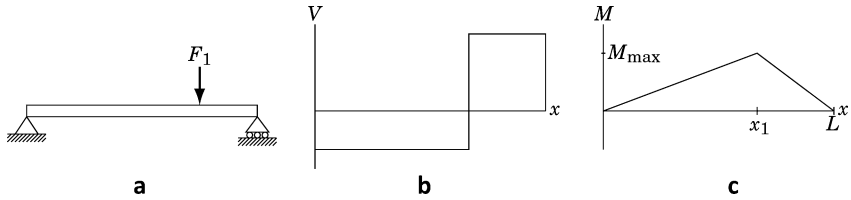

Figure 8.6. Simply supported beam under a single concentrated load: (a) loading, (b) shear diagram, (c) moment diagram

If the beam is simply supported (the span being L), as in Fig. 8.6a, elementary statics (see Example 2.2.9, page 82) leads to the force reactions at $x = 0$ and $x = L$ being $F_1(1 - x_1/L)$ and $F_1 x_1/L$, respectively. Consequently, since the shear force is constant in each of the two segments $0 < x < x_1$ and $x_1 < x < L$, it is given by $V(x) = -F_1(1 - x_1/L)$ and $V(x) = F_1 x_1/L$, respectively (it is easy to see the difference between these two values is just F_1). Since the moment vanishes at $x = 0$, for $x < x_1$ we have $M(x) = F_1(1 - x_1/L)x$. Similarly, since $M(L) = 0$, we have $M(x) = F_1(x_1/L)(L - x)$. The resulting moment diagram is seen in Fig. 8.6b, with $M_{\max} = M(x_1) = F_1 x_1(1 - x_1/L)$. In the special case $x_1 = L/2$, $M_{\max} = F_1 L^2/4$.

When several concentrated forces act on the beam, the analogy with the corresponding cable problem (see Fig. 3.37a) implies that the resulting moment diagram will be polygonal. Its determination is greatly simplified with the use of singularity functions, whose application is introduced in Sect. 8.1.5.

8.1.4 Concentrated Couples

If a concentrated couple (or moment) M_1 acts on the beam at $x = x_1$, then the moment equilibrium of a section containing its point of application (disregarding any loading by forces) is shown in Fig. 8.7a. Clearly, $\Delta M = -M_1$, that is, the moment diagram exhibits a downward discontinuity equal to the magnitude of the couple if it is counterclockwise (upward if clockwise). The corresponding moment diagrams for a cantilever and a simply supported beam are shown in Fig. 8.7b and c, respectively. If a concentrated couple M_1 acts at an end of the beam (the free end of a cantilever or either end of a simply supported beam), the corresponding moment diagrams are obtained by letting $x_1 = L$ in Fig. 8.7b and either $x_1 = 0$ or $x_1 = L$ Fig. 8.7c. But (as with a concentrated force at the free end of a cantilever) it is often simpler to ex-

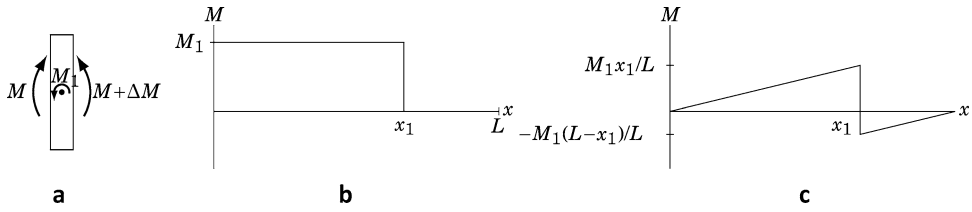

Figure 8.7. Beam with a concentrated couple: (**a**) local equilibrium; moment diagrams for (**b**) cantilever, (**c**) simply supported beam

clude it from the loading and instead to replace the end condition $M = 0$ with $M = \pm M_1$.

8.1.5 Application of Singularity Functions

With the help of the singularity functions defined in Appendix A (page 513), a set of discrete loads can be written as if it were a distributed load given by a linear combination of Dirac delta functions. Specifically, a beam under a set of concentrated forces F_1, F_2, ... acting respectively at x_1, x_2, ... can be analyzed as though it were loaded by a distributed force given by

$$w(x) = F_1\delta(x-x_1)+F_2\delta(x-x_2)+\dots . \tag{8.8}$$

Given that, according to (A.10) the Dirac delta function is the derivative of the Heaviside step function, we may use Eq. (8.2) and integrate Eq. (8.8) to obtain the shear as

$$V(x) = -A+F_1H(x-x_1)+F_2H(x-x_2)+\dots . \tag{8.9}$$

Further, (since by (A.8) the Heaviside step function is the derivative of the ramp function), we may use Eq. (8.5) to express the moment as

$$M(x) = Ax+B-F_1\langle x-x_1\rangle-F_2\langle x-x_2\rangle+\dots , \tag{8.10}$$

where A and B are constants of integration. In the just-discussed special case of a simply supported beam with a concentrated force at $x = x_1$, the boundary conditions $M(0) = M(L) = 0$ lead to $B = 0$ and $A = F_1(L-x_1)/L$, so that

$$M(x) = \frac{F_1}{L}[(L-x_1)x-L\langle x-x_1\rangle] . \tag{8.11}$$

It is left to an exercise to show that this expression is equivalent to those obtained above for $x < x_1$ and $x > x_1$.

We now revisit Examples 8.1.3 and 8.1.4 with the aid of singularity functions.

Example 8.1.5: Example 8.1.3 revisited.
Here we have

$$w(x) \;=\; F_1\delta(x-x_1)$$

and therefore, since $V(x) = M(x) = 0$ for $x > x_1$, we can integrate this equation in the form

$$V(x) \;=\; -F_1H(x_1-x) \quad , \quad M(x) \;=\; -F_1\langle x_1-x\rangle \; .$$

The special case $x_1 = L$ represents an end-loaded cantilever. Since in this case $x_1 - x$ is never negative, the Heaviside step function has the constant value 1, and the Macaulay brackets can be replaced by parentheses, so that the preceding equations can be written more simply as $V(x) = -F_1$, $M(x) = -F_1(L-x)$.

Example 8.1.6: Example 8.1.4 revisited.
Here we need a constant of integration when we integrate for the shear:

$$V(x) \;=\; C + F_1H(x-x_1) \; ,$$

so that, since $M(0) = 0$,

$$M(x) \;=\; -Cx - F_1\langle x-x_1\rangle \; .$$

The condition that $M(L) = 0$ leads to $C = -F_1(L-x_1)/L$, so that

$$M(x) \;=\; F_1\left(\frac{(L-x_1)x}{L} - \langle x-x_1\rangle\right) \; .$$

More generally, singularity functions may be used to express any combination of loads, concentrated or distributed (but not necessarily continuous or smooth), by means of a single function $w(x)$ that is a linear combination of singularity functions of various degrees. Some examples are given below.

Example 8.1.7: Beam with concentrated couple.
A concentrated couple $\overline{M}$ at $x = x_1$ can be represented by the dipole function discussed in Eq. (A.11) of Appendix A (page 515), that is, $w(x) = M_1\delta'(x-x_1)$. It follows that $V(x) = -A + M_1\delta(x-x_1)$ and $M(x) = Ax + B - M_1H(x-x_1)$.

For a cantilever beam fixed at $x = 0$ and free at $x = L$, $V(L) = 0$ implies $A = 0$, and $M(L) = 0$ implies $B = M_1$, so that $M(x) = M_1[1 - H(x-x_1)] = M_1H(x_1-x)$, consistent with the moment diagram of Fig. 8.7a, while $V(x) = 0$ except for the singularity at $x = x_1$. For a simply supported beam, $M(0) = 0$ gives $B = 0$, while $M(L) = 0$ leads to $A = M_1/L$, resulting in $M(x) = M_1[x/L - H(x-x_1)]$, as illustrated by Fig. 8.7b, and $V(x) = -M_1/L$ except at the singular point.

Example 8.1.8: Cantilever with a nonuniformly distributed load.
We consider a cantilever beam of length L, built in at $x = 0$ and carrying a distributed load whose intensity grows linearly from $x = a$ to $x = L$, with $0 < x < a$ unloaded, and the total load equal to W.

It is clear that the loading must be given by $w(x) = k<x-a>$, with k a constant to be determined by the requirement that $\int_0^L w(x)dx = W$. It follows that

$$W = k\int_0^L <x-a>dx = \frac{k}{2}[<L-a>^2 - <-a>^2] = \frac{k(L-a)^2}{2},$$

since $<L-a> = L-a$ and $<-a> = 0$ if $0 < a < L$, and therefore $k = 2W/(L-a)^2$. Eq. (8.2) now reads

$$\frac{dV}{dx} = \frac{2W}{(L-a)^2}<x-a>,$$

which upon integration yields

$$V(x) = -A + \frac{W}{(L-a)^2}<x-a>^2,$$

A being a constant of integration that is necessarily equal to the (upward) force reaction at $x = 0$. It is determined by the requirement that the shear force is zero at the free end, that is, $V(L) = 0$, so that $A = W$, just as would have been obtained from the vertical force equilibrium of the whole beam.
For Eq. (8.5) we now have

$$\frac{dM}{dx} = W = \frac{W}{(L-a)^2}<x-a>^2,$$

leading to

$$M(x) = B + Wx - \frac{W}{3(L-a)^2}<x-a>^3,$$

where B is another constant of integration (equal to M_0, the moment reaction at $x = 0$) determined by the end condition $M(L) = 0$, so that $B = -WL + W(L-a)/3 = -W(2L+a)/3$. It is easy to show that if the distributed force were to be replaced by a statically equivalent concentrated force, that force would be acting at $x = a + (2/3)(L-a) = (2L+a)/3$, so that the result is, once again, consistent with statics.
The loading and the results are shown in Fig. 8.8.

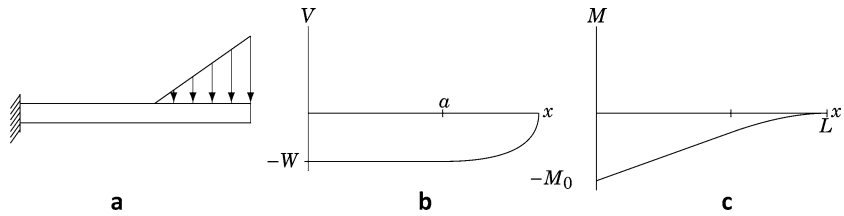

Figure 8.8. Example 8.1.8: (a) loading, (b) shear diagram, (c) moment diagram

Example 8.1.9: Partially loaded simply supported beam.
A simply supported beam carries a uniformly distributed load $\overline{w}$ over its middle half, and no other load. The loading is consequently given by

$$w(x) = \overline{w}[H(x-L/4) - H(x-3L/4)],$$

and the shear and bending moment by

$$V(x) = -A + \overline{w}\left[<x - L/4> - <x - 3L/4>\right]$$

and

$$M(x) = Ax + B - \frac{\overline{w}}{2}\left[<x - L/4>^2 - <x - 3L/4>^2\right],$$

respectively. The end condition $M(0) = 0$ yields $B = 0$, while $M(L) = 0$ leads to

$$A = \frac{\overline{w}}{2L}[(3L/4)^2 - (L/4)^2] = \frac{\overline{w}L}{4},$$

so that the shear and moment are

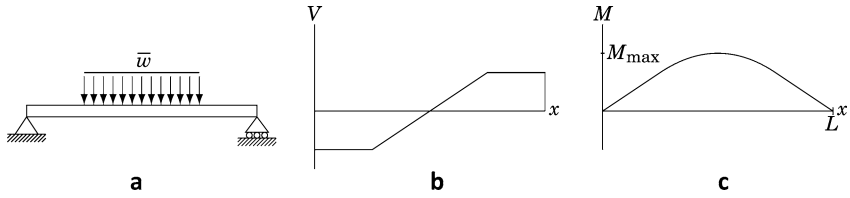

Figure 8.9. Example 8.1.9: (**a**) loading, (**b**) shear diagram, (**c**) moment diagram

$$V(x) = \overline{w}\left[<x - L/4> - <x - 3L/4> - L/4\right]$$

and

$$M(x) = \frac{\overline{w}}{4}\left[Lx - 2<x - L/4>^2 + 2<x - 3L/4>^2\right],$$

with $M_{\max} = M(L/2) = (3/32)\overline{w}L^2$. The results are shown in Fig. 8.9.

Beam with Overhang

Bodies with overhangs were mentioned in Sect. 2.2 (page 72). For a beam with an overhang, as pictured in Fig. 8.10, the use of singularity functions is particularly convenient. The solution method involves adding the force reaction at B (R_B, assumed positive upward) as an unknown load to the applied loading w. The differential equation of transverse force equilibrium now becomes

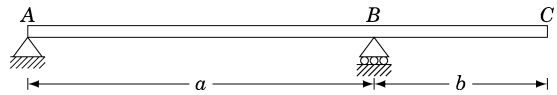

Figure 8.10. Beam with overhang

$$\frac{dV}{dx} = w(x) - R_B\delta(x - a) \tag{8.12}$$

instead of Eq. (8.2), and the second-order differential equation for the bending moment becomes

$$\frac{d^2M}{dx^2} = -w(x) + R_B\delta(x - a) \tag{8.13}$$

instead of Eq. (8.6). When this equation is integrated twice, R_B is a third unknown in addition to the two constants of integration, and the three unknowns are obtained from the three end conditions $M(0) = 0$, $V(L) = 0$ and $M(L) = 0$ (suitably modified if there are concentrated loads at the ends), with $L = a + b$. As was already noted in Sect. 2.2, if the supported span AB is short compared to the overhang BC then the beam is often referred to as cantilevered, and if in fact a goes to zero then shear and moment diagrams become those of a cantilever. Conversely, if $b = 0$ then the beam is just simply supported. Both limiting cases are recovered in the following example.

Example 8.1.10: Uniformly loaded beam with an overhang.
If the beam is under a uniformly distributed load of intensity $\overline{w}$, then Eq. (8.13), when integrated twice, yields

$$M(x) = C_1 x + C_2 - \frac{\overline{w}x^2}{2} + R_B <x-a>\ ,$$

and the condition $M(0) = 0$ immediately gives $C_2 = 0$. The conditions at $x = L$ lead to

$$C_1 + R_B = \overline{w}L\ ,$$

from which it is obvious that C_1 is just the force reaction R_A, and

$$C_1 L + R_B\, b = \frac{\overline{w}L^2}{2}\ .$$

We find that $C_1 = \overline{w}L(a-b)/2a$ and $R_B = \overline{w}L^2/2a$, so that

$$M(x) = \frac{\overline{w}}{2a}[(a-b)Lx - ax^2 + L^2 <x-a>]\ .$$

The shear and bending-moment diagrams for the special case $a = 2b = 2L/3$ are shown in Fig. 8.11. It can be seen that if the support B were to move toward the

Figure 8.11. Example 8.1.10 with $a = 2b = 2L/3$: (**a**) shear diagram, (**b**) moment diagram

right end, the diagrams would tend to those of Fig. 8.2, while if it were to move toward the left end, the diagrams would become those of Fig. 8.3.

Exercises

8.1-1. Determine the shear and bending-moment distributions and sketch the shear and bending-moment diagrams for the cantilever beam of the figure, where the load distribution has the shape of a parabola with the vertex at the tip and with $w_{\max} = 200$ lb/ft.

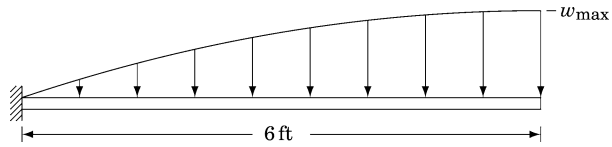

8.1-2. Determine the shear and bending-moment distributions and sketch the shear and bending-moment diagrams for the simply supported beam of the figure, where the load distribution has the shape of a sine curve and $w_{\max} = 50$ N/cm.

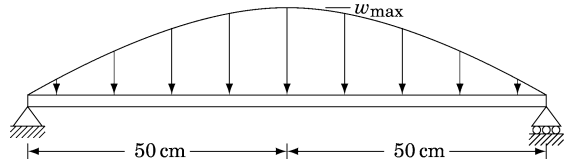

8.1-3. Without using singularity functions, determine the shear and bending-moment distributions and sketch the shear and bending-moment diagrams for the cantilever beam of the figure, where $\overline{w} = 20$ N/cm.

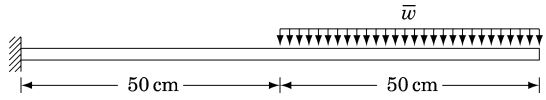

8.1-4. Do the preceding exercise using singularity functions.

8.1-5. Without using singularity functions, determine the shear and bending-moment distributions and sketch the shear and bending-moment diagrams for the cantilever beam of the figure, where the distributed load has a maximum value $w_{\max} = 15$ lb/in.

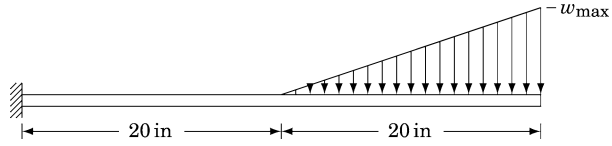

8.1-6. Do the preceding exercise using singularity functions.

8.1-7. Without using singularity functions, determine the shear and bending-moment distributions and sketch the shear and bending-moment diagrams for the simply supported beam of the figure, where the distributed load has a maximum value $w_{\max} = 10$ lb/in.

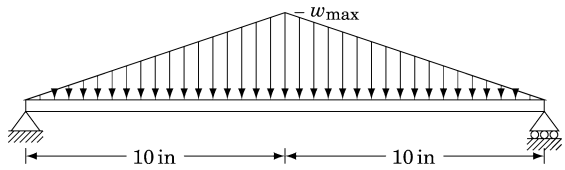

8.1-8. Do the preceding exercise using singularity functions.

8.1-9. Determine the shear and bending-moment distributions and sketch the shear and bending-moment diagrams for the cantilever beam of the figure, where $\overline{w} = 1.5$ kN/m and $F = 2.2$ kN.

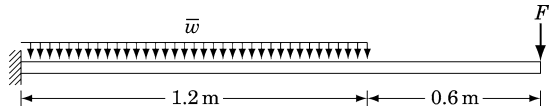

8.1-10. Determine the shear and bending-moment distributions and sketch the shear and bending-moment diagrams for the simply supported beam of the figure, where $F = 600$ lb.

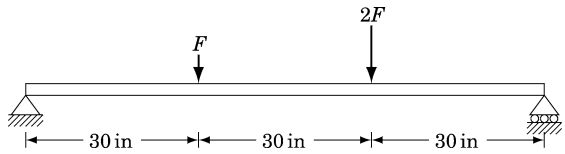

8.1-11. Determine the shear and bending-moment distributions and sketch the shear and bending-moment diagrams for the simply supported beam of the figure, where $F = 100$ N and $\overline{w} = 10$ N/cm.

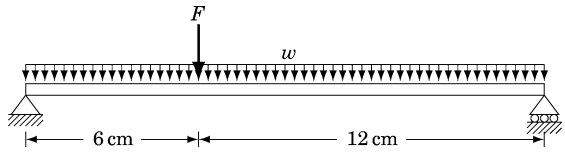

8.1-12. Determine the shear and bending-moment distributions and sketch the shear and bending-moment diagrams for the cantilever beam of the figure, where $\overline{M} = 1.50$ kN·m.

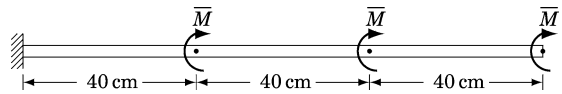

8.1-13. Determine the shear and bending-moment distributions and sketch the shear and bending-moment diagrams for the simply supported beam of the figure, where $\overline{M} = 100$ N·m and $\overline{w} = 150$ N/m.

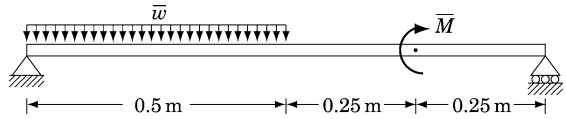

8.1-14. For the beam of Example 8.1.10, sketch the shear and bending=moment diagrams for the limiting cases $b \ll a$ and $a \ll b$, and show that in the limit they become those for a simply supported beam and a cantilever, respectively.

8.1-15. Determine the shear and bending-moment distributions and sketch the shear and bending-moment diagrams for the beam of the figure, where $F = 200$ N and $\overline{w} = 250$ N/m.

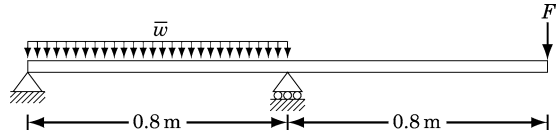

8.2 Pure Bending of Beams

8.2.1 Fundamentals of Bending

Kinematics

As we already know from Sect. 2.2, a beam is a straight bar designed to carry primarily transverse loads, and, as we learned in the preceding section, the internal force resultants caused by such a loading consist of shear force and bending moment. The ensuing deformation of the beam consists primarily of *bending*, though the presence of a shear force implies shear stresses that also cause some shearing deformation. In the special case when the shear force is zero (so that, in accordance with Eq. (8.5), the bending moment is constant) over some span of the beam (as, for example, between the supports of the beam in Fig. 8.12a, or over the entire cantilever of Fig. 8.12b), the span is said to be in a state of *pure bending*; a generic span in such a state is shown in Fig. 8.12c. We will now consider a prismatic beam with the x-axis as its

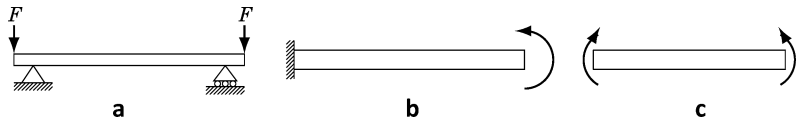

Figure 8.12. Beam in pure bending: (**a**–**b**) examples; (**c**) generic span

longitudinal axis and with a cross-section $\mathscr{A}$ (of area A in the yz-plane) that is symmetric about the y-axis (it may or may not be also symmetric about the z-axis), as shown in Fig. 8.13. The origin of the yz-plane is placed at the

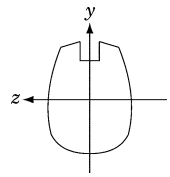

Figure 8.13. Symmetric cross-section

centroid of the cross-section, so that, by Eqs. (1.67),

$$\int_{\mathscr{A}} y\,dA \;=\; \int_{\mathscr{A}} z\,dA \;=\; 0\,. \tag{8.14}$$

We will furthermore assume that the bending moment is about the z-axis and make this explicit by denoting it M_z. By symmetry, then, all the fibers in the xy-plane will bend only in that plane. Since the bending moment is the same at every cross-section, it follows that, except possibly near the ends of the span, all segments should deform identically. This means that, along any fiber parallel to the x-axis in the plane of symmetry, all points must curve the same

way, hence the curvature will be constant. In other words, such a fiber will deform into a circular arc whose radius is called the *radius of curvature*. If we now consider any two such fibers, originally as shown in Fig. 8.14a, we may ask: after bending, where are the centers of the respective arcs in relation to each other? If they are at two different points, then there is a nonzero vector from one point to the other, but there is no reason why such a vector would have one particular direction and not another (see Fig. 8.14b–c). Moreover, if the two centers were only vertically apart, then the fibers would get in each other's way upon bending. Consequently, the two centers must coincide. That is, all the fibers in the plane of symmetry bend into *concentric* circular arcs, as in Fig. 8.14d. What this result means is that the points located on the

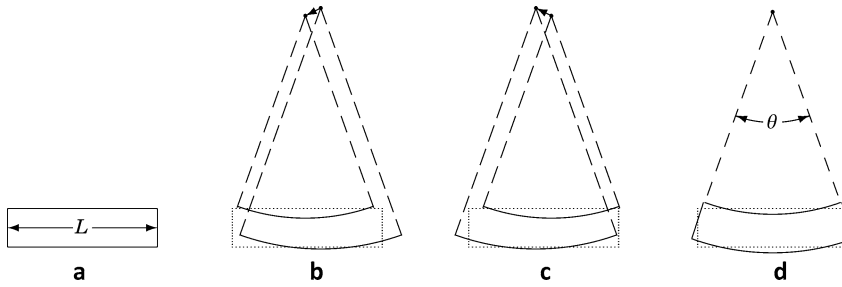

Figure 8.14. Bending of fibers into circular arcs

axis of symmetry remain on a straight line, and when the result is extended (as a hypothesis) to the entire cross-section of the beam, it can be framed as "plane sections remain plane." By observing Fig. 8.14d, we see that, in the course of bending, the fibers closer to the center of the concentric arcs shorten while those farther from the center lengthen. We may assume that there is a particular fiber whose total length L remains the same, so that its radius of curvature, to be denoted ρ, must satisfy $\rho\theta = L$, where θ is the angle formed by connecting the two end-points of the fiber to the center of the circular arc, as illustrated in Fig. 8.15. Suppose that the y-coordinate of this fiber (known as

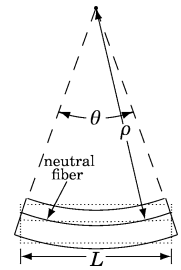

Figure 8.15. Definition of neutral fiber

the *neutral fiber*) in the unbent configuration is y_0. Then, for any other fiber

(with y-coordinate y), the radius of curvature is $\rho-(y-y_0)$, and its change in length, as seen in Fig. 8.16, is

$$\Delta L \;=\; L'-L \;=\; [\rho-(y-y_0)]\theta - L \;=\; -(y-y_0)\theta\;, \tag{8.15}$$

so that its longitudinal strain is

$$\varepsilon_x \;=\; \frac{\Delta L}{L} \;=\; -\frac{y-y_0}{\rho}\;. \tag{8.16}$$

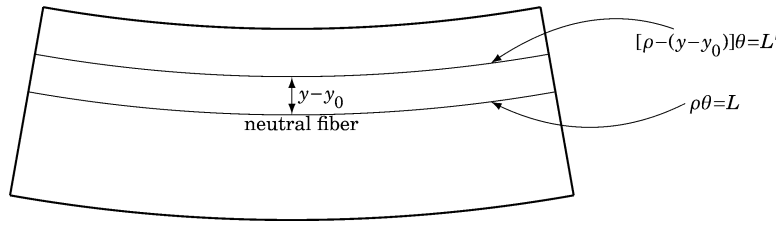

Figure 8.16. Change in length of a fiber in pure bending

Defining the *curvature* κ as the reciprocal of the radius of curvature, that is, $\kappa = 1/\rho$, we may rewrite the last equation as

$$\varepsilon_x \;=\; -\kappa(y-y_0)\;. \tag{8.17}$$

Stress and Bending Moment

We assume that Eq. (8.17) can be extended from the line of symmetry to the entire cross-section, implying that all the fibers in the plane $y = y_0$ remain unchanged in length (this plane is accordingly called the *neutral plane*). If the beam material is homogeneous and linearly elastic, with Young's modulus E, and if the fibers are assumed to be in a state of uniaxial stress, then

$$\sigma_x \;=\; E\varepsilon_x \;=\; -E\kappa(y-y_0)\;, \tag{8.18}$$

with all other stress components equal to zero. This stress distribution (with the third member of Eq. (8.18) independent of x) clearly satisfies the local equilibrium equations (4.39–4.41) in the absence of body force. It should be noted that a state of uniaxial stress σ_x implies the presence, through the Poisson's ratio (see Eq. $(6.10)_{2,3}$), of transverse strains ε_y and ε_z, and these strains imply a deformation of the cross-section in its plane. Since this phenomenon does not affect the bending behavior, we need not concern ourselves with it here. For equilibrium with the resultant moment M_z, we must first ascertain that the *force* resultant of the stress distribution given by Eq. (8.18) is zero, that is,

$$\int_{\mathscr{A}} \sigma_x\, dA \;=\; -E\kappa \int_{\mathscr{A}} (y-y_0)dA \;=\; -E\kappa\left[\int_{\mathscr{A}} y\, dA - y_0 A\right] \;=\; 0\;. \tag{8.19}$$

But, by the first of Eqs. (8.14), the integral inside the square brackets is zero, implying that $y_0 = 0$. This means that *in a homogeneous linearly elastic beam in pure bending, the neutral fiber coincides with the centroidal fiber*. Eq. (8.18) may now be replaced by

$$\sigma_x = -E\kappa y \,. \tag{8.20}$$

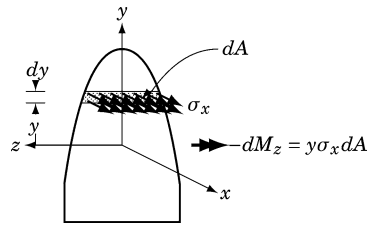

Figure 8.17. Moment due to axial stresses in a beam

To find the resultant moment about the z-axis, we note from Fig. 8.17 that a positive stress σ_x on a strip of the cross-section contained between y and $y+dy$, with y assumed positive, makes the negative contribution $-dM_z = y\sigma_x dA$, so that the total moment is

$$M_z = -\int_{\mathscr{A}} y\sigma_x \, dA \,. \tag{8.21}$$

On combining Eqs. (8.20) and (8.21), we obtain

$$M_z = EI_z\kappa \,, \tag{8.22}$$

where

$$I_z = \int_{\mathscr{A}} y^2 \, dA \tag{8.23}$$

is the *second moment of area* of the cross-section about the z-axis. As long as only bending in the plane perpendicular to the z-axis is considered, the z-subscripts can be omitted and Eq. (8.22) can be simplified to

$$M = EI\kappa \,. \tag{8.24}$$

Eq. (8.24) implies that the moment is proportional to the curvature that it induces under pure bending, just as the axial force is proportional to the elongation in bars (see Eq. (6.59)) and the torque if proportional to the twist in shafts (see Eq. (7.9). The product EI is known as the *flexural rigidity* of the beam.

We may now eliminate κ between Eqs. (8.20) and (8.24) to obtain

$$\sigma_x = -\frac{My}{I} \,. \tag{8.25}$$

Eq. (8.25) resembles Eq. (7.11) of Sect. 7.1, describing the linear distribution of the shear stress in the torsion of an elastic circular shaft. In both equations, the denominator is a quantity of dimension $[\mathrm{L}]^4$ derived from the geometry of the section, and the numerator is the product of a moment and a distance from the center or centroid. In both cases we must remember that, though the elastic modulus does not appear, the formula is limited to homogeneous, linearly elastic beams or shafts. For the maximum bending stress, there is an analogue to Eq. (7.12), namely, the widely used formula

$$\sigma_{\max} = \frac{Mc}{I} , \tag{8.26}$$

where, by convention, $\sigma_{\max}$ is actually $|\sigma_x|_{\max}$ and M is actually $|M|$, while $c = |y|_{\max}$. But the applicability of Eq. (8.26) in stress-based design is limited to materials (such as ductile metals) in which the allowable stress is the same in tension and compression. If this is not so, then separate maximum tensile and compressive stresses must be determined, and their respective location depends on the sign of M. With the definition of the *section modulus* $S = I/c$, Eq. (8.26) can be rewritten as

$$\sigma_{\max} = \frac{M}{S} . \tag{8.27}$$

The section modulus can be interpreted as a measure of the *strength* of a cross-section, since it gives the moment-carrying capacity of a beam with the given cross-section when the allowable stress σ_{all} is known. Since beams are not typically designed to carry a uniform bending moment (that is, to be in a state of pure bending), the discussion of the stress-based design of beams will be postponed to Sect. 8.3, which deals with beams under variable moment.

8.2.2 The Second Moment of Area or "Moment of Inertia"

The second moment of area I_z is often called "moment of inertia," because its definition is mathematically similar to that of the moment of inertia in dynamics. In fact, for a flat disk whose shape is that of the cross-section of the beam, with uniform mass per unit area, the moment of inertia (about an axis in the plane of the disk) is just the product of the mass per unit area and the second moment of area. For relatively simple cross-sections, especially ones with double symmetry, the calculation of the second moment of area is generally straightforward, as we will see in the next few examples. In particular, if the width of the cross-section at a given value of y is $b(y)$, while y ranges from y_1 to y_2, then the area integral of Eq. (8.23) may be rewritten as

$$I_z = \int_{y_1}^{y_2} b(y)\, y^2\, dy . \tag{8.28}$$

Example 8.2.1: Second moment of area of a rectangle.
If the cross-section is a rectangle defined by $-h/2 < y < h/2$, $-b/2 < z < b/2$ (with the width b constant, while h the *depth*[*] of the cross-section), then (8.28) reduces to

$$I_z = \int_{-h/2}^{h/2} y^2 b\, dy = \frac{b}{3} y^3 \Big|_{-h/2}^{h/2} = \frac{b}{3}\left[\left(\frac{h}{2}\right)^3 - \left(-\frac{h}{2}\right)^3\right] = \frac{bh^3}{12} . \tag{8.29}$$

Since $c = h/2$, we also have $S = bh^2/6$.

Example 8.2.2: Second moment of area of a circle.
We observe that, by symmetry, $I_z = I_y$, so that

$$I_z = \frac{1}{2}(I_z + I_y) = \frac{1}{2}\int_{\mathscr{A}} (y^2 + z^2) dA = \frac{1}{2}\int_{\mathscr{A}} r^2\, dA . \tag{8.30}$$

But in polar coordinates we can write $dA = r\, dr\, d\theta$, with the integration going over $0 < r < c$ (where c is the radius of the circle), $0 < \theta < 2\pi$, so that

$$I_z = I_y = \frac{1}{2}\int_0^c r^3 dr \int_0^{2\pi} d\theta = \frac{1}{2}\frac{c^4}{4} 2\pi = \frac{\pi c^4}{4} . \tag{8.31}$$

If we use Cartesian coordinates, then we may use Eq. (8.28) with $b(y) = 2\sqrt{c^2 - y^2}$, so that

$$I_z = 2\int_{-c}^{c} \sqrt{c^2 - y^2}\, y^2\, dy . \tag{8.32}$$

Introducing the change of variable $y = c\sin\theta$, we find that

$$\sqrt{c^2 - y^2}\, y^2\, dy = c\cos\theta \cdot c^2 \sin^2\theta \cdot \cos\theta\, d\theta . \tag{8.33}$$

so that

$$I_z = c^4 \int_{-\pi/2}^{\pi/2} \cos^2\theta \sin^2\theta\, d\theta . \tag{8.34}$$

But $cos^2\theta = (1 + \cos 2\theta)/2$ and $sin^2\theta = (1 - \cos 2\theta)/2$, so that $\cos^2\theta \sin^2\theta = (1 + \cos 2\theta)(1 - \cos 2\theta)/4 = (1 - \cos^2 2\theta)/4 = \sin^2 2\theta/4$. Hence,

$$I_z = \frac{c^4}{4}\int_{-\pi}^{\pi} \sin^2 2\theta\, d(2\theta) . \tag{8.35}$$

Lastly, $\sin^2 2\theta = (1 - \cos 4\theta)/2$, so that

$$\begin{aligned} I_z &= \frac{c^4}{8}\left[\int_{-\pi}^{\pi} d(2\theta) - \frac{1}{2}\int_{-2\pi}^{2\pi} \cos 4\theta\, d(4\theta)\right] = \frac{c^4}{8}\left[2\pi + \frac{\sin 2\pi - \sin(-2\pi)}{2}\right] \\ &= \frac{\pi c^4}{4} , \end{aligned}$$

as before. The section modulus for a circle is $S = I_z/c = \pi c^3/4$.

Note that, because of the double symmetry, it would have been sufficient in the two preceding examples to perform the integration over one half (or one quadrant) of the area and multiply the result by two (or four).

[*]Defined as the largest dimension parallel to the plane of bending

Example 8.2.3: Second moment of area of a rhombus.
A rhombus of width $2a$ and depth $2c$ is composed of four right triangles of base a and height c, with $b(y) = a(1 - y/c)$. Consequently,

$$\begin{aligned} I_z &= 4a \int_0^c y^2 \left(1 - \frac{y}{c}\right) dy = 4a \left(\frac{c^3}{3} - \frac{c^3}{4}\right) \\ &= \frac{ac^3}{3}, \end{aligned}$$

and the section modulus is $S = ac^2/3$.

In the case of cross-sections that are doubly symmetric combinations of simple geometric shapes, we can take advantage of the fact that integration is an additive operation, that is, if a region $\mathscr{A}$ consists of disjoint subregions $\mathscr{A}_1$, $\mathscr{A}_2$, …, all of which have their centroids on the z-axis, then $I_z = \sum_i I_{z_i}$, with $I_{z_i} = \int_{\mathscr{A}_i} y^2 dA$. Examples are seen in Fig. 8.18a–b. But this additive property can also be used for the subtraction of second moments of area. To wit, if a region $\mathscr{A}_3$ consists of disjoint subregions $\mathscr{A}_1$ and $\mathscr{A}_2$, so that $I_{z3} = I_{z1} + I_{z2}$, then obviously $I_{z1} = I_{z3} - I_{z2}$. Thus, if the cross-section of interest covers $\mathscr{A}_1$— while $\mathscr{A}_2$ is hollow— then the desired second moment of area I_z is found by subtracting the second moment of the hollow region (shown as shaded in Fig. 8.18c–d) from that of the larger region. If, for instance, the

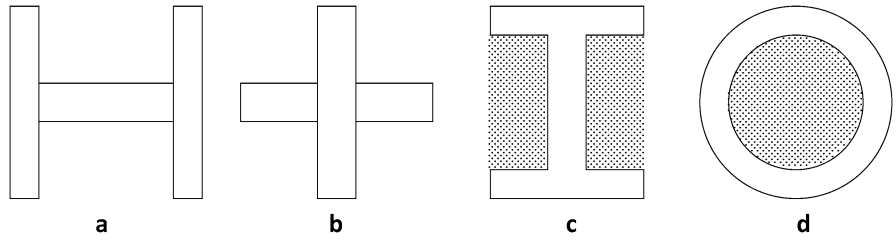

Figure 8.18. Sections whose second moment of area can be determined by addition (a–b) or subtraction (c–d)

inner and outer radii of the tube in Fig. 8.18d are b and c, respectively, then Example 8.2.2 implies that

$$I_z = \frac{\pi(c^4 - b^4)}{2}. \tag{8.36}$$

Similar results are obtained when the section is symmetric about the z-axis, and the moment is about the y-axis. If the cross-section is doubly symmetric, then the axis with the larger value of the section modulus S is called the *strong axis*, while the other is called the *weak axis*.

8.2.3 Parallel-Axis Theorem

If the cross-section (or a subregion thereof) is not symmetric about the z-axis, it is often mathematically easier to calculate the second moment of area about some axis (say z') parallel to the z-axis. The relation between this second moment $I_{z'}$ and I_z is known as the *parallel-axis theorem*. Suppose that the z'-axis intersects the y-axis at $y = d$, as depicted in Fig. 8.19. Then the second moment of area about the z'-axis is defined as

$$I_{z'} = \int_{\mathscr{A}} (y-d)^2 dA = \int_{\mathscr{A}} y^2 dA - 2d \int_{\mathscr{A}} y\, dA + d^2 \int_{\mathscr{A}} dA \,. \tag{8.37}$$

It follows from (8.23) and the first of (8.14) that

$$I_{z'} = I_z + d^2 A \,. \tag{8.38}$$

This result is the parallel-axis theorem (note that it is independent of the sign of d).

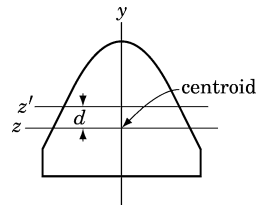

Figure 8.19. Parallel-axis theorem

Example 8.2.4: Second moment of area of an isosceles triangle.
We may regard an isosceles triangle of base b and height h as the upper half of the rhombus of Example 8.2.3, with $b = 2a$ and $h = c$. If the z'-axis coincides with the base, then we may use the result for the rhombus to obtain

$$I_{z'} = \frac{1}{2} \cdot \frac{(b/2)h^3}{3} = \frac{bh^3}{12} \,. \tag{8.39}$$

As we know from Example 1.5.2 of Sect. 1.5, the distance from the base to the centroid is $h/3$. Consequently,

$$I_z = I_{z'} - d^2 A = \frac{bh^3}{12} - \frac{(h/3)^2 bh}{2} = \frac{bh^3}{36} \,. \tag{8.40}$$

Example 8.2.5: Second moment of area of an I-beam.
For the I-beam shown in Fig. 8.18c, the second moment of area I_z can be found simply by the subtraction method: if b and h are the overall width and depth of

the section, t_w and t_f the web and flange thicknesses, and $d = h - 2t_f$ the depth of the web alone, then

$$I_z = \frac{1}{12}[bh^3 - (b - t_w)d^3] . \tag{8.41}$$

This may be rewritten as

$$I_z = \frac{1}{12}t_w d^3 + \frac{1}{12}b(h^3 - d^3) . \tag{8.42}$$

The first term is obviously the second moment of area of the web alone, and the second term must accordingly be the contribution of the flanges. Now

$$h^3 - d^3 = h^3 - (h - 2t_f)^3 = 6h^2 t_f - 12ht_f^2 + 8t_f^3 = 6t_f(h - t_f)^2 + 2t_f^3 . \tag{8.43}$$

Consequently, the second term in the equation for I_z may be rewritten as

$$2\left[bt_f\left(\frac{h - t_f}{2}\right)^2 + \frac{bt_f^3}{12}\right] , \tag{8.44}$$

where the second term inside the brackets is the second moment of area of each flange about its own centroid, and the first is its contribution through the parallel-axis theorem. If the flanges are thin in comparison with the depth ($t_f \ll h$), then the second term can be neglected and the first term simplified as $A_f h^2/4$ (with $A_f = bt_f$ being the flange area), so that the total second moment of area can be approximated as $I_z \doteq (A_w + 6A_f)h^2/12$. The approximation is even better if h is taken as not the overall depth but the distance between the centers of the flanges. If, say, $h = 12$, $b = 9$ and $t_f = t_w = 1$, then the exact value of I_z is 629, while the approximation with $h = 11$ is 645, off by 2.5%. Note, further, that the contribution of the web to the second moment (and hence to the rigidity and strength of the beam) is only around 15%.

8.2.4 Work and Energy in Pure Bending

We may consider, with no loss of generality, a beam of length L that is built-in at the left end with the right end free, with a moment M applied there. It is clear that this beam is in a state of pure bending. If the beam is bent into an arc with curvature κ (so that the free end is at an angle κL with respect to the x-axis), then a virtual displacement compatible with pure bending can consist only of a change $\delta\kappa$ in the arc curvature, so that the free end accordingly rotates by the angle $\delta\kappa L$ (see Fig. 8.20). The virtual work of the applied load

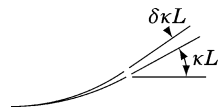

Figure 8.20. Virtual displacement in pure bending

is therefore $\delta W_{\text{ext}} = ML\,\delta\kappa$. Recall that the internal virtual work per unit length of a bar in pure tension is given by Eq. (5.18) (page 220). With ε_x

given by Eq. (8.17) with $y_0 = 0$, we have $\delta\varepsilon_x = -\delta\kappa\, y$, and the internal virtual work per unit length is obtained by integrating $\sigma_x \delta\varepsilon_x$ over the cross-sectional area, that is,

$$\delta W'_{\text{int}} = \int_{\mathscr{A}} \sigma_x(-\delta\kappa\, y)dA = \delta\kappa \left[-\int_{\mathscr{A}} \sigma y dA\right] = M\,\delta\kappa\,. \tag{8.45}$$

When this is multiplied by L to get the total internal virtual work δW_{int}, it equals the external virtual work, as required by the principle of virtual work. The actual work done by the moment M as the beam is bent from a straight configuration to one with curvature κ is

$$W = \int_0^{\kappa} M(\kappa')d(\kappa' L)\,, \tag{8.46}$$

which, on substituting the moment-curvature relation (8.24), becomes

$$W = \frac{EI\kappa^2 L}{2}\,. \tag{8.47}$$

Consequently,

$$U'_{\text{b}} = \frac{EI\kappa^2}{2} \tag{8.48}$$

is the strain energy of bending, per unit length, stored in the beam. By the same token, the complementary energy per unit length is

$$\overline{U}'_{\text{b}} = \frac{M^2}{2EI}\,. \tag{8.49}$$

8.2.5 Initially Curved Beams

If the beam has a slight initial curvature κ_0 before any moment is applied, then the length of the fibers is not the same to begin with, but is given by $L - (y - y_0)\kappa_0$. The strain, then, is due to the additional elongation and is consequently given by

$$\varepsilon_x = -(\kappa - \kappa_0)(y - y_0)\,, \tag{8.50}$$

rather than by Eq. (8.17). Consequently, in Eqs. (8.18), (8.20), (8.22) and (8.24) the curvature κ needs to be replaced by $\kappa - \kappa_0$.

Exercises

8.2-1. Find the smallest radius of curvature to which a steel wire of diameter 0.08 in, initially straight, can be bent without exceeding a maximum normal stress of 24 ksi. Assume $E = 30 \times 10^3$ ksi.

8.2-2. A strip of wood with rectangular cross-section 0.5 cm×2.0 cm and length 2.0 m, is bent about the weak axis into a semicircle. If $E = 12.0$ GPa, find the bending moment and the maximum normal stress.

8.2-3. Find the second moment of area I_z about the centroidal z-axis, as well as the section modulus S, for the ellipse given by $(y/b)^2 + (z/c)^2 = 1$.

8.2-4. For an equilateral triangle with sides of length a, find the second moment of area about a centroidal axis (a) parallel to one of the sides, (b) perpendicular to one of the sides.

8.2-5. Find the second moment of area I_z about the centroidal z-axis, as well as the section modulus S, for the solid semicircle of radius c shown in the figure.

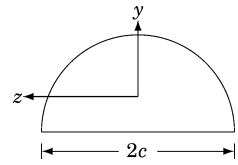

8.2-6. Find the second moment of area I_z about the centroidal z-axis, as well as the section modulus S, for the thick-walled tube of the figure on the left. Use this result to also find the second moment of area $I_{z'}$ about the centroidal z'-axis of the open cross-section of the figure on the right.

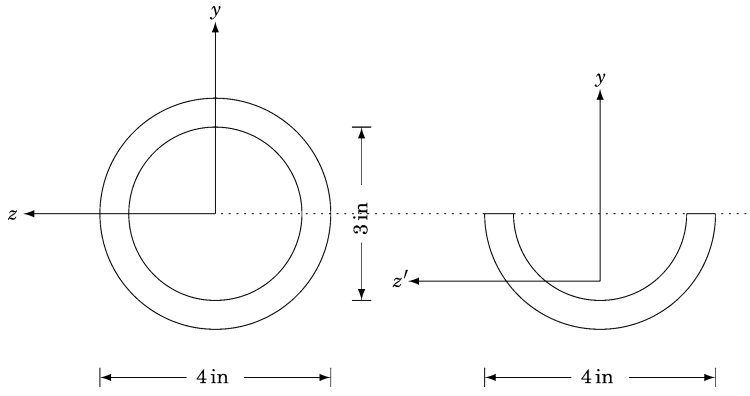

8.2-7. Find the second moment of area I_z about the centroidal z-axis, as well as the section modulus S, for the square thick-walled cross-section of

the figure on the left. Use this result to also find the second moment of area $I_{z'}$ about the centroidal z'-axis of the open cross-section of the figure on the right.

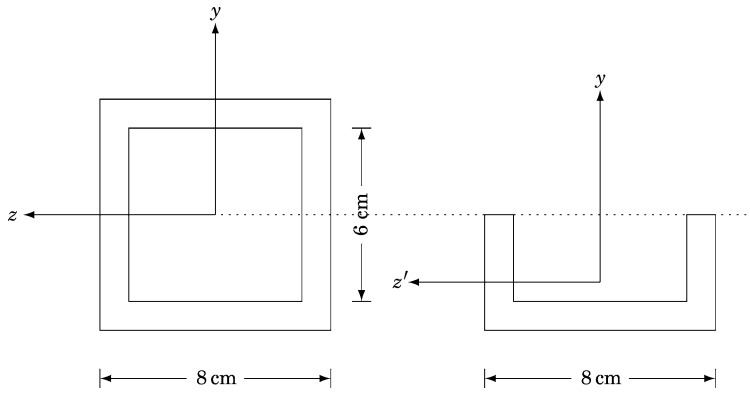

8.2-8. Find the second moment of area I_z about the centroidal z-axis, as well as the section modulus S, for the regular hexagon of the figure on the left. Use the result, and the parallel-axis theorem, to obtain the same result for the trapezoid of the figure on the right.

8.2-9. For the wide-flange beam shown in the figure, with $t_f = t_w = t$ and $t \ll b$, $t \ll h$, find the ratio b/h such that the beam is (a) equally stiff about both axes (that is, $I_y = I_z$), (b) equally strong about both axes (that is, $2I_y/b = 2I_z/h$).

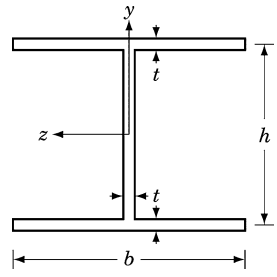

8.2-10. For the I-beam of Fig. 8.18c, suppose that the overall depth and width are 100 mm and 70 mm, respectively, while the flange and web thicknesses are 15 mm and 20 mm, respectively. Find the second moment

of area I_z about the centroidal z-axis using (a) subtraction, (b) addition and the parallel-axis theorem. Also find the section modulus S.

8.2-11. A rectangular strip of steel ($E = 200\,\text{GPa}$) with rectangular cross-section $1\,\text{mm} \times 10\,\text{mm}$ and length $10\,\text{cm}$ is used as a rotational spring as illustrated in Fig. 6.1e (page 248). Find (a) the rotational spring constant $\overline{k}$, (b) the energy stored in the spring when it is bent to an angle of $5°$.

8.2-12. Consider a simply-supported I-beam subject to the two end moments $\overline{M} = 100$ kip·ft, as in the figure. Suppose that the thickness of the web and flanges is $t_w = t_f = 2$ in, the depth of the web is $d = 16$ in, and the width of the flanges is $b = 10$ in, as discussed in Example 8.2.5. If the beam is made of a linearly elastic material with $E = 1.6 \times 10^3$ ksi, find

(a) the maximum normal stress and strain in the web and in the flanges,

(b) the radius of curvature of the neutral fiber,

(c) the rotation of the one end relative to the other,

(d) the energy stored in the beam.

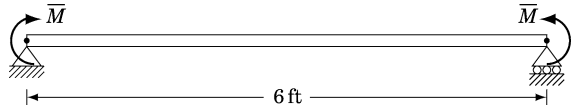

8.3 Bernoulli–Euler Beam Theory

8.3.1 Introduction

As we noted in the preceding section, beams are not typically designed to carry a uniform bending moment. Instead (as we noted much earlier, in Sect. 2.2, page 82) they are used primarily to carry transverse forces, and are therefore rarely in a state of pure bending. Nevertheless, the theory we have just developed can still be applied, to a large extent, to actual beams, as we will discuss below. The so-called *engineering* (or *technical*) *theory of beams*, also

Figure 8.21. Daniel Bernoulli

known as the *Bernoulli–Euler beam theory*[*], is based on the assumption that, for sufficiently slender beams, the basic results in pure bending are valid *locally* (meaning, at each point x) in a beam with variable bending moment $M(x)$. This means that the longitudinal strain and axial stress are still given by Eqs. (8.17) and (8.18), respectively, with $y_0 = 0$ in the absence of axial force, and with $\kappa(x)$ being the *local* curvature of the curve assumed by the neutral fiber (known as the *elastic curve* or *elastica*). The local relations between moment and curvature, and between stress and moment, are still assumed to be given by Eqs. (8.22) and (8.25), respectively.

It is important to note that, with M in Eq. (8.25) being a function of x, σ_x is no longer independent of x, so that the local equilibrium equations (4.39–4.42) are not satisfied in the absence of other stress components. (The presence of shear stresses is necessarily implied by that of a shear force.) The Bernoulli–Euler theory makes no attempt to satisfy these equations, and it is consequently not an "exact" but rather an *approximate* theory, whose validity must be confirmed by experience. Such confirmation is abundant for

[*]Named for two noted Swiss mathematicians, Daniel Bernoulli (1700–1782) and the aforementioned (page 57) Leonhard Euler, who developed it around 1750, though engineers did not get around to using it for another century.

sufficiently slender beams, which in practice means beams with a span-to-depth ratio of 10 or more.[†] The width must also be small in comparison to the length.

8.3.2 Stress Analysis and Stress-Based Design of Beams

Stress analysis is the calculation of stresses in a given structure or structural element, under prescribed or expected loading, as already done for axially loaded bars in Sect. 6.3 and for shafts in torsion in Chap. 7. Just as with variable axial force and variable torque, when the bending moment in a beam varies with x, the maximum stress for the purpose of stress-based design must be found not only over the cross-section but over the length of the beam. Consequently, instead of Eq. (8.26), we have, for a prismatic beam,

$$\sigma_{\max} = \frac{M_{\max} c}{I} = \frac{M_{\max}}{S}, \tag{8.51}$$

where $\sigma_{\max}$ is in fact $|\sigma|_{\max}$ and $M_{\max}$ is $|M|_{\max}$. Again, Eq. (8.51) is valid only for those materials (typically, ductile metals such steel, aluminum and so on) for which the allowable stress σ_{all} is the same in tension and in compression. When designing with such materials, it makes sense to use beams (if they are loaded in the xy-plane) with cross-sections that are symmetric about the z-axis, so that the maximum stresses in tension and compression are numerically the same. It also makes sense, in the interest of economizing on material, for such sections to have as much area as possible far away from the neutral fibers, in order to maximize the second moment of the area, and hence also the moment-carrying capacity for a given maximum stress. For these two reasons, I-beams (as introduced in Example 8.2.5, page 373) are among the most common structural elements in large structures. It is common practice to select I-beams (as well as other structural shapes) from readily available tables that detail their geometric properties.

In the United States, the most commonly used I-beam sections are designated W $xx \times yy$ (for example, W 24×146), where xx denotes the approximate depth in inches and yy the approximate unit weight in pounds per foot. In Europe the most common wide-flange I-beams are designated HEA xxx or HE xxx A (for example HEA 160 or HE 160 A), where xxx is the width in millimeters.

Example 8.3.1: Stress-based design of a uniformly loaded simply supported I-beam.
A steel beam, with an allowable stress of 175 MPa, is to carry a uniformly distributed load of 5 kN/m over a span of 8 m. We wish to find the lightest HEA

[†]A better measure of slenderness than the span-to-depth ratio is the *slenderness ratio*, which will be discussed in the next chapter.

section does not exceed 20 cm from the table below, where all lineal dimensions are in millimeters, the unit weight w_b is in kg_f/m, and I and S (about the strong axis) are in cm^4 and cm^3, respectively.

HEA	h	b	t_w	t_f	w_b	I	S
100	96	100	5	8	16.7	349	72.8
120	114	120	5	8	19.9	606	106
140	133	140	5.5	8.5	24.7	1030	155
160	152	160	6	9	30.4	1670	220
180	171	180	6	9.5	35.5	2510	294
200	190	200	6.5	10	42.3	3690	389
220	210	220	7	11	50.5	5410	515
240	230	240	7.5	12	60.3	7760	875
260	250	260	7.5	12.5	68.2	10450	836
280	270	280	8	13	76.4	13670	1010
300	290	300	8.5	14	88.3	18260	1260

If, to begin with, we neglect the weight of the beam, then the maximum moment is found, from Eq. (8.1.1), as

$$M_{\max} = \frac{5\,\mathrm{kN/m}\cdot 10^2\,\mathrm{m}^2}{8} = 62.5\,\mathrm{kN}\cdot\mathrm{m}.$$

The minimum section modulus required is therefore

$$S_{\min} = \frac{M_{\max}}{\sigma_{\mathrm{all}}} = \frac{62.5\times 10^3\,\mathrm{N}\cdot\mathrm{m}}{175\times 10^6\,\mathrm{N}\cdot\mathrm{m}^{-2}} = 357\,\mathrm{cm}^3.$$

We find that the beam of section HEA 200, with a depth of 19 cm and a section modulus of 389 cm^3, meets our requirements. The weight of this beam per unit length is 42.3 kg_f/m or 0.414 kN/m. The actual load per unit length is therefore 5.41 kN/m, and therefore the minimum section modulus is now, in cm^3, (5.41/5)357=387. The selected shape still works.

In timber, the practice is to prescribe an allowable stress in bending, to be used in conjunction with Eq. (8.51), that is not necessarily the same as the tensile or compressive allowable stress that might be used in the design of axial-force members (it is usually greater than either). The value of the right-hand side of Eq. (8.51) at failure, regardless of whether the behavior leading up to it is elastic, is conventionally known as the *modulus of rupture*, and is denoted σ_U^{b}. The allowable stress is obtained by dividing this quantity by the safety factor.

The first known analysis of a beam, though based on incorrect assumptions, was performed by Galileo in his final book[‡] and is illustrated in the figures taken from this book. Fig. 8.22a shows a cantilevered timber carrying a concentrated load at its free end. In Fig. 8.22b, Galileo showed that a rectangular beam with the narrow sides horizontal and the wide sides vertical

[‡]*Discorsi e Dimostrazioni Matematiche, intorno á Due Nuove Scienze* (Discourses and Mathematical Demonstrations Concerning Two New Sciences) was published in 1638.

a b

Figure 8.22. Galileo's illustrations of beam analysis: (**a**) illustration of end-loaded cantilever, (**b**) comparison of strong and weak configurations

(the configuration on the left) can carry a greater weight than in the other configuration, by a ratio equal to that of the sides, which is just what the theory of beams tells us, since the ratio of the section moduli for a rectangular beam is $(bh^2/6)/(hb^2/6) = h/b$. The stress-based design of a timber beam will be illustrated in the following example.

Example 8.3.2: Design of a cantilevered rectangular timber beam under an end load.
We consider a cantilever beams of span $L = 4$ ft and carrying a concentrated force $F = 500$ lb at its tip, made of wood with an allowable flexural stress of 1.8 ksi. The beam is to be selected from the "two-by" series ($2\times n$), whose width is $b = 1.5$ in and whose depth is $h = n - 0.5$ in, with n an even integer. The specific weight of the wood is taken as 35 lb/ft^3. The quantity to determine is the depth of the beam. From

$$S_{\min} = \frac{bh_{\min}^2}{6} = \frac{M_{\max}}{\sigma_{\text{all}}} = \frac{FL}{\sigma_{\text{all}}}$$

we find

$$h_{\min} = \sqrt{\frac{6FL}{b\sigma_{\text{all}}}} = \sqrt{\frac{6\cdot 0.5\,\text{kip}\cdot 48\,\text{in}}{1.5\,\text{in}\cdot 1.8\,\text{kip}\cdot\text{in}^{-2}}} = 10.3\,\text{in}\,.$$

Consequently the beam will be a 2×12, with a depth of 11.5 in. The weight of the beam per unit length is accordingly 35 lb/ft$^3\cdot(1.5\cdot 11.5/144)$ ft^2 = 42 lb/ft, equivalent to an addition of 84 lb to the end load, and therefore requiring an increase in the minimum section modulus by a factor of 584/500 = 1.168, and in the minimum depth by a factor of $\sqrt{1.168} = 1.08$, making it 11.1 in. The selected beam still works.

In materials that are brittle (see Sect. 11.1), for example cast iron, in which the allowable stress in tension is considerably smaller than in compression, it is not economical to use doubly symmetric sections, but rather sections such that the distance from the neutral fibers to the extreme fibers in tension is significantly smaller than to those in compression. A typical design is that of a T-beam, as in the following example.

Example 8.3.3: Stress analysis of a T-beam shelf.

The cantilevered T-beam shown in the figure (where all dimensions shown are in inches) is 24 inches long, is made of cast iron and is to be used as a shelf carrying a uniformly distributed load $\overline{w}$ per unit length. We wish to find the largest value of $\overline{w}$ for the maximum stress not to exceed 18 ksi in tension or 60 ksi in compression.

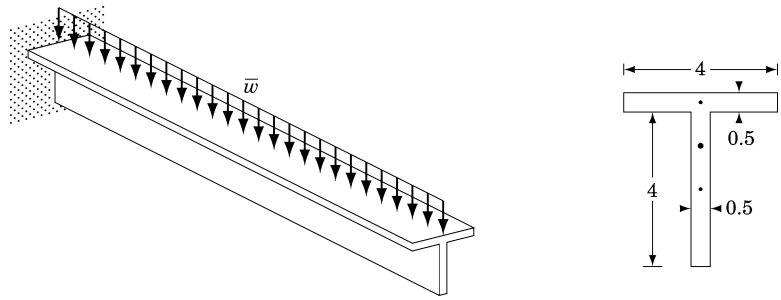

Because the stem and the flange are both 4 in × 0.5 in rectangles, the centroid of the whole section is located halfway between those of the rectangles, the distance between them being 2.25 in. The centroid is consequently 1.375 in from the top and 3.125 in from the bottom. For the purposes of the parallel-axis theorem, $d = 1.125$ in for both subregions. The second moment of area is accordingly

$$I_z = \left[\frac{4\cdot 0.5^3}{12} + \frac{0.5\cdot 4^3}{12} + 2(4\cdot 0.5\cdot 1.125^2)\right] \text{in}^4 = 7.77 \text{ in}^4 . \tag{8.52}$$

Since the moment is negative, the fibers above the neutral plane will intension and those below it in compression. For the tension zone $c = 1.375$ in, and therefore the allowable moment is

$$M^{\text{t}}_{\text{all}} = \frac{18 \text{ k}\cdot\text{in}^{-2}\cdot 7.77 \text{ in}^4}{1.375 \text{ in}} = 102 \text{ k}\cdot\text{in} , \tag{8.53}$$

while the allowable moment for compression is

$$M^{\text{c}}_{\text{all}} = \frac{60 \text{ k}\cdot\text{in}^{-2}\cdot 7.77 \text{ in}^4}{3.125 \text{ in}} = 149 \text{ k}\cdot\text{in} , \tag{8.54}$$

and it is the former, being smaller, that governs; that is, $M_{\text{all}} = 102\text{k}\cdot\text{in}$. Since we know from Sect. 8.1 (Example 8.1.2, page 355) that $M_{\max} = wL^2/2$, it follows that $\overline{w}_{\text{all}} = 2M_{\text{all}}/L^2 = 2\cdot 102 \text{ k}\cdot\text{in}/24^2 \text{ in}^2 = 0.354$ k/in.

8.3.3 Curvature and Deflection

Let a curve in the (x, y)-plane be described by the equation $y = v(x)$. We define the *inclination* of the curve as the angle

$$\theta = \tan^{-1} v' , \tag{8.55}$$

where $v'(x) = dy/dx$ is the slope of the curve. Now consider two infinitesimally close points on the curve, $(x, v(x))$ and $(x+dx, v(x+dx))$. If we write $d\theta = \theta(x+dx) - \theta(x)$, then, as shown in Fig. 8.23, the portion of the curve between the two points is approximately a small circular arc (shown thick in the figure) subtending the angle $d\theta$. If the arc length of this portion of the curve is ds, then its radius ρ must satisfy $\rho d\theta = ds$. Recalling that the curvature κ is the

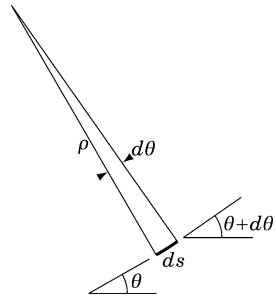

Figure 8.23. Small arc of an elastic curve

reciprocal of the radius of curvature ρ, we obtain

$$\kappa = \frac{d\theta}{ds} . \tag{8.56}$$

Starting from Eq. (8.55), it follows that[§]

$$\frac{d\theta}{dx} = \frac{v''}{1+v'^2} . \tag{8.57}$$

Furthermore, appealing to the Pythagorean theorem $ds = \sqrt{(dx)^2 + (dy)^2}$, and recalling that $dy = v'dx$, it follows that

$$\frac{ds}{dx} = \sqrt{1+v'^2} . \tag{8.58}$$

By dividing Eq. (8.57) by Eq. (8.58), the curvature in Eq. (8.56) may be expressed as

$$\kappa = \frac{v''}{\left(1+(v')^2\right)^{3/2}} . \tag{8.59}$$

If we limit our attention to curves for which $|v'(x)| \ll 1$ (that is, ones whose slope does not deviate much from the x-axis), Eq. (8.59) may be replaced by its linearized *small-deflection* counterpart

$$\kappa \doteq v'' = \frac{d^2v}{dx^2} . \tag{8.60}$$

[§]This derivation relies on the identity $d(\tan^{-1}x)/dx = 1/(1+x^2)$.

Eq. (8.60), when combined with Eq. (8.24), forms a second-order differential equation for the determination of beam deflections when the moment is known, that is, when the beam is statically determinate. When, however, this equation is further combined with the equilibrium equation (8.5), the result is a fourth-order equation for the deflection in terms of the loading, and represents an application of the displacement method, in which, as we know from Sect. 6.4, the static determinacy of the body does not play a role. The calculation of beam-deflection curves (also known as *elastic curves*) will be pursued in Sect. 8.4. In the present section, we limit our consideration to the calculation of deflections and/or rotations[¶] at discrete points, for which we can use energy methods.

8.3.4 Work and Energy

Since the basic idea of the Bernoulli–Euler theory is that the *local* behavior of the beam is very nearly like pure bending, the internal virtual work per unit length is given by Eq. (8.45), with κ (which we now write as v'') obtained from Eq. (8.60). Thus, the total internal virtual work is

$$\delta W_{\text{int}} = \int_0^L M \delta v'' dx \,, \tag{8.61}$$

where L is the span of the beam. Since, as was pointed out in Sect. 2.1, the δ operator defining virtual displacements is distributive, it can be interchanged with differentiation, so that $\delta v'' = (\delta v)''$. Accordingly, we may use integration by parts to express the integral in Eq. (8.61) as

$$\int_0^L M(\delta v)'' dx = M \delta v' \Big|_0^L - \int_0^L M'(\delta v)' dx \tag{8.62}$$

$$= M \delta v' \Big|_0^L - M' \delta v \Big|_0^L + \int_0^L M'' \delta v \, dx \,. \tag{8.63}$$

The external virtual work of the loading w is

$$\delta W_{\text{ext}} = -\int_0^L w \delta v \, dx \,, \tag{8.64}$$

since w is defined as positive downward and v as positive upward. Consequently, by the principle of virtual work (Eq. (2.30)), which requires that, at equilibrium, $\delta W_{\text{ext}} = \delta W_{\text{int}}$, we obtain, on letting $M' = V$ from Eq. (8.5),

$$\int_0^L (M'' + w) \delta v \, dx - M \delta v' \Big|_0^L - V \delta v \Big|_0^L = 0 \,. \tag{8.65}$$

[¶]Since the beam is assumed to behave locally as if it were in pure bending, the cross-section is assumed to be perpendicular to the deflection curve, and therefore the inclination θ of the latter is also the rotation of the cross-section. This assumption is, however, an approximation.

The integral in Eq. (8.65) vanishes identically as a result of Eq. (8.6), and for the vanishing of the boundary terms it is required at each end that

(a) either (i) the bending moment vanish or (ii) the slope be prescribed, and

(b) either (iii) the shear force vanish or (iv) the deflection be prescribed.

The combination (i)+(iii) describes a free end, (ii)+(iv) a built-in end, and (i)+(iv) a simply supported end.

8.3.5 Elastic Energy

For the strain energy of bending, we use Eq. (8.48) for the local value per unit length, replace κ by v'', and integrate over the length of the beam to obtain

$$U_{\mathrm{b}} = \frac{1}{2}\int_0^L EIv''^2\,dx\,. \tag{8.66}$$

Similarly, the complementary energy is deduced from Eq. (8.49) as

$$\overline{U}_{\mathrm{b}} = \int_0^L \frac{M^2}{2EI}\,dx\,. \tag{8.67}$$

For statically determinate beams carrying a single load, we can use the principle of conservation of energy, Eq. (6.134), in conjunction with Eq. (8.49) to find the displacement (deflection or rotation) conjugate to the applied load, be it a force or a moment.

Example 8.3.4: Tip deflection of an end-loaded cantilever.
In a cantilever carrying a force F at the tip, the bending moment is $M(x) = \pm F(L-x)$, and therefore

$$\overline{U}_{\mathrm{b}} = \frac{F^2}{2EI}\int_0^L (L-x)^2\,dx = \frac{F^2L^3}{6EI}\,. \tag{8.68}$$

Equating this to the work done by the force, $W = \frac{1}{2}F\Delta$ (where $\Delta = |v(L)|$), immediately leads to $\Delta = FL^3/3EI$, so that the spring constant of the spring illustrated in Fig. 6.1c is $k = 3EI/L^3$.

When more than one load is present, we can use Castigliano's second theorem, Eq. $(6.138)_2$, to determine the deflections conjugate to the loads. We can do this even for points where no load is acting: we place a fictitious concentrated force there, and, after differentiating with respect to it to obtain the deflection, we set its value equal to zero. Moreover, Castigliano's theorems refer to *generalized* forces and displacements, that is, either forces or moments and either deflections or angles of rotation (which, in the context of small-deflection analysis, are the same as slopes). Thus, a fictitious concentrated

couple will enable us to calculate the slope at its location. With the complementary energy given by Eq. (8.67), it is convenient to apply Castigliano's second theorem, that is, differentiate with respect to the concentrated force, say F, (and, if appropriate, then set $F = 0$) *before* carrying out the integration. Thus

$$\Delta = \int_0^L M \frac{\partial M}{\partial F}\, dx \,. \tag{8.69}$$

Example 8.3.5: Tip deflection of a uniformly loaded cantilever.
If a cantilever carries both a uniformly distributed load of intensity $\overline{w}$ and a downward concentrated force F at its tip, the moment is given by

$$M(x) = -\frac{\overline{w}}{2}(L-x)^2 - F(L-x)\,,$$

so that

$$\frac{\partial M}{\partial F} = -(L-x)\,, \tag{8.70}$$

it follows that that, with F now set to zero, the tip deflection (assumed downward) of a uniformly loaded homogeneous prismatic beam, with flexural rigidity EI, is

$$\Delta = \frac{\overline{w}}{2EI}\int_0^L (L-x)^3\, dx = \frac{\overline{w}L^4}{8EI}\,.$$

If instead of a concentrated force we place a clockwise concentrated couple $\overline{M}$ at the tip, the moment is

$$M(x) = -\frac{\overline{w}}{2}(L-x)^2 - \overline{M}$$

so that $\partial M/\partial \overline{M} = -1$ and therefore the slope (assumed downward) at the tip is

$$\theta = \frac{\overline{w}}{2EI}\int_0^L (L-x)^2\, dx = \frac{\overline{w}L^3}{6EI}\,.$$

It should be noted that the partial derivative $\partial M/\partial F$ given by Eq. (8.70) is just what the bending moment at x would be if the only loading were by a concentrated force *of magnitude 1* acting at the tip. This moment is usually written as $m(x)$, and if there are several (say N) possible points x_i at which a force (or, possibly, couple) of unit magnitude may be applied, the corresponding moments are written as $m_i(x)$. If, now, there are actual forces F_i acting at these points, then, by the principle of superposition, the actual bending moment is given by

$$M(x) = \sum_{i=1}^{N} F_i m_i(x)\,, \tag{8.71}$$

and, consequently, the complementary energy, from Eq. (8.67), is

$$\overline{U}_{\rm b} = \int_0^L \frac{1}{2EI}\left[\sum_{i=1}^{N} F_i m_i(x)\right]\left[\sum_{j=1}^{N} F_j m_j(x)\right] dx \tag{8.72}$$

$$= \frac{1}{2}\sum_{i=1}^{N}\sum_{j=1}^{N}\left(\int_0^L \frac{m_i(x)m_j(x)}{EI}\, dx\right) F_i F_j. \tag{8.73}$$

By comparison with Eq. (6.133)$_2$ (page 304), we see that the integrals inside the parentheses of the last expression are just the flexibility coefficients of a discretely loaded beam viewed as an elastic system, that is,

$$f_{ij} = \int_0^L \frac{m_i(x)m_j(x)}{EI}\,dx\,. \tag{8.74}$$

Accordingly, they form a basis for the solution of statically indeterminate beam problems by the force method, as discussed in Sect. 6.4 (page 293).

Example 8.3.6: Flexibility matrix for an end-loaded cantilever.
We consider a cantilever that can be loaded at its tip either by a concentrated force F or a concentrated couple $\overline{M}$. Accordingly we let $F_1 = F$ and $F_2 = \overline{M}$, and the conjugate general displacements Δ_1 and Δ_2 are respectively the tip deflection Δ and the tip rotation θ. Since, as we already know, $m_1(x) = -(L-x)$, and (see Fig. 8.12b) $m_2(x) = 1$, we have (assuming constant EI)

$$f_{11} = \frac{1}{EI}\int_0^L (L-x)^2\,dx = \frac{L^3}{3EI}\,,\; f_{12} = f_{21} = -\frac{1}{EI}\int_0^L (L-x)\,dx = -\frac{L^2}{2EI}\,,\; f_{22} = \frac{L}{EI}\,.$$

Note that the result for $f_{12} = f_{21}$ gives *both* the rotation due to a force *and* the deflection due to a couple.

Exercises

8.3-1. Find the maximum tensile and the maximum compressive stress in the beam of Exercise **8.1-1**, assuming that it has the cross-section of Exercise **8.2-5**, with $c = 3$ in, and that it is made of a linearly elastic material.

8.3-2. Find the maximum tensile and the maximum compressive stress in the beam of Exercise **8.1-2**, assuming that it has the open cross-section of Exercise **8.2-7** and that it is made of a linearly elastic material.

8.3-3. Find the maximum tensile and the maximum compressive stress in the beam of Exercise **8.1-3**, assuming that it has the open cross-section of Exercise **8.2-7** and that it is made of a linearly elastic material.

8.3-4. Find the maximum tensile and the maximum compressive stress in the beam of Exercise **8.1-5**, assuming that it has the open cross-section of Exercise **8.2-6** and that it is made of a linearly elastic material.

8.3-5. Find the maximum tensile and the maximum compressive stress in the beam of Exercise **8.1-7**, assuming that its cross-section is an isosceles triangle as in Example 8.2.4, with $b = 1$ in and $h - 2$ in, and that it is made of a linearly elastic material.

8.3-6. Find the maximum tensile and the maximum compressive stress in the beam of Exercise **8.1-9**, assuming that it has the open cross-section of Exercise **8.2-7** and that it is made of a linearly elastic material.

8.3-7. Find the maximum tensile and the maximum compressive stress in the beam of Exercise **8.1-10**, assuming that it has the open cross-section of Exercise **8.2-6** and that it is made of a linearly elastic material.

8.3-8. Find the maximum tensile and the maximum compressive stress in the beam of Exercise **8.1-11**, assuming that its cross-section is an isosceles triangle as in Example 8.2.4, with $b = 2$ cm and $h = 3$ cm, and that it is made of a linearly elastic material.

8.3-9. Suppose that the concentrated force $F = 100$ N of Exercise **8.1-11** traverses the length of the beam, while the distributed force $\overline{w} = 10$ N/cm (downwards) remains constant. Find the maximum normal stress at the center of the beam (along its length) as a function of the position $\bar{x}$ of F, where $\bar{x} = 0$ corresponds to the leftmost point of the beam. Assume that the beam is made of a linearly elastic material and that the cross-section is rectangular with width $b = 0.1$ cm and depth $h = 0.5$ cm.

8.3-10. Use conservation of energy to determine the rotation at B of the simply supported beam (with flexural rigidity EI) loaded as shown in the figure.

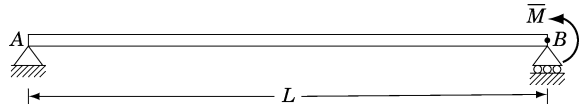

8.3-11. Use Castigliano's second theorem to determine the rotation at B of the simply supported beam (with flexural rigidity EI) loaded as shown in the figure.

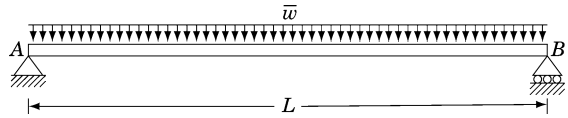

8.4 Calculation of Elastic Beam Deflections

8.4.1 General Procedure

The moment in a homogeneous and linearly elastic beam may be related to the deflection of the neutral fiber (which is taken to represent the deflection of the beam and is illustrated in Figure 8.24) by combining the curvature-deflection relation (8.60) with the moment-curvature relation (8.24), leading to

$$EI\frac{d^2v}{dx^2} = M\,. \tag{8.75}$$

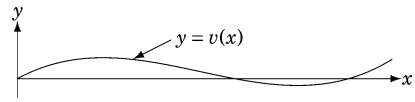

Figure 8.24. Illustration of beam deflection

Once the bending-moment distribution $M(x)$ is determined, it may be put into the right-hand side of Eq. (8.75) and integrated twice to yield the deflection $v(x)$. The solution will have two constants of integration, which can be determined from the two constraints on the deflection that are necessary for a statically determinate beam. At a fixed end, these constraints (boundary conditions) are $v = 0$ and $v' = 0$. At a simple support (assumed to lie on the x-axis), it is just $v = 0$.

Example 8.4.1: Simply supported beam under a uniform load.
On the basis of Eq. (8.1.1), the governing equation is

$$\frac{d^2v}{dx^2} = \frac{\overline{w}}{2EI}x(L-x)\,. \tag{8.76}$$

Integrating this twice yields

$$v(x) = C_1x + C_2 + \frac{\overline{w}}{2EI}\left(\frac{Lx^3}{6} - \frac{x^4}{12}\right)\,. \tag{8.77}$$

The condition $v(0) = 0$ yields $C_2 = 0$, while $v(L) = 0$ implies $C_1L + (\overline{w}L^4/2EI)$ $[(1/6) - (1/12)]$, that is, $C_1 = -\overline{w}L^3/24EI$. The deflection is therefore given by

$$v(x) = -\frac{\overline{w}}{24EI}(L^3x - 2Lx^3 + x^4)\,. \tag{8.78}$$

To find the (numerical) maximum we normally need to find the point x where $v'(x) = 0$, but in this case the symmetry tells us that this has to be at $x = L/2$. Inserting this value, we find that $|v|_{\max} = -v(L/2) = (5/384)\overline{w}L^4/EI$.

Example 8.4.2: Simply supported beam under a concentrated force.
On the basis of the result of Example 8.1.6 (page 359), we have

$$\frac{d^2v}{dx^2} = \frac{F_1}{EI}\left(\frac{(L-x_1)x}{L} - <x-x_1>\right) . \tag{8.79}$$

Integrating twice leads to

$$v(x) = C_1x + C_2 + \frac{F_1}{6EI}\left[\frac{(L-x_1)x^3}{L} - <x-x_1>^3\right] . \tag{8.80}$$

The end conditions $v(0) = v(L) = 0$ lead to $C_2 = 0$ and

$$C_1 = -\frac{F_1(L-x_1)}{6EIL}[L^2-(L-x_1)^2] = -\frac{F_1(L-x_1)(2L-x_1)x_1}{6EIL}$$

Consequently

$$v(x) = -\frac{F_1}{6EIL}\left[(L-x_1)(2L-x_1)x_1x - (L-x_1)x^3 + L<x-x_1>^3\right] . \tag{8.81}$$

For the special case $x_1 = L/2$, we find $v(L/2) = -F_1L^3/48EI$.

Alternatively, Eq. (8.75) may be combined with the equilibrium equation (8.6) to yield the fourth-order differential equation

$$\frac{d^2}{dx^2}\left(EI\frac{d^2v}{dx^2}\right) = -w(x) , \tag{8.82}$$

which for homogeneous prismatic beams becomes

$$EI\frac{d^4v}{dx^4} = -w(x) . \tag{8.83}$$

The solution of this equation includes four integration constants and therefore requires four boundary conditions in terms of the deflection v and its derivatives. These are not necessarily the constraint conditions discussed above, but may also be specifications of zero (or prescribed nonzero) bending moment or shear force. A condition of zero moment is given, through Eq. (8.75), by $EIv'' = 0$ (or more simply by $v'' = 0$), while that of zero shear is given, through combining Eq.s (8.75) and (8.5), by $(EIv'')' = 0$ and by $EIv''' = 0$ (or more simply $v''' = 0$) for a prismatic beam. The standard end conditions are accordingly specified as

$$\begin{array}{lll} v'' = v''' = 0 & & \text{free} \\ v = v' = 0 & & \text{built-in} \\ v = v'' = 0 & & \text{simply supported} \end{array} , \tag{8.84}$$

provided that no shear force or bending moment is applied at the end of the beam (if such forces are applied, then the homogeneous boundary conditions

are replaced by inhomogeneous counterparts). Note that the applicability of this method is independent of whether the beam is statically determinate or not. This independence, as pointed out in Sect. 6.4, is characteristic of the displacement method, of which this is an instance. Note that the end conditions discussed here are consistent with those derived by the virtual-work method after Eq. (8.65) (page 385).

Example 8.4.3: End-loaded cantilever.
We will solve Eq. (8.83) with $w(x) = 0$, subject to the boundary conditions $v(0) = v'(0) = 0$, $v''(L) = 0$ and $v'''(L) = F/EI$, the last of these representing the condition $V(L) = -F$ for a downward force F applied at the end. The general solution is

$$v(x) = C_1 x^3 + C_2 x^2 + C_3 x + C_4 \,. \tag{8.85}$$

The conditions at $x = 0$ immediately lead to $C_3 = C_4 = 0$, while those at $x = L$ give $6C_1 L + 2C_2 = 0$, $6C_1 = F/EI$, so that

$$v(x) = -\frac{F}{6EI}(3Lx^2 - x^3) \,. \tag{8.86}$$

The maximum deflection is thus $|v|_{\max} = |v(L)| = FL^3/3EI$, as was already found by the method of conservation of energy in Sect. 8.3.

Example 8.4.4: Center-loaded doubly built-in beam.
The fourth-order differential equation to be solved is

$$\frac{d^4 v}{dx^4} = -\frac{F}{EI}\delta(x - L/2) \,. \tag{8.87}$$

A solution satisfying the end conditions $v(0) = v'(0) = 0$ is

$$v(x) = C_1 x^3 + C_2 x^2 - \frac{F}{6EI}\langle x - L/2\rangle^3 \,. \tag{8.88}$$

The conditions $v(L) = v'(L) = 0$ are satisfied by

$$C_1 L^3 + C_2 L^2 = \frac{FL^3}{48EI} \quad , \quad 3C_1 L^2 + 2C_2 L = \frac{FL^2}{8EI} \,, \tag{8.89}$$

leading to

$$C_1 = \frac{F}{12EI} \quad , \quad C_2 = -\frac{FL}{16EI} \,. \tag{8.90}$$

The midpoint deflection is accordingly

$$v(L/2) = C_1(L/2)^3 + C_2(L/2)^2 = -\frac{FL^3}{192EI} \,. \tag{8.91}$$

The end moments are equal to $2EIC_2 = -FL/8$, while the midpoint moment is $2EIC_2 + 6EIC_1(L/2) = +FL/8$. Since the shear is constant (and equal to $\pm F/2$) in each half of the beam, it follows that the quarter-points are points of zero

moment and therefore points of inflection of the elastic curve. It follows further that each half of the beam is antisymmetric about the quarter points, and each quarter of the beam deflects like a cantilever of length $L/4$ and carrying an end load $F/2$, so that the magnitude of the deflection of each quarter is $(F/2)(L/4)^3/3EI = FL^3/384$. The midpoint deflection of the beam is just twice that, as derived above. It can also be noted that the portion of the beam between the quarter points behaves just like a center-loaded simply supported beam of length $L/2$. Since the deflection of this portion (relative to the quarter points) is $FL^3/384EI = F(L/2)^3/48EI$. Consequently, the midpoint deflection of a center-loaded simply supported beam of length L is $FL^3/48EI$.

8.4.2 Beams with Overhangs and Continuous Beams

For a beam with an overhang, as treated in Sect. 8.1 (page 361), combining Eq.s (8.13) and (8.75) leads to

$$EI\frac{d^4v}{dx^4} = -w(x) + R_B\delta(x-a)\,, \tag{8.92}$$

which replaces Eq. (8.83). The reaction R_B can be treated as an unknown in addition to the constants of integration $C_1, \ldots C_4$ obtained on integrating Eq. (8.92) four times, since the condition $v(L) = 0$ provides an additional equation besides the end conditions at $x = 0$ and $x = L$. The same method can be used to treat beams with more than two supports, known as *continuous beams* and exemplified in Fig. 8.25. The reactions at the intermediate supports

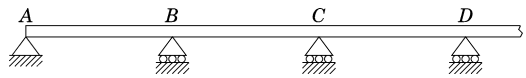

Figure 8.25. Continuous beam

are added as unknown loads to the applied loading, and the condition that the deflection is zero at these supports furnishes the additional equations necessary for the determination of the unknowns.

Example 8.4.5: Symmetric, uniformly loaded beam on three supports. We consider a uniformly loaded, simply supported beam of span $2L$ to which an intermediate support has been added at $x = L$. Eq. (8.92) becomes

$$EI\frac{d^4v}{dx^4} = -\overline{w} + R_B\delta(x-L)\,,$$

which, upon integration, leads to

$$v(x) = C_1x^3 + C_2x^2 + C_3x + C_4 - \frac{\overline{w}x^4}{24EI} + \frac{R_B}{6EI}<x-L>^3\,.$$

The conditions $v(0) = 0$ and $v''(0) = 0$ imply $C_2 = C_4 = 0$. The remaining equations, resulting from $v(L) = 0$, $v(2L) = 0$ and $v''(2L) = 0$, respectively, are

$$\begin{aligned} L^3C_1 + LC_3 &= \frac{\overline{w}L^4}{24EI} \\ 8L^3C_1 + 2LC_3 + \frac{L^3}{6EI}R_B &= \frac{2\overline{w}L^4}{3EI} \\ 12LC_1 + \frac{L}{EI}R_B &= \frac{2\overline{w}L^2}{EI} \end{aligned}$$

whose solution is $C_1 = \overline{w}L/16EI$, $C_3 = -\overline{w}L^3/48EI$, and $R_B = 5\overline{w}L/4$. It follows from the last result that, for equilibrium, each of the end reactions is $(3/8)\overline{w}L$. The shear, bending-moment and deflection diagrams are shown in Fig. 8.26.

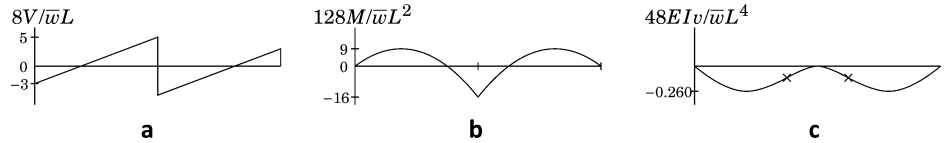

Figure 8.26. Example 8.4.5: (a) shear, (b) bending moment, (c) deflection

Note that, given the symmetry of the problem, it is equivalent (for each half-span) to that of a uniformly loaded beam that is simply supported at one end and built-in at the other.

When the number of supports is large, the number of simultaneous equations to be solved becomes proportionately large. When the solution of a large system is difficult (as was generally the case before high-speed computers) it may be more convenient to treat the values of the bending moment at the intermediate supports, and not the reactions, as the unknowns. The reason is that, according to a classical result due to Clapeyron* and known as the *theorem of three moments*, each such moment is related only to the moments at the two neighboring supports, so that the equations can be tackled sequentially. This result is treated in an exercise.

8.4.3 Beam Deflections by Superposition

The results of the last example, as well as those for many other beam problems, including especially statically indeterminate ones, may also be obtained by applying the principle of superposition, since, as discussed in Sect. 6.2 (page 258), all the governing differential equations are linear. Specifically, if, for a beam with given support conditions, two different loadings (say 1 and 2) produce the respective deflection functions $v_1(x)$ and $v_2(x)$, then, if the two loadings are added, the resulting deflection is $v_1(x) + v_2(x)$. Thus if, for example, a simply supported beam carries both a concentrated force F at the

*Émile Clapeyron (1799–1864) was a French engineer and physicist.

midpoint (for which the midpoint deflection was derived in Example 8.4.4) and a uniformly distributed load $\overline{w}$ (as in Example 8.4.1), the resultant midpoint deflection is

$$|v(L/2)| = \frac{5\overline{w}L^4}{384EI} + \frac{FL^3}{48EI} . \tag{8.93}$$

Note that the absolute value in the preceding equation is due to the fact that the deflection at $x = L/2$ is negative (recall from Fig. 8.1 that the positive vertical axis points upwards). We may use the result in Eq. (8.93) to alternatively determine the reaction R_B at the center support in Example 8.4.5. With L replaced by $2L$ as in the example, and F by $-R_B$, the requirement that the midpoint deflection be zero is given by

$$0 = \frac{5\overline{w}(2L)^4}{384EI} - \frac{R_B(2L)^3}{48EI} , \tag{8.94}$$

leading to $R_B = 5\overline{w}L/4$, as we found in Example 8.4.5. If we recall that each half-span of the beam of Example 8.4.5 is equivalent to a uniformly loaded beam that is built-in at one end and simply supported at the other, as in Fig. 8.27a, we can use superposition to solve the problem in other ways, analogous to those discussed in Sect. 6.4 in conjunction with the force method, as in the following example.

Example 8.4.6: A uniformly loaded beam that is built-in at one end and simply supported at the other

We consider the beam shown in Fig. 8.27a. If we choose the reaction at the sim-

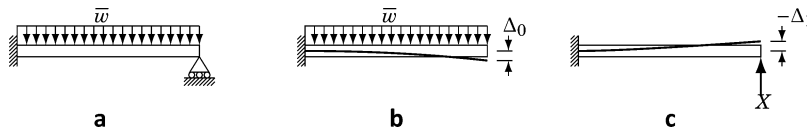

Figure 8.27. Example 8.4.6

ple support as the redundant, then the reduced system is the cantilever shown in Fig. 8.27b, with the elastic curve exhibiting a tip deflection (as we found in the preceding section, Example 8.3.5, page 387) of $\overline{w}L^4/8EI$, which we will label Δ_0 (as in Sect. 6.4). We now apply an as yet unknown upward force X at the tip, producing an elastic curve with an upward tip deflection that we well call $-\Delta_1$ and which we know from Example 8.4.3 to be $XL^3/3$. The compatibility condition $v(L) = 0$ is equivalent to $\Delta_0 + \Delta_1 = 0$ (a special case of Eq. (6.113) with one redundant), leading to $X = 3\overline{w}L/8$, as we already found in Example 8.4.5. An alternative choice of redundant is the moment at the built-in end, making the reduced system a uniformly loaded simply supported beam. The compatibility condition is then that the sum of the rotation θ_0 at one end (say $x = 0$) of the reduced system and the rotation θ_1 due to a counterclockwise concentrated couple X at the same end add to zero. Since these results have not yet been derived, we may apply Castigliano's second theorem directly to the combined loading. The

moment is given by

$$M(x) = \frac{\overline{w}}{2}x(L-x) - (X/L)(L-x)\,,$$

so that $\partial M/\partial X = -(L-x)/L$, and therefore

$$\theta_0+\theta_1 = 0 = \frac{\partial \overline{U}_\mathrm{b}}{\partial X} = -\frac{1}{EIL}\int_0^L (L-x)\left[\frac{\overline{w}}{2}x(L-x) - \frac{X}{L}(L-x)\right]dx = \frac{1}{EIL}\left(\frac{XL}{3} - \frac{\overline{w}L^3}{12}\right),$$

leading to $X = \overline{w}L^2/4$.

A more general approach to superposition is based on the solution for a concentrated force as found, for the case of a simply supported beam, in Example 8.81. If we write Eq. (8.81) as $v(x) = -F_1 g(x,x_1)$, then, clearly, for any combination of concentrated forces F_i acting at $x = x_i$ $(i = 1,2,\ldots,n)$,

$$v(x) = -\sum_{i=1}^{n} F_i g(x,x_i)\,, \tag{8.95}$$

and, since a distributed loading $w(x)$ may be approximated by a combination of concentrated loads $w(x)\Delta x$ if Δx is sufficiently small, in the limit we can write, for an arbitrary loading $w(x)$ (which may include concentrated forces),

$$v(x) = -\int_0^L w(x')g(x,x')dx'\,. \tag{8.96}$$

Similar functions $g(x,x')$ can be found for beams with other end conditions. Such functions are known as *fundamental solutions* or *Green's*[†] *functions*. By the Maxwell-Betti reciprocal theorem (see Sect. 6.5.3, page 301), such a function must satisfy $g(x,x') = g(x',x)$; the proof is left to an exercise.

8.4.4 Approximate Calculation of Deflections by the Energy Method

In view of the definition of the external virtual work in Eq. (8.64), we can also define the external potential energy V_b, which was discussed in Sect. 6.5 (and is not to be confused with the shear force V), as

$$V_\mathrm{b} = \int_0^L wv\,dx\,, \tag{8.97}$$

so that the total potential energy in bending is

$$\Pi_\mathrm{b} = \frac{1}{2}\int_0^L EI_z v''^2\,dx + \int_0^L wv\,dx\,. \tag{8.98}$$

[†]George Green (1793–1841) was a British mathematical physicist.

As indicated in Sect. 6.5, we may use the principle of minimum total potential energy in order to find displacement fields (in the present case elastic curves) that are approximations to be exact solution. This entails defining a parametric family of curves that satisfy the boundary conditions of the beam bending problem and exploiting the minimum property of the total potential energy to determine all parameters needed to fully specify the elastic curve. A simple example of this method is presented below.

Example 8.4.7: Approximating beam deflections by sinusoidal curves. An elastic curve in the form

$$v(x) = A \sin \frac{\pi x}{L} \tag{8.99}$$

satisfies the conditions $v(0) = v(L) = 0$, so that it obeys the constraints for a simply supported beam of span L. Since $v''(x) = -(\pi/L)^2 A \sin(\pi x/L$, it follows that the value of Π for this deflection is

$$\Pi_b = \frac{EI_z A^2}{2}\left(\frac{\pi}{L}\right)^4 \int_0^L \sin^2 \frac{\pi x}{L}\, dx + A \int_0^L w(x) \sin \frac{\pi x}{L}\, dx\,. \tag{8.100}$$

We minimize this expression by setting $d\Pi/dA = 0$, and, since the integral in the first term on the right-hand side is just $L/2$, it follows that the value of A that minimizes Π is

$$A = -\left(\frac{2}{\pi^4}\right)\frac{L^3}{EI_z}\int_0^L w(x) \sin \frac{\pi x}{L}\, dx\,. \tag{8.101}$$

In the case of a center-loaded simply supported beam, $V_\mathrm{b} = Fv(L/2) = FA$, so that $A = -(2/\pi^4)FL^3/EI$. Now, $\pi^4/2 = 48.70$, so that the result is within 1.5% of the previously calculated value.

If the loading is not symmetric about the center, then it would be unreasonable to approximate the deflection by a simple sine curve. In that case we can add sine curves of higher frequency to the assumed deflection curve, resulting in an expression of the form

$$v(x) = A_1 \sin \frac{\pi x}{L} + A_2 \sin \frac{2\pi x}{L} + \ldots\,. \tag{8.102}$$

Such sine functions are *orthogonal* to one another in the sense that

$$\int_0^L \sin \frac{m\pi x}{L} \sin \frac{n\pi x}{L}\, dx = \begin{cases} 0, & m \neq n \\ L/2, & m = n \end{cases}\,. \tag{8.103}$$

Consequently,

$$U_\mathrm{b} = \frac{EI_z}{2}\left(\frac{\pi}{L}\right)^4 \frac{L}{2}(A_1^2 + 2^4 A_2^2 + \ldots) \tag{8.104}$$

and

$$V_\mathrm{b} = A_1 \int_0^L w(x) \sin \frac{\pi x}{L}\, dx + A_2 \int_0^L w(x) \sin \frac{2\pi x}{L}\, dx + \ldots \tag{8.105}$$

It will be noted that, because of the aforementioned orthogonality of the sine functions, the minimum conditions $\partial \Pi_b/\partial A_i = 0$ $(i = 1, 2, \ldots)$ will yield *uncoupled* equations for the parameters A_i.

8.4.5 Beams with Initial Deflection

As was noted in Sect. 8.2, if a beam has initial curvature, say κ_0, then κ must be replaced in the moment-curvature relation by $\kappa - \kappa_0$. In the Bernoulli–Euler theory, accordingly, EIv'' is replaced by $EI(v'' - v_0'')$ if the beam has an initial deflection curve given by $y = v_0(x)$. If the beam is homogeneous and prismatic, in place of Eq. (8.83) we would therefore write

$$EI\left(\frac{d^4v}{dx^4} - \frac{d^4v_0}{dx^4}\right) = -w(x)\,. \tag{8.106}$$

The preceding equation may be rewritten as

$$EI\frac{d^4v}{dx^4} = -w(x) + EI\frac{d^4v_0}{dx^4}\,, \tag{8.107}$$

so that the effect of the initial deflection is like that of an additional distributed loading, except that any boundary conditions involving the bending moment must be given in terms of $v'' - v_0''$ rather than simply v''.

Exercises

8.4-1. Determine the deflection $v(x)$ of the beam shown in the figure due to the effect of the moment $M = 100$ N·m, assuming that the beam in made of a linearly elastic material with $E = 10$ GPa and that its cross-section is circular with radius $c = 3$ cm. What is the value of the maximum deflection and at which point of the beam it is experienced?

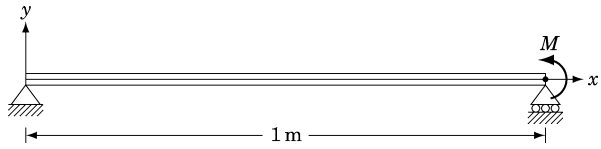

8.4-2. Determine the deflection $v(x)$ of the cantilever beam shown in the figure due to the effect of the uniform load $w = 25$ kips/in. Assume that the beam is made of a linearly elastic material and that $EI = 20$ kips·in^2. Obtain the deflection in two ways: (a) using the second-order differential equation (8.75) and (b) using the fourth-order differential equation (8.83).

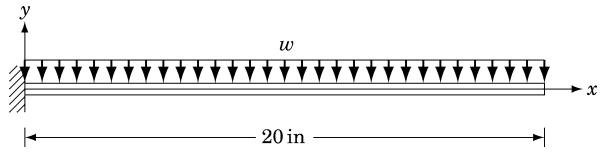

8.4-3. Find an expression of the deflection of the beam shown in the figure, when $w = 5$ kN/m. Assume that the beam is made of a linearly elastic material with $E = 25$ GPa and that the cross-section is square with side $a = 2$ cm. Find the deflection *without* using singularity functions.

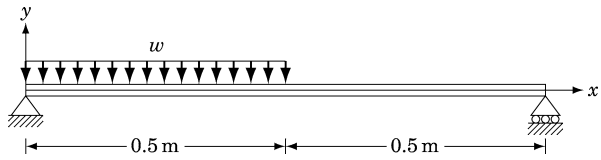

8.4-4. Do the preceding exercise using singularity functions.

8.4-5. Determine the deflection $v(x)$ of the statically indeterminate beam shown in the figure due to the effect of the uniform load $w = 10$ kips/in. Assume that the beam is made of a linearly elastic material and that $EI = 30$ kips·in^2. Use the deflection $v(x)$ to calculate the reactions at the two ends of the beam.

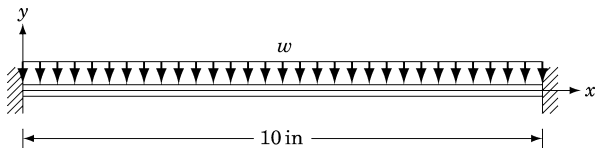

8.4-6. Use singularity functions to find the deflection $v(x)$ of the simply-supported beam with an overhang due to the loads $F = 50$ kN and $M = 20$ kN·m, as in the figure. Assume that the beam has a square cross-section of side $a = 2$ cm, and is made of a linearly elastic material with $E = 10$ GPa.

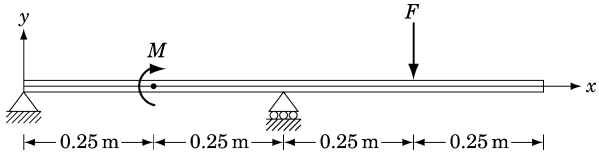

8.4-7. Find the deflection $v(x)$ for the statically indeterminate beam shown in the figure, and show that it is equivalent to that of the right-hand half of the continuous beam of Example 8.4.5.

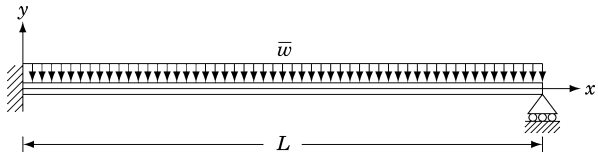

8.4-8. Consider a statically indeterminate elastic beam which is subject to two concentrated loads, each of magnitude F, as in the figure.

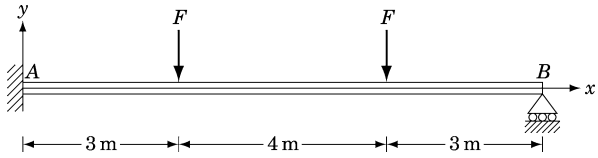

(a) Write a mathematical expression for the applied loads using singularity functions.

(b) Write the boundary conditions that apply to the two end-points A and B of the beam.

(c) Use the results of part (a) and (b) to determine the deflection v of the beam as a function of x.

(d) Locate the point of maximum downward deflection in the beam and find the magnitude of this deflection.

(e) Determine all the reactions at A and B.

In all calculations, assume that the beam has constant Young's modulus E and second moment of area I_z.

8.4-9. Consider a simply-supported elastic beam subject to a distributed load $w = 1.0$ kN/m and a concentrated load $F = 10$ kN, as in the figure.

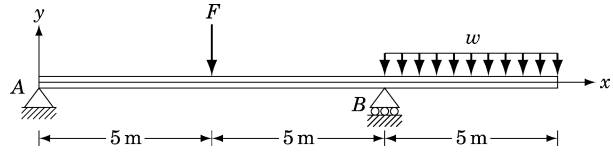

(a) Determine the reactions at points A and B.

(b) Write a mathematical expression for the applied loads using singularity functions.

(c) Use the expression in part (c) to determine the deflection v of the beam as a function of x.

(d) Locate the point of maximum downward deflection in the segment AB and determine the magnitude of this deflection.

8.4-10. Show that, if Eq. (8.81) is written as $v(x) = -F_1 g(x, x_1)$, then $g(x, x_1) = g(x_1, x)$.

8.4-11. Use Eq.s (8.81) and (8.96) with $w(x) = \overline{w}$ to determine the deflection of a uniformly loaded simply supported beam.

8.4-12. Repeat Example 8.4.7 for the case of a uniformly loaded simply supported beam, and find the percentage error of the maximum deflection with respect to the result of Example 8.4.1.

8.4-13. (a) Use the energy method to find an approximation to the center deflection of a simply supported beam of span L carrying a concentrated force F at $x = L/3$ by assuming the deflection to be given by the sum of the two terms shown on the right-hand side of Eq. (8.102).

(b) For a simply supported beam carrying concentrated forces F at $x = L/3$ and $x = 2L/3$, find an approximation to the center deflection by: (i) by superposition of the results from (a), (ii) assuming $v(x) = A \sin(\pi x/L)$. Is there a difference between the two results? Why?

8.4-14. Consider any two points (say, at $x = x_1$ and $x = x_2$) on the neutral fiber of a beam, as shown in the figure.

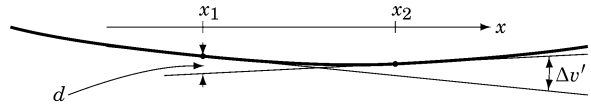

(a) Show that the change $\Delta v'$ in the slope of the neutral fiber from x_1 to x_2 is equal to the integral of M/EI from x_1 to x_2.

(b) Show that the vertical distance d between the point at x_1 on the neutral fiber and the point at x_1 of the tangent to the neutral fiber at x_2 is equal to the integral of the "moment" of M/EI about x_1 from x_1 to x_2.

The results in parts (a) and (b) are known as *Mohr's first and second theorem*, respectively.

8.4-15. Consider a structure consisting of two linearly elastic beams with Young's modulus E and second moment of area I, and a linearly elastic bar of the same Young's modulus, cross-sectional area A and coefficient of thermal expansion α, as shown in the figure. The bar is inserted midway along the span of the beams and initially fits precisely between the beams without generating any forces. Subsequently the temperature of the bar is uniformly increased by ΔT.

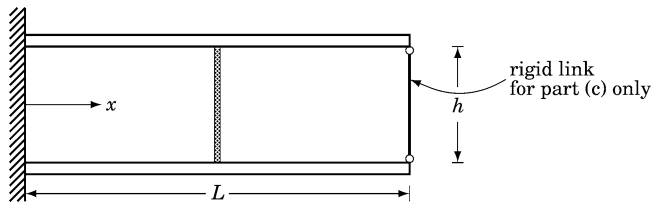

(a) Determine the forces applied by the bar to the two beams. (*Hint:* you will first need to determine the displacement of the midpoint of each beam due to a concentrated load at that point.)

(b) Find the deflection $v(x)$ for any one of the two beams due to the temperature increase in the bar.

(c) Suppose that the end-points of the two beams are now connected by a rigid link, as in the figure. What are the forces applied by the bar and the rigid link to the two beams? (*Hint:* It may be easier to answer this part of the problem using singularity functions to describe the load on each beam.)

Chapter 9

Additional Topics in Bending

9.1 Composite Cross-Sections

9.1.1 Introduction

A *composite beam* is defined analogously to a composite bar as in Sect. 6.3.3 (page 278) and a composite shaft as in Sect. 7.1.5 (page 328): it is assumed to be made up of two or more materials, so that the Young's modulus E varies over the cross-section $\mathscr{A}$. We express this variation as $E(y,z)$, although, in fact, $\mathscr{A}$ comprises subregions (say $\mathscr{A}_1, \mathscr{A}_2, \ldots$) within which E has a constant value ($E_1, E_2, \ldots$).

We assume, as in Chapter 8, that the cross-section is symmetric about the y-axis, with regard to both geometry and the variation of E (so that $E(y,-z) = E(y,z)$), and that the bending moment has only the component M_z, so that bending takes place in the xy-plane.

9.1.2 Doubly Symmetric Sections

If the cross-section is also symmetric about the z-axis, with regard to both geometry and the variation of E, then it follows from the symmetry that the centroid is located at $(0,0)$ and that, in pure bending (and, by extension, in Bernoulli–Euler bending), the z-axis is also the neutral axis. Consequently, recalling Eq. (8.20), we find that the stress is given by

$$\sigma_x(y,z) \;=\; -E(y,z)\kappa y \tag{9.1}$$

and the moment, in accordance with Eq. (8.21), by

$$M_z \;=\; \left(\int_{\mathscr{A}} E(y,z)y^2 dA\right)\kappa \;, \tag{9.2}$$

where the integral in parentheses, which may be denoted $\overline{EI}$, is the effective flexural rigidity of the beam in the same sense as the effective axial and

© Springer International Publishing Switzerland 2017

J. Lubliner, P. Papadopoulos, *Introduction to Solid Mechanics*,
DOI 10.1007/978-3-319-18878-2_9

torsional rigidities discussed in Sects. 6.3 and 7.1, respectively.

Since the symmetry requires that each of the subregions (not necessarily connected) of constant Young's modulus also be symmetric about the z-axis, the integral in Eq. (9.2) may be expressed as the sum of integrals over the subregions. If

$$I_i = \int_{\mathscr{A}_i} y^2 dA \tag{9.3}$$

is the second moment of area about the z-axis of the i-th subregion, then

$$\overline{EI} = \sum_i E_i I_i \ . \tag{9.4}$$

If c_i denotes the maximum value of $|y|$ in $\mathscr{A}_i$, then the maximum stress in this i-th subregion is

$$\sigma_{\max(i)} = E_i \kappa c_i = \frac{M}{S_i} \ , \tag{9.5}$$

where

$$S_i = \frac{\overline{EI}}{E_i c_i} \ . \tag{9.6}$$

If we require that $\sigma_{\max(i)} \le \sigma_{\text{all}(i)}$, then the allowable moment is given by

$$M_{\text{all}} = \min_i \left(S_i \sigma_{\text{all}(i)} \right) \ . \tag{9.7}$$

Example 9.1.1: Steel-clad wooden beam
We consider a wooden beam, of width b and depth h, that is clad on the top and bottom edges with steel plates of width b and thickness t, as shown in Fig. 9.1. We define $\mathscr{A}_1$ as comprising the wood and $\mathscr{A}_2$ as comprising *both* steel plates.

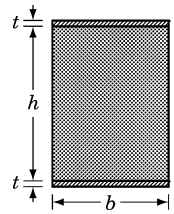

Figure 9.1. Example 9.1.1

Thus

$$I_1 = \frac{bh^3}{12} \quad , \quad I_2 = \frac{b[(h+2t)^3 - h^3]}{12} \ .$$

Supposing that $b = 4$ in, $h = 6$ in, $t = 0.20$ in, $E_1 = 1.45 \times 10^3$ ksi and $E_2 = 29.0 \times 10^3$ ksi, it follows that $I_1 = 72\ \text{in}^4$ and $I_2 = 15.4\ \text{in}^4$, so that $\overline{EI} = 5.50 \times 10^5$ k·in^2. Note that the steel, though it occupies only 6.25% of the area, contributes over 80% of the rigidity.
The partial section moduli S_i are given, according to Eq. (9.6), by

$$S_1 = \frac{5.50 \times 10^5 \,\text{kip} \cdot \text{in}^2}{1.45 \times 10^3 \,\text{kip} \cdot \text{in}^{-2} \times 3 \,\text{in}} = 126 \,\text{in}^3$$

and

$$S_2 = \frac{5.50 \times 10^5 \,\text{kip}\cdot\text{in}^2}{29 \times 10^3 \,\text{kip}\cdot\text{in}^{-2} \times 3.2\,\text{in}} = 5.93\,\text{in}^3 .$$

If the allowable stresses are 4 ksi in the wood and 22 ksi in the steel, then the allowable moment is the lesser of $126 \times 4 = 504$ kip·in and $5.93 \times 22 = 130$ kip·in, that is, 130 kip·in, and it is the steel that fails first. This does not mean, however, that the steel does not strengthen the beam: without it, the allowable moment would have been $(4 \times 72/3)$ kip·in = 96 kip·in.

9.1.3 Transformed section

For beam cross-sections that are not symmetric about the z-axis with regard to either geometry or the variation of E (though, as we said earlier, they are still symmetric about the y-axis), a convenient method for treating bending problems is provided by the concept of the *transformed section*.

We begin by noting that, if $E(y,z)$ is not symmetric about the z-axis, then, in an elastic bar with nonuniform Young's modulus $E = E(y,z)$ whose values are symmetric about the y-axis (that is, $E(y,z) = E(y,-z)$), the line of action of an axial force producing purely axial deformation does not, in general, coincide with the centroidal axis of the cross-section. If we choose to define the x-axis as being along this line of action, then, since $\sigma(y,z) = E(y,z)\varepsilon$, it follows that the resultant moment about the z-axis must be zero, implying that

$$\int_{\mathscr{A}} yE(y,z)dA = 0 . \tag{9.8}$$

Now, suppose that the width of the section at y is given by $b(y)$; then, the preceding equation may be expressed as

$$\int_{y_{\min}}^{y_{\max}} \int_{-b(y)/2}^{b(y)/2} yE(y,z)dz\,dy = \int_{y_{\min}}^{y_{\max}} \left(\int_{-b(y)/2}^{b(y)/2} E(y,z)dz \right) y\,dy = 0 . \tag{9.9}$$

If we choose a certain value of E as a reference value and call it E_{ref}, then we can define a *transformed width* $\bar{b}(y)$ by

$$\bar{b}(y) = \frac{1}{E_{\text{ref}}} \int_{-b(y)/2}^{b(y)/2} E(y,z)dz , \tag{9.10}$$

and Eq. (9.9) may be rewritten as

$$E_{\text{ref}} \int_{y_{\min}}^{y_{\max}} y\,\bar{b}(y)dy = 0 . \tag{9.11}$$

If we now define a *transformed section* $\overline{\mathscr{A}}$, of area $\overline{A}$, as one in which $\bar{b}(y)$ replaces $b(y)$ at every y, then the area increment in this section is $d\overline{A} = \bar{b}(y)dy$, and Eq. (9.11) finally leads to

$$\int_{\overline{\mathscr{A}}} y\,d\overline{A} = 0 . \tag{9.12}$$

The line of action of an axial force producing purely axial deformation therefore passes through the *centroid of the transformed section*. In the case of bending with no axial force, the neutral axis also passes through this point. If $\bar{I}_z$ is the second moment of area of the transformed section about its centroidal axis, then the moment-curvature relation is

$$M = \overline{EI}\kappa\,, \tag{9.13}$$

where the previously defined effective flexural rigidity is $\overline{EI} = E_{\text{ref}}\bar{I}_z$.

Example 9.1.2: Rectangular beam made of two materials.
We consider a beam of width b and depth h such that the upper half $y > 0$ is made of material 1, with $E = E_1$, and the lower half $y < 0$ is made of material 2, with $E = E_2 = 3E_1$. If we let $E_{\text{ref}} = E_1$, then in the upper half $\bar{b} = b$, while in

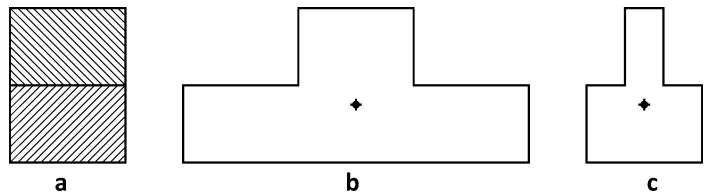

Figure 9.2. Example 9.1.2

the upper half $\bar{b} = 3b$, as in Fig. 9.2b. If, conversely, $E_{\text{ref}} = E_2$, then $\bar{b} = b$ in the lower half and $\bar{b} = b/3$ in the upper half, as in Fig. 9.2c. Note that the location of the effective centroid is the same location ($3h/8$ from the bottom, $5h/8$ from the top) in both transformed sections.

For the transformed section of Fig. 9.2b, we calculate $\bar{I}_z$ as follows:

$$\bar{I}_z = \frac{b(h/2)^3}{12} + \frac{3b(h/2)^3}{12} + (bh/2)(3h/8)^2 + (3bh/2)(h/8)^2 = \frac{13}{96}bh^3,$$

where the first and second terms in the middle members are the values of I_z for the upper and lower rectangles, and the third and fourth terms their contributions by the parallel-axis theorem. The effective flexural rigidity is consequently $\overline{EI} = (13/96)E_1bh^3 = (13/288)E_2bh^3$.

9.1.4 Reinforced Concrete

Concrete is far weaker in tension than in compression. For this reason, it is standard practice to place steel reinforcing bars (often called *rebars*) inside the concrete near the side of the beam that is expected to be in tension. In the usual method of analysis, we assume that the concrete undergoes no tensile stress at all, and if it is linearly elastic in compression, then the compressive stress increases linearly from the neutral axis. We also assume that the zone between the neutral axis and the reinforcement (which is modeled as a thin

band of steel with area equal to that of the cross-section of all the reinforcing bars) carries no axial stress, but merely acts as a kind of "web" holding the beam together. Thus, the rectangular cross-section of width b and height d depicted in Fig. 9.3a (with bottom reinforcement only, based on an assumption of positive bending moment) is modeled as in Fig. 9.3b, with the stress distribution shown in Fig. 9.3c.

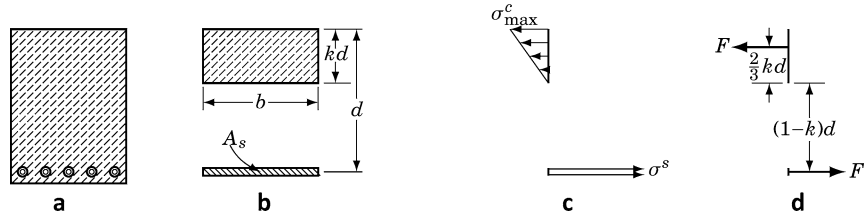

Figure 9.3. Reinforced-concrete beam: (**a**) cross-section, (**b**) model, (**c**) stress distribution, (**d**) force resultants

In the absence of axial load, equilibrium requires that the force resultant F be equal and opposite in the steel and the concrete regions, as shown in Fig. 9.3d. This implies that

$$\sigma^s A_s \;=\; \frac{1}{2}\sigma^c_{\max} bkd \;, \tag{9.14}$$

where σ^s is the stress in the steel reinforcement, σ^c is the stress in the concrete (with $\sigma^c_{\max}$ being its maximum value)*, and k $(0<k<1)$ is a parameter which defines the portion of the section that is in compression. The assumption that plane sections remain plane necessitates that the strain be proportional to the distance from the neutral axis, that is

$$\frac{\sigma^s/E_{\rm s}}{(1-k)d} \;=\; \frac{\sigma^c_{\max}/E_{\rm c}}{kd} \;. \tag{9.15}$$

Eliminating the stresses between Eqs. (9.14) and (9.15) yields a quadratic equation in k which may be expressed in terms of the dimensionless parameter $r = E_{\rm s}A_s/E_{\rm c}bd$ as

$$k^2 - 2r(1-k) \;=\; 0 \;. \tag{9.16}$$

The only positive solution of this equation is

$$k \;=\; \sqrt{r^2+2r} - r \;, \tag{9.17}$$

with $0<1<k$ valid for all positive r.

The moment-curvature relation for the reinforced concrete beam is found by multiplying the resultant force F, expressed as either $E_{\rm s}(1-k)d\kappa$ or $\frac{1}{2}E_{\rm c}(bkd)\kappa$, by the moment arm $(1-\frac{1}{3}k)d$. Hence the effective flexural rigidity is

$$\overline{EI} \;=\; \frac{1}{2}k^2\left(1-\frac{k}{3}\right)E_{\rm c}bd^3 \;=\; (1-k)\left(1-\frac{k}{3}\right)E_{\rm s}A_s d^2 \;. \tag{9.18}$$

*Structural engineers usually write f_s for σ^s and f_c for $\sigma^c_{\max}$.

Finally, the maximum stresses can be related to the moment by the section moduli S_s and S_c as

$$\sigma^s = \frac{M}{S_s} \quad , \quad \sigma^c_{\max} = \frac{M}{S_c} \, , \tag{9.19}$$

where

$$S_s = \left(1 - \frac{k}{3}\right) A_s d \quad , \quad S_c = \frac{k}{2}\left(1 - \frac{k}{3}\right) b d^2 \, . \tag{9.20}$$

Example 9.1.3: Analysis of a reinforced-concrete beam.
We consider a beam cross-section with $d = 11$ in and $b = 6$ in, with 5 #4 (US) reinforcing bars, each with an area of 0.2 in^2, so that $A_s = 1.00$ in^2. The values of the Young's modulus are $E_c = 4.20 \times 10^3$ ksi and $E_s = 29.0 \times 10^3$ ksi, so that $r = 29.0 \cdot 1.00/(4.20 \cdot 11 \cdot 6) = 0.105$, and $k = 0.365$. We can now calculate $\overline{EI} = 1.96 \times 10^6 \text{k} \cdot \text{in}^2$, $S_s = 9.66$ in^3, and $S_c = 116$ in^3. For a bending moment of, say, 100 k$\cdot$in, the respective maximum stresses are $\sigma^s = 10.35$ ksi and $\sigma^c_{\max} = 0.862$ ksi.

In stress-based design (specifically, *allowable-stress design*), the allowable bending moment is the smaller of those corresponding to the allowable stress being reached in the concrete and the steel:

$$M_{\text{all}} = \min(\sigma^s_{\text{all}} S_s, \sigma^c_{\text{all}} S_c) \, . \tag{9.21}$$

If, for example, the allowable stresses are $\sigma^s_{\text{all}} = 24$ ksi and $\sigma^c_{\text{all}} = 2.25$ ksi, then in the preceding example we would have $M^s_{\text{all}} = 232$ k$\cdot$in and $M^c_{\text{all}} = 261$ k$\cdot$in, and therefore $M_{\text{all}} = 232$ k$\cdot$in; in other words, it is the steel that limits the moment-bearing capacity, and the beam is regarded as *underreinforced*. This is the preferred design criterion, since failure by yielding of the steel (which will be discussed in Chapter 11) is less destructive than failure by crushing of the concrete.

Exercises

9.1-1. A wooden beam of rectangular cross-section, with width 7 cm and depth 12 cm, is covered on all four sides with copper plate that is 0.3 cm thick. If $E_w = 10$ GPa and $E_c = 120$ GPa, find the effective flexural rigidity $\overline{EI}$ (in kN·cm^2) of the beam. If the allowable stresses are $\sigma_{all(w)} = 30$ MPa and $\sigma_{all(c)} = 45$ MPa, find the allowable moment M_{all} in kN·m.

9.1-2. Compare (a) the flexural rigidity and (b) the allowable moment of a solid aluminum bar with a circular cross-section of 2-in diameter with that of an aluminum tube of the same outer diameter if the inner diameter is 1.5 in and the tube is filled with nylon. Let $E = 10 \times 10^3$ ksi and $\sigma_{all} = 25$ ksi for the aluminum, while $E = 450$ ksi and $\sigma_{all} = 7$ ksi for the nylon.

9.1-3. Consider a sandwich beam like that in Fig. 9.1, but with the Young's modulus E_c of the core so small compared to that of the faceplates (E_f) that it does not contribute to the flexural rigidity, and with the faceplate thickness t so small compared to h that only the highest-order term in t need be retained.

(a) Find the effective flexural rigidity.

(b) Find the condition in terms of E_c, E_f and the allowable stresses $\sigma_{all(c)}$ and $\sigma_{all(f)}$ that determines whether the allowable moment is governed by the stress in the core or the faceplate.

9.1-4. Find the effective flexural rigidity $\overline{EI}$ in Example 9.1.1 using transformed sections, with both the wood and steel values of E as the reference value.

9.1-5. Find the effective flexural rigidity $\overline{EI}$ of the composite beam shown in the figure below, with dimensions in centimeters. If the allowable stresses (tension and compression) are 150 MPa in aluminum and 50 MPa in copper, find the allowable moment M_{all}.

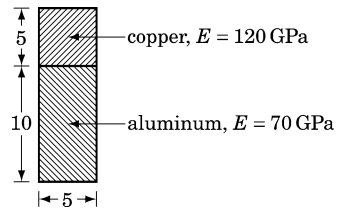

9.1-6. A floor consists of a precast concrete slab set on parallel Douglas-fir joists 6 ft apart, with the 6-ft-wide section shown in the figure below (with dimensions in inches) acting as a beam. (The concrete is reinforced only in the direction perpendicular to the joists.)

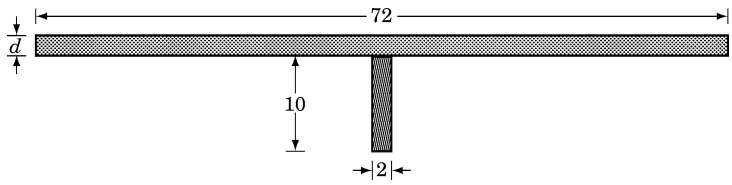

(a) If E is 1,900 ksi in the wood and 3,800 ksi in the concrete, determine the slab thickness d that will place the neutral axis just at the joist-slab interface.

(b) With d as found in (a), if σ_{all} is 1.5 ksi for the wood and 2 ksi for the concrete, determine the allowable moment M_{all}.

(c) If the joists span 10 ft and are simply supported, find the load in pounds per square foot that the floor can carry, after subtracting the weight of the slab (assuming the specific weight of concrete as 150 lb/ft^3).

9.1-7. Prove that for all positive r, k as given by Eq. (9.17) satisfies $0 < k < 1$.

9.1-8. Redo Example 9.1.3 with $d = 300$ mm, $b = 160$ mm, three #3 bars (each with an area of 0.11 in^2), and with $E_c = 5{,}500$ ksi and $E_s = 29{,}000$ ksi. Find the allowable moment. Is this beam over- or underreinforced?

9.1-9. Redo Example 9.1.3 with $d = 9$ in, $b = 5$ in, four 20-mm bars (each with an area of 314 mm^2), and with $E_c = 30.0$ GPa and $E_s = 200$ GPa. Find the allowable moment. Is this beam over- or underreinforced?

9.1-10. Redo Example 9.1.3 with $d = 250$ mm, $b = 100$ mm, three 16-mm bars (each with an area of 201 mm^2), and with $E_c = 40.0$ GPa and $E_s = 200$ GPa. Find the allowable moment. Is this beam over- or underreinforced?

9.2 Asymmetric Bending of Beams

9.2.1 Plane of Bending, Curvature Vector

If the transverse loading is not in the plane of symmetry of the beam cross-section $\mathscr{A}$, then it can no longer be assumed, as done in Sect. 8.2, that the plane of bending is the same as the plane perpendicular to the moment. (In the usual case of loading by transverse forces only, this is the plane of the loading.) If, then, we suppose that the bending moment is $\mathbf{M} = M_y\mathbf{j} + M_z\mathbf{k}$, then we have to assume that the plane of bending has some inclination α with respect to the xy-plane, as shown in Fig. 9.4. We label this plane xy^*, with

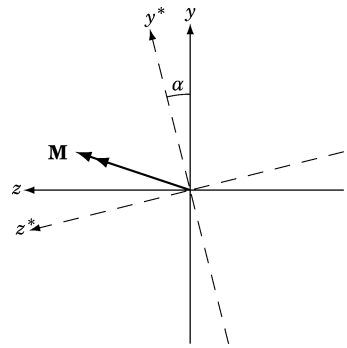

Figure 9.4. Plane of bending

$y^* = y\cos\alpha + z\sin\alpha$, and, in view of Eq. (8.17) (with $y_0 = 0$), the longitudinal strain is given by

$$\varepsilon_x = -\kappa(y\cos\alpha + z\sin\alpha)\,, \tag{9.22}$$

so that the normal stress is now

$$\sigma_x = -E\kappa(y\cos\alpha + z\sin\alpha)\,. \tag{9.23}$$

In this case, the neutral plane is the xz^*-plane, defined by

$$y\cos\alpha + z\sin\alpha = 0\,. \tag{9.24}$$

Taking into account Eq. (9.23), we find the resulting moment as

$$\begin{aligned}\mathbf{M} = -\int_{\mathscr{A}} \mathbf{r}\times\mathbf{i}\sigma_x\,dA &= E\kappa\int_{\mathscr{A}}(\mathbf{j}y+\mathbf{k}z)\times\mathbf{i}(y\cos\alpha+z\sin\alpha)\,dA\\ &= E\kappa\int_{\mathscr{A}}(\mathbf{k}y-\mathbf{j}z)(y\cos\alpha+z\sin\alpha)\,dA\,,\end{aligned} \tag{9.25}$$

so that

$$\begin{aligned}M_y &= -E\kappa\left(\sin\alpha\int_{\mathscr{A}} z^2\,dA + \cos\alpha\int_{\mathscr{A}} yz\,dA\right),\\ M_z &= E\kappa\left(\sin\alpha\int_{\mathscr{A}} yz\,dA + \cos\alpha\int_{\mathscr{A}} y^2\,dA\right).\end{aligned} \tag{9.26}$$

Note that if $\alpha = 0$, then the curvature is entirely about the z-axis (that is, the bending is in the xy-plane) and if $\alpha = \pi/2$ then it is entirely about the y-axis (bending in the xz-plane). We can accordingly define a *curvature vector* $\boldsymbol{\kappa}$ whose direction is normal to the plane of bending xy^* (and therefore pointing along the z^*-axis), such that

$$\kappa_y = -\kappa \sin\alpha\,, \quad \kappa_z = \kappa\cos\alpha\,. \tag{9.27}$$

In view of (9.23) and (9.27), the normal stress can now be expressed as

$$\sigma_x = E(\kappa_y z - \kappa_z y)\,. \tag{9.28}$$

In Eqs. (9.26), the integrals $\int_{\mathscr{A}} z^2 dA$ and $\int_{\mathscr{A}} y^2 dA$ are the familiar second moments of area about the y- and z-axes, I_y and I_z, respectively. The integral $\int_{\mathscr{A}} yz\,dA$ is the *mixed second moment of area*[*] and will be denoted $-I_{yz}$. It follows that, with the aid of Eqs. (9.27), the moment-curvature relations in Eqs. (9.26) can be expressed in matrix form as

$$\left\{ \begin{array}{c} M_y \\ M_z \end{array} \right\} = E \left[\begin{array}{cc} I_y & I_{yz} \\ I_{yz} & I_z \end{array} \right] \left\{ \begin{array}{c} \kappa_y \\ \kappa_z \end{array} \right\}. \tag{9.29}$$

When Eq. (9.29) is solved for κ_y and κ_z, then Eqs. (9.27) can be used to determine the angle $\alpha = \tan^{-1}(-\kappa_y/\kappa_z)$.

9.2.2 Principal Axes of Area

In view of the definition of a tensor given in Sect. 4.4 (page 182), it follows from Eq. (9.29) that the matrix $[I]$ of the second moments of area represents a tensor. It is, moreover, symmetric, just like the two-dimensional stress matrix discussed in Sect. 4.6, and its transformation to another set of axes y', z' (rotated by an angle θ with respect to y, z) is given by an equation analogous to Eq. (4.48). Just as with stresses, a pair of *principal axes* can be found such that with respect to those axes the mixed second moment is zero. Also, just as with stresses, either there is a unique pair of mutually perpendicular principal axes, or else every axis is a principal axis, and in that case the second moment or area is the same about every axis. Furthermore, the second moments of area about the principal axes are the eigenvalues of the square matrix in Eq. (9.29), and they are the maximum and minimum values of I about all possible centroidal axes. If one of the axes (say y or z) is an axis of symmetry, then I_{yz} is necessarily zero, since every area element dA has a mirror image where the product yz has the opposite sign (see Fig. 9.5), and therefore $\int_{\mathscr{A}} yz\,dA = 0$. This means, of course, that an axis perpendicular to an axis of symmetry is also a principal axis. Furthermore, in any area with two or more *non-perpendicular* axes of symmetry (such as any regular polygon), all axes are principal axes.

[*]Also called "product of inertia" (see page 370).

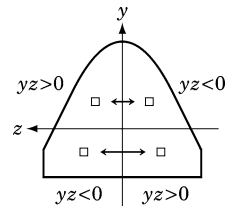

Figure 9.5. Explanation of the vanishing of I_{yz} for a symmetric section

Example 9.2.1: Second moment of area of a square.
For a square with sides of length b, the second moment of area about the axes bisecting the sides is, as we know, $b^4/12$. For an axis along the diagonal we can regard the section as a rhombus (Example 8.2.3), with $a = c = b/\sqrt{2}$, so that $I = (b/\sqrt{2})(b/\sqrt{2})^3/3 = b^4/12$. It follows that $I = b^4/12$ about *any* axis passing through the center.

For a section with no axis of symmetry, the principal axes are determined by first calculating I_y, I_z and I_{yz}, and then using a procedure similar to that of Sect. 4.6, as illustrated in the following example.

Example 9.2.2: Non-isosceles right triangle.
We consider the right triangle shown in Fig. 9.6, with the origin of the y- and z-axes at its centroid, and with vertices at $(y,z) = (-2,-2)$, $(-2,1)$ and $(4,1)$. Since such a triangle is just the right half (or the upper half) of an isosceles triangle, we can use the previously derived results to find $I_z = 3\cdot 6^3/36 = 18$ and $I_y = 6\cdot 3^3/36 = 4.5$. To determine I_{yz}, we define new axes $\bar{y} = y+2$ and $\bar{z} = z-1$; the

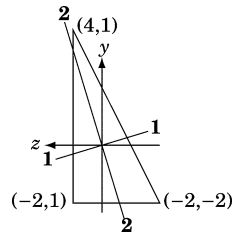

Figure 9.6. Principal axes of a non-isosceles right triangle

triangle is then bounded by $\bar{y} = 0$, $\bar{z} = 0$ and $\bar{y} = 6+2\bar{z}$. Consequently,

$$I_{yz} \;=\; -\int_{\mathscr{A}} yz\,dA \;=\; -\int_{-3}^{0}\int_{0}^{6+2\bar{z}} (\bar{z}+1)(\bar{y}-2)\,d\bar{y}\,d\bar{z} \;=\; -4.5\,. \tag{9.30}$$

(The details of the integration are omitted.) The principal directions are given, by analogy with Eq. (4.56) (with θ_p measured counterclockwise from the y-axis), by

$$\tan 2\theta_p \;=\; \frac{2I_{yz}}{I_y - I_z} \;=\; \frac{2\cdot(-4.5)}{4.5-18} \;=\; \frac{2}{3}\,, \tag{9.31}$$

leading to $\theta_{p1} = 16.85°$; the principal axes are shown as the lines **1-1** and **2-2** in the figure. We further calculate the principal second moments, I_1 and I_2, by

analogy with Eq. (4.60), as

$$I_{1,2} = \frac{I_y + I_z}{2} \pm \sqrt{\left(\frac{I_y - I_z}{2}\right)^2 + I_{yz}^2} = 19.36,\ 3.14\ . \tag{9.32}$$

If y and z are principal axes, the moment-curvature relations given by Eqs. (9.29) are uncoupled:

$$M_y = EI_y\kappa_y \quad , \quad M_z = EI_z\kappa_z\ , \tag{9.33}$$

that is, *if the moment is about a principal axis, then the plane of bending coincides with that of the moment.* In other words, bending about one principal axis is uncoupled from bending about the other, a fact that can also be motivated (in accordance with the discussion in Sect. 6.5) by showing that the strain energy per unit length is the sum of terms depending respectively on κ_y and κ_z alone, with no mixed terms:

$$U_{\rm b}' = \frac{1}{2}\int_{\mathscr{A}} E\varepsilon^2\, dA = \frac{E}{2}\int_{\mathscr{A}} (\kappa_y z - \kappa_z y)^2\, dA = \frac{EI_y\kappa_y^2}{2} + \frac{EI_z\kappa_z^2}{2}\ , \tag{9.34}$$

since $\int_{\mathscr{A}} yz\, dA = 0$. Substituting the expressions for the components of the curvature vector from (9.33) in (9.28), it follows that the stress can be expressed as

$$\sigma_x = \frac{M_y z}{I_y} - \frac{M_z y}{I_z}\ , \tag{9.35}$$

that is, it is simply the sum of the stresses due to each moment acting in its own plane. Now, the neutral plane is defined by the equation

$$\frac{M_y z}{I_y} - \frac{M_z y}{I_z} = 0\ . \tag{9.36}$$

Furthermore, taking into account (9.27) and (9.33) (or, alternatively, (9.24) and (9.36)), the angle α satisfies

$$\tan\alpha = -\frac{M_y I_z}{M_z I_y}\ . \tag{9.37}$$

9.2.3 Determination of Stresses

While it is possible to calculate the stress in an asymmetric cross-section from Eq. (9.28), with κ_y and κ_z obtained by solving Eqs. (9.29) (the derivation of the corresponding equation is left to an exercise), it is usually simpler to do so by using Eq. (9.35) with respect to the principal axes. Once the neutral plane is found from Eq. (9.36), then the points in the cross-section that are farthest from it, on either side, are the locations of the maximum tensile and compressive stresses, as will be illustrated in the following example.

Example 9.2.3: Stresses in the triangle of Example 9.2.2.
Suppose that the dimensions shown in Fig. 9.6 are in inches, and that a moment $M = 10$ k·in acts about the z-axis of that figure. We now redefine the y- and z-axes to coincide with the principal axes **1-1** and **2-2**, respectively, as shown in Fig. 9.7 (with the coordinates of the vertices relabeled in terms of the redefined axes), so that $I_y = 3.14$ in^4 and $I_z = 19.36$ in^4, while $M_y = M \sin 16.85° = 2.90$ k·in and $M_z = M \cos 16.85° = 9.57$ k·in.

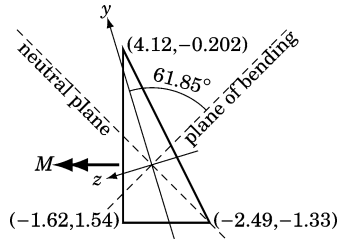

Figure 9.7. Plane of bending and neutral plane in the triangle of Example 9.2.2

The neutral plane is accordingly described by $(2.90/3.14)z - (9.57/19.36)y = 0$ and is shown in the figure, with $\alpha = \tan^{-1}(-2.90 \cdot 19.36/9.57 \cdot 3.14) = -61.85°$. By inspection, the maximum tensile and compressive stresses act at the lower left and upper vertices, respectively, and are given, in accordance with Eq. (9.35) by

$$\sigma^{\mathrm{t}}_{\max} = \left(\frac{2.90 \cdot 1.54}{3.14} - \frac{9.57 \cdot (-1.62)}{19.36} \right) \text{ksi} = 2.22 \text{ ksi}$$

and

$$\sigma^{\mathrm{c}}_{\max} = \left(\frac{2.90 \cdot (-0.202)}{3.24} - \frac{9.57 \cdot 4.12}{19.36} \right) \text{ksi} = -2.22 \text{ ksi} .$$

Note that the values are numerically equal, since it so happens that the neutral plane is at 45°with respect to the original y- and z-axes of Fig. 9.6, and it can easily be checked that the critical vertices are equidistant from that plane.

Exercises

9.2-1. Solve Eqs. (9.29) for κ_y and κ_z, and substitute the expressions into Eq. (9.28) to show that the stress σ_x due to asymmetric bending when the y- and z-axes are not necessarily principal axes is given by

$$\sigma_x = \frac{(M_y I_z - M_z I_{yz})z - (M_z I_y - M_y I_{yz})y}{I_y I_z - I_{yz}^2} .$$

9.2-2. For an isosceles right triangle with legs of length a, find the second moments of area I_y, I_z and I_{yz} about axes going through the centroid that are (a) parallel to the legs, (b) parallel and perpendicular to the hypotenuse.

9.2-3. Show that, if the y- and z-axes are principal axes, then the complementary energy per unit length, $\overline{U}'_{\mathrm{b}}$, can be expressed as the sum of terms depending respectively on M_y and M_z alone.

9.2-4. A beam of square cross-section, with sides of length 3.5 in oriented along the y- and z-axes, is subjected to a bending moment of magnitude 5 k·in and direction $-(1/2)\mathbf{j} + (\sqrt{3}/2)\mathbf{k}$. Find the maximum tensile and compressive stresses in the cross-section and the points at which they act.

9.2-5. A beam of rectangular cross-section, with sides of length 14 cm along the y-axis and 9 cm along the z-axis, is subjected to a bending moment with $M_y = 0.5$ kN·m and $M_z = 2.5$ kN·m. Find:

(a) an equation describing the neutral plane;

(b) the angle α between the xy-plane and the plane of bending due to the applied moment;

(c) the maximum tensile and compressive stresses in the cross-section and the points at which they act.

9.2-6. A beam whose cross-section is an isosceles right triangle, with legs of length 10 cm along the y- and z-axes, is subjected to a bending moment $M = 6$ kN·m about the z-axis. Find:

(a) an equation describing the neutral plane;

(b) the angle α between the xy-plane and the plane of bending due to the applied moment;

(c) the maximum tensile and compressive stresses in the cross-section and the points at which they act.

9.2-7. A T-beam with the cross-section shown in the figure (with all dimensions in centimeters) is subjected to a moment $\mathbf{M} = 10\mathbf{j} - 20\mathbf{k}$ kN·m. Find:

(a) the principal second moments of area for the cross-section;

(b) the distribution of axial stress over the cross-section;

(c) an equation describing the neutral plane;

(d) the angle α between the xy-plane and the plane of bending due to the applied moment;

(e) the maximum tensile stress in the cross-section and the point(s) at which it acts;

(f) the maximum compressive stress in the cross-section and the point(s) at which it acts.

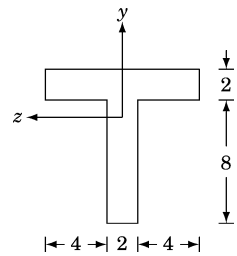

9.2-8. An equal-legged angle beam having the cross-section shown in the figure, with the leg thickness t assumed small compared to the length d, is subjected to a bending moment $\mathbf{M} = M\mathbf{k}$. Find:

(a) approximate expressions (retaining only the terms of the lowest order in t) for the second moments of area I_y, I_z and I_{yz};

(b) approximate expressions for the principal second moments of area I_1 and I_2, and their corresponding axes;

(c) an equation describing the neutral axis;

(d) the angle α between the xy-plane and the plane of bending due to the applied moment;

(e) the maximum tensile stress in the cross-section and the point(s) at which it acts;

(f) the maximum compressive stress in the cross-section and the point(s) at which it acts.

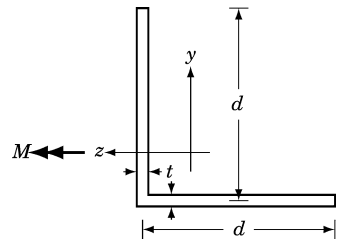

9.2-9. Redo Example 9.2.3 for a moment of 10 k·in about the y-axis, including a figure analogous to 9.2.3.

9.2-10. Redo Exercise **9.2-8** for the unequal-legged angle beam shown in the figure below.

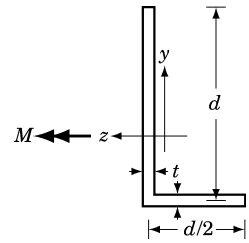

9.2-11. Redo the preceding exercise for a moment M acting about the y-axis.

9.3 Shear Stresses in Beams

9.3.1 Introduction

When a shear force, say $V = V_y$ (with the y-axis assumed to be a principal axis), acts on a beam cross-section, as in Fig. 9.8, then the distribution of shear stress τ_{yx} on the cross-section $\mathscr{A}$ must be such that

$$V = \int_{\mathscr{A}} \tau_{yx}\, dA \,. \tag{9.38}$$

By the same token, since in the presence of a shear force the bending moment necessarily depends on x (see Eq. (8.5), page 354), then so does the axial stress σ_x, as given by Eq. (8.25) (page 369). Consequently, since $\partial\sigma_x/\partial x \neq 0$, the local equilibrium Eq. (4.39) (page 190) cannot be satisfied without a shear stress τ_{xy}.

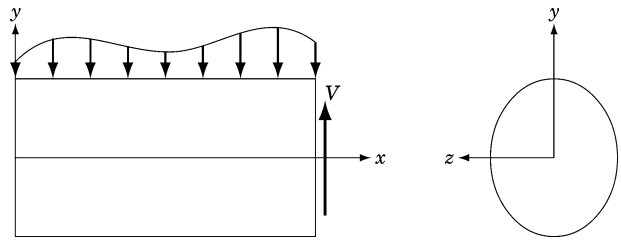

Figure 9.8. Shear force on a cross-section of a beam

Assuming at the outset that the boundary of the cross-section is free of any shear traction, the distribution of the shear stress in the cross-section must have the property that at the boundary of the cross-section its direction is always tangential to the boundary, as seen in Fig. 9.9; otherwise there would be longitudinal shear stress on the lateral surface of the beam. This means that, unless the shear stress vanishes at the boundary, there must in general be a component τ_{zx} as well, except when the boundary is locally parallel to the y-axis.

9.3.2 Beam with Rectangular Cross-Section

If the cross-section is rectangular, as in Fig. 9.10a, then, assuming that the lateral surface of the beam is free of shear stress, we have

$$\tau_{xy} = 0 \quad \text{at} \quad y = \pm\frac{h}{2} \,. \tag{9.39}$$

Since $\tau_{zx} = \tau_{xz} = 0$ on the boundaries $z = \pm b/2$, as discussed above, we can also assume that this holds throughout the cross-section, and in the absence

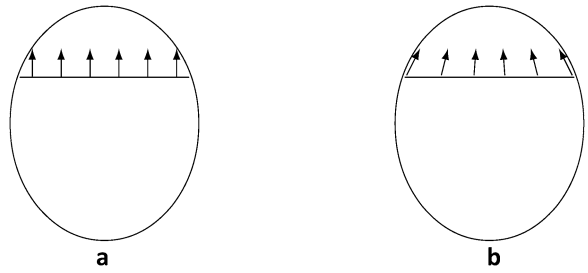

Figure 9.9. Distribution of shear stress on a cross-section: (**a**) inconsistent with shear-traction-free beam, (**b**) consistent with shear-traction-free beam

of body forces the local equilibrium equation in the x-direction, Eq. (4.39) (page 190), becomes

$$\frac{\partial \tau_{xy}}{\partial y} = -\frac{\partial \sigma_x}{\partial x} = \frac{dM}{dx}\frac{y}{I} = -V\frac{y}{I} = -\frac{12V}{bh^3}y\,, \tag{9.40}$$

where we use Eqs. (8.5), (8.25), (8.5), and (8.29). If the solution of the differential equation formed by the first and last members of Eq. (9.40) is assumed independent of z, then it satisfies the boundary conditions (9.39) if

$$\tau_{xy} = \frac{6V}{bh^3}\left[\left(\frac{h}{2}\right)^2 - y^2\right] = \frac{3V}{2A}\left[1-\left(\frac{2y}{h}\right)^2\right], \tag{9.41}$$

where $A = bh$ is the cross-sectional area of the beam. Eq. (9.41) implies that the distribution of shear stress is parabolic in y, as seen in Fig. 9.10b. Clearly, the maximum value of the shear stress occurs at $y = 0$, and is given by

$$\tau_{\max} = \tau_{xy}\Big|_{y=0} = \frac{3}{2}\tau_{\text{av}}\,, \tag{9.42}$$

where $\tau_{\text{av}} = V/bh$ is the average shear stress over the whole cross-section.

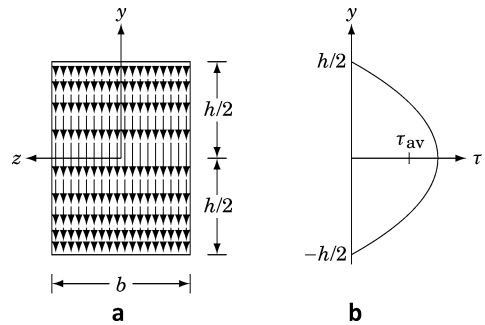

Figure 9.10. Shear stress in a rectangular cross-section: (**a**) visualization in the plane of the cross-section, (**b**) distribution with respect to y

If the shear force V varies with x (as it would, for instance, under a distributed load), then the term $\partial\tau_{xy}/\partial x$ is non-zero, and hence other stress components must be present for compliance with the equilibrium equation (4.40). The present approach must, therefore, be viewed as an approximation. Exact theories of shear (which will not be discussed here) show that the approximation becomes more accurate as the rectangular cross-section becomes narrower.

The derivation of a shear-stress distribution τ_{zx} due to a shear force V_z is completely analogous.

9.3.3 Elastic Energy Due to Shear Stresses

The presence of shear stresses gives rise to additional terms in the elastic energy, as discussed in Sect. 6.5. With a single shear-stress component τ in the rectangular cross-section of Fig. 9.10, the additional term in the complementary energy per unit volume is $\overline{U}^0_{\rm sh} = \tau^2/2G$. If we integrate this term over the area, using Eq. (9.41) for $\tau = \tau_{xy}$ we obtain the complementary energy per unit length,

$$\overline{U}'_{\rm sh} = \frac{1}{2G}\left(\frac{3V}{2bh}\right)^2 b\int_{-h/2}^{h/2}\left[1-\left(\frac{2y}{h}\right)^2\right]^2 dy = \frac{3}{5}\frac{V^2}{2GA}\,. \tag{9.43}$$

For other cross-sections the result can also be written in the form $\overline{U}'_{\rm sh} = \alpha V^2/2GA$, where $V^2/2GA$ is what $\overline{U}'_{\rm sh}$ would be if the shear-stress distribution were uniform, and α is the *shear correction factor* which is not always easy to determine but which is typically not very different from 1.*

Example 9.3.1: Energy due to shear stress in end-loaded cantilever. We may study the influence of this energy by revisiting the end-loaded cantilever (Example 8.3.4, page 386) and adding $\overline{U}_{\rm sh} = \alpha F^2 L/2GA$ (since $|V(x)| = F$) to the previously found $\overline{U}_b = F^2L^3/6EI$. If we now equate the combined $\overline{U}$ to the external work $F\Delta/2$, then the result may be expressed, after dividing by $F/2$, as

$$\Delta = \Delta_{\rm b} + \Delta_{\rm sh}\,. \tag{9.44}$$

where $\Delta_{\rm b} = FL^3/3EI$ and $\Delta_{\rm sh} = \alpha FL/GA$. The ratio is

$$\frac{\Delta_{\rm sh}}{\Delta_{\rm b}} = \frac{3\alpha EI}{GAL^2} = \frac{6\alpha(1+\nu)}{(L/r)^2}\,, \tag{9.45}$$

where $r = \sqrt{I/A}$ is called the *radius of gyration*† (in this case about the z-axis), which for a rectangular section is $\sqrt{bh^3/12bh} = h/\sqrt{12}$, and L/r is the already mentioned *slenderness ratio*. Since the numerator in the third member of the

*Sometimes a *shear-corrected area* $A_{\rm sh} = A/\alpha$ is used.

†The term is borrowed from rigid-body dynamics, as is "moment of inertia."

last equation is around 10, it follows that for slenderness ratios greater than 30 (which, for a rectangular beam, mean span-to-depth ratios greater than about 9) the shear correction to the deflection is less than 1%, justifying the assumption of the Bernoulli–Euler theory that the local deformation in a beam is essentially like that in pure bending.

9.3.4 General Cross-Sections: Shear Flow

For non-rectangular cross-sections, the Bernoulli–Euler theory allows the determination of only the average, over a cut in the cross-section, of the shear-stress component normal to the cut. Consider the beam cross-section shown in Fig. 9.11a, and imagine a line (shown here as straight, but not necessarily so in general) that sections the region $\mathscr{A}$ into subregions $\mathscr{A}'$ and $\mathscr{A}''$. Now

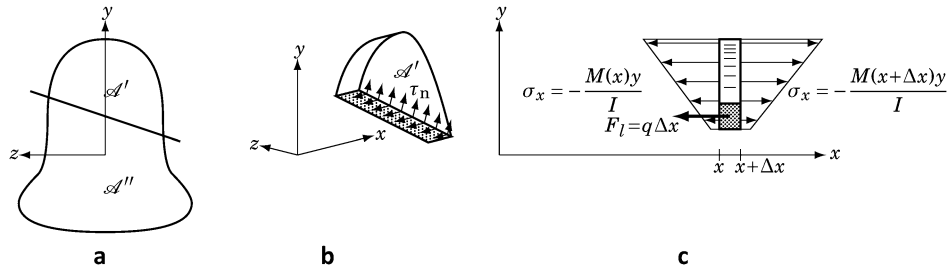

Figure 9.11. Shear flow in a beam: (**a**) cross-section, (**b**) free body, (**c**) x-force equilibrium

suppose that a slice of the beam (between x and $x + \Delta x$) is further cut along the plane formed by that line and the x-axis, producing the free body shown in Fig. 9.11b, where only the shear stress τ_n normal to the cut line (not necessarily constant along the line) is shown on the two perpendicular planes meeting there, namely the plane of the cross-section and that of the longitudinal cut. We define the *shear flow* q by

$$q = \int_{\text{cut}} \tau_n \, ds \,, \tag{9.46}$$

the integration being taken over the longitudinal cut shown as shaded in Fig. 9.11b so that the average value of τ_n is

$$\tau_{av} = \frac{q}{l} \,, \tag{9.47}$$

where l is the length of the cut. Now, if the variation of q with x is neglected, the shear stress over the longitudinal cut produces a longitudinal force $F_l = q\Delta x$ in the negative x-direction if the sign of the shear stress is as shown in Fig. 9.11b. This force must be balanced by the resultants of the normal stress

on $\mathscr{A}'$ on both faces of the section, as shown in Fig. 9.11c, so that

$$q\Delta x = \int_{\mathscr{A}'} \left(-\frac{M(x+\Delta x)y}{I}\right) dA - \int_{\mathscr{A}'} \left(-\frac{M(x)y}{I}\right) dA \,, \tag{9.48}$$

which can be simplified by noting that, as Δx becomes infinitesimal, then, by Eq. (8.5),

$$q = \frac{V}{I} \int_{\mathscr{A}'} y \, dA \,. \tag{9.49}$$

The integral in the preceding equation is the *first moment* of the area $\mathscr{A}'$ about the z-axis and is usually denoted Q, resulting in the *shear-flow equation*

$$q = \frac{VQ}{I} \,. \tag{9.50}$$

It is easy to determine Q if both the area and the location of the centroid of $\mathscr{A}'$ are known, because it then just equals the product of the area of $\mathscr{A}'$ and the distance of this centroid from the z-axis. The same operation could have been performed using the region $\mathscr{A}''$ instead of $\mathscr{A}'$, with the resulting Q being the negative of that found by using $\mathscr{A}'$, since, by definition, the first moment of an area (in this case, that of the whole cross-section) about its centroid is zero.

To confirm that Eq. (9.50) is consistent with the previously derived result for rectangular beams, we note that if we define $\mathscr{A}'$ as set of points satisfying $y > y_1$, then the centroid of $\mathscr{A}'$ is at $y = \frac{1}{2}(y_1 + h/2)$, and its area is $b(h/2 - y_1)$. Consequently,

$$q = \frac{Vb(h/2-y_1)(y_1+h/2)/2}{bh^3/12} = \frac{6V}{h^3}\left[\left(\frac{h}{2}\right)^2 - y_1^2\right] \,, \tag{9.51}$$

consistent with Eq. (9.41) if $\tau_{xy} = q/b$.

Example 9.3.2: Shear stress in isosceles triangle.
Let the base and height of the triangle be b and h, respectively. If we perform a cut parallel to the z-axis at $y = y_1$, then A' is an isosceles triangle of base $(b/h)(\frac{2}{3}h - y_1)$ and height $\frac{2}{3}h - y_1$. Consequently, the area is $(b/2h)(\frac{2}{3}h - y_1)^2$, and the centroid is at $y_1 + \frac{1}{3}(\frac{2}{3}h - y_1) = \frac{2}{3}(y_1 + \frac{1}{3}h)$. If we use Eq. (9.50) to determine q and divide the result by the length of the cut, $l = (b/h)(\frac{2}{3}h - y_1)$, to obtain the average vertical shear, we find (using the previously derived result $I = bh^3/36$)

$$\tau_{\text{av}} = \frac{12V}{bh^3}\left(\frac{2h}{3} - y_1\right)\left(\frac{h}{3} + y_1\right) \,.$$

As expected, this expression vanishes at the apex ($y_1 = 2h/3$) and at the base ($y_1 = -h/3$), while the maximum is reached at $y_1 = h/6$ and equals $3V/bh$, which happens to be $(3/2)V/A$ as in the rectangle, but it is of course not the true maximum shear stress, though it can be expected to be close to it if the triangle is narrow.

9.3.5 Shear Stresses in I-Beams and Built-Up Beams

Rolled sections, such as I-beams and wide-flange beams, and built-up sections, such as box beams, are regarded as very efficient structural shapes, especially when made of ductile materials, because as much as possible of the material is in the flanges, as far as possible from the center, where the compressive and tensile axial stresses are highest. The web, as we have already seen in Example 8.2.5 (page 373), contributes a relatively small part of the flexural rigidity and strength; its main function is to hold the flanges together by resisting the longitudinal shear (shown in Fig. 9.11b) that would otherwise make the flanges slide past each other. Such sliding would also occur in beams built up of planks or similar elements; these must be held together by glue or by fasteners, such as nails or bolts. The shear-flow equation (9.50) can be used not only to calculate the average shear stress at a glued joint, but also the shear force carried by a fastener.

In thin-walled sections, such as the I-beam and the box beam shown in Fig. 9.12, we can employ the shear-flow equation (9.50) to estimate the average shear strain at any given point. Indeed, we may assume that, since at the walls the direction of the shear must be parallel to the walls, it is very nearly the same across the section. Thus, in the flanges the shear stress consists

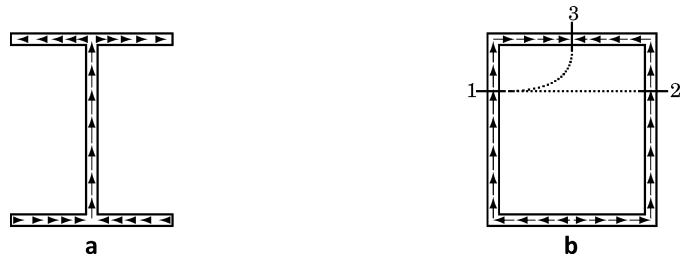

Figure 9.12. Shear flow in an I-beam (**a**) and a box beam (**b**)

primarily of τ_{zx}. Because of the symmetry of the section, this shear stress is algebraically antisymmetric about the y-axis (that is, it is an odd function of z). Hence, the resultant of the shear stresses in the flanges is very nearly zero, except to the slight extent that these stresses may contribute to V_y; it is primarily the web that resists the shear force V_y. The antisymmetry of τ_{zx} is convenient when analyzing a multiply connected section like the box beam of Fig. 9.12b, since to isolate a free body the section material must be cut twice. The double cut by line 1-2 creates shear flows in two places, 1 and 2, equal by symmetry, but in the double cut by line 1-3 there is nonzero shear flow only at 1. Since the value of Q for cut 1-2 is twice that for cut 1-3, it is clear that these cuts produce the same shear flow.

Example 9.3.3: Approximate calculation of maximum shear stress in an I-beam.
It is obvious that, the web being rectangular, the shear-stress distribution there will parabolic like the one derived for the simple rectangle, except that the shear stress will not be zero at the extreme ends of the web. If we use the approximate expression for I derived in Example 8.2.5, and if we assume (as in the example) that the flange and web thicknesses are relatively small, then for a cut along the z-axis the first moment of the area above it is approximately $Q \doteq (A_w/2)(h/4) + A_f(h/2) = (A_w + 4A_f)h/8$. Since $t_w \doteq A_w/h$, the maximum shear stress is approximately

$$\tau_{\max} = \frac{q_{\max}}{t_w} \doteq V\frac{h}{A_w}\frac{(A_w+4A_f)h/8}{(A_w+6A_f)h^2/12} = \frac{1+A_w/4A_f}{1+A_w/6A_f}\frac{3V}{2A_w}. \qquad (9.52)$$

For the section with the dimensions given in Example 8.2.5, with the effective depth taken as 11 (so that $A_w = 11$), the result of the calculation is $\tau_{\max} = V/10.145$, while an exact calculation leads to $\tau_{\max} = V/10.142$, a negligible difference. For wide-flange beams, in which the flange area is significantly larger than the web area, the first fraction in the last member of the above equation is not very different from 1, and $\tau_{\max} = 3V/2A_w$ is a good approximation.

Shear in Fasteners

If a cut is made along a glued surface, the analysis is exactly as for the continuous material discussed so far. The difference arises in stress-based design, since the allowable shear stress transmitted by the glue is, in general, different from that of the material. When the beam is built up from separate elements held together with discrete fasteners (such as nails, screws, bolts or rivets) with a longitudinal spacing of, say, d, then the slice used for equilibrium analysis, as in Fig. 9.11c, is not taken arbitrarily, but precisely so that it contains one fastener (or one set of fasteners, if there is more than one at a given x). In other words, Δx is not taken such that it goes to zero, but it equals d, with F_l being the shear force transmitted by the fastener (or set of fasteners) crossed by the cut. The shear-flow equation (9.50) can then be used to calculate F_l through the relation $F_l = q\Delta x = qd$, so that

$$F_l = \frac{VQd}{I}. \qquad (9.53)$$

Eq. (9.53) can be invoked to calculate the minimum fastener spacing for a given beam geometry and loading when the shear-force capacity of the fasteners is known. Fig. 9.13 shows examples of built-up cross-sections held together with fasteners, and the cuts that may be used to calculate the forces transmitted by them.

Example 9.3.4: Nailed box beam.
In the box beam in figure 9.13a, let the dimensions of the vertical planks be

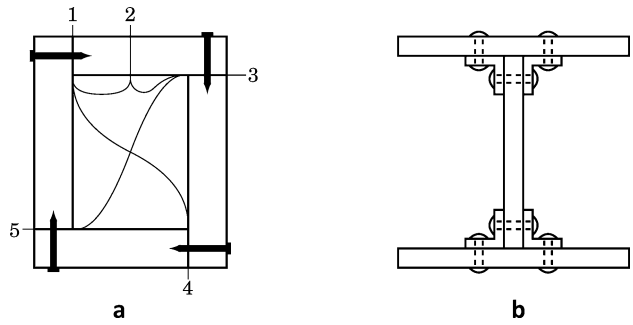

Figure 9.13. Built-up sections: (**a**) nailed box, (**b**) riveted I-beam

2 in by 10 in, and those of the horizontal planks 2 in by 8 in. (Note that the asymmetric placement of the nails does not affect the geometric symmetry of the cross-section and hence the validity of the method followed here.) For the second moment of area we therefore have, by the subtraction method

$$I_z = \frac{1}{12}(10\cdot 12^3 - 6\cdot 8^3)\,\text{in}^4 = 1280\,\text{in}^4\,. \tag{9.54}$$

For the cut 1-2, which will give the shear in the horizontal nails, we have $Q = (2\cdot 3)\cdot 5\text{in}^3 = 30\ \text{in}^3$, while for the cut 2-3, $Q = (2\cdot 5)\cdot 5\text{in}^3 = 50\ \text{in}^3$. (It will be left to an exercise to show that equivalent results will be produced by using cuts 1-4 and 3-5.) If the longitudinal nail spacing is, say, $d = 12$ in, then the forces in the horizontal and vertical nails are $0.281V$ and $0.469V$, respectively. Clearly, the horizontal nailing is more efficient than the vertical. If the nails are all the same size (and hence have the same shear strength), for a given shear force the horizontal nails can be spaced farther apart (by a factor of 5/3) than the vertical ones. Alternatively, the box could accordingly be redesigned with two 2-by-12 and two 2-by-6 planks.

9.3.6 Shear Stress in Reinforced-Concrete Beams

As we discussed in Sect. 9.1, in a reinforced-concrete beam the concrete that would carry tension is modeled as a shear zone that carries no axial stress but acts as a "web" connecting the "flanges" constituted by the compression concrete and the reinforcing steel. Since the moment arm of the resultant compressive and tensile forces is $(1-\frac{1}{3}k)d$, it can be shown by an analysis similar to that of Fig. 9.11 (page 424) that the shear flow over a horizontal cut anywhere in this zone is $q = V/(1-\frac{1}{3}k)d$. Therefore the average shear stress there is $\tau = V/(1-\frac{1}{3}k)bd$, which can be approximated for estimation purposes as V/bd. The shear strength of concrete is of the order of magnitude of its tensile strength and therefore much smaller than its compressive strength, but then shear stresses in beams are typically much smaller in magnitude than axial stresses. If, however, the shear force at a section of the beam is too great for the shear strength of the concrete, bent steel bars known as *stirrups* are inserted as shown in a plan view in the cross-section plane in Fig. 9.14a;

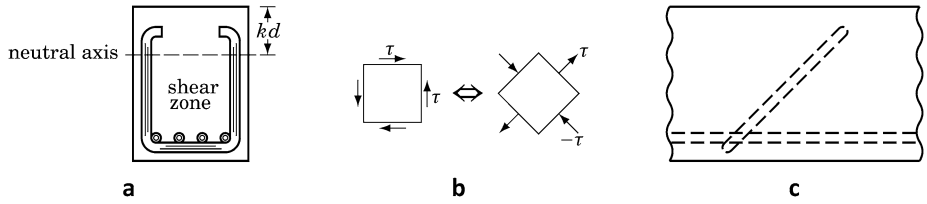

Figure 9.14. Stirrups in a reinforced-concrete beam: (**a**) view in the plane of the cross-section, (**b**) principal stresses in the shear zone, (**c**) diagonal placement

they act essentially as fasteners between the two "flanges." However, in view of the orientation of the principal stresses in the shear zone shown in Fig. 9.14b (with V assumed positive), it is more efficient to orient the stirrups diagonally as shown in Fig. 9.14c so that they act as tensile reinforcement.

9.3.7 Asymmetric Thin-Walled Sections: Shear Center

In sections for which the y-axis is a principal axis but not an axis of symmetry, the previously derived results for the shear flow and average shear stress are still a necessary consequence of force equilibrium, but the stresses so generated will not, in general, produce zero moment about the x-axis. We can see this by considering the channel section shown in Fig. 9.15. If, for

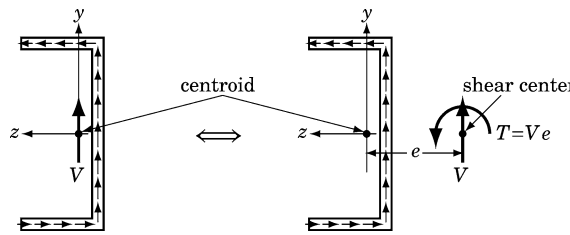

Figure 9.15. Shear force acting asymmetrically on a channel section

example, the line of action of the shear force V along the y-axis goes through the centroid, then the shear flows add up to a positive moment about the centroid (that is, a torque) consisting of the counterclockwise couple formed by the shear flows in the flanges and the likewise counterclockwise moment of the shear flow in the web. In order for the flange and web moments to cancel, the line of action of the shear force would have to be outside the web, on the right as shown in the figure. The point where this line intersects the z-axis is known as the *shear center* of the section. Its distance e from the centroid along the z-axis is found by requiring that the torque of V relative to the centroid be equal to the torque due to the shear stresses in the cross-section.

This translates to an equation of the form

$$\mathbf{i} \cdot \int_{\mathscr{C}} \mathbf{r} \times t\boldsymbol{\tau}\, ds = Ve\,, \tag{9.55}$$

where $\mathscr{C}$ denotes the mean curve of the cross-section as in Sec. 7.2, $\mathbf{r}$ is position vector of a point on $\mathscr{C}$, $\boldsymbol{\tau}$ is the shear stress (in vectorial form) and t is the (possibly variable) thickness of the cross-section. It follows, then, that a beam undergoing shear forces will bend without twisting only if the line of action of the shear force is everywhere through the shear center. Otherwise the shear force must be replaced, for the purpose of analysis, by the statically equivalent system of a shear force that does so and the corresponding torque. The beam, consequently, undergoes torsion in addition to bending, and to the shear stresses found by the method of this section must be added the torsional shear stresses, component by component. This approach works mainly for thin-walled sections, in which the direction of the shear stresses is approximately known.

The same superposition must also be applied in the case of symmetric sections if the shear force does not pass through the centroid, or if a torque is applied independently of the transverse loading. The superposition of stresses is the subject of Sect. 9.4.

If neither principal axis is an axis of symmetry, then the shear center is at the intersection of the non-moment-producing lines of action for V_y and V_z.

Exercises

9.3-1. Determine the distribution of the average shear stress with respect to the y-axis in a beam with circular cross-section of radius c, subject to a shear force V_y, as in the figure.

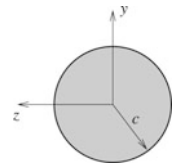

9.3-2. Show that the calculation of shear stress in Example 9.3.3 on the basis of the cuts 1-4 and 3-5 is equivalent to that in the example.

9.3-3. Find the maximum shear stress acting on the cross-section of the beam of Exercise **8.1-1**, assuming that the beam has a rectangular cross-section with width $b = 1$ cm and depth $h = 2$ cm.

9.3-4. An I-beam spanning the region $0 < x < 2$ (x in meters), with the cross-section shown in the figure (with all dimensions in centimeters), is subject to a moment M, which varies quadratically according to $M(x) = ax(2 - x)$ in N·m. If the flanges of the I-beam are glued to the web such that the maximum allowable shear stress at the locations of the glue is $\tau_{\text{al}} = 50$ MPa, estimate the maximum allowable value of the loading parameter $a > 0$. Assume that the beam is made of a linearly elastic material.

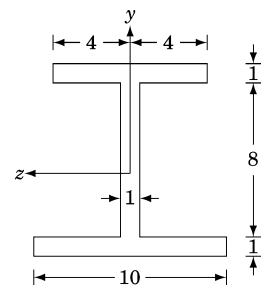

9.3-5. Consider a beam with a cross-section in the shape of an isosceles triangle of base b and height h, as in the figure.

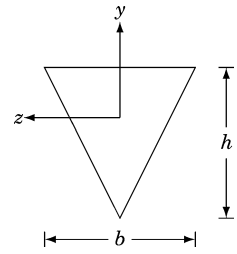

(a) Calculate the second moment of area I_z of the cross-section with respect to the horizontal neutral axis.

(b) Suppose that a vertical resultant shear of magnitude V is applied downwards at a given cross-section of the beam. Determine and sketch the distribution of the shear stress along the y-axis using the conventional shear-flow equation.

(c) Find the location and magnitude of the maximum shear stress due to V.

9.3-6. A simply supported beam of span 10 ft, carrying a uniformly distributed load $\overline{w}$, is made of a W12×50 section, which weighs 50 lb/ft and for which $I_z = 394\,\text{in}^4$, $h = 12.2\,\text{in}$, $b = 8.08\,\text{in}$, $t_f = 0.64\,\text{in}$ and $t_w = 0.37\,\text{in}$. Find the maximum loading $\overline{w}_{\max}$ (taking the beam weight into account) if the normal stress is not to exceed 24 ksi and the shear stress 14 ksi.

9.3-7. A rectangular box beam is made by gluing to vertical strips of plywood to two horizontal planks, with the dimensions (in centimeters) shown in the figure. The beam is to be used as a simply supported beam of length 3 m, carrying a concentrated force of 40 kN at the midpoint. Let $\sigma_{\text{all}} = 10$ MPa and $\tau_{\text{all}} = 3.5$ MPa. Making reasonable approximations, find the minimum values of the plank with b (in whole centimeters) and the plywood thickness t (in whole millimeters) so that the allowable stresses are not exceeded.

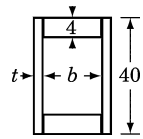

9.3-8. Suppose that, in the riveted beam of Fig. 9.13b, the web and the flanges are made of steel plate of width 20 cm and thickness 2 cm, while the angles have the dimensions (in centimeters) shown in the figure, with the rivet holes centered at 1.5 cm from the edges.

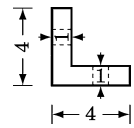

Given a vertical shear force of 10 kN·m, find the average shear stress in the horizontal and the vertical rivets, and specify whether it is single shear or double shear.

9.3-9. A square box beam is made by vertically nailing two horizontal 2 in×14 in planks to two vertical 2 in×10 in planks, one nail per joint.

(a) If the allowable shear stress in the wood is 550 psi, find the maximum allowable shear force.

(b) If the shear force found in (a) is constant over a certain length of the beam, find the minimum nail spacing required if the allowable shear force in each nail is 280 lb.

9.3-10. A square box beam is made by gluing two horizontal 5 cm×35 cm planks to two vertical 5 cm×25 cm planks. If the allowable shear stress is 5 MPa in the wood and 1.6 MPa in the glue, find the maximum allowable shear force.

9.3-11. Consider a beam with the cross-section shown in the figure below, with all dimensions in inches. The beam is assumed to be linearly elastic with Young's modulus $E = 10^4$ ksi.

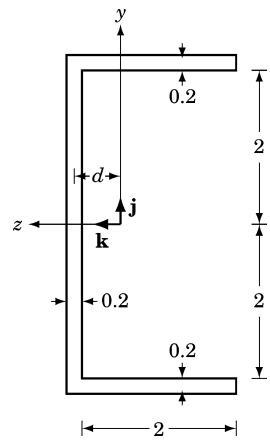

(a) Find the distance d of the centroidal y-axis from the web.

(b) Determine the second moments of area I_y and I_z.

(c) Given a moment $\mathbf{M} = 5\mathbf{j} + 10\mathbf{k}$ in kip·ft, find the magnitude and locations of the maximum tensile and compressive stress σ_x in the cross-section.

(d) Given a shear force $\mathbf{V} = -50\mathbf{j}$ in kips, determine and sketch the distribution of the shear flow on the web and flanges of the cross-section (use the thin-wall approximation for this calculation).

9.4 Stresses in Beams Under Combined Loading

9.4.1 Bending with an Axial Force

When a homogeneous beam is simultaneously subjected to a bending moment M_z and an axial force P passing through the center of the cross-section, there is nothing to prevent us from assuming that plane sections remain plane and therefore the axial stress is still given by Eq. (8.18), provided the yz-axes are principal axes and the curvature is constant and equal to κ. The axial force is then

$$P = \int_{\mathcal{A}} \sigma_x \, dA = -E\kappa \int_{\mathcal{A}} (y - y_0) dA = E\kappa y_0 A \,, \tag{9.56}$$

where the line $y = y_0$ defines all the points of the cross-section where the axial strain and stress are zero, although, because of the axial force P, the centroid of the cross-section is not on this line. It follows immediately from (9.56) that

$$y_0 = \frac{P}{EA\kappa} \,. \tag{9.57}$$

The bending moment is, as before, defined by Eq. (8.21), and is given by Eq. (8.22) regardless of the value of y_0, which implies that the latter can now be expressed as

$$y_0 = \frac{P}{A} \frac{I_z}{M_z} \,. \tag{9.58}$$

With Eqs. (8.22) and (9.58) taken into account, the axial stress, defined as in (8.18), takes the form

$$\sigma_x = -\frac{M_z y}{I_z} + \frac{P}{A} \,. \tag{9.59}$$

This means that the stress is the result of the superposition of the previously found bending stress and the average stress due to the axial force. Axial deformation and bending are thus uncoupled, as can also be verified by means of an energy argument (as discussed in Sect. 6.5, page 300); the derivation is left to an exercise.

If the moment has non-zero components M_y and M_z, the same superposition can be used with Eq. (9.35), yielding

$$\sigma_x = -\frac{M_z y}{I_z} + \frac{M_y z}{I_y} + \frac{P}{A} \,. \tag{9.60}$$

A bending moment can be also created by an axial force whose line of action does not go through the centroid of the cross-section (taken here to be at the origin of the coordinate system), but through some other point with coordinates (y_1, z_1). This is the case of *eccentric loading*, in which

$$\mathbf{M} = (y_1 \mathbf{j} + z_1 \mathbf{k}) \times P\mathbf{i} = P z_1 \mathbf{j} - P y_1 \mathbf{k} \,, \tag{9.61}$$

so that the axial stress is given by

$$\sigma_x = P\left(\frac{1}{A} + \frac{y_1}{I_z}y + \frac{z_1}{I_y}z\right) . \tag{9.62}$$

In this case, the neutral axis is defined by the equation

$$1 + \frac{y_1 A}{I_z}y + \frac{z_1 A}{I_y}z \;=\; 0 . \tag{9.63}$$

This is a line that intersects the y-axis at $-\dfrac{I_z}{y_1 A}$ and the z-axis at $-\dfrac{I_y}{z_1 A}$. Clearly, the position of the neutral axis is independent of the magnitude of the normal force P.

The neutral axis may or may not intersect the cross-section. If it does not, then all material points of the cross-section are subject to normal stress of the same sense (that is, either tensile or compressive).

Example 9.4.1: Rectangular beam bending under axial load. If a beam of rectangular cross-section, with $-h/2 < y < h/2$ and $-b/2 < z < b/2$, is subject to an axial load P passing through a point with coordinates (y_1, z_1), it follows from (9.62) with the aid of (8.29) that

$$\sigma_x \;=\; \left(1 + \frac{12y_1}{h^2}y + \frac{12z_1}{b^2}z\right)\frac{P}{bh} . \tag{9.64}$$

The location of the numerically largest stress depends on the quadrant containing (y_1, z_1). If we suppose this to be the first quadrant (that is, $y_1 \geq 0, z_1 \geq 0$), then the maximum stress will be at the corner of that quadrant, that is, at $y = h/2$, $z = b/2$, and therefore

$$\sigma_{\max} \;=\; \left(1 + \frac{6y_1}{h} + \frac{6z_1}{b}\right)\frac{P}{bh} ; \tag{9.65}$$

in the general case this result is valid with y_1 and z_1 replaced by their absolute values. The minimum stress is at the opposite corner, that is,

$$\sigma_{\min} \;=\; \left(1 - \frac{6|y_1|}{h} - \frac{6|z_1|}{b}\right)\frac{P}{bh} . \tag{9.66}$$

Whether this minimum has the same sign as $\sigma_{\max}$ depends on the magnitudes of y_1 and z_1. In some structural situations (for example, in the voussoirs of a masonry arch) it is desirable that the stress be compressive throughout the cross-section, so that, with $P < 0$, the quantity inside the parentheses must be positive. That is,

$$\frac{6|y_1|}{h} + \frac{6|z_1|}{b} \;<\; 1 , \tag{9.67}$$

meaning that the line of action of the thrust must be inside a rhombus whose vertices are at $(\pm h/6, 0)$ and $(0, \pm b/6)$, shown in Fig. 9.16. This result is known as the *middle-third rule*.

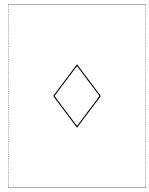

Figure 9.16. Illustration of the middle-third rule

9.4.2 Shear and Torsion

Similarly to the way that axial stress can be produced by a bending moment and/or an axial force, shear stress can be due to a torsional moment (torque) and/or a shear force*. The difference is that while axial stresses can be superposed algebraically, shear stresses, being vectorial in nature (as discussed in Sect. 4.2), have to be superposed vectorially, that is, component by component. Since, with few exceptions, the methods used here (Chap. 8 and Sect. 9.3) do not provide for the derivation of the complete shear-stress distribution, the problems in which such superposition can be used are few in number. One class of such problems includes thin-walled sections, both open and closed. Here we can assume that the shear stresses, both direct and torsional, are parallel to the wall. The direct shear stress can, moreover, be assumed to be practically uniform through the thickness, as can the torsional shear stress in a thin-walled tube (but not, of course, in an open section).

Example 9.4.2: Square tube with an eccentric shear force.
We consider a thin-walled square tube or box beam of uniform thickness t and sides of length $2c$, and carrying a shear force V whose line of action is parallel to a pair of sides and at a distance e from the centerline. For the purpose of calculating the direct shear we may treat the section as an I-beam with web area $A_w = 4ct$ and flange area $A_f = 2ct$, and use the formula of Example 9.3.3 to obtain $\tau^d_{\max} = 9V/32ct$. For the torsional shear stress we use Eq. (7.35) with $\overline{A} = 4c^2$, and therefore $\tau^t = Ve/8c^t$. Consequently,

$$\tau_{\max} = \frac{9V}{32ct}\left(1+\frac{4e}{9c}\right) . \tag{9.68}$$

The preceding example shows that when the eccentricity of the shear force is of the order of magnitude of the cross-section dimensions, then in a closed cross-section the torsional and direct shear stresses are of the same order of magnitude. The same can be said about solid cross-sections. In open cross-sections the situation is different.

*The shear stresses produced by a shear force are known as *direct shear stresses*

Example 9.4.3: I-beam with an eccentric shear force.
We consider an I-beam with $b = h = 2c$, $t_f = t$ and $t_w = 2t$, so that the maximum direct shear stress is the same as in the preceding example. For the maximum torsional shear stress we use Eq. (7.55) with $t_{\max} = 2t$ and

$$J = \frac{1}{3}[2c(2t)^3 + 2(2c)t^3] = \frac{20}{3}ct^3 . \tag{9.69}$$

Consequently, $\tau^t_{\max} = 3Ve/10ct^2$, and this is of the same order as the direct shear stress only if e is of the same order as t, that is, if the force is only slightly eccentric. Otherwise torsion predominates over direct shear. The much greater torsional resistance of box beams (shown in Example 7.4.1, page 349) is one of the reasons why in certain constructions they are preferred to I-beams.

Exercises

9.4-1. Show that, in a beam undergoing bending about the z-axis and axial deformation, the strain energy per unit length can be expressed as the sum of terms depending on κ_z and the average longitudinal strain ε_0 alone, respectively.

9.4-2. Show that, in a beam simultaneously subject to a bending moment M_z and an axial force P, the complementary energy per unit length can be expressed as the sum of terms depending on P and M_z alone, respectively.

9.4-3. A beam of rectangular cross-section with $-3 \le y \le 3$ and $-2 \le z \le 2$ (in inches) is subject to a compressive force $P = 400$ kips acting at a point with coordinates $(-2, -1)$, as in the figure. Find the maximum and minimum values of the normal stress on the cross-section and specify whether they are tensile or compressive.

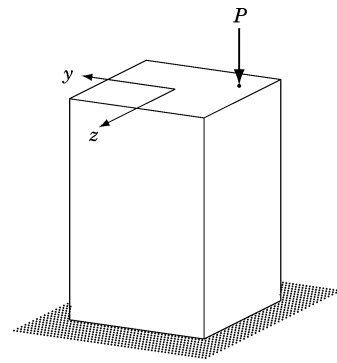

9.4-4. A bar of circular cross-section with radius c carries an axial load whose line of action is at a distance r_1 from the center. Find the limit on r_1 that will make the axial stress keep the same sign throughout the cross-section.

9.4-5. A stone column has the cross-section of an equilateral triangle with sides of length of a. Find the figure within which a compressive axial force must act for the column to sustain no tensile stress.

9.4-6. An I-beam with a cross-section as in Exercise **9.3-4** is made of a linearly elastic material that cannot sustain any tensile stress. Suppose that a compressive force acts on the beam at some point along the y-axis. How far away from the centroid is the force allowed to act?

9.4-7. A circular bar of radius c is subject to a shear force V and a torque T.

(a) Use the shear-flow formula to estimate the maximum direct shear stress due to V.

(b) Estimate the location and magnitude of the maximum shear stress due to the combined effect of V and T.

9.4-8. A thin-walled circular bar of radius c and thickness t is subject to an eccentric shear force V acting along the circumference, that is, with $e = c$.

(a) Find the maximum direct shear stress due to the shear force V.

(b) Find the location and magnitude of the maximum shear stress due to the combined effect of the shear force V and the torque Vc.

9.4-9. A thin-walled rectangular tube, with uniform thickness $2t$, is subject to an eccentric shear force V as shown in the figure.

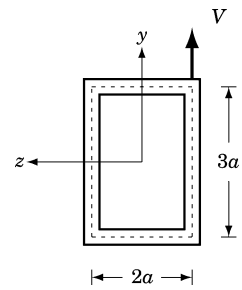

(a) Use the conventional shear formula to find and sketch the distribution of the shear stress τ_{xy} along the y-axis due to the shear force V.

(b) Use the thin-walled approximation to find and sketch the distribution of the shear stress throughout the cross section due to the torque Va.

(c) What is the location and magnitude of the maximum shear stress τ_{xy} due to the combined effect of the shear force V and the torque Va?

9.4-10. A solid bar of square cross-section with sides of length a is subject to an eccentric shear force V as shown in the figure. If it is known that the maximum shear stress due to a torque T is given by $\tau^{\mathrm{t}}_{\max} = 4.81T/a^3$ and acts at the midpoints of the sides, estimate the location and magnitude of the maximum shear stress due to the combined effect of the shear force and the torque.

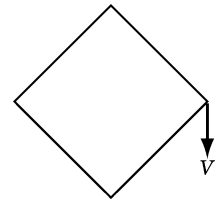
V

Chapter 10

Elastic Stability and Buckling

10.1 Buckling Fundamentals and Simple Models

10.1.1 Introduction

As we already mentioned in Chap. 2, and as is known from everyday experience (for example, compressing a short plastic ruler or the like between thumb and middle finger, as seen in Fig. 10.1), a slender bar subject to a compressive axial force is likely to buckle (that is, assume a bent shape) if the force is sufficiently large. This phenomenon is called *buckling* and will be studied in the present chapter. Buckling is typically undesirable in structural and mechanical systems. Therefore, when designing such systems, an effort is made, wherever relevant, to prevent its occurrence.

Figure 10.1. Simple illustration of buckling: (**a**) before, (**b**) after

The mechanism of buckling can be understood as follows: if a bar carrying an axial force deviates ever so slightly from being straight, then the deviation provides a moment arm for the axial force, generating a bending moment. If the force is tensile, as in Fig. 10.2a, then this moment is opposite to the curvature and tends to straighten the bar, reducing the moment arm. If, how-

© Springer International Publishing Switzerland 2017

J. Lubliner, P. Papadopoulos, *Introduction to Solid Mechanics*,
DOI 10.1007/978-3-319-18878-2_10

Figure 10.2. Effect of axial force on a deflected column: (**a**) tensile, (**b**) compressive

ever, the force is compressive, as in Fig. 10.2b, then the moment increases the deflection and hence the moment arm, resulting in more and more bending. Similar considerations apply if the force is eccentric, that is, not exactly aligned with the neutral axis of the bar.

Even in the ideal case of a perfectly straight bar with a perfectly axial force, a momentary transverse disturbance may occur when the load is in place. The question is then whether the equilibrium of the bar is stable, in which case the bar returns to the initial configuration, or unstable, in which case it buckles. The answer turns out to depend on whether the load is below or above a critical value.

Slender members whose primary function is to transmit a compressive axial force are variously known (depending on their use) as columns, posts, studs or struts. In this chapter we refer to all such members as columns (members that carry both axial compression and transverse loading are accordingly called *beam-columns*.) An analytical theory of the buckling of linearly elastic columns was first developed by Euler in the 18th century. Here we discuss only a linearized version of this theory. But first we will illustrate buckling by means of some simplified models.

10.1.2 Simple Bar-Spring Models

The most essential aspect of buckling is the existence of a critical compressive load that depends on the geometry and the elastic properties of the member (and below which no buckling occurs). This can be studied by means of simple models in which hinged rigid bars (assumed weightless) are supported by simple linear springs, either translational (as in Fig. 10.3a), or rotational (as in Fig. 10.3b), the spring constants being k and $\bar{k}$, respectively. For each kind of spring, a possible deflected configuration is shown in Figs. 10.3a′ and 10.3b′, respectively. In both cases, the spring applies to the bar a *restoring force*, that is, one that tends to bring the bar back to its upright position. The external force is, on the contrary, a *disturbing force*, which tends to upset the

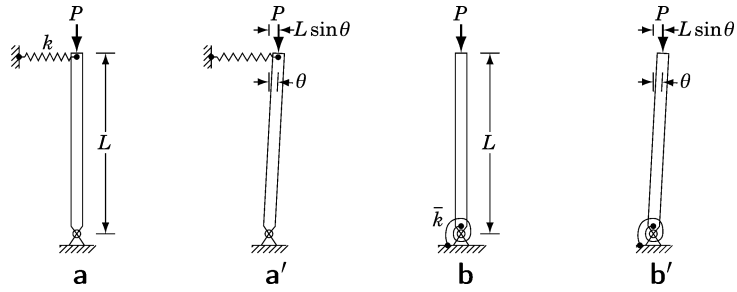

Figure 10.3. Simple bar-spring models of buckling: (**a**) and (**b**) straight configuration; (a′) and (b′) deflected configuration

original equilibrium position. Force equilibrium yields the reactions at the hinge, but these are of no interest, and therefore the only equilibrium equation that needs to be satisfied is that of moment equilibrium about the hinge, since it is assumed that in the straight configuration the line of the action of the applied force goes through the hinge. In the case of the translational spring in Figs. 10.3**a** and 10.3**a**′, we note that the spring rotates (slightly at first) about the fixed pin as the bar deflects, and so the relation between the spring elongation and the bar deflection is nonlinear. However, when the deflection is slight, that is, when $\theta \ll 1$, so that $\sin\theta \doteq \theta$, the spring force is essentially horizontal and its moment arm is essentially L. Consequently, the moment-equilibrium equation about the hinge, subject to the limitation of small θ, is*

$$P(L\theta) = (kL\theta)L \,, \tag{10.1}$$

or

$$(P - kL)\theta = 0 \,. \tag{10.2}$$

This equation can be satisfied in two ways: either $\theta = 0$, in which case P can have any value, or $P = kL$, in which case θ can have any value (as long as it remains small). The latter solution is shown in the P-θ diagram of Fig. 10.4**a**, and kL is seen as the *critical load* P_{cr} below which no buckling can occur.

In the model with the rotational spring, as long the moment-rotation relation of the spring is linear, it is not necessary for the angle θ to be limited to small values. For this case, the moment-equilibrium equation is

$$PL\sin\theta = \bar{k}\theta \,. \tag{10.3}$$

Again, $\theta = 0$ is a solution, and in fact, since $|\sin\theta| < |\theta|$, it is the only possible solution when $P \le \bar{k}/L$. The critical load is thus $P_{\text{cr}} = \bar{k}/L$, since, for $P > \bar{k}/L$, two equal and opposite nonzero values of θ are also possible, as shown in the diagram of Fig. 10.4**b**. This diagram illustrates the phenomenon known as

*Note that throughout this chapter the axial force P will be treated as positive in compression.

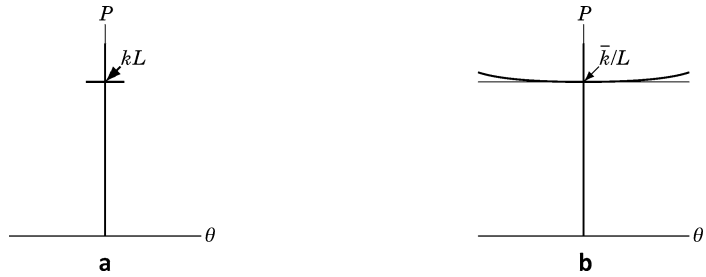

Figure 10.4. Load-deflection (P-θ) diagrams for bar-spring models: (**a**) translational spring, (**b**) rotational spring

bifurcation. Some non-trivial solutions of (10.3) are shown in the following table:

$P/(\bar{k}/L)$	θ (rad)
1.01	±0.244
1.02	±0.344
1.04	±0.483
1.10	±0.749
1.20	±1.027

It is shown in the next section that, for $P > P_{\text{cr}}$, the equilibrium at $\theta = 0$ is *unstable*, while at $\theta \neq 0$ it is *stable*. Eq. (10.3) can, of course, be linearized for small θ, and it then becomes

$$(P - \frac{\bar{k}}{L})\theta \;=\; 0\,. \tag{10.4}$$

This is equivalent in form to Eq. (10.2), so that the equations for both kinds of springs can be written more generally as

$$(P - P_{\text{cr}})\theta \;=\; 0\,. \tag{10.5}$$

10.1.3 Effect of Imperfections: Eccentric Load and Initial Deflection

Eccentric Load

If the axial load in the models of Sect. 10.1.2 is applied with a lateral eccentricity e in the initial (straight) configuration, then in the deflected configuration its moment arm is $L\sin\theta + e\cos\theta$, as can be seen from Fig. 10.5. The linearized equilibrium equation is then, in place of Eq. (10.5),

$$(P - P_{\text{cr}})\theta + P\eta \;=\; 0\,, \tag{10.6}$$

Figure 10.5. Details of the loaded end of an eccentrically loaded bar: (**a**) initial configuration, (**b**) deflected configuration

where $\eta = e/L$. The solution of Eq. (10.6) is

$$\frac{P}{P_{\text{cr}}} = \frac{\theta}{\theta + \eta}\,, \tag{10.7}$$

and is described by the hyperbolas shown in Fig. 10.6a, asymptotic to the line $P = P_{\text{cr}}$. This figure shows that the smaller the value of η, the closer the load must get to the critical value before the deflection becomes significant. The

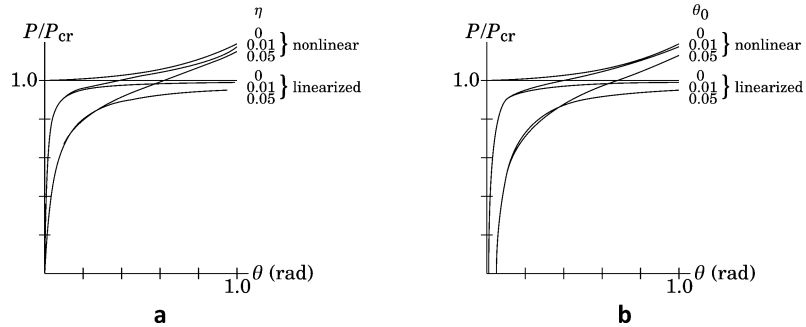

Figure 10.6. Load-deflection (P-θ) diagrams for simple bar-spring models with imperfections: (**a**) eccentric load, (**b**) initial deflection

nonlinear equation for the rotational spring, Eq. (10.3), is similarly replaced by

$$P(L\sin\theta + e\cos\theta) = \bar{k}\theta\,, \tag{10.8}$$

with the solution

$$\frac{P}{P_{\text{cr}}} = \frac{\theta}{\sin\theta + \eta\cos\theta}\,. \tag{10.9}$$

For a given η and for small θ, the curve describing this solution is very close to the hyperbola describing the solution of Eq. (10.6). As θ increases, the corresponding curve is asymptotic to the curve of Fig. 10.4b. In particular, the curve crosses the line $P = P_{\text{cr}}$ at a finite value of θ, which, for $\eta = 0.01$, is (to our customary three-digit precision) 0.383 rad.

Initial Deflection

When the bar has a uniform initial deflection of angle θ_0, then, if θ is still measured from the vertical line as in Fig. 10.3, the resisting moment of the rotational spring is $\bar{k}(\theta-\theta_0)$, while that exerted by the translational spring, when linearized, is $kL^2(\theta-\theta_0)$. For both springs it may therefore be written as $P_{\rm cr}L(\theta-\theta_0)$, where, as before, $P_{\rm cr}=kL$ (or $\bar{k}/L$). The moment equilibrium equation accordingly becomes

$$PL\sin\theta \;=\; P_{\rm cr}L(\theta-\theta_0) \tag{10.10}$$

or, equivalently,

$$\frac{P}{P_{\rm cr}} \;=\; \frac{\theta-\theta_0}{\sin\theta}\;. \tag{10.11}$$

When linearized (which, in this case, requires that both θ_0 and θ be small), the equilibrium equation takes the form

$$\frac{P}{P_{\rm cr}} \;=\; 1-\frac{\theta_0}{\theta}\;. \tag{10.12}$$

Some curves describing Eqs. (10.11) and (10.12), with θ_0 as a parameter, are shown in Fig. 10.6b. Qualitatively, these solutions are quite similar to those of Fig. 10.6a, except, of course, that $P=0$ when $\theta=\theta_0$.

10.1.4 Multi-Bar-Spring Models

While the simple models discussed thus far in this section elucidate the significance of the critical load, with and without linearization, as well as with and without imperfections, they provide no information about the possible buckled shapes of real columns. For example, while the model of Fig. 10.3**b**

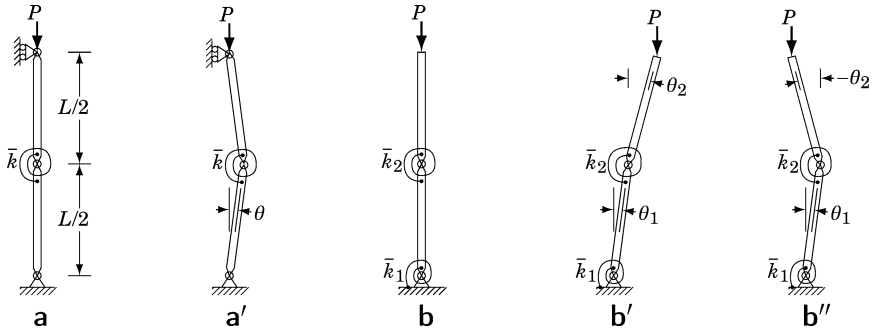

Figure 10.7. Examples of multi-bar-spring models

may be a reasonable, if rough, representation of a free-standing column (the

equivalent of a cantilever beam), a column that is the equivalent of a simply supported beam (usually referred to by the somewhat confusing term "pinned-pinned") is represented much better by the two-bar model of Fig. 10.7a. In the deflected configuration shown in Fig. 10.7a′, it is clear that the total rotation of the spring is 2θ, so that the moment transmitted there is $2\bar{k}\theta$, and moment equilibrium of either the upper or the lower bar requires that this be equal to the external moment $P(L/2)\sin\theta$, or, when linearized, $PL\theta/2$. The critical load is, therefore, $P_{\rm cr} = 4\bar{k}/L$. A model with two or more rotational springs, like the one in Fig. 10.7b, is a multi-degree-of-freedom system. As illustrated in Figs. 10.7b′–b″, the two bars can rotate independently of each other.

Example 10.1.1: Two-bar model of a free-standing column.
We will suppose for simplicity that $\bar{k}_1 = \bar{k}_2 = \bar{k}$. By defining the signs of θ_1 and θ_2 as in Fig. 10.7b′, the configuration of Fig. 10.7b″ is covered as well. The rotation of the upper spring is $\theta_2 - \theta_1$, so that the spring moment acting on the upper bar is $\bar{k}(\theta_2 - \theta_1)$, and the equilibrium of the upper bar requires that this be equal to the external moment (linearized) $P(L/2)\theta_2$. In the lower bar the external moment is $P(L/2)\theta_1$, and it is opposed by both the upper and the lower springs, with moments $\bar{k}(\theta_1 - \theta_2)$ and $\bar{k}(\theta_1)$, respectively. The equilibrium equation for this bar is therefore

$$\bar{k}(2\theta_1 - \theta_2) \;=\; P(L/2)\theta_1 \,, \tag{10.13}$$

while for the upper bar it is

$$\bar{k}(\theta_2 - \theta_1) \;=\; P(L/2)\theta_2 \,. \tag{10.14}$$

Each of these equations can be solved for the ratio θ_2/θ_1, and the requirement that the solutions agree,

$$\frac{\theta_2}{\theta_1} \;=\; 2 - \lambda = \frac{1}{1-\lambda} \,, \tag{10.15}$$

(where $\lambda = PL/2\bar{k}$), leads to the condition

$$(2-\lambda)(1-\lambda) = 1. \tag{10.16}$$

Alternatively, the two equations can be written in matrix form as

$$\begin{bmatrix} 2-\lambda & -1 \\ -1 & 1-\lambda \end{bmatrix} \begin{Bmatrix} \theta_1 \\ \theta_2 \end{Bmatrix} = \begin{Bmatrix} 0 \\ 0 \end{Bmatrix}, \tag{10.17}$$

and this equation constitutes an *eigenvalue problem* similar to the problem of the principal axes of stress (Sect. 4.6) and of the second moment of area (Sect. 9.2). Nonzero values of θ_1 and θ_2 will be possible if and only if the determinant of the square matrix in the last equation is zero, that is, if

$$(2-\lambda)(1-\lambda) - 1 \;=\; 0 \,, \tag{10.18}$$

which is the same as Eq. (10.16). The possible values of λ (the eigenvalues) are the roots of this quadratic equation (known as the *characteristic equation* of the eigenvalue problem), namely $\lambda_1 = 0.382$ and $\lambda_2 = 2.618$; thus the critical load has the possible values $0.764\bar{k}/L$ and $5.236\bar{k}/L$. The corresponding ratios θ_2/θ_1 are 1.618 and −0.618, respectively, represented qualitatively in Figs. 10.7b′ and b″; these are the *buckling modes* (more generally the eigenvectors of the problem).

The preceding example can be generalized to other multi-bar-spring models with several (say n) degrees of freedom. As a rule, each spring adds another degree of freedom, and the eigenvalue problem for an n-degree-of-freedom system leads to an algebraic equation of degree n for the critical load; to each value of this load there corresponds a distinct buckling mode. For practical purposes, of course, all that matters is the lowest value of the critical load, corresponding to the *fundamental mode* of buckling, unless the system can somehow be rigged to prevent buckling in this mode. This notion is explored in connection with the buckling of elastic columns in Sect. 10.3.

Exercises

10.1-1. Verify that, given the definitions of the translational and rotational spring constants, kL and $\bar{k}/L$ have the dimensions of force.

10.1-2. Derive the equilibrium equation for the bar-spring model shown in Fig. 10.3a′ without linearization, assuming that the pin at the left end of the spring remains fixed.

10.1-3. Derive the equilibrium equation for the bar-spring model shown in Fig. 10.3a′ without linearization, assuming that the pin at the left end of the spring is free to move vertically so that the spring remains horizontal.

10.1-4. Calculate values of θ that satisfy Eq. (10.3) for $P/(\bar{k}/L) = 1.05$ and 1.15.

10.1-5. Calculate values of θ that satisfy Eq. (10.9) with $P = P_{\text{cr}}$ for $\eta = 0.02$ and 0.05.

10.1-6. Calculate values of θ that satisfy Eq. (10.11) with $P = P_{\text{cr}}$ for $\theta_0 = 0.02$ and 0.05.

10.1-7. Determine the critical load for the two-bar-spring model in the figure below, assuming that the angles of rotation are small.

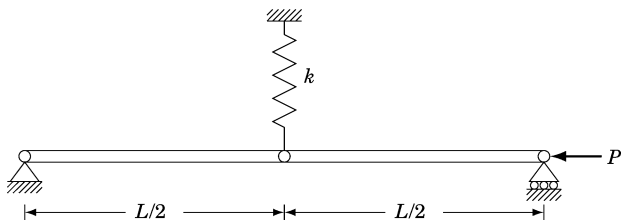

10.1-8. Consider a multi-bar-spring model with the end conditions as in Fig. 10.7a, but consisting of three bars of length $L/3$, with a rotational spring of spring constant $\bar{k}$ at each of the two joints. Find the critical loads and sketch the corresponding buckling modes.

10.1-9. Consider a multi-bar-spring model with the end conditions as in Fig. 10.7b, but consisting of three bars of length $L/3$, with a rotational spring of spring constant $\bar{k}$ at the bottom pin and each of the two joints. Derive the characteristic equation, calculate the critical loads and sketch the corresponding buckling modes.

10.1-10. Consider a multi-bar-spring model with the end conditions as in Fig. 10.7a, but consisting of four bars of length $L/4$, with a rotational spring of spring constant $\bar{k}$ at each of the three joints. Derive the characteristic equation, calculate the critical loads and sketch the corresponding buckling modes.

10.2 Stability and Energy

10.2.1 Introduction

It was already noted in Sects. 3.5 and 6.5 that in a stable equilibrium position the total potential energy attains a minimum. This can be conceptualized with the help of Fig. 10.8, where a rigid round solid subject to gravity rolls on a curved surface and comes to rest at places where the slope of the surface is zero. It is intuitively obvious that only position (a) is stable in the sense that

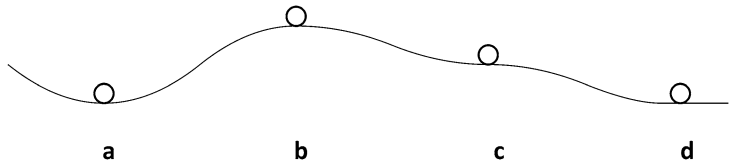

Figure 10.8. Equilibrium positions of a round object on a curved surface

moving the solid away from it to a nearby position on the surface requires work done by an external agency; the others are unstable (b), semistable (c) and neutral (d) see Exercise **10.2-1**. This can be explained physically by examining the total potential energy Π of the solid (which, here, equals the gravitational potential energy defined, to within an additive constant, by the weight times the height with respect to an arbitrary datum). The function Π is *stationary* whenever its derivative with respect to vertical displacement is zero, and is a minimum only if its *second* derivative is positive, which is the case in position (a). This, in turn, means that any neighboring positions have a higher potential energy, and so work must be done to achieve it. Thus, if q is a generalized coordinate in a conservative one-degree-of-freedom system, then the necessary and sufficient condition for stable equilibrium is

$$\frac{d\Pi}{dq} = 0 \quad , \quad \frac{d^2\Pi}{dq^2} > 0 \, . \tag{10.19}$$

10.2.2 Stability of a Simple Bar-Spring Model

As discussed in Sect. 6.5, the elastic energy of a simple rotational spring is $\frac{1}{2}\bar{k}\theta^2$, while that of the translational spring of Fig. 10.3a, when linearized, is $\frac{1}{2}k(L\theta)^2$. Following the discussion in Sect. 10.1, this can be expressed, in the present case, as $U = \frac{1}{2}P_{\text{cr}}L\theta^2$ for both kinds of spring.

For the potential energy of the load we have $V = -P\Delta$, where Δ is the displacement conjugate to the load, that is—if P acts downward—the downward displacement of the point of application of the load, given by $\Delta = L(1-\cos\theta)$.

Consequently, the total potential energy $\Pi(= U + V)$ is given by

$$\Pi = \left[\frac{1}{2}P_{\text{cr}}\theta^2 - P(1-\cos\theta)\right]L \,. \tag{10.20}$$

For equilibrium we have

$$\frac{d\Pi}{d\theta} = (P_{\text{cr}}\theta - P\sin\theta)L = 0 \,, \tag{10.21}$$

which is equivalent to Eq. (10.3). To check for stability, we determine the second derivative, which is

$$\frac{d^2\Pi}{d\theta^2} = (P_{\text{cr}} - P\cos\theta)L \,. \tag{10.22}$$

At $\theta = 0$ this is clearly positive (stable equilibrium) when $P < P_{\text{cr}}$ and negative (unstable equilibrium) when $P > P_{\text{cr}}$. At the nonzero values of θ that satisfy Eq. (10.21), the value of the second derivative is $P_{\text{cr}}L[1-(\theta/\tan\theta)]$. Since the ratio $\theta/\tan\theta$ is algebraically less than 1 for all nonzero values of θ, the second derivative is positive, so that the equilibrium at the deflected positions is stable, as we indicated in Sect. 10.1.

10.2.3 Stability in Multi-Degree-of-Freedom Systems

As shown in Sect. 6.5, in a conservative system with n degrees of freedom described by the generalized coordinates q_i $(i = 1,\ldots,n)$, a necessary condition for equilibrium is given by Eqs. (6.144), which will be rewritten here (in terms of the q_i) as

$$\frac{\partial\Pi}{\partial q_i} = 0, \quad i = 1,\ldots,n \,. \tag{10.23}$$

These can be further rewritten by introducing the generalized virtual displacements δq_i and defining the *first variation* of Π as

$$\delta\Pi = \sum_{i=1}^{n}\frac{\partial\Pi}{\partial q_i}\delta q_i \,, \tag{10.24}$$

so that we can restate the equations in (10.23) as

$$\delta\Pi = 0 \,, \tag{10.25}$$

where it is understood that Eq. eqrefeq:dePi holds for *any* combination of δq_i. If we now consider a specific point $(q_1,\ldots,q_n)$ in the space of the generalized coordinates, by Taylor's theorem we have

$$\Pi(q_1+\delta q_1,\ldots,q_n+\delta q_n) - \Pi(q_1,\ldots,q_n) = \delta\Pi + \frac{1}{2}\sum_{i=1}^{n}\sum_{j=1}^{n}\frac{\partial^2\Pi}{\partial q_i\partial q_j}\delta q_i\delta q_j + \ldots \,. \tag{10.26}$$

The double sum on the right-hand side of this equation (without the factor $\frac{1}{2}$) is called the *second variation* of Π and is denoted $\delta^2\Pi$. In view of the preceding discussion of the requirement that the potential energy attain a minimum for stable equilibrium—that is, that *any* change of configuration requires positive work—it follows that the necessary and sufficient conditions for stable equilibrium in a multi-degree-of-freedom system are Eq. (10.25) and

$$\delta^2\Pi > 0 , \tag{10.27}$$

where it is understood, once again, that the inequality holds for all combinations of δq_i. This can be expressed in mathematical language by saying that $\delta^2\Pi$ constitutes a *positive-definite quadratic form*, or equivalently that the square matrix composed of the second partial derivatives $\partial^2\Pi/\partial q_i \partial q_j$ (evaluated at the equilibrium values of the q_i) is a *positive-definite matrix*. A necessary and sufficient condition for this is that all the eigenvalues of the matrix are positive.

Example 10.2.1: Stability of the two-bar model of Example 10.1.1. In the model shown in the deflected configuration in Fig. 10.7b′, with $\bar{k}_1 = \bar{k}_2 = \bar{k}$,the elastic energy of the springs is just

$$U = \frac{\bar{k}}{2}[\theta_1^2 + (\theta_2 - \theta_1)^2] .$$

The downward displacement of the load is $L - (L/2)\cos\theta_1 - (L/2)\cos\theta_2$, which can be approximated for small angles as $(L/4)(\theta_1^2 + \theta_2^2)$. Using the previously introduced parameter $\lambda = PL/2\bar{k}$, we can write the potential energy as

$$\Pi(\theta_1, \theta_2) = \frac{\bar{k}}{2}[(2-\lambda)\theta_1^2 - 2\theta_1\theta_2 + (1-\lambda)\theta_2^2] .$$

The matrix of second partial derivatives is (to within the factor $\bar{k}$) just the one seen in Example 10.1.1, and its determinant is positive for $\lambda < 0.382$ and $\lambda > 2.618$. In the latter case, however, the diagonal elements $2-\lambda$ and $1-\lambda$ are negative, so that the equilibrium is stable only for $\lambda < 0.382$. It is consequently only the lower critical load that constitutes the limit of stability.

10.2.4 Another Minimum Principle: Rayleigh's Method

Since $\Pi = U - P\Delta$, Eq. (10.25) can be written as

$$\delta U - P\delta\Delta = 0 , \tag{10.28}$$

where both U and Δ are functions of the generalized coordinates $(q_1, \ldots, q_n)$. Now consider the quotient $R = U/\Delta$ (a special case of what is known in mathematics as the *Rayleigh quotient*[*]). If we seek its minimum value, for which

[*]John William Strutt, 3rd Baron Rayleigh (1842–1919) was a British physicist (Fig. 10.9).

Figure 10.9. Lord Rayleigh

a necessary condition is

$$\delta R = 0 , \tag{10.29}$$

we may use the chain rule to express Eq. (10.29) as

$$\frac{1}{\Delta}\left(\delta U - \frac{U}{\Delta}\delta\Delta\right) = 0 , \tag{10.30}$$

which, when multiplied by Δ, can be written as

$$\delta U - R\delta\Delta = 0 . \tag{10.31}$$

It can be seen that Eq. (10.31) is the same as Eq. (10.28) when we identify the minimum value of R with the smallest value of P for which the latter equation has a solution, that is, the critical load P_{cr}. Consequently, another definition of the critical load is

$$P_{\text{cr}} = \left(\frac{U}{\Delta}\right)_{\text{min}} , \tag{10.32}$$

the minimum being taken over all possible values of the generalized coordinates. Like other minimum principles, the one embodied in Eq. (10.32) can be used to find approximate solutions, as will be shown in the following example. The procedure is known as *Rayleigh's method*.

Example 10.2.2: Approximate critical loads for the model of Example 10.1.1. If, instead of solving the problem as in Example 10.1.1, we *assume* a deflected shape and calculate the corresponding U/Δ, we should, in view of Eq. (10.32), get an approximation *from above* to P_{cr}. If we suppose, for example, that $\theta_2 = 2\theta_1$, then (with the factors of $\frac{1}{2}$ omitted in both numerator and denominator)

$$R = \frac{\bar{k}[\theta_1^2 + (2\theta_1 - \theta_1)^2]}{L[\theta_1^2 + (2\theta_1)^2]} = 0.4\frac{\bar{k}}{L} .$$

With $\theta_2 = 1.5\theta_1$, we have

$$R = \frac{\bar{k}[\theta_1^2 + (1.5\theta_1 - \theta_1)^2]}{L[\theta_1^2 + (1.5\theta_1)^2]} = 0.385\frac{\bar{k}}{L} .$$

Both results are greater than the exact value of $0.382\bar{k}/L$, but not by much.

Exercises

10.2-1. Using Fig. 10.8, propose definitions of unstable, semistable and neutral equilibrium.

10.2-2. Suppose that the fixed pin supporting the spring in Fig. 10.3a is replaced by one that can slide vertically along the wall, so that the spring remains horizontal. Determine the possible equilibrium positions (without linearizing the equations) and check their stability.

10.2-3. Consider the simple chain of Fig. 3.33 (page 142), with the link lengths (as defined on page 143) $l_{01} = 3L/4$, $l_{12} = l_{23} = L/2$ (L being the span), and subject to the downward forces $F_1 = 2F$ and $F_2 = F$. Find the equilibrium configurations, and show that the "arch" and "cable" configurations of Fig. 3.36 (page 145) are unstable and stable, respectively.

10.2-4. Following Example 10.2.1, examine the stability of the buckling modes of the three-bar model described in Exercise **10.1-8**.

10.2-5. In Example 10.2.2, use trial and error to determine a value of θ_2/θ_1 for which Rayleigh's quotient R agrees with the result of Example 10.1.1 to three significant figures.

10.2-6. Use Rayleigh's method to find an approximation to the critical load of the two-bar model of Fig. 10.7b.

10.2-7. Use Rayleigh's method to find an approximation to the critical load of the four-bar model described in Exercise **10.1-10**, assuming the fundamental buckling mode to be symmetric.

10.3 Buckling of Elastic Columns

10.3.1 Bending with an Axial Force

When a bent column is subjected to an axial force P, the deflection (as we discussed at the beginning of the chapter) provides a moment arm for the axial force, in the same way as for the bar-spring models of Sect. 10.1. In applying the method of sections, then, we must consider the equilibrium state in which the deflection of the column included explicitly, as in Fig. 10.10, rather than the undeformed equilibrium state depicted in Fig. 8.1b (page 354). When the deflection of the column is taken into account, we see that, in

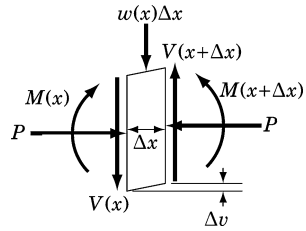

Figure 10.10. Forces and moments on section $(x, x+\Delta x)$ in the presence of bending and axial force

addition to the moments considered in Sect. 8.1, there is also a moment $P\Delta v$ due to the force couple formed by the compressive forces acting on the two cross sections at x and $x+\Delta x$ that must be added to the moment-equilibrium equation. As a result, this equation now becomes

$$\frac{dM}{dx} + P\frac{dv}{dx} + V(x) = 0\,, \tag{10.33}$$

in place of Eq. (8.5) (note that we continue this chapter's convention of treating P as positive in compression). Since the transverse force equilibrium is unaffected by the axial force, Eqs. (8.2) and (10.33) constitute the equilibrium equations of what is often called a *beam-column*.

If the axial load varies, then Eq. (6.86) must be added as well. This would happen if, for example, a vertical column's own weight contributed significantly to the axial load. For slender columns this is rarely the case.

If a column is linearly elastic, then (as we found in Sect. 9.4) the moment-curvature relation holds independently of the presence of an axial force. Consequently, this is also true of the moment-deflection relation, Eq. (8.75). Combining this equation with Eqs. (10.33) and (8.2) leads, if the axial force P is constant, to the beam-column deflection equation

$$\frac{d^2}{dx^2}\left(EI\frac{d^2v}{dx^2}\right) + P\frac{d^2v}{dx^2} = -w(x)\,, \tag{10.34}$$

or, for a prismatic homogeneous beam-column,

$$EI\frac{d^4v}{dx^4}+P\frac{d^2v}{dx^2} \;=\; -w(x)\,. \tag{10.35}$$

This is a fourth-order equation for the deflection v, just like (8.83) (page 392), and requires four boundary conditions to be satisfied. It should be noted that the condition of zero shear at a free end must be expressed, in view of Eq. (10.33), as $EIv''' + Pv' = 0$ rather than simply $v''' = 0$. Aside from this, the boundary conditions are the same as those of Eq. (8.84) (page 392). An example will now be considered.

Example 10.3.1: Simply supported beam-column under uniformly distributed transverse loading and an axial load.
Setting the right-hand side of Eq. (10.35) equal to $-w_0$, we find that a particular solution of the equation is $v_p(x) = w_0x^2/2P$. To obtain the general solution we add to it the general solution of the *homogeneous* equation obtained by setting the right-hand side equal to zero, that is, $EIv'''' + Pv'' = 0$. Possible solutions of this equation are: (i) a constant, (ii) a constant times x, and (iii)–(iv) a constant times $\cos(\lambda x)$ or $\sin(\lambda x)$, where $\lambda = \sqrt{P/EI}$. Since these functions are linearly independent of one another, we know from the theory of ordinary differential equations that the general solution of the homogeneous equation is an arbitrary linear combination of these functions. The general solution of Eq. (10.35) with $w(x) = w_0$ is therefore

$$v(x) \;=\; -w_0\frac{x^2}{2P}+C_1+C_2x+C_3\sin(\lambda x)+C_4\cos(\lambda x)\,, \tag{10.36}$$

where $C_1,\ldots,C_4$ are constants to be determined by the end conditions. The conditions $v(0) = 0$ and $v''(0) = 0$ lead to $C_1 + C_4 = 0$ and $-w_0/P - \lambda^2C_4 = 0$, so that $C_1 = -C_4 = w_0/\lambda^2P$. The conditions $v(L) = 0$ and $v''(L) = 0$ produce, after some manipulation, $C_2 = w_0L/2P$ and $C_3 = -(w_0/2P)[1-\cos(\lambda L)]/\sin(\lambda L)$. It can be shown, however, that

$$\frac{1-\cos(\lambda L)}{\sin(\lambda L)} \;=\; \frac{\sin(\lambda L/2)}{\cos(\lambda L/2)}\,, \tag{10.37}$$

and, with the help of other trigonometric identities, the deflection can be expressed as

$$v(x) \;=\; \frac{w_0}{\lambda^2P}\left[\frac{\lambda^2}{2}x(L-x)+1-\frac{\cos[\lambda(x-L/2)]}{\cos(\lambda L/2)}\right]\,, \tag{10.38}$$

a form that clearly exhibits the vanishing of the deflection at $x = 0$ and $x = L$ and its symmetry about $x = L/2$. The maximum (midpoint) deflection, $v_{\max} = |v(L/2)|$, is given by

$$v_{\max} \;=\; \frac{w_0}{\lambda^2P}\left[\sec(\lambda L/2)-1-\frac{(\lambda L/2)^2}{2}\right]\,. \tag{10.39}$$

The power-series expansion of the secant function is $\sec u = 1+u^2/2+5u^4/24\ldots...$, so that for small values of $\lambda L/2$ we can write

$$v_{\max} \;\doteq\; \frac{w_0}{\lambda^2P}\cdot\frac{5(\lambda L/2)^4}{24}\,, \tag{10.40}$$

which, in view of the definition of λ, can be rewritten as $5w_0L^4/384EI$ and denoted $v_{0\max}$; it is just the maximum deflection of a uniformly loaded simply supported beam, as derived in Example 8.4.1 (page 391). The maximum deflection can now be written in the form

$$\frac{v_{\max}}{v_{0\max}} = \frac{24}{5(\lambda L/2)^4}\left[\sec(\lambda L/2) - 1 - \frac{(\lambda L/2)^2}{2}\right]. \tag{10.41}$$

The most striking feature of the quantity in brackets is that it goes to infinity as $\lambda L \to \pi$, since $\sec(\pi/2) = \infty$. This corresponds to $P = \pi^2 EI/L^2$, and, by analogy with the results for the linearized bar-spring model with initial deflection (Fig. 10.6b), this value of P may be regarded as the critical load P_{cr}. The corresponding plot of P/P_{cr} against $v_{\max}/v_{0\max}$ is shown in Fig. 10.11.

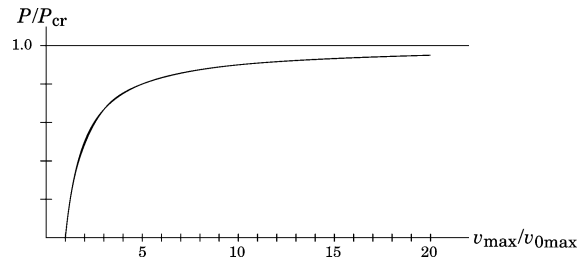

Figure 10.11. Load-deflection curves for a simply supported beam-column

The calculations of the preceding example would have been much simpler if the loading, rather than uniform, had been taken in the sinusoidal form $w(x) = w_0 \sin(\pi x/L)$. This is because the deflection could then have been assumed in the form $v(x) = -v_{\max}\sin(\pi x/L)$, which satisfies all the boundary conditions and which, when inserted in Eq. (10.35), leads (with the definition $v_{0\max} = w_0L^4/\pi^4 EI$) to the hyperbola defined by

$$\frac{P}{P_{\text{cr}}} = 1 - \frac{v_{0\max}}{v_{\max}}. \tag{10.42}$$

This has exactly the same form as Eq. (10.12) (page 446) for the linearized bar-spring model with initial deflection, and is also shown in Fig. 10.11. Note that the two curves are practically indistinguishable.

Initially Curved Column

As we pointed out in Sect. 8.4.5 (page 399), the effect of an initial deflection v_0 is equivalent to that of a transverse loading $-EIv_0''''$, except that in boundary conditions involving moments $v'' - v_0''$ must be used. The insensitivity of the load-deflection relation to the precise nature of the transverse loading means that a similar simplifying assumption can be made for the case of an initially deflected column. If, for a simply supported prismatic column, the

initial deflection is assumed as $v_0(x) = v_{0\max}\sin(\pi x/L)$, this is equivalent to a transverse loading given by

$$w(x) \;=\; -EI(\pi/L)^4 v_{0\max}\sin(\pi x/L)\,, \tag{10.43}$$

with exactly the same load-deflection relation as above.

10.3.2 The Euler Load

If we now wish to treat the problem of a column under a compressive axial load as a buckling problem, then we must find nonzero solutions P of Eq. (10.34) or (for a prismatic column) (10.35) with $w(x) = 0$. For a prismatic

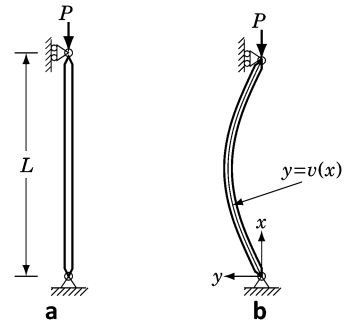

Figure 10.12. Simply supported column: (**a**) before buckling, (**b**) after buckling

simply supported column, as shown in Fig. 10.12 (the continuum analogue of Fig. 10.7a–a′), we have already found the general solution in Example 10.3.1, namely,

$$v(x) \;=\; C_1 + C_2 x + C_3\sin(\lambda x) + C_4\cos(\lambda x)\,, \tag{10.44}$$

where the constants $C_1,\ldots,C_4$, in order to satisfy the boundary conditions $v(0) = v(L) = v''(0) = v''(L) = 0$, must obey the equations

$$\begin{aligned} C_1 + C_4 &= 0\,,\\ C_1 + C_2 L + C_3\sin(\lambda L) + C_4\cos(\lambda L) &= 0\,,\\ -\lambda^2 C_4 &= 0\,,\\ -\lambda^2[C_3\sin(\lambda L) + C_4\cos(\lambda L)] &= 0\,. \end{aligned} \tag{10.45}$$

For any $\lambda \neq 0$, it follows from Eqs. $(10.45)_1$ and $(10.45)_3$ that $C_1 = C_4 = 0$, and when $(10.45)_4$ is combined with $(10.45)_2$, it follows further that $C_2 = 0$. The only remaining constant is C_3, and it obeys the condition

$$C_3\sin(\lambda L) \;=\; 0\,. \tag{10.46}$$

This equation can be satisfied either if $C_3 = 0$, in which case there is no deflection, or else if $\sin(\lambda L) = 0$, which is possible only if $\lambda = n\pi/L$, with

$n = 1, 2, \ldots$. Since, by definition, $\lambda = \sqrt{P/EI}$, P must have one of the values $P_n = n^2\pi^2 EI/L^2$, and the corresponding deflection is given by

$$v(x) = C_3 \sin \frac{n\pi x}{L} , \tag{10.47}$$

with C_3 undetermined. For each n, the deflection given by Eq. (10.47) describes the *buckling mode* corresponding to the buckling load P_n. However, just as in the case of the previously considered multi-bar-spring models, the undeflected configuration is in stable equilibrium only for $P < P_1$, so that P_1 is the critical load $P_{\text{cr}} = \pi^2 EI/L^2$, as was already found in Example 10.3.1. It is commonly known as the *Euler load* and denoted P_E.

While the presence of a transverse load or an initial deflection predetermines the plane of the additional deflection, an initially straight column, unless it is somehow constrained to buckle in a particular plane, may do so in any plane containing its axis. In keeping with the *principle of least resistance*[*], then, the column will buckle in the plane corresponding to the smallest critical load (if there is such a unique plane), and that load is determined by the smallest principal second moment of area. The buckling is then said to be about the *weak axis*. It is this value of I that will henceforth be implied when the Euler load is defined for a simply supported column as

$$P_E = \frac{\pi^2 EI}{L^2} . \tag{10.48}$$

Example 10.3.2: Calculation of the Euler load.
We consider a 12-ft steel column made of a W12×50 section, for which the second moment of area about the weak axis is 56.3 in^4. The Euler load is accordingly

$$P_E = \frac{\pi^2 \times 29 \times 10^3 \,\text{kip}\cdot\text{in}^{-2} \times 56.3\,\text{in}^4}{(12\times 12)^2\,\text{in}^2} = 777\,\text{kip} .$$

According to the same principle of least resistance, if the column can fail by some mechanism other than buckling, it will do so if the load required for such failure is less than the buckling load. Suppose, for example, that a compressive stress σ_{f} provokes crushing of the material; if this stress occurs when the column is straight, then the load that will crush the column is $P_c = \sigma_{\text{f}} A$ (where A is the cross-section area), and, if $P_c < P_E$, then crushing takes place before buckling. This last inequality can be written as

$$\sigma_{\text{f}} < \pi^2 E \frac{I}{L^2 A} \tag{10.49}$$

or, in terms of the *slenderness ratio* L/r defined in Sect. 9.3 (page 423),

$$(L/r) < \pi\sqrt{E/\sigma_{\text{f}}} = (L/r)_{\text{cr}} . \tag{10.50}$$

[*]First formulated by the English scientist Henry Moseley (1802–1872), whose namesake son (1844–1891) and grandson (1887–1915) were also prominent scientists. A special case of this principle, applicable to systems in series, is known as the *principle of the weakest link*.

The right-hand side of Eq. (10.50) defines the *critical slenderness ratio* and thus differentiating between "short" or "stubby" columns and "long" or "slender" ones. If the *critical stress* is defined as $\sigma_{\rm cr} = \min(\sigma_{\rm f}, P_E/A)$, then it can be plotted against the slenderness ratio, as in Fig. 10.13; the resulting plot (made up of the heavy line and curve) is often called a *column curve*.

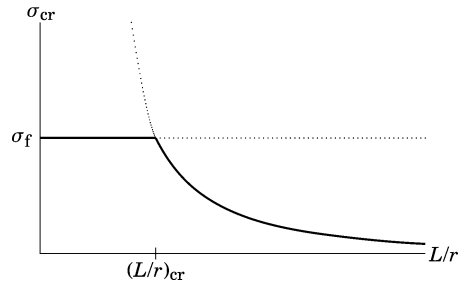

Figure 10.13. Column curve (critical stress against slenderness ratio): simple case

Eqs. (10.45) for the coefficients $C_1, \ldots, C_4$ can be written in matrix form as

$$\begin{bmatrix} 1 & 0 & 0 & 1 \\ 1 & L & \sin(\lambda L) & \cos(\lambda L) \\ -\lambda^2 & 0 & 0 & 0 \\ 0 & 0 & -\lambda^2 \sin(\lambda L) & -\lambda^2 \cos(\lambda L) \end{bmatrix} \begin{Bmatrix} C_1 \\ C_2 \\ C_3 \\ C_4 \end{Bmatrix} = \begin{Bmatrix} 0 \\ 0 \\ 0 \\ 0 \end{Bmatrix} . \tag{10.51}$$

As in the eigenvalue problems encountered before, most recently in Sect. 10.1, what we need here is to find non-trivial solutions to Eq. (10.51), meaning that the determinant of the square matrix must be zero. Since the determinant equals $\lambda^4 L \sin(\lambda L)$, it follows that the values of λL that allow such solutions are the roots of $\sin(\lambda L) = 0$, as we found above. The difference between this case and those encountered previously is that the characteristic equation is now a transcendental equation and not, as for the finite-degree-of-freedom systems in Sect. 10.1, an algebraic one. The number of eigenvalues (and possible buckling modes) is thus infinite, but, as we discussed earlier, what interests us here is primarily the lowest eigenvalue and the corresponding fundamental buckling mode.

10.3.3 Columns with Different End Conditions

When columns with end conditions other than simply supported are considered, the lowest eigenvalue $\lambda_1 L$ provides the critical load by the relation

$$P_{\rm cr} = \frac{(\lambda_1 L)^2 EI}{L^2} . \tag{10.52}$$

However, it is common to use the Euler-load formula (10.48), with L replaced by the length of the simply supported column having the same critical load.

This length is called the *effective length* and is denoted L_e, so that

$$P_{\text{cr}} = \frac{\pi^2 EI}{L_e^2} . \tag{10.53}$$

It follows from Eqs. (10.52) and (10.53) that

$$\frac{L_e}{L} = \frac{\pi}{\lambda_1 L} . \tag{10.54}$$

Fixed-Free (Cantilever) Column

For a column that is fixed at $x = 0$ and free at $x = L$, the boundary conditions are

$$v(0) = 0 \quad , \quad v'(0) = 0 \quad , \quad v''(L) = 0 \quad , \quad v'''(L) + \lambda^2 v'(L) = 0 , \tag{10.55}$$

the last equation representing zero shear as derived from Eq. (10.33). With the solution assumed in the form (10.44), the equations for the coefficients $C_1, \ldots, C_4$ are written in matrix form as

$$\begin{bmatrix} 1 & 0 & 0 & 1 \\ 0 & 1 & \lambda & 0 \\ 0 & 0 & -\lambda^2 \sin(\lambda L) & -\lambda^2 \cos(\lambda L) \\ 0 & \lambda^2 & 0 & 0 \end{bmatrix} \begin{Bmatrix} C_1 \\ C_2 \\ C_3 \\ C_4 \end{Bmatrix} = \begin{Bmatrix} 0 \\ 0 \\ 0 \\ 0 \end{Bmatrix} . \tag{10.56}$$

We readily see from (10.56) that $C_2 = C_3 = 0$, $C_1 = -C_4$ and $C_4 \cos(\lambda L) = 0$. The last equation has the non-trivial solution $\lambda_n L = (2n-1)\pi/2$, $n = 1, 2, \ldots$, so that $\lambda_1 L = \pi/2$. Alternatively, the determinant of the square matrix in (10.56) is $-\lambda^5 \cos(\lambda L)$, and the eigenvalues are accordingly $\lambda_n L = (2n-1)\pi/2$, $n = 1, 2, \ldots$. Either way, we conclude that

$$P_{\text{cr}} = \frac{\pi^2 EI}{4L^2} , \tag{10.57}$$

and, in view of Eq. (10.54), that $L_e = 2L$. This result may also be deduced intuitively from Fig. 10.14a: the buckled shape assumed by the column, along with its reflection, forms the shape assumed by a simply supported column of length $2L$.

Fixed-Pinned Column

If the column is fixed at $x = 0$ and pinned at $x = L$, the end conditions are

$$v(0) = 0 \quad , \quad v'(0) = 0 \quad , \quad v(L) = 0 \quad , \quad v''(L) = 0 , \tag{10.58}$$

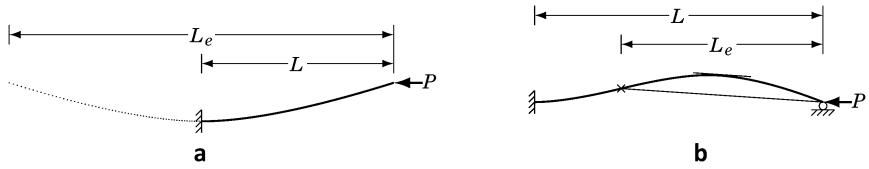

Figure 10.14. Fundamental buckling mode and effective length: (**a**) fixed-free, (**b**) fixed-pinned

giving rise to a system of equations written in matrix form as

$$\begin{bmatrix} 1 & 0 & 0 & 1 \\ 0 & 1 & \lambda & 0 \\ 1 & L & \sin(\lambda L) & \cos(\lambda L) \\ 0 & 0 & -\lambda^2 \sin(\lambda L) & -\lambda^2 \cos(\lambda L) \end{bmatrix} \begin{Bmatrix} C_1 \\ C_2 \\ C_3 \\ C_4 \end{Bmatrix} = \begin{Bmatrix} 0 \\ 0 \\ 0 \\ 0 \end{Bmatrix}. \tag{10.59}$$

When Eqs. (10.59)$_{1,2,4}$ are used to express all the unknowns in Eq. (10.59)$_3$ in terms of C_3, this last equation takes (for $C_3 \neq 0$) the form $C_3(\tan(\lambda L - \lambda L) = 0$, which is satisfied by values of λL obeying

$$\lambda L \;=\; \tan(\lambda L)\,. \tag{10.60}$$

The same result can be obtained by considering the characteristic equation

$$\begin{vmatrix} 1 & 0 & 0 & 1 \\ 0 & 1 & \lambda & 0 \\ 1 & L & \sin(\lambda L) & \cos(\lambda L) \\ 0 & 0 & -\lambda^2 \sin(\lambda L) & -\lambda^2 \cos(\lambda L) \end{vmatrix} = \lambda^2[\sin(\lambda L) - \lambda L \cos(\lambda L)] \;=\; 0\,. \tag{10.61}$$

The roots of Eq. (10.60) can be found graphically, by trial and error with a calculator, or by using a computer program, and the smallest positive one is 4.49, corresponding to an effective length, by Eq. (10.54), of $L_e = 0.699L$. The deflected shape for the fundamental buckling mode of a fixed-pinned column is shown in Fig. 10.14b, and it is clear that the portion between the pinned end and the inflection point (that is, the point where $v'' = 0$, marked by $\times$) at $x = 0.301L$ bends like a simply supported column. (The fact that is slanted with respect to the original axis is immaterial.)

Fixed-Fixed Column

A column that is absolutely fixed at both ends would, in principle, not be able to buckle. When speaking of the buckling of a fixed-fixed column, then, we usually consider two possibilities. In either case, the ends do not rotate. But in one case at least one of the ends can move longitudinally (along the axis) toward the other, while in the other the ends can also displace laterally (a

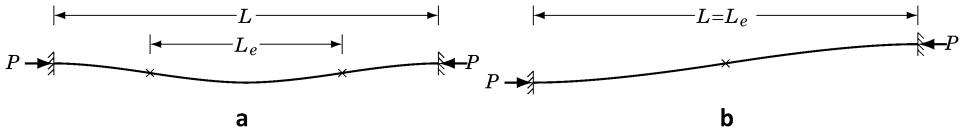

Figure 10.15. Fundamental buckling mode and effective length for a fixed-fixed column: (**a**) without sidesway, (**b**) with sidesway

movement known as *sidesway*). The corresponding buckling shapes in the fundamental mode can be drawn intuitively as in Fig. 10.15, though this figure does not show the longitudinal movement of the ends; a more accurate illustration, for the case of Fig. 10.15a, is that given in Exercise **10.3-8** (page 470). The column without sidesway, shown in Fig. 10.15a, takes the shape of a whole cosine wave, and that the portion between the inflection points, occupying half the wavelength, bends like a simply supported column, so that $L_e = L/2$. With sidesway allowed, on the other hand, as in Fig. 10.15b, each half buckles—like a cantilever—into a quarter wave, so that the length of the column is half a wavelength, and therefore $L_e = L$. These observations may be confirmed analytically by enforcing suitable boundary conditions to the general solution of Eq. (10.34).

10.3.4 Eccentric Load

Let us suppose, next, that the line of action of P is at a distance e from the axis of the column (assumed simply supported). As we can see from the free-body diagram in Fig. 10.16a, the only equilibrium equation to be satisfied, in the absence of any transverse force, is the moment equilibrium equation

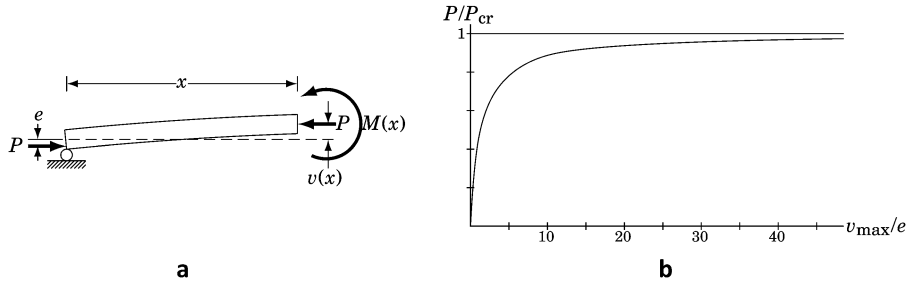

Figure 10.16. Eccentrically loaded simply supported column: (**a**) free-body diagram, (**b**) load-deflection curve

$$M(x) + P[e + v(x)] = 0 \,. \tag{10.62}$$

In view of Eq. (8.75), the deflection $v(x)$ satisfies the differential equation

$$EI\frac{d^2v}{dx^2} + P(v + e) = 0 \,, \tag{10.63}$$

whose general solution is

$$v(x) \;=\; -e + C_1 \sin(\lambda x) + C_2 \cos(\lambda x)\,. \tag{10.64}$$

In order to satisfy the end conditions $v(0) = v(L) = 0$, the coefficients in (10.64) are

$$C_1 \;=\; e\frac{1-\cos(\lambda L)}{\sin(\lambda L)} \;=\; e\frac{\sin(\lambda L/2)}{\cos(\lambda L/2)} \quad , \quad C_2 \;=\; e\,, \tag{10.65}$$

and, with the help of trigonometric transformations similar to those used in Example 10.3.1, the deflection may be written as

$$v(x) \;=\; e\left(\frac{\cos[\lambda(x-L/2)]}{\cos(\lambda L/2)} - 1\right)\,. \tag{10.66}$$

The maximum (midpoint) deflection is thus given by

$$v_{\max} \;=\; v(L/2) \;=\; e[\sec(\lambda L/2) - 1]\,, \tag{10.67}$$

an equation known as the *secant formula*. The corresponding graph of $P/P_{\rm cr}$ against $v_{\max}/e$ is shown in Fig. 10.16b. Note that it resembles the linearized graphs of Fig. 10.6a (page 445).

10.3.5 Practical Column Curves

The theoretical column curve shown in Fig. 10.13, consisting of a horizontal straight line for short columns (representing material failure) and the "Euler hyperbola" (representing elastic buckling) for long columns, is usually replaced in engineering practice by one which recognizes that the two failure criteria are not always sharply separated. A typical example is shown in Fig. 10.17. (Note that the abscissa is the *effective* slenderness ratio.) Here, an in-

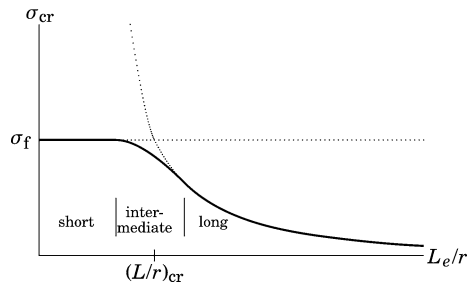

Figure 10.17. Typical column curve (critical stress against effective slenderness ratio)

termediate class of columns is shown, in which the two criteria may interact. For example, in a metal column that has residual stresses from the manufacturing process, some fibers may be subject to material failure, while other remain elastic. Consequently, a smooth transition between the two extremes

is introduced. Various engineering or manufacturing organizations have their own column curves, or formulas from which such curves can be generated. It is also common for such formulas to incorporate a safety factor (which may be different in different ranges), in which case the abscissa is the allowable stress rather than the critical stress.

10.3.6 Approximations by Rayleigh's Method

Rayleigh's method, discussed in the preceding section, can be used not only for systems with a finite number of degrees of freedom, as in Sect. 10.2.4, but also for continua (such as elastic columns). In the latter case we use $U = U_b$, as given by Eq. (8.66) (page 386), that is,

$$U = \frac{1}{2}\int_0^L EIv''^2\,dx\,. \tag{10.68}$$

For the displacement Δ of the axial load, we assume that the shortening of the fibers due to the direct effect of the compressive stress is negligible, so that, as the column buckles, the arc length of the neutral fibers remains L, and therefore

$$\Delta = L - \int_0^L \frac{dx}{ds}\,ds\,, \tag{10.69}$$

as illustrated in Fig. 10.18. Now $ds = \sqrt{(dx)^2 + (dv)^2}$, so that $dx =$

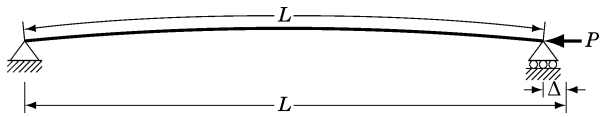

Figure 10.18. Axial-load displacement in a buckled column

$\sqrt{1-(dv/ds)^2}\,ds$. If $|v'|$ is small, then $dv/ds \doteq v'$, and the square root in the expression for dx can be replaced by $1 - \frac{1}{2}v'^2$. Consequently,

$$\Delta = L - \int_0^L \left(1 - \frac{v'^2}{2}\right)dx = \frac{1}{2}\int_0^L v'^2\,dx\,, \tag{10.70}$$

and Rayleigh's quotient becomes

$$R = \frac{\int_0^L EIv''^2\,dx}{\int_0^L v'^2\,dx}\,. \tag{10.71}$$

We can easily verify that when v is given by the exact shape of the fundamental buckling mode of a prismatic simply supported column, $v(x) = C\sin(\pi x/L)$ (where C is an arbitrary amplitude), then, if EI is constant, R equals the Euler load P_E. If, now, we assume a different shape for v, provided it satisfies the geometric boundary conditions $v(0) = v(L) = 0$, then R will approximate P_E

from above. If, for example, we assume a parabola given by $v(x) = Cx(L-x)$, so that $v'(x) = C(L-2x)$ and $v''(x) = -2C$, then

$$R = \frac{4EIC^2L}{C^2\int_0^L (L^2-4Lx+4x^2)\,dx} = \frac{4EIL}{L^3(1-2+\frac{4}{3})} = 12\frac{EI}{L^2}\,. \qquad (10.72)$$

This is more than 20% above the Euler load, and can only be said to give the right order of magnitude. In situations where no exact solution for the buckling shape is available, however, as for example in columns with variable EI, Rayleigh's method is often the simplest recourse.[†]

Example 10.3.3: Column with entasis
In classical Greek and Roman architecture columns are usually not cylindrical but have a bulge at the base and taper toward the top, a feature known as *entasis*, illustrated in Fig. 10.19a.[‡] While in reality such columns are too stubby

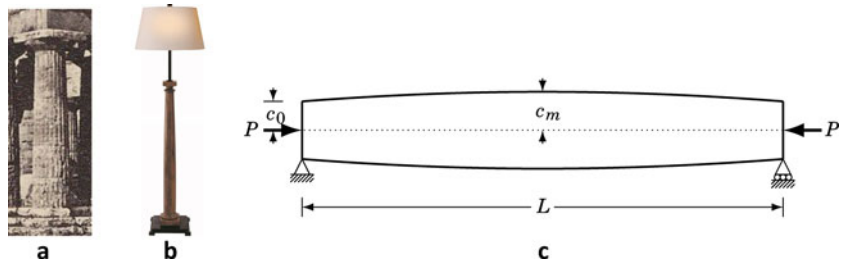

Figure 10.19. Column with entasis: (**a**) classical illustration, (**b**) modern illustration, (**c**) equivalent simply supported column

to buckle, in modern design entasis is sometimes applied to slender columns for aesthetic reasons, as in Fig. 10.19b. If we model the actual column as fixed-free, then it is equivalent to half of the simply supported column drawn in Fig. 10.19c. In order to make the problem mathematically tractable, we suppose that the variation of the column radius c with the axial coordinate x (measured from the left end) is given by $c(x) = c_0[1+\alpha\sin(\pi x/L)]$, where $\alpha = (c_m - c_0)/c_0$. Consequently the second moment of area is given by $I(x) = I_0[1+\alpha\sin(\pi x/L)]^4$, where $I_0 = \pi c_0^4/4$. If we assume $v(x) = C\sin(\pi x/L)$, then the denominator of Rayleigh's quotient is $(\pi C/L)^2 L/2$. To determine the numerator we need to evaluate integrals of the form $\int_0^L \sin^n(\pi x/L)\,dx$ for $n = 2,\ldots,6$, which are given in the following table.

n	2	3	4	5	6
$\int_0^L \sin^n(\pi x/L)\,dx$	$L/2$	$4L/3\pi$	$3L/8$	$16L/15\pi$	$5L/16$

[†]There exists a refinement of Rayleigh's method, known as the *Rayleigh–Ritz* method (Walter Ritz (1878–1909) was a Swiss physicist), in which the assumed shape is taken as a linear combination of several functions with undetermined coefficients, and R is minimized with respect to these coefficients.

[‡]It has long been believed that the reason for it was to create an illusion of straightness, but recent psychological studies have shown that no such illusion takes place.

After carrying out the integrations we find that, if the approximation to the critical load produced by Rayleigh's method is denoted $\tilde{P}_{\text{cr}}$ and if $P_{E0} = \pi^2 E I_0 / L^2$ (that is, the Euler load for a cylindrical column of radius c_0),

$$\tilde{P}_{\text{cr}} = P_{E0}\left(1 + \frac{8}{3\pi}\alpha + \frac{3}{4}\alpha^2 + \frac{32}{15\pi}\alpha^3 + \frac{5}{8}\alpha^4\right) .$$

Exercises

10.3-1. A wooden yardstick is 36 in long and of 0.25 in×1 in rectangular cross-section. If it is initially bowed with a maximum deflection of 0.25 in, and if the Young's modulus of the wood is 1.3×10^3 ksi, find the axial force needed to increase the deflection by (a) 0.25 in, (b) 1 in, (c) 2 in.

10.3-2. An aluminum meter stick is 1 m long and of 1.5 mm×27 mm rectangular cross-section. If it is initially bowed with a maximum deflection of 2 mm, and if the Young's modulus of the aluminum is 70 GPa, find the axial force needed to increase the deflection by (a) 1.5 mm, (b) 15 mm, (c) 30 mm.

10.3-3. Calculate the Euler load (in kN) for a 4-m-tall wooden post of rectangular cross-section with dimensions 10 cm by 5 cm if $E = 12$ GPa.

10.3-4. Calculate the Euler load (in kips) for a 20-ft column made of aluminum structural pipe with outer diameter 6.625 in and wall thickness 0.280 in if $E = 10 \times 10^3$ ksi.

10.3-5. Determine the critical buckling load for the fixed-fixed column shown in Fig. 10.15a.

10.3-6. Determine the critical buckling load for the elastic column shown in the figure, assuming that $EI_1 = 2EI_2$. Which of the two parts of the column becomes unstable first?

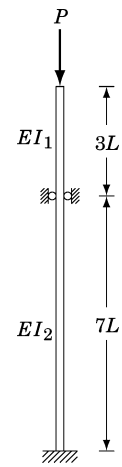

10.3-7. Find the critical value $P = P_{cr}$ that leads to buckling in the truss of the figure, assuming that all three bars have the same value of EI. Which bar buckles first? How would the answer to this problem change if the pin and roller supports were interchanged?

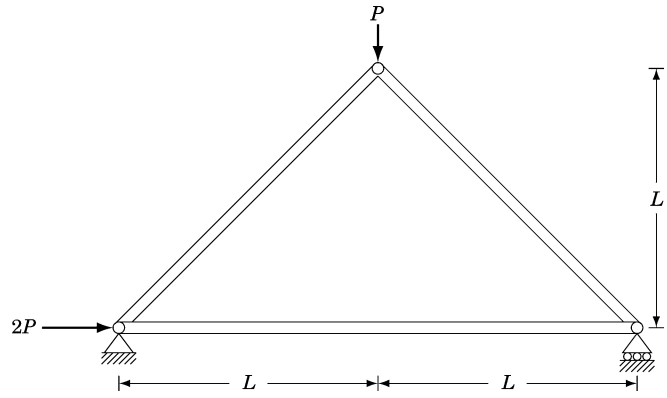

10.3-8. Consider an elastic column that is fixed at point B and guided (that is, prevented from rotating or moving normal to its axis, as in Fig. 2.15d, page 71) at point A. The column is subjected to a compressive force P at point A and undergoes a small deflection, as shown by the dotted line in the figure.

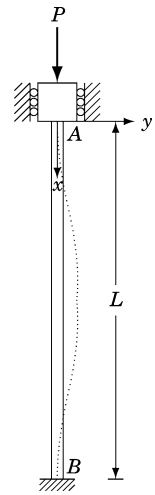

(a) Draw the free-body diagram of the column and show that both end-points are subject to the same moment M_0.

(b) Write the second-order differential equation which governs the deflection v of the column in terms of Young's modulus E, the moment of inertia I, the moment M and the force P.

(c) Solve the differential equation of part (b) and apply the boundary conditions at end-points A and B.

(d) Determine the critical buckling load P_{cr} for this column.

(e) What is the effective length L_e of this column?

10.3-9. For a simply supported prismatic column that is loaded by an axial force P with an eccentricity e, find the value of P/P_E needed to produce a maximum deflection of (a) e, (b) $2e$, (c) $5e$, (d) $15e$.

10.3-10. Using the data of Table B-5 or B-6, and identifying σ_f with σ_Y for metals and with σ_U^c for wood and concrete, find the critical slenderness ratio $(L_e/r)_{cr}$ for (a) 6061 aluminum, (b) A36 steel, (c) Douglas fir, (d) regular-strength concrete.

10.3-11. Let $\bar{d}$ denote the cross-sectional dimension of a beam along the weakest axis. Find a relation between $L_e/\bar{d}$ and L_e/r for the following cross-sections: (a) circle of radius c, (b) $t \times b$ rectangle with $t < b$, (c) equilateral triangle with sides of length a.

10.3-12. Find the ratio between the Euler load of a prismatic column whose cross-section is a square and that of a circular column if the cross-sectional areas are the same.

10.3-13. Find the ratio between the Euler load of a prismatic column whose cross-section is an equilateral triangle and that of a circular column if the cross-sectional areas are the same.

10.3-14. Find the ratio between the Euler load of a prismatic column whose cross-section is a regular hexagon and that of a circular column if the cross-sectional areas are the same.

10.3-15. Suppose that intermediate columns are defined as those with $\frac{2}{3}(L_e/r)_{cr} < (L_e/r) < \frac{4}{3}(L_e/r)_{cr}$, and that in that range σ_{cr}/σ_f is given by a cubic function of $(L_e/r)/(L_e/r)_{cr}$. Find this function such that the corresponding curve, as in Fig. 10.17, is tangent to both the horizontal line and the Euler hyperbola at the appropriate points.

10.3-16. Show that if $v(x) = C\sin(\pi x/L)$ is substituted in Eq. (10.71), R equals the Euler load P_E.

10.3-17. In Example 10.3.3, determine the volume of the column and find the radius c_e of the cylindrical column having the same volume. If the Euler load for this column is P_{Ee}, find the ratio $\tilde{P}_{cr}/P_{Ee}$ as a function of α, and calculate it for $\alpha = 0.1$, 0.25 and 0.5.

Chapter 11

Inelasticity and Material Failure

11.1 Stress-Strain Diagrams

11.1.1 Introduction

The load-displacement diagrams for simple springs shown in Fig. 6.2 (page 248) have their counterpart (as was already noted in Example 6.1.2, page 251) in *stress-strain diagrams*. These represent the properties of the material for, on the one hand, uniaxial normal stress (tensile and compressive) and the conjugate longitudinal strain and, on the other hand, shear stress and the conjugate shear strain. Such diagrams may represent linearly elastic, nonlinearly elastic or inelastic behavior, as discussed in Sect. 6.1. However, as we remarked in that section, nonlinear elasticity does not normally occur in the range of strains considered infinitesimal (as defined in Sect. 5.1, page 216), but only in certain materials—such as rubber—that are capable of large deformations.

Stress-strain diagrams in tension, compression and shear are obtained from appropriate tests, which are discussed below. The results of tensile and compressive tests can be plotted in the same stress-strain plane, occupying respectively the first and third quadrants, in accordance with the usual sign convention for stress and strain. However, it is more common (and space-saving) to plot the diagrams in the first quadrant only, with tension and compression duly marked.

11.1.2 Tension and Compression Tests

As we discussed in Sect. 4.1, when a straight bar (or wire or cable or the like) is subjected to a tensile axial force, it stretches and, as the force is in-

© Springer International Publishing Switzerland 2017

J. Lubliner, P. Papadopoulos, *Introduction to Solid Mechanics*,
DOI 10.1007/978-3-319-18878-2_11

creased, eventually breaks. The breaking may happen suddenly after a relatively slight amount of stretching, or it may be preceded by the sudden or gradual onset of a large amount of elongation with relatively little resistance (yielding). In the latter case, at some point the elongation may become confined to a limited segment of the bar that narrows considerably and is said to experience *necking*.

A solid that breaks suddenly without appreciable yielding is called *brittle*, while a material that allows significant yielding is called *ductile* (as already noted in Sect. 4.1). It is conventional to refer to the breaking of a brittle material as *fracture*, and to that of a ductile material as *rupture*. Among biological materials, bone is brittle while soft tissue is ductile, and medical terminology observes a similar distinction between fracture and rupture.

As we noted in Sect. 4.1, the maximum stress attained before fracture or rupture is known as the *ultimate strength* (tensile, compressive, or shear) of the material.

A standard tension test uses a specimen—if the material allows the fabrication of such a specimen, by shaping or casting—that is either circularly symmetric (in other words, a solid of revolution or flat, with a profile that typically looks as in Fig. 11.1. The specimen's shoulders are held by the grips of a testing machine as it stretches the specimen, and the elongation of the gage length L in the narrow cylindrical portion is measured by means of an extensometer or similar device. At the same time, the applied force is measured by a load cell, that is, a transducer which converts a force into an electrical signal). The gage marks must, of course, be far enough away from the shoulders for Saint-Venant's principle to apply.

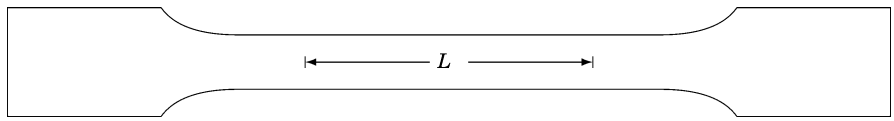

Figure 11.1. Typical tension-test specimen with gage length L

A similar procedure can be used for compression tests, provided that care is taken so that no buckling occurs.

In materials such as concrete and rock, the fabrication of such specimens is not practicable. Compression tests are performed by direct pressure on circular or rectangular cylinders. It is important that the contact between the pressure plates and the cylinders be as nearly frictionless as possible, to allow free lateral expansion and prevent transverse tensile stresses.

One way of measuring the *tensile* behavior (at least the strength) of concrete is to force such tensile stresses, eventually resulting in the splitting of

the cylinder (a procedure known as the *Brazilian test*). Here, a right circular cylinder made of concrete is placed with its curved surface between two (nearly) rigid flat solids and squeezed until it splits apart, as illustrated in Fig. 11.2a. In a modified version of the test the contact surface between the

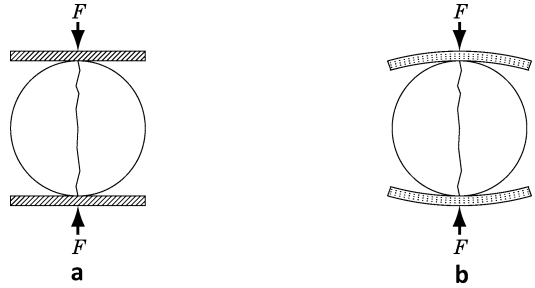

Figure 11.2. Brazilian test: (**a**) traditional, (**b**) modified

rigid solids and the specimen is concave, as in Fig. 11.2b.) If the applied load F is assumed to be uniformly distributed along the length of the cylinder, then the theory of elasticity predicts that the tensile stress across the diameter between the loading points attains a maximum value of

$$\sigma_{\max} = \frac{2F}{\pi L d}, \tag{11.1}$$

where L and d are respectively the length and the diameter of the cylinder. The value of F at splitting thus gives, through Eq. (11.1), a nominal tensile strength of the material.

The technology of *direct* tension testing of concrete and rock is still evolving.

Another method of determining tensile strength is through a flexure (bending) test, with the specimen typically in the shape of a rectangular beam of width b, depth h, and span L, which is simply supported near the ends and with a concentrated transverse force F applied in the middle of the span, as seen in Fig. 11.3. This is known as a *three-point flexural test*. If the force

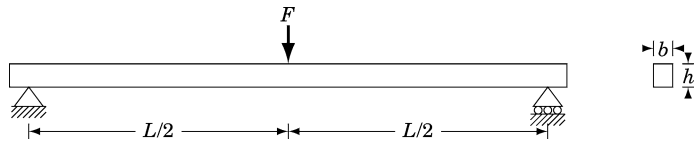

Figure 11.3. Three-point flexural test

when rupture begins (at the outermost tensile fibers) is F_U, then, assuming linearly elastic behavior, we can readily calculate the tensile stress in those fibers to be $M_{\max}/S = (F_U L/4)/(bh^2/6) = 3F_U L/bh^2$. This is just the modulus of rupture already defined in Sect. 8.3 (page 381), also known as *flexural strength*, and is usually somewhat higher than the ultimate tensile strength

found from direct tension tests, if such tests are practicable. It is this value that is given as σ_U^{t} for wood in Tables B-5 and B-6.

All the tests described above can be performed with a machine known as a *universal testing machine* (UTM), as shown in Fig. 11.4.

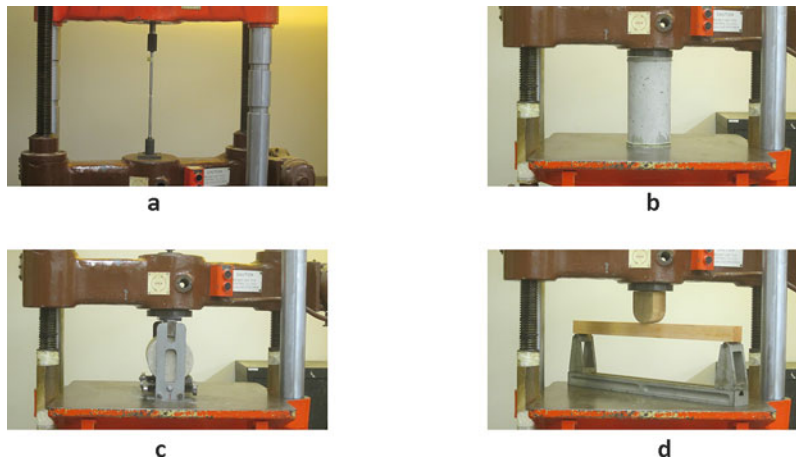

Figure 11.4. Universal testing machine: (a) tension, (b) compression, (c) Brazilian, (d) three-point flexure

11.1.3 Shear Tests

As we discussed in Sect. 4.2, the most direct way of generating a state of uniform shear stress is by applying a torque to a thin-walled tube. As we learned in Sect. 7.1, in such a tube torque and twist can be related to shear stress and shear strain, respectively, independently of material properties. The downside of applying such loading is the possibility of crumpling of the tube. How this may occur can be explained if we recall from Sect. 4.6 that a simple shear stress is equivalent to equal tensile and compressive stresses along mutually perpendicular axes at 45° to the shear axes. Then, by imagining the tube as constituting a network of helical fibers with a helix angle of 45°, the crumpling may be regarded as the buckling of the compressive fibers, as illustrated in Fig. 11.5. Fig. 11.6 shows the result of an attempt to twist a cardboard tube.

A testing method based on shear produced in conjunction with bending is known as the *Iosipescu shear test*[*], illustrated in Fig. 11.7. If the forces are such that the inner couple balances the outer couple, then in the section between the notches the bending moment is zero, while the presence of

[*]Nicolae Iosipescu (1905–1978) was a Romanian engineer.

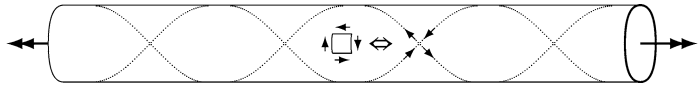

Figure 11.5. Crumpling of a thin-walled tube as buckling of compressive helical fibers

Figure 11.6. Crumpling as a result of twisting a cardboard tube

the notches makes the shear stress more or less uniform through the cross-section.

Alternative "direct" or "simple" shear tests (called *shear-box tests*) are used in geotechnical engineering for soil and very weak rocks. Schematics of such tests are shown in Fig. 11.8.

11.1.4 Brittle Materials—Tension and Shear

Conventionally brittle materials, such as glass and many ceramics, behave in a linearly elastic fashion all the way to fracture (marked by ×), as shown in Fig. 11.9a for the case of a typical glass. Other brittle materials, including concrete and many hard plastics (specifically thermosetting polymers such as bakelite and melamine resin), show some inelastic deformation before fracture.

A tensile stress-strain diagram for a typical concrete is shown in Fig. 11.9b. Unloading in the inelastic range (that is, at stresses greater than the *elastic limit* σ_E[†]), and subsequent reloading usually takes place more or less elastically, as shown in the same figure. After unloading to zero stress, some strain is seen to remain, but whether it remains permanently (in which case it is called *plastic strainn*) or fades away in time depends on the material and on other factors such as the temperature and the rate of the initial loading.[‡]

[†]In some discussions a distinction is made between the elastic limit and the *proportional limit*, referring to the limit of *linear* elasticity, but in the range of small strains there is no justification for such a distinction.

[‡]There are also materials in which unloading follows a different path from that of loading but results immediately in zero strain at zero stress. This behavior is called *pseudoelastic*, and among the materials exhibiting it are those known as *shape-memory alloys*.

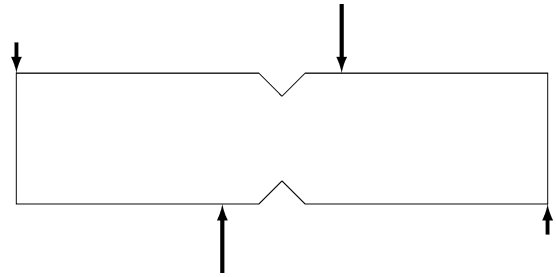

Figure 11.7. Test specimen and loading for the Iosipescu shear test

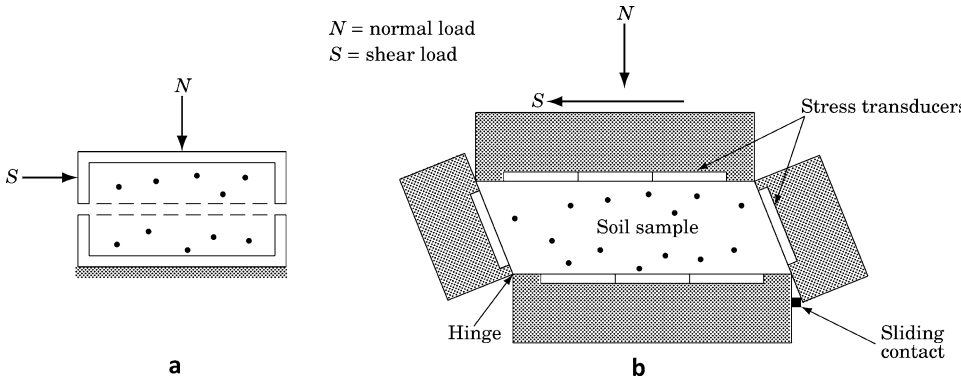

Figure 11.8. Shear-box tests: (**a**) "direct," (**b**) "simple"

In gray cast iron, whose stress-strain diagram is shown in Fig. 11.9c, inelastic deformation is present almost from the outset. For such materials there is no unequivocal definition of the Young's modulus. When elastic analysis is applied to bodies made of such a material, the choice of Young's modulus depends on the application. Besides the *initial* modulus E_0 (equal to the slope of the stress-strain curve at the origin), at any given point on the stress-strain curve there are also (1) the *secant* modulus $E_s = \sigma/\varepsilon$, (2) the *tangent* modulus $E_t = d\sigma/d\varepsilon$, and (3) the *unloading-reloading* modulus E_u equal to the average slope of the unloading and reloading curves. Similar definitions can be applied to other materials having no well-defined linearly elastic range.

The behavior of brittle materials in shear is, as a rule, quite similar to that in tension.

11.1.5 Brittle Materials—Compression

It is characteristic of brittle materials that the ultimate compressive strength is typically many times greater than the ultimate tensile strength, with the factor ranging from about 3 or 4 for gray cast iron to 10 or more for concrete

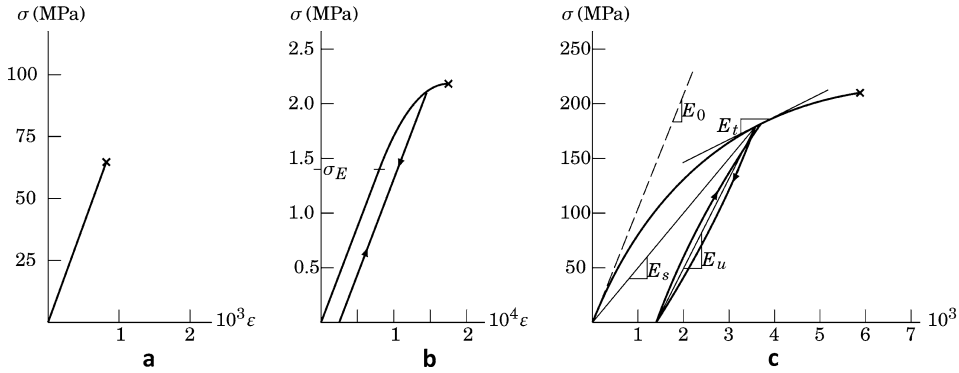

Figure 11.9. Tensile stress-strain diagrams for representative brittle materials: (**a**) glass, (**b**) concrete, (**c**) gray cast iron

and about 20 for glass. Compressive stress-strain diagrams for glass, concrete and gray cast iron are shown in Fig. 11.10. The tensile curves in Fig. 11.9 are shown alongside the compressive ones for comparison.

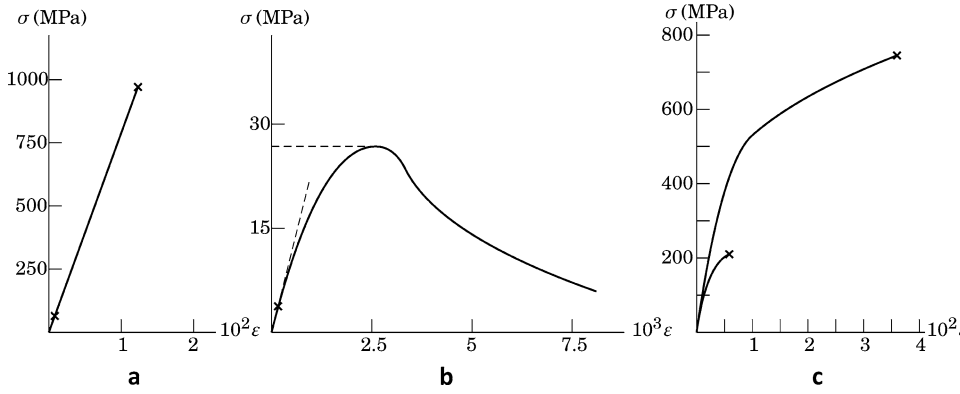

Figure 11.10. Compressive stress-strain diagrams for representative brittle materials: (**a**) glass, (**b**) concrete, (**c**) gray cast iron

In concrete and rock, the decrease in stress after the ultimate compressive strength is reached (but before complete fracture) is known as *softening* (or *strain-softening*), and is due to the coalescence of microscopic cracks (microcracks) that are formed during the prior loading. The softening portion of the stress-strain curve is, in general, influenced by testing conditions and specimen dimensions.

11.1.6 Ductile Materials

For most ductile materials, by contrast to brittle materials, the stress-strain diagrams in tension and compression are most often nearly the same, at least in the range of small strains. Fig. 11.11a shows tensile stress-strain diagrams for a selection of ductile metals, while Fig. 11.11b shows tensile *and* compressive stress-strain diagrams for one of the most common engineering materials, mild (low-carbon) steel (also included in Fig. 11.11a). As already mentioned in Sect. 4.1, the stress at the onset of yielding, if it can be determined to some degree of precision, is called the *yield stress* or *yield strength*; it is denoted σ_Y.

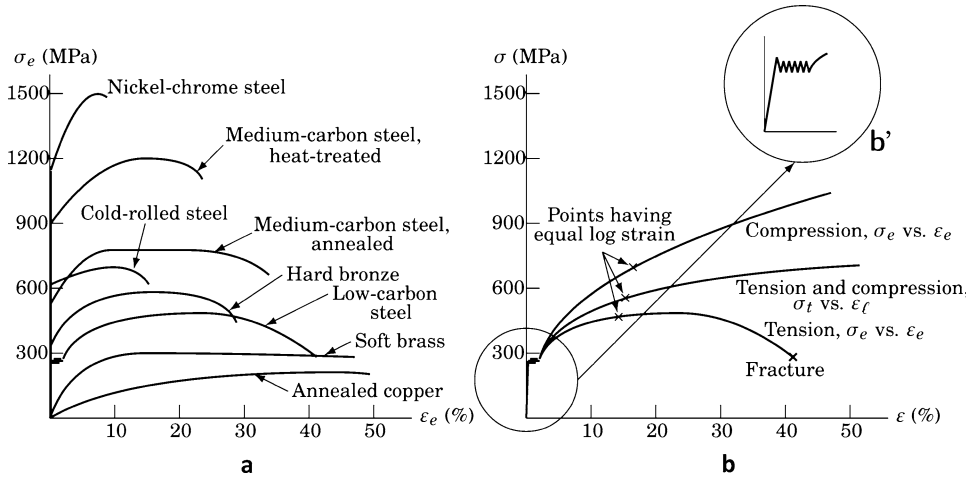

Figure 11.11. Stress-strain diagrams for ductile metals: (**a**) various metals (tensile), (**b**) low-carbon steel (tensile and compressive)

The apparent softening seen on several of the stress-strain curves in Fig. 11.11a is due to the fact that the ordinate is given by the engineering stress (denoted σ_e), defined (see Sect. 4.1) as the force divided by the *original* area, and in the range of large strains the actual area decreases significantly as the specimen is stretched, so that the true stress (denoted σ_t) becomes greater than the engineering stress. The converse is true in a compression test. In the range of large strains, it is generally found that the volume remains constant, that is $L'A' = LA$ (where A and L are the initial, and A' and L' the subsequent, values of the area and length, respectively). Thus, if ε is the engineering strain (see Sect. 5.1), then $L' = L(1+\varepsilon)$, so that $A'(1+\varepsilon) = A$, and therefore $\sigma_t = \sigma_e(1+\varepsilon)$. When the stress-strain diagrams in tension and compression for low-carbon steel, shown in Fig. 11.11b as engineering stress against engineering strain, are converted to true stress against logarithmic strain ε_ℓ (see Sect. 5.1), they are found to coincide.

Note that the strains shown on the abscissa are quite large, so that the

strain at the elastic limit (of the order of 0.1%) is too small to be seen, and the straight line representing the elastic range almost coincides with the stress axis.

The inset labeled b′ in Fig. 11.11 shows the peculiar property of mild steel (and a few other alloys, as well as thermoplastic polymers such as nylon) of a drop in the stress after the initial yielding, and then some oscillation (up to a strain of about 2%) about a stress plateau before the increase in stress known as *work-hardening* (also *strain-hardening* or simply *hardening*) begins. Since in a typical structure or machine a strain of this magnitude already represents displacements that may be regarded as failure, it is common to confine the analysis of members made of this metal to the range of the plateau and to describe the behavior of the metal (ignoring the oscillations) as *elastic–perfectly plastic*, shown in Fig. 11.12.

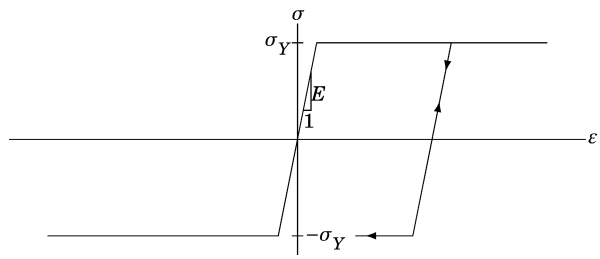

Figure 11.12. Elastic–perfectly plastic stress-strain diagram

The model represented by Fig. 11.12 is often applied to materials (not only metals) that do not exhibit this behavior in reality and, in particular, have no well-defined yield stress. For such materials it is conventional to define the yield stress as the stress corresponding to a certain predefined *offset*, that is, a permanent strain (called *plastic strain*) remaining after the stress is completely removed, as shown in Fig. 11.13. Common values of the offset

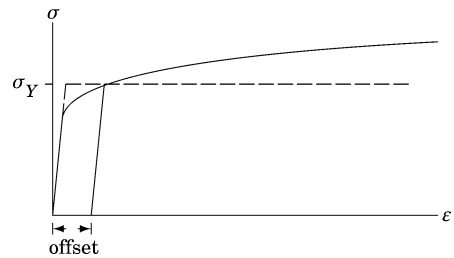

Figure 11.13. Offset yield stress

are 0.1% and 0.2%, and the yield stress thus defined is accordingly called the 0.1% or 0.2% offset (or proof) yield stress. The dashed diagram in the figure

corresponds to the elastic–perfectly plastic representation of the stress-strain diagram, ignoring the work-hardening.

An alternative representation of the stress-strain relation of a solid without a well-defined elastic range is by means of an empirical formula. The best-known such formula, the *Ramberg–Osgood formula*[§], is discussed in the following example.

Example 11.1.1: *The Ramberg–Osgood formula.*
The formula is

$$\varepsilon = \frac{\sigma}{E} + \alpha \frac{\sigma_0}{E} \left(\frac{\sigma}{\sigma_0} \right)^n , \tag{11.2}$$

where E, α, σ_0 and n are curve-fitting parameters, with $n > 1$. It is clear that

$$\left. \frac{d\varepsilon}{d\sigma} \right|_{\sigma=0} = \frac{1}{E} ,$$

so that E is the initial elastic modulus. σ_0 may be identified with an offset yield stress, the offset strain being $\alpha\sigma_0/E$. The exponent n is chosen so as to optimize the fit at large values of the strain.

Necking

The range of apparent softening in the tensile engineering stress-strain diagrams corresponds to necking, shown in Fig. 11.14, and rupture occurs in the narrowest portion of the neck.

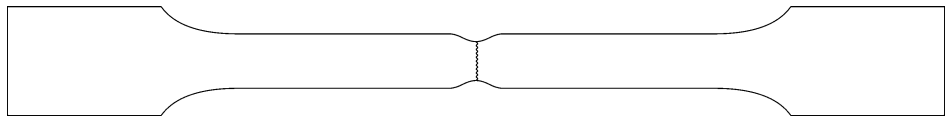

Figure 11.14. Necking and tensile rupture in a ductile metal

In ductile polymers, on the other hand, necking begins right at the yield point, and the neck is then drawn out until, just before rupture (which occurs when the ultimate tensile strength is reached, with no subsequent softening), it extends over most of the narrow portion of the specimen, as shown in Fig. 11.15.

Toughness

We observe from the diagrams shown in Fig. 11.11a that the strongest metals tend to be the least ductile in the sense of having the smallest strain attained

[§]Walter Ramberg (1904-1985) was an American physicist and William R. Osgood (1895–1977) was an American Engineer.

Figure 11.15. Necking in a ductile polymer: (**a**) at yield, (**b**) in the drawing phase, (**c**) just before rupture

at rupture (often called *percent elongation* when expressed in percent, and denoted $\varepsilon_{\max}$ in Tables B-5 and B-6), and vice versa. A property that is intermediate between strength and ductility is *toughness*, defined by the area under the entire stress-strain curve. It is left to an exercise to show that this value is virtually the same whether the curve used is engineering stress and strain or true stress and logarithmic strain.

We recall, from Eq. (5.17) (page 220), that $\sigma\delta\varepsilon$ is the internal virtual work per unit volume. Accordingly, $\sigma d\varepsilon$ is the actual work per unit volume done in the course of an infinitesimal strain increment $d\varepsilon$, and the integral $\int \sigma d\varepsilon$ is the total work per unit volume (on the average) done on the specimen. Toughness thus measures the capacity of the material to absorb energy (for example upon impact) before breaking. (Recall that the product of stress and strain has the dimensions of work or energy per unit volume.)

Rough estimates for the toughness of a few of the metals represented in Fig. 11.11a give about 110 MPa for nickel-chrome steel, 130 MPa for soft brass, and 220 and 250 MPa, respectively, for annealed and heat-treated medium-carbon steel.

Exercises

11.1-1. A four-point test of flexural strength is performed on a Douglas-fir plank of depth 1 in and width 2 in, spanning 3 ft between supports and loaded by two concentrated forces F at points that are 1 ft away from either end. If the plank begins to break at $F = 3.7$ kip, find the modulus of rupture.

11.1-2. A three-point test of flexural strength is performed on a nylon rod of circular cross-section with a diameter of 20 mm, spanning 80 cm between supports and loaded by a concentrated force F at midspan. If the material is meant to exhibit a modulus of rupture of at least 90 MPa, find the smallest value of F that would cause failure.

11.1-3. For materials whose stress-strain diagrams are significantly different in tension and compression, even in the range of infinitesimal strains, an estimate of Young's modulus is often made by means of the three-point flexure test described in the preceding exercise. If a force F produces a midspan deflection Δ, find E in terms of F, Δ and the geometric properties of the specimen.

11.1-4. In the Iosipescu shear test shown in Fig. 11.7, assign dimensions to the beam and the load points, as well as magnitudes to the forces, and determine the relation between them that will make the section between the notches free of bending moment.

11.1-5. In the Ramberg–Osgood formula, Eq. (11.2), show that only three of the four parameters are independent.

11.1-6. For a material whose stress-strain relation is described by the Ramberg–Osgood formula, find the secant and tangent moduli (E_s and E_t) at a given value of σ.

11.1-7. Assume that the relation between true stress and logarithmic strain for an aluminum alloy is described by the Ramberg–Osgood formula. If the initial Young's modulus is 80 GPa and the 0.2% offset yield stress is 250 MPa, find the exponent n such that $\sigma_t = 400$ MPa when $\varepsilon_\ell = 0.30$.

11.1-8. A wire made of low-carbon steel, with the stress-strain relations shown in Fig. 11.11b, has an original diameter of 2 mm and is subjected to a tensile force of 1.2 kN. From the stress-strain diagram, estimate the diameter of the wire after the application of the force.

11.1-9. Show that the toughness is virtually the same whether calculated from an engineering stress-strain diagram or from one of true stress against logarithmic strain.

11.1-10. From Fig. 11.11a, find estimates of the toughness of (a) cold-rolled steel, (b) annealed copper.

11.2 Material Failure

11.2.1 Basic Failure Mechanisms

The differences between brittle and ductile failure are due to the internal mechanisms at work on the microstructural level in the material. The elastic behavior of solids is largely determined by the primary atomic or molecular structure. While solid-state, glass and polymer physics allow the prediction of the stresses required to break the atomic or molecular bonds, these stresses are normally many times greater than the observed strengths of the materials. In fact, inelasticity and failure are determined by structural imperfections such as microscopic cracks and dislocations. It is possible to produce very thin fibers ("whiskers") that are relatively free of such imperfections, and they exhibit tensile strengths that are much higher than those of the bulk material. This is why, for example, while bulk glass is rather weak in tension (see Fig. 11.9a), high-strength glass fibers can used as tensile reinforcement in a polymer matrix.

The two main failure mechanisms in solids are cleavage, which is resisted by tensile stress, and slip, resisted by shear stress. The latter may or may not involve internal friction.

Cleavage failure is typical of brittle materials in tension. It is caused by the presence of preexisting microscopic cracks. A crack perpendicular to the applied tensile force causes a *stress concentration* in the material just outside the tip of the crack, that is, the tensile stress there is many times greater than the average stress, and when this stress reaches a critical value it causes the crack to open and spread. This phenomenon can be tested by trying, first, to tear a sheet of paper by pulling on when it is intact, as in Fig. 11.16a, and then to do the same after a small tear or cut has been made in a side of the sheet, as in Fig. 11.16b.

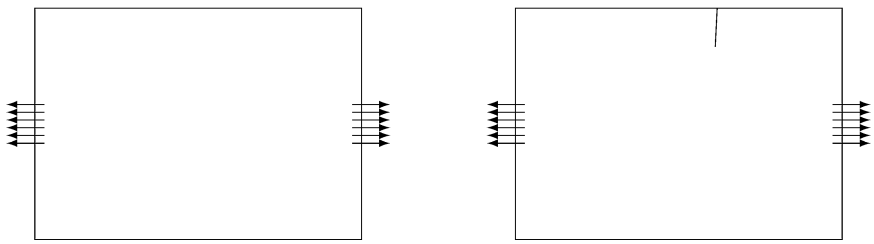

Figure 11.16. "Tear in a sheet of paper" analogy for the effect of cracks on tensile fracture

Slip is the primary mechanism of plastic deformation and failure in ductile materials. In crystalline materials this is facilitated by misalignments

in the atomic structure known as *dislocations*, much as a rug can be moved across a floor by introducing a ripple in it and then moving the ripple, far more easily than by sliding the whole rug, as illustrated in Fig. 11.17.

Figure 11.17. "Ripple in a rug" analogy for the effect of dislocations on slip

Slip, however, is also one of the main mechanisms in the failure of brittle materials in compression, through the coalescence of cracks into *shear faults*. Another such mechanism stems from the opening of cracks that are parallel to the compressive force, resulting in *splitting*, and if splitting occurs on enough surfaces parallel to the force, the result is the local formation of columns that eventually buckle. In the compression testing of concrete or rock cylinders, both mechanisms are often observed, as shown schematically in Fig. 11.18a; the shear fault often forms a cone, as seen in Fig. 11.18b. For comparison, splitting and shear failures are shown in Figs. 11.18c and 11.18d, respectively. The occurrence of one or another failure mode in a test is influenced

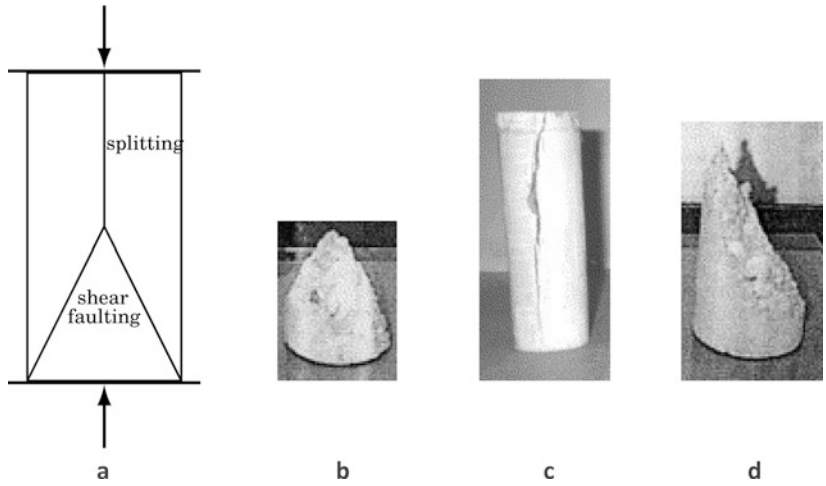

Figure 11.18. Splitting and shear faulting in test cylinders: (**a**) schematic drawing, (**b**) cone from combined failure, (**c**) splitting failure, (**d**) shear failure

by the nature of the contact between the cylinder and the end plates of the testing machine, with "smooth" contact favoring splitting and "rough" contact favoring shearing.

11.2.2 Failure Criteria

As we remarked in Sect. 10.3, Fig. 10.13 (page 461) is an illustration of the principle of least resistance, according to which, when there are two or more

modes of failure—in that case buckling and material failure—then the one that requires the least force or stress will occur first.

In the column case, both mechanisms are governed by the same stress component, namely the (average) axial compressive stress. When different mechanisms are governed by different stress components or combinations thereof, it is necessary to describe the failure criteria as surfaces in the Cartesian space of the stress components. Here, each such surface defines a boundary between the "safe region" and the failure region for the particular mechanism. According to the principle of least resistance, then, the overall safe region is the intersection of the safe regions for all the criteria.

For a general state of stress, the symmetry of the stress components, as given by Eq. (4.42) (page 191), implies that the Cartesian space of stresses is six-dimensional: its coordinates may be the independent components of stress ($\sigma_x,\ldots,\tau_{yz}$, or $\sigma_1,\ldots,\sigma_6$ in the column-matrix notation of Sect. 6.2.10), but, equivalently, they may also be the three principal stresses and the three angles giving the directions of the principal axes. For plane stress, the space is three-dimensional—*either* the space of the stress components σ_x, σ_y, τ_{xy} *or* that of the two principal stresses σ_1, σ_2 and the angle giving the direction of one of the principal axes.

In general, the failure surfaces may be parametrically dependent on additional variables such as the rate of loading and the temperature. (In the case of column failure, the slenderness ratio is also such a parameter.)

If the material is isotropic (as defined in Sect. 6.2), then its properties are the same regardless of the directions of the principal axes, and therefore the failure criterion depends only on the principal stresses. Moreover, the dependence must be symmetric in the sense that the numbering of the principal stresses plays no role. In plane stress, for example, if the failure surface is given by $F(\sigma_1,\sigma_2)=0$, then $F(\sigma_1,\sigma_2)=F(\sigma_2,\sigma_1)$.

Brittle tensile failure is described simply by

$$\sigma_{\max} = \sigma_{\text{br}} , \tag{11.3}$$

where $\sigma_{\max}$ is the *algebraically* greatest stress (positive in tension) and σ_{br} is the breaking stress, or, in terms of principal stresses

$$\max(\sigma_1,\sigma_2,\sigma_3) = \sigma_{\text{br}} . \tag{11.4}$$

Its plane-stress projection (corresponding to $\sigma_3=0$) is shown in Fig. 11.19a.

The simplest shear-failure criterion is known as the *Tresca criterion*[¶], and is given by

$$\tau_{\max} = \tau_{\text{cr}} , \tag{11.5}$$

where $\tau_{\max}$ is the *numerically* largest shear stress and τ_{cr} is the critical shear stress for slip (for ductile materials this is the yield stress in shear, τ_Y). In

[¶]Henri Tresca (1814–1885) was a French mechanical engineer.

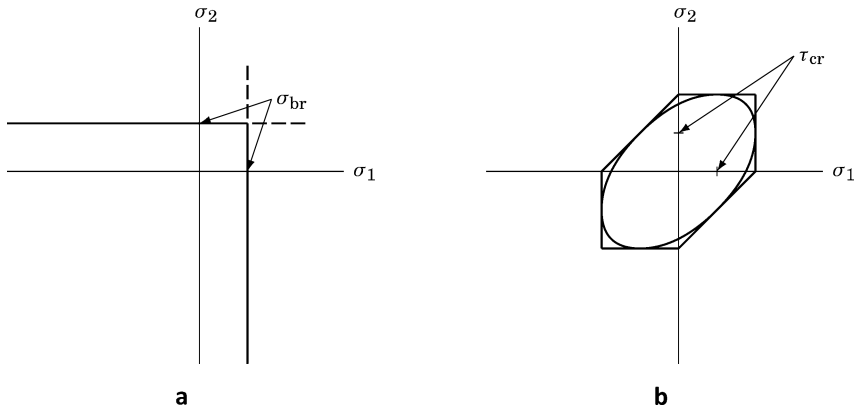

Figure 11.19. Failure criteria in the $\sigma_1\sigma_2$ plane: (**a**) tensile brittle failure, (**b**) shear failures

the space of the principal stresses, this is given, in accordance with Eq. (4.85) (page 208), by

$$\max(|\sigma_1-\sigma_2|,|\sigma_1-\sigma_3|,|\sigma_2-\sigma_3|) \;=\; 2\tau_{cr} \tag{11.6}$$

and in plane stress ($\sigma_3 = 0$) it reduces to

$$\max(|\sigma_1-\sigma_2|,|\sigma_1|,|\sigma_2|) \;=\; 2\tau_{cr}\,, \tag{11.7}$$

taking the form of the hexagon shown in Fig. 11.19b. Note that in a state of uniaxial tension or compression, the critical stress is equal to $2\tau_{cr}$. In other words, the Tresca criterion predicts that in a ductile metal the uniaxial yield stress σ_Y is twice the yield stress in shear. However, we know from experiments that in most metals this ratio is between 1.7 and 1.8, in keeping with the criterion depicted by the ellipse in Fig. 11.19b and represented for a general state of stress by

$$(\sigma_1-\sigma_2)^2+(\sigma_1-\sigma_3)^2+(\sigma_2-\sigma_3)^2 \;=\; 6\tau_{cr}^2\,, \tag{11.8}$$

so that $\sigma_Y = \sqrt{3}\tau_Y$. This is known as the *(von) Mises criterion*[||]. Note that the left-hand side of Eq. (11.8) is proportional to the deviatoric invariant J_2 defined in Eq. (6.32) (page 263), as well as to the octahedral shear stress defined in Eq. (4.89) (page 209). In fact, the criterion is often written as

$$J_2 \;=\; \tau_{cr}^2\,. \tag{11.9}$$

Since, in addition, J_2 is also proportional to the distortional strain or complementary energy (Sect. 6.5, page 310), the Mises criterion is also known as the distortional-energy criterion.

[||] Richard von Mises (1883–1953) was an Austrian-American mathematician and engineering scientist.

Example 11.2.1: Tube under combined axial force and torsion.
A thin-walled circular tube of mean radius r and wall thickness t is subjected simultaneously to an axial force P, producing an axial normal stress $\sigma = P/2\pi rt$, and a torque T, producing a shear stress $\tau = T/2\pi r^2 t$, with no other stresses. We wish to find the combinations of σ and τ that produce yielding.
(a) If we apply the Mises criterion in the form (11.9), with J_2 given by Eq. (6.33) (with $\sigma_x = \sigma$ and $\sigma_y = \sigma + z = 0$), we readily see that

$$\frac{\sigma^2}{3} + \tau^2 = \tau_Y^2 .$$

(b) For the Tresca criterion we need to determine the principal stresses, which, since the state is locally one of plane stress, are easily found from Eq. (4.60) to be

$$\sigma_{1,2} = \frac{\sigma}{2} \pm \sqrt{\left(\frac{\sigma}{2}\right)^2 + \tau^2} ,$$

and, since $\sigma_1 > 0$ and $\sigma_2 < 0$, Eq. (11.7) becomes

$$2\sqrt{\left(\frac{\sigma}{2}\right)^2 + \tau^2} = 2\tau_Y ,$$

or, equivalently,

$$\frac{\sigma^2}{4} + \tau^2 = \tau_Y^2 .$$

We see that both criteria are represented by ellipses in the $\sigma\tau$ plane, but with different eccentricities, as illustrated (with only one quadrant shown) in Fig. 11.20.

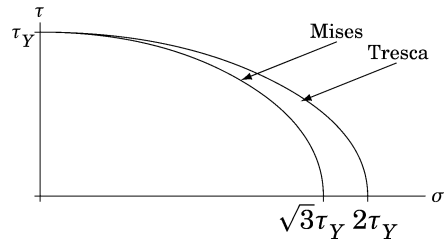

Figure 11.20. Example 11.2.1

11.2.3 Internal Friction

In many rocks and soils, as well as concrete, slip is resisted both by internal friction and by cohesion. Let us designate the critical shear stress due to cohesion by c; it is the equivalent of τ_{cr} in the Tresca criterion, and is often called simply the *cohesion*. Now, on a plane with a compressive stress $-\sigma$ acting across it, slip can occur only when the shear stress reaches $c + \mu(-\sigma)$, where μ is the *coefficient of internal friction*. Equivalently, this condition can be written as

$$|\tau| + \mu\sigma = c , \tag{11.10}$$

where the absolute value is needed to include both senses of the relative sliding motion. If the material is isotropic, then slip occurs on *some* plane when

$$\max_{\text{all planes}} (|\tau| + \mu\sigma) \;=\; c \;. \tag{11.11}$$

It is left to an exercise to show that, in terms of the principal stresses σ_i ($i = 1,2,3$), this can be rewritten as

$$\max_{i\neq j} \left[\sqrt{1+\mu^2}|\sigma_i - \sigma_j| + \mu(\sigma_i + \sigma_j) \right] \;=\; 2c \tag{11.12}$$

or yet again as

$$\sqrt{1+\mu^2}(\sigma_{\max} - \sigma_{\min}) + \mu(\sigma_{\max} + \sigma_{\min}) \;=\; 2c \;, \tag{11.13}$$

where $\sigma_{\max}$ and $\sigma_{\min}$ are respectively the *algebraic* maximum and minimum normal stresses. Eq. (11.13) describes what is known as the *Mohr–Coulomb* failure criterion. It is often expressed in terms of the *angle of internal friction* $\phi = \tan^{-1}\mu$, and written as

$$(1+\sin\phi)\sigma_{\max} - (1-\sin\phi)\sigma_{\min} \;=\; 2c\cos\phi \;. \tag{11.14}$$

Note that the critical stress τ_{cr} in simple shear (where $\sigma_{\max} = -\sigma_{\min} = \tau_{\text{cr}}$) is not c but $c\cos\phi$. The critical stresses (interpreted as a yield stresses) in uniaxial tension (where $\sigma_{\max} = \sigma_Y^{\text{t}}$, $\sigma_{\min} = 0$) and compression (where $\sigma_{\max} = 0$, $\sigma_{\min} = -\sigma_Y^{\text{c}}$) are, respectively,

$$\sigma_Y^{\text{t}} \;=\; 2c(\sqrt{1+\mu^2} - \mu) \;=\; 2c\frac{1-\sin\phi}{\cos\phi} \;=\; 2c\tan\left(\frac{\pi}{4} - \frac{\phi}{2}\right) \tag{11.15}$$

and

$$\sigma_Y^{\text{c}} \;=\; 2c(\sqrt{1+\mu^2} + \mu) \;=\; 2c\frac{1+\sin\phi}{\cos\phi} \;=\; 2c\tan\left(\frac{\pi}{4} + \frac{\phi}{2}\right) \;. \tag{11.16}$$

Consequently, the criterion can also be written as

$$\frac{\sigma_{\max}}{\sigma_Y^{\text{t}}} - \frac{\sigma_{\min}}{\sigma_Y^{\text{c}}} \;=\; 1 \;. \tag{11.17}$$

In plane stress, the Mohr–Coulomb criterion is depicted by the hexagon of Fig. 11.21a.

The Mohr–Coulomb criterion is commonly used to describe soils, ranging from loose ones (like dry sand) that are *cohesionless* ($c = 0$) to dense ones (like clay) in which friction plays virtually no role ($\phi = 0$). In the former case, Eq. (11.14) can be satisfied only if all three principal stresses are compressive, as is intuitively obvious.

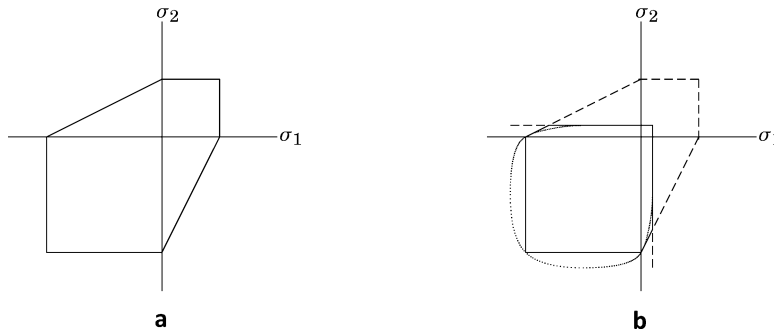

Figure 11.21. Mohr–Coulomb criterion in plane stress: (**a**) by itself, (**b**) with tensile brittle fracture

For rocks and concrete, however, it is necessary to combine the Mohr–Coulomb criterion for slip with one for tensile brittle failure, as in Fig. 11.21b, illustrating yet again the principle of least resistance. Here, the solid hexagon is a composite of the one of Fig. 11.21a and of the lines of Fig. 11.19a. The dotted curves in the second and fourth quadrants show a smoothing in the region of the transition between the two criteria, which may not be abrupt since the two failure mechanisms may interact.

The dotted curve in the third quadrant is a smoothing of the Mohr–Coulomb criterion in the domain of biaxial compression, similar to the way the Mises criterion smooths the Tresca criterion, bringing the failure criterion more in line with experimental observations. It will be noted that stress states corresponding to simple shear, as discussed in Example 4.6.5 (page 208), that is, where $\sigma_1 = -\sigma_2 = \pm\tau$, are governed by brittle fracture, as seen in Fig. 11.21b. Since the principal planes are oriented at 45°to the shearing plane, it follows that brittle specimens that are locally in a state of simple shear, such as a bar in torsion, will break along planes at 45°to the axis. This can be ascertained experimentally by twisting a piece of chalk until it breaks, and is illustrated in Fig. 11.22.

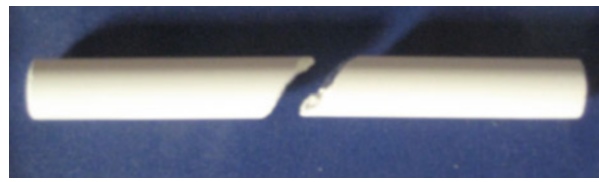

Figure 11.22. Fracture of a twisted piece of chalk

11.2.4 Effect of Temperature and Loading Rate

It is important to recognize that the mechanisms of brittle (cleavage) fracture and shear failure are independent of each other. Accordingly, the values of the critical tensile and shear stresses in Figs. 11.19a and 11.19b, respectively, are also independent of each other. For any given material, the surface shown in 11.19a may or may not intersect that of 11.19b. If it so happens, for a given material, that the surface shown in 11.19a is completely outside that of 11.19b, then brittle fracture never occurs and the material is ductile.

In general, however, the two mechanisms have very different sensitivities to temperature. It is well known that the yield stress of a metal decreases with increasing temperature (which makes hot forging possible) and, conversely, increases with decreasing temperature, meaning that the hexagon or ellipse of Fig. 11.19b *expands* as the temperature drops.

The effect of loading rate (as long as it is slow enough for inertial effects to be negligible) is similar: higher temperatures are equivalent to slower loading, and vice versa. This similarity can be explained physically by the fact that temperature, as we discussed in Sect. 1.1, represents the kinetic energy of the random motion of the atoms and molecules; a higher temperature thus corresponds to a greater frequency of vibration, giving the particles more opportunity to change their state, and a slower rate of loading does the same.

In some materials, as the yield surface expands with decreasing temperature, at a certain temperature (known as the *transition temperature*, denoted T_{tr}) it may cross the lines of Fig. 11.19b, which are much less temperature-sensitive. When that happens, at any state state of stress dominated by tension the failure will be brittle. The situation is illustrated in Fig. 11.23, where

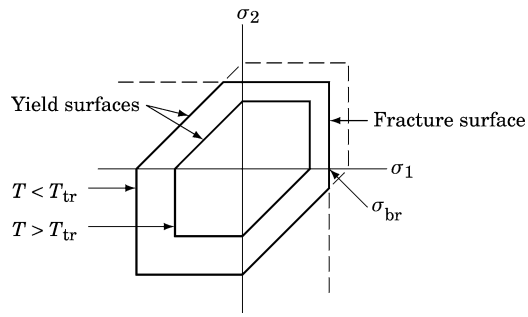

Figure 11.23. Temperature dependence of failure criterion

for simplicity the Tresca criterion is shown for yielding and where, in each temperature range, the governing criterion is given by the solid lines, σ_{br} denoting the ultimate stress in brittle fracture. Among the materials with this property is common structural steel. Knowledge of the transition temperature is therefore essential when designing structures for cold climates, since brittle failure can be much more catastrophic than yielding. One of the most

striking demonstrations of this fact may be the sinking of the RMS Titanic in 1912, which is now, at least partially, attributed to the brittle fracture of the hull (made of steel) and rivets (made of wrought iron) due to the combination of high velocity of impact with the iceberg and the extremely low water temperature.

An effect similar to that of the transition temperature, but involving loading rate, can be observed experimentally by pulling on a piece of silicone putty: in slow pulling (equivalent to a higher temperature) the putty yields like clay, but a quick pull (equivalent to a lower temperature) results in an abrupt break.

The effect of temperature and loading rate on stress-strain curves of a typical inelastic material is illustrated qualitatively in Fig. 11.24. The fact

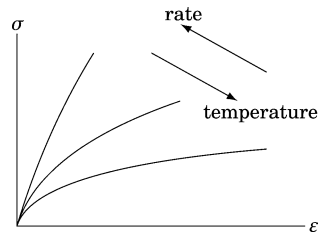

Figure 11.24. Effect of temperature and rate on stress-strain curve

that rapid loading will, for a given value of the stress, produce a smaller strain that slow loading implies that, if the stress is maintained after loading, the strain will spontaneously increase, a phenomenon known as *creep*. If, on the other hand, it is the strain that is maintained then the stress will decrease; this is known as *relaxation*.

11.2.5 Viscoelasticity

Whether creep or relaxation constitutes failure (in the form of excessive deformation or loss of load-carrying capacity, respectively) is a matter of degree. An example: the reason that bus stops are often paved with concrete while the rest of the road is asphalt is that the creep of concrete is much less than that of asphalt, and the prolonged time that buses spend there might otherwise deform the pavement more than is desirable.

As we already mentioned in Sect. 6.1, materials in which the relation between stress and strain is influenced by loading rate are called *rate-dependent*; they are also known as *rate-sensitive*. Many aspects of rate dependence, including but not limited to creep and relaxation, can be described by means of a linear theory, known as *linear viscoelasticity theory*, in which the strain is assumed to depend linearly on the stress *history*, and vice versa. The rate-dependent behavior of polymers, asphalt, concrete

and other materials can often be adequately described, within limits, by this linear theory.

The following discussion will be limited to the case of uniaxial stress but can be extended to other states in the same way as for elastic behavior, as in Sect. 6.2.

It is common to represent inelastic behavior by decomposing the strain additively into an elastic strain ε^{e} and and an inelastic strain ε^{i},

$$\varepsilon = \varepsilon^{\mathrm{e}} + \varepsilon^{\mathrm{i}}, \tag{11.18}$$

where $\varepsilon^{\mathrm{e}} = \sigma/E$. (The plastic strain defined in Sect. 11.1 is a special case of inelastic strain.) Since the decomposition (11.18) introduces the additional variable ε^{i}, it is clear that at least one additional equation are required, and this is usually assumed to be a *rate equation*, that is, a differential equation that determines the rate (time derivative) of the inelastic strain. The simplest such equations are of the form

$$\dot{\varepsilon}^{\mathrm{i}} = g(\sigma, \varepsilon^{\mathrm{i}}). \tag{11.19}$$

A linear form of Eq. (11.19) is provided by the so-called *standard solid* model of viscoelasticity, illustrated by the mechanical model shown in Fig. 11.25a, where each spring represents a linearly elastic (Hookean) relation between its extension and the force acting on it, while the "dashpot" represents a linearly viscous (Newtonian) relation between its extension *rate* and the force acting on it. As in the transition from the behavior of springs to that of elastic solids in Sect. 6.1, so we also suppose here that relation between force and displacement models that between stress and strain. With the extension

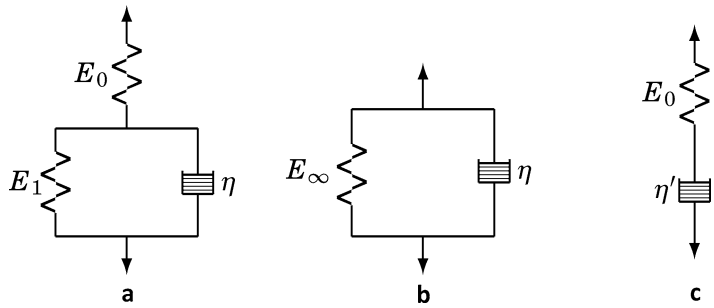

Figure 11.25. Simple models of viscoelasticity: (**a**) standard solid, (**b**) Kelvin, (**c**) Maxwell

of the top spring representing the elastic part $\varepsilon^{\mathrm{e}} = \sigma/E_0$ and with $\varepsilon^{\mathrm{i}} = \varepsilon - \varepsilon^{\mathrm{e}}$, the relation is

$$\sigma = E_0\varepsilon^{\mathrm{e}} = E_1\varepsilon^{\mathrm{i}} + \eta\dot{\varepsilon}^{\mathrm{i}},$$

or

$$\dot{\varepsilon}^{\mathrm{i}} = \frac{1}{\eta}\sigma - \frac{1}{\lambda}\varepsilon^{\mathrm{i}}, \tag{11.20}$$

where η is the viscosity of the dashpot element, and $\lambda = \eta/E_1$ is a characteristic time. Eq. (11.20) is, clearly, the linear form of Eq. (11.19).

Given an input of stress in time, Eq. (11.20) can be solved for $\varepsilon^{\mathrm{i}}(t)$ with the help of the integrating factor $e^{t/\lambda}$:

$$e^{t/\lambda}\varepsilon^{\mathrm{i}}(t) = e^{t_0/\lambda}\varepsilon^{\mathrm{i}}(t_0) + \frac{1}{\eta}\int_{-t_0}^{t} e^{t'/\lambda}\sigma(t')\,dt',$$

where t_0 is an initial time. It is often convenient to let $t_0 = -\infty$, so that the initial condition is unnecessary, and the solution takes the form

$$\varepsilon^{\mathrm{i}}(t) = \frac{1}{\eta}\int_{-\infty}^{t} e^{-(t-t')/\lambda}\sigma(t')\,dt'.$$

Of course, this formulation implies that the stress history must be prescribed for all past times, $-\infty < t' < t$, but in fact the factor $e^{-(t-t')/\lambda}$ in the integrand damps out the values of $\sigma(t')$ for $t - t' \gg \lambda$, so that the strain at time t is not significantly influenced by the stress history in the distant past; this property of materials is known as *fading memory*.

In particular, if $\sigma(t) = 0$ for $t < 0$ and $\sigma(t) = \sigma_0$ (constant) for $t > 0$, then $\varepsilon^{\mathrm{i}}(t) = (1 - e^{-t/\lambda})\sigma_0/E_1$, and the total strain is given by

$$\varepsilon(t) = \left[\frac{1}{E_0} + \frac{1 - e^{-t/\lambda}}{E_1}\right]\sigma_0, \tag{11.21}$$

where the function in brackets is the *creep function*. A plot of strain against time is a *creep curve*—in this case a simple exponential curve with positive but declining slope. At very short times (compared to λ) the inelastic strain is negligible and the body responds like an elastic solid with modulus E_0 (the *instantaneous* or *unrelaxed* modulus); after a very long time, the inelastic strain becomes σ/E_1, so that the total strain becomes $(1/E_0 + 1/E_1)\sigma_0$, and the body again responds like an elastic solid but with the *asymptotic* or *relaxed* modulus $E_\infty = E_0E_1/(E_0 + E_1)$; note that $E_\infty < E_0$.

Let the creep function be denoted $J(t)$, so that the creep strain described by Eq. (11.21) can be written more simply as

$$\varepsilon(t) = \sigma_0 J(t)\,. \tag{11.22}$$

If the stress is removed at a time $t = t_1 > 0$, then the removal is equivalent to the application of a stress $-\sigma_0$ in addition to the previously applied stress σ_0, and the strain at $t > t_1$ is consequently given, in accordance with the principle of superposition, by

$$\varepsilon(t) = \sigma_0[J(t) - J(t - t_1)], \quad t > t_1\,. \tag{11.23}$$

The curves representing Eqs. (11.21) (shown dotted for $t > t_1$) and (11.23) are shown in Fig. 11.26. The solid curve for $t > t_1$ represents *creep recovery*.

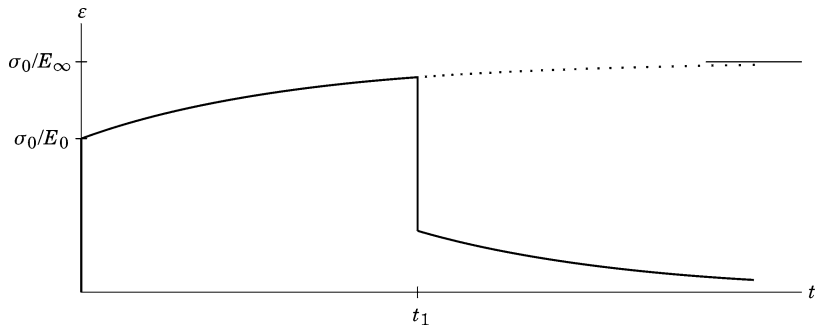

Figure 11.26. Creep and creep recovery

Some limiting cases of the standard solid model are also shown in Fig. 11.25. Fig. 11.25b shows the *Kelvin* (or *Kelvin–Voigt*) model, corresponding to the limit as $E_0 \to \infty$; here the deformation has no instantaneous elastic response but exhibits *delayed elasticity* with the asymptotic modulus E_∞; the governing equation is

$$\sigma = E_\infty \varepsilon + \eta \dot{\varepsilon},$$

and the creep function is $(1 - e^{-t/\lambda})/E_\infty$.

The case $E_1 = 0$ with E_0 finite represents the *Maxwell* model, shown in Fig. 11.25c, in which the instantaneous response is that of an elastic solid, but the asymptotic response is that of a viscous fluid, and creep curves are straight lines, the creep function being $1/E_0 + t/\eta$, as may derived from that of the standard solid in the limit as $\lambda \to 0$, or directly from the governing equation

$$\dot{\varepsilon} = \frac{\dot{\sigma}}{E_0} + \frac{\sigma}{\eta}.$$

In order to obtain the stress response to a given strain history for the standard solid model, it is necessary to eliminate the inelastic strain in order to obtain a relation between the stress, the total strain, and their rates; this relation becomes a differential equation for the stress when the strain is a given function of time, and in the particular case where $\varepsilon(t) = 0$ for $t < 0$ and $\varepsilon(t) = \varepsilon_0$ (constant) for $t > 0$, the result is

$$\sigma(t) = \left[E_\infty + (E_0 - E_\infty) e^{-t/\lambda'} \right] \varepsilon_0,$$

where $\lambda' = (E_\infty/E_0)\lambda = \eta/(E_0 + E_1)$, and the function in brackets is the *relaxation function* (or *relaxation-modulus function*) corresponding to the standard solid model; λ' if often called the *relaxation time*. For the special case of the Maxwell model, the relaxation function is $E_0 e^{-t/\lambda'}$, with the relaxation time $\lambda' = \eta/E_0$. The Kelvin model, on the other hand, has no relaxation function, since it cannot be subjected to an arbitrary strain input—in particular, an input in which the strain is discontinuous in time, requiring an infinite stress.

The simple exponential curve of the standard solid and Kelvin models describes creep that is *bounded*, while the straight line of the Maxwell model describes *unbounded* creep. More complicated models can be formed by combining a number of simple models with different values of the parameters, either Maxwell models in parallel (the *generalized Maxwell model*) or Kelvin models in series (the *generalized Kelvin model*), possibly with an additional spring and/or dashpot. Asymptotically, however, the creep curves produced by these models are the same as those of the simple models, namely, straight lines with either zero slope (bounded creep) or positive slope (asymptotically steady creep). Many solids, however, exhibit long-time creep which is unbounded, but at an ever-decreasing rate, for example as $\log t$ or t^α. Such materials the long-time response cannot be represented by the functions derived from spring-dashpot models. But of course it is always possible to describe the experimentally observed creep curve by some function by means of curve-fitting.

The principle of superposition (Sect. 6.2.4) can be applied to the behavior of linearly viscoelastic solids as a superposition *over time*, and in this form it is known as the *Boltzmann*[**] *superposition principle*. In accordance with Eq. (11.22), a stress increment $d\sigma(t')$ applied at a past time t' produces, at the present time t, the strain increment $d\varepsilon(t) = J(t-t')d\sigma(t')$. Consequently the strain due to an arbitrary stress history is

$$\begin{aligned}\varepsilon(t) &= \int_{-\infty}^{t} J(t-t')\,d\sigma(t') \\ &= J(0)\sigma(t) + \int_{-\infty}^{t} \dot{J}(t-t')\sigma(t')\,dt,\end{aligned} \tag{11.24}$$

where $\dot{J} = dJ/dt$; the two expressions can be obtained from each other by integration by parts.

Similarly, if the relaxation function is denoted $R(t)$, then then for an arbitrary strain history $\varepsilon(t)$ the stress response is

$$\begin{aligned}\sigma(t) &= \int_{-\infty}^{t} R(t-t')\,d\varepsilon(t') \\ &= R(0)\varepsilon(t) + \int_{-\infty}^{t} \dot{R}(t-t')\varepsilon(t')\,dt.\end{aligned} \tag{11.25}$$

By combining the two superpositions it can be shown that the creep and relaxation functions are related to each other by

$$\int_0^t R(t')J(t-t')\,dt' = t. \tag{11.26}$$

From this relation follow the results

$$\lim_{t\to 0} R(t)J(t) = \lim_{t\to\infty} R(t)J(t) = 1, \tag{11.27}$$

[**]Ludwig Boltzmann (1844–1906) was an Austrian physicist

and if $J(0) > 0$ then $R(0) = 1/J(0)$ is the instantaneous elastic modulus E_0, while if $J(\infty) < \infty$ then $R(\infty) = 1/J(\infty)$ is the asymptotic elastic modulus E_∞.

Exercises

11.2-1. A long cylindrical pressure vessel, or mean radius r and wall-thickness t (with $t << r$), is subjected to an internal pressure p and an axial force P. If the uniaxial yield stress is σ_Y, find the relation between p and P at yield according to (a) the Mises criterion, (b) the Tresca criterion.

11.2-2. A long cylindrical pressure vessel, or mean radius r and wall-thickness t (with $t << r$), is subjected to an internal pressure p and a torque T. If the yield stress in shear is τ_Y, find the relation between p and T at yield according to (a) the Mises criterion, (b) the Tresca criterion.

11.2-3. Consider a ductile solid in a state of triaxial compression such that $\sigma_2 = \sigma_3 = -p$ (where p is the confining pressure) and $\sigma_1 = \sigma$ (where σ is the applied compressive stress). If the uniaxial yield stress is σ_Y, find the value of σ required for the yielding of the confined solid according to (a) the Mises criterion, (b) the Tresca criterion.

11.2-4. Derive Eqs. (11.12) and (11.13) from Eq. (11.11).

11.2-5. For a material governed by the Mohr–Coulomb criterion in which the yield stresses in tension and compression are found to be σ_Y^{t} and σ_Y^{c}, respectively, find the yield stress in simple shear in terms of σ_Y^{t} and σ_Y^{c}.

11.2-6. For a material governed by the Mohr–Coulomb criterion in which the yield stresses in tension and compression are found to be σ_Y^{t} and σ_Y^{c}, respectively, show that the angle of internal friction is given by $\phi = \sin^{-1}[(\sigma_Y^{\mathrm{c}} - \sigma_Y^{\mathrm{t}})/(\sigma_Y^{\mathrm{c}} + \sigma_Y^{\mathrm{t}})]$.

11.2-7. Do Exercise **11.2-3** for the Mohr–Coulomb criterion with the compressive yield stress σ_Y^{c} and the angle of internal friction ϕ as parameters.

11.2-8. For the twisted piece of chalk of Fig. 11.22, show the sense of the torque that produced the fracture.

11.2-9. If the Tresca hexagon in Fig. 11.23 is replaced by a Mises ellipse, find the combinations of σ_1 and σ_2 at which, as the temperature drops, the Mises yield criterion first coincides with brittle fracture.

11.2-10. Show that if a Maxwell element with a spring of modulus E_0' and a dashpot of viscosity η' is placed in parallel with a spring of modulus E_∞, the resulting model is equivalent to the standard solid shown in Fig. 11.25a. Find the relations between the parameters of the respective models.

11.3 Structural failure

11.3.1 Introduction

As we discussed in Sect. 3.1, if, in an articulated assemblage of rigid (or quasi-rigid) members, the number of members is insufficient to satisfy Eq. (3.1) (in two dimensions) or (3.2) (in three dimensions), then the assemblage becomes a mechanism. If the assemblage is, to begin with, a statically determinate load-carrying structure, then it collapses as soon as one member fails. By *failure* we mean not only outright fracture or rupture (in which case the member, in effect, ceases to exist) but also deformation large enough so that the member can no longer be regarded as rigid—whether by yielding (if the member is made of a ductile material) or buckling (if it is a slender compression member)—and the geometry of the structure is changed to a significant degree. We can think of such a change as constituting a partial collapse, while fracture or rupture can bring about a total collapse. Moreover, a member that has yielded or buckled maintains, at least initially, the capacity of transmitting a load. This is why, as we mentioned at the end of the preceding section, brittle failure is usually much more catastrophic than yielding.

For a statically determinate structure carrying a single load (or, if there are additional loads, these are all proportional to the nominal load), the principle of least resistance dictates that the ultimate load (collapse load or failure load) is the smallest load required for the failure of any one member. The first member to fail is, of course, the weakest member for the given loading, and the principle of least resistance can here also be referred to here as that of the weakest link, by analogy with the fact that a chain carrying a load at its end breaks when the weakest link fails.

The following example demonstrates the failure of a simple truss.

Example 11.3.1: Collapse of a simple truss.
Let us consider the simple truss shown in Fig. 11.27a. We will assume that

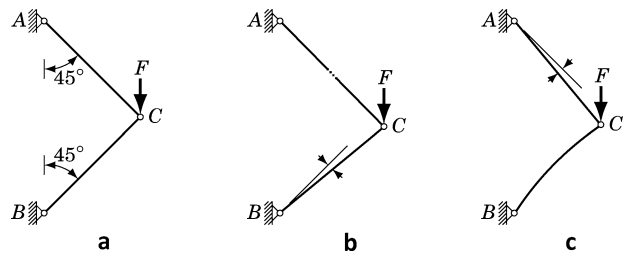

Figure 11.27. Collapse of a simple truss: (**a**) initial configuration, (**b**) failure (yielding or fracture) of tension member AC, (**c**) buckling of compression member BC

the compression member BC is slender, so that it will buckle before undergoing

material failure. The truss will collapse either if the tension member AC fails (either by yielding or by brittle fracture, depending on the material), as shown in Fig. 11.27b, or if the compression member buckles, as in Fig. 11.27c. In either case the structure becomes a mechanism with one degree of freedom: in the former case joint C rotates about B, and in the latter case about A. An elementary analysis by the method of joints gives $P_{AC} = F/\sqrt{2}$ and $P_{BC} = -F/\sqrt{2}$ The structure will consequently collapse when $F/\sqrt{2}$ reaches the smaller of $P^{\mathrm{t}}_{\mathrm{cr}(AC)}$ and $P^{\mathrm{c}}_{\mathrm{cr}(BC)}$, being respectively the tensile breaking or yield force in AC and the buckling load of BC. That is, the ultimate load is given by

$$F_U = \sqrt{2}\min\left(P^{\mathrm{t}}_{\mathrm{cr}(AC)},\, P^{\mathrm{c}}_{\mathrm{cr}(BC)}\right) .$$

As we already noted in Sect. 2.2, a statically determinate structure can also be turned into a mechanism by increasing the number of joints and/or reducing the number of constraints; either way, the left-hand side of Eq. (3.1) (page 111) becomes smaller than the right-hand side. Obviously, if one of the pin supports in the preceding example were to become a roller, the assemblage would collapse, as it would if the pin at C were to fail. Collapse through the formation of internal degrees of freedom is especially important in the case of beams, as we indicated in Sect. 2.2 (page 72) and as we will now discuss.

11.3.2 Failure of Beams

The simplest way to understand the failure of a beam is to grab a wooden stick by its ends and bend it over your knee (it is then, practically speaking, a simply supported beam with a concentrated load) until it breaks. Typically, the break will not be complete: some fibers on what was the compression edge will remain unbroken and keep the two halves of the stick connected, but these halves can now be rotated with respect to each other, with the unbroken fibers acting like a hinge, as shown in Fig. 11.28a. If a similar experiment is done

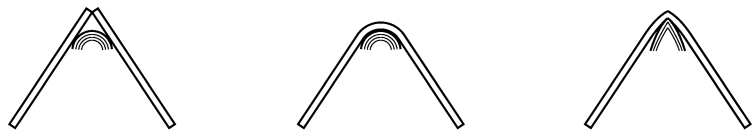

Figure 11.28. Beam failure by hinge formation: (**a**) fracture hinge, (**b–c**) plastic hinge

with a thin steel or aluminum rod, then the rod will bend around the knee, as in Fig. 11.28b. If, however, the rod (or a piece of copper tubing, or even a short piece of wire) is bent around an object presenting a corner, as in Fig. 11.28c, then a kink will form, acting almost like a hinge (with some, but not much, resistance) in the direction of continued bending, though not necessarily in that of straightening. The phenomena illustrated in Figs. 11.28a and 11.28c involve the formation of a fracture hinge and a plastic hinge, respectively.

The formation of a fracture hinge can be understood by simply considering that, in a material whose tensile strength is less than its compressive strength, at the section of greatest bending moment the outermost tensile fibers will break when the critical stress is reached, correspondingly increasing the stress in the neighboring fibers so that they also break, and so on, until the capacity to carry a transverse load is lost. The moment required to produce the hinge (the *ultimate moment*, denoted M_U) is therefore the moment at which the ultimate tensile stress σ_U^{t} is first reached, and can be assumed to be given by

$$M_U = S\sigma_U^{\mathrm{t}} , \tag{11.28}$$

where S is the section modulus, even if the material behavior is not strictly elastic up to fracture. If σ_U^{t} is taken to be the modulus of rupture discussed in Sect. 8.3 (page 381), then Eq. (11.28) is of course valid by definition.

The conventional theory of the plastic hinge is based on the elastic–perfectly plastic model illustrated in Fig. 11.12 (page 481). If the behavior at any section of the beam is assumed to be like that in pure bending (as discussed in Sect. 8.2), then the longitudinal strain ε_x is given by Eq. (8.17) (page 368), that is, its variation with respect to y is linear. Consequently, so is the variation of the axial stress σ_x (given by Eq. (8.20), page 369) as long as the material in the entire section is linearly elastic, that is, as long as $\sigma_{\max} < \sigma_Y$. This also means, by Eq. (8.27) (page 370), that $|M| < S\sigma_Y \stackrel{\text{def}}{=} M_Y$. When this value of the moment (the *yield moment*) is exceeded, the distribution of stress begins to resemble the stress-strain diagram of Fig. 11.12: in the outer fibers (those where $|\varepsilon_x| > \sigma_Y/E$, constituting the *plastic zones*) the stress is constant at $\pm\sigma_Y$, while in the *elastic core* is still varies linearly with y. As the moment is increased, more stress is required to resist it, and the plastic zones expand inward while the elastic core shrinks. In general, the neutral axis may move during this process, but if we limit ourselves to sections in which symmetry guarantees that $y_0 = 0$ (where, as in Sect. 8.2.1, y_0 denotes the y-coordinate of the neutral fibers), then, since $\varepsilon_x = -\kappa y$, the boundary between the elastic core and the plastic zones is given by $y = \pm y_p$, where $y_p = \sigma_Y/E|\kappa|$. The ultimate moment M_U thus corresponds to the state at which the elastic core has shrunk to a negligible thickness and hence, in accordance with the last formula, the curvature approaches infinity. An infinite curvature corresponds to a discontinuity in the slope, that is, a kink in the deflected shape of the beam, and this is just what is meant by a plastic hinge as seen in Fig. 11.28c.

The value of the ultimate moment can be easily calculated from the fact that, if the yield stress is the same in tension and compression, the vanishing of the axial force means that in the ultimate state one half of the area is in tension and the other half is in compression. Now, the resultant forces of magnitude $\sigma_Y A/2$ act at the centroids of the half-areas, and if the distance

between these centroids is d, then

$$M_U = \sigma_Y A d/2 \,. \tag{11.29}$$

The quantity $M_U/\sigma_Y = Ad/2$ is often called the *plastic modulus* of the section and is denoted Z. In a rectangular beam with a cross-section of width b and height h (with the latter dimension parallel to the plane of bending), $A = bh$ and $d = h/2$, so that $Z = bh^2$. Since for such a beam the elastic section modulus is $S = bh^2/6$, the ratio of ultimate moment to yield moment is $M_U/M_Y = Z/S = 1.5$. In general this ratio depends on the shape of the cross-section and is accordingly known as the *shape factor*. It tends to be larger than 1.5 if there is more material near the neutral plane (where the stress is low) than away from it, and smaller (though never less than 1) if there is more material in the zones of high stress; for I-beams bending around the strong axis it typically ranges between 1.1 and 1.2. The successive stress distributions as the moment is increased are shown in Fig. 11.29. At each of

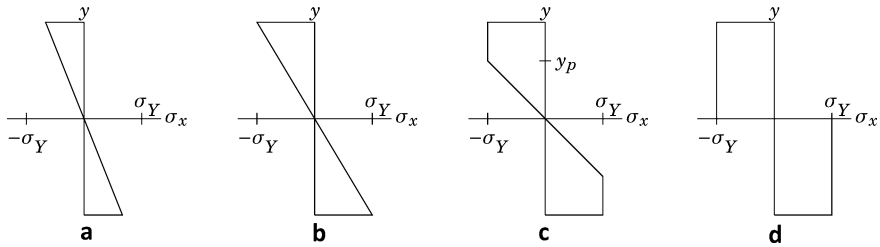

Figure 11.29. Stress distributions in an elastic–perfectly plastic beam under increasing moment: (a) $M < M_Y$, (b) $M = M_Y$, (c) $M_Y < M < M_U$, (d) $M = M_U$

the states represented in Fig. 11.29c we can calculate not only the moment but also the curvature κ, on the basis of the definition of y_p. In particular, when $y_p = h/2$, $|\kappa| = 2\sigma_Y/Eh \stackrel{\text{def}}{=} \kappa_Y$, so that we can also write $y_p = h\kappa_Y/2|\kappa|$. For a rectangular cross-section the moment for $0 < y_p < h/2$ (or, equivalently, $|\kappa| > \kappa_Y$) can be shown to be

$$M = \sigma_Y b \left(\frac{h^2}{4} - \frac{y_p^2}{3} \right) = M_U \left[1 - \frac{1}{3} \left(\frac{\kappa_Y}{\kappa} \right)^2 \right] . \tag{11.30}$$

In the elastic range ($M < M_Y$, $\kappa < \kappa_Y$), the moment-curvature relation (8.24) (page 369) can be replaced by $M = (M_Y/\kappa_Y)\kappa$, and it can be represented graphically together with Eq. (11.30) as in Fig. 11.30.

Note that the ultimate moment is attained asymptotically as the curvature goes to infinity, consistent with our previous characterization of a plastic hinge. Since a statically determinate structure turns into a mechanism as soon as one hinge is added, a statically determinate beam collapses as soon

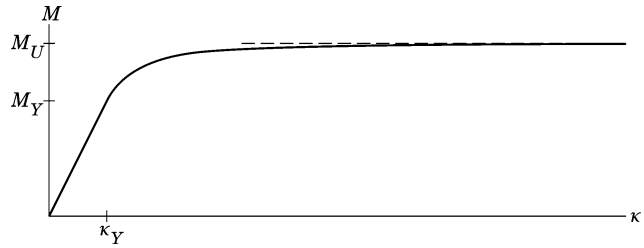

Figure 11.30. Elastic–perfectly plastic moment-curvature relation for a rectangular beam

as the ultimate moment is reached at one section, that is, when

$$M_{\max} = M_U \,, \tag{11.31}$$

where, as in Chapter 8, $M_{\max}$ is written to mean $|M|_{\max}$.

Example 11.3.2: Collapse loads for various statically determinate beams. We will apply Eq. (11.31) to determine the collapse loads of the most common cases of statically determinate beams, as considered in Examples 8.1.1–8.1.4 (pages 355–357).

- Simply supported beam with a uniformly distributed load: $(q_0 L)_U = 8M_U/L$.
- Cantilever beam with a uniformly distributed load: $(q_0 L)_U = 2M_U/L$.
- Cantilever beam with a point load at a distance a from the built-in end: $F_U = M_U/a$.
- Simply supported beam with a point load at a distance a from one of the supports: $F_U = M_U L/a(L-a)$.

11.3.3 Effect of Static Indeterminacy

When a statically indeterminate structure becomes inelastic, the governing equations are no longer linear, and the reactions and member forces no longer vary linearly with the applied loads. It thus becomes very difficult to determine the stresses, and stress-based design is no longer practicable. What is done instead is to determine the collapse load (or ultimate load) and to design the structure by applying an appropriate safety factor to the load rather than to the stress. (As we mentioned in Sect. 4.3, in statically determinate structures stress factor and load factor are equivalent, while in statically indeterminate structures the redundancy allows the structure to remain stable even if some members or connections have failed.)

For the determination of collapse loads in statically indeterminate structures, it is convenient to use the principle of virtual work, Eq. (2.30), by assuming a possible mechanism and expressing the displacement conjugate

to the applied load, as well as the elongations of the failed axial members and the rotations in the plastic hinges, in terms of the degree of freedom corresponding to the given mechanism. As before, it is assumed that collapse occurs before any significant change in the geometry of the structure, and that elastic deformation can be ignored.

Example 11.3.3: Collapse of a statically indeterminate assemblage. Let us suppose that the truss of Fig. 11.27a is modified by adding a bar CD, as shown in Fig. 11.31a. If the angle of rotation about B shown in the mechanism

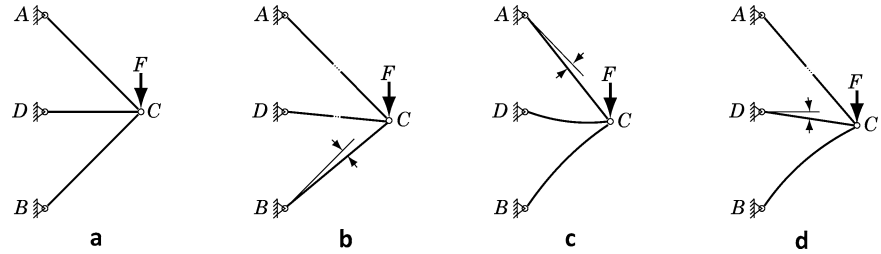

Figure 11.31. Statically indeterminate assemblage: (**a**) initial configuration, (**b–d**) possible collapse mechanisms and their corresponding degrees of freedom

of Fig. 11.31b is θ, and if the lengths $\overline{AD}$, $\overline{BD}$ and $\overline{CD}$ are all equal to L (so that $\overline{AC} = \overline{BC} = \sqrt{2}L$), then the downward virtual displacement of C is $L\delta\theta$, as is the virtual elongation of member CD, while that of AC is $\sqrt{2}L\delta\theta$, as seen in the figure.

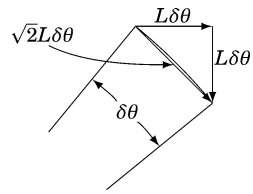

Consequently,

$$FL\delta\theta \;=\; P^{\mathrm{t}}_{\mathrm{cr}(AC)}\sqrt{2}L\delta\theta + P^{\mathrm{t}}_{\mathrm{cr}(CD)}L\delta\theta \;,$$

and after we divide by the common factor $L\delta\theta$ we obtain $F = \sqrt{2}P^{\mathrm{t}}_{\mathrm{cr}(AC)} + P^{\mathrm{t}}_{\mathrm{cr}(CD)}$. A similar analysis of the other two mechanisms leads to

$$F_U \;=\; \min\left[(\sqrt{2}P^{\mathrm{t}}_{\mathrm{cr}(AC)} + P^{\mathrm{t}}_{\mathrm{cr}(CD)}),\; (\sqrt{2}P^{\mathrm{c}}_{\mathrm{cr}(BC)} + P^{\mathrm{c}}_{\mathrm{cr}(CD)}),\; (P^{\mathrm{t}}_{\mathrm{cr}(AC)} + P^{\mathrm{c}}_{\mathrm{cr}(BC)})/\sqrt{2}\right] .$$

It should be noted that in the absence of the bar CD, that is, when $P^{\mathrm{t}}_{\mathrm{cr}(CD)} = P^{\mathrm{c}}_{\mathrm{cr}(CD)} = 0$, this result is the same as that of Example 11.3.1, since the third quantity in the brackets is then the average of the first two and hence cannot be less than the smaller of them.

The collapse of beams occurs, as discussed above, through the formation of plastic hinges, and in statically indeterminate beams the number of plastic hinges must be sufficient to create a mechanism. This means that there needs to be one more plastic hinge than the degree of static indeterminacy. In some cases only one mechanism is possible; in other cases, a finite number of mechanisms, as in the preceding example; and in yet other cases, when distributed loads are present, there is an infinity of possible mechanisms. The principle of least resistance is used to find the actual collapse mechanism. The first and third of these types of cases will be illustrated in the following examples.

Example 11.3.4: Collapse of a statically indeterminate beam carrying a concentrated load.
The beam shown in Fig. 11.32a is statically indeterminate of degree 1 (see page 111), and therefore, if the material is assumed to be elastic–perfectly plastic, collapse requires two plastic hinges. Given the nature of the supports and loading,

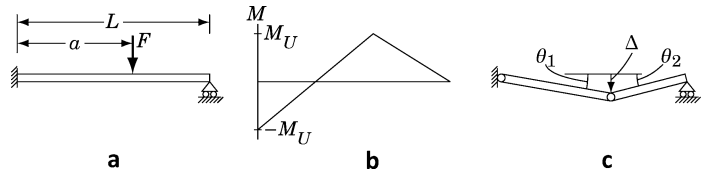

Figure 11.32. Statically indeterminate beam carrying a concentrated load: (**a**) geometry and loading, (**b**) moment diagram at collapse, (**c**) collapse mechanism

the only possible locations of the hinges are the two points at which the moment attains a local maximum, namely, the built-in end and the load point. We further know, from the expected deflection, that these moments are negative and positive, respectively. The moment diagram at collapse is therefore necessarily that shown in Fig. 11.32b. The shear force in the segment between the hinges is therefore, by Eq. (8.5) (page 354), given by $V = -2M_U/a$, and the force reaction at the left end is accordingly $2M_U/a$ (upward). The condition of zero moment at the roller then implies

$$M_U - (2M_U/a)L + F(L-a) \;=\; 0\,,$$

from which we obtain the collapse load as

$$F_U \;=\; M_U \frac{2L-a}{a(L-a)}\,.$$

If we wish to apply the principle of virtual work to this problem, we observe from the geometry of the collapse mechanism shown in Fig. 11.32c that, as long as the deflection Δ is small, the angles shown are

$$\theta_1 \doteq \frac{\Delta}{a} \quad , \quad \theta_2 \doteq \frac{\Delta}{L-a}\,.$$

Now, the angles of rotation of the two hinges are θ_1 and $\theta_1+\theta_2$, respectively, so that the internal virtual work in a virtual displacement $\delta\Delta$ is

$$\delta W_{\text{int}} = M_U\left(\frac{2}{a}+\frac{1}{L-a}\right)\delta\Delta\ . \tag{11.32}$$

Equating this to the external virtual work $F\delta\Delta$ loads to the same collapse load as before.

Example 11.3.5: Collapse of a statically indeterminate beam carrying a distributed load.
When a beam with the same supports as in the previous example carries a uniformly distributed load as shown in Fig. 11.33a, we know that the moment diagram has a parabolic shape and that at collapse it will have the form shown in Fig. 11.33b, but the location of plastic hinge in the interior of the beam (that is, the distance a shown in the figure) is not known. Wherever that hinge is,

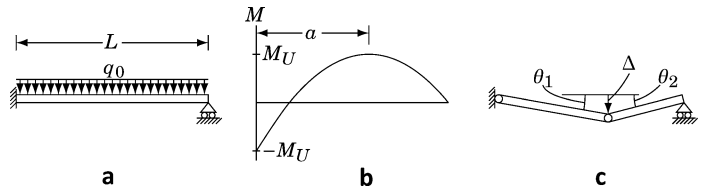

Figure 11.33. Statically indeterminate beam carrying a uniformly distributed load: (**a**) geometry and loading, (**b**) moment diagram at collapse, (**c**) collapse mechanism

the collapse mechanism will be the one shown in Fig. 11.33c, the same as in Fig. 11.32c, and the internal virtual work is given by Eq. (11.32). The external virtual work in a virtual displacement $\delta\Delta$ is $\frac{1}{2}q_0L\delta\Delta$, since the the resultant of the distributed load on each segment has undergoes the displacement $\frac{1}{2}\Delta$. Consequently the collapse load, for a given value of a, is

$$(q_0L)_{Ua} \;=\; 2M_U\frac{2L-a}{a(L-a)}\ .$$

We now invoke the principle of least resistance: we expect that, as load is gradually increased, as soon as *some* value of a exists for which a collapse mechanism can form, and this value is that which corresponds to the smallest $(q_0L)_{Ua}$ given by the preceding equation. The fraction on the right-hand side can be rewritten as $\dfrac{2}{a}+\dfrac{1}{L-a}$, and minimizing this with respect to a leads to

$$-\frac{2}{a^2}+\frac{1}{(L-a)^2} \;=\; 0\ ,$$

or, equivalently, to $a^2=2(L-a)^2$, which can be rewritten as the quadratic equation $a^2-4La+2L^2=0$. The only solution for a between 0 and L is $(2-\sqrt{2})L$, and inserting this value into the expression for $(q_0L)_{Ua}$ yields $(q_0L)_U = 11.66M_U/L$

11.3.4 Torsional Failure

The failure of shafts undergoing torsion can be analyzed in a similar manner to that of beams. If the shaft material is brittle, then, as we discussed in Sect. 11.2 (page 492), the failure is in tension. Thus, when at the points of maximum shear stress the critical value is reached, the material there undergoes fracture on planes that, locally, are at 45°to the shaft axis. The fracture reduces the amount of material capable of resisting the torque and hence increases the stress there, and so on, so that the fracture will quickly propagate until the entire shaft breaks on a helical surface, as illustrated in Fig. 11.22.

If the shaft material is ductile and is modeled as elastic–perfectly plastic, then, if T_Y denotes (by analogy with M_Y) the torque at which the maximum shear stress in the cross-section first attains τ_Y, then as torque is increased above T_Y a plastic zone forms and spreads. In a circular cross-section this zone is an annulus, but otherwise it will, at least at first, consist of two or more disconnected regions. As the plastic zone spreads the elastic core shrinks. In a solid shaft it shrinks to a point, which is when the ultimate or fully plastic state is reached; the torque is then the ultimate torque T_U. In a hollow shaft, on the other hand, this state as reached when the elastic-plastic boundary coincides with the inner boundary of the shaft.

What characterizes the ultimate state is that the magnitude of the shear stress (viewed as a vector, as in Sect. 4.2, page 163) is everywhere equal to τ_Y. In terms of the Prandtl stress function discussed in Example 4.5.3 (page 192), this means that

$$\sqrt{\left(\frac{\partial \chi}{\partial x}\right)^2 + \left(\frac{\partial \chi}{\partial y}\right)^2} \;=\; \tau_Y \;. \tag{11.33}$$

But if we envision a surface in xyz-space described by $z = \chi(x, y)$, the left-hand side of Eq. (11.33) gives the slope of the surface, and if χ is required to be zero on the outer boundary (so that the torque is given by Eq. (4.44)), then such a surface can be obtained experimentally by heaping sand onto a horizontal figure having the shape of the cross-section until the maximal heap is reached, with any further sand sliding off. The angle formed by such a heap is known as the *angle of repose*, but in the case of sand it is the same as the angle of internal friction discussed in Sect. 11.2 (page 491), and the slope is therefore equal to the coefficient of internal friction μ. If, then, the volume of the heap is V, then the torque is, by Eq. (4.44) (page 193) and with scaling, given by $2(\tau_Y/\mu)V$. The correspondence between the ultimate state of the cross-section in torsion and the heaping of sand is referred to as the *sand-heap analogy*.

If the cross-section has the shape of a convex polygon, then the maximal sand heap takes the form of a solid whose plan view, in general, is like the one shown in Fig. 11.34a. The slope is the same on all sides, with the light

lines representing contours (lines joining points of equal elevation), while the heavy lines represent ridge lines where the slope changes abruptly. If the polygon is regular, then the solid is a pyramid, as shown in Fig. 11.34b.

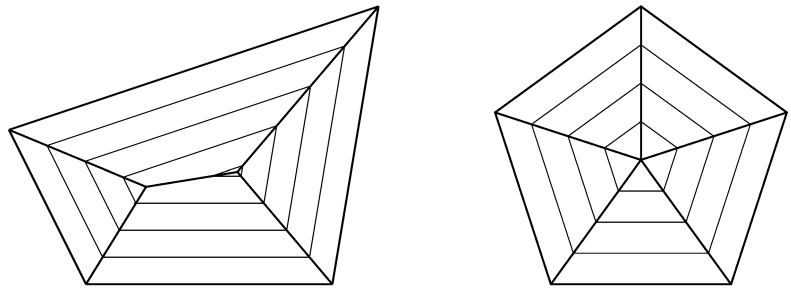

Figure 11.34. Ridge lines and contours of the maximal sand heap on a convex polygon: (**a**) irregular, (**b**) regular

The limit of a regular polygon as the number of sides goes to infinity is of course a circle, and for a solid circular cross-section of radius c, the maximal sand heap is therefore a cone of height μc, with volume equal to $\pi\mu c^3/3$. The ultimate torque is therefore

$$T_U = 2\pi c^3 \tau_Y/3 \,. \tag{11.34}$$

We would obtain the same result, of course, by setting $\tau(r) = \tau_Y$ in Eq. (7.3) (page 324) with $b = 0$. The yield torque is obtained by setting $\tau_{\max}$ as given by Eq. (7.13) (page 327) equal to τ_Y, resulting in

$$T_Y = \pi c^3 \tau_Y/2 \,. \tag{11.35}$$

The shape factor for a circular cross-section is thus 4/3.

Lastly, the sand-heap analogy can be combined with the membrane analogy discussed in Sect. 7.4 (page 347) to study the partially plastic state of the shaft (when $T_Y < T < T_U$). To that end, we envision a roof whose shape is that of the ultimate sand heap, and then begin to pressurize, from below, an initially horizontal soap film. The onset of plasticity corresponds to the moment when the film begins to adhere to the underside of the roof. As the pressure is further increased, the zone of adhesion represents the plastic zone, and the free membrane the elastic core. For circular shafts it is simple to derive a torque-twist relation analogous to the moment-curvature relation for a beam. For a solid cross-section the resulting diagram is quite similar to Fig. 11.30, except for the different shape factor. For a hollow cross-section, on the other hand, the ultimate torque is attained not asymptotically but at a finite value of the twist ϕ'. For comparison, the torque–twist diagrams for a solid circular shaft of outer radius c and a hollow one with inner radius $b = c/2$ are shown in Fig. 11.35.

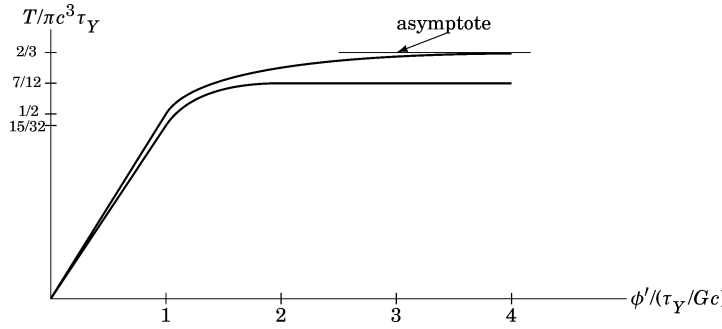

Figure 11.35. Elastic–plastic torque–twist diagram for circular shafts, solid ($b = 0$) and hollow ($b = c/2$)

Exercises

11.3-1. By analogy with Example 11.3.1, find the collapse value of the load F in the simple truss shown in the figure.

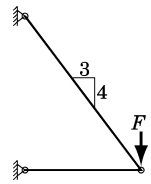

11.3-2. Explain qualitatively why the shape factor M_U/M_Y should be less for an I-beam than for a rectangular beam.

11.3-3. Determine the shape factor M_U/M_Y for a beam of solid cross-section.

11.3-4. Determine the shape factor M_U/M_Y for a beam with a cross-section of a circular tube whose inner diameter is half the outer diameter.

11.3-5. Determine the shape factor M_U/M_Y for a beam of square cross-section bending in the plane of the diagonal.

11.3-6. Determine the shape factor M_U/M_Y for the I-beam of Exercise **8.2-10** (page 378).

11.3-7. Determine the shape factor M_U/M_Y for the box beam having the dimensions of the one in Example 9.3.4 (page 427).

11.3-8. Derive Eq. (11.30) for the moment at a section of a rectangular beam that is partly plastic.

11.3-9. Show that the curve of representing Eq. (11.30) has the same slope at (M_Y, κ_Y) as the elastic line.

11.3-10. For the beam in Example 11.3.4, find the value of a/L for which F_U is smallest.

11.3-11. Replace the beam shown in Fig. 11.32a (Example 11.3.4) by one that is built in at both ends, and find the corresponding value of F_U.

11.3-12. Replace the beam shown in Fig. 11.33a (Example 11.3.5) by one that is built in at both ends, and find the corresponding value of $(q_0 L)_U$.

11.3-13. Determine the ultimate torque, yield torque and torsional shape factor T_U/T_Y for a hollow circular shaft of outer radius c and inner radius b.

11.3-14. Find the torque-twist relation for the shaft of the preceding exercise, and draw the diagram representing it for $b = c/2$.

11.3-15. Determine the ultimate torque T_U for a shaft of square cross-section with sides of length a.

Appendix A: Singularity Functions

Singularity functions are used in the solution of differential equations in which the known terms are non-smooth in the independent variable. In particular, these functions are particularly useful in the study of bars, shafts and beams subjected to non-smooth loading, such as point loading and distributed loading that exhibits finite jumps. Indeed, singularity functions permit the direct use of equations such as (6.86), (7.49), (8.2), (8.5), (8.6), (8.75) and (8.82) when determining axial-force, torque, bending-moment and shear distributions, as well as deflections in beams with such non-smooth loading.

One of the most common singularity functions is the *Heaviside*[*] *step function* $H(x)$, defined as

$$H(x) = \begin{cases} 0, & x < 0 \\ 1, & x > 0 \end{cases} , \tag{A.1}$$

and shown in Fig. A.1. Note that the Heaviside function $H(x)$ is undefined at $x = 0$, although it is sometimes taken to be equal to $\frac{1}{2}$. Clearly, the Heaviside

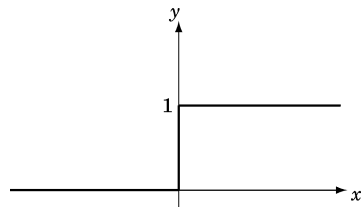

Figure A.1. The Heaviside step function $H(x)$

function $H(x-a)$ is analogous to the function plotted in Fig. A.1, only shifted so as to undergo the step at $x = a$.

The integral of the Heaviside step function is the *ramp function* written as $<x>$, where $<\cdot>$ are known as the *Macaulay*[†] *brackets*. With Eq. (A.1) taken into account, the ramp function is given by

$$<x> = \begin{cases} 0, & x \le 0 , \\ x, & x > 0 , \end{cases} \tag{A.2}$$

and plotted in Fig. A.2.

It is easy to see that the ramp function can be raised to any positive power, with

$$<x>^n = \begin{cases} 0, & x \le 0 , \\ x^n, & x > 0 . \end{cases} \tag{A.3}$$

[*]Oliver Heaviside (1850-1925) was a self-taught British engineer, mathematician and physicist.

[†]Francis Sowerby Macaulay (1862-1937) was a British mathematician

© Springer International Publishing Switzerland 2017

J. Lubliner, P. Papadopoulos, *Introduction to Solid Mechanics*,
DOI 10.1007/978-3-319-18878-2

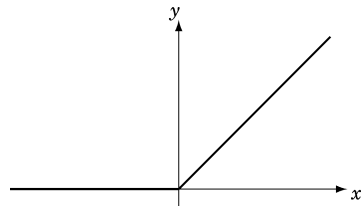

Figure A.2. The ramp function $<x>$

and that, for $n > 1$,

$$\frac{d}{dx}<x>^n = n<x>^{n-1}, \tag{A.4}$$

while[‡]

$$\frac{d}{dx}<x> = H(x) \tag{A.5}$$

and, for $n > 0$,

$$\int <x>^n dx = \frac{1}{n+1}<x>^{n+1}. \tag{A.6}$$

While $H(x)$ does not have a derivative in the usual sense of a smooth function, such a derivative can be defined as what in mathematics is termed a *distribution* from the limit of a sequence of continuous approximations to the discontinuous step function, as shown, for example, in Fig. A.3. The

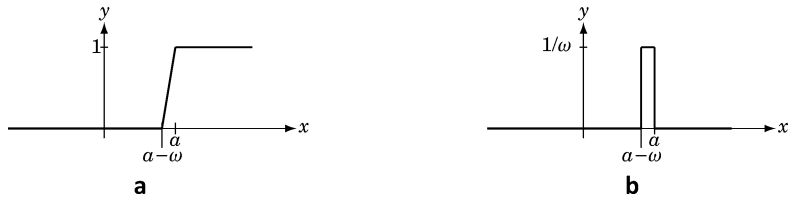

Figure A.3. Ramp approximation to the step function and its derivative

function depicted in Fig. A.3a may be expressed as

$$H_\omega(x-a) = \frac{1}{\omega}[<x-a+\omega> - <x-a>], \tag{A.7}$$

and it becomes $H(x-a)$ in the limit as $\omega \to 0$, that is,

$$H(x-a) = \frac{d<x-a>}{dx}. \tag{A.8}$$

The derivative of $H_\omega(x-a)$ (depicted in Fig. A.3b) is, in accordance with Eq. (A.5),

$$\frac{d}{dx}H_\omega(x-a) = \frac{1}{\omega}[H(x-a+\omega) - H(x-a)], \tag{A.9}$$

[‡]In some books the Heaviside function is written as $<x>^0$ (so that Eq. (A.4) would seem to apply also when $n = 1$), but this notation leads to the indeterminate 0^0 for $x \le 0$.

and in the limit as $\omega \to 0$ it formally becomes (by the standard definition of the derivative) the derivative of $H(x-a)$, that is,

$$\frac{d}{dx}H(x-a) \;=\; \delta(x-a)\,. \tag{A.10}$$

(What happens is that, as ω decreases, the rectangle in Fig. A.3b becomes narrower and taller, but its area remains 1, as can be seen from the figure.) This limit is known as the *Dirac*[§] *delta function* and is usually denoted $\delta(x-a)$.[¶]

It must be emphasized again that the Dirac delta function is not a function in the usual mathematical sense, since it has the anomalous behavior of having the value of infinity at one point and zero elsewhere. To understand why it represents a finite concentrated force we must remember that such a force is idealized as acting on a stretch of zero length and its intensity (the force divided by the length over which it acts) is consequently infinite.

When two quantities described by delta functions (be they forces, electric charges, magnetic poles or the like), of equal magnitude and opposite sign, are located a short distance apart, they are said to form a *dipole*. Suppose that there is a "force" $-F$ at $x=a$ and a "force" F at $x=a-d$, and let $C=Fd$ denote the *dipole strength*. The corresponding intensity may then be written as

$$p(x) \;=\; \frac{C}{d}[\delta(x-a+d)-\delta(x-a)]\,. \tag{A.11}$$

We see that, in the limit as $d \to 0$, the quantity multiplying C formally becomes the derivative of $\delta(x-a)$, to be denoted $\delta'(x-a)$ (and called the *dipole function* or the *unit doublet*), in the same way that $\delta(x-a)$ is the derivative of $H(x-a)$.

[§]Paul A.M. Dirac (1902-1984) was a British physicist.

[¶]In some Mechanics of Materials textbooks the strange notation $<x-a>_*^{-1}$ can be found; the subscript asterisk is there to tell us that the superscript -1 does not denote the power -1.

Appendix B: Tables

List of Tables

Table B-1 Unit conversions: US to SI 517
Table B-2 Unit conversions: SI to US 517
Table B-3 Geometric properties of some plane figures 518
Table B-4 Geometric properties of some three-dimensional figures 518
Table B-5 Physical properties of some solids, SI 519
Table B-6 Physical properties of some solids, US 520

$1\,\text{lb}_m$	$1\,\text{lb}_f$	1 ft	1 in	1 psf	1 ksi
0.454 kg	4.45 N	0.3048 m	25.4 mm	47.9 Pa	6.89 MPa

Table B-1. Unit conversions: US to SI

1 kg	1 N	1 m	1 cm	1 kPa	1 MPa
$2.20\,\text{lb}_m$	$0.225\,\text{lb}_f$	3.28 ft	0.394 in	20.9 psf	0.145 ksi

Table B-2. Unit conversions: SI to US

© Springer International Publishing Switzerland 2017
J. Lubliner, P. Papadopoulos, *Introduction to Solid Mechanics*,
DOI 10.1007/978-3-319-18878-2

Figure	Area	I_z	I_y	S	d
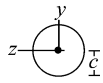	πc^2	$\frac{\pi c^4}{4}$	$\frac{\pi c^4}{4}$	$\frac{\pi c^3}{4}$	
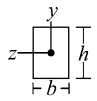	bh	$\frac{bh^3}{12}$	$\frac{b^3h}{12}$	$\frac{bh^2}{6}$	
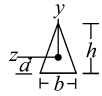	$\frac{bh}{2}$	$\frac{bh^3}{36}$	$\frac{b^3h}{48}$	$\frac{bh^2}{24}$	$\frac{h}{3}$
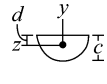	$\frac{\pi c^2}{2}$	$\left(\frac{\pi}{8}-\frac{8}{9\pi}\right)c^4$	$\frac{\pi c^4}{8}$		$\frac{4c}{3\pi}$
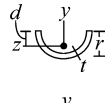	πrt	$\left(\frac{\pi}{2}-\frac{4}{\pi}\right)r^3t$	$\frac{\pi r^3 t}{2}$		$\frac{2r}{\pi}$
	πbc	$\frac{\pi bc^3}{4}$	$\frac{\pi b^3 c}{4}$	$\frac{\pi bc^2}{4}$	

Table B-3. Geometric properties of some plane figures

Figure perspective	Figure side view	Volume	d
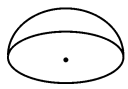	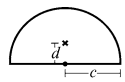	$\frac{2\pi c^3}{3}$	$\frac{3c}{8}$
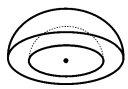	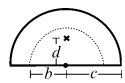	$\frac{2\pi(c^3-b^3)}{3}$	$\frac{3(b+c)(b^2+c^2)}{8(b^2+bc+c^2)}$
	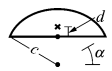	$\frac{(1-\sin\alpha)^2(2+\sin\alpha)\pi c^3}{3}$	$\frac{(3+\sin\alpha)(1-\sin\alpha)c}{4(2+\sin\alpha)}$
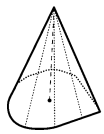	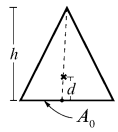	$\frac{A_0 h}{3}$	$\frac{h}{4}$
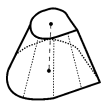	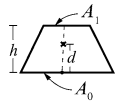	$\frac{\left(A_0+\sqrt{A_0A_1}+A_1\right)h}{3}$	$\frac{\left(A_0+2\sqrt{A_0A_1}+3A_1\right)h}{4\left(A_0+\sqrt{A_0A_1}+A_1\right)}$

Table B-4. Geometric properties of some three-dimensional figures (× denotes centroid)

Material	σ_U^t MPa	ε_{max} %	σ_Y MPa	σ_{all}^t MPa	σ_{all}^c MPa	τ_Y MPa	τ_{all} MPa	E GPa	G GPa	ν	α $10^{-6}/°K$	ρ kg/L
Aluminum alloy (6061-T6)	300	9	241	146	146	138	84	69	26	0.33	23.6	2.7
Aluminum alloy (7075-T6)	570	7	500	300	300	280	170	70	28	0.34	23.2	2.7
Brass (30% Zn)	255	65	120			70		100	38	0.31	20.5	8.49
Copper	70	45	70			40		120	45	0.33	16.8	8.9
Nylon	95	30	80			45		3.1	1.1	0.42	80	1.14
Polypropylene	45	100	35			20		1.4	0.5	0.4	85	0.89
Steel, mild (ASTM A36)	400	25	250	150	150	145	87	200	79	0.27	11.7	7.88
Steel, high-strength (AISI 1045)	585	12	450			250		200	78	0.29	10.5	7.87
Titanium	390	25	250			200		116	44	0.32	8.6	4.5

Ductile materials

Material	σ_U^t MPa	ε_{max} %	σ_U^c MPa	σ_{all}^t MPa	σ_{all}^c MPa	τ_U MPa	τ_{all} MPa	E GPa	G GPa	ν	α $10^{-6}/°K$	ρ kg/L
Bone, cortical (wet, longitudinal)	150	1.5	190					17	3.5		27	1.6–1.9
Cast iron, gray (ASTM 30)	210	0.1	750			275		100	40	0.23	10.5	7.2
Concrete, normal-strength	2.2	0.1	27	0	9	2.2	0.7	24	10	0.2	12	2.4
Concrete, high-strength	3.5+	0.1	40+	0	13+	3.5+	0.9+	30+	12	0.2	12	2.4
Glass	65	0.1	950			65		70	30	0.22	3.3	2.2
Phenolic (glass-fiber-reinforced)	70	1.5	200			70		4	1.5	0.35	15	1.8
Wood, Douglas fir (dry, longitudinal)	85	0.5	48			7.8		13	0.83–1.1	0.29–0.45	3.1	0.48
Wood, Oak (dry, longitudinal)	100	0.5	50			13		12	1.0–1.1	0.35–0.45	4.9	0.66
Wood, Pine (dry, longitudinal)	78	0.5	43			9		10.5	0.7–0.8	0.28–0.40	5.0	0.47

Brittle materials

Table B-5. Mechanical properties of some solids, SI (typical values)

Material	σ_U^{t} ksi	$\varepsilon_{\max}$ %	σ_Y ksi	$\sigma_{\mathrm{all}}^{\mathrm{t}}$ ksi	$\sigma_{\mathrm{all}}^{\mathrm{c}}$ ksi	τ_Y ksi	τ_{all} ksi	E 10^3 ksi	G 10^3 ksi	ν	α $10^{-6}/^{\circ}\mathrm{R}$	γ lb/ft^3
Aluminum alloy (6061-T6)	44	9	35	21	21	20	12	10	3.8	0.33	13.1	170
Aluminum alloy (7075-T6)	83	7	72	44	44	40	25	10	4	0.34	12.9	170
Brass (30% Zn)	37	65	17				10	14	5.4	0.31	11.4	530
Copper	10	45	10			6		17	6.5	0.33	9.3	555
Nylon	14	30	12			6.5		0.45	0.16	0.42	44	71
Polypropylene	6.5	100	5			3		0.2	0.07	0.4	47	55
Steel, mild (ASTM A36)	58	25	36	22	22	21	12.5	29	11.5	0.27	6.5	492
Steel, high-strength (AISI 1045)	85	12	65			36		29	11.3	0.29	5.8	490
Titanium	56	25	36			29		17	6.4	0.32	4.8	280

Ductile materials

Material	σ_U^{t} ksi	$\varepsilon_{\max}$ %	σ_U^{c} ksi	$\sigma_{\mathrm{all}}^{\mathrm{t}}$ ksi	$\sigma_{\mathrm{all}}^{\mathrm{c}}$ ksi	τ_U ksi	τ_{all} ksi	E 10^3 ksi	G 10^3 ksi	ν	α $10^{-6}/^{\circ}\mathrm{R}$	γ lb/ft^3
Bone, cortical (wet, longitudinal)	22	1.5	28					2.5	0.5		15	100–120
Cast iron, gray (ASTM 30)	29	0.1	65			40		14.5	5.8	0.23	5.8	450
Concrete, normal-strength	0.3	0.1	3.9	0	1.3	0.3	0.1	3.5	1.5	0.2	6.7	150
Concrete, high-strength	0.5+	0.1	6+	0	2+	0.5+	0.13+	4.4+	1.8+	0.2	6.7	150
Glass	9	0.1	140			9		10	4.3	0.22	1.8	140
Phenolic (glass-fiber-reinforced	10	1.5	30			10		0.58	0.22	0.35	8.3	110
Wood, Douglas fir (dry, longitudinal)	12	0.5	7.0			1.1		1.9	0.12–0.16	0.29–0.45	1.7	31
Wood, Oak (dry, longitudinal)	14.5	0.5	7.2			0.9		1.7	0.14–0.16	0.35–0.45	2.7	41
Wood, Pine (dry, longitudinal)	11	0.5	6.2			1.3		1.5	0.10–0.12	0.28–0.40	2.8	29

Brittle materials

Table B-6. Mechanical properties of some solids, US (typical values)

Photo Credits

Chapter 1:

Fig. 1.1. Portrait of Galileo. This picture was accessed in February 2012 from http://en.wikipedia.org/wiki/File:Justus_Sustermans_-Portrait_of_Galileo_Galilei,_1636.jpg. This work is in the public domain.

Fig. 1.2. Portrait of Newton. This picture was accessed in February 2012 from http://en.wikipedia.org/wiki/File:GodfreyKneller-IsaacNewton-1689.jpg. This work is in the public domain.

Chapter 2:

Fig. 2.6. Portrait of Euler. This picture was accessed in February 2012 from http://en.wikipedia.org/wiki/File:Leonhard_Euler_2.jpg. This work is in the public domain.

Fig. 2.14, 2.15. Greatly cropped from various sources

Chapter 3:

Fig. 3.23. Truss Bridge in Walnut Creek, CA. This picture was taken in January, 2006, by Leonard G. Barton and accessed in January, 2010, from http://en.wikipedia.org/wiki/File:RRTrussBridgeSideView.jpg. This work is in the public domain.

Fig. 3.24b. Shane 3-m Telescope. This picture was accessed in January, 2010, from http://mthamilton.ucolick.org/techdocs/telescopes/Shane/index.html. This work is ©UC Regents/Lick Observatory and is used by permission.

Fig. 3.25. Authors' photo

Fig. 3.32c. Patellofemoral (knee) joint. This picture was accessed in November, 2012, from http://blog.affinityhealth.org/wp-content/uploads/2011/11/patellofemoral-joint1.jpg and in January, 2013, from

© Springer International Publishing Switzerland 2017

J. Lubliner, P. Papadopoulos, *Introduction to Solid Mechanics*,
DOI 10.1007/978-3-319-18878-2

http://www.physios-online.com/Resources/Articles/Patello-femoral-joint--or-steam-train-.aspx. The source is unknown.

Exercise 3.4-10. Authors' photo

Chapter 4:

Fig. 4.26. Portrait of Cauchy. This picture was accessed in January, 2010, from http://en.wikipedia.org/wiki/File:Augustin-Louis_Cauchy_1901.jpg. This work is in the public domain.

Fig. 4.40. Portrait of Mohr. This picture was accessed in January, 2010, from http://fr.wikipedia.org/wiki/Fichier:Christian_Otto_Mohr.jpg. This work is in the public domain.

Chapter 6:

Fig. 6.16b. Authors' photo

Chapter 8:

Fig. 8.21. Portrait of Daniel Bernoulli. This picture was accessed in January, 2010, from http://en.wikipedia.org/wiki/File:Daniel_Bernoulli_001.jpg. This work is in the public domain.

Chapter 10:

Fig. 10.1. Authors' photo.

Fig. 10.9. Portrait of Lord Rayleigh. This picture was accessed in January, 2010, from http://en.wikipedia.org/wiki/File:John_William_Strutt.jpg. This work is in the public domain.

Fig. 10.19a. Column of the Temple of Neptune, Paestum (Italy). This picture was cropped from one taken in or before 1868 by Giorgio Sommer (1834-1914) and accessed in January, 2013, from http://commons.wikimedia.org/wiki/File:Sommer,_Giorgio_%281834-1914%29_-_n._0283_-_Tempio_di_Nettuno_-_Pesto_%28Napoli%29_%28dated_1868%29_2.jpg. This work is in the public domain.

Fig. 10.19b. Sandy Chapman entasis floor lamp. This picture was obtained from Visual Comfort & Co. (www.visualcomfort.com) and is used by permission.

Chapter 11:

Fig. 11.4. Photos made for authors by Cruz Carlos (Dept. of Civil and Environmental Engineering, University of California, Berkeley).

Fig. 11.6. Authors' photo.

Fig. 11.18b. Failure cone. This picture was cropped from one accessed in November, 2012, from `http://ars.els-cdn.com/content/image/1-s2.0-S1359836800000433-gr9.jpg` and is used by permission of the publisher, Elsevier.

Fig. 11.18c. Splitting failure. This picture was accessed in January, 2013, from `http://ars.els-cdn.com/content/image/1-s2.0-S0261306904003309-gr1.jpg` and is used by permission of the publisher, Elsevier.

Fig. 11.18d. Shear failure. This picture was cropped from one accessed in November, 2012, from `http://ars.els-cdn.com/content/image/1-s2.0-S1359836800000433-gr9.jpg` and is used by permission of the publisher, Elsevier.

Fig. 11.22. Authors' photo

Index

acceleration, 2, 16
action-reaction law, *see* Newton's Third Law
allowable stress, 173–176, 282, 370, 410, 466
Amontons-Coulomb law, *see* Coulomb's law
amorphous, 267
angle of repose, 509
angle of twist, 324, 328, 342
  diagram, 343
angular velocity, 58, 330
arch, 103, 174, 435
  three-hinged or three-pinned, 72, 76, 103, 111, 115, 134, 275
    rise, 77
    span, 77
articulation, 107
axial rigidity, 274
  effective, 279, 329
axial stiffness, 274

bar
  composite, 278
  definition, 100
beam
  cantilever, 247, 355–357, 359, 393, 394, 447
  composite, 405
  continuous, 394
  definition, 82, 100
  initially curved, 375, 399
  simply supported, 82, 355, 357, 360, 391, 392, 394, 398, 447
beam-column, 442, 456
bearing stress, 175
bending
  pure, 366
Bernoulli–Euler beam theory, 379, 424
biaxial stress, 159
bifurcation, 444
body
  continuous, 1
  definition, 1
  deformable, 1
  finite, 1
  homogeneous, 260
  overconstrained, 72
  rigid, 1, 65
  three-force, 68
  two-force, 68, 70, 77, 107
  underconstrained, 72
body force, 24, 183, 188, 195
Brazilian test, 475
brittle material, 474, 477, 478, 480
buckling, 441
  mode, 447, 460
built-in support, 71
bulk modulus, 262

cable, 108, 142, 145
  catenary, 150
  sag, 147
Cartesian coordinate system
  basis, 17
Castigliano's theorems, 305, 386, 396
Cauchy tetrahedron, 185
Cauchy's equations, 191
center of gravity, 43

© Springer International Publishing Switzerland 2017
J. Lubliner, P. Papadopoulos, *Introduction to Solid Mechanics*,
DOI 10.1007/978-3-319-18878-2

center of mass, 45
centroid, 45, 274
  effective (axial force), 279
chain, 108, 142, 145
  simple, 143
chain rule, 240
chord
  bottom, 116
  top, 116
cohesion, 490
column, 100, 175, 253, 281, 283, 442, 446–448, 456, 458–466, 487, 488
compatibility, 143, 144, 147, 233, 274, 290–293, 295, 307, 317, 325, 344
complementary energy, 301, 329, 337
  bending, Euler–Bernoulli, 386
  bending, pure, 375
compliance, 266
composite bar, 278
compound shaft, 342
configuration, 1
conjugate, 58, 61, 236, 247, 293, 304
conservation of energy, 304
constraint, 58
  external, 59, 69
  internal, 59
continuum, 1
coordinates
  generalized, 61, 247, 292, 296, 305
coplanar
  forces, 27, 65
Coulomb's law, 74
couple, 35
creep, 494
  curve, 496
  function, 496
critical load, 442, 443, 458, 460
cross product, 16
crystalline, 267
curvature, 368
  radius, 367
curve, 383
  inclination, 383

deformation, 1, 65, 112, 215, 218, 224, 230, 235, 249, 258, 501
degrees of freedom, 69
  internal, 72
design, 172
deviatoric, 263
diagram
  axial-force, 102, 280
  bending-moment, 102
  shear-force, 102
dilatation, 245, 264, 310
dimensionless, 8
dipole function, 359, 515
Dirac delta function, 358, 515
direction cosines, 19
dislocation, 487
displacement, 1, 55, 219, 247, 290, 291
  axial, 219
  generalized, 247, 292, 293, 296, 300, 310
  infinitesimal, 59
  rigid, 1, 230
  vector, 230
  virtual, 59–61, 220, 284, 374, 385, 451, 506
displacement field, 230, 295, 310
displacement method, 276, 290–292, 305, 385, 393
distortion, 245, 264, 310
distribution (mathematics), 514
dot product, 16
ductile material, 155, 156, 426, 474, 480

eccentric loading, 434
effective centroid
  axial force, 279
effective flexural rigidity, 405, 408
eigenvalue, 203, 414, 447, 461
eigenvector, 203

elastic curve, 379, 385
elastic energy, 301
  bending, Euler–Bernoulli, 386
elastic limit, 477
elastic–perfectly plastic, 481, 482, 503, 507, 509
elasticity
  linear, 248
elasticity matrix, 265, 267, 309
elongation diagram, 283
energy, 7
  complementary, 301, 329, 337
  conservation of, principle, 304
  elastic, 301
  free, 318
  per unit volume, 308
  strain, 301
  thermal, 7, 315
equilibrium, 3, 53, 54, 56, 58–60, 66–68, 74, 76, 78–80, 82, 88, 89, 93, 98, 99, 101–104, 107, 109–111, 117–122, 136, 137, 142, 144–146, 148, 150, 162, 165, 170, 181, 189–191, 195, 224, 279, 280, 295, 296, 307, 317, 324, 338, 354, 357, 360, 385, 395, 409, 427, 429, 442, 444, 447, 450–452, 456, 460
  definition, 51
  equation(s), 55, 65–67, 72, 73, 75–77, 80, 98, 101, 104, 110, 111, 118–120, 122, 134, 135, 142, 144, 147, 170, 183, 188, 190, 192, 197, 198, 216, 259, 274–276, 281, 284, 289–292, 343, 353, 354, 361, 368, 379, 385, 392, 421, 423, 443, 444, 446, 447, 456, 464
  local, 188, 281, 421
  stable, 145, 307, 442, 444, 450–452, 460
  unstable, 145, 442, 444, 451
Euler load, 460
Euler's laws, 56
external constraint, 59

fiber
  neutral, 367
finite-element method, 295, 310
first variation, 451
fixed support, 71
flexibility
  axial, 280
flexibility coefficients, 293, 302, 388
flexibility matrix, 302
flexural rigidity, 369, 387
  effective, 405, 408
flexural strength, 475
force, 24
  axial, 100
    diagrams, 102
  body, 24, 183, 188, 195
  central, 54
  collinear, 27
  concentrated, 27
  concurrent, 27
  contact, 24
  definition, 2
  distributed, 27
  disturbing, 442
  equal and opposite, 26
  external, 52, 56
  frictional, 74
  generalized, 61, 247, 293, 300, 305
  intensity, 27
  internal, 55
  lever arm, 30
  line of action, 24
  moment arm, 30
  restoring, 442
  resultant, 24
  shear, 100
force couple, 34
force method, 276, 290–292, 306, 344, 347, 388, 396

force system, 40
  definition, 40
  planar, 65, 68, 75
  statically equivalent, 40
fracture, 474, 477, 479, 492, 493, 501–503, 509
frame, 108, 134
free energy, 318
free-body diagram, 75
frequency, 330
friction, 73
  angle of kinetic, 79
  angle of static, 79
  dry, 73
  fluid, 73
  internal, 486, 490
  wet, 73
friction coefficient
  kinetic, 74
  static, 74

generalized coordinates, 61, 247, 292, 296, 305
generalized displacement, 247, 292, 293, 296, 300, 310
generalized force, 61, 247, 293, 300, 305
gravity
  center of, 27, 43
  specific, 27
guided support, 71

hardening
  work- or strain-, 481
Heaviside step function, 358, 359, 513
hertz, 330
Hooke's law, 248
  uniaxial, 250
horsepower, 7
hyperstatic, 110
hypostatic, 112

improper supports, 70
incompressible, 245, 252, 262, 308
inelastic strain, 495
initial modulus, 478
internal constraint, 59
internal friction, 486, 490
  angle of, 491, 509
  coefficient of, 490, 509
Iosipescu shear test, 476
isostatic, 110
isotropic, 257, 262, 264, 265, 267, 268, 308–310, 315, 318, 488, 491
  transversely, 269
isotropy, 257–260
  transverse, 269

joint
  ball-and-socket, 90

Kelvin model, 497, 498
  generalized, 498

Lamé coefficients, 262
Lamé stress ellipsoid, 213
line of action, 24
linear elasticity, 248
link
  of a chain, 142
load, 75
  critical, 442, 443, 458, 460
  dead, 173
  design, 173
  Euler, 460
  live, 173
load factor, 173, 505
longitudinal strain, 216, 473

Macaulay brackets, 359, 513
machine, 108, 134, 136
mass
  center of, 45
mass density, 45
material
  anisotropic, 257
  auxetic, 258
  brittle, 382, 474, 477, 478, 480

ductile, 155, 156, 426, 474, 480
rate-dependent, 249
rate-independent, 249
Maxwell model, 497, 498
generalized, 498
Maxwell–Betti reciprocal theorem, 303, 397
mean stress, 203, 262
mechanics, 1
solid, 1
mechanism, 72, 108, 112, 137, 138, 142, 248, 441, 486, 501, 502, 504–507
collapse, 507, 508
failure, 486–488, 492, 493
member, 107
force, 107
method of joints, 109, 502
method of sections, 77, 98, 280
microstrain, 217
middle-third rule, 435
minimum total potential energy, principle of, 307, 398
Mises criterion, 489, 490, 492
modulus of rupture, 381, 475, 503
Mohr's circle, 205, 207, 208
strain, 243, 244
Mohr's first theorem, 403
Mohr's second theorem, 403
Mohr–Coulomb criterion, 491, 492
moment, 7, 30
bending, 100, 413
diagrams, 102
resultant, 33, 34
torsional, 100
twisting, 100
moment of inertia, *see* second moment of area
motion, 2
accelerated, 2
uniform, 2

necking, 474, 482
neutral fiber, 367
neutral plane, 368, 413
Newton's First Law, 51
Newton's law of universal gravitation, 63
Newton's laws of motion, 51
Newton's Second Law, 51
Newton's Third Law, 52, 53, 78, 109
nonlinearity
geometric, 142
normal stress, 156, 157, 180, 181, 473

octahedral planes, 208
octahedral shear stress, 209
overhang, 71, 394

parallel-axis theorem, 373
particle, 1
definition, 51
Pascal's law, 191, 203
planar force system, 65, 68, 75
plane
neutral, 368
plane strain, 232, 260, 266, 312
plane stress, 188, 191, 195, 201, 203, 207, 260, 266, 488, 489, 491
plastic modulus, 504
plastic strain, 477
Poisson's ratio, 258, 368
positive-definite, 452
potential energy
minimum total, principle of, 307, 398
power, 57
pressure, 6, 27, 203
pressure vessel, 169, 266
principal invariants, 202
principle of conservation of energy, 304
principle of least resistance, 460, 487, 488, 492, 501
principle of superposition, 258, 283, 293, 316, 387, 395, 496
principle of transmissibility, 33

principle of virtual work, 296
proper supports, 70, 108
pseudoelasticity, 477
pure bending, 366
pure shear, 208

Ramberg–Osgood formula, 482, 484
ramp function, 513
Rayleigh quotient, 452
Rayleigh's method, 452, 453, 466
reaction, 69, 75
  internal, 98, 107
  redundant, 290
rebar, 408
reciprocal theorem (Maxwell–Betti), 303, 397
redundancy, 111
redundant reaction, 290
relaxation, 494
right-hand rule, 100
rigid
  body, 1
  particle system, 55
rigid body, 65
rigidity
  axial, 274
  effective axial, 279, 329
  effective torsional, 329
  torsional, 326, 348, 349
roller support, 70
rosette
  delta, 241
  rectangular, 241
rupture, 474, 475, 482, 483, 501
  modulus of, 381, 475, 503

safety factor, 173, 505
Saint-Venant's principle, 159, 174, 253, 274, 323, 474
sand-heap analogy, 509
scalar, 8
scalar product, 16
secant formula, 465
secant modulus, 251, 478
second moment of area, 369, 414
  mixed, 414
  polar, 326
second variation, 452
section modulus, 370, 503
shaft
  compound, 342
  definition, 100
shape factor, 504
shear
  double, 165
  force
    diagrams, 102
  single, 165
shear center, 429
shear flow, 335, 424
shear modulus, 253
shear strain, 473
shear stress, 162–164, 180, 181, 473
  average, 164
  direct, 436
  maximum in-plane, 204
  octahedral, 209
sign convention, 100
significant digits, 8
simple shear, 191, 208, 235, 253, 308, 329, 337, 476, 491
simple stress state, 169, 173, 192, 336
simply supported body, 71
singularity functions, 282, 343, 344, 513
slenderness ratio, 380, 423, 460
  critical, 461
softening, 479, 480, 482
solid, 1
span, 143
specific weight, 27, 283
spherical angles, 20
spring, 247
  inelastic, 248
  linear, 247
  linearly elastic, 247
  nonlinearly elastic, 248

rotational, 247
translational, 247
spring constant
torsional, 328
standard solid model, 495, 497, 498
statically determinate, 72, 75, 110, 385
externally, 110, 324
locally, 169, 192
statically indeterminate, 72, 110, 111, 147, 289, 388, 395
degree, 111
externally, 147
locally, 324
statically underdeterminate, 112
statics
definition, 3
stiffness
axial, 274
torsional, 328
stiffness coefficients, 291, 293
stiffness matrix, 302
global, 312
stirrup, 428
strain
area, 244
average, 218
conventional, 216
deviatoric, 264, 309
engineering, 216, 480
finite, 216
inelastic, 495
infinitesimal, 216, 473
local, 218
logarithmic, 217, 480
longitudinal, 216, 231, 232, 473
normal, 232
plane, 232, 260, 266, 312
plastic, 477
shear, 224, 473
engineering, 225, 232
tensor, 233
thermal, 315
true, 217
volumetric, 245, 262, 315
strain energy, 301
bending, Euler–Bernoulli, 386
bending, pure, 375
strain ga(u)ge, 218
strain-gauge rosette, 241
strain-hardening, 481
strength
compressive, ultimate, 156, 478, 479
flexural, 475
shear, ultimate, 163
tensile, ultimate, 156, 251, 474, 475, 478, 482
ultimate, 174
stress, 6
allowable bearing, 175
allowable normal, 173–175, 282, 370, 410, 466
allowable shear, 175, 176
average normal, 157
bearing, 175
biaxial, 159
components, 182
compressive, 157
critical, 173
deviatoric, 263, 309
engineering, 156
equibiaxial, 159, 170
equitriaxial, 159
hydrostatic, 159
mean, 203, 262
mean in-plane, 201, 203, 204
nominal, 156
non-uniform, 158
normal, 156, 157, 180, 181, 473
plane, 188, 191, 195, 201, 203, 207, 260, 266, 488, 489, 491
principal, 199
shear, 162–164, 180, 181, 473
average, 164
state of, 182
tensile, 157

tensor, 182
thermal, 317
triaxial, 159
true, 156, 251, 480, 483
uniaxial, 159, 368
uniform, 157
yield, 480
stress factor, 173, 505
stress field
normal, 157
shear, 164
stress function, 347
stress state
hydrostatic, 203
simple, 169, 173, 192, 336
triaxial, 207
stress vector, 183
stress-strain diagram, 251, 473
stretch, 215, 252
local, 219
structure, 108
nonlinear, 144
subbody, 98
superposition, principle of, 258, 283, 293, 316, 387, 395, 496
Boltzmann, 498
support, 69
1-dof, 70
built-in or fixed, 71
guided, 71
pin or hinge, 71
roller, 70
simple, 71
supports
improper, 70
proper, 70, 108

tangent modulus, 251, 478
temperature, 7
absolute, 7
Celsius, 7
tensor, 414
rotation, 234
strain, 233
stress, 182
thermal expansion, linear coefficient of, 315
thermal strain, 315
thermal stress, 317
thin-walled, 169
definition, 169
three-point flexural test, 475
torque, 36, 100, 171, 193
torque-twist relation, 325, 326
torsional rigidity, 326, 348, 349
effective, 329
torsional spring constant, 328
torsional stiffness, 328
toughness, 483
traction vector, 183
transformed section, 407
Tresca criterion, 488–490, 492, 493
triaxial stress, 159
tribology, 74
triple product
scalar, 21
vector, 21, 186
truss, 108, 115
cantilevered, 116
flat, 116
Howe, 116
open, 116
pitched, 116
Pratt, 116, 129
Serrurier, 130
space, 127
simple, 127
statically determinate, 117
twist, 325
angle of, 324, 328, 342
two-force body, 68, 70, 77, 107

ultimate load, 501, 502, 505
ultimate moment, 503–505
ultimate strength, 174
compressive, 474, 478, 479

shear, 163, 474
tensile, 251, 474, 475, 478, 482
uniaxial stress, 159, 368
unit doublet, 515
units
imperial, 4
metric, 4
US customary, 4
unloading-reloading modulus, 478

variation
first, 451
second, 452
Varignon's theorem, 33
vector, 14
Cartesian components, 18
Cartesian coordinate system, 17
cross product, 16
differentiation with respect to a scalar variable, 15
dot product, 16
equal and opposite, 14
free, 35
orthogonal, 16
parallel, 17
parallelogram rule, 14
scalar multiplication, 14
scalar product, 16
unit, 16
vector product, 16
zero, 14
vector product, 16
velocity, 2, 16
virtual displacement, 59–61, 220, 284, 374, 385, 451, 506
virtual strain
longitudinal, 220
shear, 235
virtual work, 57, 59, 60, 227
definition, 59
external, 60, 508
external (axial), 284
external (Euler–Bernoulli), 385, 397
external (pure bending), 374, 375
external (torsion), 329
internal, 60, 220, 236, 265, 508
internal (axial), 283, 374, 483
internal (bending), 375, 385
internal (shear), 228, 235, 308
internal (torsion), 329
principle of, 58, 60, 220, 284, 296, 375, 385, 505, 507
viscoelasticity, 494
Kelvin model, 497, 498
Maxwell model, 497, 498
standard solid model, 495, 497, 498
volume
center of, 45
volumetric strain, 245, 262, 315

warping, 325
web, 116
weight
specific, 27, 283
work, 7, 57
actual, 51, 57, 221, 329, 375, 483
infinitesimal, 57
virtual, 51, 57–60, 220, 221, 227, 283, 284, 329, 374, 385, 483, 505
work-hardening, 481, 482

yield moment, 503
yield stress, 156, 174, 480
yielding, 155, 474
Young's modulus, 250–252, 273, 278, 282, 368, 405–407, 410, 478

zero-force member, 117